

C5320 Theoretical Concepts of NMR

Lukáš Židek

May 16, 2020

Contents

I	Classical Introduction	1
	Before we start	3
0.1	Classical electromagnetism	3
0.1.1	Electric field, electric charge, electric dipole	3
0.1.2	Magnetic field and magnetic dipole	4
0.1.3	Source of the electric field	4
0.1.4	Origin of the magnetic field	5
0.1.5	Electrodynamics and magnetodynamics	7
0.1.6	Potential energy of an electric dipole	8
0.1.7	Current loop as a magnetic dipole	8
0.1.8	Precession	10
0.1.9	Electromotoric voltage	11
0.2	Classical mechanics: Newton, Lagrange, Hamilton	13
0.2.1	Legendre transformation	16
0.2.2	Lagrangian and Hamiltonian including magnetism	16
0.3	Diffusion	19
0.3.1	Translational diffusion	20
0.3.2	Isotropic rotational diffusion	21
	Nuclear magnetic resonance	23
1.1	Nuclear magnetic moments in chemical substances	23
1.2	Polarization	23
1.3	Coherence	24
1.4	Chemical shift	25
1.5	DERIVATIONS	30
1.5.1	Polarization and bulk magnetization	30
1.5.2	Rotating coordinate frame	31
1.5.3	Chemical shift tensor	32
1.5.4	Offset effects	33
1.5.5	Evolution of magnetization in \vec{B}_0	35

Relaxation	37
2.1 Relaxation due to chemical shift anisotropy	37
2.2 Adiabatic contribution to relaxation	38
2.3 Including non-adiabatic contribution to relaxation	40
2.4 Internal motions, structural changes	42
2.5 Bloch equations	43
2.6 DERIVATIONS	44
2.6.1 Loss of coherence	44
2.6.2 Time correlation function	47
2.6.3 Return to equilibrium	50
Signal acquisition and processing	55
3.1 NMR experiment	55
3.1.1 Setting up the experiment	55
3.1.2 Quadrature detection	56
3.1.3 Analog-digital conversion	57
3.1.4 Signal averaging and signal-to-noise ratio	57
3.2 Fourier transformation	57
3.2.1 Properties of continuous Fourier transformation	64
3.2.2 Consequence of finite signal acquisition	64
3.2.3 Discrete Fourier transformation	66
3.2.4 Consequence of discrete signal acquisition	67
3.3 Phase correction	68
3.4 Zero filling	68
3.5 Apodization	71
3.6 DERIVATIONS	73
3.6.1 Resonator impedance	73
3.6.2 Power and attenuation	73
3.6.3 Quadrature detection and complex signal	73
3.6.4 Noise accumulation	73
3.6.5 Mathematical description of Fourier transformation	74
3.6.6 Fourier transformation of an ideal NMR signal	75
3.6.7 Causality and reconstruction of imaginary signal	75
3.6.8 Spectral width, resolution, and sampling	75
3.6.9 Discrete ideal signal	77
3.6.10 Dolph–Chebyshev window	77
II Quantum description	79
Review of quantum mechanics	81
4.1 Wave function and state of the system	81
4.2 Superposition and localization in space	82

4.3	Operators and possible results of measurement	82
4.4	Expected result of measurement	85
4.5	Operators of position and momentum, commutators	86
4.6	Operator of energy and equation of motion	88
4.7	Operator of angular momentum	89
4.8	Operator of orbital magnetic moment	91
4.9	DERIVATIONS	92
4.9.1	Calculating square	92
4.9.2	Orthogonality and normalization of monochromatic waves	92
4.9.3	Eigenfunctions and eigenvalues, operator of momentum	93
4.9.4	Operator of position	93
4.9.5	Commutation relations of the position and momentum operators	94
4.9.6	Schrödinger equation	95
4.9.7	Limitation of wave equation to first time derivative	96
4.9.8	Angular momentum and rotation	98
4.9.9	Commutators of angular momentum operators	99
Spin		101
5.1	Dirac equation	101
5.2	Operator of the spin magnetic moment	102
5.3	Operators of spin angular momentum	103
5.4	Eigenfunctions and eigenvalues of \hat{I}_z	104
5.5	Evolution, eigenstates and energy levels	105
5.6	Real particles	107
5.7	DERIVATIONS	109
5.7.1	Relativistic quantum mechanics	109
5.7.2	Finding the matrices	112
5.7.3	Solution of the Dirac equation	114
5.7.4	Relation between Dirac and Schrödinger equations	116
5.7.5	Hamiltonian of spin magnetic moment	116
5.7.6	The factor of one half in the eigenvalues of \hat{I}_z	119
5.7.7	Eigenfunctions of \hat{I}_x and \hat{I}_y	120
5.7.8	Stationary states and energy level diagram	122
5.7.9	Oscillatory states	122
Ensemble of non-interacting spins		125
6.1	Mixed state	125
6.2	Populations	129
6.3	Coherence	130
6.4	Basis sets	131
6.5	Liouville - von Neumann equation	132
6.6	General strategy of analyzing NMR experiments	133
6.7	DERIVATIONS	135

6.7.1	Indistinguishable particles	135
6.7.2	Separation of variables	136
6.7.3	Phases and coherences	137
6.7.4	From Schrödinger to Liouville - von Neumann equation	138
6.7.5	Rotation in operator space	139
Chemical shift, one-pulse experiment		141
7.1	Operator of the observed quantity	141
7.2	Hamiltonian of the static field \vec{B}_0	141
7.3	Hamiltonian of the radio-frequency field \vec{B}_1	141
7.4	Hamiltonian of chemical shift	142
7.5	Secular approximation and averaging	143
7.6	Thermal equilibrium as the initial state	144
7.7	Relaxation due to chemical shift anisotropy	144
7.8	One-pulse experiment	146
7.8.1	Part 1: excitation by radio wave pulses	146
7.8.2	Part 2: evolution of chemical shift after excitation	147
7.9	Conclusions	148
7.10	DERIVATIONS	150
7.10.1	Decomposition of chemical shift Hamiltonian	150
7.10.2	Density matrix in thermal equilibrium	150
7.10.3	Bloch-Wangsness-Redfield theory	151
7.10.4	Spectrum and signal-to-noise ratio	153
Dipolar coupling, product operators		157
8.1	Dipolar coupling	157
8.2	Quantum states of magnetic moment pairs	159
8.3	Product operators	160
8.4	Density matrix of a two-spin system	163
8.5	Evolution of coupled spin states	163
8.6	Operator of the observed quantity for more nuclei	166
8.7	Dipolar relaxation	166
8.8	Thermal equilibrium with dipolar coupling	168
8.9	DERIVATIONS	170
8.9.1	Tensor and Hamiltonian of dipolar coupling	170
8.9.2	Secular approximation and averaging of dipolar Hamiltonian	171
8.9.3	Interacting and non-interacting magnetic moments	172
8.9.4	Commutators of product operators	174
8.9.5	Dipole-dipole relaxation	175
8.9.6	Two magnetic moments in thermal equilibrium	180

Two-dimensional spectroscopy, NOESY	183
9.1 Two-dimensional spectroscopy	183
9.2 Evolution in the absence of dipolar coupling	184
9.3 Signal modulation in a two-dimensional experiment	185
9.4 NOESY	188
9.5 DERIVATIONS	190
9.5.1 Quantitative analysis of cross-relaxation in NOESY	190
9.5.2 Intensity of NOESY cross-peaks	190
<i>J</i>-coupling, spin echoes	193
10.1 Through-bond coupling	193
10.2 Secular approximation, averaging, and relaxation	194
10.3 Density matrix evolution in the presence of <i>J</i> -coupling	196
10.4 Homo- and heteronuclear magnetic moment pairs	201
10.5 Spin echoes	202
10.6 Refocusing echo	205
10.7 Decoupling echo	206
10.8 Simultaneous echo	206
10.9 DERIVATIONS	208
10.9.1 Interaction between nuclei mediated by bond electrons	208
10.9.2 Two electrons in a sigma orbital	210
10.9.3 Two <i>J</i> -coupled nuclei in thermal equilibrium	213
Correlated spectroscopy using <i>J</i>-coupling	217
11.1 INEPT	217
11.2 HSQC	220
11.3 Decoupling trains	224
11.4 Benefits of HSQC	224
11.5 COSY	226
11.6 DERIVATIONS	233
11.6.1 APT	233
11.6.2 Double-quantum filtered COSY	233
Strong coupling	237
12.1 Strong <i>J</i> -coupling	237
12.2 Magnetic equivalence	239
12.3 TOCSY	241
12.4 DERIVATIONS	245
12.4.1 Diagonalization of the <i>J</i> -coupling Hamiltonian matrix	245
12.4.2 Strong <i>J</i> -coupling and density matrix evolution	248
12.4.3 \mathcal{H}_j and operators of components of total \vec{I} commute	249
12.4.4 <i>J</i> -coupling of magnetically equivalent nuclei	249
12.4.5 Commutation relations of the TOCSY mixing Hamiltonian	250

12.4.6	Density matrix evolution in the TOCSY experiment	250
Field gradients		257
13.1	Pulsed field gradients in NMR spectroscopy	257
13.2	Magnetic resonance imaging	261
13.3	Weighting	264
13.4	DERIVATIONS	268
13.4.1	Coherence dephasing and slice selection by field gradients	268
13.4.2	Field gradients with smooth amplitude	269
13.4.3	Frequency encoding gradients	269
13.4.4	Phase encoding gradients	270

Part I

Classical Introduction

Before we start

0.1 Classical electromagnetism

Literature: Discussed in¹ L2 and B11, with mathematical background in B4.

0.1.1 Electric field, electric charge, electric dipole

Objects having a property known as the *electric charge* (Q) experience forces (\vec{F}) described as the *electric field*. Since the force depends on both charge and field, a quantity $\vec{E} = \vec{F}/Q$ known as *electric intensity* has been introduced:

$$\vec{F} = Q\vec{E}. \quad (1)$$

Field lines are often used to visualize the fields: direction of the line shows the direction of \vec{E} , density of the lines describes the size of \vec{E} ($|E|$). A homogeneous static electric field is described by straight parallel field lines.

Two point electric charges of the same size and opposite sign ($+Q$ and $-Q$) separated by a distance $2r$ constitute an *electric dipole*. Electric dipoles in a homogeneous static electric field experience a *moment of force*, or *torque* $\vec{\tau}$:

$$\vec{\tau} = 2\vec{r} \times \vec{F} = 2\vec{r} \times Q\vec{E} = 2Q\vec{r} \times \vec{E} = \vec{\mu}_e \times \vec{E}, \quad (2)$$

where $\vec{\mu}_e$ is the *electric dipole moment*.

$$\vec{\tau} = \vec{\mu}_e \times \vec{E}, \quad (3)$$

is another possible definition of \vec{E} . As derived in Section 0.1.6, potential energy of an electric dipole is

$$\mathcal{E} = -\vec{\mu}_e \cdot \vec{E}. \quad (4)$$

¹The references consist of a letter specifying the textbook and a number specifying the section. The letters refer to the following books: **B**, Brown: Essential mathematics for NMR and MRI spectroscopists, Royal Society of Chemistry 2017; **C**, Cavanagh et al., Protein NMR spectroscopy, 2nd. ed., Academic Press 2006; **K**, Keeler, Understanding NMR spectroscopy, 2nd. ed., Wiley 2010; **L** Levitt: Spin dynamics, 2nd. ed., Wiley 2008.

0.1.2 Magnetic field and magnetic dipole

There is no "magnetic charge", but magnetic moments exist:

$$\vec{\tau} = \vec{\mu}_m \times \vec{B}, \quad (5)$$

where $\vec{\mu}_m$ is the *magnetic dipole moment* (because this course is about magnetic resonance, we will write simple $\vec{\mu}$). This is the *definition* of the *magnetic induction* \vec{B} as a quantity describing magnetic field. As a consequence, potential energy of a magnetic dipole can be derived as described by Eq. 27 for the electric dipole.

Potential energy of a magnetic moment $\vec{\mu}$ is

$$\mathcal{E} = -\vec{\mu} \cdot \vec{B}. \quad (6)$$

The magnetic induction \vec{B} is related to the force acting on a charged object, but in a different way than the electric intensity \vec{E} (cf. Eq. 1). The magnetic force depends not only on the electric charge Q but also on the speed of the charge \vec{v} (i.e., on the *electric current*)

$$\vec{F} = Q(\vec{v} \times \vec{B}). \quad (7)$$

Therefore, the torque $\vec{\tau}$ cannot be described by an equation similar to Eq. 3. Instead,

$$\vec{\tau} = \vec{r} \times \vec{F} = Q\vec{r} \times (\vec{v} \times \vec{B}). \quad (8)$$

Due to the fundamental difference between Eqs. 3 and 8, it is more difficult to describe relation between the magnetic force, magnetic moment and energy. We experience it in Sections 0.1.7 and 0.2.

0.1.3 Source of the electric field

The source of the electric field is the *electric charge*. The charge (i) feels (a surrounding) field and (ii) makes (its own) field. Charge at rest is a source of a static electric field. Parallel plates with homogeneous distribution of charges (a capacitor) are a source of a homogeneous static electric field.

Force between charges is described by the *Coulomb's law*. The force between two charges is given by

$$\vec{F} = \frac{1}{4\pi\epsilon_0} \frac{Q_1 Q_2}{r^2} \frac{\vec{r}}{|r|}, \quad (9)$$

where $\epsilon_0 = 8.854187817 \times 10^{-12} \text{ F m}^{-1}$ is the vacuum electric permittivity. Consequently, the electric intensity generated by a point charge is

$$\vec{E} = \frac{1}{4\pi\epsilon_0} \frac{Q}{r^2} \frac{\vec{r}}{|r|}. \quad (10)$$

The electric intensity generated by a charge density ρ is

$$\vec{E} = \frac{1}{4\pi\epsilon_0} \int_V dV \frac{\rho}{r^2} \frac{\vec{r}}{|r|} \quad (11)$$

Coulomb's law implies that electric fields lines of a resting charge

1. are going out of the charge (diverge), i.e., the static electric field has a source (the charge)
2. are not curved (do not have curl or rotation), i.e., the static electric field does not circulate

This can be written mathematically in the form of *Maxwell equations*²:

$$\operatorname{div} \vec{E} = \frac{\rho}{\epsilon_0}, \quad (12)$$

$$\operatorname{rot} \vec{E} = 0. \quad (13)$$

where $\operatorname{div} \vec{E}$ is a scalar equal to $\frac{\partial E_x}{\partial x} + \frac{\partial E_y}{\partial y} + \frac{\partial E_z}{\partial z}$ and $\operatorname{rot} \vec{E}$ is a vector with the x, y, z components equal to $\frac{\partial E_z}{\partial y} - \frac{\partial E_y}{\partial z}$, $\frac{\partial E_x}{\partial z} - \frac{\partial E_z}{\partial x}$, $\frac{\partial E_y}{\partial x} - \frac{\partial E_x}{\partial y}$, respectively. These expressions can be written in a much more compact form, if we introduce a vector operator $\vec{\nabla} = \left(\frac{\partial}{\partial x}, \frac{\partial}{\partial y}, \frac{\partial}{\partial z} \right)$. Using this formalism, the Maxwell equations have the form

$$\vec{\nabla} \cdot \vec{E} = \frac{\rho}{\epsilon_0}, \quad (14)$$

$$\vec{\nabla} \times \vec{E} = 0. \quad (15)$$

0.1.4 Origin of the magnetic field

Electric charge at rest does not generate a magnetic field, but a *moving* charge does. The magnetic force is a *relativistic effect* (consequence of the contraction of distances in the direction of the motion, described by Lorentz transformation).³ Magnetic field of a moving point charge is moving with the charge. Constant *electric current* generates a stationary magnetic field. Constant electric current in an *ideal solenoid* generates a *homogeneous* stationary magnetic field inside the solenoid.

Magnetic induction generated by a current density \vec{j} (*Biot-Savart law*):

$$\vec{B} = \frac{1}{4\pi\epsilon_0 c^2} \int_V dV \frac{\vec{j}}{r^2} \times \frac{\vec{r}}{|r|} = \frac{\mu_0}{4\pi} \int_V dV \frac{\vec{j}}{r^2} \times \frac{\vec{r}}{|r|} \quad (16)$$

Biot-Savart law implies that magnetic field lines of a constant current in a straight wire

²The first equation is often written using *electric induction* \vec{D} as $\operatorname{div} \vec{D} = \rho$. If electric properties are described in terms of individual charges in vacuum, $\vec{D} = \epsilon_0 \vec{E}$. If behavior of charges bound in molecules is described in terms of polarization \vec{P} of the material, $\vec{D} = \epsilon_0 \vec{E} + \vec{P}$.

³A charge close to a very long straight wire which is uniformly charged experiences an electrical force F_\perp in the direction perpendicular to the wire. If the charges in the wire move with a velocity v_0 and the charge close to the wire moves along the wire with a velocity v_1 , the perpendicular force changes to $F_\perp (1 - \frac{v_0 v_1}{c^2})$, where c is the speed of light in vacuum. The modifying factor is clearly relativistic (B11.5).

1. do not diverge, i.e., the static magnetic field does not have a source
2. make closed loops around the wire (have curl or rotation), i.e., the magnetic field circulates around the wire

This can be written mathematically in the form of *Maxwell equations*⁴:

$$\vec{\nabla} \cdot \vec{B} = 0, \quad (17)$$

$$\vec{\nabla} \times \vec{B} = \mu_0 \vec{j}. \quad (18)$$

A simple example of a moving charge is a circular loop with an electric current. As derived in Section 0.1.7, magnetic moment of a current loop is proportional the angular momentum of the circulating charge.

Magnetic dipolar moment $\vec{\mu}$ is proportional to the angular momentum \vec{L}

$$\vec{\mu} = \gamma \vec{L}, \quad (19)$$

where γ is known as the *magnetogyric ratio*.

The classical theory does not explain why particles like electrons or nuclei have their own magnetic moments, even when they do not move in circles (because the classical theory does not explain why such particles have their own angular momenta). However, if we take the nuclear magnetic moment as a fact (or if we obtain it using a better theory), the classical results are useful. It can be shown that the magnetic moment is *always* proportional to the angular momentum⁵, but the proportionality constant is not always $Q/2m$; it is difficult to obtain for nuclei.

Analysis of the current loop in a static homogeneous external magnetic field, presented in Section 0.1.7, shows that if the direction of the magnetic moment $\vec{\mu}$ of the loop differs from the direction of \vec{B} , a torque trying to align $\vec{\mu}$ with \vec{B} . However, the magnetic dipole does not adopt the energetically most favored orientation (with the same direction of $\vec{\mu}$ as \vec{B}), but rotates around \vec{B} without changing the angle between $\vec{\mu}$ and \vec{B} . This motion on a cone is known as *precession*.

This is not a result of quantum mechanics, but a classical consequence of the relation between the magnetic moment and angular momentum of the current loop. The spinning top also precess in the Earth's gravitational field and riding a bicycle is based on the same effect.⁶ The precession frequency can be derived easily for the classical current loop in a magnetic field (see Section 0.1.8):

Angular frequency of the precession of a magnetic dipolar moment $\vec{\mu}$ in a magnetic field \vec{B} is

$$\vec{\omega} = -\gamma \vec{B}. \quad (20)$$

⁴The second equation is often written using *magnetic intensity* \vec{H} as $\vec{\nabla} \times \vec{H} = \vec{j}$. If magnetism is described as behavior of individual charges and magnetic moments in vacuum, $\vec{H} = \vec{B}/\mu_0$. If properties of a magnetic materials are described in terms of its *magnetization* \vec{M} , then $\vec{H} = \vec{B}/\mu_0 - \vec{M}$.

⁵A consequence of the rotational symmetry of space described mathematically by the Wigner-Eckart theorem.

⁶If you sit on a bike which does not move forward, gravity soon pulls you down to the ground. But if the bike has a certain speed and you lean to one side, you do not fall down, you just turn a corner. A qualitative discussion of precession using the spinning top and riding a bicycle is presented in L2.4–L2.5.

0.1.5 Electrodynamics and magnetodynamics

Similarly to the electric charge, the magnetic dipole (i) feels the surrounding magnetic field and (ii) generates its own magnetic field. The magnetic field generated by a precessing magnetic dipole is not stationary, it varies. To describe variable fields, the Maxwell equations describing rotation must be modified⁷:

$$\vec{\nabla} \times \vec{E} = -\frac{d\vec{B}}{dt}, \quad (21)$$

$$\vec{\nabla} \times \vec{B} = \frac{1}{c^2} \frac{d\vec{E}}{dt} + \mu_0 \vec{j}. \quad (22)$$

Note that electric and magnetic fields are coupled in the dynamic equations. Not only electric currents current, but also temporal variation of \vec{E} induces circulation of \vec{B} , and circulation of \vec{E} is possible if \vec{B} varies. This has many important consequences: it explains electromagnetic waves in vacuum and has numerous fundamental applications in electrical engineering, including those used in NMR spectroscopy.

Eq. 21 shows us how the frequency of the precession motion can be measured. A magnetic dipole in a magnetic field \vec{B}_0 generates a magnetic field \vec{B}' with the component $\parallel \vec{B}_0$ constant and the component $\perp \vec{B}_0$ rotating around \vec{B}_0 . If we place a loop of wire next to the precessing dipole, with the axis of the loop perpendicular to the axis of precession, the rotating component of \vec{B}' induces circulation of \vec{E} which creates a measurable oscillating electromotoric force (voltage) in the loop (see Section 0.1.9).

$$U = \frac{\mu_0}{4\pi} \frac{2|\mu|S}{r^3} \omega \sin(\omega t). \quad (23)$$

As a consequence, an oscillating electric current flows in the loop (L2.8).

⁷The second equation can be written as $\vec{\nabla} \times \vec{H} = \frac{d\vec{D}}{dt} + \vec{j}$.

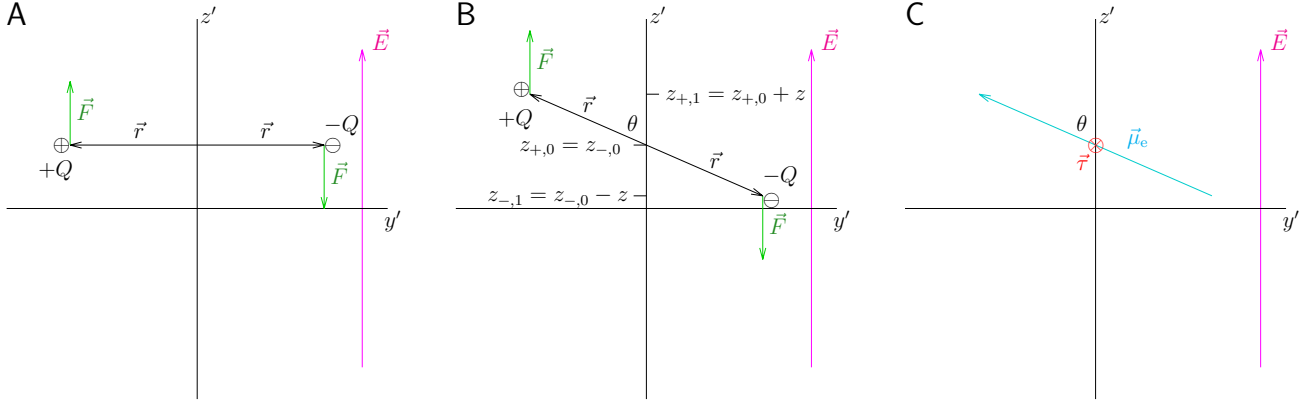


Figure 1: Potential energy of an electric dipole in a homogeneous electric field described by the intensity \vec{E} . The reference position of the dipole (0) is shown in Panel A, the actual position of the dipole (1) is shown in Panel B. Individual charges and forces are shown in panels A and B, the dipolar moment $\vec{\mu}_e$ and the torque $\vec{\tau}$ (its direction $-x$ is depicted using the symbol \otimes) are shown in Panel C. Note that the direction of $\vec{\mu}_e$ follows the convention used in physics, the convention used in chemistry is opposite.

DERIVATIONS

0.1.6 Potential energy of an electric dipole

Potential energy⁸ of the electric dipole can be calculated easily as a sum of potential energies of the individual charges. Potential energy is defined as the work done by the field moving the charge from a position (1) to a reference position (0). If we choose a coordinate system as defined in Figure 1), then the force acts only in the z' -direction ($F_{z'} = |\vec{F}| = Q|\vec{E}|$ for the positive charge and $F_{z'} = -|\vec{F}| = -Q|\vec{E}|$ for the negative charge). Therefore, it is sufficient to follow only how the z' -coordinates of the charges change because changes of other coordinates do not change the energy. The natural choice of the reference position is that the z' coordinates are the same for both charges, $z_{+,0} = z_{-,0}$. Changing the z' coordinate of the positive charge from $z_{+,0}$ to $z_{+,1} = z_{+,0} + z$ results in a work

$$Q|\vec{E}|(z_{+,0} - z_{+,1}) = -Q|\vec{E}|z. \quad (24)$$

Changing the z' coordinate of the negative charge from $z_{-,0}$ to $z_{-,1} = z_{-,0} - z$ results in a work

$$-Q|\vec{E}|(z_{-,0} - z_{-,1}) = -Q|\vec{E}|z. \quad (25)$$

Adding the works

$$\mathcal{E} = -2Q|\vec{E}|z = -2Q|\vec{E}|r \cos \theta = -\vec{\mu}_e \cdot \vec{E}, \quad (26)$$

where θ is the angle between \vec{E} and $\vec{\mu}_e$.

Equivalently, the potential energy can be defined as the work done by the torque $\vec{\tau}$ on $\vec{\mu}_e$ (Figure 1C) when rotating it from the reference orientation to the orientation described by the angle θ (between \vec{E} and $\vec{\mu}_e$). The reference angle for $z_{+,0} = z_{-,0}$ is $\pi/2$, therefore,

$$\mathcal{E} = \int_{\frac{\pi}{2}}^{\theta} |\vec{\tau}| d\theta' = \int_{\frac{\pi}{2}}^{\theta} |\vec{\mu}_e| |\vec{E}| \sin \theta' d\theta' = -|\vec{\mu}_e| |\vec{E}| \cos \theta = -\vec{\mu}_e \cdot \vec{E}. \quad (27)$$

0.1.7 Current loop as a magnetic dipole

Now we derive what is the magnetic dipole of a circular loop with an electric current. The magnetic moment is defined by the torque $\vec{\tau}$ it experiences in a magnetic field \vec{B} (Eq. 5):

$$\vec{\tau} = \vec{\mu} \times \vec{B}, \quad (28)$$

⁸Do not get confused: \mathcal{E} (scalar) is the energy and \vec{E} (vector) is electric intensity.

Therefore, we can calculate the magnetic moment of a current loop if we place it in a magnetic field \vec{B} . Let us first define the geometry of our setup. Let the axis z is the normal of the loop and let \vec{B} is in the xz plane ($\Rightarrow B_y = 0$). The vector product in Eq. 5 then simplifies to

$$\tau_x = \mu_y B_z, \quad (29)$$

$$\tau_y = \mu_z B_x - \mu_x B_z, \quad (30)$$

$$\tau_z = -\mu_y B_x. \quad (31)$$

Note that we assume that the electric current in the loop and the magnetic field are independent. The current is not induced by \vec{B} but has another (unspecified) origin, and \vec{B} is not a result of the current, but is introduced from outside.

As the second step, we describe the electric current in the loop. The electric current is a motion of the electric charge. We describe the current as a charge Q homogeneously distributed in a ring (loop) of a mass m which rotates with a circumferential speed v . Then, each element of the loop of a infinitesimally small length $dl = r d\varphi$ contains the same fraction of the mass dm and of the charge dQ , moving with the velocity \vec{v} . The direction of the vector \vec{v} is tangent to the loop and the amount of the charge per the length element is $Q/2\pi r$. The motion of the charge element dQ can be described, as any circular motion, by the *angular momentum*

$$d\vec{L} = \vec{r} \times d\vec{p} = dm(\vec{r} \times \vec{v}), \quad (32)$$

where r is the vector defining the position of the charge element dQ (Figure 2A). In our geometry, \vec{r} is radial and therefore always perpendicular to \vec{v} . Since both \vec{r} and \vec{v} are in the xy plane, $d\vec{L}$ must have the same direction as the normal of the plane. Therefore, the x and y components of $d\vec{L}$ are equal to zero and the z component is constant and identical for all elements (note that \vec{r} and \vec{v} of different elements differ, but $\vec{r} \times \vec{v}$ is constant, oriented along the normal of the z axis and with the size equal to rv for all elements). It is therefore easy to integrate $d\vec{L}$ and calculate \vec{L} of the loop

$$L_x = 0, \quad (33)$$

$$L_y = 0, \quad (34)$$

$$L_z = rv \int_{\text{loop}} dm = mrv. \quad (35)$$

As the third step, we examine forces acting on dQ . The force acting on a moving charge in a magnetic field (the Lorentz force) is equal to

$$\vec{F} = Q(\vec{E} + \vec{v} \times \vec{B}), \quad (36)$$

but we are now only interested in the magnetic component $\vec{F} = Q(\vec{v} \times \vec{B})$. The force acting on a single charge element dQ is

$$d\vec{F} = dQ(\vec{v} \times \vec{B}) = \frac{Q}{2\pi r} dl(\vec{v} \times \vec{B}) = \frac{Q}{2\pi} (\vec{v} \times \vec{B}) d\varphi. \quad (37)$$

The key step in our derivation is the definition of the torque

$$\vec{\tau} = \vec{r} \times \vec{F} = Q\vec{r} \times (\vec{v} \times \vec{B}), \quad (38)$$

which connects our analysis of the circular motion with the definition of $\vec{\mu}$ (Eq. 5). The torque acting on a charge element is (Figure 2B)

$$d\vec{\tau} = \vec{r} \times d\vec{F} = \frac{Q}{2\pi} \vec{r} \times (\vec{v} \times \vec{B}) d\varphi = \frac{Q}{2\pi} \left(\vec{v}(\vec{r} \cdot \vec{B}) - \vec{B} \underbrace{(\vec{r} \cdot \vec{v})}_{=0} \right) d\varphi = \frac{Q}{2\pi} (\vec{r} \cdot \vec{B}) \vec{v} d\varphi. \quad (39)$$

where a useful vector identity $\vec{a} \times (\vec{b} \times \vec{c}) = (\vec{a} \cdot \vec{c})\vec{b} - (\vec{a} \cdot \vec{b})\vec{c}$ helped us to simplify the equation because $\vec{r} \perp \vec{v}$. Eq. 39 tells us that the torque has the same direction as the velocity \vec{v} (\vec{v} is the only vector on the right-hand side because $\vec{r} \cdot \vec{B}$ is a scalar). In our coordinate frame, $v_x = -v \sin \varphi$, $v_y = v \cos \varphi$, $v_z = 0$, and $\vec{r} \cdot \vec{B} = r_x B_x + r_y B_y + r_z B_z = r_x B_x = B_x r \cos \varphi$ ($\vec{r} \cdot \vec{B}$ is reduced to $r_x B_x$ in our coordinate frame because $B_y = 0$ and $r_z = 0$). Therefore, we can calculate the components of the overall torque $\vec{\tau}$ as (Figure 2C)

$$\tau_x = -\frac{Qrv}{2\pi} B_x \int_0^{2\pi} \sin \varphi \cos \varphi d\varphi = -\frac{Qrv}{4\pi} B_x \int_0^{2\pi} \sin(2\varphi) d\varphi = 0, \quad (40)$$

$$\tau_y = \frac{Qrv}{2\pi} B_x \int_0^{2\pi} \cos^2 \varphi d\varphi = \frac{Qrv}{4\pi} B_x \int_0^{2\pi} (1 + \cos(2\varphi)) d\varphi = \frac{Qrv}{2} B_x, \quad (41)$$

$$\tau_z = 0. \quad (42)$$

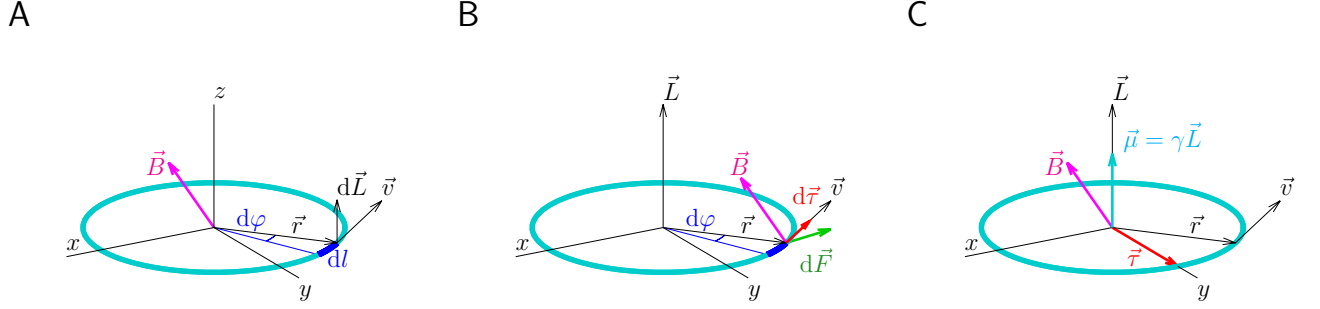


Figure 2: Current loop as a magnetic dipole. The loop of radius r and length $2\pi r$, charge Q and mass m is shown in cyan. A magnetic induction \vec{B} of an external field is shown in magenta. The coordinates are chosen such that the loop is placed in the xy plane and \vec{B} in the xz . An element of charge dQ (moving with the velocity \vec{v}), mass dm and length $dl = r d\varphi$ is shown in blue. The angular momentum of the blue element is $d\vec{L} = \vec{r} \times \vec{v} dm$ (Panel A). The total angular momentum is $\vec{L} = \vec{r} \times \vec{v} m$ (Panel B). The force $d\vec{F} = \vec{v} \times \vec{B} dQ$ and the torque $d\vec{\tau} = \vec{r} \times d\vec{F}$ acting on the blue element are depicted as the green and red arrows in Panel B. The torque acting on the whole loop and the magnetic moment experiencing the torque in the field \vec{B} are shown as the red and cyan arrows in Panel C.

Comparison with Eqs. 29–31 immediately shows that

$$\mu_x = 0, \quad (43)$$

$$\mu_y = 0, \quad (44)$$

$$\mu_z = \frac{Qrv}{2} \quad (45)$$

and comparison with Eqs. 33–35 reveals that the magnetic dipole moment of the current loop is closely related to the angular momentum $\vec{L} = \vec{r} \times m\vec{v}$:

$$\vec{\mu} = \frac{Q}{2m} \vec{L}. \quad (46)$$

0.1.8 Precession

Angular momentum of a particle moving in a circle is defined as $\vec{L} = m\vec{r} \times \vec{v}$ (Eq. 32), where \vec{r} defines position of the particle and m and \vec{v} are the mass and the velocity of the particle, respectively (Figure 3A). The change of \vec{L} is described by the time derivative of \vec{L} .

$$\frac{d\vec{L}}{dt} = m \frac{d(\vec{r} \times \vec{v})}{dt} = m \frac{d\vec{r}}{dt} \times \vec{v} + m\vec{r} \times \frac{d\vec{v}}{dt} = m \underbrace{(\vec{v} \times \vec{v})}_0 + \vec{r} \times m\vec{a}. \quad (47)$$

According the second Newton's law, $m\vec{a}$ is equal to the force acting on the particle (changing \vec{L})

$$\frac{d\vec{L}}{dt} = \vec{r} \times m\vec{a} = \vec{r} \times \vec{F} = \vec{\tau}, \quad (48)$$

where \vec{F} is the force and $\vec{\tau}$ is the corresponding torque. The change of the angular momentum of a current loop due to an external force can be calculated in the same manner (Figure 3). For an infinitesimal element of the loop,

$$\frac{d(d\vec{L})}{dt} = \vec{r} \times \vec{a} dm = \vec{r} \times d\vec{F} = d\vec{\tau}. \quad (49)$$

In a homogeneous magnetic field, the force acting on all elements is the same and integration of the individual elements is as easy as in Eq. 35, resulting in Eq. 48, where the force \vec{F} and the torque $\vec{\tau}$ now act on the angular momentum of the whole loop. Because $\vec{\mu} = \gamma \vec{L}$ (Eq. 19) and $\vec{\tau} = \vec{\mu} \times \vec{B}$ (Eq. 5, the the magnetic moment of a current loop in a homogeneous magnetic field changes as

$$\frac{d\vec{\mu}}{dt} = \gamma \vec{r} \times \vec{F} = \gamma \vec{\tau} = \gamma \vec{\mu} \times \vec{B} = -\gamma \vec{B} \times \vec{\mu}. \quad (50)$$

Rotation of any vector, including $\vec{\mu}$ can be described using the angular frequency $\vec{\omega}$ (its magnitude is the speed of the rotation in radians per second and its direction is the axis of the rotation):

$$\frac{d\vec{\mu}}{dt} = \vec{\omega} \times \vec{\mu}. \quad (51)$$

Comparison with Eq. 50 immediately shows that $\vec{\omega} = -\gamma \vec{B}$.

0.1.9 Electromotoric voltage

We can use a simple example to analyze the induced voltage quantitatively. This voltage (the electromotoric force) is an integral of the electric intensity along the detector loop. Stokes' theorem (see B9) allows us to calculate such integral from Eq. 21.

$$\oint_L \vec{E} d\vec{l} = - \int_S \frac{\partial \vec{B}}{\partial t} d\vec{S} = S \frac{\partial \vec{B}}{\partial t} \cdot \vec{n}, \quad (52)$$

where S is the area of the loop and \vec{n} is the normal vector to the loop. If the distance r of the magnetic moment from the detector is much larger than the size of the loop, the magnetic induction of a field which is generated by a magnetic moment $\vec{\mu}$ rotating in a plane perpendicular to the detector loop and which crosses the loop (let us call it B_x) is⁹

$$B_x = \frac{\mu_0}{4\pi} \frac{2\mu_x}{r^3}. \quad (53)$$

As $\vec{\mu}$ rotates with the angular frequency ω , $\mu_x = |\mu| \cos(\omega t)$, and

$$\frac{\partial B_x}{\partial t} = -\frac{\mu_0}{4\pi} \frac{2}{r^3} |\mu| \omega \sin(\omega t). \quad (54)$$

Therefore, the oscillating induced voltage is

$$\oint_L \vec{E} d\vec{l} = \frac{\mu_0}{4\pi} \frac{2|\mu|S}{r^3} \omega \sin(\omega t). \quad (55)$$

⁹We describe the field generated by a magnetic moment in more detail later in Section 8.1 when we analyze mutual interactions of magnetic moments of nuclei.

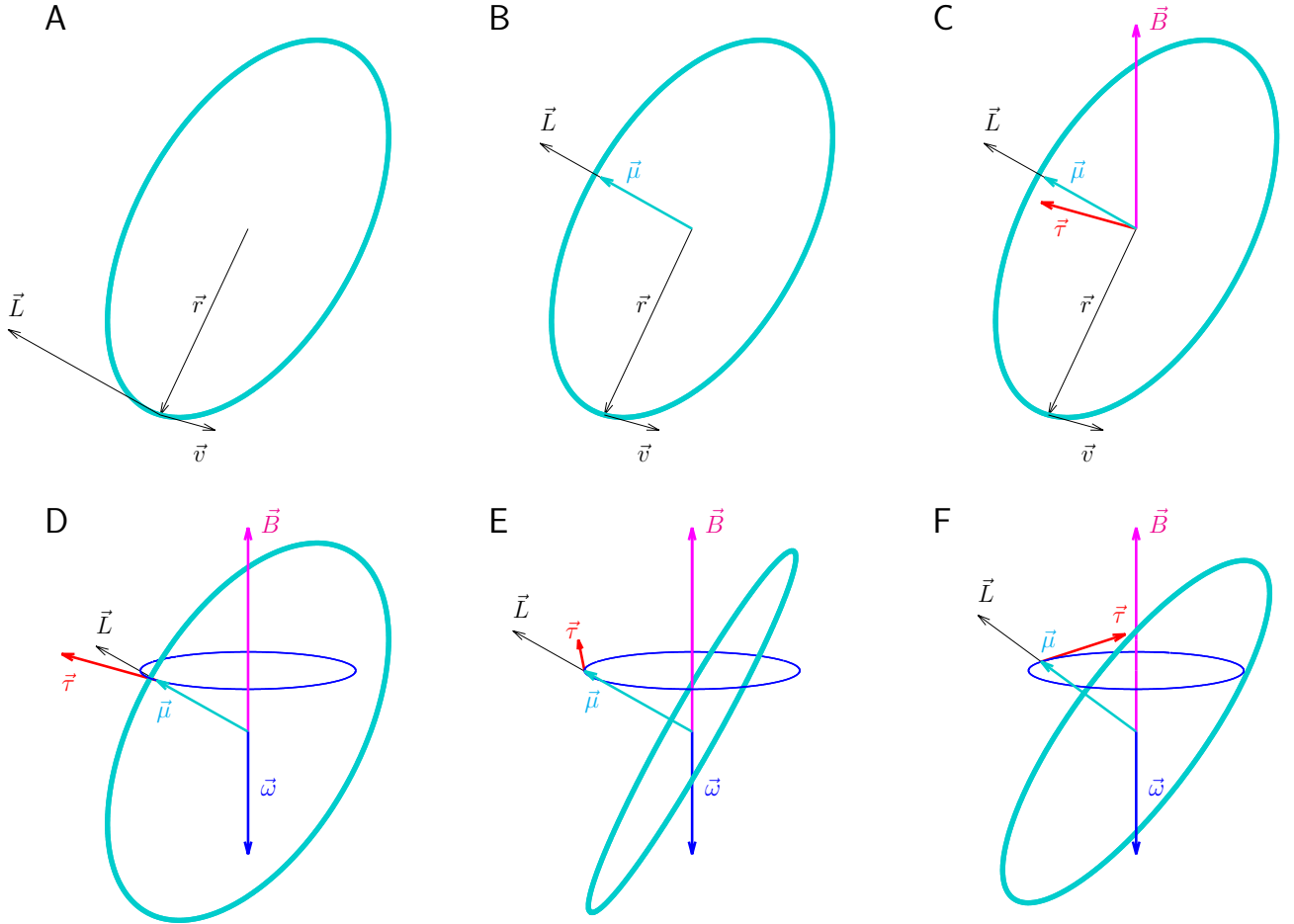


Figure 3: Classical description of precession of a current loop in a homogeneous magnetic field. Angular momentum \vec{L} of a charged particle of the mass m moving in a circular loop (shown in cyan in Panel A) randomly oriented in space is given by the vector product of the actual position vector of the particle \vec{r} and the actual particle's velocity \vec{v} ($\vec{L} = m\vec{r} \times \vec{v}$). Note that size and direction of \vec{L} is the same for all positions of the particle along the circle (for all possible vectors \vec{r}). The angular momentum \vec{L} of a current loop of the same mass and the magnetic moment $\vec{\mu}$ (cyan arrow), proportional to \vec{L} are shown in Panel B. The proportionality constant is γ (Eq. 19). In a presence of a vertical static magnetic field \vec{B} (magenta arrow in Panel C), the loop experiences a torque $\vec{\tau} = \vec{\mu} \times \vec{B}$ (Eq. 5), shown as the red arrow in Panel C. This torque (red arrow moved to the tip of the cyan arrow in Panel D) acts on $\vec{\mu}$, which precesses about \vec{B} . Two snapshots of the precessing $\vec{\mu}$ (with the loop) are shown in Panels E and F. The tip of the cyan arrow representing $\vec{\mu}$ rotates about \vec{B} (the blue circle) with the angular frequency $\vec{\omega} = -\gamma\vec{B}$.

0.2 Classical mechanics: Newton, Lagrange, Hamilton

Newton's laws describe mechanics using *forces*. In the presence of a force \vec{F} , motion of a particle of a mass m is described by the second Newton's law

$$m\vec{a} = \vec{F}. \quad (56)$$

As an alternative, the Newton mechanics be reformulated in terms of *energies*. The total kinetic energy of a body consisting of N particles is

$$\mathcal{E}_{\text{kin}} = \frac{1}{2} \sum_{k=1}^N \vec{v}_k \cdot \vec{v}_k \quad (57)$$

and depends only on the velocities of the particles \vec{v}_k , not on their positions \vec{r}_k . The total kinetic energy can be related to the accelerations as follows

$$\frac{\partial \mathcal{E}_{\text{kin}}}{\partial v_{kl}} = \frac{1}{2} m (2v_{kl}) = mv_{kl} = p_{kl}, \quad (58)$$

$$ma_{kl} = \frac{d}{dt}(mv_{kl}) = \frac{d}{dt} \frac{\partial \mathcal{E}_{\text{kin}}}{\partial v_{kl}}, \quad (59)$$

where k is the particle number and l is the direction (x , y , or z). In the presence of forces that depend only on the coordinates (x , y , or z) and can be calculated as gradients of potential energy, the formulation of the second Newton's law is straightforward

$$ma_{kl} = \frac{d}{dt} \frac{\partial \mathcal{E}_{\text{kin}}}{\partial v_{kl}} = \frac{\partial \mathcal{E}_{\text{pot}}}{\partial r_{kl}} = F_{kl}. \quad (60)$$

Since our \mathcal{E}_{kin} depends only on velocities and not on position in space, and \mathcal{E}_{pot} depends only on position in space and not on velocities, \mathcal{E}_{kin} and \mathcal{E}_{pot} can be combined into one variable called *Lagrangian* \mathcal{L} :

$$0 = ma_{kl} - F_{kl} = \frac{d}{dt} \frac{\partial \mathcal{E}_{\text{kin}}}{\partial v_{kl}} - \frac{\partial \mathcal{E}_{\text{pot}}}{\partial r_{kl}} = \frac{d}{dt} \frac{\partial (\mathcal{E}_{\text{kin}} - \mathcal{E}_{\text{pot}})}{\partial v_{kl}} - \frac{\partial (\mathcal{E}_{\text{kin}} - \mathcal{E}_{\text{pot}})}{\partial r_{kl}} \equiv \frac{d}{dt} \frac{\partial \mathcal{L}}{\partial v_{kl}} - \frac{\partial \mathcal{L}}{\partial r_{kl}}. \quad (61)$$

A set of Eq. 61 for all values of k and l ($3N$ combinations) describes well a set of N free particles, which has $3N$ degrees of freedom. If the mutual positions of particles are constrained by C constraints (e.g. atoms in a molecule), the number of degrees of freedom is lower ($3N - C$) and the number of equations can be reduced. It is therefore desirable to replace the $3N$ values of r_{kl} by $3N - C$ values *generalized coordinates* q_j . Each value of r_{kl} is then a combination of q_j values, and

$$dr_{kl} = \sum_{j=1}^{3N-C} \frac{\partial r_{kl}}{\partial q_j} dq_j, \quad (62)$$

and (if the constraints do not depend on time)

$$v_{kl} = \frac{dr_{kl}}{dt} = \sum_{j=1}^{3N-C} \frac{\partial r_{kl}}{\partial q_j} \frac{dq_j}{dt} \equiv \sum_{j=1}^{3N-C} \frac{\partial r_{kl}}{\partial q_j} \dot{q}_j, \quad (63)$$

where the dot represents time derivative. The equation of motion can be thus rewritten as

$$\frac{d}{dt} \frac{\partial \mathcal{L}}{\partial \dot{q}_j} = \frac{\partial \mathcal{L}}{\partial q_j}. \quad (64)$$

We obtained Eq. 64 starting from the second Newton's law. However, mechanics can be also built in the opposite direction, starting from the following statement. *Equation of motion describing a physical process that starts at time t_1 and ends at time t_2 must be such that the integral $\int_{t_1}^{t_2} \mathcal{L} dt$ is stationary, in other words, that the variation of the integral is zero.* This statement is known as the *least action principle* and, using calculus of variation (as nicely described in The Feynman Lectures on Physics, Vol. 2, Chapter 19), Eq. 64 can be derived from it.¹⁰ There is, however, no general rule how to express the Lagrangian as an explicit function of generalized coordinates and velocities. Finding the Lagrangian may be a demanding task, requiring experience and physical intuition.

Lagrangian can be converted to yet another energy-related function, known as *Hamiltonian*. Lagrangian and Hamiltonian are related by the *Legendre transformation* (see Section 0.2.1).

$$\mathcal{H}(q_j, p_j) + \mathcal{L}(q_j, \dot{q}_j) = \sum_j (p_j \cdot \dot{q}_j), \quad (65)$$

where

$$p_j = \frac{\partial \mathcal{L}}{\partial \dot{q}_j}. \quad (66)$$

For our set of N unconstrained particles exposed to forces that do not depend on the particle velocities, $q_j = r_{kl}$ and $p_j = \frac{\partial \mathcal{L}}{\partial \dot{q}_j}$ is the linear momentum of the k -th particle in the direction l (cf. Eq. 58) and the Hamiltonian is simply the sum of total kinetic and potential energy ($\mathcal{H} = \mathcal{E}_{\text{kin}} + \mathcal{E}_{\text{pot}}$). In general, p_j is called the *canonical momentum*.

The introduction of Lagrangian and Hamiltonian approaches may seem to be an unnecessarily complication of the description of classical mechanics. However, Hamiltonians and Lagrangians become essential when we search for quantum mechanical description of particles observed in magnetic resonance experiments because Hamiltonian describes evolution of quantum states in time.¹¹

Derivation of the Hamiltonian (classical or quantum) for magnetic particles in magnetic fields is much more demanding because the magnetic force depends on the velocity of moving charged particles. Therefore, velocity enters the Lagrangian not only through the kinetic energy and the

¹⁰Richard Feynman showed that quantum mechanics can be reformulated by using

$$e^{i \int_{t_1}^{t_2} \mathcal{L} / \hbar dt}$$

as a probability amplitude (*path integral approach*).

¹¹The Hamiltonian can be also used to describe time evolution in classical mechanics.

canonical momentum is no longer identical with the linear momentum. Careful analysis, presented in Section 0.2.2, shows that the classical Hamiltonian

$$\mathcal{H} = \frac{(\vec{p} - Q\vec{A})^2}{2m} + QV, \quad (67)$$

where V is the electric potential and \vec{A} is a so-called *vector potential*, defined as $\vec{b} = \vec{\nabla} \times \vec{A}$ (for more details, see Section 0.2.2). We use Eq. 67 in Section 5.7.5 as a starting point of quantum mechanical description of the spin magnetic moment.

DERIVATIONS

0.2.1 Legendre transformation

The Legendre transformation has a simple graphical representation (Figure 4). If we plot a function of a variable x , e.g. $f(x)$, slope at a certain value of $x = \xi$ is equal to $s(\xi) = (\partial f / \partial x)_\xi$. A tangent line $y(\xi)$ touching the plotted f for $x = \xi$ is described by the slope $s(\xi)$ and intercept $g(\xi)$ as $y = g + s(\xi)x$. The value of the intercept for all possible values of ξ can be expressed as a function of the slope $g(s) = y(\xi) - s(\xi)\xi = f(\xi) - s(\xi)\xi$ (y and f are equal at $x = \xi$ because they touch each other). If we identify x with \dot{q} , f with \mathcal{L} , and $-g$ with \mathcal{H} , we get Eq. 65 for a one-dimensional case ($j = 1$).

0.2.2 Lagrangian and Hamiltonian including magnetism

We start our analysis by searching for a classical Lagrangian describing motion of a charged particle in a magnetic field, and then convert it to the Hamiltonian using Legendre transformation.

We know that the Lagrangian should give us the Lorentz force

$$\vec{F} = Q(\vec{E} + \vec{v} \times \vec{B}). \quad (68)$$

We know that a velocity-independent force is a gradient of the corresponding potential energy. For the electric force,

$$\vec{F} = \vec{\nabla} \mathcal{E}_{\text{el}} = Q \vec{\nabla} V, \quad (69)$$

where the electric potential energy \mathcal{E}_{el} and the electric potential V are scalar quantities. Intuitively, we expect the magnetic force to be also a gradient of some scalar quantity (some sort of magnetic potential energy or magnetic potential). The magnetic force is given by $Q\vec{v} \times \vec{B}$, so the magnetic energy should be proportional to the velocity. But the velocity is a vector quantity, not a scalar. We may guess that the scalar quantity resembling the electric potential may be a scalar product of velocity with another vector. This tells us that the search for the electromagnetic Lagrangian is a search for a vector that, when included in the Lagrangian, correctly reproduces the Lorentz force, expressed in terms of \vec{E} and \vec{B} in Eq. 69. The information about \vec{E} and \vec{B} can be extracted from the following Maxwell equations

$$\vec{\nabla} \cdot \vec{B} = 0 \quad (70)$$

$$\vec{\nabla} \times \vec{E} = -\frac{\partial \vec{B}}{\partial t}, \quad (71)$$

but we have to employ our knowledge of vector algebra to handle the divergence in Eq. 70 and the curl in Eq. 71.

First, note that we look for a scalar product, but Eq. 69 contains a vector product. The useful identity $\vec{a} \times (\vec{b} \times \vec{c}) = \vec{b}(\vec{a} \cdot \vec{c}) - (\vec{a} \cdot \vec{b})\vec{c}$ tells us that it would be nice to replace \vec{B} with a curl of another vector because it would give us, after inserting in Eq. 69, the desired gradient of scalar product:

$$\vec{v} \times (\vec{\nabla} \times \vec{A}) = \vec{\nabla}(\vec{v} \cdot \vec{A}) - (\vec{v} \cdot \vec{\nabla})\vec{A}. \quad (72)$$

Another identity says that $\vec{a} \cdot (\vec{a} \times \vec{b}) = 0$ for any vectors \vec{a} and \vec{b} because $\vec{a} \times \vec{b} \perp \vec{a}$. As a consequence, we can really replace \vec{B} by a curl (rotation) of some vector \vec{A} because $\vec{\nabla} \cdot (\vec{\nabla} \times \vec{A}) = 0$ as required by Eq. 70. The first step thus gives us a new definition of \vec{B}

$$\vec{B} = \vec{\nabla} \times \vec{A} \quad (73)$$

which can be inserted into Eq. 69

$$\vec{F} = Q(\vec{E} + \vec{v} \times \vec{B}) = Q(\vec{E} + \vec{v} \times (\vec{\nabla} \times \vec{A})), \quad (74)$$

and using the aforementioned identity $\vec{a} \times (\vec{b} \times \vec{c}) = \vec{b}(\vec{a} \cdot \vec{c}) - (\vec{a} \cdot \vec{b})\vec{c}$,

$$\vec{F} = Q(\vec{E} + \vec{v} \times \vec{B}) = Q(\vec{E} + \vec{v} \times (\vec{\nabla} \times \vec{A})) = Q(\vec{E} + \vec{\nabla}(\vec{v} \cdot \vec{A}) - (\vec{v} \cdot \vec{\nabla})\vec{A}). \quad (75)$$

Second, we use our new definition of \vec{B} and rewrite Eq. 71 as

$$0 = \frac{\partial \vec{B}}{\partial t} + \vec{\nabla} \times \vec{E} = \vec{\nabla} \times \frac{\partial \vec{A}}{\partial t} + \vec{\nabla} \times \vec{E} = \vec{\nabla} \times \left(\frac{\partial \vec{A}}{\partial t} + \vec{E} \right). \quad (76)$$

Third, we notice that that for any vector \vec{a} and constant c , $\vec{a} \times (c\vec{a}) = 0$ because $\vec{a} \parallel c\vec{a}$. As a consequence, we can replace $(\partial \vec{A} / \partial t + \vec{E})$ by a gradient of some scalar V because $\vec{\nabla} \times (\vec{\nabla}(\partial \vec{A} / \partial t + \vec{E})) = \vec{\nabla} \times (-\vec{\nabla} V) = 0$ as required by Eq. 71. The scalar V is the well-known electric potential and allows us to express \vec{E} as

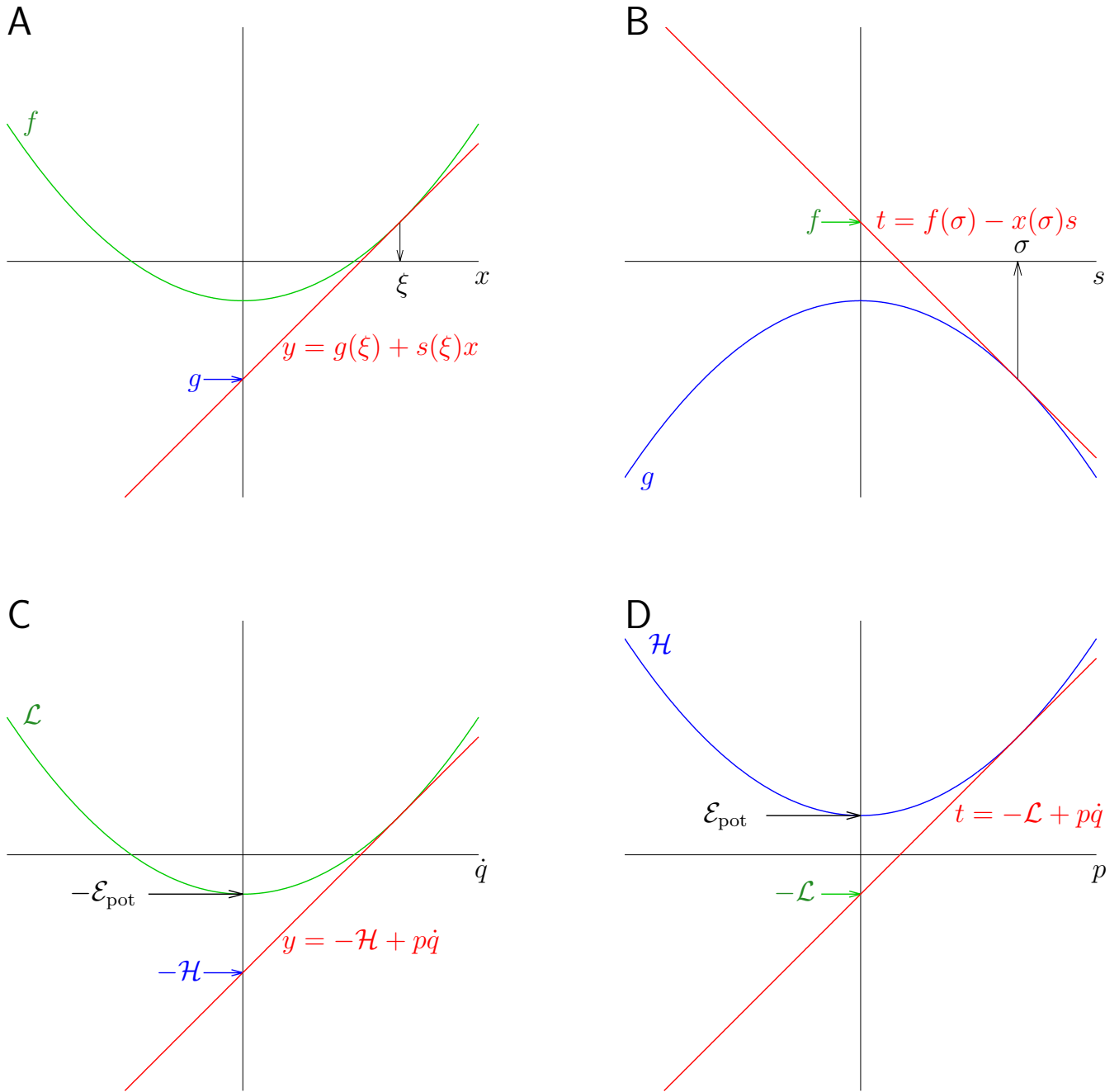


Figure 4: Legendre transformation (A) and inverse Legendre transformation (B) of general functions $f(x)$ and $g(s)$. Legendre transformation (C) and inverse Legendre transformation (D) of one-dimensional Lagrangian \mathcal{L} and Hamiltonian \mathcal{H} describing forces independent of the velocity.

$$\vec{E} = -\frac{\partial \vec{A}}{\partial t} - \vec{\nabla}V. \quad (77)$$

which can be also inserted into Eq. 69

$$\vec{F} = Q(\vec{E} + \vec{v} \times \vec{B}) = Q\left(-\frac{\partial \vec{A}}{\partial t} - \vec{\nabla}V + \vec{\nabla}(\vec{v} \cdot \vec{A}) - (\vec{v} \cdot \vec{\nabla})\vec{A}\right). \quad (78)$$

Finally, we notice that

$$\frac{d\vec{A}}{dt} = \frac{\partial \vec{A}}{\partial t} + \frac{\partial \vec{A}}{\partial x} \frac{dx}{dt} + \frac{\partial \vec{A}}{\partial y} \frac{dy}{dt} + \frac{\partial \vec{A}}{\partial z} \frac{dz}{dt} = \frac{\partial \vec{A}}{\partial t} + (\vec{v} \cdot \vec{\nabla})\vec{A} \Rightarrow \frac{\partial \vec{A}}{\partial t} = \frac{d\vec{A}}{dt} - (\vec{v} \cdot \vec{\nabla})\vec{A}, \quad (79)$$

which shows that $(\vec{v} \cdot \vec{\nabla})\vec{A}$ in Eq. 78 can be included into $d\vec{A}/dt$

$$\vec{F} = Q(\vec{E} + \vec{v} \times \vec{B}) = Q\left(-\frac{\partial \vec{A}}{\partial t} - \vec{\nabla}V + \vec{\nabla}(\vec{v} \cdot \vec{A}) - (\vec{v} \cdot \vec{\nabla})\vec{A}\right) = Q\left(-\frac{d\vec{A}}{dt} - \vec{\nabla}V + \vec{\nabla}(\vec{v} \cdot \vec{A})\right). \quad (80)$$

Let us now try to write \mathcal{L} as

$$\mathcal{L} = \mathcal{E}_{\text{kin}} - \mathcal{E}_{\text{el}} + \mathcal{E}_{\text{magn}} = \frac{1}{2}mv^2 - QV + \mathcal{E}_{\text{magn}}, \quad (81)$$

where \mathcal{E}_{el} is a typical potential energy dependent on position but not on speed, and $\mathcal{E}_{\text{magn}}$ can depend on both position and speed. For this Lagrangian,

$$\frac{\partial \mathcal{L}}{\partial x} = \frac{\partial \mathcal{E}_{\text{el}}}{\partial x} + \frac{\partial \mathcal{E}_{\text{magn}}}{\partial x} = -Q \frac{\partial V}{\partial x} + \frac{\partial \mathcal{E}_{\text{magn}}}{\partial x} \quad (82)$$

$$\frac{d}{dt} \frac{\partial \mathcal{L}}{\partial v_x} = \frac{d}{dt} \left(\frac{\partial \mathcal{E}_{\text{kin}}}{\partial v_x} + \frac{\partial \mathcal{E}_{\text{magn}}}{\partial v_x} \right) = ma_x + \frac{d}{dt} \frac{\partial \mathcal{E}_{\text{magn}}}{\partial v_x}. \quad (83)$$

If we use $\mathcal{E}_{\text{magn}} = Q\vec{v} \cdot \vec{A}$, Eqs. 82 and 83 with Eq. 64 for $q = x$ give us

$$ma_x = -Q \left(\frac{dA_x}{dt} - \frac{\partial V}{\partial x} + \frac{\partial(\vec{v} \cdot \vec{A})}{\partial x} \right) \quad (84)$$

and a sum with similar y - and z -components is equal to the Lorentz force

$$m\vec{a} = F = Q \left(-\frac{d\vec{A}}{dt} - \vec{\nabla}V + \vec{\nabla}(\vec{v} \cdot \vec{A}) \right) = Q(\vec{E} + \vec{v} \times \vec{B}). \quad (85)$$

We have found that our (classical and non-relativistic) Lagrangian has the form

$$\mathcal{L} = \frac{1}{2}mv^2 - QV + Q(\vec{v} \cdot \vec{A}). \quad (86)$$

According to Eq. 66, the canonical momentum has the following components

$$p_x = \frac{\partial \mathcal{L}}{\partial v_x} = mv_x + QA_x \quad p_y = \frac{\partial \mathcal{L}}{\partial v_y} = mv_y + QA_y \quad p_z = \frac{\partial \mathcal{L}}{\partial v_z} = mv_z + QA_z. \quad (87)$$

The Hamiltonian can be obtained as usually as the Legendre transform

$$\mathcal{H} = \sum_{j=x,y,z} p_j v_j - \mathcal{L} = \vec{p} \cdot \vec{v} - \mathcal{L}. \quad (88)$$

In order to express \mathcal{H} as a function of \vec{p} , we express \vec{v} as $(\vec{p} - Q\vec{A})/m$:

$$\mathcal{H} = \frac{2\vec{p} \cdot (\vec{p} - Q\vec{A}) - (\vec{p} - Q\vec{A})^2 - 2Q(\vec{p} - Q\vec{A}) \cdot \vec{A}}{2m} + QV = \frac{(\vec{p} - Q\vec{A})^2}{2m} + QV. \quad (89)$$

0.3 Diffusion

Diffusion can be viewed as a result of collisions of the observed molecule with other molecules. Collisions change position of the molecule in space (cause *translation*) and orientation of the molecule (cause *rotation*). *Rotational diffusion* is important for NMR relaxation. *Translational diffusion* influences NMR experiments only if the magnetic field is inhomogeneous. Translational diffusion can be described as a random walk in a three-dimensional space, rotational diffusion can be described as a random walk on a surface of a sphere. Although we are primarily interested in relaxation and we do not discuss magnetic field inhomogeneity at this moment, we start our discussion with the random walk in a three-dimensional space (Section 0.3.1) because the random walk on a surface of a sphere is just a special case of the general walk in three directions. Then we continue with the analysis of the simplest example of the random walk on a spherical surface, i.e., of the *isotropic rotational diffusion* (Section 0.3.2). The analysis shows that the isotropic rotational diffusion is described by a simple exponential time dependence (Eq. 97). This relation will serve as a starting point for derivation of the key component of the theory of NMR relaxation, of the *time correlation function*, described in Section 2.6.2.

DERIVATIONS

0.3.1 Translational diffusion

We start with several definitions. Let us assume that the position of our molecule is described by coordinates x, y, z and its orientation is described by angles φ, ϑ, χ .

- Probability that the molecule is inside a cubic box of a volume $\Delta V = \Delta x \Delta y \Delta z$ centered around x, y, z is

$$P(x, y, z, t, \Delta x, \Delta y, \Delta z) = \int_{x-\frac{\Delta x}{2}}^{x+\frac{\Delta x}{2}} \int_{y-\frac{\Delta y}{2}}^{y+\frac{\Delta y}{2}} \int_{z-\frac{\Delta z}{2}}^{z+\frac{\Delta z}{2}} \rho(x, y, z, t) dx dy dz,$$

where $\rho(x, y, z, t)$ is *probability density* at x, y, z , corresponding to local concentration in a macroscopic picture. If the box is small enough so that $\rho(x, y, z, t)$ does not change significantly inside the box, the equation with the triple integral can be simplified to

$$P(x, y, z, t, \Delta x, \Delta y, \Delta z) = \rho(x, y, z, t) \Delta V.$$

- Probability that the molecule crosses one side of the box centered around x, y, z and jumps into the box centered around $x + \Delta x, y, z$ during a time interval δt is proportional to the area of the side between boxes centered around x, y, z and around $x + \Delta x, y, z$. This area is equal to $\Delta y \Delta z = \Delta V / \Delta x$ and the probability of jumping from the box centered around x, y, z to the box centered around $x + \Delta x, y, z$ can be written as

$$P(x \rightarrow x + \Delta x; x, y, z, t, \Delta x, \Delta y, \Delta z, \Delta t) = \Phi_{x \rightarrow x + \Delta x} \Delta y \Delta z = \Phi_{x \rightarrow x + \Delta x} \Delta V / \Delta x,$$

where $\Phi_{x \rightarrow x + \Delta x}$ is the *flux* from the box centered around x, y, z to the box centered around $x + \Delta x, y, z$ (per unit area). The corresponding *probability density* is

$$\rho(x \rightarrow x + \Delta x; x, y, z, t, \Delta t) = P(x \rightarrow x + \Delta x; x, y, z, t, \Delta x, \Delta y, \Delta z, \Delta t) / \Delta V = \Phi_{x \rightarrow x + \Delta x} / \Delta x.$$

The probability of jumping to the box centered around $x + \Delta x, y, z$ is also proportional to the probability that the molecule is inside the box centered around x, y, z (equal to $\rho(x, y, z, t) \Delta V$ if the box is small enough). If the probability of escaping the box is the same in all directions,

$$\begin{aligned} \rho(x \rightarrow x + \Delta x; x, y, z, t, \Delta t) &= \xi \rho(x, y, z, t), \\ \rho(y \rightarrow y + \Delta y; x, y, z, t, \Delta t) &= \xi \rho(x, y, z, t), \\ \rho(z \rightarrow z + \Delta z; x, y, z, t, \Delta t) &= \xi \rho(x, y, z, t), \end{aligned}$$

where ξ is a proportionality constant describing frequency of crossing a side of a box (per unit volume and including the physical description of the collisions).

- The *net flux* in the x direction is given by

$$\Phi_x = \Phi_{x \rightarrow x + \Delta x} - \Phi_{x + \Delta x \rightarrow x} = \xi \Delta x (\rho(x, y, z, t) - \rho(x + \Delta x, y, z, t)) = -\xi \Delta x \Delta \rho = -\xi (\Delta x)^2 \frac{\partial \rho}{\partial x} = -D^{\text{tr}} \frac{\partial \rho}{\partial x},$$

where $D^{\text{tr}} = \xi (\Delta x)^2$ is the *translational diffusion coefficient*.

- The net flux in all directions is

$$\vec{\Phi} = -D^{\text{tr}} \vec{\nabla} \rho,$$

which is the *first Fick's law*.

- The *continuity equation*

$$\int_V \frac{\partial \rho}{\partial t} dV + \oint_S \vec{\Phi} dS = 0$$

states that any time change of probability that the molecule is in a volume V is due to the total flux through a surface S enclosing the volume V (molecules are not created or annihilated). Using the divergence theorem,

$$0 = \frac{\partial \rho}{\partial t} + \vec{\nabla} \cdot \vec{\Phi} = \frac{\partial \rho}{\partial t} + \vec{\nabla} \cdot (-D^{\text{tr}} \vec{\nabla} \rho) \Rightarrow \frac{\partial \rho}{\partial t} = D^{\text{tr}} \nabla^2 \rho,$$

which is the *second Fick's law*.

- If the diffusion is not isotropic, the diffusion coefficient is replaced by a diffusion tensor. If we define a coordinate frame so that the diffusion tensor is represented by a diagonal matrix with elements $D_{xx}^{\text{tr}}, D_{yy}^{\text{tr}}, D_{zz}^{\text{tr}}$, the second Fick's law has the following form:

$$\frac{\partial \rho}{\partial t} = D_{xx}^{\text{tr}} \frac{\partial}{\partial x} \frac{\partial \rho}{\partial x} + D_{yy}^{\text{tr}} \frac{\partial}{\partial y} \frac{\partial \rho}{\partial y} + D_{zz}^{\text{tr}} \frac{\partial}{\partial z} \frac{\partial \rho}{\partial z} = \left(D_{xx}^{\text{tr}} \frac{\partial^2}{\partial x^2} + D_{yy}^{\text{tr}} \frac{\partial^2}{\partial y^2} + D_{zz}^{\text{tr}} \frac{\partial^2}{\partial z^2} \right) \rho.$$

0.3.2 Isotropic rotational diffusion

Isotropic rotational diffusion can be viewed as random motions of a vector describing orientation of the molecule. Such motions are equivalent to a random wandering of a point particle on a surface of a sphere with a unit diameter. In order to describe such a random walk on a spherical surface, it is convenient to express the second Fick's law in spherical coordinates

$$\frac{\partial \rho}{\partial t} = \frac{D^{\text{rot}}}{r^2 \sin \vartheta} \left(\frac{\partial}{\partial r} \left(r^2 \sin \vartheta \frac{\partial}{\partial r} \right) + \frac{\partial}{\partial \vartheta} \left(\sin \vartheta \frac{\partial}{\partial \vartheta} \right) + \frac{\partial}{\partial \varphi} \left(\frac{1}{\sin \vartheta} \frac{\partial}{\partial \varphi} \right) \right) \rho. \quad (90)$$

Since r is constant and equal to unity,

$$\frac{\partial \rho}{\partial t} = \frac{D^{\text{rot}}}{\sin \vartheta} \left(\frac{\partial}{\partial \vartheta} \left(\sin \vartheta \frac{\partial}{\partial \vartheta} \right) + \frac{\partial}{\partial \varphi} \left(\frac{1}{\sin \vartheta} \frac{\partial}{\partial \varphi} \right) \right) \rho. \quad (91)$$

Using the substitution $u = \cos \vartheta$ (and $\partial u = -\sin \vartheta \partial \vartheta$),

$$\frac{\partial \rho}{\partial t} = D^{\text{rot}} \left((1-u^2) \frac{\partial^2}{\partial u^2} - 2u \frac{\partial}{\partial u} + \frac{1}{1-u^2} \frac{\partial^2}{\partial \varphi^2} \right) \rho. \quad (92)$$

Let us now try if time and space coordinates can be separated, i.e. if ρ can be expressed as a product $\rho(\vartheta, \varphi, t) = f(\vartheta, \varphi)g(t)$.

$$f \frac{\partial g}{\partial t} = g D^{\text{rot}} \left((1-u^2) \frac{\partial^2}{\partial u^2} - 2u \frac{\partial}{\partial u} + \frac{1}{1-u^2} \frac{\partial^2}{\partial \varphi^2} \right) f. \quad (93)$$

Dividing both sides of the equation by $D^{\text{rot}} \rho = D^{\text{rot}} fg$,

$$\frac{1}{D^{\text{rot}}} \frac{1}{g} \frac{\partial g}{\partial t} = \frac{1}{f} \left((1-u^2) \frac{\partial^2}{\partial u^2} - 2u \frac{\partial}{\partial u} + \frac{1}{1-u^2} \frac{\partial^2}{\partial \varphi^2} \right) f. \quad (94)$$

If the separation of time and space coordinates is possible, i.e., if Eq. 94 is true for any t and any ϑ, φ independently, both sides of the equation must be equal to the same constant (called λ below).

$$\frac{1}{D^{\text{rot}}} \frac{1}{g} \frac{\partial g}{\partial t} = \lambda \quad (95)$$

$$\frac{1}{f} \left((1-u^2) \frac{\partial^2}{\partial u^2} - 2u \frac{\partial}{\partial u} + \frac{1}{1-u^2} \frac{\partial^2}{\partial \varphi^2} \right) f = \lambda. \quad (96)$$

Solution of the first equation is obviously

$$g(t) = g(0)e^{\lambda D^{\text{rot}} t}, \quad (97)$$

where λ is obtained by solving the second equation. We solve a simplified version of the second equation in Section 2.6.2.

Lecture 1

Nuclear magnetic resonance

Literature: A general introduction can be found in L2.6 and L2.7. A nice and detailed discussion, emphasizing the importance of relaxation, is in Szántay et al.: *Anthropic awareness*, Elsevier 2015, Section 2.4. A useful review of relevant statistical concepts is presented in B6. Chemical shift is introduced by Levitt in L3.7 and discussed in detail in L9.1 (using a quantum approach, but the classical treatment can be obtained simply by using energy \mathcal{E}_j instead of \hat{H}_j and magnetic moment $\vec{\mu}_{jk}$ instead of $\gamma_j \hat{I}_{jk}$ in Eqs. 9.11–9.14). A nice discussion of the offset effects (and more) can be found in K4.

1.1 Nuclear magnetic moments in chemical substances

The aim of this course is to describe physical principles of the most frequent version of NMR spectroscopy, NMR analysis of chemical compounds dissolved in suitable solvents. The classical theory does not explain why some nuclei in such solutions have a magnetic moment, but it describes macroscopic effects of the nuclear magnetic moments in bulk samples (i.e., in macroscopic systems composed of billions of billions of molecules). It should be emphasized that classical (non-quantum) physics provides much more relevant description of the macroscopic samples than quantum mechanics of individual particles (electrons or nuclei).

Nuclei have permanent microscopic magnetic moments, but the macroscopic magnetic moment of non-ferromagnetic chemical substances is induced only in the magnetic field. This is the effect of symmetry. Outside a magnet, all orientations of the microscopic magnetic moments have the same energy and are equally probable. Therefore, the bulk magnetic moment is zero and the bulk magnetization \vec{M} (magnetic moment per unit volume) is zero (Fig. 1.1).

1.2 Polarization

In a static homogeneous magnetic field \vec{B}_0 , the orientations of $\vec{\mu}$ are no longer equally probable: the orientation of $\vec{\mu}$ along \vec{B}_0 is energetically most favored and the opposite orientation is least favored. The symmetry is broken in the direction of \vec{B}_0 , this direction is used to define the z axis of a coordinate system we work in. However, the state with all magnetic moments in the energetically most favorable orientation is not most probable. Orienting all magnetic moments along the magnetic field

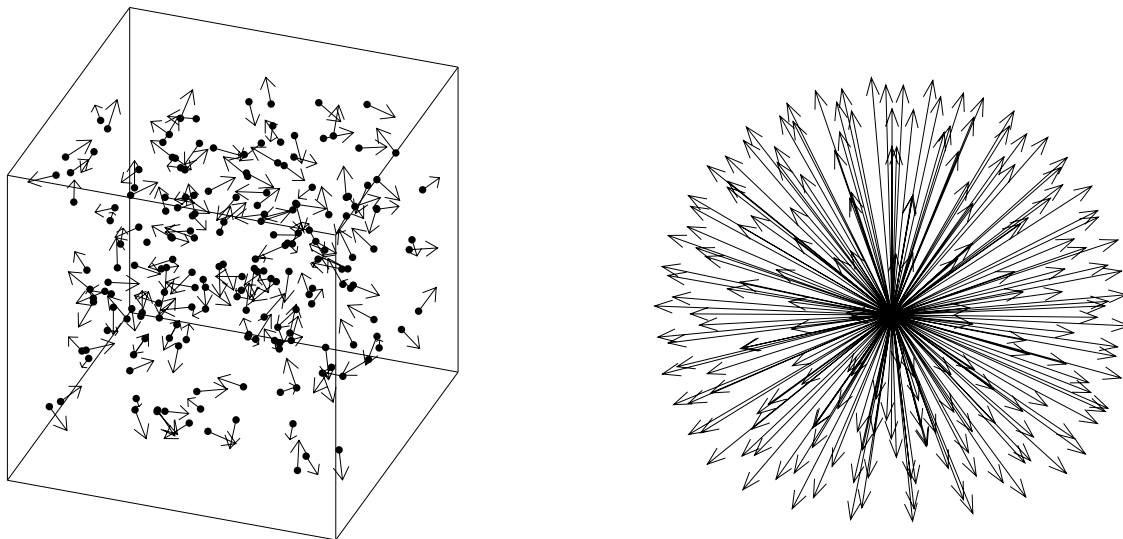


Figure 1.1: Distribution of magnetic moments in the absence of a magnetic field. Left, a schematic representation of an NMR sample. Dots represent molecules, arrows represent magnetic moments (only one magnetic moment per molecule is shown for the sake of simplicity, like e.g. in compressed $^{13}\text{C}^{16}\text{O}_2$). Right, the molecules are superimposed to make the distribution of magnetic moments visible.

represents only one *microstate*. In contrast, there exist a large number of microstates with somewhat higher energy. The correct balance between energy and probability is described by the Boltzmann distribution law, which can be derived from purely statistical arguments. Thermodynamics thus helps us to describe the polarization along z quantitatively.¹ Calculation of the average magnetic moment, presented in Section 1.5.1, shows that the bulk magnetization of the NMR sample containing nuclei with $\vec{\mu}$:

$$M_x^{\text{eq}} = 0 \quad M_y^{\text{eq}} = 0 \quad M_z^{\text{eq}} = \frac{\mathcal{N} |\mu|^2 |B_0|}{3 k_B T}, \quad (1.1)$$

where \mathcal{N} is the number of dipoles per unit volume.

In summary, dipoles are polarized in the static homogeneous magnetic fields. In addition, all dipoles precess² with the frequency $\vec{\omega} = -\gamma \vec{B}_0$, but the precession cannot be observed at the macroscopic level because the bulk magnetization is parallel with the axis of precession (Fig. 1.2).

1.3 Coherence

In order to observe precession, we need to break the axial symmetry and introduce a *coherent* motion of magnetic moments. This is achieved by applying another magnetic field \vec{B}_1 perpendicular to \vec{B}_0 and

¹Thermodynamics also tells us that the energy of the whole (isolated) system must be conserved. Decreased energy of magnetic moments is compensated by increased rotational kinetic energy of molecules of the sample, coupled with the magnetic moments via magnetic fields of the tumbling molecules, as discussed in the next chapter.

²Precession is described in Background section 0.1.8.

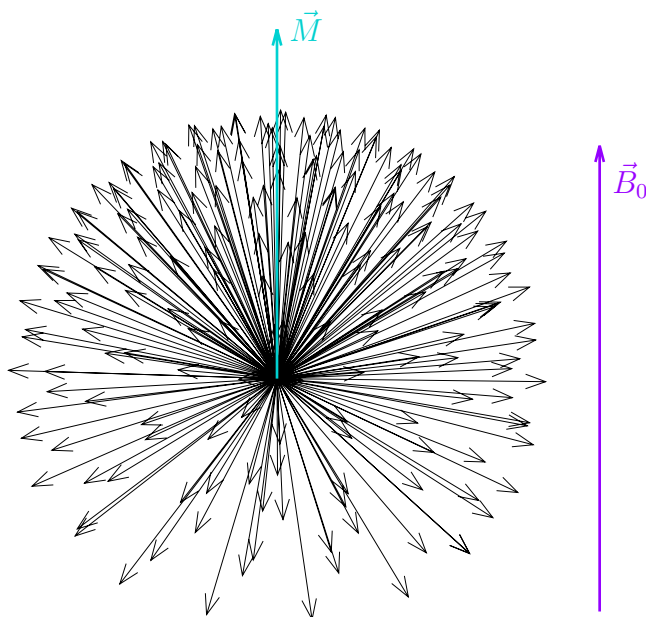


Figure 1.2: Distribution of magnetic moments in a homogeneous magnetic field B_0 . The cyan arrow represents the bulk magnetization.

oscillating with the frequency close to (ideally equal to) $\gamma|B_0|/2\pi$. In NMR, sources of the oscillatory field are radio waves.³ Figure 1.3 shows why a static perpendicular magnetic field cannot be used, whereas the desired effect of an oscillating perpendicular magnetic field is depicted in Figure 1.4.

If the radio waves are applied exactly for the time needed to rotate the magnetization by 90° , they create a state with \vec{M} perpendicular to \vec{B}_0 . The magnetization vector (left panel in Fig. 1.4) describe a new distribution of magnetic moments (right panel in Fig. 1.4). Such magnetization vector then rotates with the precession frequency, also known as the *Larmor frequency*. The described rotation corresponds to a coherent motion of nuclear dipoles polarized in the direction of \vec{M} and generates measurable electromotoric force in the detector coil. When describing the effect of radio waves, the oscillating magnetic field of the waves is often approximated by a rotating magnetic field. Such treatment is presented in detail in Section 1.5.2.

1.4 Chemical shift

The description of the motions of the bulk nuclear magnetization presented in the previous section is simple but boring. What makes NMR useful for chemists and biologists is the fact that the energy of the magnetic moment of the observed nucleus is influenced by magnetic fields associated with motions of nearby electrons. In order to understand this effect, we need to describe the magnetic fields of moving electrons.

³In the context of the NMR spectroscopy, it is important that the field *oscillates in time*, not that it travels in space as a wave.

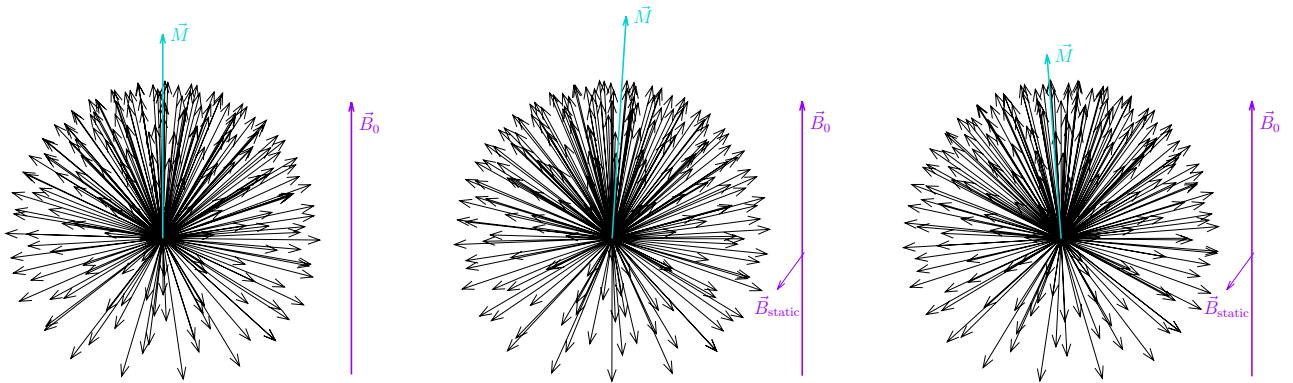


Figure 1.3: Distribution of magnetic moments in the presence of an external homogeneous magnetic field \vec{B}_0 (vertical violet arrow) is such that the bulk magnetization of nuclei (shown in cyan) is oriented along \vec{B}_0 (left). Application of an another static magnetic field \vec{B}_1 rotates magnetization away from the original vertical orientation down in a clockwise direction (middle). However, the magnetization also precesses about \vec{B}_0 . After a half-turn precession (right), the clockwise rotation by the additional magnetic field \vec{B}_1 returns the magnetization towards its original vertical direction. Therefore, a static field cannot be used to turn the magnetization from the vertical direction to a perpendicular orientation.

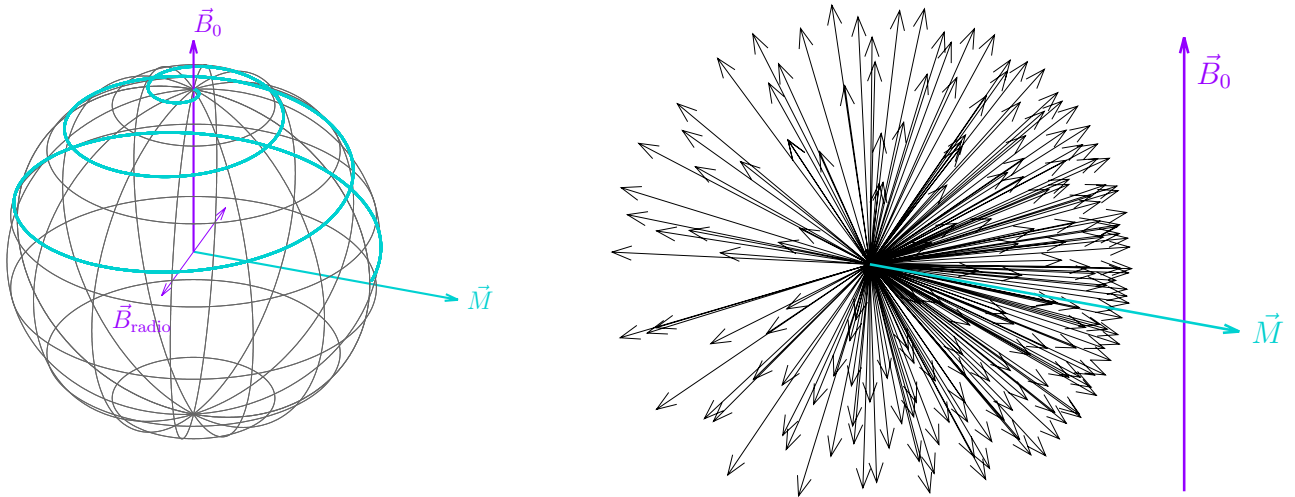


Figure 1.4: Effect of the radio waves on the bulk magnetization (left) and distribution of magnetic moments after application of the radio-wave pulse. The thin purple line shows oscillation of the magnetic induction vector of the radio waves, the cyan trace shows evolution of the magnetization during irradiation. If the perpendicular magnetic field oscillates with a frequency equal to the precession frequency of magnetization, it rotates the magnetization clockwise then it is tilted to the right, but counter-clockwise when the magnetization is tilted to the left. Therefore, the magnetization is more and more tilted down from the original vertical direction. The total duration of the irradiation by the radio wave was chosen so that the magnetization is rotated to the plane perpendicular to \vec{B}_0 (cyan arrow). Note that the ratio $|\vec{B}_0|/|\vec{B}_{\text{radio}}|$ is much higher in a real experiment.

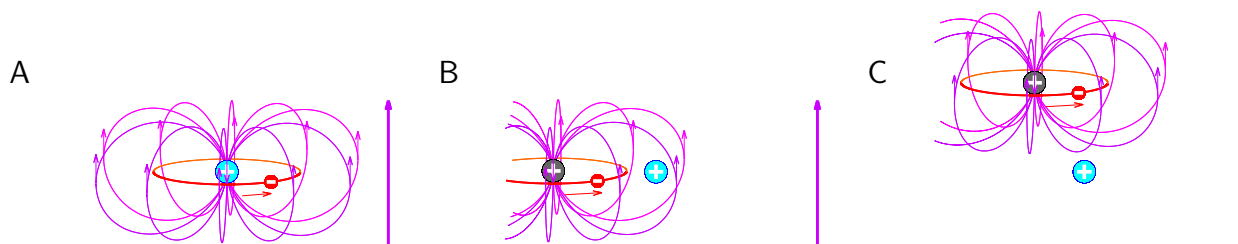


Figure 1.5: A, Classical description of interaction of an observed magnetic moment with the orbital magnetic moment of an electron of the same atom. The observed nucleus and the electron are shown in cyan and red, respectively. The thick purple arrow represents \vec{B}_0 , the thin purple induction lines represent the magnetic field of the electron (the small purple arrows indicate its direction). The electron in \vec{B}_0 moves in a circle shown in red, direction of the motion is shown as the red arrow. The field of the orbital magnetic moment of the electron in the same atom decreases the total field in the place of the observed nucleus (the small purple arrow in the place of the cyan nucleus is pointing down). B, Interaction of an observed magnetic moment with the orbital magnetic moment of an electron of the another atom (its nucleus is shown in gray). In the shown orientation of the molecule, the field of the orbital magnetic moment of the electron in the other atom increases the total field in the place of the observed nucleus (the small purple arrow close the cyan nucleus is pointing up). C, As the molecule rotates, the cyan nucleus moves to a position where the field of the orbital magnetic moment of the electron in the other atom starts to decrease the total field (the induction lines reverse their direction in the place of the cyan nucleus).

If a moving electron enters a homogeneous magnetic field, it experiences a Lorentz force and moves in a circle in a plane perpendicular to the field (cyclotron motion). Such an electron represents an electric current in a circular loop, and is a source of a magnetic field induced by the homogeneous magnetic field. The homogeneous magnetic field \vec{B}_0 in NMR spectrometers induces a similar motion of electrons in atoms, which generates microscopic magnetic fields (Figure 1.5A).

The observed nucleus feels the external magnetic field \vec{B}_0 slightly modified by the microscopic fields of electrons. If the electron distribution is spherically symmetric, with the observed nucleus in the center (e.g. electrons in the 1s orbital of the hydrogen atom), the induced field of the electrons decreases the effective magnetic field felt by the nucleus in the center. Since the induced field of electrons \vec{B}_e is proportional to the inducing external field \vec{B}_0 , the effective field can be described as

$$\vec{B} = \vec{B}_0 + \vec{B}_e = (1 + \delta)\vec{B}_0. \quad (1.2)$$

The constant δ is known as *chemical shift* and does not depend on the orientation of the molecule in such a case⁴. The precession frequency of the nucleus is equal⁵ to $(1 + \delta)\omega_0$.

Most molecules consist of multiple atoms and electron distribution is therefore not spherically symmetric around the observed nucleus. As a consequence, the effective field depends on the orienta-

⁴Instead of δ , a constant with the opposite sign defining the *chemical shielding* is sometimes used.

⁵The value of δ in Eq. 1.2 describes how much the frequency of nuclei deviates from a hypothetical frequency of free nuclei. Such a hypothetical frequency is difficult to measure. In practice, frequencies of nuclei in certain, readily accessible chemical compounds are used instead of the frequencies of free nuclei as the reference values of δ , as is described in Section 3.1.

tion of the whole molecule defining mutual positions of atoms and orientation of molecular orbitals. The currents induced in orbitals of other atoms may decrease or increase (shield or deshield) the effective magnetic field felt by the observed nucleus (Figure 1.5B,C). Therefore, the effective field fluctuates as a result of rotational diffusion of the molecule and of internal motions changing mutual positions of atoms. The induced field of electrons is still proportional to the inducing external field \vec{B}_0 , but the proportionality constants are different for each combination of components of \vec{B}_e and \vec{B}_0 in the coordination frame used. Therefore, we need six⁶ constants δ_{jk} to describe the effect of electrons:

$$B_{e,x} = \delta_{xx}B_{0,x} + \delta_{xy}B_{0,y} + \delta_{xz}B_{0,z} \quad (1.3)$$

$$B_{e,y} = \delta_{yx}B_{0,x} + \delta_{yy}B_{0,y} + \delta_{yz}B_{0,z} \quad (1.4)$$

$$B_{e,z} = \delta_{zx}B_{0,x} + \delta_{zy}B_{0,y} + \delta_{zz}B_{0,z} \quad (1.5)$$

Eqs. 1.3–1.5 can be written in more compact forms

$$\begin{pmatrix} B_{e,x} \\ B_{e,y} \\ B_{e,z} \end{pmatrix} = \begin{pmatrix} \delta_{xx} & \delta_{xy} & \delta_{xz} \\ \delta_{yx} & \delta_{yy} & \delta_{yz} \\ \delta_{zx} & \delta_{zy} & \delta_{zz} \end{pmatrix} \cdot \begin{pmatrix} B_{0,x} \\ B_{0,y} \\ B_{0,z} \end{pmatrix} \quad (1.6)$$

or

$$\vec{B}_e = \underline{\delta} \cdot \vec{B}_0, \quad (1.7)$$

where $\underline{\delta}$ is the *chemical shift tensor*.

It is always possible to find a coordinate system X, Y, Z known as the *principal frame*, where $\underline{\delta}$ is represented by a diagonal matrix. In such a system, we need only three constants (principal values of the chemical shift tensor): $\delta_{XX}, \delta_{YY}, \delta_{ZZ}$. However, three more parameters must be specified: three *Euler angles* (written as φ, ϑ , and χ in this text) defining orientation of the coordinate system X, Y, Z in the laboratory coordinate system x, y, z . Note that $\delta_{XX}, \delta_{YY}, \delta_{ZZ}$ are true constants because they do not change as the molecule tumbles in solution (but they may change due to internal motions or chemical changes of the molecule). The orientation is completely described by the Euler angles. Graphical representation of the chemical shift tensor is shown in Figure 1.6, the algebraic description is presented in Section 1.5.3. We derive a not very simple equation describing how electrons modify the external magnetic field:

$$\begin{aligned} \vec{B}_e = & \delta_i B_0 \begin{pmatrix} 0 \\ 0 \\ 1 \end{pmatrix} + \delta_a B_0 \begin{pmatrix} 3 \sin \vartheta \cos \vartheta \cos \varphi \\ 3 \sin \vartheta \cos \vartheta \sin \varphi \\ 3 \cos^2 \vartheta - 1 \end{pmatrix} \\ & + \delta_r B_0 \begin{pmatrix} -(2 \cos^2 \chi - 1) \sin \vartheta \cos \vartheta \cos \varphi + 2 \sin \chi \cos \chi \sin \vartheta \sin \varphi \\ -(2 \cos^2 \chi - 1) \sin \vartheta \cos \vartheta \sin \varphi - 2 \sin \chi \cos \chi \sin \vartheta \cos \varphi \\ +(2 \cos^2 \chi - 1) \sin^2 \vartheta \end{pmatrix}, \quad (1.8) \end{aligned}$$

⁶There are nine constants in Eqs. 1.3–1.5, but $\delta_{xy} = \delta_{yx}$, $\delta_{xz} = \delta_{zx}$, and $\delta_{yz} = \delta_{zy}$.

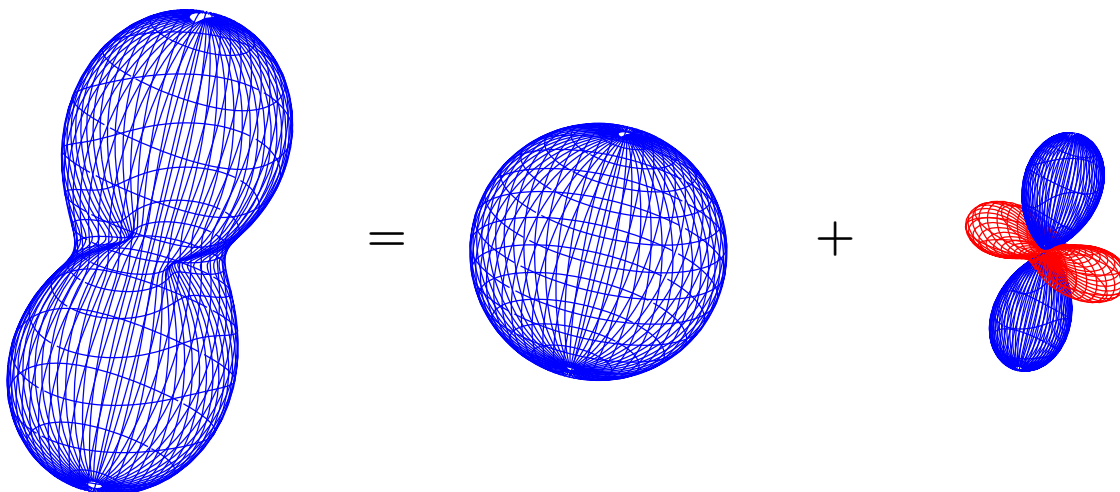


Figure 1.6: Visualization of the chemical shift tensor (left). Distance of each point at the plotted surface from its center is proportional to the magnetic induction \vec{B}_e in the given direction (given by angles θ, φ). The chemical shift tensor can be decomposed to its isotropic (middle) and anisotropic (right) contributions. The red color indicates negative values of the anisotropic contribution.

where δ_i , δ_a , and δ_r are constants describing sizes of the isotropic, axially symmetric and asymmetric (rhombic) components of the chemical shift tensor, respectively, and ϑ, φ, χ are the aforementioned Euler angles.

Do we really need such a level of complexity? The answer is "yes and no". When we analyze only the (average) value of the precession frequency, it is sufficient to consider only the isotropic component. The description of the effect of electrons then simplifies to Eq. 1.2, where δ now represents δ_i of Eq. 1.8. When we analyze also the effect of stochastic motions, the other terms become important as well. The correct quantitative analysis requires full Eq. 1.8, but the basic principles can be discussed without using the rhombic component. Therefore, we will use the axially symmetric approximation of Eq. 1.8 when we discuss effects of molecular motions in Section 1.5.5.

Practical consequences of the existence of the chemical shift, their formal description and related conventions used in the NMR literature are discussed in Section 1.5.4. In addition, Section 1.5.4 presents simplified equations of motion describing evolution of magnetization in terms of classical physics and in the absence of relaxation. Solution of these equations is described in Section 1.5.5 for a simple case of magnetization rotating in the absence of the radio waves. The classical analysis of relaxation effects is then discussed in the next lecture.

HOMework

First check that you understand Section 0.1.6. Then, derive how is the magnetic moment of a current loop related to the angular momentum (Section 0.1.7) and what defines the precession frequency of a magnetic moment of a current loop in a homogeneous magnetic field (Section 0.1.8).

1.5 DERIVATIONS

1.5.1 Polarization and bulk magnetization

The average value of the z -component of $\vec{\mu}$ is calculated as⁷

$$\bar{\mu}_z^{\text{eq}} = \int_0^\pi P^{\text{eq}}(\vartheta) \mu_z \sin \vartheta d\vartheta = \int_0^\pi P^{\text{eq}}(\vartheta) |\mu| \cos \vartheta \sin \vartheta d\vartheta, \quad (1.9)$$

where ϑ is the inclination (angle between $\vec{\mu}$ and axis z) and $P^{\text{eq}}(\vartheta)$ is the probability of $\vec{\mu}$ to be tilted by the angle ϑ . If the magnetic dipoles are in a thermodynamic equilibrium, the angular distribution of the $\vec{\mu}$ orientation is given by the Boltzmann law⁸

$$P^{\text{eq}}(\vartheta) = \frac{e^{-\frac{\mathcal{E}(\vartheta)}{k_B T}}}{\int_0^\pi e^{-\frac{\mathcal{E}(\vartheta')}{k_B T}} \sin \vartheta' d\vartheta'}, \quad (1.11)$$

where T is the thermodynamic temperature, $k_B = 1.38064852 \times 10^{-23} \text{ m}^2 \text{ kg s}^{-2} \text{ K}^{-1}$ is the Boltzmann constant, and $\mathcal{E} = -|\mu||B_0| \cos \vartheta$ is the magnetic potential energy of the dipole. The distribution is axially symmetric, all values of the azimuth φ are equally possible.

Using the substitutions

$$u = \cos \vartheta \Rightarrow du = \frac{du}{d\vartheta} d\vartheta = -\frac{d \cos \vartheta}{d\vartheta} d\vartheta = -\sin \vartheta d\vartheta \quad (1.12)$$

and

$$w = \frac{|\mu||B_0|}{k_B T}, \quad (1.13)$$

$$P^{\text{eq}}(\vartheta) = \frac{e^{-\frac{\mathcal{E}(\vartheta)}{k_B T}}}{\int_0^\pi e^{-\frac{\mathcal{E}(\vartheta')}{k_B T}} \sin \vartheta' d\vartheta'} = \frac{e^{uw}}{\int_{-1}^{-1} -e^{u'w} du'} = \frac{e^{uw}}{\int_{-1}^{-1} e^{u'w} du'} = \frac{e^{uw}}{\frac{1}{w} [e^{u'w}]_{-1}^1} = \frac{w}{e^w - e^{-w}} e^{uw} = P^{\text{eq}}(u). \quad (1.14)$$

Knowing the distribution, the average z -component of $\vec{\mu}$ can be calculated

$$\bar{\mu}_z^{\text{eq}} = \int_0^\pi P^{\text{eq}}(\vartheta) |\mu| \cos \vartheta \sin \vartheta d\vartheta = \int_{-1}^{-1} |\mu| u P^{\text{eq}}(u) du = \frac{|\mu|w}{e^w - e^{-w}} \int_{-1}^{-1} u e^{uw} du. \quad (1.15)$$

Using the chain rule,

$$\bar{\mu}_z^{\text{eq}} = \frac{|\mu|w}{e^w - e^{-w}} \left[\frac{1}{w^2} e^{uw} (uw - 1) \right]_{-1}^1 = |\mu| \left(\frac{e^w + e^{-w}}{w} - \frac{e^w - e^{-w}}{w^2} \right) = |\mu| \left(\frac{e^w + e^{-w}}{e^w - e^{-w}} - \frac{1}{w} \right) = |\mu| \left(\coth(w) - \frac{1}{w} \right). \quad (1.16)$$

The function $\coth(w)$ can be expanded as a Taylor series

$$\coth(w) \approx \frac{1}{w} + \frac{w}{3} - \frac{w^3}{45} + \frac{2w^5}{945} - \dots \Rightarrow \bar{\mu}_z \approx |\mu| \left(\frac{w}{3} - \frac{w^3}{45} + \frac{2w^5}{945} - \dots \right). \quad (1.17)$$

At the room temperature, $|\mu||B_0| \ll k_B T$ even in the strongest NMR magnets. Therefore, w is a very small number and its high powers in the Taylor series can be neglected. In summary, the angular distribution can be approximated by

⁷The integral represents summation (integration) over all possible orientations with respect to \vec{B}_0 , described by the inclination angles ϑ .

⁸Probability of a system to be in the state with the energy \mathcal{E}_j at the temperature T is given by

$$P^{\text{eq}}(\vartheta) = \frac{e^{-\frac{\mathcal{E}_j}{k_B T}}}{Z}, \quad (1.10)$$

where Z is sum of the $e^{-\frac{\mathcal{E}_k}{k_B T}}$ terms of all possible states.

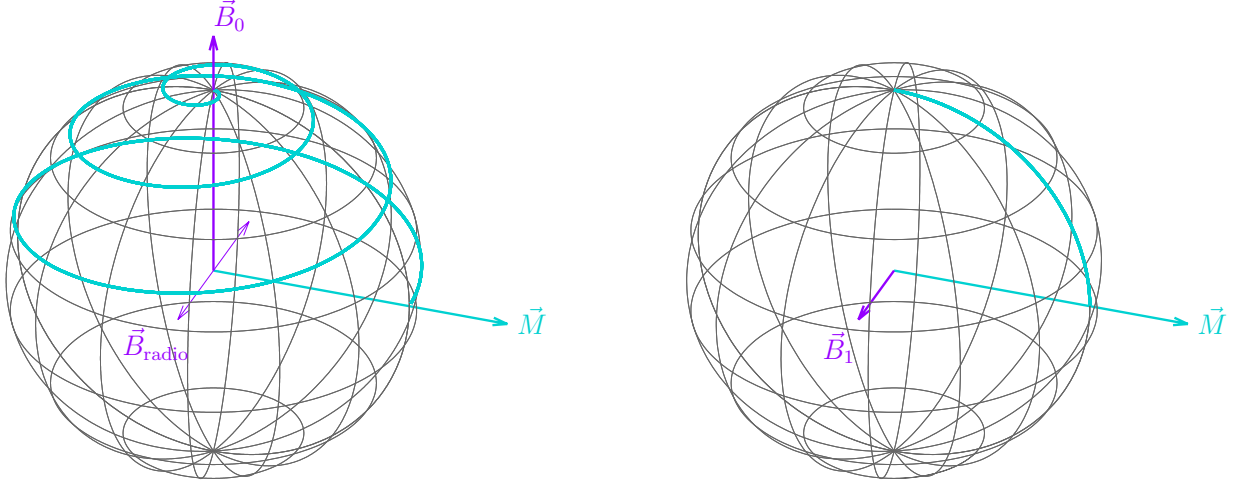


Figure 1.7: Rotation of the magnetization to direction perpendicular to \vec{B}_0 , shown in the laboratory and rotating coordinate frame in the left and right panel, respectively. The thin purple line shows oscillation of the magnetic induction vector of the radio waves, the cyan trace shows evolution of the magnetization during irradiation.

$$\bar{\mu}_z^{\text{eq}} = \frac{1}{3} \frac{|\mu|^2 |B_0|}{k_B T}, \quad (1.18)$$

while

$$\bar{\mu}_x^{\text{eq}} = \bar{\mu}_y^{\text{eq}} = 0. \quad (1.19)$$

1.5.2 Rotating coordinate frame

Mathematically, the described radio field can be decomposed into two components \vec{B}_{radio}^+ and \vec{B}_{radio}^- rotating with the same angular frequency but in opposite directions ($\vec{\omega}_{\text{radio}}$ and $-\vec{\omega}_{\text{radio}}$, respectively). The component rotating in the same direction as the precessing dipoles ($\vec{B}_{\text{radio}}^- \equiv \vec{B}_1$ in this text) tilts the magnetization vector \vec{M} from the z direction, the other component can be neglected as long as $|B_1| \ll |B_0|$. This process represents a double rotation, the first rotation is precession around the direction of \vec{B}_0 , the second rotation around \vec{B}_1 is known as *nutation*. Although this mathematical decomposition is only formal and does not reflect the physical reality, it is frequently used to facilitate the analysis of the effect of radio waves on magnetization. The description can be simplified (the effect of the precession removed), if we use \vec{B}_1 to define the x axis of our coordinate frame. As \vec{B}_1 rotates about \vec{B}_0 with an angular frequency $\vec{\omega}_{\text{radio}}$, we work in a coordinate frame rotating with a frequency $\vec{\omega}_{\text{rot}} = -\vec{\omega}_{\text{radio}}$ (*rotating frame*). In order to define the direction of x in the rotating frame, we must also define the phase ϕ_{rot} .

The components of the field \vec{B}_1 rotating with the angular frequency $-\vec{\omega}_{\text{radio}}$ are in the laboratory frame

$$B_{1,x} = |B_1| \cos(\omega_{\text{rot}} t + \phi_{\text{rot}}) = |B_1| \cos(-\omega_{\text{radio}} t + \phi_{\text{rot}}), \quad (1.20)$$

$$B_{1,y} = |B_1| \sin(\omega_{\text{rot}} t + \phi_{\text{rot}}) = |B_1| \sin(-\omega_{\text{radio}} t + \phi_{\text{rot}}), \quad (1.21)$$

$$B_{1,z} = 0 \quad (1.22)$$

and in the rotating frame

$$B_{1,x} = |B_1| \cos(\phi_{\text{rot}}), \quad (1.23)$$

$$B_{1,y} = |B_1| \sin(\phi_{\text{rot}}), \quad (1.24)$$

$$B_{1,z} = 0. \quad (1.25)$$

Consequently, the rotation of magnetization is given by the angular frequency vector

$$\vec{\omega} = \vec{\omega}_0 + \vec{\omega}_1 = -\gamma(\vec{B}_0 + \vec{B}_1) = \begin{pmatrix} 0 \\ 0 \\ -\gamma|B_0| \end{pmatrix} + \begin{pmatrix} -\gamma|B_1| \cos(-\omega_{\text{radio}}t + \phi_{\text{rot}}) \\ -\gamma|B_1| \sin(-\omega_{\text{radio}}t + \phi_{\text{rot}}) \\ 0 \end{pmatrix} = \begin{pmatrix} -\gamma|B_1| \cos(-\omega_{\text{radio}}t + \phi_{\text{rot}}) \\ -\gamma|B_1| \sin(-\omega_{\text{radio}}t + \phi_{\text{rot}}) \\ -\gamma|B_0| \end{pmatrix} \quad (1.26)$$

in the laboratory frame, and by

$$\vec{\omega} = \vec{\omega}_1 = -\gamma\vec{B}_1 = \begin{pmatrix} -\gamma|B_1| \cos(\phi_{\text{rot}}) \\ -\gamma|B_1| \sin(\phi_{\text{rot}}) \\ 0 \end{pmatrix} \quad (1.27)$$

in the coordinate frame rotating with the angular frequency $\vec{\omega}_{\text{rot}} = -\vec{\omega}_{\text{radio}} = \vec{\omega}_0$. What are the components of \vec{B}_1 in the rotating frame for different choices of ϕ_{rot} ? If $\phi_{\text{rot}} = 0$, $\cos(0) = 1$, $\sin(0) = 0$, and

$$B_{1,x} = |B_1|, \quad (1.28)$$

$$B_{1,y} = 0, \quad (1.29)$$

$$B_{1,z} = 0. \quad (1.30)$$

If $\phi_{\text{rot}} = \frac{\pi}{2}$, $\cos(\frac{\pi}{2}) = 0$, $\sin(\frac{\pi}{2}) = 1$, and

$$B_{1,x} = 0, \quad (1.31)$$

$$B_{1,y} = |B_1|, \quad (1.32)$$

$$B_{1,z} = 0. \quad (1.33)$$

If $\phi_{\text{rot}} = \pi$, $\cos(\pi) = -1$, $\sin(\pi) = 0$, and

$$B_{1,x} = -|B_1|, \quad (1.34)$$

$$B_{1,y} = 0, \quad (1.35)$$

$$B_{1,z} = 0, \quad (1.36)$$

and so on.

The typical convention is to choose $\phi_{\text{rot}} = \pi$ for nuclei with $\gamma > 0$ and $\phi_{\text{rot}} = 0$ for nuclei with $\gamma < 0$. Then, the nutation frequency is $\omega_1 = +\gamma|B_1|$ (opposite convention to the precession frequency!) for nuclei with $\gamma > 0$ and $\omega_1 = -\gamma|B_1|$ (the same convention as the precession frequency) for nuclei with $\gamma < 0$.

1.5.3 Chemical shift tensor

The chemical shift tensor in its principal frame can be also written as a sum of three simple matrices, each multiplied by one characteristic constant:

$$\begin{pmatrix} \delta_{XX} & 0 & 0 \\ 0 & \delta_{YY} & 0 \\ 0 & 0 & \delta_{ZZ} \end{pmatrix} = \delta_i \begin{pmatrix} 1 & 0 & 0 \\ 0 & 1 & 0 \\ 0 & 0 & 1 \end{pmatrix} + \delta_a \begin{pmatrix} -1 & 0 & 0 \\ 0 & -1 & 0 \\ 0 & 0 & 2 \end{pmatrix} + \delta_r \begin{pmatrix} 1 & 0 & 0 \\ 0 & -1 & 0 \\ 0 & 0 & 0 \end{pmatrix}, \quad (1.37)$$

where

$$\delta_i = \frac{1}{3} \text{Tr}\{\delta\} = \frac{1}{3}(\delta_{XX} + \delta_{YY} + \delta_{ZZ}) \quad (1.38)$$

is the *isotropic component* of the chemical shift tensor,

$$\delta_a = \frac{1}{3} \Delta_\delta = \frac{1}{6}(2\delta_{ZZ} - (\delta_{XX} + \delta_{YY})) \quad (1.39)$$

is the *axial component* of the chemical shift tensor (Δ_δ is the *chemical shift anisotropy*), and

$$\delta_r = \frac{1}{3} \eta_\delta \Delta_\delta = \frac{1}{2}(\delta_{XX} - \delta_{YY}) \quad (1.40)$$

is the *rhombic component* of the chemical shift tensor (η_δ is the *asymmetry of the chemical shift tensor*).

The chemical shift tensor written in its principle frame is relatively simple, but we need its description in the laboratory coordinate frame. Changing the coordinate systems represents a rotation in a three-dimensional space. Equations describing such a simple operation are relatively complicated. On the other hand, the equations simplify if \vec{B}_0 defines the z axis of the coordinate frame (i.e., $B_{0,z} = B_0$ and $B_{0,x} = B_{0,y} = 0$):

$$\vec{B}_e = \delta_i B_0 \begin{pmatrix} 0 \\ 0 \\ 1 \end{pmatrix} + \delta_a B_0 \begin{pmatrix} 3 \sin \vartheta \cos \vartheta \cos \varphi \\ 3 \sin \vartheta \cos \vartheta \sin \varphi \\ 3 \cos^2 \vartheta - 1 \end{pmatrix} + \delta_r B_0 \begin{pmatrix} -(2 \cos^2 \chi - 1) \sin \vartheta \cos \vartheta \cos \varphi + 2 \sin \chi \cos \chi \sin \vartheta \sin \varphi \\ -(2 \cos^2 \chi - 1) \sin \vartheta \cos \vartheta \sin \varphi - 2 \sin \chi \cos \chi \sin \vartheta \cos \varphi \\ +(2 \cos^2 \chi - 1) \sin^2 \vartheta \end{pmatrix}. \quad (1.41)$$

The first, isotropic contribution does not change upon rotation (it is a scalar). The second, axial contribution, is insensitive to the rotation about the symmetry axis \vec{a} , described by χ . Rotation of the chemical shift anisotropy tensor from its principal frame to the laboratory frame can be also described by orientation of \vec{a} in the laboratory frame:

$$\delta_a \begin{pmatrix} -1 & 0 & 0 \\ 0 & -1 & 0 \\ 0 & 0 & 2 \end{pmatrix} \longrightarrow \delta_a \begin{pmatrix} 3a_x^2 - 1 & 3a_x a_y & 3a_x a_z \\ 3a_x a_y & 3a_y^2 - 1 & 3a_y a_z \\ 3a_x a_z & 3a_y a_z & 3a_z^2 - 1 \end{pmatrix}, \quad (1.42)$$

where $a_x = \sin \vartheta \cos \varphi$, $a_y = \sin \vartheta \sin \varphi$, and $a_z = \cos \vartheta$.

1.5.4 Offset effects

The presence of electrons makes NMR a great method for chemical analysis. The measured precession frequency depends not only on the type of nucleus (e.g. ^1H) but also on the electronic environment: frequencies of protons in different chemical moieties differ and can be used to identify chemical groups in organic molecules. But how do the electrons influence the physical description of the nuclear magnetization?

The effect of the isotropic component of the chemical shift on the precession frequency is simply introducing a small correction constant $1 + \delta$ modifying γ :

$$\vec{\omega}_0 = -\gamma \vec{B}_0 \quad \rightarrow \quad \vec{\omega}_0 = -\gamma(1 + \delta) \vec{B}_0. \quad (1.43)$$

The trouble is that the correction is different for each proton (or carbon etc.) in the molecule. Therefore, the frequency of the radio waves can match $\omega_0 = -\gamma(1 + \delta)|B_0|$ only for one proton in the molecule. For example, if the radio wave resonate with the frequency of the methyl proton in ethanol, it cannot resonate with the frequency of the proton in the OH or CH_2 group. In the rotating coordinate frame, only magnetization of the methyl protons rotates about $\vec{\omega}_1 = \gamma(1 + \delta_{\text{methyl}}) \vec{B}_1 \approx \gamma \vec{B}_1$. Magnetizations of other protons rotate about other axes (Figure 1.8). Such rotations can be described by effective angular frequencies

$$\vec{\omega}_{\text{eff}} = \vec{\omega}_1 + \vec{\Omega}, \quad (1.44)$$

where

$$\vec{\Omega} = \vec{\omega}_0 - \vec{\omega}_{\text{rot}} = \vec{\omega}_0 - (-\vec{\omega}_{\text{radio}}) = \vec{\omega}_0 + \vec{\omega}_{\text{radio}} \quad (1.45)$$

is the angular frequency *offset*. As any vector in a 3D space, $\vec{\omega}_{\text{eff}}$ is characterized by three parameters: magnitude ω_{eff} , inclination ϑ , and azimuth φ .

The magnitude of the effective frequency is

$$\omega_{\text{eff}} = \sqrt{\omega_1^2 + \Omega^2}. \quad (1.46)$$

The inclination can be calculated from

$$\tan \vartheta = \frac{\omega_1}{\Omega}. \quad (1.47)$$

The azimuth is given by the phase of \vec{B}_1 ($\varphi = \varphi_{\text{rot}}$ in a single-pulse experiment).

As a result of the chemical shift, only the magnetization of the nucleus with $\Omega = 0$ (methyl protons in our case) rotates along the "meridian" in the rotating coordinate system (Figure 1.8 left). Magnetizations of other protons move in other circles⁹ (Figure 1.8 right). Therefore, if the radio transmitter is switched off when the methyl magnetization is pointing horizontally (and starts to rotate around the "equator" with the precession frequency of methyl protons), vectors of magnetizations of other protons point in different directions, and start to precess on cones with different inclinations and with different initial phases. Such effects, known as the *offset effects*, influence the measured signal.¹⁰

⁹For a certain ratio of B_1 to $-\Omega/\gamma$, the magnetization makes a full circle and returns to the original direction along \vec{B}_0 . It is therefore possible to chose such value of $\omega_1 \approx \gamma \vec{B}_1$ so that magnetization of one nucleus (with precession frequency resonating with the radio wave frequency) is flipped by 90° (Figure 1.9) or 180° (Figure 1.10), while magnetization of another nucleus (offset by Ω) is practically unaffected, being returned to the original direction.

¹⁰The result is the same as if apparent effective fields of the magnitude $B_{\text{eff}} = \sqrt{B_1^2 + (\Omega/\gamma)^2}$ were applied in the direction in the directions of $\vec{\omega}_{\text{eff}}$. The apparent effective field \vec{B}_{eff} is often used to describe the offset effects.

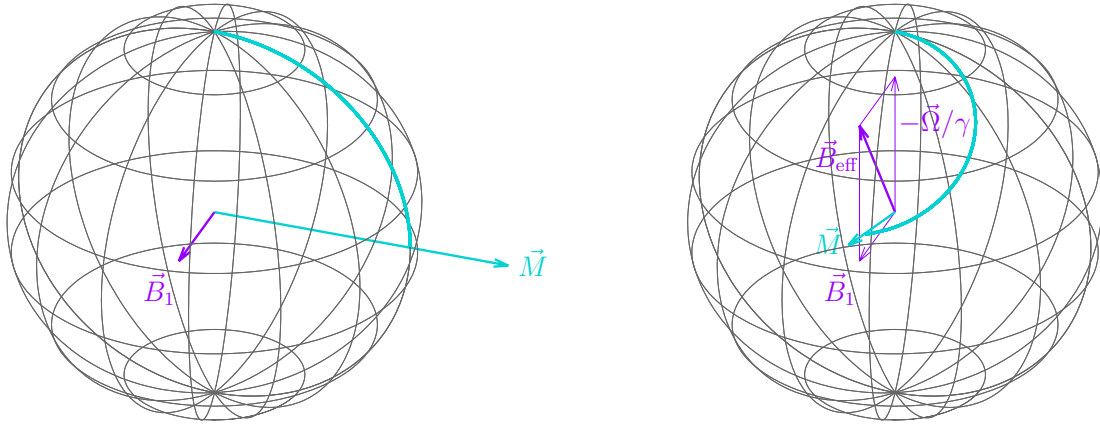


Figure 1.8: Evolution of the magnetization vectors with precession frequency exactly matching the used radio frequency (left) and slightly off-resonance (right). The evolution is shown in a coordinate frame rotating with $\vec{\omega}_{\text{rot}} = -\vec{\omega}_{\text{radio}}$.

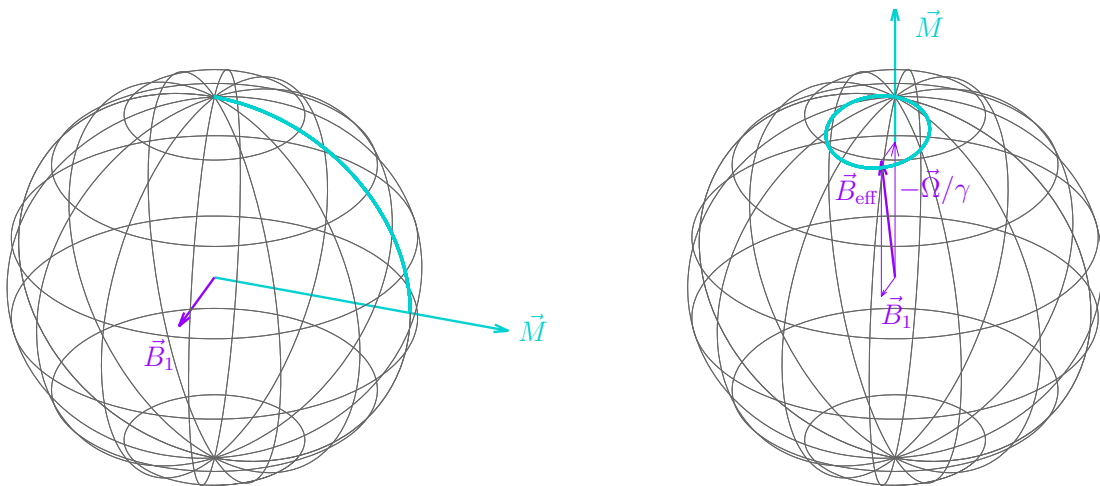


Figure 1.9: Evolution of the magnetization vectors with precession frequency exactly matching the used radio frequency (left) and with a frequency offset Ω (right), for $\omega_1 = \Omega/\sqrt{15}$. If ω_1 rotates magnetization of the former nucleus by 90° , then $\omega_{\text{eff}} = \sqrt{1 + 15}\Omega = 4\Omega$ rotates magnetization of the latter nucleus by $4 \times 90^\circ = 360^\circ$, i.e., by the full circle. The evolution is shown in a coordinate frame rotating with $\vec{\omega}_{\text{rot}} = -\vec{\omega}_{\text{radio}}$. In both cases, magnetization rotates about the thick purple arrow with the angular frequency proportional to the length of the arrow.

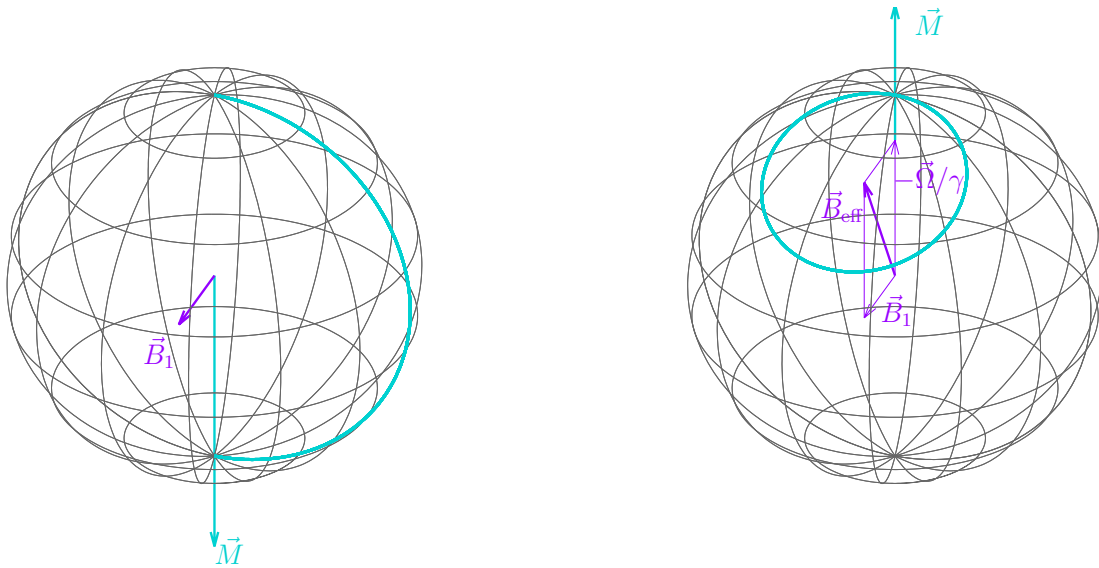


Figure 1.10: Evolution of the magnetization vectors with precession frequency exactly matching the used radio frequency (left) and with a frequency offset Ω (right), for $\omega_1 = \Omega/\sqrt{3}$. If ω_1 rotates magnetization of the former nucleus by 180° , then $\omega_{\text{eff}} = \sqrt{1+3}\Omega = 2\Omega$ rotates magnetization of the latter nucleus by $2 \times 180^\circ = 360^\circ$, i.e., by the full circle. The evolution is shown in a coordinate frame rotating with $\vec{\omega}_{\text{rot}} = -\vec{\omega}_{\text{radio}}$. In both cases, magnetization rotates about the thick purple arrow with the angular frequency proportional to the length of the arrow.

The discussed motion of the magnetization vector \vec{M} during irradiation is described by the following equations

$$\frac{dM_x}{dt} = -\Omega M_y + \omega_1 \sin \varphi M_z, \tag{1.48}$$

$$\frac{dM_y}{dt} = +\Omega M_x - \omega_1 \cos \varphi M_z, \tag{1.49}$$

$$\frac{dM_z}{dt} = -\omega_1 \sin \varphi M_x + \omega_1 \cos \varphi M_y, \tag{1.50}$$

$$\tag{1.51}$$

where φ is the azimuth of $\vec{\omega}_{\text{eff}}$. The equation can be written in a compact form as

$$\frac{d\vec{M}}{dt} = \vec{\omega}_{\text{eff}} \times \vec{M}. \tag{1.52}$$

1.5.5 Evolution of magnetization in \vec{B}_0

Eqs. 1.48–1.50 are easy to solve in the absence of \vec{B}_1 (i.e., after turning off the radio waves):

$$\frac{dM_x}{dt} = -\Omega M_y \tag{1.53}$$

$$\frac{dM_y}{dt} = \Omega M_x \tag{1.54}$$

$$\frac{dM_z}{dt} = 0 \tag{1.55}$$

The trick is to multiply the second equation by i and add it to the first equation or subtract it from the first equation.

$$\frac{d(M_x + iM_y)}{dt} = \Omega(-M_y + iM_x) = +i\Omega(M_x + iM_y) \quad (1.56)$$

$$\frac{d(M_x - iM_y)}{dt} = \Omega(-M_y - iM_x) = -i\Omega(M_x - iM_y) \quad (1.57)$$

$$M_x + iM_y = C_+ e^{+i\Omega t} \quad (1.58)$$

$$M_x - iM_y = C_- e^{-i\Omega t} \quad (1.59)$$

where the integration constants $C_+ = M_x(0) + iM_y(0) = \sqrt{M_x^2(0) + M_y^2(0)}e^{i\phi_0}$ and $C_- = M_x(0) - iM_y(0) = \sqrt{M_x^2(0) + M_y^2(0)}e^{-i\phi_0}$ are given by the initial phase ϕ_0 of \vec{M} in the coordinate system (in our case, $t = 0$ is defined by switching off the radio waves):

$$M_x + iM_y = \sqrt{M_x^2(0) + M_y^2(0)}e^{+i(\Omega t + \phi_0)} = \sqrt{M_x^2(0) + M_y^2(0)}(\cos(\Omega t + \phi_0) + i\sin(\Omega t + \phi_0)) \quad (1.60)$$

$$M_x - iM_y = \sqrt{M_x^2(0) + M_y^2(0)}e^{-i(\Omega t + \phi_0)} = \sqrt{M_x^2(0) + M_y^2(0)}(\cos(\Omega t + \phi_0) - i\sin(\Omega t + \phi_0)), \quad (1.61)$$

$$M_x = \sqrt{M_x^2(0) + M_y^2(0)} \cos(\Omega t + \phi_0) \quad (1.62)$$

$$M_y = \sqrt{M_x^2(0) + M_y^2(0)} \sin(\Omega t + \phi_0), \quad (1.63)$$

where

$$\tan \phi_0 = \frac{M_y(0)}{M_x(0)}. \quad (1.64)$$

In order to obtain ϕ_0 and $\sqrt{M_x^2(0) + M_y^2(0)}$, we must first solve Eqs. 1.48–1.50. This solution is not so easy, and we look only at the result:

$$M_x(0) = M_0 \sin(\omega_{\text{eff}}\tau_p) \sin \vartheta, \quad (1.65)$$

$$M_y(0) = M_0(1 - \cos(\omega_{\text{eff}}\tau_p)) \sin \vartheta \cos \vartheta, \quad (1.66)$$

$$M_z(0) = M_0(\cos^2 \vartheta + \cos(\omega_{\text{eff}}\tau_p) \sin^2 \vartheta), \quad (1.67)$$

where M_0 is the magnitude of the bulk magnetization in the thermodynamic equilibrium, τ_p is duration of irradiation by the radio waves, and $\tan \vartheta = \omega_1/\Omega$.

Lecture 2

Relaxation

Literature: A nice introduction is in K9.1 and K9.3, more details can be found in L19 and L20.1–L20.3.

2.1 Relaxation due to chemical shift anisotropy

The Boltzmann law allowed us to describe the state of the system in the thermal equilibrium, but it does not tell us *how is the equilibrium reached*. The processes leading to the equilibrium states are known as *relaxation*. Relaxation takes places e.g. when the sample is placed into a magnetic field inside the spectrometer or after excitation of the sample by radio wave pulses.

Spontaneous emission is completely inefficient (because energies of nuclear magnetic moments in available magnetic fields are very small). Relaxation in NMR is due to interactions with local fluctuating magnetic fields in the molecule. One source¹ of fluctuating fields is the *anisotropy of chemical shift*, described by the axial and rhombic components of the chemical shift tensor. The chemical shift tensor is given by the distribution of electrons in a molecule. Therefore, its orientation in a coordinate frame attached to the molecule is fixed. As collisions with other molecules change orientation of the observed molecule, the isotropic component of the chemical shift tensor does not change because it is spherically symmetric (cf. Figure 1.6). However, contributions to the local fields described by the axial and rhombic components fluctuate even if the constants δ_a and δ_r do not change because the axial and rhombic parts of the chemical shift depends on the orientation of the molecule (Figure 2.1).

Here, we introduce the basic idea by analyzing the effects of fluctuating magnetic fields in a classical manner. Obviously, it is not possible to describe exactly random motions of each magnetic moment. However, it is possible to describe statistically the effect of random fluctuations of magnetic fields on the bulk magnetization. For the simplest model of molecules (rigid spherical particles in an isotropic solvent), the final equation is surprisingly simple. However, the derivation is very tedious. Therefore, we limit our analysis to the axially symmetric chemical shift tensor, and divide it to two steps.

¹There are stronger sources of fluctuating fields in real molecules, but we limit our discussion to the chemical shift anisotropy in this lecture. We extend our analysis to other sources later, when we introduce quantum mechanical description of NMR.

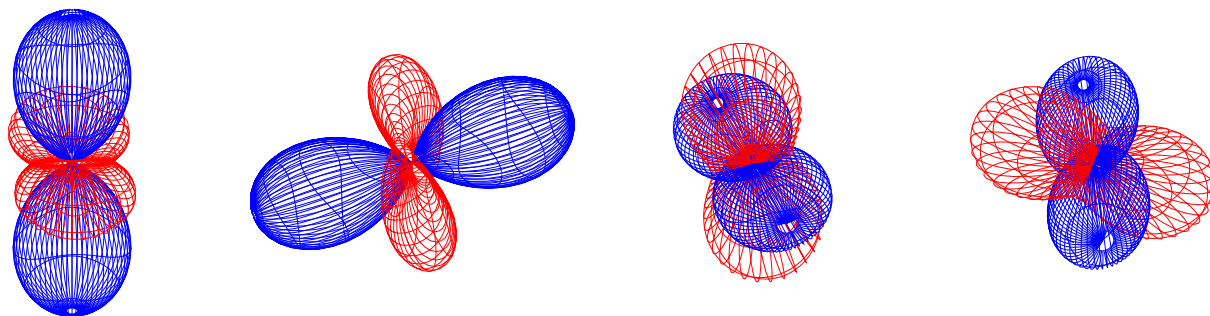


Figure 2.1: Visualization of reorientation of the anisotropic contribution to the chemical shift tensor as a result of tumbling (rotational diffusion) of the molecule.

2.2 Adiabatic contribution to relaxation

We start by the analysis of *adiabatic* contributions to relaxation. In physics, the term *adiabatic* is used for processes that do not change energy of the studied system. The adiabatic contributions to relaxation are due to fluctuations of magnetic fields parallel to \vec{B}_0 . Therefore, they do not change distribution of the z -components of magnetic moments (components parallel to \vec{B}_0). As the energy of magnetic moments is given by $-\vec{\mu} \cdot \vec{B}_0$, i.e., it depends only on the component of the magnetic moment parallel to \vec{B}_0 , the fluctuations parallel to \vec{B}_0 do not change the overall energy of magnetic moments. However, they randomize distribution of the x and y components. In other words, the adiabatic contributions to relaxation destroy *coherence* of the x and y components of magnetic moments (distributed as shown in the right panel of Figure 1.4) that was created by the radio wave pulse at the beginning of the NMR experiment.

As the molecules rotate and the anisotropic components chemical shift tensors rotate with them (Figure 2.1), the vertical magnetic fields ($B_0 + B_{e,z}$) fluctuate.² These fluctuations are random and independent for different molecules because individual molecules in solution tumble randomly (due to collisions with other molecules) and independently. Therefore, the frequency of precession of magnetic moments in individual molecules, given by $B_0 + B_{e,z}$, also fluctuates (randomly and independently for each molecule). As a consequence, the magnetic moments in individual molecules do not precess completely coherently (with the same frequency) and their distribution shown in (Figure 1.4 is slowly randomized. The cyan arrow in Figure 1.4, representing the bulk magnetization \vec{M} of the given distribution of magnetic moments, shrinks but stays in the xy plane, as long as only adiabatic relaxation (fluctuations along \vec{B}_0) are considered. Note that we observe two processes: rotation of the cyan arrow (\vec{M}) in the xy plane with the (average) precession frequency, and shrinking of the cyan arrow due to the adiabatic relaxation.

²As the molecule rotates, $B_{e,x}$ and $B_{e,y}$ of course fluctuates two. However, fluctuating $B_{e,x}$ and $B_{e,y}$ have only the non-adiabatic effect, discussed in the next section. In this section, we analyze adiabatic effects. Therefore, we can ignore what happens to $B_{e,x}$ and $B_{e,y}$. As explained in Section 2.6.1, our analysis of adiabatic contributions describes effects of molecular collisions that happen at a frequency different from the precession frequency of the observed magnetic moment.

In order to describe the adiabatic relaxation quantitatively, we express the precession frequency ω_z in terms of the components of the chemical shift tensor and angles³ describing its orientation in the laboratory coordinate frame, depending on the orientation of the given molecule in the sample (Eq 1.8):

$$\omega_z = -\gamma(B_0 + B_{e,z}) = -\gamma B_0(1 + \delta_i) - \gamma B_0 \delta_a (3 \cos^2 \vartheta - 1). \quad (2.1)$$

The analysis presented in Section 2.6.1 shows that the coherence disappears (the cyan arrow shrinks) with a rate constant (called R_0 in this text) proportional to the time integral of the *time correlation function*, i.e., of a mathematical function describing how quickly a molecule (and consequently the chemical shift tensor attached to it) loses memory of its original orientation (Eq. 2.49).

$$R_0 = (\gamma B_0 \delta_a)^2 \int_0^\infty \overline{(3 \cos^2 \vartheta(0) - 1)(3 \cos^2 \vartheta(t) - 1)} dt, \quad (2.2)$$

where the horizontal bar indicates an average value for all molecules in the sample and $\vartheta(0)$ describes orientation of the chemical shift tensor at $t = 0$. Note that statistics play the key role here: the whole analysis relies on the fact that although the product $(3 \cos^2 \vartheta(0) - 1)(3 \cos^2 \vartheta(t) - 1)$ changes randomly and differently for each molecule (and therefore cannot be described), the value of the time correlation function $\overline{(3 \cos^2 \vartheta(0) - 1)(3 \cos^2 \vartheta(t) - 1)}$ is defined statistically. If the structure of the molecule does not change (*rigid body rotational diffusion*), which is the case we analyze, the analytical form of $\overline{(3 \cos^2 \vartheta(0) - 1)(3 \cos^2 \vartheta(t) - 1)}$ can be derived. The simplest analytical form of the time correlation function is derived from the rotational diffusion equation in Section 2.6.2. The derivation shows that the time correlation function for spherically symmetric rotational diffusion is a single-exponential function:

$$\overline{\left(\frac{3}{2} \cos^2 \vartheta(0) - \frac{1}{2}\right) \left(\frac{3}{2} \cos^2 \vartheta(t) - \frac{1}{2}\right)} = \frac{1}{5} e^{-t/\tau_c} = \frac{1}{5} e^{-6D^{\text{rot}}t}, \quad (2.3)$$

where τ_c is the *rotational correlation time* and D^{rot} is the *rotational diffusion coefficient*, given by the Stokes' law

$$\frac{k_B T}{8\pi\eta(T)r^3}, \quad (2.4)$$

where r is the radius of the spherical particle, T is the temperature, and $\eta(T)$ is the dynamic viscosity of the solvent, strongly dependent on the temperature.⁴

³We need only one angle, ϑ , for our analysis of adiabatic contribution to relaxation.

⁴Dynamic viscosity of water can be approximated by

$$\eta(T) = \eta_0 \times 10^{T_0/(T-T_1)}, \quad (2.5)$$

where $\eta_0 = 2.414 \times 10^{-5} \text{ kg m}^{-1} \text{ s}^{-1}$, $T_0 = 247.8 \text{ K}$, and $T_1 = 140 \text{ K}$ (Al-Shemmeri, T., 2012. Engineering Fluid Mechanics. Ventus Publishing ApS. pp. 1718.).

Analytical solutions are also available (but more difficult to derive) for axially symmetric and asymmetric rotational diffusion, with the time correlation function in a form of three- and five-exponential functions, respectively.

For the spherically symmetric rotational diffusion, the rate constant of the loss of coherence can be calculated easily:

$$R_0 = \frac{4}{5} (\gamma B_0 \delta_a)^2 \int_0^{\infty} e^{-t/\tau_c} dt = \frac{4}{5} (\gamma B_0 \delta_a)^2 \tau_c = \frac{4}{5} (\gamma B_0 \delta_a)^2 \frac{1}{6D^{\text{rot}}}. \quad (2.6)$$

2.3 Including non-adiabatic contribution to relaxation

A much more complex analysis of the *non-adiabatic* contributions to relaxation, consequences of magnetic fields fluctuations perpendicular to \vec{B}_0 , is outlined in Section 2.6.3. Fluctuations perpendicular to \vec{B}_0 are also results of molecular tumbling, but now we are interested in how $B_{e,x}$ and $B_{e,y}$ fluctuate due to the reorientation of the chemical shift tensor. $B_{e,x}$ and $B_{e,y}$ have the same direction as the magnetic field of the radio waves used to rotate the magnetization from the equilibrium orientation (in the z direction) to the xy plane. Accidentally, the molecule may tumble for a short time with a rate close to the precession frequency of the magnetic moments. The resulting perpendicular fluctuations then act on the magnetic moments in a similar manner as the radio waves, i.e. rotate them about a horizontal axis. This of course changes the distribution of the z components of the magnetic moments and changes their energy in \vec{B}_0 . However, there is a fundamental difference between the fluctuations and the radio waves. The radio waves coherently rotate magnetic moments in all molecules, but the fluctuating fields are different in the individual molecules. And because the fluctuations are random, they randomly change distribution of magnetic moments until it returns to the equilibrium distribution. This is what happens after a sample is placed in the magnetic field of the spectrometer, and this is also what starts to happen immediately after the magnetization is tilted from the z direction by the radio waves.

The analysis in Section 2.6.3 provides values of two relaxation rates, (i) of the *longitudinal* relaxation rate R_1 describing how fast the z component of the bulk magnetization returns to its equilibrium value, and (ii) of the *transverse* relaxation rate R_2 describing how fast the x and y components of the bulk magnetization decay to zero. Note that the longitudinal and transverse relaxation are different processes. The return of M_z to its equilibrium value is identical with the process of restoring the equilibrium distribution of magnetic moments. However, the transverse relaxation has two sources, the non-adiabatic return to the equilibrium distribution of magnetic moments (with the orientation along \vec{B}_0 being slightly preferred) and the adiabatic loss of coherence. For large molecules, the loss of coherence is much faster than the return to the equilibrium distribution, which makes $R_2 \gg R_1$.

Quantitatively,

$$R_1 = 3 (\gamma B_0 \delta_a)^2 \left(\frac{1}{2} J(\omega_0) + \frac{1}{2} J(-\omega_0) \right) \approx 3 (\gamma B_0 \delta_a)^2 J(\omega_0), \quad (2.7)$$

where

$$J(\omega_0) = \int_{-\infty}^{\infty} \overline{\left(\frac{3}{2} \cos^2(\theta(0)) - \frac{1}{2}\right) \left(\frac{3}{2} \cos^2(\theta(t)) - \frac{1}{2}\right)} \cos(\omega_0 t) dt. \quad (2.8)$$

The function $J(\omega)$ is known as the *spectral density function*.

Note that

- The definition of R_1 , describing solely the non-adiabatic effects of fluctuations perpendicular to \vec{B}_0 includes the same time correlation function as the definition of R_0 , describing the adiabatic effects of fluctuations parallel to \vec{B}_0 . This is possible in *isotropic solutions*, where no orientation of the molecule is preferred. Then the distribution of the orientation of the molecules in the x or y direction should be the same as in the z direction and the same time correlation function can be used. Do not get confused! The molecules may be oriented isotropically even if their tumbling is anisotropic. The anisotropic tumbling (rotational diffusion) is a result of a non-spherical shape of the molecule, whereas anisotropic orientation is a result of an external force preferring certain orientation of the molecules. The magnetic field represents such a force, but this force is very small for diamagnetic molecules and can be often neglected when describing orientations of the molecules.⁵
- The definition of R_1 , unlike that of R_0 , includes also the value of the (average) precession frequency ω_0 . This reflects the fact that the fluctuations perpendicular to \vec{B}_0 rotate the magnetic moments about a horizontal axis only if their rate matches the precession frequency (resonance condition).
- The term in the integral defining R_0 , lacking the cosine function of ω_0 , can be also written as a value of the spectral function at the zero frequency (zero in the exponent converts the exponential function to unity).

Similarly, R_2 is given by

$$R_2 = 2(\gamma B_0 \delta_a)^2 J(0) + \frac{3}{2}(\gamma B_0 \delta_a)^2 J(\omega_0), \quad (2.9)$$

where the first term is the adiabatic contribution destroying the coherence. Note that

- The first term is the adiabatic contribution destroying the coherence.
- The second term is the non-adiabatic contribution, equal to $\frac{1}{2}R_1$. The factor of $\frac{1}{2}$ reflects the fact that fluctuations in a certain direction influence only components of magnetic moment vectors perpendicular to that direction. E.g., fluctuations along the x axis influence only μ_y , but not μ_x . Therefore, a fluctuation in the x direction that causes some longitudinal relaxation (described by R_1) by altering μ_z , is only half as effective at causing transverse relaxation described by R_2 (only μ_y is altered, not μ_x).

⁵Note, however, that the magnetic field cannot be neglected when describing the return of the magnetization to the equilibrium, as discussed in Section 2.6.3.

The *longitudinal relaxation rate* R_1 , describing the return of M_z to the equilibrium due to the chemical shift anisotropy in randomly reorienting molecules, and the *transverse relaxation rate* R_2 , describing the decay of magnetization in the xy plane, are given by

$$R_1 = \frac{3}{4}b^2J(\omega_0), \quad (2.10)$$

$$R_2 = \frac{1}{2}b^2J(0) + \frac{3}{8}b^2J(\omega_0), \quad (2.11)$$

where $b = -2\gamma B_0\delta_a$.

2.4 Internal motions, structural changes

So far, we analyzed only the rigid body motions of molecules, assuming that the structures of molecules are rigid. What happens if the structure of the molecule changes? Let us first assume that the structural changes are random internal motions which change orientation of the chemical shift tensor relative to the orientation of the whole molecule, but do not affect the size or shape of the tensor. Then, Eq. 2.36 can be still used and R_0 is still given by Eq. 2.49, but the correlation function is *not* mono-exponential even if the rotational diffusion of the molecule is spherically symmetric. The internal motions contribute to the dynamics together with the rotational diffusion, and in a way that is very difficult to describe exactly. Yet, useful qualitative conclusions can be made.

- If the internal motions are *much faster* than rotational diffusion, correlation between $3\cos^2\vartheta(0) - 1$ and $3\cos^2\vartheta(t) - 1$ is lost much faster. The faster the correlation decays, the lower is the result of integration. The internal motions faster than rotational diffusion always *decrease* the value of R_0 (make relaxation slower). Amplitude and rate of the fast internal motions can be estimated using approximative approaches.
- If the internal motions are *much slower* than rotational diffusion, the rate of the decay of the correlation function is given by the faster contribution, i.e., by the rotational diffusion. The internal motions much slower than rotational diffusion *do not change* the value of R_0 significantly. Amplitude and rate of the fast internal motions cannot be measured if the motions do not change size or shape of the diffusion tensor.

If the structural changes alter size and/or shape of the chemical shift tensor,⁶ parameters δ_i and δ_a vary and cannot be treated as constants. E.g., the parameter δ_i is not absorbed into the constant (average) precession frequency (removed by introducing the rotating coordinate frame in Section 2.6.1) and $\overline{\delta_i(0)\delta_i(t)}$ contributes to R_0 even if it decays much slower than $(3\cos^2\vartheta(0) - 1)(3\cos^2\vartheta(t) - 1)$.

- Internal motions or chemical processes changing size and/or shape of the chemical shift tensor may have a dramatic effect on relaxation even if their frequency is much slower than the rotational diffusion of the molecule. If the molecule is present in two inter-converting states

⁶Examples of such changes are internal motions changing torsion angles and therefore distribution of electrons, or chemical changes (e.g. dissociation of protons) with similar effects.

(e.g. in two conformations or in a protonated and deprotonated state), the strongest effect is observed if the differences between the chemical shift tensors of the states are large and if the frequency of switching between the states is similar to the difference in $\gamma B_0 \delta_i$ of the states. Such processes are known as *chemical* or *conformational exchange* and increase the value of R_0 and consequently R_2 .

2.5 Bloch equations

The effects of relaxation can be included in the equations describing evolution of the bulk magnetization (Eqs. 1.48–1.50). The obtained set of equations, known as *Bloch equations*, provides a general macroscopic description of NMR for proton and similar nuclei.

$$\frac{dM_x}{dt} = -R_2 M_x - \Omega M_y + \omega_1 \sin \varphi M_z, \quad (2.12)$$

$$\frac{dM_y}{dt} = +\Omega M_x - R_2 M_y - \omega_1 \cos \varphi M_z, \quad (2.13)$$

$$\frac{dM_z}{dt} = -\omega_1 \sin \varphi M_x + \omega_1 \cos \varphi M_y - R_1 (M_z - M_z^{\text{eq}}). \quad (2.14)$$

$$(2.15)$$

HOMEWORK

First check that you understand how equations describing rotation of magnetization in the absence of the radio waves (Eqs. 1.53–1.55) are solved. Then derive the rate constant R_0 (Section 2.6.1).

2.6 DERIVATIONS

2.6.1 Loss of coherence

Motion of a magnetic moment in a magnetic field is described classically as (cf. Eq. 1.52)

$$\frac{d\vec{\mu}}{dt} = \vec{\omega} \times \vec{\mu} = -\gamma \vec{B} \times \vec{\mu}, \quad (2.16)$$

or for individual components:

$$\frac{d\mu_x}{dt} = \omega_y \mu_z - \omega_z \mu_y, \quad (2.17)$$

$$\frac{d\mu_y}{dt} = \omega_z \mu_x - \omega_x \mu_z, \quad (2.18)$$

$$\frac{d\mu_z}{dt} = \omega_x \mu_y - \omega_y \mu_x. \quad (2.19)$$

Solving a set of three equations is not so easy. Therefore, we start with a simplified case. Remember what we learnt when we tried to rotate the magnetization away from the z direction by magnetic fields perpendicular to \vec{B}_0 , i.e., by fields with B_x and B_y components. Only B_x and B_y fields rotating with the frequency equal to the precession frequency of individual magnetic moments (*Larmor frequency*) have the desired effect. Let us start our analysis by assuming that the molecular motions are much slower than the Larmor frequency. Under such circumstances, the effects of $B_{e,x}$ and $B_{e,y}$ can be neglected and the equations of motion simplify to

$$\frac{d\mu_x}{dt} = -\omega_z \mu_y = \gamma B_z \mu_y \quad (2.20)$$

$$\frac{d\mu_y}{dt} = \omega_z \mu_x = -\gamma B_z \mu_x \quad (2.21)$$

$$\frac{d\mu_z}{dt} = 0 \quad (2.22)$$

Eqs. 2.20–2.22 are very similar to Eqs. 1.53–1.55, so we try the same approach and calculate

$$\frac{d\mu^+}{dt} \equiv \frac{d(\mu_x + i\mu_y)}{dt} = i\omega_z(\mu_x + i\mu_y) = -i\gamma B_z(\mu_x + i\mu_y) = -i\gamma B_z \mu^+ \quad (2.23)$$

According to Eq. 1.41,

$$B_z = B_0 + B_{e,z} = B_0(1 + \delta_1 + \delta_a(3 \cos^2 \vartheta - 1) + \delta_r(2 \cos^2 \chi - 1) \sin^2 \vartheta). \quad (2.24)$$

For the sake of simplicity, we assume that the chemical shift tensor is axially symmetric ($\delta_r = 0$). Then, ω_z can be written as

$$\omega_z = -\gamma(B_0 + B_{e,z}) = -\gamma B_0(1 + \delta_1) - \gamma B_0 \delta_a(3 \cos^2 \vartheta - 1) = \omega_0 + b\Theta^{\parallel}, \quad (2.25)$$

where

$$\omega_0 = -\gamma B_0(1 + \delta_1) \quad (2.26)$$

$$b = -2\gamma B_0 \delta_a \quad (2.27)$$

$$\Theta^{\parallel} = \frac{3 \cos^2 \vartheta - 1}{2}. \quad (2.28)$$

This looks fine, but there is a catch here: Eq. 2.23 cannot be solved as easily as we solved 1.53–1.55 because ω_z is not constant but fluctuates in time. The value of ω_z is not only changing, it is changing differently for each molecule in the sample and it is changing in a random, unpredictable way! Can we solve the equation of motion at all? The answer is "yes and no". The equation of motion cannot be solved for an individual magnetic moment. However, we can take advantage of *statistics* and solve the equation of motion for the *total magnetization* M^+ , given by the statistical ensemble of magnetic moments.

We start by assuming that for a very short time Δt , shorter than the time scale of molecular motions, the orientation of the molecule does not change and Θ^{\parallel} remains constant. We try to describe the evolution of μ^+ in such small time steps, assuming

$$\frac{\Delta \mu^+}{\Delta t} \approx \frac{d\mu^+}{dt} \approx i(\omega_0 + b\Theta^{\parallel})\mu^+ \quad (2.29)$$

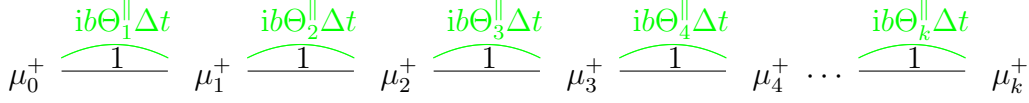


Figure 2.2: Evolution of magnetic moments due to longitudinal (parallel with \vec{B}_0) fluctuations of magnetic fields. The symbols μ_0^+ and μ_k^+ are connected by 2^k possible pathways composed of black and green segments. Each black segment represents multiplication by one, each green segment represents multiplication by $ib\Theta_j^\parallel\Delta t$, where j ranges from 1 to k . The product of binomials in Eq. 2.36 is a sum of 2^k terms. In order to obtain one term of the series, we walk along the corresponding pathway and multiply all black and green numbers written above the individual steps. The pathway composed of the black segments only gives the result of multiplication equal to one, the pathways containing just one green segment give results of multiplication proportional to Δt , the pathways containing two green segments give results of multiplication proportional to $(\Delta t)^2$, etc. In order to get the complete product in Eq. 2.36, we must walk through all possible pathways (all possible combinations of the segments) and sum all results of the multiplication.

If the initial value of μ^+ is μ_0^+ and if the values of $\omega_0, b, \Theta^\parallel$ during the first time step are $\omega_{0,1}, b_1, \Theta_1^\parallel$, respectively, the value of μ^+ after the first time step is

$$\mu_1^+ = \mu_0^+ + \Delta\mu_1^+ = \mu_0^+ + i(\omega_{0,1} + b_1\Theta_1^\parallel)\Delta t\mu_0^+ = [1 + i(\omega_{0,1} + b_1\Theta_1^\parallel)\Delta t]\mu_0^+. \quad (2.30)$$

After the second step,

$$\mu_2^+ = \mu_1^+ + \Delta\mu_2^+ = \mu_1^+ + i(\omega_{0,2} + b_2\Theta_2^\parallel)\Delta t\mu_1^+ = [1 + i(\omega_{0,2} + b_2\Theta_2^\parallel)\Delta t][1 + i(\omega_{0,1} + b_1\Theta_1^\parallel)\Delta t]\mu_0^+. \quad (2.31)$$

After k steps,

$$\mu_k^+ = [1 + i(\omega_{0,k} + b_k\Theta_k^\parallel)\Delta t][1 + i(\omega_{0,k-1} + b_{k-1}\Theta_{k-1}^\parallel)\Delta t] \cdots [1 + i(\omega_{0,2} + b_2\Theta_2^\parallel)\Delta t][1 + i(\omega_{0,1} + b_1\Theta_1^\parallel)\Delta t]\mu_0^+. \quad (2.32)$$

If the structure of the molecule does not change, the electron distribution is constant and the size and shape of the chemical shift tensor described by δ_i and δ_a does not change in time. Then, ω_0 and b are constant and the only time-dependent parameter is Θ^\parallel , fluctuating as the orientation of the molecule (described by ϑ) changes. The parameter $\omega_0 = -\gamma B_0(1 + \delta_i)$ represents a constant frequency of coherent rotation under such circumstances. The coherent rotation can be removed if we describe the evolution of μ^+ in a coordinate frame rotating with the frequency ω_0 . The transformation of μ^+ to the rotating frame is given by

$$(\mu^+)_{\text{rot}} = \mu^+ e^{-i\omega_0 t}. \quad (2.33)$$

We also need to express the derivative of $(\mu^+)_{\text{rot}}$, which is done easily by applying the chain rule:

$$\frac{d(\mu^+)_{\text{rot}}}{dt} = \frac{d(\mu^+ e^{-i\omega_0 t})}{dt} = \frac{d\mu^+}{dt} e^{-i\omega_0 t} - i\omega_0 \mu^+ e^{-i\omega_0 t}. \quad (2.34)$$

Substituting $d\mu^+/dt$ from Eq. 2.29 results in

$$\frac{d(\mu^+)_{\text{rot}}}{dt} = i(\omega_0 + b\Theta^\parallel)\mu^+ e^{-i\omega_0 t} - i\omega_0 \mu^+ e^{-i\omega_0 t} = ib\Theta^\parallel \mu^+ e^{-i\omega_0 t} = ib\Theta^\parallel (\mu^+)_{\text{rot}}. \quad (2.35)$$

When compared with Eq. 2.29, we see that ω_0 disappeared, which simplifies Eq. 2.32 to

$$(\mu_k^+)_{\text{rot}} = [1 + ib\Theta_k^\parallel\Delta t][1 + ib\Theta_{k-1}^\parallel\Delta t] \cdots [1 + ib\Theta_2^\parallel\Delta t][1 + ib\Theta_1^\parallel\Delta t](\mu_0^+)_{\text{rot}}. \quad (2.36)$$

The process of calculating the product of brackets in Eq. 2.36 is shown schematically in Figure 2.2. The final product is

$$(\mu_k^+)_{\text{rot}} = [1 + ib\Delta t(\Theta_k^\parallel + \Theta_{k-1}^\parallel + \cdots + \Theta_1^\parallel) - b^2\Delta t^2(\Theta_k^\parallel(\Theta_{k-1}^\parallel + \cdots + \Theta_2^\parallel + \Theta_1^\parallel) + \cdots + \Theta_2^\parallel\Theta_1^\parallel) - ib^3\Delta t^3(\cdots) + \cdots](\mu_0^+)_{\text{rot}}. \quad (2.37)$$

We can now return to the question how random fluctuations change μ^+ . Let us express the difference between μ^+ after k and $k-1$ steps:

$$\Delta(\mu_k^+)_{\text{rot}} = (\mu_k^+)_{\text{rot}} - (\mu_{k-1}^+)_{\text{rot}} = [ib\Delta t\Theta_k^\parallel - b^2\Delta t^2\Theta_k^\parallel(\Theta_{k-1}^\parallel + \cdots + \Theta_1^\parallel) - ib^3\Delta t^3(\cdots) + \cdots](\mu_0^+)_{\text{rot}}. \quad (2.38)$$

Dividing both sides by Δt

$$\frac{\Delta(\mu_k^+)_{\text{rot}}}{\Delta t} = [ib\Theta_k^\parallel - b^2\Delta t\Theta_k^\parallel(\Theta_{k-1}^\parallel + \cdots + \Theta_1^\parallel) - ib^3\Delta t^2(\cdots) + \cdots](\mu_0^+)_{\text{rot}} \quad (2.39)$$

and going back from Δt to dt (neglecting terms with dt^2, dt^3, \dots , much smaller than dt),

$$\frac{d(\mu^+(t_k))_{\text{rot}}}{dt} = \left[ib\Theta^{\parallel}(t_k) - b^2 \int_0^{t_k} \Theta^{\parallel}(t_k)\Theta^{\parallel}(t_k - t_j)dt_j \right] (\mu_0^+)_{\text{rot}}. \quad (2.40)$$

We see that calculating how fluctuations of B_z affect an individual magnetic moment in time t_k requires knowledge of the orientations of the molecule during the whole evolution ($\Theta^{\parallel}(t_k - t_j)$). However, we are not interested in the evolution of a single magnetic moment, but in the evolution of the total magnetization M^+ . The total magnetization is given by the sum of all magnetic moments (magnetic moments in all molecules). Therefore, we must average orientations of all molecules in the sample. In other words, we should describe Θ^{\parallel} using *two* indices, k and m , where k describes the time step and m the orientation of the given molecule. Calculation of the evolution of M^+ then should include summation of $\Theta_{k,m}^{\parallel}$ for all k and m , or integration over the angles describing orientations of the molecule in addition to the time integration. As the magnetic moments move almost independently of the molecular motions, we can average Θ^{\parallel} and μ^+ separately. In the case of the axially symmetric chemical shift tensor, the orientations of molecules are given by orientations of the symmetry axes \vec{a} of the chemical shift tensors of the observed nuclei in the molecules, described by the angles φ and ϑ . In order to simplify averaging the orientations, we assume that all orientations are equally probable. **This is a very dangerous assumption. It does not introduce any error in this section, but leads to wrong results when we analyze the effects of fluctuations of magnetic fields perpendicular to \vec{B}_0 !**

As the angle $\vartheta(t)$ is hidden in the function $\Theta^{\parallel}(t) = (3 \cos^2 \vartheta - 1)/2$ in our equation, the ensemble averaging can be written as⁷

$$\frac{d(M^+(t_k))_{\text{rot}}}{dt} = \left[ib \frac{1}{4\pi} \int_0^{2\pi} d\varphi \int_0^{\pi} \Theta^{\parallel}(t_k) \sin \vartheta d\vartheta - b^2 \int_0^{t_k} dt_j \frac{1}{4\pi} \int_0^{2\pi} d\varphi \int_0^{\pi} \Theta^{\parallel}(t_k)\Theta^{\parallel}(t_k - t_j) \sin \vartheta d\vartheta \right] (M_0^+)_{\text{rot}}, \quad (2.41)$$

where $\varphi \equiv \varphi(t_k)$ and $\vartheta \equiv \vartheta(t_k)$.

In order to avoid writing too many integration signs, we mark the averaging simply by a horizontal bar above the averaged function:

$$\frac{d(M^+(t_k))_{\text{rot}}}{dt} = \left[ib\overline{\Theta^{\parallel}(t_k)} - b^2 \int_0^{t_k} \overline{\Theta^{\parallel}(t_k)\Theta^{\parallel}(t_k - t_j)} dt_j \right] (M_0^+)_{\text{rot}}. \quad (2.42)$$

The average values of $a_z^2 = \cos^2 \vartheta$, of $a_x^2 = \cos^2 \varphi \sin^2 \vartheta$, and of $a_y^2 = \sin^2 \varphi \sin^2 \vartheta$ must be the same because none of the directions x, y, z is preferred:

$$\overline{a_x^2} = \overline{a_y^2} = \overline{a_z^2}. \quad (2.43)$$

Therefore,

$$\overline{a_x^2 + a_y^2 + a_z^2} = \overline{3a_z^2} \quad (2.44)$$

and

$$a_x^2 + a_y^2 + a_z^2 = 1 \Rightarrow \overline{a_x^2 + a_y^2 + a_z^2} = 1 \Rightarrow \overline{3a_z^2 - 1} = \overline{(3 \cos^2 \vartheta - 1)} = 2\overline{\Theta^{\parallel}} = 0 \Rightarrow \overline{\Theta^{\parallel}} = 0. \quad (2.45)$$

It explains why we did not neglect already the $b^2 dt$ term – we would obtain zero on the right-hand side in the rotating coordinate frame (this level of simplification would neglect the effects of fluctuations and describe just the coherent motions).

We have derived that the equation describing the loss of coherence (resulting in a loss of transverse magnetization) is

$$\frac{d(M^+(t_k))_{\text{rot}}}{dt} = - \left[b^2 \int_0^{t_k} \overline{\Theta^{\parallel}(t_k)\Theta^{\parallel}(t_k - t_j)} dt_j \right] (M_0^+)_{\text{rot}}, \quad (2.46)$$

where the value of $\overline{\Theta^{\parallel}(t_k)\Theta^{\parallel}(t_k - t_j)}$ is clearly defined statistically (by the averaging described above). Values of $\overline{\Theta^{\parallel}(t_k)\Theta^{\parallel}(t_k - t_j)}$ can be determined easily for two limit cases:

- $t_j = 0$: If $t_j = 0$, $\overline{\Theta^{\parallel}(t_k)\Theta^{\parallel}(t_k - t_j)} = \overline{(\Theta^{\parallel}(t_k))^2}$, i.e., $\Theta^{\parallel}(t_k)$ and $\Theta^{\parallel}(t_k - t_j)$ are *completely correlated*.

The average value of $\overline{\Theta^{\parallel}(t_k)^2}$ is

$$\overline{\Theta^{\parallel}(t_k)^2} = \frac{1}{4} \overline{(3 \cos^2 \vartheta - 1)^2} = \frac{1}{16\pi} \int_0^{2\pi} d\varphi \int_0^{\pi} d\vartheta (\sin \vartheta) (3 \cos^2 \vartheta - 1)^2 = \frac{1}{5}. \quad (2.47)$$

⁷Two integrals in the following equation represent calculation of an average of a function depending on the orientation. Geometrically, it is summation of the values of the function for individual surface elements (defined by inclination ϑ and azimuth φ) of a sphere with the radius $r = 1$, divided by the complete surface of the sphere 4π . Note that the *current* orientation of each molecule at t_k is described by $\vartheta(t_k)$ and $\varphi(t_k)$, the values $\vartheta(t_j)$ hidden in the function $\Theta^{\parallel}(t_j)$ describe only *history* of each molecule. They are *somehow* related to $\vartheta(t_k)$ and $\varphi(t_k)$ and therefore treated as an unknown function of $\vartheta(t_k)$ and $\varphi(t_k)$ during the integration.

- $t_j \rightarrow \infty$: If the changes of orientation (molecular motions) are random, the correlation between $\Theta^{\parallel}(t_k)$ and $\Theta^{\parallel}(t_k - t_j)$ is lost for very long t_j and they can be averaged separately: $\overline{\Theta^{\parallel}(t_k)\Theta^{\parallel}(t_k - t_j)} = \overline{\Theta^{\parallel}(t_k)} \cdot \overline{\Theta^{\parallel}(t_k - t_j)}$. But we know that average $\overline{\Theta^{\parallel}(t)} = \overline{3 \cos^2 \vartheta} - 1 = 0$. Therefore, $\overline{\Theta^{\parallel}(t_k)\Theta^{\parallel}(t_k - t_j)} = 0$ for $t_j \rightarrow \infty$.

If the motions are really stochastic, it does not matter when we start to measure time. Therefore, we can describe the loss of coherence for any t_k as

$$\frac{d(M^+)_{\text{rot}}}{dt} = - \left[b^2 \int_0^{\infty} \overline{\Theta^{\parallel}(0)\Theta^{\parallel}(t)} dt \right] (M^+)_{\text{rot}}, \quad (2.48)$$

which resembles a first-order chemical kinetics with the rate constant

$$R_0 = b^2 \int_0^{\infty} \overline{\Theta^{\parallel}(0)\Theta^{\parallel}(t)} dt. \quad (2.49)$$

In order to calculate the value of the rate constant R_0 , we must be able to evaluate the averaged term $\overline{\Theta^{\parallel}(0)\Theta^{\parallel}(t)}$, known as the *time correlation function*. As mentioned above, statistics play the key role here. Although the product $\Theta^{\parallel}(0)\Theta^{\parallel}(t)$ changes randomly and individually, the value of the time correlation function is defined statistically.

2.6.2 Time correlation function

Analysis of the isotropic rotational diffusion in Section 0.3.2 allows us to calculate the time correlation function $\overline{\Theta^{\parallel}(0)\Theta^{\parallel}(t)}$ for this type of diffusion (with a spherical symmetry). The ensemble-averaged product of randomly changing $(3 \cos^2 \vartheta(t) - 1)/2$, evaluated for a time difference t , can be expressed as

$$\overline{\left(\frac{3}{2} \cos^2 \vartheta(0) - \frac{1}{2} \right) \left(\frac{3}{2} \cos^2 \vartheta(t) - \frac{1}{2} \right)} \quad (2.50)$$

$$= \int_0^{2\pi} d\varphi(0) \int_0^{\pi} \sin \vartheta(0) d\vartheta(0) \rho_0 \int_0^{2\pi} d\varphi(t) \int_0^{\pi} \sin \vartheta(t) d\vartheta(t) \left(\frac{3}{2} \cos^2 \vartheta(0) - \frac{1}{2} \right) \left(\frac{3}{2} \cos^2 \vartheta(t) - \frac{1}{2} \right) G(\vartheta(0), \varphi(0) | \vartheta(t), \varphi(t)), \quad (2.51)$$

where ρ_0 is the *probability density*⁸ of the original orientation described by $\vartheta(0)$ and $\varphi(0)$, and $G(\vartheta(0), \varphi(0) | \vartheta(t), \varphi(t))$ is the *conditional probability density* or *propagator* (also known as the *Green's function*) describing what is the chance to find an orientation given by $\vartheta(t), \varphi(t)$ at time t , if the orientation at $t = 0$ was given by $\vartheta(0), \varphi(0)$.

If the molecule is present in an isotropic environment,⁹ ρ_0 plays a role of a normalization constant and can be calculated easily from the condition that the overall probability of finding the molecule in *any* orientation is equal to one:

$$\int_0^{2\pi} d\varphi(0) \int_0^{\pi} \sin \vartheta(0) d\vartheta(0) \rho_0 = 4\pi \rho_0 = 1 \quad \Rightarrow \quad \rho_0 = \frac{1}{4\pi}. \quad (2.52)$$

Evaluation of $G(\vartheta(0), \varphi(0) | \vartheta(t), \varphi(t))$ requires to solve the diffusion equation Eq. 96. We again express G as a product of time-dependent and time-independent functions $g(t)P(\vartheta)$. The function $g(t)$ is defined by Eq. 95, the function $P(\vartheta)$ is a simplified version of function $f(\vartheta, \varphi)$ from Eq. 96. Since our correlation function does not depend on φ , $\partial P / \partial \varphi = 0$, and we can further simplify Eq. 96 to

$$\left((1 - u^2) \frac{d^2}{du^2} - 2u \frac{d}{du} \right) P = \lambda P, \quad (2.53)$$

$$(1 - u^2) \frac{d^2 P}{du^2} - 2u \frac{dP}{du} - \lambda P = 0. \quad (2.54)$$

We expand P in a Taylor series

$$P = \sum_{k=0}^{\infty} a_k u^k, \quad a_k = \frac{1}{k!} \frac{d^k P(0)}{du^k}, \quad (2.55)$$

⁸Probability density is defined in Section 0.3.1.

⁹Note that in the isotropic environment, where all orientations of the molecule are equally probable, the diffusion can be very anisotropic if the shape of the molecule greatly differs from a sphere.

calculate its first and second derivatives

$$\frac{dP}{du} = \sum_{k=0}^{\infty} k a_k u^{k-1}, \quad (2.56)$$

$$\frac{d^2P}{du^2} = \sum_{k=0}^{\infty} k(k-1) a_k u^{k-2}, \quad (2.57)$$

and substitute them into Eq. 2.54

$$(1-u^2) \sum_{k=0}^{\infty} k(k-1) a_k u^{k-2} - 2 \sum_{k=0}^{\infty} k a_k u^k - \lambda \sum_{k=0}^{\infty} a_k u^k - 2u = 0 \quad (2.58)$$

$$\sum_{k=0}^{\infty} k(k-1) a_k u^{k-2} - \sum_{k=0}^{\infty} k(k-1) a_k u^k - 2 \sum_{k=0}^{\infty} k a_k u^k - \lambda \sum_{k=0}^{\infty} a_k u^k = 0. \quad (2.59)$$

Note that the first two terms of the first sum are equal to zero (the first term includes multiplication by $k=0$ and the second term includes multiplication by $k-1=0$ for $k=1$). Therefore, we can start summation from $k=2$ in the first term

$$\sum_{k=2}^{\infty} k(k-1) a_k u^{k-2} - \sum_{k=0}^{\infty} k(k-1) a_k u^k - 2 \sum_{k=0}^{\infty} k a_k u^k - \lambda \sum_{k=0}^{\infty} a_k u^k = 0. \quad (2.60)$$

We shift the index in the first sum by two to get the first sum expressed in the same power of u as the other sums

$$\sum_{k=0}^{\infty} (k+2)(k+1) a_{k+2} u^k - \sum_{k=0}^{\infty} k(k-1) a_k u^k - 2 \sum_{k=0}^{\infty} k a_k u^k - \lambda \sum_{k=0}^{\infty} a_k u^k = 0 \quad (2.61)$$

$$\sum_{k=0}^{\infty} ((k+2)(k+1) a_{k+2} - (k(k-1) + 2k + \lambda) a_k) u^k = \sum_{k=0}^{\infty} ((k+2)(k+1) a_{k+2} - (k(k+1) + \lambda) a_k) u^k = 0. \quad (2.62)$$

This equation is true only if all terms in the sum are equal to zero

$$(k+2)(k+1) a_{k+2} - (k(k+1) + \lambda) a_k = 0, \quad (2.63)$$

which gives us a recurrence formula relating a_{k+2} and a_k :

$$a_{k+2} = \frac{k(k+1) + \lambda}{(k+2)(k+1)} a_k = 0. \quad (2.64)$$

We can use the recurrence formula to express the Taylor series in terms of a_0 and a_1 :

$$P = a_0 \left(1 + \frac{0 \cdot 1 + \lambda}{1 \cdot 2} u^2 + \frac{0 \cdot 1 + \lambda}{1 \cdot 2} \cdot \frac{2 \cdot 3 + \lambda}{3 \cdot 4} u^4 + \dots \right) + a_1 \left(u + \frac{1 \cdot 2 + \lambda}{2 \cdot 3} u^3 + \frac{1 \cdot 2 + \lambda}{2 \cdot 3} \cdot \frac{3 \cdot 4 + \lambda}{4 \cdot 5} u^5 + \dots \right) = 0. \quad (2.65)$$

What is the value of λ ? Note that $a_{k+2} = 0$ for each $\lambda = -k(k+1)$, which terminates one of the series in large parentheses, while the other series grows to infinity (for $u \neq 0$). To keep P finite, the coefficient before the large parentheses in the unterminated series must be set to zero. It tells us that we can find a possible solution for each even or odd k if $a_1 = 0$ or $a_0 = 0$, respectively.

$$k=0 \quad a_1=0 \quad P=P_0=1 \quad \lambda=-k(k+1)=0 \quad (2.66)$$

$$k=1 \quad a_0=0 \quad G=P_1=u=\cos\vartheta \quad \lambda=-k(k+1)=-2 \quad (2.67)$$

$$k=2 \quad a_1=0 \quad G=P_2=\frac{3u^2-1}{2}=\frac{3\cos^2\vartheta-1}{2} \quad \lambda=-k(k+1)=-6 \quad (2.68)$$

$$k=3 \quad a_0=0 \quad G=P_3=\frac{5u^3-3u}{2}=\frac{5\cos^3\vartheta-3\cos\vartheta}{2} \quad \lambda=-k(k+1)=-12 \quad (2.69)$$

$$\vdots \quad (2.70)$$

The value of a_0 or a_1 preceding the terminated series was chosen so that $P_k(u=1) = P_k(\vartheta=0) = 1$. Which of the possible solutions is the correct one? It can be shown easily that

$$\int_{-1}^1 P_k(u)P_{k'}(u)du = \int_0^\pi P_k(\vartheta)P_{k'}(\vartheta)d\vartheta = \frac{2}{2k+1}\delta_{kk'}, \quad (2.71)$$

i.e., the integral is equal to zero for each $k \neq k'$ (P_k are orthogonal). As we are going to use $G = g(t)P(\vartheta)$ to calculate a correlation function for functions having the same form as the solutions for $k = 2$ and as the calculation of the correlation function includes the same integration as in Eq. 2.71, it is clear that the only solution which gives us a non-zero correlation function is that for $k = 2$, i.e. P_2 . Our function G is therefore given by

$$G = g_0 \frac{3 \cos^2 \vartheta - 1}{2} e^{-6D^{\text{rot}}t}. \quad (2.72)$$

Still, we need to evaluate the factor g_0 . This value must be chosen so that we fulfill the following conditions:

$$\int_0^{2\pi} d\varphi \int_0^\pi \sin \vartheta d\vartheta G = 1 \quad (2.73)$$

and

$$G(t=0) = \delta(\vartheta - \vartheta(0)), \quad (2.74)$$

where $\delta(\vartheta - \vartheta(0))$ is a so-called Dirac delta function, defined as

$$\int_{-\infty}^{\infty} f(x)\delta(x - x_0) = f(x_0). \quad (2.75)$$

The second condition says that ϑ must have its original value for $t = 0$. This is fulfilled for g_0 proportional to $(3 \cos^2 \vartheta(0) - 1)/2$:

$$g_0 = c_0 \frac{3 \cos^2 \vartheta(0) - 1}{2}. \quad (2.76)$$

We can re-write our original definition of the correlation function with the evaluated G function and in a somewhat simplified form (omitting integration over φ and $\varphi(0)$):

$$\overline{\left(\frac{3}{2} \cos^2 \vartheta(0) - \frac{1}{2}\right) \left(\frac{3}{2} \cos^2 \vartheta(t) - \frac{1}{2}\right)} = \int_{-1}^1 du_0 \rho_0 c_0 \int_{-1}^1 du \frac{(3u_0^2 - 1)^2}{4} \frac{(3u^2 - 1)^2}{4} e^{-6D^{\text{rot}}t}, \quad (2.77)$$

where ρ_0 can be evaluated from the normalization condition

$$\int_{-1}^1 du_0 \rho_0 = 2\rho_0 = 1 \Rightarrow \rho_0 = \frac{1}{2} \quad (2.78)$$

and c_0 from

$$\int_{-1}^1 du_0 \int_{-1}^1 c_0 \frac{3u_0^2 - 1}{2} \frac{3u^2 - 1}{2} \delta(u - u_0) du = \int_{-1}^1 du_0 c_0 \frac{(3u_0^2 - 1)^2}{4} = \frac{2}{5}c_0 \Rightarrow c_0 = \frac{5}{2}. \quad (2.79)$$

Finally, the correlation function can be calculated

$$\overline{\left(\frac{3}{2} \cos^2 \vartheta(0) - \frac{1}{2}\right) \left(\frac{3}{2} \cos^2 \vartheta(t) - \frac{1}{2}\right)} = \frac{5}{4} \int_{-1}^1 du_0 \int_{-1}^1 du \frac{(3u_0^2 - 1)^2}{4} \frac{(3u^2 - 1)^2}{4} e^{-6D^{\text{rot}}t} = \frac{1}{5} e^{-6D^{\text{rot}}t}. \quad (2.80)$$

We have derived that the time correlation function for spherically symmetric rotational diffusion is a single-exponential function.

2.6.3 Return to equilibrium

After introducing the correlation function, we can repeat the analysis using the same simplifications (rigid molecule, isotropic liquid), but taking the transverse (perpendicular) field fluctuations into account.

$$\frac{d\mu_x}{dt} = \omega_y \mu_z - \omega_z \mu_y \quad (2.81)$$

$$\frac{d\mu_y}{dt} = \omega_z \mu_x - \omega_x \mu_z \quad (2.82)$$

$$\frac{d\mu_z}{dt} = \omega_x \mu_y - \omega_y \mu_x \quad (2.83)$$

Expressing ω_x as $b\Theta^\perp \cos \varphi$ and ω_y as $b\Theta^\perp \sin \varphi$, where

$$b = -2\gamma B_0 \delta_a \quad (2.84)$$

$$\Theta^\perp = \frac{3}{2} \sin \vartheta \cos \vartheta, \quad (2.85)$$

gives

$$\frac{d\mu_x}{dt} = (b\Theta^\perp \sin \varphi) \mu_z - (\omega_0 + b\Theta^\parallel) \mu_y \quad (2.86)$$

$$\frac{d\mu_y}{dt} = (\omega_0 + b\Theta^\parallel) \mu_x - (b\Theta^\perp \cos \varphi) \mu_z \quad (2.87)$$

$$\frac{d\mu_z}{dt} = (b\Theta^\perp \cos \varphi) \mu_y - (b\Theta^\perp \sin \varphi) \mu_x, \quad (2.88)$$

Introducing $\mu^+ = \mu_x + i\mu_y$ and $\mu^- = \mu_x - i\mu_y$ results in

$$\frac{d\mu^+}{dt} = -ib\Theta^\perp e^{i\varphi} \mu_z + i(\omega_0 + b\Theta^\parallel) \mu^+ \quad (2.89)$$

$$\frac{d\mu^-}{dt} = ib\Theta^\perp e^{-i\varphi} \mu_z - i(\omega_0 + b\Theta^\parallel) \mu^- \quad (2.90)$$

$$\frac{d\mu_z}{dt} = \frac{i}{2} b\Theta^\perp \left(e^{-i\varphi} \mu^+ - e^{i\varphi} \mu^- \right), \quad (2.91)$$

In a coordinate frame rotating with ω_0 ,

$$\frac{d(\mu^+)_{\text{rot}}}{dt} = -ib\Theta^\perp e^{i(\varphi - \omega_0 t)} \mu_z + ib\Theta^\parallel (\mu^+)_{\text{rot}} \quad (2.92)$$

$$\frac{d(\mu^-)_{\text{rot}}}{dt} = ib\Theta^\perp e^{-i(\varphi - \omega_0 t)} \mu_z - ib\Theta^\parallel (\mu^-)_{\text{rot}} \quad (2.93)$$

$$\frac{d\mu_z}{dt} = \frac{i}{2} b\Theta^\perp \left(e^{-i(\varphi - \omega_0 t)} (\mu^+)_{\text{rot}} - e^{i(\varphi - \omega_0 t)} (\mu^-)_{\text{rot}} \right), \quad (2.94)$$

Note that now the transformation to the rotating frame did not remove ω_0 completely, it survived in the exponential terms.

Again, the set of differential equations cannot be solved because Θ^\parallel , Θ^\perp , and φ fluctuate in time, but we can analyze the evolution in time steps short enough to keep Θ^\parallel , Θ^\perp , and φ constant.

$$\mu_1^+ = \mu_0^+ + \Delta\mu_1^+ = [1 + i(\omega_0 + b\Theta_1^\parallel)\Delta t] \mu_0^+ - ib\Theta_1^\perp \Delta t e^{i(\varphi_1 - \omega_0 t_1)} \mu_{z,0} \quad (2.95)$$

$$\mu_1^- = \mu_0^- + \Delta\mu_1^- = [1 - i(\omega_0 + b\Theta_1^\parallel)\Delta t] \mu_0^- + ib\Theta_1^\perp \Delta t e^{-i(\varphi_1 - \omega_0 t_1)} \mu_{z,0} \quad (2.96)$$

$$\mu_{z,1} = \mu_{z,0} + \Delta\mu_{z,1} = \mu_{z,0} - \frac{i}{2} b\Theta_1^\perp \Delta t e^{-i(\varphi_1 - \omega_0 t_1)} \mu_0^+ + \frac{i}{2} b\Theta_1^\perp \Delta t e^{i(\varphi_1 - \omega_0 t_1)} \mu_0^-. \quad (2.97)$$

The μ^+ , μ^- , and $\mu_{z,0}$ are now coupled which makes the step-by-step analysis much more complicated. Instead of writing the equations, we just draw a picture (Figure 2.3) similar to Fig. 2.2. Derivation of the values of relaxation rates follows the procedure described for

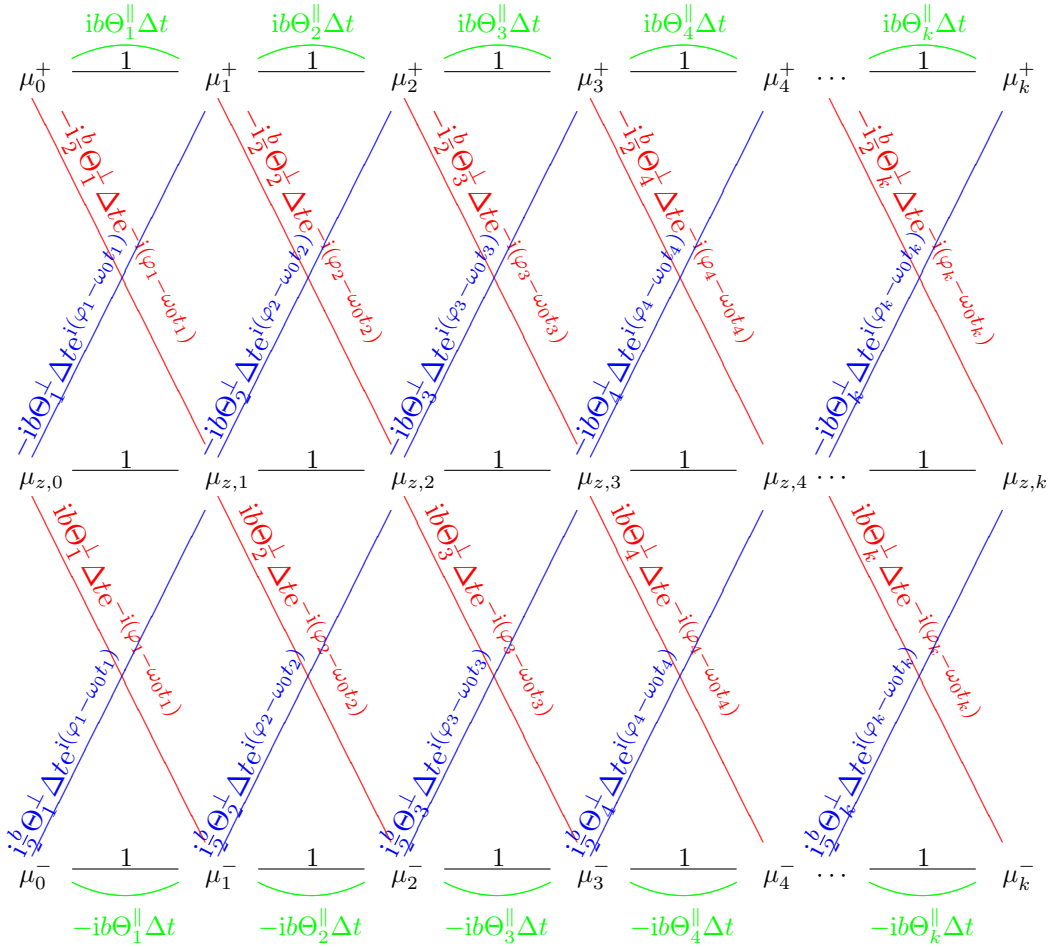


Figure 2.3: Evolution of magnetic moments due to longitudinal (parallel) and transverse (perpendicular) fluctuations of magnetic fields. The meaning of the diagram is the same as in Fig. 2.2, but additional segments (red and blue) interconnect μ_j^+ , μ_j^- , and $\mu_{z,j}$, substantially increasing the number of possible pathways. The pathway composed of the black segments only gives the result of multiplication equal to one, the pathways containing just one segment of a different color give results of multiplication proportional to Δt , the pathways containing two segments of a color different than black give results of multiplication proportional to $(\Delta t)^2$, etc.

the parallel fluctuations (Eqs. 2.36–2.41). As the number of possible pathways in Fig. 2.3 is very high, already the list of the terms proportional to Δt and Δt^2 is very long. Fortunately, we are not interested in evolution of magnetic moments in individual molecules, described in Fig. 2.3. The values of Θ_1^\parallel , Θ_1^\perp , φ_1 , etc. are different for each molecule and we are interested in what we get after averaging results of multiplications for all molecules (all possible orientations). In order to avoid writing the long expressions for magnetic moments of individual molecules, we skip steps corresponding to Eqs. 2.36–2.40 and jump directly to the calculation of the evolution of total magnetization (corresponding to Eq. 2.41).

Let us start with the terms proportional to Δt , which give us the imaginary term proportional to b when calculating dM^+/dt (and dM^-/dt , dM_z/dt). We have already seen that the average of Θ^\parallel (the green segment) is zero. The terms containing Θ^\perp (red and blue segments) contain the exponential expression with the phase including φ . If the azimuth φ is random,¹⁰ the "red" and "blue" terms average to zero.

Let us now turn to the terms proportional to Δt^2 , which give us the time integral multiplied by b^2 when calculating dM^+/dt (and dM^-/dt , dM_z/dt). The pathways containing two red segments or two blue segments correspond to Δt^2 terms with a random phase in the exponent (random sums of $\varphi_j - \omega_0 t_j$). When averaged for all orientations, such phases tend to zero. The Δt^2 terms do not average to zero only in two cases: (i) if the pathway contains two green segments (effect of longitudinal fluctuations described above) or (ii) if the pathway contains a combination of one red and one blue segment. The former case is obvious, but the latter one is more subtle.

We can distinguish two combinations of one red and one blue segment:

$$\frac{1}{2}b^2\Delta t^2\Theta_k^\perp e^{i(\varphi_k - \omega_0 t_k)}\Theta_j^\perp e^{-i(\varphi_j - \omega_0 t_j)} = \frac{1}{2}b^2\Delta t^2\Theta_k^\perp\Theta_j^\perp e^{i(\varphi_k - \varphi_j - \omega_0(t_k - t_j))} \quad (2.98)$$

(with $-\omega_0(t_k - t_j)$ in the exponent) and

$$\frac{1}{2}b^2\Delta t^2\Theta_k^\perp e^{-i(\varphi_k - \omega_0 t_k)}\Theta_j^\perp e^{i(\varphi_j - \omega_0 t_j)} = \frac{1}{2}b^2\Delta t^2\Theta_k^\perp\Theta_j^\perp e^{i(-\varphi_k + \varphi_j + \omega_0(t_k - t_j))} \quad (2.99)$$

(with $+\omega_0(t_k - t_j)$ in the exponent). As discussed in Section 2.6.1, we can replace t_k by zero and t_j by t because the molecular motions are random:

$$\frac{1}{2}b^2\Delta t^2\Theta^\perp(0)\Theta^\perp(t)e^{i(-(\varphi(t) - \varphi(0)) + \omega_0 t)} \quad (2.100)$$

(with $+\omega_0 t$ in the exponent) and

$$\frac{1}{2}b^2\Delta t^2\Theta^\perp(0)\Theta^\perp(t)e^{i(+(\varphi(0) - \varphi(t)) - \omega_0 t)} \quad (2.101)$$

(with $-\omega_0 t$ in the exponent).

In both cases, the phase is not randomly distributed for different orientations only if $\varphi(0) - \varphi(t)$ is similar to $\omega_0 t$. The average value of $\overline{\Theta^\perp(0)^2}$ is 3/10:

$$\overline{\Theta^\perp(t)^2} = \frac{9}{4}\overline{\cos^2\vartheta\sin^2\vartheta} = \frac{9}{16\pi}\int_0^{2\pi}d\varphi\int_0^\pi d\vartheta(\sin^3\vartheta\cos^2\vartheta) = \frac{3}{10} \quad (2.102)$$

for any t .

The M_z component of magnetization is given by the average of the μ_z components at t_k . In order to get to $\mu_{z,k}$ through paths giving terms proportional to Δt^2 , we must start at $\mu_{z,0}$ and pass one blue segment and one red segment in Figure 2.3. Eqs. 2.100 and 2.101 mathematically describe that orientations of magnetic moments are redistributed if the molecular motions (described by the azimuth φ) accidentally resonate for a short time with the frequencies $\omega_0 t$ and $-\omega_0 t$. Then the magnetic energy of the magnetic moments is exchanged with the rotational kinetic energy of the molecules. This energy exchange must be taken into account when we average magnetic moments of individual molecules to calculate M_z . Let us call the total rotational energy of molecules $\mathcal{E}_0^{\text{rot}}$. The exchange of the magnetic energy \mathcal{E}_μ of a magnetic moment $\vec{\mu}$ with a small amount of rotational energy of molecules $\Delta\mathcal{E}^{\text{rot}}$ can be described as

$$\mathcal{E}_0^{\text{rot}} \rightarrow \mathcal{E}_0^{\text{rot}} + \Delta\mathcal{E}^{\text{rot}} + \mathcal{E}_\mu. \quad (2.103)$$

The molecular motions have much more degrees of freedom (both directions of rotational axes and rates of rotation vary) than the magnetic moments (size is fixed, only orientation changes). We can therefore assume that the exchange perturbs distribution of the magnetic moments, but the rotating molecules stay very close to the thermodynamic equilibrium. At the equilibrium, the probability to find a molecule with the rotational kinetic energy $\mathcal{E}_0^{\text{rot}} + \Delta\mathcal{E}^{\text{rot}}$ is proportional (Boltzmann law) to

$$e^{-\Delta\mathcal{E}^{\text{rot}}} \approx 1 - \Delta\mathcal{E}^{\text{rot}}. \quad (2.104)$$

The conservation of energy requires

$$\mathcal{E}_0^{\text{rot}} + \Delta\mathcal{E}^{\text{rot}} + \mathcal{E}_\mu = \mathcal{E}_0^{\text{rot}}, \quad (2.105)$$

¹⁰Note that this is true even in the presence of \vec{B}_0 and in molecules aligned along the direction of \vec{B}_0 , for example in liquid crystals oriented by the magnetic field.

showing that $\Delta\mathcal{E}^{\text{rot}} = -\mathcal{E}_\mu$. Consequently, the population of molecules with the given rotational energy is proportional to $1 - \Delta\mathcal{E}^{\text{rot}} = 1 + \mathcal{E}_\mu$. According to Eq. 1.11, the probability of finding a magnetic moment in the orientation described by a given $u = \cos\vartheta_\mu$ is

$$P^{\text{eq}}(u) = \frac{w}{e^w - e^{-w}} e^{uw} \approx \frac{w}{1 - w - 1 + w} (1 + uw) = \frac{1}{2} (1 + uw). \quad (2.106)$$

Consequently, $\mathcal{E}_\mu = -uw = 1 - 2P^{\text{eq}}(u)$ and the probability to find a molecule with the rotational kinetic energy $\mathcal{E}_0^{\text{rot}} + \Delta\mathcal{E}^{\text{rot}}$ is proportional to

$$1 - \Delta\mathcal{E}^{\text{rot}} = 1 + \mathcal{E}_\mu = 2 - 2P^{\text{eq}}(u) = 2(1 - P^{\text{eq}}(u)), \quad (2.107)$$

where the factor of two can be absorbed to the normalization constant.

We have derived that the averaged values of μ_z are weighted by $1 - P^{\text{eq}}(u)$. How does it affect the calculation of M_z ? In the expression $\mu_z - P^{\text{eq}}(u)\mu_z$, μ_z in the first term is not weighted by anything and its average (multiplied by the number of magnetic moments per unit volume) is equal to M_z . The average value of the second term has been already calculated in Eqs. 1.15–1.1. It represents the equilibrium value of the magnetization, M^{eq} . Therefore, averaging of μ_z results in $M_z - M^{\text{eq}}$, usually abbreviated as ΔM_z .

Using the same arguments as in Section 2.6.1,

$$\frac{d\Delta M_z}{dt} = - \left(\frac{1}{2} b^2 \int_0^\infty \overline{\Theta^\perp(0)\Theta^\perp(t)e^{-i(\varphi(t)-\varphi(0))}} e^{i\omega_0 t} dt + \frac{1}{2} b^2 \int_0^\infty \overline{\Theta^\perp(0)\Theta^\perp(t)e^{i(\varphi(t)-\varphi(0))}} e^{-i\omega_0 t} dt \right) \Delta M_z \quad (2.108)$$

The relaxation rate R_1 for M_z , known as *longitudinal relaxation rate* in the literature, is the real part¹¹ of the expression in the parentheses

$$R_1 = b^2 \Re \left\{ \int_0^\infty \overline{\Theta^\perp(0)\Theta^\perp(t)e^{-i(\varphi(t)-\varphi(0))}} e^{i\omega_0 t} dt + \int_0^\infty \overline{\Theta^\perp(0)\Theta^\perp(t)e^{i(\varphi(t)-\varphi(0))}} e^{-i\omega_0 t} dt \right\}. \quad (2.109)$$

If the fluctuations are random and their statistical properties do not change in time, they are *stationary*: the current orientation of the molecule is correlated with the orientation in the past in the same manner as it is correlated with the orientation in the future. Therefore,

$$\int_0^\infty \overline{\Theta^\perp(0)\Theta^\perp(t)e^{-i(\varphi(t)-\varphi(0))}} e^{i\omega_0 t} dt = \frac{1}{2} \left(\int_0^\infty \overline{\Theta^\perp(0)\Theta^\perp(t)e^{-i(\varphi(t)-\varphi(0))}} e^{i\omega_0 t} dt + \int_{-\infty}^0 \overline{\Theta^\perp(0)\Theta^\perp(t)e^{-i(\varphi(t)-\varphi(0))}} e^{i\omega_0 t} dt \right) \quad (2.110)$$

$$= \frac{1}{2} \int_{-\infty}^\infty \overline{\Theta^\perp(0)\Theta^\perp(t)e^{-i(\varphi(t)-\varphi(0))}} e^{i\omega_0 t} dt. \quad (2.111)$$

$$\int_0^\infty \overline{\Theta^\perp(0)\Theta^\perp(t)e^{i(\varphi(t)-\varphi(0))}} e^{-i\omega_0 t} dt = \frac{1}{2} \left(\int_0^\infty \overline{\Theta^\perp(0)\Theta^\perp(t)e^{i(\varphi(t)-\varphi(0))}} e^{-i\omega_0 t} dt + \int_{-\infty}^0 \overline{\Theta^\perp(0)\Theta^\perp(t)e^{i(\varphi(t)-\varphi(0))}} e^{-i\omega_0 t} dt \right) \quad (2.112)$$

$$= \frac{1}{2} \int_{-\infty}^\infty \overline{\Theta^\perp(0)\Theta^\perp(t)e^{i(\varphi(t)-\varphi(0))}} e^{-i\omega_0 t} dt. \quad (2.113)$$

In isotropic solutions, the motions of molecules are very little affected by magnetic fields. Therefore, the choice of the z axes is arbitrary from the point of the view of the molecule (not of the magnetic moment!). Therefore, the terms with Θ^\perp can be replaced by those with Θ^\parallel , multiplied by 3/2 to match the difference between $\Theta^\parallel(0)^2 = 1/5$ with $\Theta^\perp(0)^2 = 3/10$:

$$\frac{1}{2} \int_{-\infty}^\infty \overline{\Theta^\perp(0)\Theta^\perp(t)e^{\mp i(\varphi(t)-\varphi(0))}} e^{\pm i\omega_0 t} dt = \frac{3}{4} \int_{-\infty}^\infty \overline{\Theta^\parallel(0)\Theta^\parallel(t)e^{\pm i\omega_0 t}} dt. \quad (2.114)$$

Real parts of the integrals in Eq. 2.114 are known as *spectral density functions* $J(\omega)$. Note that the real part of the integral in the right-hand side of Eq. 2.114 is

¹¹Solving Eq. 2.108 gives

$$\Delta M_z = \Delta M_z(0) e^{-(R_1 + i\omega')t} = \Delta M_z(0) e^{-R_1 t} e^{i\omega' t} = \Delta M_z(0) e^{-R_1 t} (\cos \omega' t + i \sin \omega' t),$$

where R_1 and ω' are the real and imaginary parts, respectively, of the expression in the parentheses in Eq. 2.108. Whereas R_1 describes the decay rate of ΔM_z , ω' , known as the *dynamic frequency shift*, describes an oscillation of ΔM_z , and is usually included into the value of ω_0 .

$$\Re \left\{ \frac{3}{4} \int_{-\infty}^{\infty} \overline{\Theta^{\parallel}(0)\Theta^{\parallel}(t)} e^{\pm i\omega_0 t} dt \right\} = \frac{3}{4} \int_{-\infty}^{\infty} \overline{\Theta^{\parallel}(0)\Theta^{\parallel}(t)} \cos(\omega_0 t) dt. \quad (2.115)$$

because

$$e^{\pm ix} = \cos x \pm i \sin x. \quad (2.116)$$

Also note that the integral in Eq. 2.48 in Section 2.6.1 can be also included in the definition of the spectral density function if we replace ω_0 by zero:

$$\int_0^{\infty} \overline{\Theta^{\parallel}(0)\Theta^{\parallel}(t)} dt = \frac{1}{2} \left(\int_0^{\infty} \overline{\Theta^{\parallel}(0)\Theta^{\parallel}(t)} dt + \int_{-\infty}^0 \overline{\Theta^{\parallel}(0)\Theta^{\parallel}(t)} dt \right) = \frac{1}{2} \int_{-\infty}^{\infty} \overline{\Theta^{\parallel}(0)\Theta^{\parallel}(t)} e^0 dt = \frac{1}{2} J(0). \quad (2.117)$$

Lecture 3

Signal acquisition and processing

Literature: Function of an NMR spectrometer is nicely described in L4, K13, or C3.1. More details are provided in B23. Experimental setup is discussed in C3.8.2. Signal averaging is described in L5.2, quadrature detection in L5.7 and LA.5, K13.6, and C3.2.3, Fourier transformation is introduced in K5.1–K5.3.1 and L5.8.1.–L5.8.3, and treated more thoroughly in B8 and C3.3.1. Phase correction is described nicely in K5.3.2–K5.3.4 and discussed also in C3.3.2.3 and L5.8.4–L5.8.5, zero filling is discussed in C3.3.2.1 and K5.5, and apodization is explained in K5.4 and C3.3.2.2.

3.1 NMR experiment

The real NMR experiment closely resembles FM radio broadcast. The mega-hertz radio frequency ω_{radio} plays the role of the *carrier frequency*, and is *frequency-modulated* by the offset, which usually falls in the range of kilo-hertz *audio frequencies*. In the same fashion, the carrier frequency of the FM broadcast is modulated by the audio frequency of the transmitted signal (voice, music). Like when listening to the radio, we need to know the carrier frequency to tune the receiver, but its value is not interesting. The interesting information about the chemical environment is hidden in the audio-frequency offset. Note, however, that the numerical value of Ω is arbitrary as it depends on the actual choice of the carrier frequency. What can be interpreted unambiguously, is the constant δ , given just by the electron density. But in practice, the absolute value of δ is extremely difficult to obtain because the reference $\delta = 0$ represents nuclei with no electrons – definitely not a sample we are used to produce in our labs. Therefore, more accessible references (precession frequencies ω_{ref} of stable chemical compounds) are used instead of the vacuum frequency. The value of δ is then defined as $(\omega - \omega_{\text{ref}})/\omega_{\text{ref}}$ and usually presented in the units of ppm.

3.1.1 Setting up the experiment

- *Temperature control and calibration.* Temperature affects molecular motions and chemical shifts, it should be controlled carefully to obtain reproducible spectra and to analyze them quantitatively. The sample temperature is controlled by a flow of pre-heated/cooled air or nitrogen gas. The exact temperature inside the sample is not so easy to measure. Usually, spectra of compounds with known temperature dependence of chemical shifts are recorded (e.g. methanol). The temperature is obtained by comparing a difference of two well defined

chemical shifts (of methyl and hydroxyl protons in the case of methanol) with its values reported for various temperatures. Purity of the standard samples is a critical issue.

- *Field-frequency lock.* The external magnetic field should be *stationary*. It is achieved by a feedback system known as *field-frequency lock*. A deuterated compound (usually heavy water or other deuterated solvent) is added to the sample and the deuterium frequency is measured continually and kept constant by adjusting electric current in an auxiliary electromagnet. The lock parameters for the particular deuterium compound used are selected and the deuterium spectrometer is switched on before the measurement.
- *Shimming.* The external magnetic field should be also *homogeneous*. The inhomogeneities caused e.g. by the presence of the sample are compensated by adjusting electric current in a set of correction coils called *shims*. This is usually at least partially automated.
- *Tuning.* Each radio-frequency circuit in the probe consists of a receiver coil and two adjustable capacitors. The capacitors should be adjusted for each sample. The *tuning capacitor* of the capacitance C_T and the coil of the inductance L make an LC circuit, acting as a resonator. Adjusting the value of C_T defines the resonant frequency, which should be equal to the precession frequency of the measured nucleus ω_0 . If we neglect the second capacitor, the resonant frequency is $\omega = 1/\sqrt{LC_T}$. The second, *matching capacitor* of the capacitance C_M is used to adjust the impedance of the resonator. The radio waves do not travel from the transmitter to the coil through air but through co-axial cables. In order to have minimum of the wave reflected back to the transmitter, the impedance of the resonator (defined Section 3.6.1 should match the input impedance Z_{in} .

In order to tune the circuit, C_T and C_M must be adjusted simultaneously to get (i) $Z_c = Z_{in}$ and (ii) $\omega = \omega_0$.

- *Calibration of pulse duration.* The magnitude of \vec{B}_1 cannot be set directly. Therefore, the duration of irradiation rotating \vec{M} by 360° at the given strength of radio waves is searched for empirically. This duration is equal to $2\pi/\omega_1$ and can be used to calculate ω_1 or $|\vec{B}_1| = \omega_1/\gamma$. As $|\vec{B}_1|$ is proportional to the square root of power P , durations of pulses of radio waves of other strengths need not be calibrated, but can be recalculated, as described in Section 3.6.2.

3.1.2 Quadrature detection

Precession of the magnetization vector in the sample induces a signal oscillating with the same frequency (Larmor frequency ω_0) in the coil of the NMR probe. The signal generated in the coil and amplified in the preamplifier is split into two channels. The signal in each channel is mixed with a reference wave supplied by the radio-frequency synthesizer. The reference waves have the same frequency ω_{ref} in both channels, but their phases are shifted by 90° . It is convenient to treat the signals in the individual channels as a real and imaginary component of a single complex number, denoted $y(t)$ in this text. If we ignore relaxation, the complex signal can be described as

$$y(t) = \mathcal{A} \cos(\Omega t) + i\mathcal{A} \sin(\Omega t) = \mathcal{A} e^{i\Omega t}. \quad (3.1)$$

Mathematical description of the quadrature detection is presented in Section 3.6.3.

3.1.3 Analog-digital conversion

The output of the quadrature receiver is converted to a digital form. Therefore, the information obtained from an NMR experiment is a set of complex numbers describing the signal intensities at the time points $t \in \{0, \Delta t, 2\Delta t, \dots, (N-1)\Delta t\}$.

3.1.4 Signal averaging and signal-to-noise ratio

The NMR signal induced by precession of the magnetization vector is very weak, comparable to the *noise*, generated mostly by random motions of electrons in the receiver coil. Therefore, the NMR experiments are usually repeating several times, adding the signal together. If the experiment is repeated in the same manner N -times, the evolution of the magnetization vector is identical in all repetitions (magnetization is evolving *coherently*), and the sum of the signals from the individual measurements, called *transients*, is simply $Ny(t)$. However, the absolute size of the signal is not important, what really matters is the *signal-to-noise* ratio. Therefore, it is also important how noise accumulates when adding signals of separate measurements. The analysis presented in Section 3.6.4 shows that the signal-to-noise ratio is proportional to the square root of the number of summed transients.

3.2 Fourier transformation

The effect of electrons (chemical shift) makes NMR signal much more interesting but also much more complicated. Oscillation of the voltage induced in the receiver coil is not described by a cosine function, but represents a superposition (sum) of several cosine curves (phase-shifted and dumped). It is practically impossible to get the frequencies of the individual cosine functions just by looking at the recorded interferograms. Fortunately, the signal acquired as a function of time can be converted into a frequency dependence using a straightforward mathematical procedure, known as *Fourier transformation*.

It might be useful to present the basic idea of the Fourier transformation in a pictorial form before we describe details of Fourier transformation by mathematical equations. The oscillating red dots in Figure 3.1 represent an NMR signal defined by one frequency ν . Let us assume that the signal oscillates as a cosine function but we do not know the frequency. We generate a testing set of cosine functions of different known frequencies f_j (blue curves in Figure 3.1) and we multiply each blue testing function by the red signal. The resulting product is plotted as magenta dots in Figure 3.1. Then we sum the values of the magenta points for each testing frequency getting one number (the sum) for each blue function. Finally, we plot these numbers (the sums) as the function of the testing frequency. How does the plot look like? If the testing frequency differs from ν , the magenta dots oscillate around zero and their sum is close to zero (slightly positive or negative, depending on how many points were summed). But if we are lucky and the testing frequency matches ν (f_3 in Figure 3.1), the result is always positive (we always multiply two positive numbers or two negative numbers). The sum is then also positive, the larger the more points are summed. Therefore, the sum

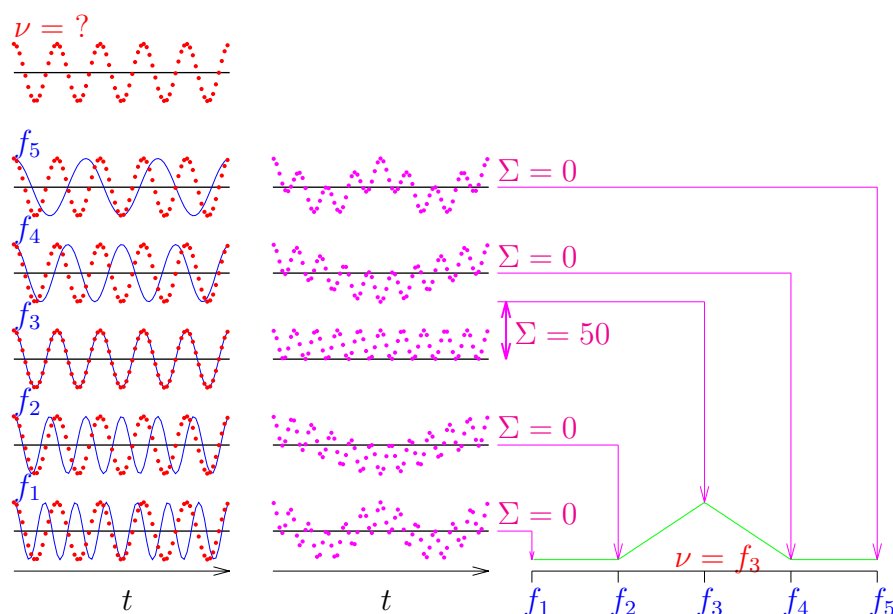


Figure 3.1: The basic idea of Fourier transformation.

for the matching frequency is much higher than the other sums, making a positive peak in the final green plot (the dependence on f_j). The final plot represents a *frequency spectrum* and the position of the peak immediately identifies the value of the unknown frequency. If the NMR signal is composed of two frequencies, the red dots oscillate in a wild interference patterns, not allowing to get the frequency simply by measuring the period of the oscillation. However, the individual components (if they are sufficiently different) just make several peaks in the final green plot and their frequencies can be easily obtained by reading the positions of the peaks.

Let us now try to describe the Fourier transformation in a bit more mathematical manner (a more detailed discussion is presented in Section 3.6.5). For a continuous signal $y(t)$ recorded using quadrature detection, i.e., stored as complex numbers, it is convenient to apply continuous complex Fourier transformation, defined as

$$Y(\omega) = \int_{-\infty}^{\infty} y(t)e^{-i\omega t} dt. \quad (3.2)$$

Although the actual NMR signal is not recorded and processed in a continuous manner, the idealized continuous Fourier transformation helps to understand the fundamental relation between the shapes of FID and frequency spectra and reveals important features of signal processing. Therefore, we discuss the continuous Fourier transformation before we proceed to the discrete analysis.

An "ideal signal" (see Figure 3.2) has the form $y(t) = 0$ for $t \leq 0$ and $y(t) = \mathcal{A}e^{-R_2 t}e^{i\Omega t}$ for $t \geq 0$, where \mathcal{A} can be a complex number (*complex amplitude*), including the real amplitude $|\mathcal{A}|$ and the initial phase ϕ_0 :

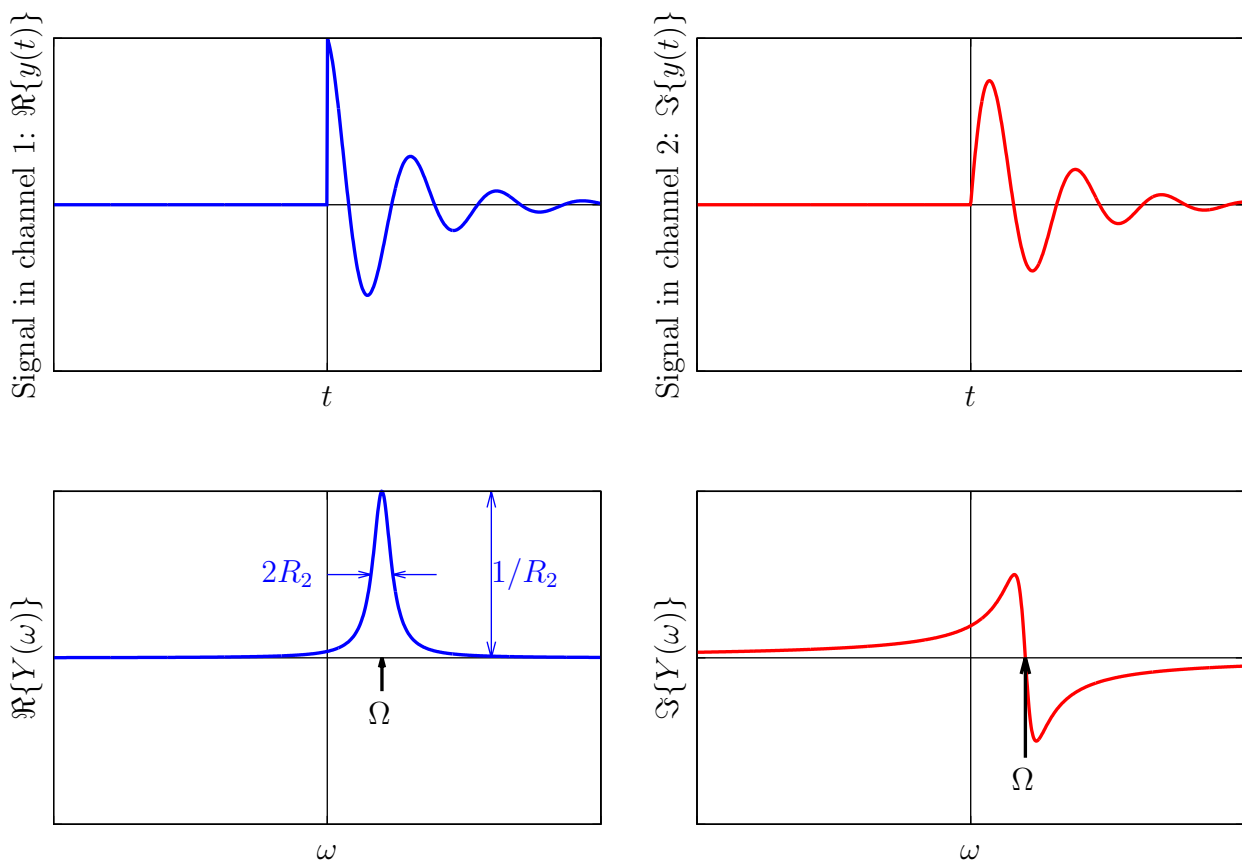


Figure 3.2: Ideal signal detected with a quadrature detection (top) and its Fourier transform (bottom).

$$\mathcal{A} = |\mathcal{A}|e^{i\phi_0}. \quad (3.3)$$

As derived in Section 3.6.6,

Fourier transform of the "ideal" signal is

$$Y(\omega) = \int_{-\infty}^{\infty} \mathcal{A}e^{-R_2t} e^{i\Omega t} e^{-i\omega t} dt = \mathcal{A} \frac{R_2}{R_2^2 + (\Omega - \omega)^2} + i\mathcal{A} \frac{\Omega - \omega}{R_2^2 + (\Omega - \omega)^2} \quad (3.4)$$

If $\phi_0 = 0$, the blue term, known as the *absorption line* is a real function ($\Re\{Y(\omega)\}$) having a shape of the *Lorentz curve* (see Figure 3.2). The shape of the absorption line is given¹ by the relaxation rate R_2 :

- Peak height $\propto 1/R_2$ ($Y = Y_{\max}$ at $\omega = \Omega \Rightarrow Y_{\max} = Y(\Omega) = \mathcal{A}/R_2$)
- Linewidth at the half-height = $2R_2$ ($Y = Y_{\max}/2$ at $\Omega - \omega = \pm R_2$)

The red term, the *dispersion line*, is purely imaginary ($\Im\{Y(\omega)\}$) if $\phi_0 = 0$. Such shape is less convenient in real spectra containing several lines because the broad wings of the dispersion line distort the shape of the neighbouring lines (see Figure 3.2).

Figure 3.3 documents that Fourier transformation allows us to immediately determine several Larmor frequencies in spectra even if the signal in the time domain (FID) is very difficult to interpret, and that the real (absorption) part of the complex spectrum is much better for such purpose.

The discussed transformation of a continuous signal is extremely useful for understanding the relation between evolution of the magnetization vector and shape of the peaks observed in the frequency spectra. But in reality, the signal is finite ($t_{\max} < \infty$) and discrete ($\Delta t > 0$):

- $t \in \{0, \Delta t, 2\Delta t, \dots, (N-1)\Delta t\}$ $y(t) \in \{y_0, y_1, y_2, \dots, y_{N-1}\}$
- $\omega \in \{0, \Delta\omega, 2\Delta\omega, \dots, (N-1)\Delta\omega\}$ $Y(t) \in \{Y_0, Y_1, Y_2, \dots, Y_{N-1}\}$

The seemingly marginal difference between ideal and real (finite and discrete) signal has several practical consequences, discussed below.

Figures 3.4 and 3.5 document the advantage of recording the signal with the quadrature detection, as a complex number. If we take only the signal from the first channel, oscillating as the cosine function if $\phi = 0$, and stored as the real part if the quadrature detection is used (Figure 3.4), and perform the Fourier transformation, we get a spectrum with two peaks with the frequency offsets Ω and $-\Omega$. Such a spectrum does not tell us if the actual Larmor frequency is $\omega_0 = \omega_{\text{radio}} - \Omega$ or $\omega_0 = \omega_{\text{radio}} + \Omega$. If we use the signal from the second channel only, oscillating as the sine function if $\phi = 0$ (Figure 3.5), a spectrum with two peaks is obtained again, the only difference is that the peaks have opposite phase (i.e., their phases differ by 180°). But if we combine both signals, the false peaks at $-\Omega$ disappear because they have opposite signs and cancel each other in the sum of the spectra.

¹In practice, it is also affected by inhomogeneities of the static magnetic field, increasing the apparent value of R_2 . This effect is known as *inhomogeneous broadening*.

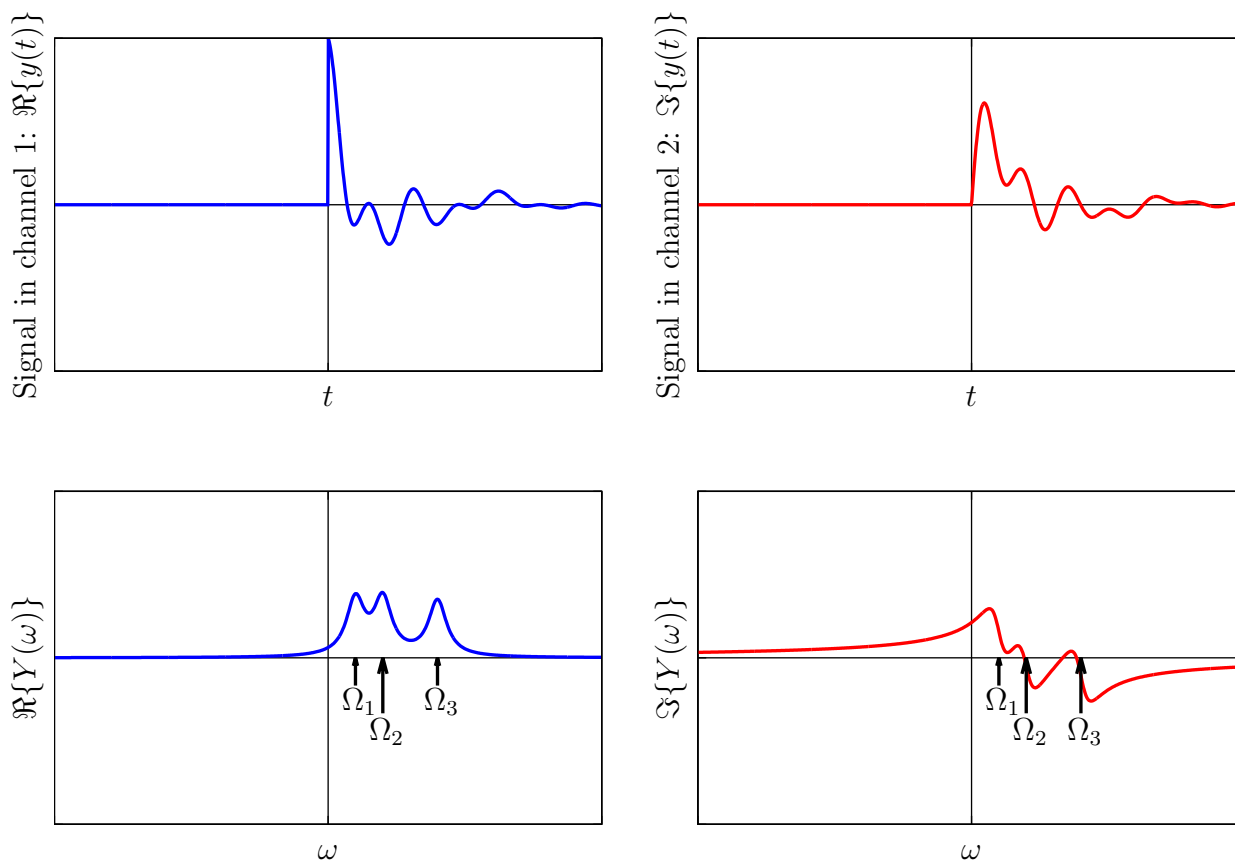


Figure 3.3: Signal (top) and frequency spectrum (bottom) with three Larmor frequencies.

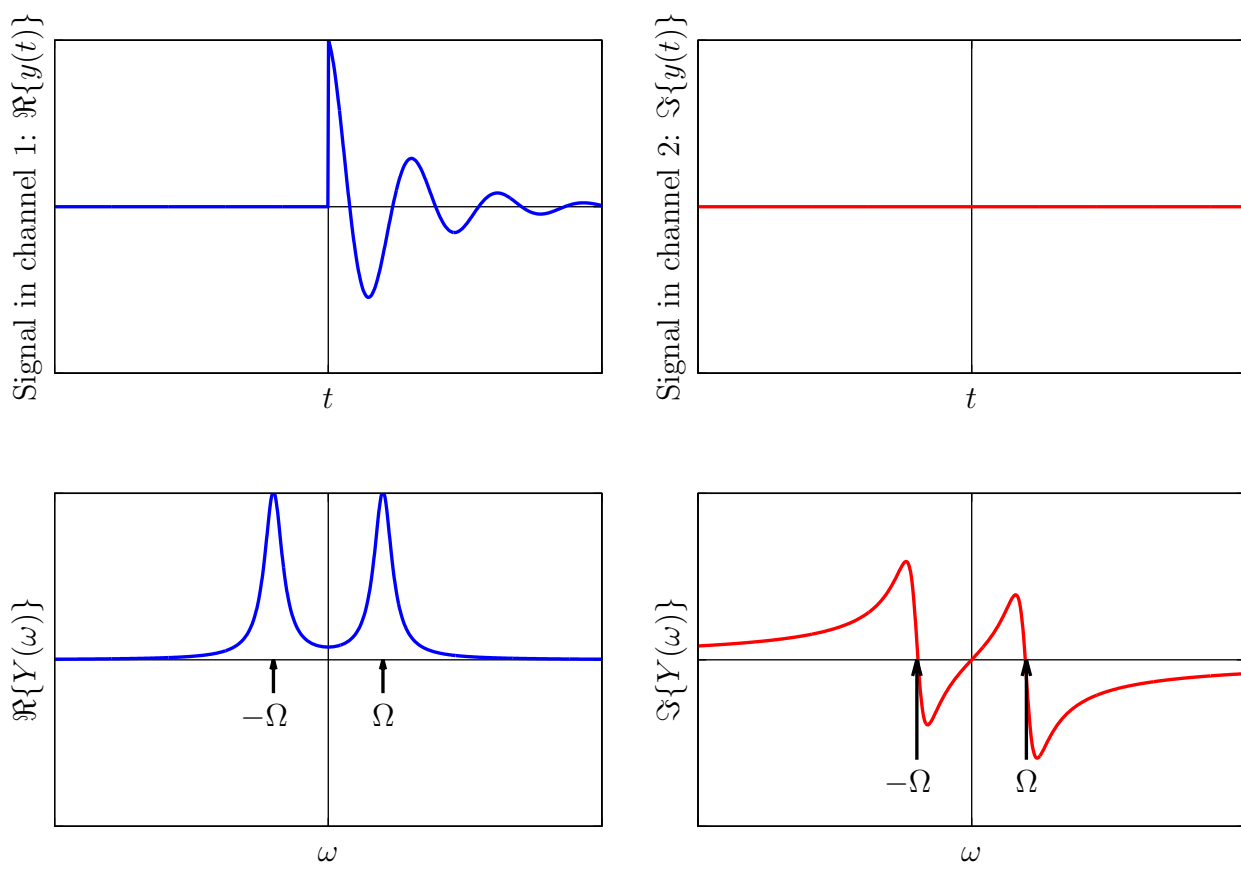


Figure 3.4: A signal detected in the first ("real") channel (top) and its Fourier transform (bottom).

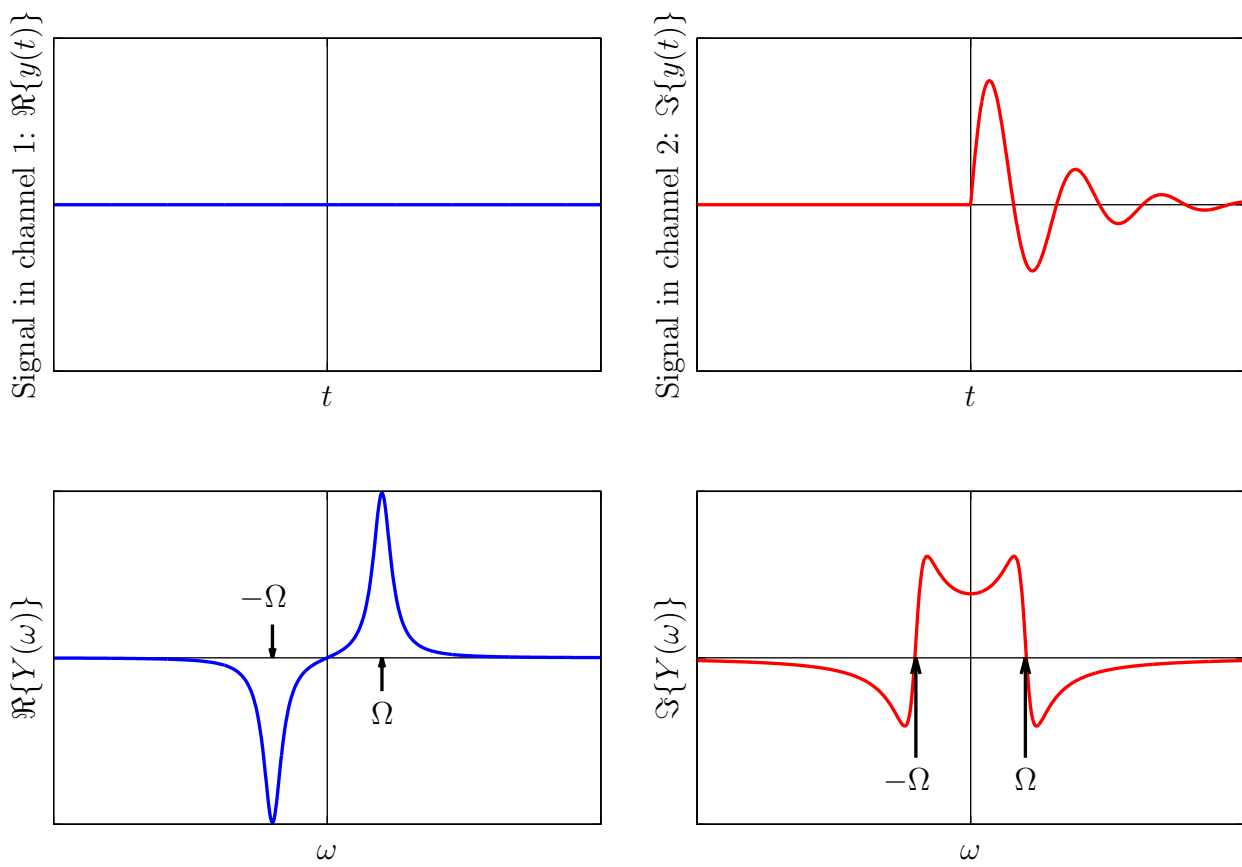


Figure 3.5: A signal detected in the second ("imaginary") channel (top) and its Fourier transform (bottom).

3.2.1 Properties of continuous Fourier transformation

The continuous Fourier transformation has several important properties:

- *Parseval's theorem* $\int_{-\infty}^{\infty} |y(t)|^2 dt = \frac{1}{2\pi} \int_{-\infty}^{\infty} |Y(\omega)|^2 d\omega$

A conservation law, documents that the signal energy (information content) is preserved by the Fourier transformation.

- *Linearity* $\int_{-\infty}^{\infty} (y(t) + z(t))e^{-i\omega t} dt = Y(\omega) + Z(\omega)$

It documents that a sum of periodic functions (difficult to be distinguished in the time domain) can be converted to a sum of resonance peaks (easily distinguishable in the frequency domain if the resonance frequencies differ).

- *Convolution* $\int_{-\infty}^{\infty} (y(t) \cdot z(t))e^{-i\omega t} dt = \int_{-\infty}^{\infty} Y(\omega)Z(\omega - \omega')d\omega'$

It provides mathematical description of apodization (Section 3.5)

- *Time shift* $\int_{-\infty}^{\infty} y(t - t_0)e^{-i\omega t} dt = Y(\omega)e^{-i\omega t_0}$

It shows that time delays result in frequency-dependent phase shifts in the frequency domain (Section 3.3)

- *Frequency modulation* $\int_{-\infty}^{\infty} y(t)e^{i\omega_0 t}e^{-i\omega t} dt = Y(\omega - \omega_0)$

It shows that the apparent frequencies can be shifted after acquisition.

- *Causality* $\int_{-\infty}^{\infty} y(t)e^{-i\omega t} dt = \int_0^{\infty} y(t)e^{-i\omega t} dt$

It says that no signal is present before the radio-wave pulse (this is why we can start integration at $t = 0$ or $t = -\infty$, $y(t) = 0$ for $t < 0$). This provides an extra piece of information allowing us to reconstruct the imaginary part of the signal from the real one and vice versa (Figure 3.6 and Section 3.6.7).

3.2.2 Consequence of finite signal acquisition

In reality, the acquisition of signal stops at a finite time t_{\max} :

$$Y(\omega) = \int_0^{t_{\max}} \mathcal{A}e^{i(\Omega - R_2)t} dt = \mathcal{A} \frac{1 - e^{-R_2 t_{\max}} e^{i(\Omega - \omega)t_{\max}}}{R_2 - i(\Omega - \omega)}. \quad (3.5)$$

It has some undesirable consequences:

Leakage: Part of the signal is lost, peak height $Y(\Omega) < \mathcal{A}/R_2$.

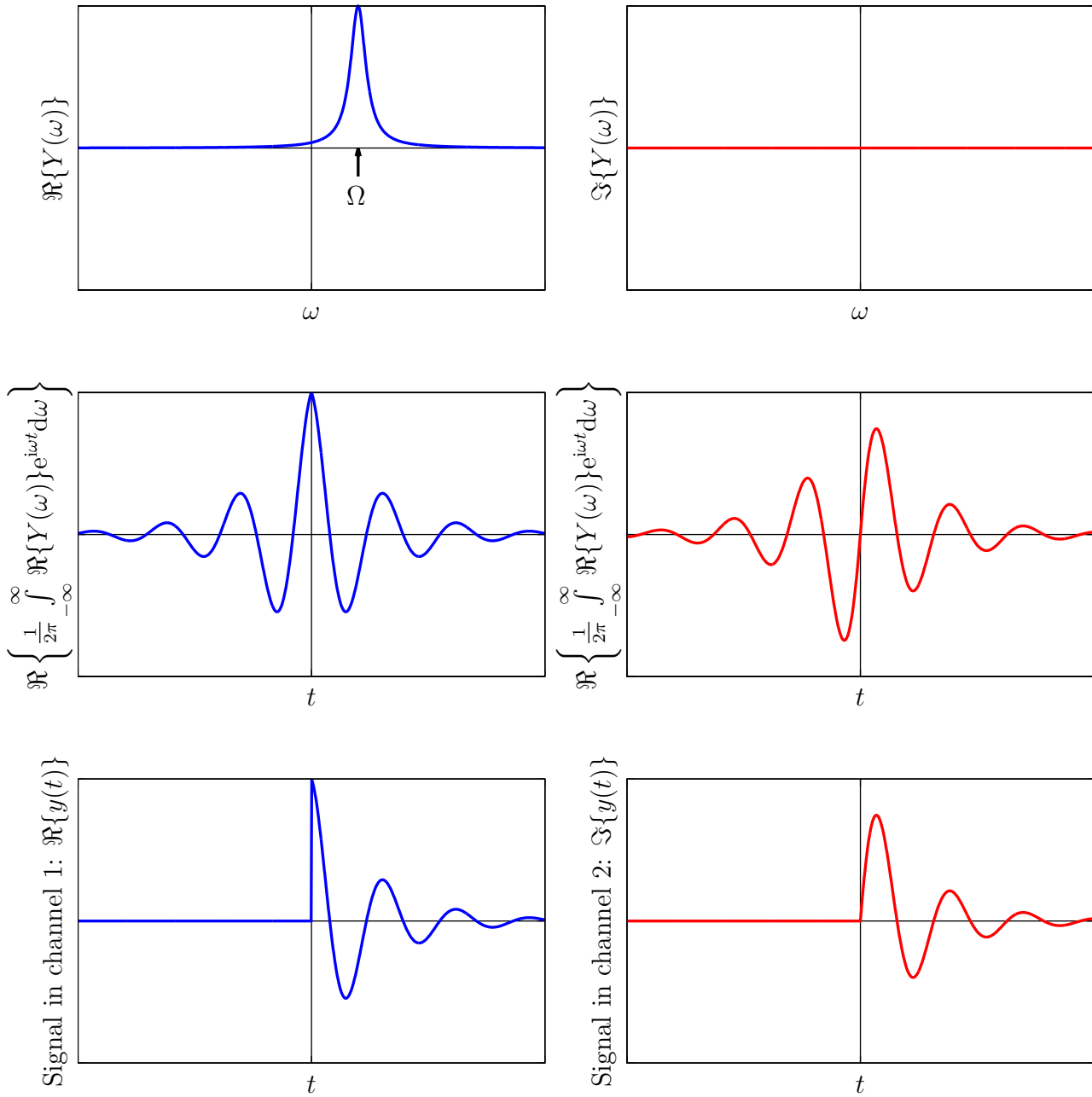


Figure 3.6: Causality of NMR signal. If we take a frequency spectrum, discard its imaginary part (the first row), and perform the inverse Fourier transformation, we do not get the original signal (starting at $t = 0$), but a set of symmetric (real part) and antisymmetric (imaginary part) functions predicting non-zero signal before $t = 0$ (the second row). However, we can apply our knowledge that no signal was present before $t = 0$ and multiply the left half of the predicted signal by zero. This recovers the actual signal (the third row). Fourier transformation of this signal provides both real and imaginary parts of the spectrum, as shown in Figure 3.2.

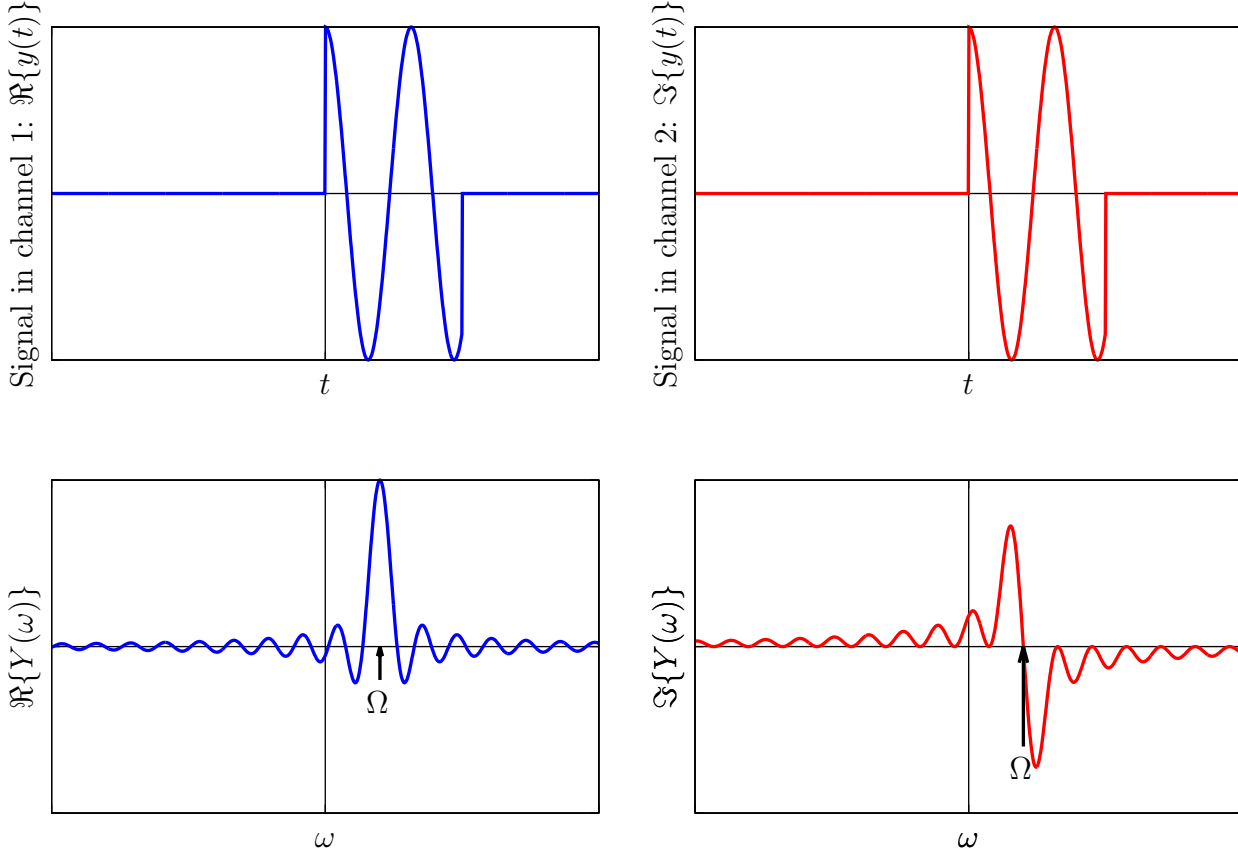


Figure 3.7: Effect of finite acquisition in the limit $R_2 \rightarrow 0$.

Truncation artifacts: For $R_2 \rightarrow 0$,

$$Y(\omega) = \int_0^{t_{\max}} \mathcal{A} e^{i(\Omega - \omega)t} dt = \mathcal{A} \frac{1 - e^{i(\Omega - \omega)t_{\max}}}{-i(\Omega - \omega)} = \mathcal{A} \frac{\sin(\Omega - \omega)t_{\max}}{\Omega - \omega} + i\mathcal{A} \frac{1 - \cos(\Omega - \omega)t_{\max}}{\Omega - \omega}. \quad (3.6)$$

If the acquisition is stopped before the signal relaxes completely, artifacts (baseline oscillation) appear. In the limit of no relaxation, the real part of the Fourier-transformed signal does not have a pure absorption shape (Lorentz curve), but has a shape of the $\sin(\Omega - \omega)t_{\max}/(\Omega - \omega)t_{\max}$ function (*sinc function*).

3.2.3 Discrete Fourier transformation

In reality, the acquired signal is finite ($t_{\max} < \infty$) and discrete ($\Delta t > 0$):

- $t \in \{0, \Delta t, 2\Delta t, \dots, (N - 1)\Delta t\}$ $y(t) \in \{y_0, y_1, y_2, \dots, y_{N-1}\}$
- $\omega \in \{0, \Delta\omega, 2\Delta\omega, \dots, (N - 1)\Delta\omega\}$ $Y(t) \in \{Y_0, Y_1, Y_2, \dots, Y_{N-1}\}$

or, expressing ω as $2\pi f$ (in Hertz)

$$\bullet f \in \{0, \Delta f, 2\Delta f, \dots, (N-1)\Delta f\} \quad Y(t) \in \{Y_0, Y_1, Y_2, \dots, Y_{N-1}\}$$

As shown in Section 3.6.8, the values of Δt , Δf and N are not independent in the discrete Fourier transformation, but they are restricted by the relation

$$\Delta f \Delta t = 1/N. \quad (3.7)$$

The consequences of the requirement $\Delta f \Delta t = 1/N$ are:

- spectral width $N\Delta f = 1/\Delta t$, it is defined by the choice of the time increment
- digital resolution $\Delta f = 1/N\Delta t$, it is defined by the choice of the maximum acquisition time

Possible definitions of the discrete Fourier transform with a correct normalization (so that $\Delta f \Delta t = 1/N$) are

$$Y_k = \sum_{j=0}^{N-1} y_j e^{-i\frac{2\pi}{N}kj} \quad y_j = \frac{1}{N} \sum_{k=0}^{N-1} Y_k e^{i\frac{2\pi}{N}kj} \quad (3.8)$$

or

$$Y_k = \frac{1}{\sqrt{N}} \sum_{j=0}^{N-1} y_j e^{-i\frac{2\pi}{N}kj} \quad y_j = \frac{1}{\sqrt{N}} \sum_{k=0}^{N-1} Y_k e^{i\frac{2\pi}{N}kj}. \quad (3.9)$$

3.2.4 Consequence of discrete signal acquisition

As derived in Section 3.6.9, the discrete "ideal" NMR signal

$$y_j = \mathcal{A} e^{-R_2 j \Delta t} e^{i2\pi \nu j \Delta t} \quad (3.10)$$

has a Fourier transform

$$Y_k = \sum_{j=0}^{N-1} \mathcal{A} e^{-R_2 j \Delta t} e^{i2\pi \nu j \Delta t} e^{-i\frac{2\pi}{N}kj} \Delta t = \mathcal{A} \Delta t \frac{1 - e^{-R_2 N \Delta t} e^{i\pi(N-2k)}}{1 + (1 - R_2 \Delta t) e^{-i2\pi \frac{k}{N}}}. \quad (3.11)$$

Since the signal is discrete, the spectral width is limited: $\Delta t > 0 \Rightarrow N\Delta f = 1/\Delta t < \infty$. The consequences of the discrete sampling are:

Aliasing: If we add a value of $N\Delta f$ to the frequency which was originally in the middle of the frequency spectrum ($\frac{1}{2}N\Delta f = \frac{1}{2\Delta t}$), i.e. add N to $k = N/2$ in Eq. 3.11, the last exponent in the sum in Eq. 3.11 changes from $i\pi j$ to $i3\pi j$, i.e. by one period (2π), and the transformed signal (the spectrum) does not change. In general, a peak of the real frequency $\nu + N\Delta f$ (outside the spectral width) appears at the apparent frequency ν in the spectrum (*Nyquist theorem:* frequencies ν and $\nu + 1/\Delta t$ cannot be distinguished).

Offset: Peak height of the continuous Fourier transform $Y(f) = \mathcal{A}/R_2$ and offset of the continuous Fourier transform $Y(\pm\infty) = 0$. Peak height of the discrete Fourier transform.

$$Y_{\frac{N}{2}} = \mathcal{A}\Delta t \frac{1 - e^{-R_2 N \Delta t}}{R_2 \Delta t} \rightarrow \mathcal{A}/R_2 \quad (3.12)$$

for $N\Delta t \rightarrow \infty$, but offset of the discrete Fourier transform

$$Y_0 = \mathcal{A}\Delta t \frac{1 - e^{-R_2 N \Delta t} e^{iN\pi}}{2 - R_2 \Delta t} \rightarrow \frac{1}{2} \mathcal{A}\Delta t = \frac{1}{2} y_0 \Delta t \quad (3.13)$$

for $N\Delta t \rightarrow \infty$ and $\Delta t \rightarrow 0$. The offset of discrete Fourier transform is non-zero, equal to half of the intensity of the signal at the first time point $y(0)$ if the signal was acquired sufficiently long to relax completely ($N\Delta t \gg 1/R_2$).

Loss of causality: The algorithm of the discrete Fourier transform assumes that the signal is periodic. This contradicts the causality theorem: a periodic function cannot be equal to zero for $t < 0$ and different from zero $t > 0$. The causality must be introduced in a sort of artificial manner. After recording N time points, another N zeros should be added to the signal² (see Section 3.4).

3.3 Phase correction

So-far, we ignored the effect of the initial phase ϕ_0 and analyzed Fourier transforms of NMR signals consisting of a collection of (damped) cosine functions, with zero initial phase. In reality, the signal has a non-zero phase, difficult to predict

$$y(t) = \mathcal{A}e^{-R_2 t} e^{i\Omega(t+t_0)} = |\mathcal{A}|e^{-R_2 t} e^{i\Omega(t+t_0)+\phi_0}. \quad (3.14)$$

The phase has a dramatic impact on the result of the Fourier transformation. Real and imaginary parts are mixtures of absorption and dispersion functions. If we plot the real part as a spectrum, it looks really ugly for a non-zero phase.

For a single frequency, the phase correction is possible (multiplication by the function $e^{-(i\Omega t_0 + \phi_0)}$, where t_0 and ϕ_0 are found empirically):

$$|\mathcal{A}|e^{-R_2 t} e^{i\Omega(t+t_0)+\phi_0} e^{-(i\Omega t_0 + \phi_0)} = |\mathcal{A}|e^{-R_2 t} e^{i\Omega t}. \quad (3.15)$$

In practice, phase corrections are applied also to signal with more frequencies – multiplication by a function $e^{-i(\vartheta_0 + \vartheta_1 \omega)}$, where ϑ_0 and ϑ_1 are zero-order and first-order phase corrections, respectively (we try to find ϑ_0 and ϑ_1 giving the best-looking spectra). **Note that phase correction is *always necessary*, but only approximative corrections are possible for a signal with multiple frequencies!**

3.4 Zero filling

Routinely, a sequence of N_Z zeros is appended to the recorded signal, mimicking data obtained at time points $N\Delta t$ to $(N + N_Z - 1)\Delta t$:

²In practice, the zeros are added *after* the last point of the measured signal, not before the first one, as one may expect based on the fact that signal should be equal to zero for $t < 0$.

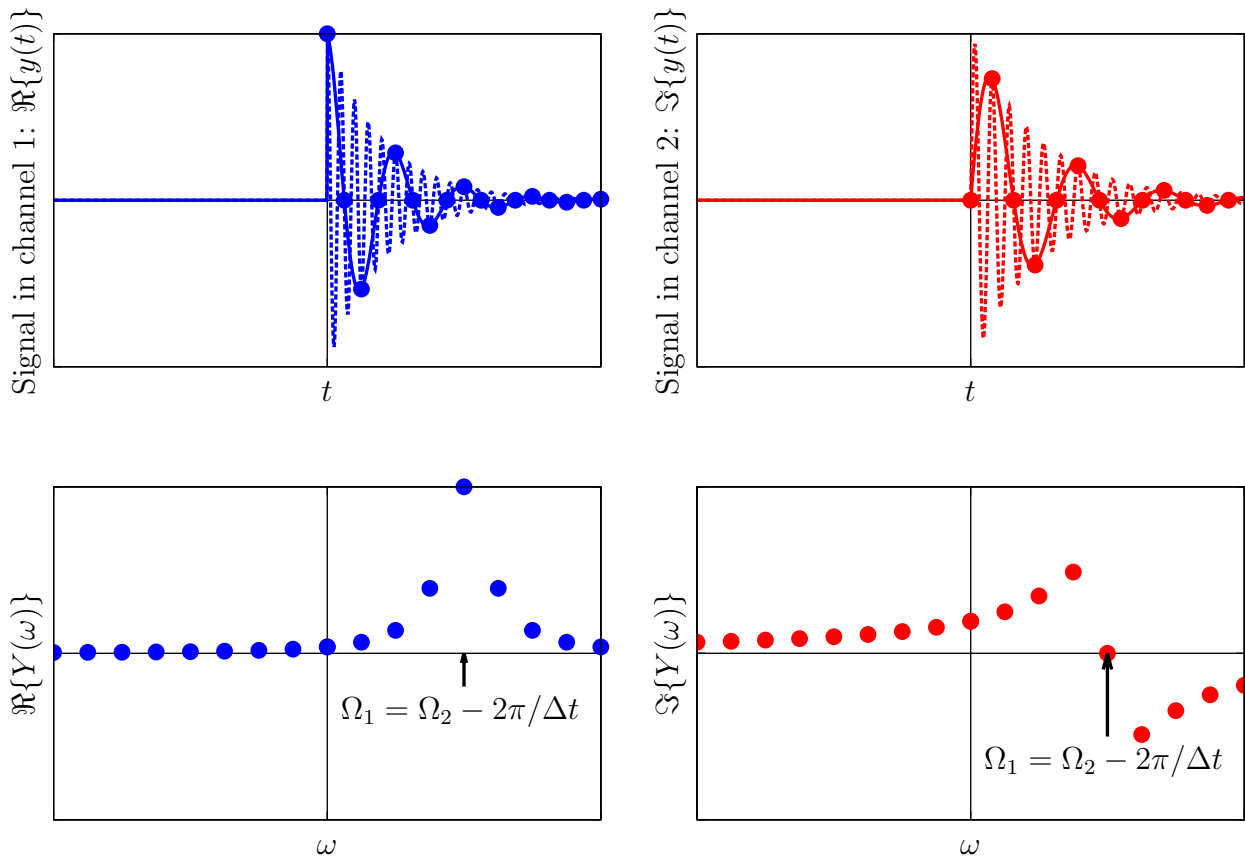


Figure 3.8: Aliasing. If the signal is acquired in discrete time intervals (dots in the top plots), the signals with frequencies different by an integer multiple of $2\pi/\Delta t$, shown by solid (Ω_1) and dotted (Ω_2) lines, cannot be distinguished. Both signals give a peak with the same frequency in the spectrum. This frequency is equal to Ω_1 and to $\Omega_2 - 2\pi/\Delta t$, where $2\pi/\Delta t$ is the width of the spectrum.

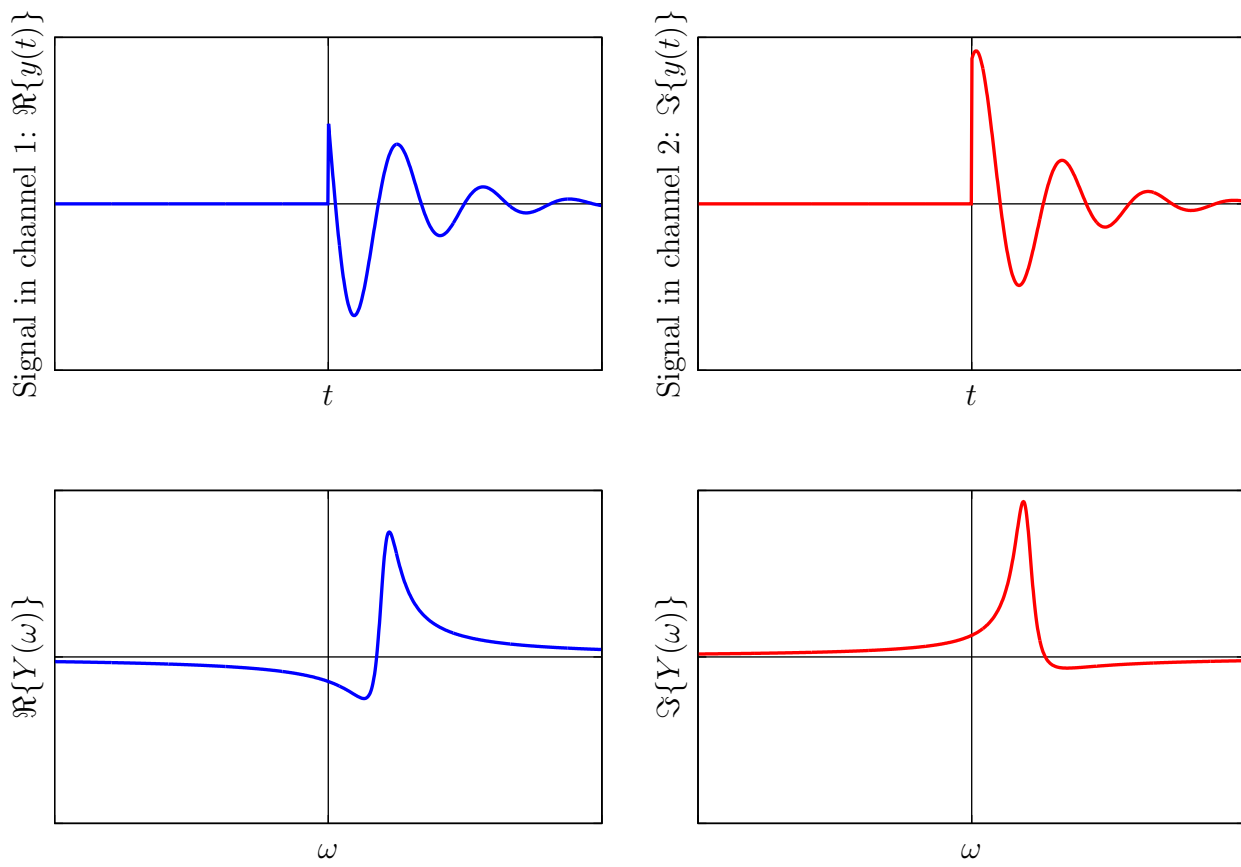


Figure 3.9: A signal with the initial phase of 60° (top) provides distorted spectra (bottom), unless a phase correction is applied.

$$\begin{array}{l}
0, \Delta t, 2\Delta t, \dots, (N-1)\Delta t \\
y_0, y_1, y_2, \dots, y_{N-1} \\
\downarrow \\
0, \Delta t, 2\Delta t, \dots, (N-1)\Delta t, N\Delta t, (N+1)\Delta t, \dots, (N+N_Z-1)\Delta t \\
y_0, y_1, y_2, \dots, y_{N-1}, \quad 0, \quad 0, \quad \dots, \quad 0
\end{array} \tag{3.16}$$

This may look like a completely artificial procedure, but there are several practical reasons to do it.

1. The very fast computational algorithm of calculating Fourier transform, known as *Cooley–Tukey FFT*, requires the number of time points to be an integer power of 2. If the number of collected time points N is not a power of 2, N_Z zeros are added to the data prior to Fourier transformation so that $N + N_Z$ is an integer power of 2.
2. In order to obtain a spectrum with the full content of information by discrete Fourier transformation, the collected data must be extended by a factor of 2 by zero-filling. As discussed in Section 3.2.4, this operation reintroduces causality and the full information content of N experimental complex points (i.e., N points of the real part and N points of the imaginary part, together $2N$ bits of information) is encoded in the spectrum (i.e., in the real part of the Fourier transform, which now consists of $2N$ frequency points because we artificially increased the maximum time from $N - 1$ to $2N - 1$ and therefore narrowed the frequency sampling step Δf from $1/N\Delta t$ to $1/2N\Delta t$).
3. The *digital resolution* $\Delta\nu$, given by $1/(N\Delta t)$, can be improved (narrowed) to $1/((N+N_Z)\Delta t)$ by zero-filling. In this manner, the visual appearance of spectra can be improved by interpolation between data points. **Note, however, that adding more than N zeros does not improve the informational content of the spectrum. Although the digital resolution is improved, the real resolution is the same, zero-filling does not help to resolve frequencies that differ less than $1/(N\Delta t)$!**

3.5 Apodization

The NMR signal is very often multiplied by a so-called *window function* prior to Fourier transformation.³ This process is known as *apodization*. The goal is to

1. *improve resolution*. As the resolution is given by $1/(N\Delta t)$, resolution is improved if the signal is multiplied by a window function that amplifies the late data points.
2. *improve sensitivity*. Due to the relaxation, signal of data acquired at later time points is lower, but the noise is the same. Therefore, the late time points decrease the signal-to-noise ratio. The sensitivity can be improved by discarding or attenuating the late time points.

³The mathematical expression describing the Fourier-transformed product of two functions, signal and window in our case, is given by the convolution theorem, presented in Section 3.2.1.

3. *suppress truncation artifacts*. We have seen that oscillations of the baseline appear if the data acquisition stops before the signal relaxes to zero (i.e., to the noise level). The desired effect of relaxation can be mimicked by a window function that smoothly converges to zero at $N\Delta t$.

Obviously, the three listed goals are in conflict, and only a compromise can be reached. **There is no "best apodization". The choice of the optimal window function depends on the actual needs.**

The simplest window function is a *rectangle*: multiplying the signal by a rectangular function equal to 1 for $j\Delta t \leq m\Delta t$ and to 0 for $j\Delta t > m\Delta t$ represents discarding data recorded for times longer than $m\Delta t$. It is a very useful way of improving signal-to-noise ratio if the signal relaxed before $m\Delta t$. Otherwise, it produces severe truncation artifacts.

The highest signal-to-noise ratio is provided by a *matched filter* window function. The matched filter has the shape of the envelope of the signal. The matched filter for our ideal signal is $e^{-R_2 j\Delta t}$. The price paid for the signal-to-noise improvement is a lower resolution: Multiplying $e^{-R_2 t} e^{i\Omega\Delta t}$ by $e^{-R_2 t}$ obviously doubles the linewidth, given by the decay rate, which is now $2R_2$. The best balance between resolution and truncation artifacts for an allowed extra line broadening λ is obtained with the *Dolph-Chebyshev* window, defined in Section 3.6.10, which is, however, not used in practice due to its very complex form. Instead, *sine-bell* windows $\sin^p\left(\frac{2\pi-\phi}{N}j + \phi\right)$ are used routinely, usually with the phase $\phi = \pi/2$ (i.e., cosine function) and with the power $p = 1$ or $p = 2$.

HOMEWORK

Derive equations describing continuous and discrete Fourier transformation of an ideal NMR signal (Sections 3.6.6 and 3.6.9, respectively), and check that you understand the consequences of using discrete Fourier transformation Section 3.2.4.

3.6 DERIVATIONS

3.6.1 Resonator impedance

The impedance of the coil circuit is given by

$$Z_c = \frac{1}{\frac{1}{Z_M} + \frac{1}{Z_T + Z_L + R}} = \frac{1}{i\omega C_M + \frac{1}{\frac{1}{i\omega C_T} + i\omega L + R}}.$$

3.6.2 Power and attenuation

Power is measured in the units of Watt, but the relative power is usually expressed on a logarithmic scale in decibells (dB). One Bell represents a ten-fold attenuation of power

$$\log_{10} \frac{P_2}{P_1} = \text{attenuation/B.} \quad (3.17)$$

Consequently,

$$10 \log_{10} \frac{P_2}{P_1} = \text{attenuation/dB} \quad (3.18)$$

and

$$20 \log_{10} \frac{P_2^2}{P_1^2} = 20 \log_{10} \frac{|\vec{B}_1|_2^2}{|\vec{B}_1|_1^2} = 10 \log_{10} \frac{|\vec{B}_1|_2}{|\vec{B}_1|_1} = \text{attenuation/dB.} \quad (3.19)$$

3.6.3 Quadrature detection and complex signal

Let us assume that the signal oscillates as a cosine function $\cos(\omega_0 t)$ and that the reference wave in the first channel is a cosine wave $\cos(\omega_{\text{ref}} t)$ and that the reference wave in the second channel is a sine wave $-\sin(\omega_{\text{ref}} t)$. Mathematically, the quadrature detection can be described as

$$\cos(\omega_0 t) \rightarrow \begin{cases} \frac{1}{2} \cos(\omega_0 t) \rightarrow \frac{1}{2} \cos(\omega_0 t) \cos(\omega_{\text{ref}} t) \\ \frac{1}{2} \cos(\omega_0 t) \rightarrow -\frac{1}{2} \cos(\omega_0 t) \sin(\omega_{\text{ref}} t) \end{cases} \quad (3.20)$$

Basic trigonometric identities show that the result of mixing in the first channel is a sum of a high-frequency cosine wave $\cos((\omega_0 + \omega_{\text{ref}})t)$ and a low-frequency cosine wave $\cos((\omega_0 - \omega_{\text{ref}})t)$, while the result of mixing in the second channel is a difference of the corresponding sine waves:

$$\frac{1}{2} \cos(\omega_0 t) \cos(\omega_{\text{ref}} t) = \frac{1}{4} \cos((\omega_0 + \omega_{\text{ref}})t) + \frac{1}{4} \cos((\omega_0 - \omega_{\text{ref}})t), \quad (3.21)$$

$$-\frac{1}{2} \cos(\omega_0 t) \sin(\omega_{\text{ref}} t) = -\frac{1}{4} \sin((\omega_0 + \omega_{\text{ref}})t) + \frac{1}{4} \sin((\omega_0 - \omega_{\text{ref}})t). \quad (3.22)$$

The high-frequency waves are filtered out by a low-pass filter, resulting in signals oscillating with a low frequency $\omega_0 - \omega_{\text{ref}}$. If $\omega_{\text{ref}} = -\omega_{\text{radio}}$, then $\omega_0 - \omega_{\text{ref}} = \Omega$. The procedure, similar to the demodulation in an ordinary radio receiver, thus produces audio signals in both channels

$$\cos(\omega_0 t) \rightarrow \begin{cases} \frac{1}{2} \cos(\omega_0 t) \rightarrow \frac{1}{2} \cos(\omega_0 t) \cos(\omega_{\text{ref}} t) \rightarrow \frac{1}{4} \cos(\Omega t) \\ \frac{1}{2} \cos(\omega_0 t) \rightarrow -\frac{1}{2} \cos(\omega_0 t) \sin(\omega_{\text{ref}} t) \rightarrow \frac{1}{4} \sin(\Omega t) \end{cases} \quad (3.23)$$

3.6.4 Noise accumulation

Here we analyze accumulation of the noise in repeated signal acquisition. The related physics is discussed later in Section 7.10.4. The noise $n(t)$ is random and so its average⁴ $\langle n(t) \rangle = 0$. The size of the noise is typically defined by the *root-mean-square* $\sqrt{\langle n(t)^2 \rangle}$. Sum of the noise from N independent experiments is

⁴To avoid writing the integrals defining averaging, we indicate the time average by the angled brackets.

$$\sqrt{\langle (n_1(t) + n_2(t) + \dots + n_N(t))^2 \rangle}. \quad (3.24)$$

Because the random motions of electrons in the individual experiments are not correlated (are independent), all terms like $\langle 2n_1(t)n_2(t) \rangle$ are equal to zero. Therefore, calculation of the square in Eq. 3.24 simplifies to

$$\sqrt{\langle (n_1(t) + n_2(t) + \dots + n_N(t))^2 \rangle} = \sqrt{\langle n_1(t)^2 \rangle + \langle n_2(t)^2 \rangle + \dots + \langle n_N(t)^2 \rangle}. \quad (3.25)$$

We can also assume that the root-mean-square is the same in all experiments, and write it as $\sqrt{\langle n(t)^2 \rangle}$. The sum of the noise can be then calculated as

$$\sqrt{N \langle n(t)^2 \rangle} = \sqrt{N} \sqrt{\langle n(t)^2 \rangle}. \quad (3.26)$$

We can now calculate the signal-to-noise ratio as

$$\frac{Ny(t)}{\sqrt{N} \sqrt{\langle n(t)^2 \rangle}} = \sqrt{N} \frac{y(t)}{\sqrt{\langle n(t)^2 \rangle}}. \quad (3.27)$$

3.6.5 Mathematical description of Fourier transformation

We start with a special case of a signal which can be described by a sum of cosine functions with frequencies that are integer multiples of some small frequency increment $\Delta\omega$. All such cosine functions must have the same value at time t and $t + 2\pi/\Delta\omega$: the whole signal is periodic with the period $2\pi/\Delta\omega$. If we record such a signal using quadrature detection, we obtain

$$y(t) = \sum_{k=-\infty}^{\infty} \mathcal{A}_k e^{i\omega_k t} = \sum_{k=-\infty}^{\infty} \mathcal{A}_k e^{ik\Delta\omega t}. \quad (3.28)$$

The mentioned periodicity allows us to determine \mathcal{A}_k by calculating the integrals

$$\int_0^{\frac{2\pi}{\Delta\omega}} y(t) e^{-i\omega_j t} dt = \sum_{j=-\infty}^{\infty} \mathcal{A}_j \int_0^{\frac{2\pi}{\Delta\omega}} e^{i(k-j)\Delta\omega t} dt = \frac{2\pi}{\Delta\omega} \mathcal{A}_k \quad (3.29)$$

(All integrated functions are periodic and their integrals are therefore equal to zero with the exception of the case when $k = j$, which is a constant function).

The same result is obtained for any integration limits which differ by $2\pi/\Delta\omega$, e.g.

$$\int_{-\frac{\pi}{\Delta\omega}}^{+\frac{\pi}{\Delta\omega}} y(t) e^{-i\omega_j t} dt = \sum_{j=-\infty}^{\infty} \mathcal{A}_j \int_{-\frac{\pi}{\Delta\omega}}^{+\frac{\pi}{\Delta\omega}} e^{i(k-j)\Delta\omega t} dt = \frac{2\pi}{\Delta\omega} \mathcal{A}_k \quad (3.30)$$

We can now continue in two different directions. We can describe the signal as it is actually measured, not as a continuous function of time, but as a discrete series of points sampled in time increments Δt . Then, the integral in Eq. 3.29 is replaced by summation of a finite number of measured signal points:

$$Y_k = \sum_{j=0}^{N-1} y_j e^{-ik\Delta\omega j \Delta t} \Delta t, \quad (3.31)$$

where $Y_k = \frac{2\pi}{\Delta\omega} \mathcal{A}_k$. As the time and frequency are treated in the same manner, we can also define the inverse operation

$$y_j = \sum_{k=0}^{N-1} Y_k e^{ik\Delta\omega j \Delta t} \Delta\omega. \quad (3.32)$$

This way of the signal analysis, discussed in more details in Section 3.2.3, handles the signal as it is measured in reality. It is also instructive to follow the other direction and to increase the period $2\pi/\Delta\omega$ by decreasing $\Delta\omega$. The series of ω_k becomes a continuous variable ω and $\pi/\Delta\omega \rightarrow \infty$ if $\Delta\omega \rightarrow 0$. The sum in Eq. 3.28 is replaced by the integral

$$y(t) = \frac{1}{2\pi} \int_{-\infty}^{\infty} Y(\omega) e^{i\omega t} d\omega \quad (3.33)$$

and the integral in Eq. 3.30 becomes

$$Y(\omega) = \int_{-\infty}^{\infty} y(t)e^{-i\omega t} dt. \quad (3.34)$$

If we apply Eq. 3.34 to a function $y(t)$ and Eq. 3.33 to the obtained result, we should get back the function $y(t)$. Such a double transformation can be written as

$$y(t) = \frac{1}{2\pi} \int_{-\infty}^{\infty} Y(\omega)e^{i\omega t} d\omega = \frac{1}{2\pi} \int_{-\infty}^{\infty} e^{i\omega t} d\omega \int_{-\infty}^{\infty} y(t')e^{-i\omega t'} dt' = \int_{-\infty}^{\infty} y(t') dt' \frac{1}{2\pi} \int_{-\infty}^{\infty} e^{i\omega(t-t')} d\omega. \quad (3.35)$$

This requires the second integral to be equal to 2π for $t' = t$ and to zero for $t' \neq t$. Therefore, the integral can be used to define the *delta* function

$$\delta(t - t') = \frac{1}{2\pi} \int_{-\infty}^{\infty} e^{i\omega(t-t')} d\omega. \quad (3.36)$$

An alternative definition

$$Y(\omega) = \frac{1}{\sqrt{2\pi}} \int_{-\infty}^{\infty} y(t)e^{-i\omega t} dt, \quad (3.37)$$

$$y(t) = \frac{1}{\sqrt{2\pi}} \int_{-\infty}^{\infty} Y(\omega)e^{i\omega t} d\omega. \quad (3.38)$$

is equally acceptable.

3.6.6 Fourier transformation of an ideal NMR signal

$$Y(\omega) = \int_{-\infty}^{\infty} y(t)e^{-i\omega t} dt = \int_0^{\infty} \mathcal{A}e^{i(\Omega-\omega)-R_2)t} dt = \frac{-\mathcal{A}}{i(\Omega-\omega) - R_2} = \mathcal{A} \frac{1}{R_2 - i(\Omega-\omega)} \frac{R_2 + i(\Omega-\omega)}{R_2 + i(\Omega-\omega)} = \mathcal{A} \frac{R_2 + i(\Omega-\omega)}{R_2^2 + (\Omega-\omega)^2} \quad (3.39)$$

3.6.7 Causality and reconstruction of imaginary signal

The mentioned consequence of causality is rather subtle. As mentioned above, the NMR signal is recorded in two channels, as a real and imaginary part of a complex number. It is because Fourier transformation of a cosine (or sine) function gives a symmetric (or antisymmetric) spectrum with two frequency peaks and thus does not allow us to distinguish frequencies higher than the carrier frequency from those lower than the carrier frequency. Once we have the transformed complex signal in the frequency domain, we can ask whether we need both its parts (real and imaginary). It looks like we do because the inverse Fourier transformation of just the real (imaginary) part produces a symmetric (antisymmetric) picture in the time domain (the second row in Figure 3.6). But the causality tells us that this is not a problem because we know that there is no signal left from the zero time – the symmetry does not bother us because we know that we can reconstruct the time signal simply by discarding the left half of the inverse Fourier image (the third row in Figure 3.6). The time signal reconstructed from the real part of the frequency spectrum only, can be then Fourier transformed to provide the missing imaginary part of the frequency spectrum.

3.6.8 Spectral width, resolution, and sampling

We may try to define the discrete Fourier transform as

$$Y_k = \sum_{j=0}^{N-1} y_j e^{-ik\Delta\omega_j \Delta t} \Delta t = \sum_{j=0}^{N-1} y_j e^{-i2\pi \Delta f \Delta t k j} \Delta t, \quad (3.40)$$

$$y_j = \sum_{k=0}^{N-1} Y_k e^{ik\Delta\omega_j \Delta t} \Delta t = \sum_{k=0}^{N-1} Y_k e^{i2\pi \Delta f \Delta t k j} \Delta f. \quad (3.41)$$

However, there is a catch here. It turns out that Δt and Δf are not independent, but closely related. The transformation can be written in a matrix form as

$$\begin{pmatrix} Y_0 \\ Y_1 \\ Y_2 \\ \vdots \\ Y_{N-1} \end{pmatrix} = \underbrace{\begin{pmatrix} F_{0,0} & F_{0,1} & F_{0,2} & \dots & F_{0,N-1} \\ F_{1,0} & F_{1,1} & F_{1,2} & \dots & F_{1,N-1} \\ F_{2,0} & F_{2,1} & F_{2,2} & \dots & F_{2,N-1} \\ \vdots & \vdots & \vdots & \ddots & \vdots \\ F_{N-1,0} & F_{N-1,1} & F_{N-1,2} & \dots & F_{N-1,N-1} \end{pmatrix}}_{\hat{F}} \begin{pmatrix} y_0 \\ y_1 \\ y_2 \\ \vdots \\ y_{N-1} \end{pmatrix} \Delta t, \quad (3.42)$$

where the elements of the matrix \hat{F} are $F_{jk} = e^{-i2\pi\Delta f\Delta t \cdot k \cdot j}$.

Let us now try to transform Y_k back to the time domain:

$$\begin{pmatrix} y_0 \\ y_1 \\ y_2 \\ \vdots \\ y_{N-1} \end{pmatrix} = \underbrace{\begin{pmatrix} F_{0,0}^{-1} & F_{0,1}^{-1} & F_{0,2}^{-1} & \dots & F_{0,N-1}^{-1} \\ F_{1,0}^{-1} & F_{1,1}^{-1} & F_{1,2}^{-1} & \dots & F_{1,N-1}^{-1} \\ F_{2,0}^{-1} & F_{2,1}^{-1} & F_{2,2}^{-1} & \dots & F_{2,N-1}^{-1} \\ \vdots & \vdots & \vdots & \ddots & \vdots \\ F_{N-1,0}^{-1} & F_{N-1,1}^{-1} & F_{N-1,2}^{-1} & \dots & F_{N-1,N-1}^{-1} \end{pmatrix}}_{\hat{F}^{-1}} \begin{pmatrix} Y_0 \\ Y_1 \\ Y_2 \\ \vdots \\ Y_{N-1} \end{pmatrix} \Delta f, \quad (3.43)$$

where the elements of the matrix \hat{F}^{-1} are $F_{jk}^{-1} = e^{+i2\pi\Delta f\Delta t \cdot k \cdot j}$. Substituting from Eq. 3.42,

$$\begin{pmatrix} y_0 \\ y_1 \\ y_2 \\ \vdots \\ y_{N-1} \end{pmatrix} = \begin{pmatrix} F_{0,0}^{-1} & F_{0,1}^{-1} & F_{0,2}^{-1} & \dots & F_{0,N-1}^{-1} \\ F_{1,0}^{-1} & F_{1,1}^{-1} & F_{1,2}^{-1} & \dots & F_{1,N-1}^{-1} \\ F_{2,0}^{-1} & F_{2,1}^{-1} & F_{2,2}^{-1} & \dots & F_{2,N-1}^{-1} \\ \vdots & \vdots & \vdots & \ddots & \vdots \\ F_{N-1,0}^{-1} & F_{N-1,1}^{-1} & F_{N-1,2}^{-1} & \dots & F_{N-1,N-1}^{-1} \end{pmatrix} \begin{pmatrix} F_{0,0} & F_{0,1} & F_{0,2} & \dots & F_{0,N-1} \\ F_{1,0} & F_{1,1} & F_{1,2} & \dots & F_{1,N-1} \\ F_{2,0} & F_{2,1} & F_{2,2} & \dots & F_{2,N-1} \\ \vdots & \vdots & \vdots & \ddots & \vdots \\ F_{N-1,0} & F_{N-1,1} & F_{N-1,2} & \dots & F_{N-1,N-1} \end{pmatrix} \begin{pmatrix} y_0 \\ y_1 \\ y_2 \\ \vdots \\ y_{N-1} \end{pmatrix} \Delta f \Delta t. \quad (3.44)$$

In order to get the original signal, the product of the transformation matrices, $\hat{F}^{-1}\hat{F}$ multiplied by $\Delta f\Delta t$, must be a unit matrix:

$$\begin{pmatrix} F_{0,0}^{-1} & F_{0,1}^{-1} & F_{0,2}^{-1} & \dots & F_{0,N-1}^{-1} \\ F_{1,0}^{-1} & F_{1,1}^{-1} & F_{1,2}^{-1} & \dots & F_{1,N-1}^{-1} \\ F_{2,0}^{-1} & F_{2,1}^{-1} & F_{2,2}^{-1} & \dots & F_{2,N-1}^{-1} \\ \vdots & \vdots & \vdots & \ddots & \vdots \\ F_{N-1,0}^{-1} & F_{N-1,1}^{-1} & F_{N-1,2}^{-1} & \dots & F_{N-1,N-1}^{-1} \end{pmatrix} \begin{pmatrix} F_{0,0} & F_{0,1} & F_{0,2} & \dots & F_{0,N-1} \\ F_{1,0} & F_{1,1} & F_{1,2} & \dots & F_{1,N-1} \\ F_{2,0} & F_{2,1} & F_{2,2} & \dots & F_{2,N-1} \\ \vdots & \vdots & \vdots & \ddots & \vdots \\ F_{N-1,0} & F_{N-1,1} & F_{N-1,2} & \dots & F_{N-1,N-1} \end{pmatrix} \Delta f \Delta t = \begin{pmatrix} 1 & 0 & 0 & \dots & 0 \\ 0 & 1 & 0 & \dots & 0 \\ 0 & 0 & 1 & \dots & 0 \\ \vdots & \vdots & \vdots & \ddots & \vdots \\ 0 & 0 & 0 & \dots & 1 \end{pmatrix}. \quad (3.45)$$

According to the matrix multiplication rule, the jl -element of the product $\hat{F}^{-1}\hat{F}$ is given by

$$\sum_{k=0}^{N-1} e^{-i2\pi\Delta f\Delta t(jk-kl)} \Delta t. \quad (3.46)$$

Clearly, the exponential terms in the sums representing the diagonal elements ($j = l$) are equal to $e^{-i2\pi\Delta f\Delta t(jk-kj)} \Delta t = e^0 = 1$. Therefore, the diagonal elements (sums of N terms $e^0 = 1$) are equal to N . Obviously, we need to set $N\Delta f\Delta t = 1$ to get the elements of the product $\hat{F}^{-1}\hat{F}$ equal to one.

What about the off-diagonal elements? For $N\Delta f\Delta t = 1$, the elements of $\hat{F}^{-1}\hat{F}$ are equal to

$$\sum_{k=0}^{N-1} e^{-i\frac{2\pi}{N}(j-l)k} \Delta t. \quad (3.47)$$

The complex numbers in the sum can be visualized as points in the Gauss plane (plane of complex numbers) with the phase of $2\pi k(l-j)/N$. Let us assume that N is an integer power of two ($N = 2^n$, a typical choice in discrete Fourier transform). Then all numbers in the series are symmetrically distributed in the Gauss plane. As a consequence, their sum is equal to zero (they cancel each other). We can therefore conclude that setting $N\Delta f\Delta t = 1$ ensures that the product $\hat{F}^{-1}\hat{F}$ is a unit matrix.

3.6.9 Discrete ideal signal

The ideal NMR signal converted to the digital form has a Fourier transform

$$Y_k = \sum_{j=0}^{N-1} \mathcal{A} e^{-R_2 j \Delta t} e^{i 2 \pi \nu j \Delta t} e^{-i \frac{2 \pi}{N} k j \Delta t}. \quad (3.48)$$

The summation formula⁵

$$\sum_{j=0}^{N-1} z^j = \frac{1 - z^N}{1 - z} \quad (3.49)$$

helps us to evaluate the sum. For the sake of simplicity, let us assume that the carrier frequency is chosen so that the peak is in the middle of the spectrum

$$\nu = \frac{1}{2} N \Delta f = \frac{1}{2 \Delta t}. \quad (3.50)$$

Then, z and z^N in the summation formula are

$$z = e^{-R_2 \Delta t} e^{i 2 \pi \left(\frac{1}{2} - \frac{k}{N} \right)} = \underbrace{e^{-R_2 \Delta t}}_{1 - R_2 \Delta t} \underbrace{e^{i \pi}}_{-1} e^{-i 2 \pi \frac{k}{N}} = -(1 - R_2 \Delta t) e^{-i 2 \pi \frac{k}{N}}, \quad (3.51)$$

$$z^N = e^{-R_2 N \Delta t} e^{i \pi (N - 2k)}. \quad (3.52)$$

Therefore,

$$Y_k = \mathcal{A} \Delta t \frac{1 - e^{-R_2 N \Delta t} e^{i \pi (N - 2k)}}{1 + (1 - R_2 \Delta t) e^{-i 2 \pi \frac{k}{N}}}. \quad (3.53)$$

3.6.10 Dolph–Chebyshev window

The Dolph–Chebyshev window function is defined as

$$\frac{1}{\sqrt{N}} \sum_{k=0}^{N-1} \frac{\cos \left(2(N-1) \arccos \frac{\cos(\pi k/N)}{\cos(\pi \lambda \Delta t/2)} \right)}{\cosh \left(2(N-1) \operatorname{arccosh} \frac{1}{\cos(\pi \lambda \Delta t/2)} \right)} e^{i \frac{2 \pi}{N} k j}. \quad (3.54)$$

⁵The summation formula can be derived easily. Write the sum

$$z^0 + z^1 + z^2 + \dots + z^{N-1} = \sum_{j=0}^{N-1} z^j$$

and multiply it by $(1 - z)$:

$$(1 - z)(z^0 + z^1 + z^2 + \dots + z^{N-1}) = z^0 - z^1 + z^1 - z^2 + z^2 - \dots - z^{N-1} + z^{N-1} - z^N = 1 - z^N = (1 - z) \sum_{j=0}^{N-1} z^j.$$

Divide the last equation on the previous line by $(1 - z)$ to obtain the summation formula.

Part II

Quantum description

Lecture 4

Review of quantum mechanics

Literature: This chapter starts with a brief review of quantum mechanics. Textbooks covering this topic represent the best source of information. Brown presents in B9 a useful review of classical mechanics, usually missing in the quantum mechanics textbooks (assuming that students learnt the classical mechanics earlier, which is true in the case of students of physics, but not so often in the case of chemistry or biology students), and reviews quantum mechanics in B13, B15, and B16. B1–B5 provides overview of the relevant mathematical tools. NMR books also provide some introduction. Keeler reviews quantum mechanics in very understandable fashion, using the concept of spin from the very beginning (K3.2 and K6). Levitt proceeds more like us (L6–7). A condensed summary is presented in C2.1 (short, rigorous, but not a good start for a novice).

4.1 Wave function and state of the system

Here we briefly review basics of quantum mechanics. Quantum mechanics was introduced because Newton mechanics did not describe experiments correctly. Quantum mechanics is postulated, not derived. It can be only tested experimentally. The basic differences between Newton and quantum mechanics are listed below.

- *Newton mechanics*: coordinates x, y, z and moments \vec{p} of all particles describe all properties of the current state and all future states
- *Quantum mechanics*: wave function Ψ describes all properties of the current state and all future states

We postulate that the state of the system is completely described by a *wave function*.

The two-slit (Young) experiment may serve as an example of motivation to use quantum mechanics to describe experimental results. The experiment (presumably known to the reader) asks the question whether the studied microscopic objects (e.g. electrons) are particles or waves. The answer is "Particles, but with probabilities combined like waves".¹ The wave function used to describe the studied object can be interpreted as a (complex) probability amplitude $\Psi = Ce^{i\phi}$. The (real) probability density is then $\rho = \Psi^*\Psi = |\Psi|^2 = |C|^2$ and the probability of finding single particle in volume

¹Quantum field theory provides more elegant description of fundamental "particles" than presented in this text. However, the relations presented in this text can be recovered from the quantum field approach.

L^3 is $\int_0^L \int_0^L \int_0^L \Psi^* \Psi dx dy dz$. We see that calculating a probability includes a calculation of square of the complex probability amplitude. Definitions of square values of different mathematical objects and the notation used in quantum mechanics are listed in Section 4.9.1.

Wave function of a free particle moving in direction x (coordinate frame can be always chosen so that x is the direction of motion of a free particle) can be written as

$$\Psi = C e^{i2\pi(\frac{x}{\lambda} - \frac{t}{T})} = C e^{\frac{i}{\hbar}(px - \mathcal{E}t)}, \quad (4.1)$$

where $h = 2\pi\hbar$ is the Planck's constant, $p = mv$ is momentum (along x), and \mathcal{E} is (kinetic) energy. Note that Ψ corresponds to a *monochromatic wave* with period equal to h/\mathcal{E} , wavelength equal to h/p , and a complex amplitude C (it may contain a phase factor $e^{i\phi}$).

4.2 Superposition and localization in space

Note that a monochromatic wave function describes exactly what is p of the particle (Figure 4.1A,B), but does not say anything about *position* of the particle because $\rho = \Psi^* \Psi = |C|^2$ is the same for any x (distribution of probability is constant from $x = -\infty$ to $x = \infty$, (Figure 4.1C). Wave function describing a particle (more) localized in space can be obtained by *superposition* of monochromatic waves (Figure 4.2).

$$\Psi(x, t) = c_1 \underbrace{A e^{\frac{i}{\hbar}(p_1 x - \mathcal{E}_1 t)}}_{\psi_1} + c_2 \underbrace{A e^{\frac{i}{\hbar}(p_2 x - \mathcal{E}_2 t)}}_{\psi_2} + \dots \quad (4.2)$$

We postulate that if possible states of our system are described by wave functions ψ_1, ψ_2, \dots , their linear combination also describes a possible state of the system.

Note that monochromatic waves are *orthogonal* and can be normalized (Section 4.9.2).

4.3 Operators and possible results of measurement

We postulated that the wave function contains a complete information about the system, but how can we extract this information from the wave function?

We postulate that any measurable property is represented by an operator (acting on the wave function) and that result of a measurement must be one of eigenvalues of the operator.

The term *eigenvalue* and a related term *eigenfunction* are explained and an example is given in Section 4.9.3.

In this text, we usually write operators with "hats", like \hat{A} . Writing $\hat{A}\Psi$ means "take function Ψ and modify it as described by \hat{A} ". It is *not* a multiplication: $\hat{A}\Psi \neq \hat{A} \cdot \Psi$, \hat{A} is not a number but an instruction what to do with Ψ !

A recipe to calculate *possible results of a measurement* is:

1. Identify the operator representing what you measure (\hat{A})

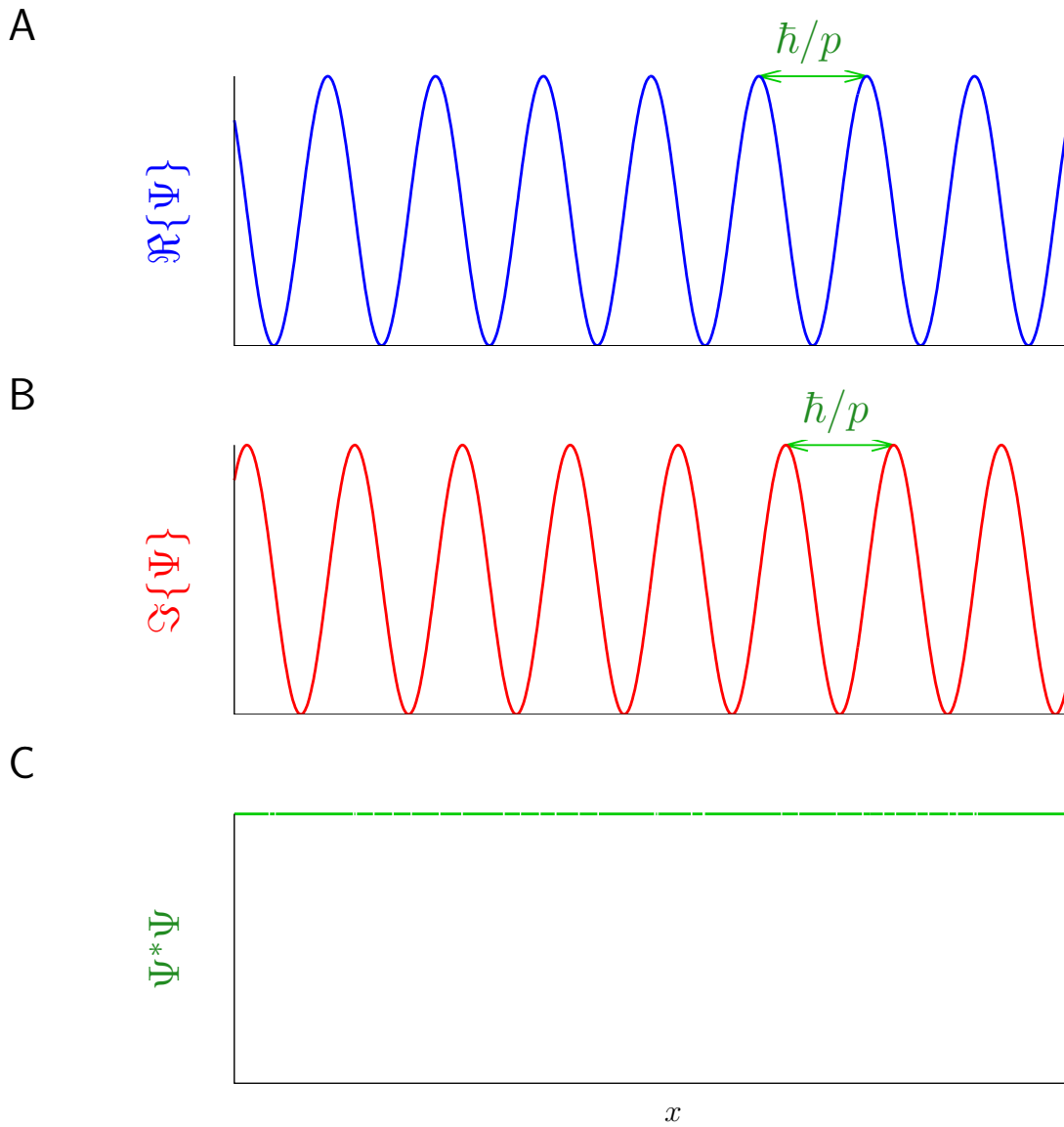
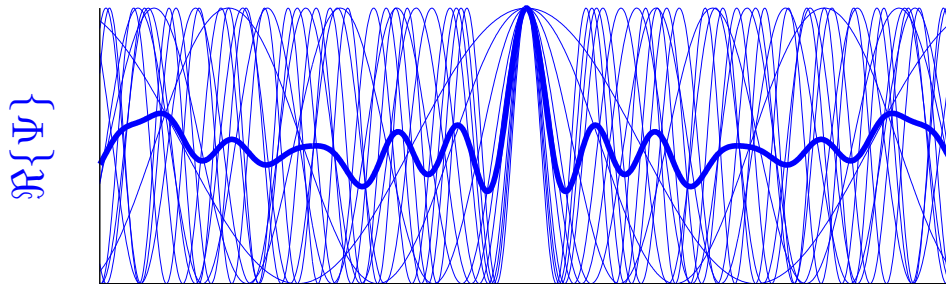
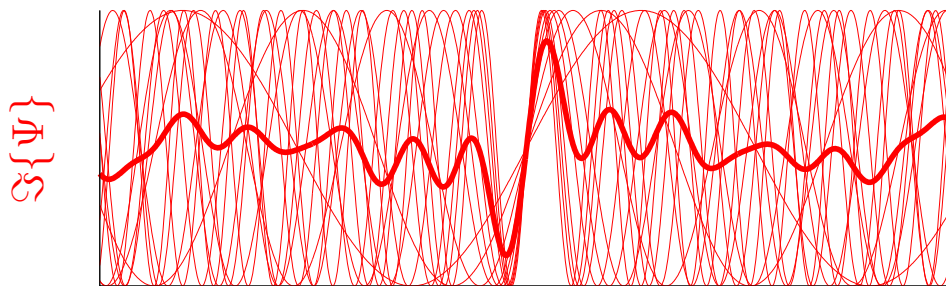


Figure 4.1: Free particle described by a monochromatic wave function Ψ . The real and imaginary parts of the wave function are plotted in Panels A and B, respectively, the probability density $\rho = \Psi^*\Psi$ is plotted in Panel C. Note that the wavelength and consequently the value of the momentum p is sharply defined (A,B), but the position of the particle is completely undefined (C).

A



B



C

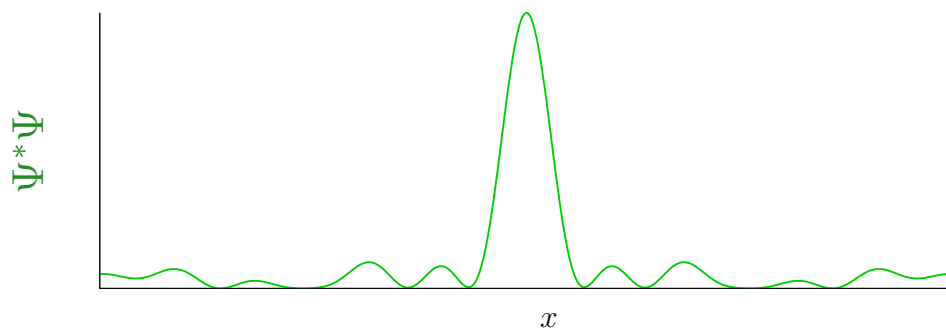


Figure 4.2: Free particle described by a superposition of ten monochromatic waves functions of the same amplitude.. The real and imaginary parts of the monochromatic wave functions (thin lines) and of the final wave function Ψ (normalized to have the same amplitude as the monochromatic wave functions, thick line) are plotted in Panels A and B, respectively, the probability density $\rho = \Psi^*\Psi$ is plotted in Panel C. Note that the position of the particle starts to be defined by the maximum of $\rho = \Psi^*\Psi$, but the wavelength and consequently the value of the momentum p is no longer well defined (A,B).

2. Find all eigenfunctions $|\psi_1\rangle, |\psi_2\rangle, \dots$ of the operator and use them as an *orthonormal basis*² for Ψ : $\Psi = c_1|\psi_1\rangle + c_2|\psi_2\rangle, \dots$
3. Calculate individual eigenvalues A_j as

$$\langle \psi_j | \hat{A} \psi_j \rangle = \langle \psi_j | A_j \cdot \psi_j \rangle = A_j \underbrace{\langle \psi_j | \psi_j \rangle}_{=1} = A_j. \tag{4.3}$$

The first equation in 4.3 follows from the definition of eigenfunctions, then A_j is just a (real) number and can be factored out of the brackets (representing integration or summation) as described by the second equation, and the last equation in 4.3 reflects orthonormality of $|\psi_j\rangle$.

4.4 Expected result of measurement

Eq. 4.3 tells us what are the *possible* results of a measurement, but it does not say which value *is actually measured*. We can only calculate probabilities of getting individual eigenvalues and predict the expected result of the measurement.

We postulate that the expected result of measuring a quantity A represented by an operator \hat{A} in a state of the system described by a wave function Ψ is

$$\langle A \rangle = \langle \Psi | \hat{A} | \Psi \rangle. \tag{4.4}$$

There are three ways how to do the calculation described by Eq. 4.4:

1. Express Ψ , calculate its complex conjugate $\Psi^* \equiv \langle \Psi |$, calculate $\hat{A}\Psi \equiv |\hat{A}\Psi\rangle$, and in the manner of Eq. 4.43

$$\langle A \rangle = \langle \Psi | \hat{A} | \Psi \rangle \equiv \langle \Psi | (\hat{A}\Psi) \rangle = \int_{-\infty}^{\infty} \Psi^*(x, \dots) \hat{A}\Psi(x, \dots) dx \dots \tag{4.5}$$

Three dots in Eq. 4.5 tell us that for anything else that a single free particle (with zero spin) we integrate over all degrees of freedom, not just over x .

2. Find eigenfunctions ψ_1, ψ_2, \dots of \hat{A} and write Ψ as their linear combination $\Psi = c_1\psi_1 + c_2\psi_2 + \dots$ (use the eigenfunctions as an *orthonormal basis* for Ψ). Due to the orthonormality of the basis functions, the result of Eq. 4.5 is $\langle A \rangle = c_1^*c_1A_1 + c_2^*c_2A_2 + \dots$, where A_1, A_2, \dots are eigenvalues of \hat{A} . We see that $\langle A \rangle$ is a *weighted average* of eigenvalues A_j with the weights equal to the squares of the coefficients ($c_j^*c_j = |c_j|^2$). The same result is obtained if we calculate

$$\langle A \rangle = (c_1^* \ c_2^* \ \dots) \begin{pmatrix} A_1 & 0 & \dots \\ 0 & A_2 & \dots \\ \vdots & \vdots & \ddots \end{pmatrix} \begin{pmatrix} c_1 \\ c_2 \\ \vdots \end{pmatrix}. \tag{4.6}$$

²The term "orthonormal basis" is described in Section 4.9.2.

We see that we can replace (i) operators by two-dimensional diagonal matrices, with eigenvalues forming the diagonal, and (ii) wave functions by one-dimensional matrices (known as *state vectors*) composed of the coefficients c_j . Eq. 4.6 shows calculation of the expected results of the measurement of A using *matrix representation* of operators and wave functions. Matrix representation is a big simplification because it allows us to calculate $\langle A \rangle$ without knowing how the operator \hat{A} and its eigenfunctions look like! We just need the eigenvalues and coefficients c_j . This simplification is possible because the right coefficients are defined by the right choice of the basis.

3. Write Ψ as a linear combination of basis functions ψ'_1, ψ'_2, \dots (not necessarily eigenfunctions of \hat{A})

$$\Psi = c'_1 \psi'_1 + c'_2 \psi'_2 + \dots \quad (4.7)$$

Build a two-dimensional matrix \hat{P}' from the products of coefficients $c'_j c'_k$:

$$\hat{P}' = \begin{pmatrix} c'_1 c'_1 & c'_1 c'_2 & \dots \\ c'_2 c'_1 & c'_2 c'_2 & \dots \\ \vdots & \vdots & \ddots \end{pmatrix}. \quad (4.8)$$

Multiply the matrix \hat{P}' by a matrix³ \hat{A}' representing the operator \hat{A} in the basis ψ'_1, ψ'_2, \dots . The sum of the diagonal elements (called *trace*) of the resulting matrix $\hat{P}'\hat{A}'$ is equal to the expected value $\langle A \rangle$

$$\langle A \rangle = \text{Tr}\{\hat{P}'\hat{A}'\}. \quad (4.9)$$

Why should we use such a bizarre way of calculating the expected value of A when it can be calculated easily from Eq. 4.6? The answer is that Eq. 4.9 is *more general*. We can use the same basis for operators with different sets of eigenfunctions.

4.5 Operators of position and momentum, commutators

We need to find operators in order to describe measurable quantities. Let us start with the most fundamental quantities, *position* of a particle x and *momentum* $p = mv$. Their operators are defined in terms of a general relation of two operator. If we apply two operators subsequently to the same wave function, order of the operators sometimes does not matter

³How can we get a matrix representation of an operator with eigenfunctions different from the basis? The complete set of N functions defines an abstract N -dimensional space ($N = \infty$ for free particles!). The wave function Ψ is represented by a vector in this space built from coefficients c'_1, c'_2, \dots , as described by Eq. 4.7, and a change of the basis is described as a rotation in this space. The same rotation describes how the matrix representing the operator \hat{A} changes upon changing the basis. Note that the matrix is not diagonal if the basis functions are not eigenfunctions of \hat{A} .

$$\hat{A}\hat{B}f = \hat{B}\hat{A}f \quad \Rightarrow \quad \hat{A}\hat{B}f - \hat{B}\hat{A}f = 0. \quad (4.10)$$

However, sometimes the order of operators makes a difference

$$\hat{A}\hat{B}f \neq \hat{B}\hat{A}f \quad \Rightarrow \quad \hat{A}\hat{B}f - \hat{B}\hat{A}f \neq 0. \quad (4.11)$$

The difference is known as the *commutator* and is written as

$$\hat{A}\hat{B}f - \hat{B}\hat{A}f = [\hat{A}, \hat{B}]f. \quad (4.12)$$

A non-zero commutator tells us that the quantities represented by \hat{A} and \hat{B} are not independent and cannot be measured exactly at the same time.

We postulate that operators of position and momentum obey the relations

$$[\hat{r}_j, \hat{p}_k] = i\hbar\delta_{jk} \quad [\hat{r}_j, \hat{r}_k] = [\hat{p}_j, \hat{p}_k] = 0. \quad (4.13)$$

Note that we only postulate relations between operators. Various choices of expressing the operators are possible and correct as long as Eq. 4.13 holds. A frequently used choice is described below.

The wave function $\Psi(x, t)$ defined by Eq. 4.2 is a function of the position of the particle, not of the momentum (it is a sum of contributions of *all* possible momenta). If we define basis as a set of functions $\psi_j = \Psi(x_j, t)$ for all possible positions x_j , operator of position is simply *multiplication by the value of the coordinate* describing the given position (see Section 4.9.4). Operators of the positions in the y and z directions are defined in the same manner.

$$\hat{x} \equiv x \cdot \quad \hat{y} \equiv y \cdot \quad \hat{z} \equiv z \cdot \quad (4.14)$$

In Section 4.9.3, an operator of momentum of a particle moving in the x direction is obtained by calculating $\partial\Psi/\partial x$ (Eq. 4.51). If a particle moves in a general direction, operators of components of the momentum tensor are derived in the same manner.

$$\hat{p}_x \equiv -i\hbar \frac{\partial}{\partial x}, \quad (4.15)$$

$$\hat{p}_y \equiv -i\hbar \frac{\partial}{\partial y}, \quad (4.16)$$

$$\hat{p}_z \equiv -i\hbar \frac{\partial}{\partial z}. \quad (4.17)$$

It is shown in Section 4.9.5 that such a choice is compatible with the postulate described by Eq. 4.13. Note that the commutator relations described in Section 4.9.5 follow from the way how we defined Ψ in Eq. 4.2. However, we can also use Eq. 4.13 as the fundamental definition and Eq. 4.2 as its consequence. This is how we postulate the definition of the position and momentum operators here.

4.6 Operator of energy and equation of motion

The arguments presented in Section 4.9.6 show that the eigenvalues of the total (kinetic and potential) energy of a free particle can be obtained by calculating $\partial\Psi/\partial t$. If the particles experience forces that depend only on the coordinates (and can be calculated as gradients of the potential energy), the sum of kinetic and potential energy is equal to the Hamiltonian \mathcal{H} in the classical mechanics (Section 0.2). The same term is used for the corresponding quantum mechanical operator, labeled \hat{H} .

The association of Hamiltonian (energy operator) with the time derivative makes it essential for analysis of dynamics of systems in quantum mechanics:

We postulate that evolution of a system in time is given by the Hamiltonian:

$$i\hbar\frac{\partial\Psi}{\partial t} = \hat{H}\Psi. \quad (4.18)$$

Note that our first postulate (the wave function completely describes the system, including its future) requires that the wave equation contains only the first time derivative (not e.g. the second time derivative). The explanation is provided in Section 4.9.7.

Eq.4.18 can be also written for matrix representation of Ψ and \hat{H} . If eigenfunctions of \hat{H} are used as a basis ($\Psi = c_1(t)\psi_1 + c_2(t)\psi_2 + \dots$), the time-independent eigenfunctions ψ_j can be factored out from $\partial\Psi/\partial t$ (left-hand side) and Ψ (right-hand side), and canceled, giving

$$i\hbar\frac{d}{dt}\begin{pmatrix} c_1 \\ c_2 \\ \vdots \end{pmatrix} = \begin{pmatrix} \mathcal{E}_1 & 0 & \dots \\ 0 & \mathcal{E}_2 & \dots \\ \vdots & \vdots & \ddots \end{pmatrix} \begin{pmatrix} c_1 \\ c_2 \\ \vdots \end{pmatrix}, \quad (4.19)$$

which is simply a set of independent differential equations

$$\frac{dc_j}{dt} = -i\frac{\mathcal{E}_j}{\hbar}c_j \quad \Rightarrow \quad c_j = a_j e^{-i\frac{\mathcal{E}_j}{\hbar}t}, \quad (4.20)$$

where the (possibly complex) integration constant a_j is given by the value of c_j at $t = 0$.

Note that the coefficients c_j evolve, but the products $c_j^*c_j = |a_j|^2$ do not change in time. Each product $c_j^*c_j$ describes the probability that the system is in the state with the energy equal to the eigenvalue \mathcal{E}_j , described by an eigenfunction ψ_j .

- States corresponding to the eigenfunctions of the Hamiltonian are *stationary* (do not vary in time).
- Only stationary states can be described by the *energy level diagram*.

Since our goal is quantum description of NMR, it is useful to see how is the evolution of a wave function influenced by the magnetic fields. Therefore, we list the equations of motions for wave functions describing a free particle, a particle in an electric field, and a particle in an electric and magnetic field. All three variants are known as the *Schrödinger equation*.

- *Free particle*. As shown in Section 4.9.6, a wave function describing a free particle evolves as

$$i\hbar \frac{\partial \Psi}{\partial t} = \underbrace{\left(-\frac{\hbar^2}{2m} \left(\frac{\partial^2}{\partial x^2} + \frac{\partial^2}{\partial y^2} + \frac{\partial^2}{\partial z^2} \right) \right)}_{\hat{H}} \Psi. \quad (4.21)$$

- *Charged particle in an electric field.* Electric forces depend only on the position of the charge in the electrical field. Therefore, the electric potential energy can be described as $QV(x, y, z)$, where Q is the electric charge and $V(x, y, z)$ is an electrostatic potential. As follows from the classical mechanics (Section 0.2), and is also shown in Section 4.9.6, the effect of an electric field is accounted for simply by adding the electric potential energy $\mathcal{E}_{\text{pot}}(x, y, z) = QV(x, y, z)$ to the Hamiltonian

$$i\hbar \frac{\partial \Psi}{\partial t} = \underbrace{\left(-\frac{\hbar^2}{2m} \left(\frac{\partial^2}{\partial x^2} + \frac{\partial^2}{\partial y^2} + \frac{\partial^2}{\partial z^2} \right) + QV(x, y, z) \right)}_{\hat{H}} \Psi. \quad (4.22)$$

- *Charged particle in an electromagnetic field.* The real challenge is to describe the effect of the magnetic field on the evolution in time. The problem is that the magnetic force does not depend solely on the position in the field, but also on the *velocity* of the charge (Eq. 69). This case is analyzed in detail in Section 0.2.2, showing that the effect of the magnetic field can be described by the *vector potential*, a vector quantity that can be used to define the magnetic induction $\vec{B} = \vec{\nabla} \times \vec{A} = \left(\frac{\partial A_z}{\partial y} - \frac{\partial A_y}{\partial z}, \frac{\partial A_x}{\partial z} - \frac{\partial A_z}{\partial x}, \frac{\partial A_y}{\partial x} - \frac{\partial A_x}{\partial y} \right)$. As shown in Section 0.2.2, the vector potential modifies the momentum $\vec{p} \rightarrow \vec{p} - Q\vec{A}$ and the resulting wave equation is

$$i\hbar \frac{\partial \Psi}{\partial t} = \underbrace{\left(-\frac{\hbar^2}{2m} \left(\left(\frac{\partial}{\partial x} + QA_x \right)^2 + \left(\frac{\partial}{\partial y} + QA_y \right)^2 + \left(\frac{\partial}{\partial z} + QA_z \right)^2 \right) + QV(x, y, z) \right)}_{\hat{H}} \Psi. \quad (4.23)$$

4.7 Operator of angular momentum

In order to understand NMR experiments, we also need to describe *rotation* in space. The fundamental quantity related to the rotation is the *angular momentum*. In a search for its operator, we start from what we know, position and momentum operators. We use classical physics and just replace the values of coordinates and momentum components by their operators.

Classical definition of the vector of angular momentum \vec{L} is

$$\vec{L} = \vec{r} \times \vec{p}. \quad (4.24)$$

The vector product represents the following set of equations:

$$L_x = r_y p_z - r_z p_y, \quad (4.25)$$

$$L_y = r_z p_x - r_x p_z, \quad (4.26)$$

$$L_z = r_x p_y - r_y p_x. \quad (4.27)$$

Going to the operators

$$\hat{L}_x = \hat{r}_y \hat{p}_z - \hat{r}_z \hat{p}_y = -i\hbar y \frac{\partial}{\partial z} + i\hbar z \frac{\partial}{\partial y}, \quad (4.28)$$

$$\hat{L}_y = \hat{r}_z \hat{p}_x - \hat{r}_x \hat{p}_z = -i\hbar z \frac{\partial}{\partial x} + i\hbar x \frac{\partial}{\partial z}, \quad (4.29)$$

$$\hat{L}_z = \hat{r}_x \hat{p}_y - \hat{r}_y \hat{p}_x = -i\hbar x \frac{\partial}{\partial y} + i\hbar y \frac{\partial}{\partial x}, \quad (4.30)$$

$$\hat{L}^2 = \hat{L}_x^2 + \hat{L}_y^2 + \hat{L}_z^2. \quad (4.31)$$

As shown in Section 4.9.9

$$[\hat{L}_x, \hat{L}_y] = i\hbar \hat{L}_z, \quad (4.32)$$

$$[\hat{L}_y, \hat{L}_z] = i\hbar \hat{L}_x, \quad (4.33)$$

$$[\hat{L}_z, \hat{L}_x] = i\hbar \hat{L}_y, \quad (4.34)$$

but

$$[\hat{L}^2, \hat{L}_x] = [\hat{L}^2, \hat{L}_y] = [\hat{L}^2, \hat{L}_z] = 0. \quad (4.35)$$

Note that

- Two components of angular momentum cannot be measured exactly at the same time
- Eqs. 4.32–4.35 can be used as a definition of angular momentum operators if the position and momentum operators are not available.⁴

Relation between the angular momentum and rotation is discussed in Section 4.9.8.

⁴Eqs. 4.32–4.35 are sometimes written in a condensed form as $[\hat{L}_j, \hat{L}_k] = i\hbar \epsilon_{jkl} \hat{L}_l$ and $[\hat{L}^2, \hat{L}_j] = 0$, where $j, k, l \in \{x, y, z\}$ and $\epsilon_{jkl} = 1$ for $jkl = xyz$ or any even permutation of x, y, z in ϵ_{xyz} (even number of exchanges of subscripts x, y, z in ϵ_{xyz} , e.g. ϵ_{yzx} is obtained by two exchanges: first $x \leftrightarrow y$ and subsequently $x \leftrightarrow z$), $\epsilon_{jkl} = -1$ for any odd permutation of x, y, z in ϵ_{xyz} , $\epsilon_{jkl} = 0$ for two or three identical subscripts (e.g. ϵ_{xyy}).

4.8 Operator of orbital magnetic moment

Knowing the operator of the angular momentum, we can easily define the operators of the orbital magnetic moment.

A moving charged particle can be viewed as an electric current. Classical definition of the magnetic moment of a charged particle travelling in a circular path (orbit) is (Section 0.1.7)

$$\vec{\mu} = \frac{Q}{2}(\vec{r} \times \vec{v}) = \frac{Q}{2m}(\vec{r} \times \vec{p}) = \frac{Q}{2m}\vec{L} = \gamma\vec{L}, \quad (4.36)$$

where Q is the charge of the particle, m is the mass of the particle, \vec{v} is the velocity of the particle, and γ is known as the *magnetogyric ratio (constant)*.⁵

Therefore, we can write the operators

$$\hat{\mu}_x = \gamma\hat{L}_x \quad \hat{\mu}_y = \gamma\hat{L}_y \quad \hat{\mu}_z = \gamma\hat{L}_z \quad \hat{\mu}^2 = \gamma^2\hat{L}^2. \quad (4.37)$$

Finally, we can define the operator of energy (Hamiltonian) of a magnetic moment in a magnetic field. Classically, the energy of a magnetic moment $\vec{\mu}$ in a magnetic field of induction \vec{B} is $\mathcal{E} = -\vec{\mu} \cdot \vec{B}$. Accordingly, the Hamiltonian of the interactions of an orbital magnetic moment with a magnetic field is

$$\hat{H} = -B_x\hat{\mu}_x - B_y\hat{\mu}_y - B_z\hat{\mu}_z = -\gamma(B_x\hat{L}_x + B_y\hat{L}_y + B_z\hat{L}_z) = -\frac{Q}{2m}(B_x\hat{L}_x + B_y\hat{L}_y + B_z\hat{L}_z). \quad (4.38)$$

In contrast to the operators of orbital angular momentum and magnetic moment, derivation of intrinsic angular momentum, known as the *spin*, and of the associated magnetic moment, requires a more fundamental (and much more demanding) approach. We discuss such approach in the next Lecture.

HOMework

As a preparation for the next lecture, derive the Dirac equation (Section 5.7.1), and check if you understand why the $\hat{\gamma}$ matrices in Dirac equation (Eq. 5.2) can have the required properties, whereas numbers cannot (Section 5.7.2).

⁵The term *gyromagnetic ratio* is also used.

4.9 DERIVATIONS

4.9.1 Calculating square

Recall how "square" is calculated for various mathematical objects: for a real number $c^2 = cc$, for a complex number $|c|^2 = cc^*$, for vector \vec{v} composed of N real numbers v_1, v_2, \dots , which can be written in a matrix form as a row or column of the numbers v_1, v_2, \dots ,

$$|v|^2 = \vec{v} \cdot \vec{v} = v_1 v_1 + v_2 v_2 + \dots = \sum_{j=1}^N v_j v_j = (v_1 \ v_2 \ \dots) \begin{pmatrix} v_1 \\ v_2 \\ \vdots \end{pmatrix}, \quad (4.39)$$

for a vector \vec{v} composed of N complex numbers $c_1 = a_1 + ib_1, c_2 = a_2 + ib_2, \dots$

$$|v|^2 = \vec{v}^\dagger \cdot \vec{v} = c_1^* c_1 + c_2^* c_2 + \dots = \sum_{j=1}^N c_j^* c_j = \sum_{j=1}^N (a_j - ib_j)(a_j + ib_j) = (c_1^* \ c_2^* \ \dots) \begin{pmatrix} c_1 \\ c_2 \\ \vdots \end{pmatrix} = (a_1 - ib_1 \quad a_2 - ib_2 \quad \dots) \begin{pmatrix} a_1 + ib_1 \\ a_2 + ib_2 \\ \vdots \end{pmatrix}, \quad (4.40)$$

for a (continuous and possibly complex) function

$$\int_{-\infty}^{\infty} f^*(x) f(x) dx \quad (4.41)$$

(function can be viewed as a vector of infinite number of infinitely "dense" elements, summation is therefore replaced by integration). Paul Dirac introduced the following notation: $\langle v|, |f\rangle$ is a vector v or function f , respectively, and

$$\langle v|v\rangle = \vec{v}^\dagger \cdot \vec{v} = \sum_{j=1}^N v_j^* v_j, \quad (4.42)$$

$$\langle f|f\rangle = \int_{-\infty}^{\infty} f^*(x) f(x) dx. \quad (4.43)$$

4.9.2 Orthogonality and normalization of monochromatic waves

Note that monochromatic waves are *orthogonal*, i.e., a scalar product of two waves differing in p is equal to zero:

$$\begin{aligned} \langle \psi_1 | \psi_2 \rangle &= \int_{-\infty}^{\infty} \psi_1^* \psi_2 dx = \int_{-\infty}^{\infty} \mathcal{A}^* e^{-\frac{i}{\hbar}(p_1 x - \mathcal{E}_1 t)} \mathcal{A} e^{\frac{i}{\hbar}(p_2 x - \mathcal{E}_2 t)} dx = |\mathcal{A}|^2 e^{\frac{i}{\hbar}(\mathcal{E}_1 - \mathcal{E}_2)t} \int_{-\infty}^{\infty} e^{\frac{i}{\hbar}(p_1 - p_2)x} dx = \\ &|\mathcal{A}|^2 e^{\frac{i}{\hbar}(\mathcal{E}_1 - \mathcal{E}_2)t} \int_{-\infty}^{\infty} \cos \frac{(p_1 - p_2)x}{\hbar} dx + i |\mathcal{A}|^2 e^{\frac{i}{\hbar}(\mathcal{E}_1 - \mathcal{E}_2)t} \int_{-\infty}^{\infty} \sin \frac{(p_1 - p_2)x}{\hbar} dx = 0 \end{aligned} \quad (4.44)$$

unless $p_1 = p_2$ (positive and negative parts of sine and cosine functions cancel each other during integration, with the exception of $\cos 0 = 1$).

Values of \mathcal{A} can be also *normalized* to give the result of Eq. 4.44 equal to 1 if $p_1 = p_2$ and $\mathcal{E}_1 = \mathcal{E}_2$. The requirement $\langle \psi_1 | \psi_2 \rangle = 0$ for $p_1 \neq p_2, \mathcal{E}_1 \neq \mathcal{E}_2$ and $\langle \psi_1 | \psi_2 \rangle = 1$ for $p_1 = p_2, \mathcal{E}_1 = \mathcal{E}_2$ can be written using the *delta function* (see Section 3.6.5):

$$|\mathcal{A}|^2 \int_{-\infty}^{\infty} e^{\frac{i}{\hbar}(p_1 - p_2)x} dx = \delta(p_1 - p_2), \quad (4.45)$$

taken into account the fact that $e^{\frac{i}{\hbar}(\mathcal{E}_1 - \mathcal{E}_2)t} = 1$ for $\mathcal{E}_1 = \mathcal{E}_2$. Repeating the analysis presented in Section 3.6.5 (replacing ω by p/\hbar , and t by x) shows that

$$|\mathcal{A}|^2 \int_{-\infty}^{\infty} e^{\frac{i}{\hbar}(p_1 - p_2)x} dx = \frac{1}{\sqrt{2\pi\hbar}} \int_{-\infty}^{\infty} e^{\frac{i}{\hbar}(p_1 - p_2)x} dx = \hbar^{-\frac{1}{2}} \int_{-\infty}^{\infty} e^{\frac{i}{\hbar}(p_1 - p_2)x} dx = \delta(p_1 - p_2) \quad (4.46)$$

(cf. Eqs. 3.36 and 3.37). The procedure can be extended to the three-dimensional case, where all three coordinates of the momentum vectors \vec{p}_1 and \vec{p}_2 must be equal to get non-zero $\langle\psi_1|\psi_2\rangle$. This can be written as

$$\begin{aligned}\langle\psi_1|\psi_2\rangle &= h^{-\frac{3}{2}} \int_{-\infty}^{\infty} \int_{-\infty}^{\infty} \int_{-\infty}^{\infty} e^{\frac{i}{\hbar}(\vec{p}_1-\vec{p}_2)\cdot\vec{r}} d\vec{r} = h^{-\frac{3}{2}} \int_{-\infty}^{\infty} e^{\frac{i}{\hbar}(p_{1,x}-p_{2,x})x} dx \int_{-\infty}^{\infty} e^{\frac{i}{\hbar}(p_{1,y}-p_{2,y})y} dy \int_{-\infty}^{\infty} e^{\frac{i}{\hbar}(p_{1,z}-p_{2,z})z} dz \\ &= \delta(\vec{p}_1-\vec{p}_2) = \delta(p_{1,x}-p_{2,x}) \cdot \delta(p_{1,y}-p_{2,y}) \cdot \delta(p_{1,z}-p_{2,z}).\end{aligned}\quad (4.47)$$

In the language of algebra, the complete set of normalized monochromatic waves constitutes an *orthonormal basis* for wave functions, in a similar way as unit vectors $\vec{i}, \vec{j}, \vec{k}$ are the orthonormal basis for all vectors in the Cartesian coordinate system x, y, z .

Also, Ψ (linear combination of ψ_1, ψ_2, \dots) can be normalized based on the condition

$$\int_{-\infty}^{\infty} \Psi^* \Psi dx = P = 1 \quad (4.48)$$

(if a particle exists, it must be somewhere). It requires

$$\int_{-\infty}^{\infty} (c_1^* c_1 + c_2^* c_2 + \dots) dx = 1. \quad (4.49)$$

4.9.3 Eigenfunctions and eigenvalues, operator of momentum

In order to understand what quantum mechanics says about measurable properties of the studied system, let us ask a question: How can we get the value of a momentum of a free particle described by Eq. 4.2? What operation should be applied to $\Psi(x)$ (a function of x) in order to get the value of the momentum? Calculation of $\partial\Psi/\partial x$ gives us a clue:

$$\frac{\partial\Psi}{\partial x} = c_1 \frac{\partial}{\partial x} e^{\frac{i}{\hbar}(p_1 x - \mathcal{E}_1 t)} + c_2 \frac{\partial}{\partial x} e^{\frac{i}{\hbar}(p_2 x - \mathcal{E}_2 t)} + \dots = \frac{i}{\hbar} p_1 c_1 e^{\frac{i}{\hbar}(p_1 x - \mathcal{E}_1 t)} + \frac{i}{\hbar} p_2 c_2 e^{\frac{i}{\hbar}(p_2 x - \mathcal{E}_2 t)} + \dots \quad (4.50)$$

It implies that

$$-i\hbar \frac{\partial}{\partial x} e^{\frac{i}{\hbar}(p_1 x - \mathcal{E}_1 t)} = p_1 e^{\frac{i}{\hbar}(p_1 x - \mathcal{E}_1 t)}, \quad -i\hbar \frac{\partial}{\partial x} e^{\frac{i}{\hbar}(p_2 x - \mathcal{E}_2 t)} = p_2 e^{\frac{i}{\hbar}(p_2 x - \mathcal{E}_2 t)}, \dots \quad (4.51)$$

We see that

1. Calculation of the partial derivative of any monochromatic wave and multiplying the result by $-i\hbar$ gives us the same wave just multiplied by a constant. The instruction to calculate the partial derivative and multiply the result by $-i\hbar$ is an example of an *operator*. If application of the operator to a function gives the same function, only multiplied by a constant, the function is called *eigenfunction* of the operator and the constant is called *eigenvalue* of the operator.
2. The eigenvalues are well-defined, measurable physical quantities – possible values of the momentum along x .
3. The eigenvalues can be obtained by applying the operator to the eigenfunctions and multiplying the results by the complex conjugates of the eigenfunctions, e.g.

$$p_1 = e^{-\frac{i}{\hbar}(p_1 x - \mathcal{E}_1 t)} \left(-i\hbar \frac{\partial}{\partial x} e^{\frac{i}{\hbar}(p_1 x - \mathcal{E}_1 t)} \right) = e^{-\frac{i}{\hbar}(p_1 x - \mathcal{E}_1 t)} p_1 e^{\frac{i}{\hbar}(p_1 x - \mathcal{E}_1 t)} = p_1 \underbrace{e^{-\frac{i}{\hbar}(p_1 x - \mathcal{E}_1 t)} e^{\frac{i}{\hbar}(p_1 x - \mathcal{E}_1 t)}}_{=1}. \quad (4.52)$$

4.9.4 Operator of position

The question we ask now is: What operation should I apply to Ψ (a function of x) in order to get the value of its coordinate? When $-i\hbar\partial/\partial x$ is used as an operator of momentum (in the x direction), applied to $\Psi(x)$, multiplication by the coordinate x is an operator of the position of the particle (in the x direction). To see how the operator acts, let us write $\Psi(x, t)$ as a series of the values $\Psi(x_j, t)$ for all possible positions x_j .⁶ Then, the product $x\Psi(x, t)$ can be written as

⁶We write the continuous function $\Psi(x)$ as a vector formally containing distinct elements $\Psi(x_1), \Psi(x_2), \dots$. In a similar fashion, we write x as a vector containing a series of all values of the coordinate $x: x_1, x_2, \dots$.

$$x \cdot \Psi(x, t) = \begin{pmatrix} x_1 c_1 e^{\frac{i}{\hbar}(p_1 x_1 - \mathcal{E}_1 t)} + x_1 c_2 e^{\frac{i}{\hbar}(p_2 x_1 - \mathcal{E}_2 t)} + x_1 c_3 e^{\frac{i}{\hbar}(p_3 x_1 - \mathcal{E}_3 t)} + \dots \\ x_2 c_1 e^{\frac{i}{\hbar}(p_1 x_2 - \mathcal{E}_1 t)} + x_2 c_2 e^{\frac{i}{\hbar}(p_2 x_2 - \mathcal{E}_2 t)} + x_2 c_3 e^{\frac{i}{\hbar}(p_3 x_2 - \mathcal{E}_3 t)} + \dots \\ x_3 c_1 e^{\frac{i}{\hbar}(p_1 x_3 - \mathcal{E}_1 t)} + x_3 c_2 e^{\frac{i}{\hbar}(p_2 x_3 - \mathcal{E}_2 t)} + x_3 c_3 e^{\frac{i}{\hbar}(p_3 x_3 - \mathcal{E}_3 t)} + \dots \\ \vdots \end{pmatrix} = \begin{pmatrix} x_1 \cdot \Psi(x_1) \\ x_2 \cdot \Psi(x_2) \\ x_3 \cdot \Psi(x_3) \\ \vdots \end{pmatrix}. \quad (4.53)$$

If the position of the particle is e.g. x_2 ,

$$\Psi(x_2, t) = \begin{pmatrix} 0 \\ c_1 e^{\frac{i}{\hbar}(p_1 x_2 - \mathcal{E}_1 t)} + c_2 e^{\frac{i}{\hbar}(p_2 x_2 - \mathcal{E}_2 t)} + c_3 e^{\frac{i}{\hbar}(p_3 x_2 - \mathcal{E}_3 t)} + \dots \\ 0 \\ \vdots \end{pmatrix} = \begin{pmatrix} 0 \\ \Psi(x_2) \\ 0 \\ \vdots \end{pmatrix} \quad (4.54)$$

and $x \cdot \Psi(x, t)$ for $x = x_2$ is

$$x_2 \cdot \Psi(x_2, t) = \begin{pmatrix} 0 \\ x_2 \left(c_1 e^{\frac{i}{\hbar}(p_1 x_2 - \mathcal{E}_1 t)} + c_2 e^{\frac{i}{\hbar}(p_2 x_2 - \mathcal{E}_2 t)} + c_3 e^{\frac{i}{\hbar}(p_3 x_2 - \mathcal{E}_3 t)} + \dots \right) \\ 0 \\ \vdots \end{pmatrix} = \begin{pmatrix} 0 \\ x_2 \cdot \Psi(x_2) \\ 0 \\ \vdots \end{pmatrix}. \quad (4.55)$$

We see that multiplication of $\Psi(x_2, t)$ by x_2 results in $x_2 \Psi(x_2)$, i.e., $\Psi(x_2)$ is an eigenfunction of the operator $\hat{x} = x \cdot$ and x_2 is the corresponding eigenvalue.

Note that multiplication by p_j does not work in the same way! We could multiply $\Psi(x_2)$ by x_2 because $\Psi(x_2)$ does not depend on any other value of the x coordinate. However, $\Psi(x_2)$ depends on all possible values of p . On the other hand, the partial derivative $\partial\Psi/\partial x$ in Eq 4.50 gave us each monochromatic wave multiplied by its value of p and ensured that the monochromatic waves acted as eigenfunctions.

4.9.5 Commutation relations of the position and momentum operators

It is easy to check that subsequently applied operators related to different coordinates commute. For example

$$\hat{x}\hat{y}\Psi = xy\Psi = yx\Psi = \hat{y}\hat{x}\Psi, \quad (4.56)$$

$$\hat{p}_x\hat{p}_y\Psi = -\hbar^2 \frac{\partial^2 \Psi}{\partial x \partial y} = -\hbar^2 \frac{\partial^2 \Psi}{\partial y \partial x} = \hat{p}_y\hat{p}_x\Psi, \quad (4.57)$$

or

$$\hat{x}\hat{p}_y\Psi = -i\hbar x \frac{\partial \Psi}{\partial y} = -i\hbar \left(\frac{\partial(x\Psi)}{\partial y} \right) = \hat{p}_y\hat{x}\Psi. \quad (4.58)$$

However,

$$\hat{x}\hat{p}_x\Psi = -i\hbar x \frac{\partial \Psi}{\partial x} \quad (4.59)$$

but

$$\hat{p}_x\hat{x}\Psi = -i\hbar \frac{\partial(x\Psi)}{\partial x} = -i\hbar\Psi - i\hbar x \frac{\partial \Psi}{\partial x}. \quad (4.60)$$

We see that

- commutators of operators of a coordinate and the momentum component in the same direction are equal to $i\hbar$ (i.e., multiplication of Ψ by the factor $i\hbar$),
- all other position and coordinate operators commute,

in agreement with Eq. 4.13.

4.9.6 Schrödinger equation

We obtained the operator of momentum by calculating $\partial\Psi/\partial x$. What happens if we calculate $\partial\Psi/\partial t$?

$$\frac{\partial\Psi}{\partial t} = c_1 \frac{\partial}{\partial t} e^{\frac{i}{\hbar}(p_1 x - \mathcal{E}_1 t)} + c_2 \frac{\partial}{\partial t} e^{\frac{i}{\hbar}(p_2 x - \mathcal{E}_2 t)} + \dots = -\frac{i}{\hbar} \mathcal{E}_1 c_1 e^{\frac{i}{\hbar}(p_1 x - \mathcal{E}_1 t)} - \frac{i}{\hbar} \mathcal{E}_2 c_2 e^{\frac{i}{\hbar}(p_2 x - \mathcal{E}_2 t)} - \dots \quad (4.61)$$

and consequently

$$i\hbar \frac{\partial}{\partial t} e^{\frac{i}{\hbar}(p_1 x - \mathcal{E}_1 t)} = \mathcal{E}_1 e^{\frac{i}{\hbar}(p_1 x - \mathcal{E}_1 t)}, \quad i\hbar \frac{\partial}{\partial t} e^{\frac{i}{\hbar}(p_2 x - \mathcal{E}_2 t)} = \mathcal{E}_2 e^{\frac{i}{\hbar}(p_2 x - \mathcal{E}_2 t)}, \quad \dots \quad (4.62)$$

1. First, we obtain the *operator of energy* from Eq. 4.62, in analogy to Eq. 4.51.
2. The second achievement is Eq. 4.61 itself. Energy of free particles is just the kinetic energy (by definition, "free" particles do not experience any forces). Therefore, all energies \mathcal{E}_j in the right-hand side of Eq. 4.61 can be written as

$$\mathcal{E}_j = \frac{mv_j^2}{2} = \frac{p_j^2}{2m}, \quad (4.63)$$

resulting in

$$\frac{\partial\Psi}{\partial t} = -\frac{i}{\hbar} \left(\frac{p_1^2}{2m} c_1 e^{\frac{i}{\hbar}(p_1 x - \mathcal{E}_1 t)} + \frac{p_2^2}{2m} c_2 e^{\frac{i}{\hbar}(p_2 x - \mathcal{E}_2 t)} + \dots \right). \quad (4.64)$$

But an equation with the p_j^2 terms can be also obtained by calculating

$$\frac{1}{2m} \frac{\partial^2\Psi}{\partial x^2} = \frac{1}{2m} \frac{\partial}{\partial x} \frac{\partial\Psi}{\partial x} = -\frac{1}{\hbar^2} \left(\frac{p_1^2}{2m} c_1 e^{\frac{i}{\hbar}(p_1 x - \mathcal{E}_1 t)} + \frac{p_2^2}{2m} c_2 e^{\frac{i}{\hbar}(p_2 x - \mathcal{E}_2 t)} + \dots \right). \quad (4.65)$$

Comparison of Eqs. 4.64 and 4.65 gives us the *equation of motion*

$$i\hbar \frac{\partial\Psi}{\partial t} = -\frac{\hbar^2}{2m} \frac{\partial^2\Psi}{\partial x^2} + \dots \quad (4.66)$$

If we extend our analysis to particles experiencing a time-independent potential energy $\mathcal{E}_{\text{pot}}(x, y, z)$, the energy will be given by

$$\mathcal{E}_j = \frac{p_j^2}{2m} + \mathcal{E}_{\text{pot}} \quad (4.67)$$

where p_j is now the absolute value of a momentum vector \vec{p}_j (we have to consider all three direction x, y, z because particles change direction of motion in the presence of a potential). The time derivative of Ψ is now

$$\frac{\partial\Psi}{\partial t} = -\frac{i}{\hbar} \left(\frac{p_1^2}{2m} c_1 e^{\frac{i}{\hbar}(\vec{p}_1 \vec{r} - \mathcal{E}_1 t)} + \frac{p_2^2}{2m} c_2 e^{\frac{i}{\hbar}(\vec{p}_2 \vec{r} - \mathcal{E}_2 t)} + \dots \right) - \frac{i}{\hbar} \mathcal{E}_{\text{pot}}(\vec{r}) \Psi \quad (4.68)$$

and

$$\left(\frac{p_1^2}{2m} c_1 e^{\frac{i}{\hbar}(\vec{p}_1 \vec{r} - \mathcal{E}_1 t)} + \frac{p_2^2}{2m} c_2 e^{\frac{i}{\hbar}(\vec{p}_2 \vec{r} - \mathcal{E}_2 t)} + \dots \right) = -\frac{\hbar^2}{2m} \left(\frac{\partial^2\Psi}{\partial x^2} + \frac{\partial^2\Psi}{\partial y^2} + \frac{\partial^2\Psi}{\partial z^2} \right). \quad (4.69)$$

Substituting Eq. 4.69 into Eq. 4.68 gives us the famous Schrödinger equation

$$i\hbar \frac{\partial\Psi}{\partial t} = \underbrace{\left(-\frac{\hbar^2}{2m} \left(\frac{\partial^2}{\partial x^2} + \frac{\partial^2}{\partial y^2} + \frac{\partial^2}{\partial z^2} \right) + \mathcal{E}_{\text{pot}}(x, y, z) \right)}_{\hat{H}} \Psi. \quad (4.70)$$

In our case, the Hamiltonian is expressed in terms of the linear momentum $\vec{p} = m\vec{v}$. This is sufficient to describe action of forces that depend only on the position in space and can be therefore calculated as the gradients of the potential energy (e.g. electric forces). However, using the linear momentum does not allow us to describe forces that depend on velocities of the particles (e.g., magnetic forces). Therefore, the *canonical* (or *generalized*) momentum should be used in general. The canonical momentum is defined by the Lagrange mechanics, reviewed in Section 0.2. We return to the description of a particle in a magnetic field in Section 5.7.5.

4.9.7 Limitation of wave equation to first time derivative

Before saying what a wave equation must fulfill in order to describe evolution of a quantum state in time, let us review similar requirements for the equation of motion in Newton mechanics. In the classical Newton mechanics, the state of the system is fully described by the coordinates x, y, z and moments mv_x, mv_y, mv_z of the particles. Therefore, the solution of the equation of motion must depend only on the starting values of the coordinates and moments, not on any additional parameter. What does it say about the equation of motion itself? It can contain only first and second derivatives in time. Why? Because:

- Solutions of equation containing only $\partial x/\partial t$ require the knowledge of $x(t=0) = x(0)$.

For example, solution of

$$\frac{\partial x}{\partial t} + kx = 0 \quad (4.71)$$

is $x = x(0)e^{-kt}$, i.e., it depends only on $x(0)$.

- Solutions of equation containing only $\partial x/\partial t$ and $\partial^2 x/\partial t^2$ require the knowledge of $x(0)$ and $\partial x/\partial t(t=0) = v_x(0)$.

For example, let us look at the wave equation

$$\frac{\partial^2 x}{\partial t^2} + \omega^2 x = 0. \quad (4.72)$$

Note that this equation corresponds to the second Newton's law, with $-m\omega^2 x$ being the force (for the sake of simplicity assumed not to change in time). The solution is well known, but we can derive it easily because we know how to play with operators:

$$\frac{\partial^2 x}{\partial t^2} + \omega^2 x = \frac{\partial}{\partial t} \left(\frac{\partial x}{\partial t} \right) + \omega^2 x = \left(\left(\frac{\partial}{\partial t} \right)^2 + \omega^2 \right) x = \left(\frac{\partial}{\partial t} + i\omega \right) \left(\frac{\partial}{\partial t} - i\omega \right) x = 0. \quad (4.73)$$

Obviously, there are two solutions of the equation

$$\left(\frac{\partial}{\partial t} - i\omega \right) x_+ = 0 \Rightarrow x_+ = C_+ e^{i\omega t} = C_+ (\cos(\omega t) + i \sin(\omega t)) \quad \left(\frac{\partial}{\partial t} + i\omega \right) x_- = 0 \Rightarrow x_- = C_- e^{-i\omega t} = C_- (\cos(\omega t) - i \sin(\omega t)), \quad (4.74)$$

but the solution must be also any linear combination of x_+ and x_- because $0 + 0 = 0$:

$$x = A_+ x_+ + A_- x_- = \underbrace{(A_+ C_+ + A_- C_-)}_{C_1} \cos(\omega t) + i \underbrace{(A_+ C_+ - A_- C_-)}_{C_2} \sin(\omega t) = C_1 \cos(\omega t) + C_2 \sin(\omega t). \quad (4.75)$$

Consequently, the velocity

$$v_x = \frac{\partial x}{\partial t} = C_1 \frac{\partial \cos(\omega t)}{\partial t} + C_2 \frac{\partial \sin(\omega t)}{\partial t} = -\omega C_1 \sin(\omega t) + \omega C_2 \cos(\omega t). \quad (4.76)$$

It is clear that the so-far unknown parameters C_1 and C_2 can be obtained by calculating x and v_x at $t=0$

$$\cos(0) = 1, \quad \sin(0) = 0 \Rightarrow x(0) = C_1 \quad v_x(0) = \omega C_2 \quad (4.77)$$

and that the evolution of x and v_x depends only on $x(0)$ and $v_x(0)$, as required in Newton mechanics:

$$x(t) = x(0) \cos(\omega t) + \frac{v_x(0)}{\omega} \sin(\omega t) \quad v_x(t) = v_x(0) \cos(\omega t) - \omega \cdot x(0) \sin(\omega t). \quad (4.78)$$

- Solutions of equations containing higher than second time derivative of x require knowledge of the initial values of higher than first time derivatives of x .

For example, let us inspect

$$\frac{\partial^3 x}{\partial t^3} + \omega^3 x = 0 \quad (4.79)$$

Following the same strategy as in Eq. 4.73

$$\frac{\partial^3 x}{\partial t^3} + \lambda^3 x = \left(\frac{\partial}{\partial t} + \lambda \right) \left(\frac{\partial^2}{\partial t^2} - \frac{\partial}{\partial t} \lambda + \lambda^2 \right) x = \left(\frac{\partial}{\partial t} + \lambda \right) \left(\frac{\partial^2}{\partial t^2} - 2 \frac{\partial}{\partial t} \lambda + \frac{1}{4} \lambda^2 + \frac{3}{4} \lambda^2 \right) x = \left(\frac{\partial}{\partial t} + \lambda \right) \left(\left(\frac{\partial}{\partial t} - \frac{\lambda}{2} \right)^2 + \frac{3}{4} \lambda^2 \right) x =$$

$$\left(\frac{\partial}{\partial t} + \lambda\right) \left(\left(\frac{\partial}{\partial t} - \frac{\lambda}{2}\right)^2 - \left(i\frac{\sqrt{3}}{2}\lambda\right)^2 \right) x = \left(\frac{\partial}{\partial t} + \lambda\right) \left(\frac{\partial}{\partial t} - \frac{1+i\sqrt{3}}{2}\lambda\right) \left(\frac{\partial}{\partial t} - \frac{1-i\sqrt{3}}{2}\lambda\right) x = 0, \quad (4.80)$$

which has three solutions

$$x_0 = C_0 e^{-\lambda t}, \quad x_+ = C_+ e^{\frac{1+i\sqrt{3}}{2}\lambda t}, \quad x_- = C_- e^{\frac{1-i\sqrt{3}}{2}\lambda t} \quad (4.81)$$

and any of their linear combinations is also a valid solution

$$x = A_0 x_0 + A_+ x_+ + A_- x_- = C_1 e^{-\lambda t} + C_2 e^{\frac{1+i\sqrt{3}}{2}\lambda t} + C_3 e^{\frac{1-i\sqrt{3}}{2}\lambda t} \quad (4.82)$$

where $C_1 = A_0 C_0$, $C_2 = A_+ C_+$, $C_3 = A_- C_-$. In order to determine C_1 , C_2 , and C_3 , we need three initial conditions, not only $x(0)$ and $v_x(0)$, but also the initial acceleration $a(0) = \partial^2/\partial t^2$. However, the acceleration should not represent an additional degree of freedom. In Newton mechanics, the acceleration should be completely defined by the initial coordinates and velocities, and by forces that are already incorporated in the constants in the equation. Therefore, the equation containing the third time derivative is not a Newton's equation of motion.

After making sure that we understand the Newton mechanics, we can return to the quantum mechanics. We have postulated that the wave function Ψ contains the *complete* information about the studied particle (or system in general). In contrast to the Newton mechanics, we must require that the wave equation describing the evolution of the system must depend only on Ψ at $t = 0$. Therefore, our wave function must contain only first derivative in time. If it contained e.g. also $\partial^2\Psi/\partial t^2$, the evolution in time would depend also on $\partial\Psi/\partial t$ at $t = 0$, which is against our first postulate.

Another problem of an equation containing second time derivative is related to our interpretation of the wave function. We interpret $\Psi(x, y, z)^*\Psi(x, y, z)$ as a distribution of the probability that the particle's coordinates are x, y, z . How is this related to the wave equation? The Schrödinger's equation Eq. 4.21 and its complex conjugate are

$$i\hbar \frac{\partial\Psi}{\partial t} = \hat{H}\Psi \quad -i\hbar \frac{\partial\Psi^*}{\partial t} = \hat{H}^*\Psi^*. \quad (4.83)$$

When we multiply the equations by Ψ^* and Ψ , respectively, subtract them, and divide the result by $i\hbar$, we obtain

$$\begin{aligned} \Psi^* \frac{\partial\Psi}{\partial t} + \Psi \frac{\partial\Psi^*}{\partial t} &= \frac{1}{i\hbar} (\Psi^* \hat{H}\Psi - \Psi \hat{H}^*\Psi^*) \\ \frac{\partial(\Psi^*\Psi)}{\partial t} &= \frac{1}{i\hbar} (\Psi^* \hat{H}\Psi - \Psi \hat{H}^*\Psi^*). \end{aligned} \quad (4.84)$$

If we assume that a free particle does not move (has a zero momentum and therefore zero Hamiltonian), we find that

$$\frac{\partial(\Psi^*\Psi)}{\partial t} = 0. \quad (4.85)$$

The result is expected, if the particle does not move, $\rho = \Psi^*\Psi$ does not change in time. But if we repeat the procedure with the equations containing the second time derivative (i.e., when the operator $i\hbar\partial/\partial t$ is applied twice)

$$- \hbar^2 \frac{\partial^2\Psi}{\partial t^2} = \hat{H}\Psi \quad - \hbar^2 \frac{\partial^2\Psi^*}{\partial t^2} = \hat{H}^*\Psi^*, \quad (4.86)$$

we get

$$\begin{aligned} -\Psi^* \frac{\partial^2\Psi}{\partial t^2} + \Psi \frac{\partial^2\Psi^*}{\partial t^2} &= \frac{1}{\hbar^2} (\Psi^* \hat{H}\Psi - \Psi \hat{H}^*\Psi^*) \\ \frac{\partial}{\partial t} \left(\Psi \frac{\partial\Psi^*}{\partial t} \right) - \frac{\partial}{\partial t} \left(\Psi^* \frac{\partial\Psi}{\partial t} \right) &= \frac{1}{\hbar^2} (\Psi^* \hat{H}\Psi - \Psi \hat{H}^*\Psi^*) \\ \frac{\partial}{\partial t} \left(\Psi \frac{\partial\Psi^*}{\partial t} - \Psi^* \frac{\partial\Psi}{\partial t} \right) &= \frac{1}{\hbar^2} (\Psi^* \hat{H}\Psi - \Psi \hat{H}^*\Psi^*). \end{aligned} \quad (4.87)$$

If we now assume that a free particle does not move (has a zero momentum and therefore zero Hamiltonian), the conserved quantity is not $\Psi^*\Psi$, but $\Psi \frac{\partial\Psi^*}{\partial t} - \Psi^* \frac{\partial\Psi}{\partial t}$, containing both Ψ and its time derivative. This contradicts our interpretation of the wave function as a probability amplitude.

4.9.8 Angular momentum and rotation

Let us first find eigenvalues $L_{z,j}$ and eigenfunctions ψ_j of \hat{L}_z . As described in B15.3 (and in textbooks discussing quantum mechanics), the operator \hat{L}_z written in the spherical coordinates (r, ϑ, φ) is $\hat{L}_z = -i\hbar \frac{\partial}{\partial \varphi}$ and we can assume that the part of its eigenfunctions dependent on the coordinate φ (azimuth) can be separated: $\psi_j = Q(r, \vartheta)R_j(\varphi)$. Eigenvalues and eigenfunctions of \hat{L}_z are defined by

$$\hat{L}_z \psi_j = L_{z,j} \psi_j, \quad (4.88)$$

$$-i\hbar \frac{\partial(QR_j)}{\partial \varphi} = L_{z,j}(QR_j), \quad (4.89)$$

$$-i\hbar Q \frac{dR_j}{d\varphi} = L_{z,j} QR_j, \quad (4.90)$$

$$-i\hbar \frac{d \ln R_j}{d\varphi} = L_{z,j}, \quad (4.91)$$

$$R_j = e^{i \frac{L_{z,j}}{\hbar} \varphi}. \quad (4.92)$$

Note that $\psi_j(\varphi)$ and $\psi_j(\varphi + 2\pi k)$ are equal for any integer k :

$$e^{i \frac{L_{z,j}}{\hbar} (\varphi + 2\pi)} = e^{i \frac{L_{z,j}}{\hbar} \varphi} \underbrace{e^{i 2\pi \frac{L_{z,j}}{\hbar}}}_{= 1} \quad (4.93)$$

if $\frac{L_{z,j}}{\hbar}$ is integer

Therefore,

- value of the z -component of the angular momentum must be an integer multiple of \hbar .

There is a close relation between the angular momentum operators and description of rotation in quantum mechanics. Rotation of a point defined by the position vector \vec{r} about an axis given by the angular frequency vector $\vec{\omega}$ can be described as

$$\frac{d\vec{r}}{dt} = \vec{\omega} \times \vec{r}, \quad (4.94)$$

or more explicitly

$$\frac{dr_x}{dt} = \omega_y r_z - \omega_z r_y, \quad (4.95)$$

$$\frac{dr_y}{dt} = \omega_z r_x - \omega_x r_z, \quad (4.96)$$

$$\frac{dr_z}{dt} = \omega_x r_y - \omega_y r_x. \quad (4.97)$$

If a coordinate frame is chosen so that $\vec{\omega} = (0, 0, \omega)$

$$\frac{dr_x}{dt} = -\omega r_y, \quad (4.98)$$

$$\frac{dr_y}{dt} = \omega r_x, \quad (4.99)$$

$$\frac{dr_z}{dt} = 0. \quad (4.100)$$

We already know (see Section 1.5.5) that such a set of equation can be solved easily: multiply the second equation by i and add it to the first equation or subtract it from the first equation.

$$\frac{d(r_x + ir_y)}{dt} = \omega(-r_y + ir_x) = +i\omega(r_x + ir_y), \quad (4.101)$$

$$\frac{d(r_x - ir_y)}{dt} = \omega(-r_y - ir_x) = -i\omega(r_x - ir_y), \quad (4.102)$$

$$r_x + ir_y = C_+ e^{+i\omega t}, \quad (4.103)$$

$$r_x - ir_y = C_- e^{-i\omega t}, \quad (4.104)$$

where the integration constants $C_+ = r_x(0) + ir_y(0) = re^{i\phi_0}$ and $C_- = r_x(0) - ir_y(0) = re^{-i\phi_0}$ are given by the initial phase ϕ_0 of \vec{r} in the coordinate system:

$$r_x + ir_y = re^{+i(\omega t + \phi_0)} = r(\cos(\omega t + \phi_0) + i(\sin(\omega t + \phi_0))), \quad (4.105)$$

$$r_x - ir_y = re^{-i(\omega t + \phi_0)} = r(\cos(\omega t + \phi_0) - i(\sin(\omega t + \phi_0))). \quad (4.106)$$

The angle of rotation φ is obviously given by $\omega t + \phi_0$.

$$r_x + ir_y = re^{+i\varphi} = r(\cos(\varphi) + i(\sin(\varphi))), \quad (4.107)$$

$$r_x - ir_y = re^{-i\varphi} = r(\cos(\varphi) - i(\sin(\varphi))). \quad (4.108)$$

Comparison with Eq. 4.92 documents the relation between \hat{L}_z and rotation:

- Eigenfunction of \hat{L}_z describes rotation about z .

4.9.9 Commutators of angular momentum operators

The operators of angular momentum components are

$$\hat{L}_x = \hat{r}_y \hat{p}_z - \hat{r}_z \hat{p}_y = -i\hbar y \frac{\partial}{\partial z} + i\hbar z \frac{\partial}{\partial y}, \quad (4.109)$$

$$\hat{L}_y = \hat{r}_z \hat{p}_x - \hat{r}_x \hat{p}_z = -i\hbar z \frac{\partial}{\partial x} + i\hbar x \frac{\partial}{\partial z}, \quad (4.110)$$

$$\hat{L}_z = \hat{r}_x \hat{p}_y - \hat{r}_y \hat{p}_x = -i\hbar x \frac{\partial}{\partial y} + i\hbar y \frac{\partial}{\partial x}, \quad (4.111)$$

$$\hat{L}^2 = \hat{L}_x^2 + \hat{L}_y^2 + \hat{L}_z^2. \quad (4.112)$$

Therefore,

$$\begin{aligned} [\hat{L}_x, \hat{L}_y] &= (\hat{r}_y \hat{p}_z - \hat{r}_z \hat{p}_y)(\hat{r}_z \hat{p}_x - \hat{r}_x \hat{p}_z) - (\hat{r}_z \hat{p}_x - \hat{r}_x \hat{p}_z)(\hat{r}_y \hat{p}_z - \hat{r}_z \hat{p}_y) \\ &= \hat{r}_y \hat{p}_z \hat{r}_z \hat{p}_x - \hat{r}_z \hat{p}_y \hat{r}_z \hat{p}_x - \hat{r}_y \hat{r}_x \hat{p}_z \hat{p}_z + \hat{r}_z \hat{p}_y \hat{r}_x \hat{p}_z - \hat{r}_z \hat{p}_x \hat{r}_y \hat{p}_z + \hat{r}_x \hat{p}_z \hat{r}_y \hat{p}_z + \hat{r}_z \hat{p}_x \hat{r}_z \hat{p}_y - \hat{r}_x \hat{p}_z \hat{r}_z \hat{p}_y \end{aligned} \quad (4.113)$$

The commutation relations postulated in Eq. 4.13 allow us to exchange some of the operators and write first the operators that commute

$$[\hat{L}_x, \hat{L}_y] = \hat{r}_y \hat{p}_x \hat{p}_z \hat{r}_z - \hat{r}_z \hat{r}_z \hat{p}_x \hat{p}_y - \hat{r}_y \hat{p}_x \hat{r}_z \hat{p}_z + \hat{r}_x \hat{p}_y \hat{r}_z \hat{p}_z - \hat{r}_y \hat{p}_x \hat{r}_z \hat{p}_z + \hat{r}_x \hat{r}_y \hat{p}_z \hat{p}_z + \hat{r}_z \hat{r}_z \hat{p}_x \hat{p}_y - \hat{r}_x \hat{p}_y \hat{p}_z \hat{r}_z \quad (4.114)$$

The red terms cancel each other and using Eq. 4.13

$$[\hat{L}_x, \hat{L}_y] = (\hat{r}_y \hat{p}_x - \hat{r}_x \hat{p}_y)(\hat{p}_z \hat{r}_z - \hat{r}_z \hat{p}_z) = (-\hat{L}_z)(-i\hbar) = i\hbar \hat{L}_z. \quad (4.115)$$

The other commutators can be derived in the same manner.

Lecture 5

Spin

Literature: Introduction to the special theory of relativity can be found in B10, but relativistic quantum mechanics is not discussed in the literature recommended for this course or in general physical chemistry textbooks (despite the important role of spin in chemistry). Therefore, more background information is presented here than in the other chapters. NMR can be correctly described if the spin is introduced *ad hoc*. The purpose of Section 5.7.1 is to show how the spin emerges naturally. Origin of nuclear magnetism is touched in L1.3 and L1.4. Quantum mechanics of spin angular momentum is reviewed in K6, L7, and L10.

5.1 Dirac equation

The angular momentum discussed in Section 4.7 is associated with the change of direction of a moving particle. However, the theory discussed so-far does not explain the experimental observation that even point-like particles moving along straight lines possess a well defined angular momentum, so-called *spin*.

The origin of the spin is a consequence of the symmetry of Nature that is taken into account in the theory of relativity. The Schrödinger equation is not relativistic and does not describe the spin naturally. In this lecture, we describe spin using relativistic quantum mechanics, a theory which is in agreement with two fundamental postulates of the special theory of relativity:

- The laws of physics are invariant (i.e. identical) in all inertial systems (non-accelerating frames of reference).
- The speed of light in a vacuum is the same for all observers, regardless of the motion of the light source.

The arguments presented in Sections 5.7.1 and 5.7.2 lead to the wave equation

$$\left(i\hbar \frac{\partial}{\partial t} \hat{\gamma}^0 + i\hbar \frac{\partial}{\partial x} \hat{\gamma}^1 + i\hbar \frac{\partial}{\partial y} \hat{\gamma}^2 + i\hbar \frac{\partial}{\partial z} \hat{\gamma}^3 - m_0 c^2 \hat{1} \right) \Psi = 0, \quad (5.1)$$

where $\hat{\gamma}^j$ are the following 4×4 matrices

$$\hat{\gamma}^0 = \begin{pmatrix} 1 & 0 & 0 & 0 \\ 0 & 1 & 0 & 0 \\ 0 & 0 & -1 & 0 \\ 0 & 0 & 0 & -1 \end{pmatrix} \quad \hat{\gamma}^1 = \begin{pmatrix} 0 & 0 & 0 & 1 \\ 0 & 0 & 1 & 0 \\ 0 & -1 & 0 & 0 \\ -1 & 0 & 0 & 0 \end{pmatrix} \quad \hat{\gamma}^2 = \begin{pmatrix} 0 & 0 & 0 & -i \\ 0 & 0 & i & 0 \\ 0 & i & 0 & 0 \\ -i & 0 & 0 & 0 \end{pmatrix} \quad \hat{\gamma}^3 = \begin{pmatrix} 0 & 0 & 1 & 0 \\ 0 & 0 & 0 & -1 \\ -1 & 0 & 0 & 0 \\ 0 & 1 & 0 & 0 \end{pmatrix}. \quad (5.2)$$

The solution of Eq. 5.1 is a wave function consisting of four components

$$\Psi = \begin{pmatrix} \psi_1 \\ \psi_2 \\ \psi_3 \\ \psi_4 \end{pmatrix}. \quad (5.3)$$

The explicit form of the solution for a free particle is presented in Section 5.7.3. Note that the solution is written as a four-component vector, but the indices 1, 2, 3, 4 are not related to time and space coordinate. Instead, they represent *new degrees of freedom*, distinguishing different spin states and particles from antiparticles.

When postulated by Dirac, Eq. 5.1 naturally explained the behavior of particles with spin number 1/2 and predicted existence of antiparticles, discovered a few years later. Relation of Eq. 5.1 to the non-relativistic Schrödinger equation is described in Section 5.7.4.

After describing the free particle, we should move to the description of particles interacting with their surroundings, in particular with the electromagnetic fields. Strictly speaking, both spin-1/2 particles and the fields should be treated in the same manner, i.e., as quantum particles or, more precisely, as states of various quantum fields. Such approach is reviewed in Engelke, *Concepts Magn. Reson.* **36(A)** (2010) 266-339, DOI 10.1002/cmr.a.20166. However, the energy of the electromagnetic quanta (photons) used in NMR spectroscopy is low and their number is very high. As a consequence, the quantum and classical¹ description of the fields give almost identical results. As we try to keep the theoretical description as simple as possible in this text, we follow with the classical description of the electromagnetic field.²

5.2 Operator of the spin magnetic moment

The Dirac equation allows us to find the operator of the spin magnetic moment. We start by deriving the Hamiltonian describing the energy of the spin magnetic moment in a magnetic field (Section 5.7.5). In a limit of energies much lower than the rest-mass energy m_0c^2 , the Hamiltonian is

¹Here, "classical" means "non-quantum, but relativistic" because the Maxwell equations are consistent with the special theory of relativity.

²A consequence of the classical treatment of the electromagnetic fields is that we derive a value of the magnetogyric ratio slightly lower than observed and predicted by the fully quantum approach. This fact is mentioned in Section 5.6.

$$\hat{H} \approx \frac{1}{2m_0} \left(\left(i\hbar \frac{\partial}{\partial x} + QA_x \right)^2 + \left(i\hbar \frac{\partial}{\partial y} + QA_y \right)^2 + \left(i\hbar \frac{\partial}{\partial z} + QA_z \right)^2 + QV \right) \begin{pmatrix} 1 & 0 \\ 0 & 1 \end{pmatrix} - \frac{\hbar Q}{2m_0} \left(B_x \begin{pmatrix} 0 & 1 \\ 1 & 0 \end{pmatrix} + B_y \begin{pmatrix} 0 & -i \\ i & 0 \end{pmatrix} + B_z \begin{pmatrix} 1 & 0 \\ 0 & -1 \end{pmatrix} \right). \quad (5.4)$$

The Hamiltonian contains a part (shown in green on the first line) which is identical with the non-relativistic Hamiltonian in the Schrödinger equation describing a particle in an electromagnetic field (Eq. 4.23), but it also contains a new part (shown in red on the second line), which appears only in the relativistic treatment (and survives the simplification to the low-energy limit. This "relativistic" component closely resembles the Hamiltonian of the interaction of the orbital magnetic moment with the magnetic field (Eq. 4.38) and, as we discuss below, has all properties expected for the Hamiltonian of the *spin* magnetic moment, despite the fact that we analyze a point-like particle which cannot spin. Comparison of Eqs. 5.4 and 4.38 helps us to identify the operator of the components of the *spin magnetic moment*:

$$\hat{\mu}_x = \frac{\hbar Q}{2m_0} \begin{pmatrix} 0 & 1 \\ 1 & 0 \end{pmatrix}, \quad (5.5)$$

$$\hat{\mu}_y = \frac{\hbar Q}{2m_0} \begin{pmatrix} 0 & -i \\ i & 0 \end{pmatrix}, \quad (5.6)$$

$$\hat{\mu}_z = \frac{\hbar Q}{2m_0} \begin{pmatrix} 1 & 0 \\ 0 & -1 \end{pmatrix}. \quad (5.7)$$

5.3 Operators of spin angular momentum

Our final task is to find the operators of the components of the *spin angular momentum*, which also gives us the value of the magnetogyric ratio. Eq. 5.4 itself is not sufficient because it does not say which constants belong to the spin angular momentum and which constitute the magnetogyric ratio. We cannot use the classical definition either because our case does not have a classical counterpart. But we can use

- the general relation between magnetic moment and angular momentum $\vec{\mu} = \gamma \vec{L}$ and
- the commutation relations Eqs. 4.32–4.35, which define operators of x, y, z components of *any* angular momentum.

In order to distinguish it from the orbital angular momentum \vec{L} , we label the spin angular momentum \vec{I} , whereas we use the symbol $\vec{\mu}$ for the spin magnetic moment. The operators of μ_x, μ_y, μ_z are given by

$$\hat{\mu}_x = \gamma \hat{I}_x, \quad \hat{\mu}_y = \gamma \hat{I}_y, \quad \hat{\mu}_z = \gamma \hat{I}_z, \quad (5.8)$$

and the operators of I_x, I_y, I_z must fulfill the same commutation relations as the operators of L_x, L_y, L_z :

$$\hat{I}_x \hat{I}_y - \hat{I}_y \hat{I}_x = i\hbar \hat{I}_z, \quad \hat{I}_y \hat{I}_z - \hat{I}_z \hat{I}_y = i\hbar \hat{I}_x, \quad \hat{I}_z \hat{I}_x - \hat{I}_x \hat{I}_z = i\hbar \hat{I}_y. \quad (5.9)$$

Comparison with Eqs. 5.103–5.105 shows that the right choice of the spin operators is

$$\hat{I}_x = \frac{\hbar}{2} \begin{pmatrix} 0 & 1 \\ 1 & 0 \end{pmatrix} \quad \hat{I}_y = \frac{\hbar}{2} \begin{pmatrix} 0 & -i \\ i & 0 \end{pmatrix} \quad \hat{I}_z = \frac{\hbar}{2} \begin{pmatrix} 1 & 0 \\ 0 & -1 \end{pmatrix} \quad \hat{I}^2 = \frac{3\hbar^2}{4} \begin{pmatrix} 1 & 0 \\ 0 & 1 \end{pmatrix}. \quad (5.10)$$

Comparison of Eq. 5.4 with Eq. 4.38 shows that the magnetogyric ratio differs by a factor of 2 from the value for orbital magnetic moment:

$$\gamma = 2 \frac{Q}{2m}. \quad (5.11)$$

For more details, see Section 5.7.6.

5.4 Eigenfunctions and eigenvalues of \hat{I}_z

The fact that \hat{I}_z is diagonal tells us that we have written the matrix representations of the operators of the spin angular momentum in the basis formed by the eigenfunctions of \hat{I}_z . This basis is a good choice if the matrix representing Hamiltonian is also diagonal in this basis and, therefore, eigenfunctions of \hat{I}_z are the same as eigenfunctions of the Hamiltonian.³ These eigenfunctions can be

$$\sqrt{\frac{1}{\hbar^3}} \begin{pmatrix} \psi \\ 0 \end{pmatrix}, \quad \sqrt{\frac{1}{\hbar^3}} \begin{pmatrix} 0 \\ \psi \end{pmatrix}, \quad (5.12)$$

i.e., the two-component variants of the free-particle wave functions from Eq. 5.85 in the low-energy approximation (the explicit form of the four-component wave function and the normalization factor $\hbar^{-3/2}$ are described in Section 5.7.3). The normalization coefficient $\hbar^{-3/2}$ and ψ can be canceled out in the eigenvalue equations and the eigenfunctions can be replaced by the vectors

$$\begin{pmatrix} 1 \\ 0 \end{pmatrix}, \quad \begin{pmatrix} 0 \\ 1 \end{pmatrix} \quad (5.13)$$

corresponding to the first and second wave functions in Eq. 5.85.

The states represented by the eigenfunctions of \hat{I}_z (*eigenstates*) are traditionally called states α and β and are further discussed in Section 5.5. The eigenfunctions of \hat{I}_z are usually labeled as $|\alpha\rangle$ or $|\uparrow\rangle$ and $|\beta\rangle$ or $|\downarrow\rangle$:

$$\hat{I}_z |\alpha\rangle = +\frac{\hbar}{2} |\alpha\rangle \quad \hat{I}_z |\uparrow\rangle = +\frac{\hbar}{2} |\uparrow\rangle \quad \frac{\hbar}{2} \begin{pmatrix} 1 & 0 \\ 0 & -1 \end{pmatrix} \begin{pmatrix} 1 \\ 0 \end{pmatrix} = +\frac{\hbar}{2} \begin{pmatrix} 1 \\ 0 \end{pmatrix}, \quad (5.14)$$

³This is a good choice, because such eigenfunctions represent states that are stationary, as was shown in Section 4.6 and is further discussed in Section 5.5.

$$\hat{I}_z|\beta\rangle = -\frac{\hbar}{2}|\beta\rangle \quad \hat{I}_z|\downarrow\rangle = -\frac{\hbar}{2}|\downarrow\rangle \quad \frac{\hbar}{2} \begin{pmatrix} 1 & 0 \\ 0 & -1 \end{pmatrix} \begin{pmatrix} 0 \\ 1 \end{pmatrix} = -\frac{\hbar}{2} \begin{pmatrix} 0 \\ 1 \end{pmatrix}. \quad (5.15)$$

Note that the vectors used to represent $|\alpha\rangle$ and $|\beta\rangle$ in Eqs. 5.14 and 5.15 are not the only choice. Vectors in Eqs. 5.14 and 5.15 have a phase set to zero (they are made of real numbers). Any other phase ϕ would work as well, e.g.

$$\begin{pmatrix} 1 \\ 0 \end{pmatrix} \rightarrow \begin{pmatrix} e^{i\phi} \\ 0 \end{pmatrix}. \quad (5.16)$$

The postulates of quantum mechanics, discussed in the preceding lecture, tell us that measurement of spin angular momentum or spin magnetic moment of a single particle is limited by *quantum indeterminacy*, described below and shown in Figure 5.1.

- If the particle is in state $|\alpha\rangle$, the result of measuring I_z is *always* $+\hbar/2$. The expected value is

$$\langle I_z \rangle = \langle \alpha | I_z | \alpha \rangle = (1 \ 0) \frac{\hbar}{2} \begin{pmatrix} 1 & 0 \\ 0 & -1 \end{pmatrix} \begin{pmatrix} 1 \\ 0 \end{pmatrix} = +\frac{\hbar}{2}. \quad (5.17)$$

- If the particle is in state $|\beta\rangle$, the result of measuring I_z is *always* $-\hbar/2$. The expected value is

$$\langle I_z \rangle = \langle \beta | I_z | \beta \rangle = (0 \ 1) \frac{\hbar}{2} \begin{pmatrix} 1 & 0 \\ 0 & -1 \end{pmatrix} \begin{pmatrix} 0 \\ 1 \end{pmatrix} = -\frac{\hbar}{2}. \quad (5.18)$$

- Any state $c_\alpha|\alpha\rangle + c_\beta|\beta\rangle$ is possible, but the result of a single measurement of I_z is *always* $+\hbar/2$ or $-\hbar/2$. However, the expected value of I_z is

$$\langle I_z \rangle = \langle \alpha | I_z | \beta \rangle = (c_\alpha^* \ c_\beta^*) \frac{\hbar}{2} \begin{pmatrix} 1 & 0 \\ 0 & -1 \end{pmatrix} \begin{pmatrix} c_\alpha \\ c_\beta \end{pmatrix} = (|c_\alpha|^2 - |c_\beta|^2) \frac{\hbar}{2}. \quad (5.19)$$

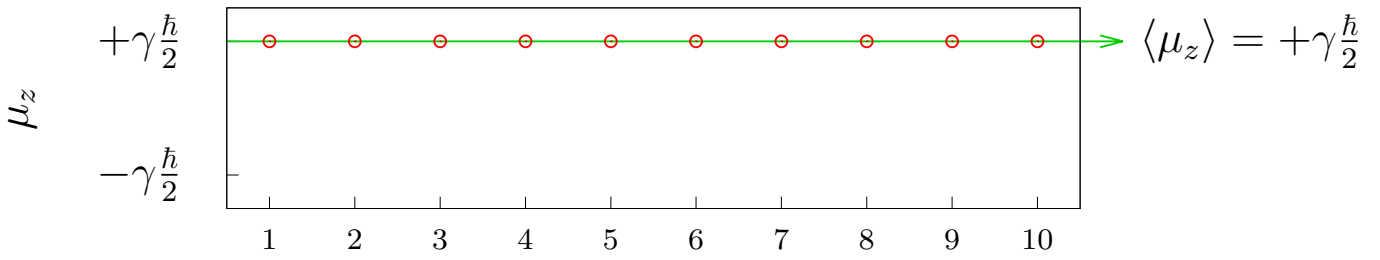
Wave functions $|\alpha\rangle$ and $|\beta\rangle$ are *not* eigenfunctions of \hat{I}_x or \hat{I}_y . Eigenfunctions of \hat{I}_x and \hat{I}_y are presented in Section 5.7.7

5.5 Evolution, eigenstates and energy levels

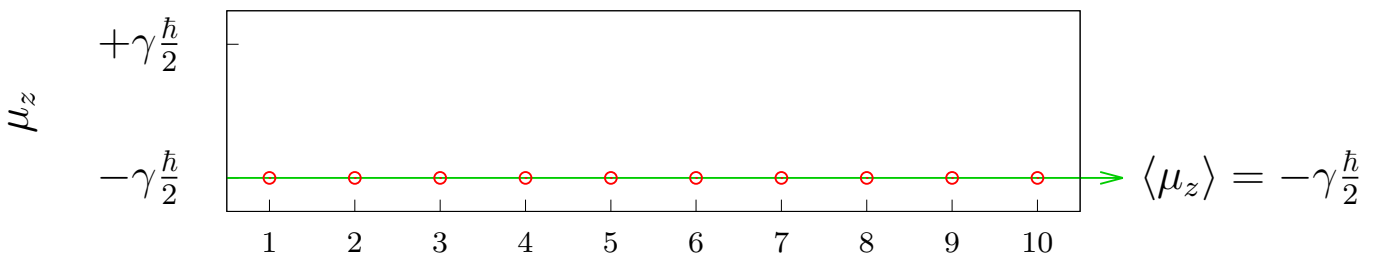
Knowledge of the Hamiltonian allows us to describe how the studied system evolves. We have learnt in Section 4.6 that states corresponding to eigenfunctions, i.e., the *eigenstates*, are stationary. This is shown for the eigenfunctions of \hat{I}_z in Section 5.7.8 and in Figure 5.2. If the system is in the stationary state, its eigenvalue does not change in time. Therefore, a system in a state described by an eigenfunction of the Hamiltonian can be associated with a certain eigenvalue of the Hamiltonian, i.e., with a certain *energy*.

The states described by basis functions which are eigenfunctions of the Hamiltonian do not evolve (are stationary). It makes sense to draw *energy level diagram* for such states, with energy of each state given by the corresponding eigenvalue of the Hamiltonian. Energy of the $|\alpha\rangle$ state is $-\hbar\omega_0/2$ and energy of the $|\beta\rangle$ state is $+\hbar\omega_0/2$. The measurable quantity is the energy difference $\hbar\omega_0$, corresponding to the angular frequency ω_0 .

A $|\Psi\rangle = |\alpha\rangle$



B $|\Psi\rangle = |\beta\rangle$



C $|\Psi\rangle = \frac{1}{\sqrt{2}}|\alpha\rangle + \frac{1}{\sqrt{2}}|\beta\rangle$

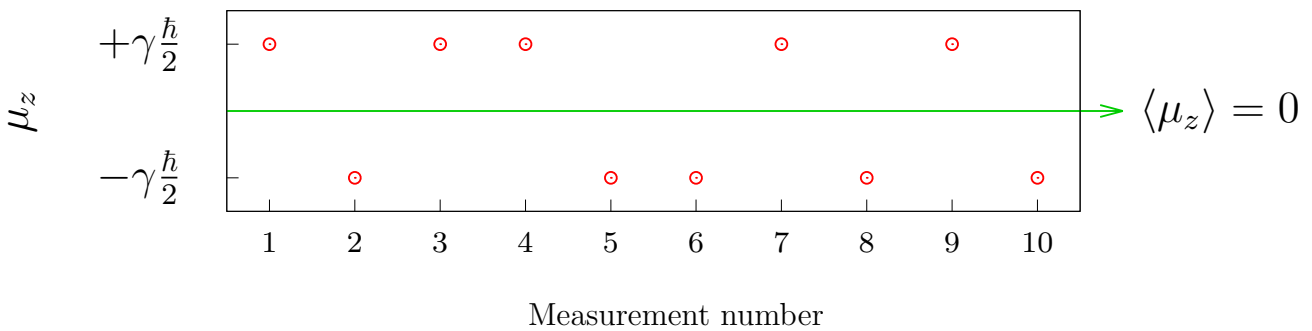


Figure 5.1: Plot of hypothetical results of individual measurements of the z components of the magnetic moment of a spin-1/2 particle in a vertical magnetic field \vec{B}_0 . Individual measured values (equal to one of eigenvalues of $\hat{\mu}_z$) and average measured values (equal to the expectation value $\langle \mu_z \rangle$) are shown as red circles and green arrows, respectively, for a particle in the α eigenstate (A), in the β eigenstate (B) and in the superposition state described by $\frac{1}{\sqrt{2}}|\alpha\rangle + \frac{1}{\sqrt{2}}|\beta\rangle$ (C).

In general, the studied system can be present in a state that is not described by a single eigenfunction, but by a linear combination (superposition) of eigenfunctions. As shown in Section 5.7.9 and in Figure 5.2, such a *superposition state* evolves in time and cannot be associated with a single energy.

The states described by basis functions different from eigenfunctions of the Hamiltonian are not stationary but oscillate between $|\alpha\rangle$ and $|\beta\rangle$ with the angular frequency ω_1 , given by the difference of the eigenvalues of the Hamiltonian ($-\hbar\omega_1/2$ and $\hbar\omega_1/2$).

It should be stressed that eigenstates of individual magnetic moments are not eigenstates of the macroscopic ensembles of nuclear magnetic moments. Eigenstates of individual magnetic moments do not determine the possible result of measurement of bulk magnetization. We present the correct description of large ensembles in the next lecture.

5.6 Real particles

Eq. 5.4, used to derive the value of γ , describes interaction of a particle with an external electromagnetic field. However, charged particles are themselves sources of electromagnetic fields. Therefore, γ is not exactly twice $Q/2m$. In general, the value of γ is

$$\gamma = g \frac{Q}{2m}, \quad (5.20)$$

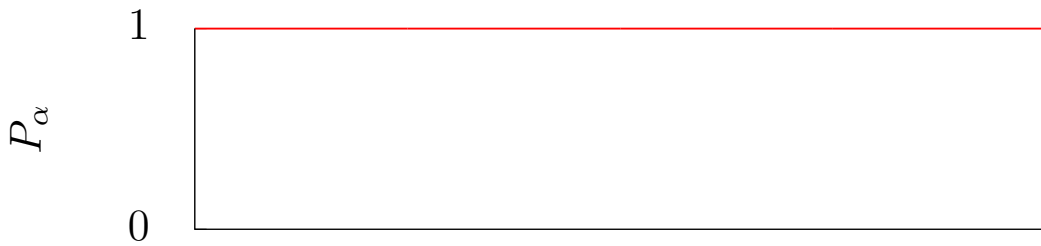
where the constant g include corrections for interactions of the particle with its own field (and other effects). For electron, the corrections are small and easy to calculate in the fully quantum approach (*quantum electrodynamics*). The current theoretical prediction is $g = 2.0023318361(10)$, compared to a recent experimental measured value of $g = 2.0023318416(13)$. On the other hand, "corrections" for the constituents of atomic nuclei, quarks, are two orders of magnitude higher than the basic value of 2! It is because quarks are not "naked" as electrons, they are confined in protons and nucleons, "dressed" by interactions, not only electromagnetic, but mostly strong nuclear with gluon. Therefore, the magnetogyric ratio of the proton is difficult to calculate and we rely on its experimental value. Everything is even more complicated when we go to higher nuclei, consisting of multiple protons and neutrons. In such cases, adding spin angular momenta represents another level of complexity. Fortunately, all equations derived for the electron also apply to nuclei with the same eigenvalues of spin magnetic moments (spin-1/2 nuclei), if the value of γ is replaced by the correct value for the given nucleus.⁴ Magnetogyric ratios of the nuclei observed most frequently are listed in Table 5.1

HOMework

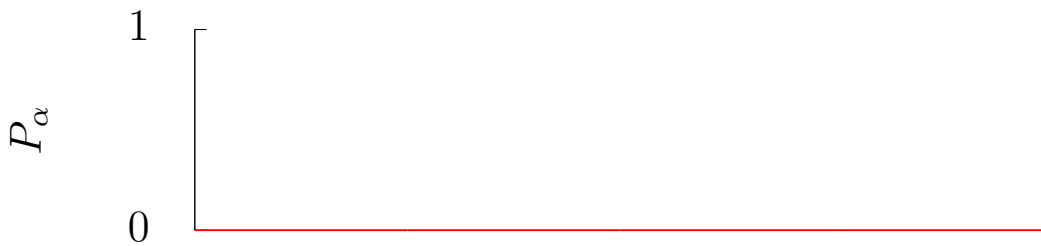
Check that you understand how commutators of the operator of the orbital angular momentum are derived (Section 4.9.9) and derive the Hamiltonian of the spin magnetic moment (Section 5.7.5).

⁴NMR in organic chemistry and biochemistry is usually limited to spin-1/2 nuclei because signal decays too fast if the spin number is greater than 1/2.

A $|\Psi\rangle(t=0) = |\alpha\rangle; \quad \hat{H} = -\gamma B_0 \hat{I}_z = \omega_0 \hat{I}_z$



B $|\Psi\rangle(t=0) = |\beta\rangle; \quad \hat{H} = -\gamma B_0 \hat{I}_z = \omega_0 \hat{I}_z$



C $|\Psi\rangle(t=0) = |\alpha\rangle; \quad \hat{H} = -\gamma B_1 \hat{I}_x = \omega_1 \hat{I}_x$

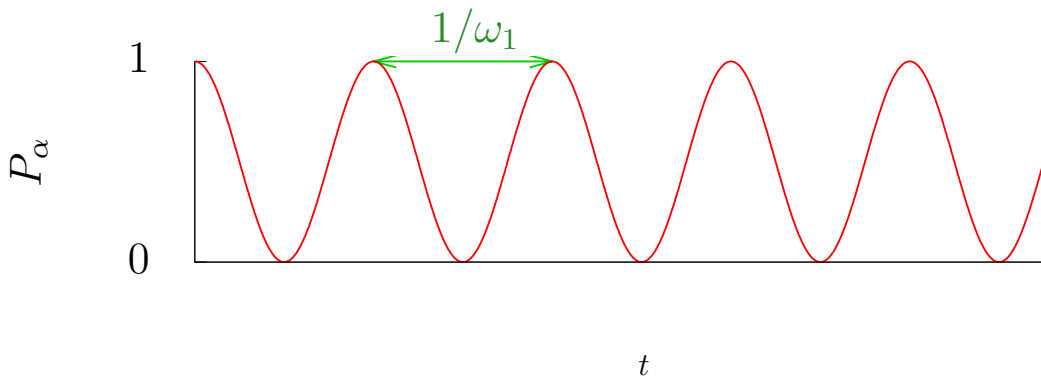


Figure 5.2: Evolution of the probability P_α that a spin-1/2 particle is found in the α state: for a particle in a vertical magnetic field \vec{B}_0 and in the α eigenstate at $t = 0$ (A), for a particle in a vertical magnetic field \vec{B}_0 and in the β eigenstate at $t = 0$ (B), and for a particle in a horizontal magnetic field \vec{B}_1 and in the α state at $t = 0$ (C). The states α and β are represented by eigenfunctions of \hat{I}_z (Panels A and B), but $|\alpha\rangle$ is not an eigenfunction of \hat{I}_x .

Table 5.1: Values of the magnetogyric ratios of selected nuclei

Nucleus	magnetogyric ratio
${}^1_1\text{H}$	$267.513 \times 10^6 \text{ rad.s}^{-1}.\text{T}^{-1}$
${}^{13}_6\text{C}$	$67.262 \times 10^6 \text{ rad.s}^{-1}.\text{T}^{-1}$
${}^{15}_7\text{N}$	$-27.116 \times 10^6 \text{ rad.s}^{-1}.\text{T}^{-1}$
${}^{19}_9\text{F}$	$251.662 \times 10^6 \text{ rad.s}^{-1}.\text{T}^{-1}$
${}^{31}_{15}\text{P}$	$108.291 \times 10^6 \text{ rad.s}^{-1}.\text{T}^{-1}$

5.7 DERIVATIONS

5.7.1 Relativistic quantum mechanics

Imagine that we wish describe a particle moving at a speed v in two coordinate frames, one attached to us (let us call it "our frame") and the other one attached to the particle ("particle's frame"). According to the special theory of relativity, time is slower and mass (closely related to the energy) is higher relative to a "our" coordinate frame than relative to the "particle's frame":

$$t = \frac{t_0}{\sqrt{1-v^2/c^2}} \quad m = \frac{m_0}{\sqrt{1-v^2/c^2}} \quad \mathcal{E}_t = mc^2 = \frac{m_0c^2}{\sqrt{1-v^2/c^2}}, \quad (5.21)$$

where m_0 is the rest mass, m_0c^2 is the rest energy, t_0 is the proper time (i.e., mass, energy, and time in the coordinate frame moving with the particle), and \mathcal{E}_t is the total energy. The first equation can be used to express dt^2

$$dt^2 = \frac{dt_0^2}{1-v^2/c^2} = \frac{m^2c^4 dt_0^2}{m^2c^4 - m^2c^2v^2}, \quad (5.22)$$

where numerator and denominator were multiplied by $\mathcal{E}_t^2 = m^2c^4$ in the second step. Eqs. 5.21 show that $t_0/t = m_0/m$. Therefore

$$dt^2 = \frac{m_0^2c^4 dt^2}{m^2c^4 - m^2c^2v^2}, \quad (5.23)$$

$$m^2c^4 - (m_0c^4) = (m_0c^4) - (m_0c^4) = m_0^2c^4, \quad (5.24)$$

$$\mathcal{E}_t^2 - c^2p_x^2 - c^2p_y^2 - c^2p_z^2 = m_0^2c^4, \quad (5.25)$$

$$0 = -\mathcal{E}_t^2 + c^2p_x^2 + c^2p_y^2 + c^2p_z^2 + m_0^2c^4. \quad (5.26)$$

We see that the special theory of relativity requires that the quantity $-\mathcal{E}_t^2 + c^2p_x^2 + c^2p_y^2 + c^2p_z^2 + m_0^2c^4$ is equal to zero. Let us look for an operator which represents the quantity $-\mathcal{E}_t^2 + c^2p_x^2 + c^2p_y^2 + c^2p_z^2 + m_0^2c^4$. We know that for a monochromatic wave function

$$\psi = e^{\frac{i}{\hbar}(p_x x + p_y y + p_z z - \mathcal{E}_t t)}, \quad (5.27)$$

partial derivatives of ψ serve as operators of energy and momentum:

$$i\hbar \frac{\partial \psi}{\partial x} = p_x \psi \quad i\hbar \frac{\partial \psi}{\partial y} = p_y \psi \quad i\hbar \frac{\partial \psi}{\partial z} = p_z \psi \quad i\hbar \frac{\partial \psi}{\partial t} = \mathcal{E}_t \psi. \quad (5.28)$$

Therefore, the operator of $-\mathcal{E}_t^2 + c^2p_x^2 + c^2p_y^2 + c^2p_z^2 + m_0^2c^4$ should have a form

$$\hbar^2 \frac{\partial^2}{\partial t^2} - c^2 \hbar^2 \frac{\partial^2}{\partial x^2} - c^2 \hbar^2 \frac{\partial^2}{\partial y^2} - c^2 \hbar^2 \frac{\partial^2}{\partial z^2} + (m_0c^2)^2. \quad (5.29)$$

Eq. 5.29 fulfills the requirements of the special theory of relativity, but it contains the second time derivative. As discussed in Section 4.9.7, an attempt to use Eq. 5.29 to describe evolution of the quantum system in time is not consistent with our first postulate of quantum mechanics and with our interpretation of $\Psi^*\Psi$ as the probability density. Therefore, we look for an operator that contains only the first time derivative and allows us to formulate the equation(s) of motion that is in agreement with the special theory of relativity and with the postulates of quantum mechanics. As this problem is not easy to solve, we will proceed step by step. Let us first assume that particles do not move, i.e., $\vec{p} = 0$. Then, Eq. 5.26 simplifies to

$$-\mathcal{E}_t^2 + m_0^2c^4 = 0, \quad (5.30)$$

which can be written as

$$(-\mathcal{E}_t + m_0c^2)(\mathcal{E}_t + m_0c^2) = 0, \quad (5.31)$$

Using the operator of energy,

$$\hbar^2 \frac{\partial^2 \psi}{\partial t^2} + (m_0c^2)^2 \psi = (-\mathcal{E}_t^2 + m_0^2c^4) \psi = 0 \quad (5.32)$$

if ψ is an eigenfunction of the energy operator. The operator of $\mathcal{E}_t^2 - m_0^2c^4$ (let us call it \hat{O}^2) can be obtained by a subsequent application of operators \hat{O}^+ and \hat{O}^- in the following equations of motion:

$$\left(i\hbar \frac{\partial}{\partial t} - m_0c^2 \right) \psi = \hat{O}^+ \psi = 0, \quad (5.33)$$

$$\left(-i\hbar \frac{\partial}{\partial t} - m_0c^2 \right) \psi = \hat{O}^- \psi = 0. \quad (5.34)$$

The operators \hat{O}^- and \hat{O}^+ can be viewed as "square roots" of \hat{O}^2 :

$$\hat{O}^2 \psi \equiv \hbar^2 \frac{\partial^2 \psi}{\partial t^2} + (m_0c^2)^2 \psi = \left(i\hbar \frac{\partial}{\partial t} - m_0c^2 \right) \left(-i\hbar \frac{\partial}{\partial t} - m_0c^2 \right) \psi = \hat{O}^+ \left(\hat{O}^- \psi \right) = 0. \quad (5.35)$$

What are the eigenfunctions? One solution is the monochromatic wave described by Eq. 5.27 (with $p_x = p_y = p_z = 0$). We can prove it by checking that calculating the time derivatives give us the eigenvalues (see the green terms in the following equation):

$$\begin{aligned} & \left(i\hbar \frac{\partial}{\partial t} - m_0c^2 \right) \left(-i\hbar \frac{\partial}{\partial t} - m_0c^2 \right) e^{\frac{i}{\hbar}(-\mathcal{E}_t t)} = \left(i\hbar \frac{\partial}{\partial t} - m_0c^2 \right) (-\mathcal{E}_t - m_0c^2) e^{\frac{i}{\hbar}(-\mathcal{E}_t t)} \\ & = (-\mathcal{E}_t - m_0c^2) \left(i\hbar \frac{\partial}{\partial t} - m_0c^2 \right) e^{\frac{i}{\hbar}(-\mathcal{E}_t t)} = (-\mathcal{E}_t - m_0c^2) (\mathcal{E}_t - m_0c^2) e^{\frac{i}{\hbar}(-\mathcal{E}_t t)} = (m_0^2c^4 - \mathcal{E}_t^2) e^{\frac{i}{\hbar}(-\mathcal{E}_t t)} = 0. \end{aligned} \quad (5.36)$$

But the complex conjugate of the monochromatic wave described by Eq. 5.27 is another possible solution:

$$\begin{aligned} & \left(i\hbar \frac{\partial}{\partial t} - m_0c^2 \right) \left(-i\hbar \frac{\partial}{\partial t} - m_0c^2 \right) e^{\frac{i}{\hbar}(\mathcal{E}_t t)} = \left(i\hbar \frac{\partial}{\partial t} - m_0c^2 \right) (\mathcal{E}_t - m_0c^2) e^{\frac{i}{\hbar}(\mathcal{E}_t t)} \\ & = (\mathcal{E}_t - m_0c^2) \left(i\hbar \frac{\partial}{\partial t} - m_0c^2 \right) e^{\frac{i}{\hbar}(\mathcal{E}_t t)} = (\mathcal{E}_t - m_0c^2) (-\mathcal{E}_t - m_0c^2) e^{\frac{i}{\hbar}(\mathcal{E}_t t)} = (m_0^2c^4 - \mathcal{E}_t^2) e^{\frac{i}{\hbar}(\mathcal{E}_t t)} = 0. \end{aligned} \quad (5.37)$$

The second eigenfunction can be interpreted as a particle with a positive energy moving backwards in time, or as an *antiparticle* moving forward in time.

Let us now turn our attention to particles that can move ($\vec{p} \neq 0$). For the most interesting particles as electron or quarks, the operator \hat{O}^2 should have the form described by Eq. 5.29

$$\hat{O}^2 \psi = \left(\hbar^2 \frac{\partial^2}{\partial t^2} - c^2 \hbar^2 \frac{\partial^2}{\partial z^2} - c^2 \hbar^2 \frac{\partial^2}{\partial x^2} - c^2 \hbar^2 \frac{\partial^2}{\partial y^2} + (m_0c^2)^2 \right) \psi. \quad (5.38)$$

Let us try to find "square roots" of the operator \hat{O}^2 for a particle with a momentum \vec{p} . In Eq. 5.35, \hat{O}^+ and \hat{O}^- were complex conjugates. A similar choice for a particle with a momentum \vec{p} , i.e.,⁵

$$\hat{O}^+ \psi = \left(i\hbar \frac{\partial}{\partial t} + i\hbar \frac{\partial}{\partial x} + i\hbar \frac{\partial}{\partial y} + i\hbar \frac{\partial}{\partial z} - m_0c^2 \right) \psi \quad (5.39)$$

$$\hat{O}^- \psi = \left(-i\hbar \frac{\partial}{\partial t} - i\hbar \frac{\partial}{\partial x} - i\hbar \frac{\partial}{\partial y} - i\hbar \frac{\partial}{\partial z} - m_0c^2 \right) \psi \quad (5.40)$$

gives

$$\begin{aligned} \hat{O}^- \hat{O}^+ \psi = \hat{O}^2 \psi = & \hbar^2 \frac{\partial^2 \psi}{\partial t^2} + ch^2 \frac{\partial \psi}{\partial t} \frac{\partial \psi}{\partial x} + ch^2 \frac{\partial \psi}{\partial t} \frac{\partial \psi}{\partial y} + ch^2 \frac{\partial \psi}{\partial t} \frac{\partial \psi}{\partial z} - im_0c^2 \hbar \frac{\partial \psi}{\partial t} \\ & + ch^2 \frac{\partial \psi}{\partial x} \frac{\partial \psi}{\partial t} + \hbar^2 \frac{\partial^2 \psi}{\partial x^2} + ch^2 \frac{\partial \psi}{\partial x} \frac{\partial \psi}{\partial y} + ch^2 \frac{\partial \psi}{\partial x} \frac{\partial \psi}{\partial z} - im_0c^2 \hbar \frac{\partial \psi}{\partial x} \\ & + ch^2 \frac{\partial \psi}{\partial y} \frac{\partial \psi}{\partial t} + ch^2 \frac{\partial \psi}{\partial y} \frac{\partial \psi}{\partial x} + \hbar^2 \frac{\partial^2 \psi}{\partial y^2} + ch^2 \frac{\partial \psi}{\partial y} \frac{\partial \psi}{\partial z} - im_0c^2 \hbar \frac{\partial \psi}{\partial y} \\ & + ch^2 \frac{\partial \psi}{\partial z} \frac{\partial \psi}{\partial t} + ch^2 \frac{\partial \psi}{\partial z} \frac{\partial \psi}{\partial x} + ch^2 \frac{\partial \psi}{\partial z} \frac{\partial \psi}{\partial y} + \hbar^2 \frac{\partial^2 \psi}{\partial z^2} - im_0c^2 \hbar \frac{\partial \psi}{\partial z} \\ & + im_0c^2 \hbar \frac{\partial \psi}{\partial t} + im_0c^2 \hbar \frac{\partial \psi}{\partial x} + im_0c^2 \hbar \frac{\partial \psi}{\partial y} + im_0c^2 \hbar \frac{\partial \psi}{\partial z} + (m_0c^2)^2 \psi \end{aligned} \quad (5.41)$$

⁵It make sense to look for an operator which depends on time and space coordinates in a similar manner because time and space play similar roles in quantum mechanics. As the first time derivative is our requirement, the equation should contain also the first derivatives $\partial/\partial x, \partial/\partial y, \partial/\partial z$.

with the correct five square terms shown in blue, but also with additional twenty unwanted mixed terms shown in red.

As the second trial, let us try (naïvely) to get rid of the unwanted mixed terms by introducing coefficients γ_j that hopefully cancel them:

$$\hat{O}^+\psi = \left(i\hbar \frac{\partial}{\partial t} \gamma_0 + i\hbar \frac{\partial}{\partial x} \gamma_1 + i\hbar \frac{\partial}{\partial y} \gamma_2 + i\hbar \frac{\partial}{\partial z} \gamma_3 - m_0 c^2 \right) \psi \quad (5.42)$$

$$\hat{O}^-\psi = \left(-i\hbar \frac{\partial}{\partial t} \gamma_0 - i\hbar \frac{\partial}{\partial x} \gamma_1 - i\hbar \frac{\partial}{\partial y} \gamma_2 - i\hbar \frac{\partial}{\partial z} \gamma_3 - m_0 c^2 \right) \psi. \quad (5.43)$$

Then,

$$\begin{aligned} \hat{O}^-\hat{O}^+\psi = \hat{O}^2\psi = & \gamma_0^2 \hbar^2 \frac{\partial^2 \psi}{\partial t^2} + \gamma_0 \gamma_1 \hbar^2 \frac{\partial \psi}{\partial t} \frac{\partial \psi}{\partial x} + \gamma_0 \gamma_2 \hbar^2 \frac{\partial \psi}{\partial t} \frac{\partial \psi}{\partial y} + \gamma_0 \gamma_3 \hbar^2 \frac{\partial \psi}{\partial t} \frac{\partial \psi}{\partial z} - i\gamma_0 m_0 c^2 \hbar \frac{\partial \psi}{\partial t} \\ & + \gamma_1 \gamma_0 \hbar^2 \frac{\partial \psi}{\partial x} \frac{\partial \psi}{\partial t} + \gamma_1^2 \hbar^2 \frac{\partial^2 \psi}{\partial x^2} + \gamma_1 \gamma_2 \hbar^2 \frac{\partial \psi}{\partial x} \frac{\partial \psi}{\partial y} + \gamma_1 \gamma_3 \hbar^2 \frac{\partial \psi}{\partial x} \frac{\partial \psi}{\partial z} - i\gamma_1 m_0 c^2 \hbar \frac{\partial \psi}{\partial x} \\ & + \gamma_2 \gamma_0 \hbar^2 \frac{\partial \psi}{\partial y} \frac{\partial \psi}{\partial t} + \gamma_2 \gamma_1 \hbar^2 \frac{\partial \psi}{\partial y} \frac{\partial \psi}{\partial x} + \gamma_2^2 \hbar^2 \frac{\partial^2 \psi}{\partial y^2} + \gamma_2 \gamma_3 \hbar^2 \frac{\partial \psi}{\partial y} \frac{\partial \psi}{\partial z} - i\gamma_2 m_0 c^2 \hbar \frac{\partial \psi}{\partial y} \\ & + \gamma_3 \gamma_0 \hbar^2 \frac{\partial \psi}{\partial z} \frac{\partial \psi}{\partial t} + \gamma_3 \gamma_1 \hbar^2 \frac{\partial \psi}{\partial z} \frac{\partial \psi}{\partial x} + \gamma_3 \gamma_2 \hbar^2 \frac{\partial \psi}{\partial z} \frac{\partial \psi}{\partial y} + \gamma_3^2 \hbar^2 \frac{\partial^2 \psi}{\partial z^2} - i\gamma_3 m_0 c^2 \hbar \frac{\partial \psi}{\partial z} \\ & + i\gamma_0 m_0 c^2 \hbar \frac{\partial \psi}{\partial t} + i\gamma_1 m_0 c^2 \hbar \frac{\partial \psi}{\partial x} + i\gamma_2 m_0 c^2 \hbar \frac{\partial \psi}{\partial y} + i\gamma_3 m_0 c^2 \hbar \frac{\partial \psi}{\partial z} + (m_0 c^2)^2 \psi. \end{aligned} \quad (5.44)$$

Obviously, the green terms with $-i\gamma_j m_0 c^2 \hbar$ cancel each other, which removes eight unwanted terms. Can we also remove the remaining dozen of unwanted mixed derivative terms? In order to do it, we need the following conditions to be fulfilled:

$$\gamma_0^2 = 1, \quad (5.45)$$

$$\gamma_1^2 = -1 \quad \gamma_2^2 = -1 \quad \gamma_3^2 = -1 \quad (5.46)$$

and

$$\gamma_j \gamma_k + \gamma_k \gamma_j = 0 \text{ for } j \neq k. \quad (5.47)$$

These conditions are clearly in conflict. The first four condition require γ_j to be ± 1 or $\pm i$, but the last condition requires them to be zero. There are no complex numbers that allow us to get the correct operator \hat{O}^2 . However, there are mathematical objects, that can fulfil the listed conditions simultaneously. Such objects are *matrices*.

Let us replace the coefficients γ_j in Eqs. 5.42–5.44 by matrices⁶ $\hat{\gamma}^j$:

$$\hat{O}^+\Psi = \left(i\hbar \frac{\partial}{\partial t} \hat{\gamma}^0 + i\hbar \frac{\partial}{\partial x} \hat{\gamma}^1 + i\hbar \frac{\partial}{\partial y} \hat{\gamma}^2 + i\hbar \frac{\partial}{\partial z} \hat{\gamma}^3 - m_0 c^2 \hat{1} \right) \Psi = 0 \quad (5.48)$$

$$\hat{O}^-\Psi = \left(-i\hbar \frac{\partial}{\partial t} \hat{\gamma}^0 - i\hbar \frac{\partial}{\partial x} \hat{\gamma}^1 - i\hbar \frac{\partial}{\partial y} \hat{\gamma}^2 - i\hbar \frac{\partial}{\partial z} \hat{\gamma}^3 - m_0 c^2 \hat{1} \right) \Psi = 0. \quad (5.49)$$

We need a set of four matrices $\hat{\gamma}^j$ with the following properties:

$$\hat{\gamma}^0 \cdot \hat{\gamma}^0 = \hat{1}, \quad (5.50)$$

$$\hat{\gamma}^1 \cdot \hat{\gamma}^1 = -\hat{1} \quad \hat{\gamma}^2 \cdot \hat{\gamma}^2 = -\hat{1} \quad \hat{\gamma}^3 \cdot \hat{\gamma}^3 = -\hat{1} \quad (5.51)$$

and

$$\hat{\gamma}^j \cdot \hat{\gamma}^k + \hat{\gamma}^k \cdot \hat{\gamma}^j = \hat{0} \text{ for } j \neq k. \quad (5.52)$$

In addition, there is a physical restriction. We know that the operator of energy (Hamiltonian) is

$$\hat{H} = i\hbar \frac{\partial}{\partial t} \quad (5.53)$$

We can get the *Dirac Hamiltonian* by multiplying Eq. 5.48 by $\hat{\gamma}^0$ from left:

⁶In relativistic quantum mechanics, these matrices can be treated as four components of a *four-vector*. There are two types of four-vectors (contravariant and covariant) which transform differently. There is a convention to distinguish these two types by writing components of covariant vectors with lower indices and components of contravariant vectors with upper indices. To keep this convention, we label the gamma matrices with upper indices, do not confuse them with power!

$$i\hbar \frac{\partial}{\partial t} \hat{\Psi} = \left(-i\hbar \frac{\partial}{\partial x} \hat{\gamma}^0 \cdot \hat{\gamma}^1 - i\hbar \frac{\partial}{\partial y} \hat{\gamma}^0 \cdot \hat{\gamma}^2 - i\hbar \frac{\partial}{\partial z} \hat{\gamma}^0 \cdot \hat{\gamma}^3 + m_0 c^2 \hat{\gamma}^0 \right) \Psi = 0. \quad (5.54)$$

Operator of any measurable quantity must be *Hermitian* ($\langle \psi | \hat{O} \psi \rangle = \langle \hat{O} \psi | \psi \rangle$) in order to give real values of the measured value. Since the terms in the Hamiltonian are proportional to $\hat{\gamma}^0$ or to $\hat{\gamma}^0 \cdot \hat{\gamma}^j$, all these matrices must be Hermitian (the elements in the j -th row and k -th column must be equal to the complex conjugates of the elements in the k -th row and j -th column for each j and k).

5.7.2 Finding the matrices

Our task is to find Hermitian matrices fulfilling the criteria imposed by Eqs. 5.50–5.52. We have a certain liberty in choosing the matrices. A matrix equation is nothing else than a set of equations. One of the matrices can be always chosen to be diagonal. Let us assume that $\hat{\gamma}^0$ is diagonal.⁷ How should the diagonal elements of $\hat{\gamma}^0$ look like? In order to fulfill Eq. 5.50, the elements must be +1 or –1.

Another requirement follows from a general property of matrix multiplication: Trace (sum of the diagonal elements) of the matrix product $\hat{A} \cdot \hat{B}$ is the same as that of $\hat{B} \cdot \hat{A}$. Let us assume that $\hat{A} = \hat{\gamma}^j$ and $\hat{B} = \hat{\gamma}^0 \cdot \hat{\gamma}^j$. Then,

$$\text{Tr}\{\hat{\gamma}^j \cdot \hat{\gamma}^0 \cdot \hat{\gamma}^j\} = \text{Tr}\{\hat{\gamma}^j \cdot \hat{\gamma}^j \cdot \hat{\gamma}^0\}. \quad (5.55)$$

But Eq. 5.52 tells us that $\hat{\gamma}^0 \cdot \hat{\gamma}^j = -\hat{\gamma}^j \cdot \hat{\gamma}^0$. Therefore, the left-hand side of Eq. 5.55 can be written as $\text{Tr}\{\hat{\gamma}^j \cdot (-\hat{\gamma}^j) \cdot \hat{\gamma}^0\}$, resulting in

$$-\text{Tr}\{\hat{\gamma}^j \cdot \hat{\gamma}^j \cdot \hat{\gamma}^0\} = \text{Tr}\{\hat{\gamma}^j \cdot \hat{\gamma}^j \cdot \hat{\gamma}^0\}, \quad (5.56)$$

and using Eq. 5.52

$$\text{Tr}\{\hat{\gamma}^0\} = -\text{Tr}\{\hat{\gamma}^0\}. \quad (5.57)$$

It can be true only if the trace is equal to zero. Consequently, the diagonal of $\hat{\gamma}^0$ must contain the same number of +1 and –1 elements. It also tells us that the dimension of the $\hat{\gamma}^j$ matrices must be even. Can they be two-dimensional?

No, for the following reason. The four $\hat{\gamma}^j$ matrices must be linearly independent, and it is impossible to find four linearly independent 2×2 matrices so that all fulfill Eq. 5.52.⁸

Is it possible to find four-dimensional $\hat{\gamma}^j$ matrices? Yes. We start by choosing

$$\hat{\gamma}^0 = \begin{pmatrix} 1 & 0 & 0 & 0 \\ 0 & 1 & 0 & 0 \\ 0 & 0 & -1 & 0 \\ 0 & 0 & 0 & -1 \end{pmatrix} \quad (5.58)$$

(the diagonal must contain two +1 elements and two –1 elements, their order is arbitrary, but predetermines forms of the other matrices).

Being diagonal, $\hat{\gamma}^0$ is of course Hermitian. The $\hat{\gamma}^0 \cdot \hat{\gamma}^j$ products

$$\begin{pmatrix} 1 & 0 & 0 & 0 \\ 0 & 1 & 0 & 0 \\ 0 & 0 & -1 & 0 \\ 0 & 0 & 0 & -1 \end{pmatrix} \cdot \begin{pmatrix} \gamma_{1,1}^j & \gamma_{1,2}^j & \gamma_{1,3}^j & \gamma_{1,4}^j \\ \gamma_{2,1}^j & \gamma_{2,2}^j & \gamma_{2,3}^j & \gamma_{2,4}^j \\ \gamma_{3,1}^j & \gamma_{3,2}^j & \gamma_{3,3}^j & \gamma_{3,4}^j \\ \gamma_{4,1}^j & \gamma_{4,2}^j & \gamma_{4,3}^j & \gamma_{4,4}^j \end{pmatrix} = \begin{pmatrix} \gamma_{1,1}^j & \gamma_{1,2}^j & \gamma_{1,3}^j & \gamma_{1,4}^j \\ \gamma_{2,1}^j & \gamma_{2,2}^j & \gamma_{2,3}^j & \gamma_{2,4}^j \\ -\gamma_{3,1}^j & -\gamma_{3,2}^j & -\gamma_{3,3}^j & -\gamma_{3,4}^j \\ -\gamma_{4,1}^j & -\gamma_{4,2}^j & -\gamma_{4,3}^j & -\gamma_{4,4}^j \end{pmatrix} \quad (5.59)$$

must be also Hermitian, i.e.,

$$\begin{pmatrix} \gamma_{1,1}^j & \gamma_{1,2}^j & \gamma_{1,3}^j & \gamma_{1,4}^j \\ \gamma_{2,1}^j & \gamma_{2,2}^j & \gamma_{2,3}^j & \gamma_{2,4}^j \\ -\gamma_{3,1}^j & -\gamma_{3,2}^j & -\gamma_{3,3}^j & -\gamma_{3,4}^j \\ -\gamma_{4,1}^j & -\gamma_{4,2}^j & -\gamma_{4,3}^j & -\gamma_{4,4}^j \end{pmatrix} = \begin{pmatrix} (\gamma_{1,1}^j)^* & (\gamma_{2,1}^j)^* & -(\gamma_{3,1}^j)^* & -(\gamma_{4,1}^j)^* \\ (\gamma_{1,2}^j)^* & (\gamma_{2,2}^j)^* & -(\gamma_{3,2}^j)^* & -(\gamma_{4,2}^j)^* \\ (\gamma_{1,3}^j)^* & (\gamma_{2,3}^j)^* & -(\gamma_{3,3}^j)^* & -(\gamma_{4,3}^j)^* \\ (\gamma_{1,4}^j)^* & (\gamma_{2,4}^j)^* & -(\gamma_{3,4}^j)^* & -(\gamma_{4,4}^j)^* \end{pmatrix}. \quad (5.60)$$

⁷This is a good choice because it results in a diagonal matrix representing the Hamiltonian, which is convenient.

⁸If the $\hat{\gamma}^j$ matrices are linearly independent, they can be used as a basis. If they constitute a basis, there must exist a linear combination of $\hat{\gamma}^j$ giving any 2×2 matrix, e.g., the unit matrix $\hat{1}$: $\hat{1} = c_0 \hat{\gamma}^0 + c_1 \hat{\gamma}^1 + c_2 \hat{\gamma}^2 + c_3 \hat{\gamma}^3$. Let us now multiply this equation by $\hat{\gamma}^0$ from left (and use Eq. 5.50)

$$\hat{\gamma}^0 = c_0 \hat{1} + c_1 \hat{\gamma}^0 \cdot \hat{\gamma}^1 + c_2 \hat{\gamma}^0 \cdot \hat{\gamma}^2 + c_3 \hat{\gamma}^0 \cdot \hat{\gamma}^3,$$

then from right

$$\hat{\gamma}^0 = c_0 \hat{1} + c_1 \hat{\gamma}^1 \cdot \hat{\gamma}^0 + c_2 \hat{\gamma}^2 \cdot \hat{\gamma}^0 + c_3 \hat{\gamma}^3 \cdot \hat{\gamma}^0,$$

and sum both equations. If the matrices fulfill Eq. 5.52, the result must be $2\hat{\gamma}^0 = 2c_0 \hat{1}$, but this cannot be true because we need $\hat{\gamma}^0$ with a zero trace and the trace of the unit matrix $\hat{1}$ is obviously not zero.

At the same time, Eq. 5.52 requires $\hat{\gamma}^0 \cdot \hat{\gamma}^j = -\hat{\gamma}^j \cdot \hat{\gamma}^0$

$$\begin{pmatrix} \gamma_{1,1}^j & \gamma_{1,2}^j & \gamma_{1,3}^j & \gamma_{1,4}^j \\ \gamma_{2,1}^j & \gamma_{2,2}^j & \gamma_{2,3}^j & \gamma_{2,4}^j \\ -\gamma_{3,1}^j & -\gamma_{3,2}^j & -\gamma_{3,3}^j & -\gamma_{3,4}^j \\ -\gamma_{4,1}^j & -\gamma_{4,2}^j & -\gamma_{4,3}^j & -\gamma_{4,4}^j \end{pmatrix} = - \begin{pmatrix} \gamma_{1,1}^j & \gamma_{1,2}^j & \gamma_{1,3}^j & \gamma_{1,4}^j \\ \gamma_{2,1}^j & \gamma_{2,2}^j & \gamma_{2,3}^j & \gamma_{2,4}^j \\ \gamma_{3,1}^j & \gamma_{3,2}^j & \gamma_{3,3}^j & \gamma_{3,4}^j \\ \gamma_{4,1}^j & \gamma_{4,2}^j & \gamma_{4,3}^j & \gamma_{4,4}^j \end{pmatrix} \cdot \begin{pmatrix} 1 & 0 & 0 & 0 \\ 0 & 1 & 0 & 0 \\ 0 & 0 & -1 & 0 \\ 0 & 0 & 0 & -1 \end{pmatrix} = \begin{pmatrix} -\gamma_{1,1}^j & -\gamma_{1,2}^j & \gamma_{1,3}^j & \gamma_{1,4}^j \\ -\gamma_{2,1}^j & -\gamma_{2,2}^j & \gamma_{2,3}^j & \gamma_{2,4}^j \\ -\gamma_{3,1}^j & -\gamma_{3,2}^j & \gamma_{3,3}^j & \gamma_{3,4}^j \\ -\gamma_{4,1}^j & -\gamma_{4,2}^j & \gamma_{4,3}^j & \gamma_{4,4}^j \end{pmatrix}, \quad (5.61)$$

which is possible only if the red elements are equal to zero. Eq. 5.60 shows that the blue elements form two adjoint 2×2 matrices for each $j > 0$:

$$\hat{\gamma}^j = \begin{pmatrix} 0 & 0 & \gamma_{1,3}^j & \gamma_{1,4}^j \\ 0 & 0 & \gamma_{2,3}^j & \gamma_{2,4}^j \\ \gamma_{3,1}^j & \gamma_{3,2}^j & 0 & 0 \\ \gamma_{4,1}^j & \gamma_{4,2}^j & 0 & 0 \end{pmatrix} = \begin{pmatrix} 0 & 0 & \gamma_{1,3}^j & \gamma_{1,4}^j \\ 0 & 0 & \gamma_{2,3}^j & \gamma_{2,4}^j \\ -(\gamma_{1,3}^j)^* & -(\gamma_{2,3}^j)^* & 0 & 0 \\ -(\gamma_{1,4}^j)^* & -(\gamma_{2,4}^j)^* & 0 & 0 \end{pmatrix} = \begin{pmatrix} \hat{0} & \hat{\sigma}^j \\ -(\hat{\sigma}^j)^\dagger & \hat{0} \end{pmatrix}. \quad (5.62)$$

Now we use Eqs. 5.51 and 5.52 to find the actual forms of three $\hat{\sigma}^j$ (and consequently $\hat{\gamma}^j$) matrices for $j > 0$. Eq. 5.51 requires

$$\begin{pmatrix} \hat{0} & \hat{\sigma}^j \\ -(\hat{\sigma}^j)^\dagger & \hat{0} \end{pmatrix} \cdot \begin{pmatrix} \hat{0} & \hat{\sigma}^j \\ -(\hat{\sigma}^j)^\dagger & \hat{0} \end{pmatrix} = \begin{pmatrix} -\hat{\sigma}^j \cdot (\hat{\sigma}^j)^\dagger & \hat{0} \\ \hat{0} & -(\hat{\sigma}^j)^\dagger \cdot \hat{\sigma}^j \end{pmatrix} = - \begin{pmatrix} \hat{1} & \hat{0} \\ \hat{0} & \hat{1} \end{pmatrix} = \begin{pmatrix} -\hat{1} & \hat{0} \\ \hat{0} & -\hat{1} \end{pmatrix}, \quad (5.63)$$

i.e.,

$$\hat{\sigma}^j \cdot (\hat{\sigma}^j)^\dagger = (\hat{\sigma}^j)^\dagger \cdot \hat{\sigma}^j = \hat{1} \quad (5.64)$$

Eq. 5.64 is obviously true if the $\hat{\sigma}^j$ matrices are Hermitian ($\hat{\sigma}^j = (\hat{\sigma}^j)^\dagger$), i.e. $\sigma_{m,n}^j = (\sigma_{n,m}^j)^*$. It implies that the $\hat{\sigma}^j$ matrices have the following form:

$$\hat{\sigma}^j = \begin{pmatrix} a_j & c_j \\ c_j^* & b_j \end{pmatrix}, \quad (5.65)$$

where a_j and b_j are real, and c_j is complex. Eq. 5.64 can be then written as

$$\hat{\sigma}^j \cdot (\hat{\sigma}^j)^\dagger = \hat{\sigma}^j \cdot \hat{\sigma}^j = \begin{pmatrix} a_j & c_j \\ c_j^* & b_j \end{pmatrix} \cdot \begin{pmatrix} a_j & c_j \\ c_j^* & b_j \end{pmatrix} = \begin{pmatrix} a_j^2 + |c_j|^2 & (a_j + b_j)c_j \\ (a_j + b_j)c_j^* & b_j^2 + |c_j|^2 \end{pmatrix} = \begin{pmatrix} 1 & 0 \\ 0 & 1 \end{pmatrix}. \quad (5.66)$$

The off-diagonal terms of the product matrix must be equal to zero, which is true if $a_j = -b_j$ or $|c_j| = 0$. In the former case, matrices $\hat{\sigma}^j$ can be written as

$$\hat{\sigma}^j = \begin{pmatrix} \sqrt{1 - |c_j|^2} & c_j \\ c_j^* & -\sqrt{1 - |c_j|^2} \end{pmatrix}, \quad (5.67)$$

in the latter case, there are only two possibilities how to construct the $\hat{\sigma}^j$ matrix:

$$\hat{\sigma}^j = \begin{pmatrix} 1 & 0 \\ 0 & 1 \end{pmatrix} \quad \text{or} \quad \hat{\sigma}^j = \begin{pmatrix} 1 & 0 \\ 0 & -1 \end{pmatrix} \quad (5.68)$$

(note that $|c_j|^2 = 0 \Rightarrow a_j^2 = b_j^2 = 1$.) Eq. 5.52 shows that the second option is correct. Eq. 5.52 requires

$$\begin{pmatrix} \hat{0} & \hat{\sigma}^j \\ -(\hat{\sigma}^j)^\dagger & \hat{0} \end{pmatrix} \cdot \begin{pmatrix} \hat{0} & \hat{\sigma}^k \\ -(\hat{\sigma}^k)^\dagger & \hat{0} \end{pmatrix} + \begin{pmatrix} \hat{0} & \hat{\sigma}^k \\ -(\hat{\sigma}^k)^\dagger & \hat{0} \end{pmatrix} \cdot \begin{pmatrix} \hat{0} & \hat{\sigma}^j \\ -(\hat{\sigma}^j)^\dagger & \hat{0} \end{pmatrix} = - \begin{pmatrix} \hat{\sigma}^j \cdot (\hat{\sigma}^k)^\dagger + \hat{\sigma}^k \cdot (\hat{\sigma}^j)^\dagger & \hat{0} \\ \hat{0} & (\hat{\sigma}^j)^\dagger \cdot \hat{\sigma}^k + (\hat{\sigma}^k)^\dagger \cdot \hat{\sigma}^j \end{pmatrix} = \begin{pmatrix} \hat{0} & \hat{0} \\ \hat{0} & \hat{0} \end{pmatrix}, \quad (5.69)$$

therefore no $\hat{\sigma}^j$ can be a unit matrix.

As Eq. 5.68 unambiguously defines one sigma matrix (let us call it $\hat{\sigma}^3$), the other two ($\hat{\sigma}^1$ and $\hat{\sigma}^2$) are given by Eq. 5.67. According to Eq. 5.52,

$$\begin{pmatrix} 1 & 0 \\ 0 & -1 \end{pmatrix} \cdot \begin{pmatrix} \sqrt{1 - |c_j|^2} & c_j \\ c_j^* & -\sqrt{1 - |c_j|^2} \end{pmatrix} + \begin{pmatrix} \sqrt{1 - |c_j|^2} & c_j \\ c_j^* & -\sqrt{1 - |c_j|^2} \end{pmatrix} \cdot \begin{pmatrix} 1 & 0 \\ 0 & -1 \end{pmatrix} = \begin{pmatrix} 2\sqrt{1 - |c_j|^2} & 0 \\ 0 & -2\sqrt{1 - |c_j|^2} \end{pmatrix} = \begin{pmatrix} 0 & 0 \\ 0 & 0 \end{pmatrix}, \quad (5.70)$$

showing that $|c_j|^2 = 1$ and the diagonal elements of $\hat{\sigma}^1$ and $\hat{\sigma}^2$ are equal to zero. Therefore, these equations can be written as

$$\hat{\sigma}^1 = \begin{pmatrix} 0 & e^{i\phi_1} \\ e^{-i\phi_1} & 0 \end{pmatrix} \quad \hat{\sigma}^2 = \begin{pmatrix} 0 & e^{i\phi_2} \\ e^{-i\phi_2} & 0 \end{pmatrix} \quad (5.71)$$

According to Eq. 5.52,

$$\begin{aligned} \begin{pmatrix} 0 & e^{i\phi_1} \\ e^{-i\phi_1} & 0 \end{pmatrix} \cdot \begin{pmatrix} 0 & e^{i\phi_2} \\ e^{-i\phi_2} & 0 \end{pmatrix} + \begin{pmatrix} 0 & e^{i\phi_2} \\ e^{-i\phi_2} & 0 \end{pmatrix} \cdot \begin{pmatrix} 0 & e^{i\phi_1} \\ e^{-i\phi_1} & 0 \end{pmatrix} &= \begin{pmatrix} 0 & e^{i(\phi_1-\phi_2)} + e^{-i(\phi_1-\phi_2)} \\ e^{-i(\phi_1-\phi_2)} + e^{i(\phi_1-\phi_2)} & 0 \end{pmatrix} = \\ \begin{pmatrix} 0 & 2\cos(\phi_1-\phi_2) \\ 2\cos(\phi_1-\phi_2) & 0 \end{pmatrix} &= \begin{pmatrix} 0 & 0 \\ 0 & 0 \end{pmatrix}. \end{aligned} \quad (5.72)$$

The off-diagonal elements of the sum of the matrix products are equal to zero if the phases differ by $\pi/2$. Choosing $\phi_1 = 0$, the set of three sigma matrices is

$$\hat{\sigma}^1 = \begin{pmatrix} 0 & 1 \\ 1 & 0 \end{pmatrix} \quad \hat{\sigma}^2 = \begin{pmatrix} 0 & -i \\ i & 0 \end{pmatrix} \quad \hat{\sigma}^3 = \begin{pmatrix} 1 & 0 \\ 0 & -1 \end{pmatrix} \quad (5.73)$$

and the set of the four gamma matrices is

$$\hat{\gamma}^0 = \begin{pmatrix} 1 & 0 & 0 & 0 \\ 0 & 1 & 0 & 0 \\ 0 & 0 & -1 & 0 \\ 0 & 0 & 0 & -1 \end{pmatrix} \quad \hat{\gamma}^1 = \begin{pmatrix} 0 & 0 & 0 & 1 \\ 0 & 0 & 1 & 0 \\ 0 & -1 & 0 & 0 \\ -1 & 0 & 0 & 0 \end{pmatrix} \quad \hat{\gamma}^2 = \begin{pmatrix} 0 & 0 & 0 & -i \\ 0 & 0 & i & 0 \\ 0 & i & 0 & 0 \\ -i & 0 & 0 & 0 \end{pmatrix} \quad \hat{\gamma}^3 = \begin{pmatrix} 0 & 0 & 1 & 0 \\ 0 & 0 & 0 & -1 \\ -1 & 0 & 0 & 0 \\ 0 & 1 & 0 & 0 \end{pmatrix}. \quad (5.74)$$

With the help of the $\hat{\gamma}^j$ matrices, we can modify our definition of \hat{O}^+ and \hat{O}^- to get the correct operator \hat{O}^2 :

$$\begin{aligned} \left(i\hbar \frac{\partial}{\partial t} \begin{pmatrix} 1 & 0 & 0 & 0 \\ 0 & 1 & 0 & 0 \\ 0 & 0 & -1 & 0 \\ 0 & 0 & 0 & -1 \end{pmatrix} + i\hbar \frac{\partial}{\partial z} \begin{pmatrix} 0 & 0 & 1 & 0 \\ 0 & 0 & 0 & -1 \\ -1 & 0 & 0 & 0 \\ 0 & 1 & 0 & 0 \end{pmatrix} + i\hbar \frac{\partial}{\partial x} \begin{pmatrix} 0 & 0 & 0 & 1 \\ 0 & 0 & 1 & 0 \\ 0 & -1 & 0 & 0 \\ -1 & 0 & 0 & 0 \end{pmatrix} + i\hbar \frac{\partial}{\partial y} \begin{pmatrix} 0 & 0 & 0 & -i \\ 0 & 0 & i & 0 \\ 0 & i & 0 & 0 \\ -i & 0 & 0 & 0 \end{pmatrix} \right. \\ \left. - m_0 c^2 \begin{pmatrix} 1 & 0 & 0 & 0 \\ 0 & 1 & 0 & 0 \\ 0 & 0 & 1 & 0 \\ 0 & 0 & 0 & 1 \end{pmatrix} \right) \begin{pmatrix} \psi_1 \\ \psi_2 \\ \psi_3 \\ \psi_4 \end{pmatrix} = \hat{O}^+ \Psi = 0, \end{aligned} \quad (5.75)$$

$$\begin{aligned} \left(-i\hbar \frac{\partial}{\partial t} \begin{pmatrix} 1 & 0 & 0 & 0 \\ 0 & 1 & 0 & 0 \\ 0 & 0 & -1 & 0 \\ 0 & 0 & 0 & -1 \end{pmatrix} - i\hbar \frac{\partial}{\partial z} \begin{pmatrix} 0 & 0 & 1 & 0 \\ 0 & 0 & 0 & -1 \\ -1 & 0 & 0 & 0 \\ 0 & 1 & 0 & 0 \end{pmatrix} - i\hbar \frac{\partial}{\partial x} \begin{pmatrix} 0 & 0 & 0 & 1 \\ 0 & 0 & 1 & 0 \\ 0 & -1 & 0 & 0 \\ -1 & 0 & 0 & 0 \end{pmatrix} - i\hbar \frac{\partial}{\partial y} \begin{pmatrix} 0 & 0 & 0 & -i \\ 0 & 0 & i & 0 \\ 0 & i & 0 & 0 \\ -i & 0 & 0 & 0 \end{pmatrix} \right. \\ \left. - m_0 c^2 \begin{pmatrix} 1 & 0 & 0 & 0 \\ 0 & 1 & 0 & 0 \\ 0 & 0 & 1 & 0 \\ 0 & 0 & 0 & 1 \end{pmatrix} \right) \begin{pmatrix} \psi_1 \\ \psi_2 \\ \psi_3 \\ \psi_4 \end{pmatrix} = \hat{O}^- \Psi = 0. \end{aligned} \quad (5.76)$$

5.7.3 Solution of the Dirac equation

Introducing matrices means that we do not have a single equation of motion, but a set of four equations for four coupled wave functions. The complete wave function Ψ is therefore a vector consisting of four components. The operators \hat{O}^+ and \hat{O}^- consist of partial derivative operators summarized in Eq. 5.28, and Eq. 5.28 also shows that a monochromatic wave $\psi = e^{\frac{i}{\hbar}(p_x x + p_y y + p_z z - \mathcal{E}_t t)}$ is an eigenfunction of the partial derivative operators, with the eigenvalues equal to $\mathcal{E}_t, p_x, p_y, p_z$. Also note that the 2×2 sub-matrices, which form the $\hat{\gamma}^j$ matrices, always appear with the opposite sign on the first and last two lines, except for the unit matrix associated with the $m_0 c^2$ term. It is therefore useful to use a complex conjugate of the aforementioned monochromatic wave as an eigenfunction on the last two lines, in order to get eigenvalues with opposite signs. Possible solutions of the Dirac equation can be then assumed to have a form

$$\Psi = \begin{pmatrix} u_1 \psi \\ u_2 \psi \\ v_1 \psi^* \\ v_2 \psi^* \end{pmatrix}, \quad (5.77)$$

where u_1, u_2, v_1, v_2 are coefficients to be determined. The Dirac equation⁹ can be written as

⁹Actually, two equations, one for \hat{O}^+ and another one for \hat{O}^- .

$$\left(i\hbar \frac{\partial}{\partial t} \begin{pmatrix} 1 & 0 & 0 & 0 \\ 0 & 1 & 0 & 0 \\ 0 & 0 & -1 & 0 \\ 0 & 0 & 0 & -1 \end{pmatrix} + i\hbar \frac{\partial}{\partial z} \begin{pmatrix} 0 & 0 & 1 & 0 \\ 0 & 0 & 0 & -1 \\ -1 & 0 & 0 & 0 \\ 0 & 1 & 0 & 0 \end{pmatrix} + i\hbar \frac{\partial}{\partial x} \begin{pmatrix} 0 & 0 & 0 & 1 \\ 0 & 0 & 1 & 0 \\ 0 & -1 & 0 & 0 \\ -1 & 0 & 0 & 0 \end{pmatrix} + i\hbar \frac{\partial}{\partial y} \begin{pmatrix} 0 & 0 & 0 & -i \\ 0 & 0 & i & 0 \\ 0 & i & 0 & 0 \\ -i & 0 & 0 & 0 \end{pmatrix} \right. \\ \left. - m_0 c^2 \begin{pmatrix} 1 & 0 & 0 & 0 \\ 0 & 1 & 0 & 0 \\ 0 & 0 & 1 & 0 \\ 0 & 0 & 0 & 1 \end{pmatrix} \right) \begin{pmatrix} u_1 \psi \\ u_2 \psi \\ v_1 \psi^* \\ v_2 \psi^* \end{pmatrix} = \hat{O}^+ \Psi = 0, \quad (5.78)$$

$$\left(-i\hbar \frac{\partial}{\partial t} \begin{pmatrix} 1 & 0 & 0 & 0 \\ 0 & 1 & 0 & 0 \\ 0 & 0 & -1 & 0 \\ 0 & 0 & 0 & -1 \end{pmatrix} - i\hbar \frac{\partial}{\partial z} \begin{pmatrix} 0 & 0 & 1 & 0 \\ 0 & 0 & 0 & -1 \\ -1 & 0 & 0 & 0 \\ 0 & 1 & 0 & 0 \end{pmatrix} - i\hbar \frac{\partial}{\partial x} \begin{pmatrix} 0 & 0 & 0 & 1 \\ 0 & 0 & 1 & 0 \\ 0 & -1 & 0 & 0 \\ -1 & 0 & 0 & 0 \end{pmatrix} - i\hbar \frac{\partial}{\partial y} \begin{pmatrix} 0 & 0 & 0 & -i \\ 0 & 0 & i & 0 \\ 0 & i & 0 & 0 \\ -i & 0 & 0 & 0 \end{pmatrix} \right. \\ \left. - m_0 c^2 \begin{pmatrix} 1 & 0 & 0 & 0 \\ 0 & 1 & 0 & 0 \\ 0 & 0 & 1 & 0 \\ 0 & 0 & 0 & 1 \end{pmatrix} \right) \begin{pmatrix} u_1 \psi \\ u_2 \psi \\ v_1 \psi^* \\ v_2 \psi^* \end{pmatrix} = \hat{O}^- \Psi = 0, \quad (5.79)$$

or shortly

$$\left(i\hbar \frac{\partial}{\partial t} \hat{\gamma}^0 + i\hbar \frac{\partial}{\partial x} \hat{\gamma}^1 + i\hbar \frac{\partial}{\partial y} \hat{\gamma}^2 + i\hbar \frac{\partial}{\partial z} \hat{\gamma}^3 - m_0 c^2 \hat{1} \right) \begin{pmatrix} u_1 \psi \\ u_2 \psi \\ v_1 \psi^* \\ v_2 \psi^* \end{pmatrix} = \hat{O}^+ \Psi = 0 \quad (5.80)$$

$$\left(-i\hbar \frac{\partial}{\partial t} \hat{\gamma}^0 - i\hbar \frac{\partial}{\partial x} \hat{\gamma}^1 - i\hbar \frac{\partial}{\partial y} \hat{\gamma}^2 - i\hbar \frac{\partial}{\partial z} \hat{\gamma}^3 - m_0 c^2 \hat{1} \right) \begin{pmatrix} u_1 \psi \\ u_2 \psi \\ v_1 \psi^* \\ v_2 \psi^* \end{pmatrix} = \hat{O}^- \Psi = 0. \quad (5.81)$$

For our wavefunctions,

$$\hat{O}^+ \Psi = \begin{pmatrix} \mathcal{E}_t u_1 \psi - c p_x v_2 \psi^* + i c p_y v_2 \psi^* - c p_z v_1 \psi^* - m_0 c^2 u_1 \psi \\ \mathcal{E}_t u_2 \psi - c p_x v_1 \psi^* - i c p_y v_1 \psi^* + c p_z v_2 \psi^* - m_0 c^2 u_2 \psi \\ \mathcal{E}_t v_1 \psi^* - c p_x u_2 \psi^* + i c p_y u_2 \psi^* - c p_z u_1 \psi^* - m_0 c^2 v_1 \psi^* \\ \mathcal{E}_t v_2 \psi^* - c p_x u_1 \psi^* - i c p_y u_1 \psi^* + c p_z u_2 \psi^* - m_0 c^2 v_2 \psi^* \end{pmatrix} = 0 \quad (5.82)$$

and

$$\hat{O}^2 \Psi = \hat{O}^- \hat{O}^+ \Psi = \begin{pmatrix} \mathcal{E}_t^2 - c^2 p^2 - (m_0 c^2)^2 \\ \mathcal{E}_t^2 - c^2 p^2 - (m_0 c^2)^2 \\ \mathcal{E}_t^2 - c^2 p^2 - (m_0 c^2)^2 \\ \mathcal{E}_t^2 - c^2 p^2 - (m_0 c^2)^2 \end{pmatrix} \begin{pmatrix} u_1 \psi \\ u_2 \psi \\ v_1 \psi^* \\ v_2 \psi^* \end{pmatrix} = (\mathcal{E}_t^2 - c^2 p^2 - (m_0 c^2)^2) \Psi \quad (5.83)$$

in agreement with Eq. 5.26.

Eq. 5.82 can be also used to find four explicit solutions of the Dirac equation, treating u_1, u_2, v_1, v_2 as unknown variables to be determined. The solutions are found by setting one of the coefficients u_1, u_2, v_1, v_2 to zero, and calculating the other coefficients so that the following normalization condition is fulfilled (as discussed in Section 4.9.2)

$$\int_{-\infty}^{\infty} \int_{-\infty}^{\infty} \int_{-\infty}^{\infty} \Psi^* \Psi dx dy dz = 1 \quad (5.84)$$

(other normalizations could be used as well). The solutions have the following form (origin of the factor h^3 is explained in Section 4.9.2).

$$\Psi_1 = \sqrt{\frac{\mathcal{E}_t + m_0 c^2}{2\mathcal{E}_t h^3}} \begin{pmatrix} \psi \\ 0 \\ \frac{c p_z}{\mathcal{E}_t + m_0 c^2} \psi^* \\ \frac{c(p_x + i p_y)}{\mathcal{E}_t + m_0 c^2} \psi^* \end{pmatrix}, \quad \Psi_2 = \sqrt{\frac{\mathcal{E}_t + m_0 c^2}{2\mathcal{E}_t h^3}} \begin{pmatrix} 0 \\ \psi \\ \frac{c(p_x - i p_y)}{\mathcal{E}_t + m_0 c^2} \psi^* \\ \frac{-c p_z}{\mathcal{E}_t + m_0 c^2} \psi^* \end{pmatrix},$$

$$\Psi_3 = \sqrt{\frac{\mathcal{E}_t + m_0 c^2}{2\mathcal{E}_t h^3}} \begin{pmatrix} \frac{c p_z}{\mathcal{E}_t + m_0 c^2} \psi \\ \frac{c(p_x + i p_y)}{\mathcal{E}_t + m_0 c^2} \psi \\ \psi^* \\ 0 \end{pmatrix}, \quad \Psi_4 = \sqrt{\frac{\mathcal{E}_t + m_0 c^2}{2\mathcal{E}_t h^3}} \begin{pmatrix} \frac{c(p_x - i p_y)}{\mathcal{E}_t + m_0 c^2} \psi \\ \frac{-c p_z}{\mathcal{E}_t + m_0 c^2} \psi \\ 0 \\ \psi^* \end{pmatrix}, \quad (5.85)$$

where $\psi = e^{\frac{i}{\hbar}(p_x x + p_y y + p_z z - \mathcal{E}_t t)}$.

5.7.4 Relation between Dirac and Schrödinger equations

How is the Dirac equation related to the Schrödinger equation? We came to the Schrödinger equation using the relation $\mathcal{E} = p^2/2m$ (energy of a free particle, i.e., kinetic energy), which is only an approximation for low speeds, obtained by neglecting the \mathcal{E}^2 term ($\mathcal{E}^2 \ll (m_0 c^2)^2$ for $v^2 \ll c^2$) in Eq. 5.26:

$$(m_0 c^2)^2 = \mathcal{E}_t^2 - c^2 p^2 = (m_0 c^2 + \mathcal{E})^2 - c^2 p^2 = (m_0 c^2)^2 + 2\mathcal{E}(m_0 c^2) + \mathcal{E}^2 - c^2 p^2 \approx (m_0 c^2)^2 + 2\mathcal{E}(m_0 c^2) - c^2 p^2 \quad (5.86)$$

$$\Rightarrow \quad \mathcal{E} = \frac{p^2}{2m_0}. \quad (5.87)$$

A similar simplification can be applied to particles in an electromagnetic fields if the potential electrostatic and magnetic energy is much lower than $m_0 c^2$. We use this approximation in Section 5.7.5.

5.7.5 Hamiltonian of spin magnetic moment

Our next goal is to find Hamiltonian for a relativistic charged particle in a magnetic field. When we compare the classical Hamiltonian of a particle in an electromagnetic field (Eq. 67) with the classical Hamiltonian of a free particle $\mathcal{H} = (\vec{p})^2/(2m)$ outside the field, we see that the presence of an electromagnetic field requires the following modifications:

$$\mathcal{H} \rightarrow \mathcal{H} - QV \quad \vec{p} \rightarrow \vec{p} - Q\vec{A}, \quad (5.88)$$

Accordingly, the operators of energy and momentum in the quantum description change to

$$i\hbar \frac{\partial}{\partial t} \rightarrow i\hbar \frac{\partial}{\partial t} - QV \quad -i\hbar \frac{\partial}{\partial x} \rightarrow -i\hbar \frac{\partial}{\partial x} - QA_x \quad -i\hbar \frac{\partial}{\partial y} \rightarrow -i\hbar \frac{\partial}{\partial y} - QA_y \quad -i\hbar \frac{\partial}{\partial z} \rightarrow -i\hbar \frac{\partial}{\partial z} - QA_z. \quad (5.89)$$

This modifies Eq. 5.54 to

$$\left(i\hbar \frac{\partial}{\partial t} - QV\right) \hat{1}\Psi = \left(-c \left(i\hbar \frac{\partial}{\partial x} + QA_x\right) \hat{\gamma}^0 \hat{\gamma}^1 - c \left(i\hbar \frac{\partial}{\partial y} + QA_y\right) \hat{\gamma}^0 \hat{\gamma}^2 - c \left(i\hbar \frac{\partial}{\partial z} + QA_z\right) \hat{\gamma}^0 \hat{\gamma}^3 + m_0 c^2 \hat{\gamma}^0\right) \Psi \quad (5.90)$$

In order to obtain the Hamiltonian describing energy of our particle in a magnetic field, we return to our operator \hat{O}^2 , which represents the quantity defining the correct relativistic relation between \mathcal{E}_t^2 , p^2 , and $(m_0 c^2)^2$ (note that now we are interested in the energy, not in the evolution in time). To get \hat{O}^2 for a particle in an electromagnetic field, we apply the operator $(i\hbar \partial/\partial t - QV)$ twice

$$\begin{aligned} & \left(i\hbar \frac{\partial}{\partial t} - QV\right) \left(i\hbar \frac{\partial}{\partial t} - QV\right) \hat{1}\Psi = \left(i\hbar \frac{\partial}{\partial t} - QV\right)^2 \Psi \\ & = \left(c^2 \left(i\hbar \frac{\partial}{\partial x} + QA_x\right)^2 \hat{\gamma}^0 \hat{\gamma}^1 \hat{\gamma}^0 \hat{\gamma}^1 + c^2 \left(i\hbar \frac{\partial}{\partial y} + QA_y\right)^2 \hat{\gamma}^0 \hat{\gamma}^2 \hat{\gamma}^0 \hat{\gamma}^2 + c^2 \left(i\hbar \frac{\partial}{\partial z} + QA_z\right)^2 \hat{\gamma}^0 \hat{\gamma}^3 \hat{\gamma}^0 \hat{\gamma}^3 + m_0^2 c^4 \hat{\gamma}^0 \hat{\gamma}^0\right) \Psi \\ & - m_0 c^3 \left(\left(i\hbar \frac{\partial}{\partial x} + QA_x\right) \hat{\gamma}^0 \hat{\gamma}^1 \hat{\gamma}^0 + \left(i\hbar \frac{\partial}{\partial y} + QA_y\right) \hat{\gamma}^0 \hat{\gamma}^2 \hat{\gamma}^0 + \left(i\hbar \frac{\partial}{\partial z} + QA_z\right) \hat{\gamma}^0 \hat{\gamma}^3 \hat{\gamma}^0 \right) \Psi \\ & - m_0 c^3 \left(\left(i\hbar \frac{\partial}{\partial x} + QA_x\right) \hat{\gamma}^0 \hat{\gamma}^0 \hat{\gamma}^1 + \left(i\hbar \frac{\partial}{\partial y} + QA_y\right) \hat{\gamma}^0 \hat{\gamma}^0 \hat{\gamma}^2 + \left(i\hbar \frac{\partial}{\partial z} + QA_z\right) \hat{\gamma}^0 \hat{\gamma}^0 \hat{\gamma}^3 \right) \Psi \\ & + c^2 \left(\left(i\hbar \frac{\partial}{\partial x} + QA_x\right) \left(i\hbar \frac{\partial}{\partial y} + QA_y\right) \hat{\gamma}^0 \hat{\gamma}^1 \hat{\gamma}^0 \hat{\gamma}^2 + \left(i\hbar \frac{\partial}{\partial y} + QA_y\right) \left(i\hbar \frac{\partial}{\partial x} + QA_x\right) \hat{\gamma}^0 \hat{\gamma}^2 \hat{\gamma}^0 \hat{\gamma}^1 \right) \Psi \\ & + c^2 \left(\left(i\hbar \frac{\partial}{\partial y} + QA_y\right) \left(i\hbar \frac{\partial}{\partial z} + QA_z\right) \hat{\gamma}^0 \hat{\gamma}^2 \hat{\gamma}^0 \hat{\gamma}^3 + \left(i\hbar \frac{\partial}{\partial z} + QA_z\right) \left(i\hbar \frac{\partial}{\partial y} + QA_y\right) \hat{\gamma}^0 \hat{\gamma}^3 \hat{\gamma}^0 \hat{\gamma}^2 \right) \Psi \\ & + c^2 \left(\left(i\hbar \frac{\partial}{\partial z} + QA_z\right) \left(i\hbar \frac{\partial}{\partial x} + QA_x\right) \hat{\gamma}^0 \hat{\gamma}^3 \hat{\gamma}^0 \hat{\gamma}^1 + \left(i\hbar \frac{\partial}{\partial x} + QA_x\right) \left(i\hbar \frac{\partial}{\partial z} + QA_z\right) \hat{\gamma}^0 \hat{\gamma}^1 \hat{\gamma}^0 \hat{\gamma}^3 \right) \Psi. \quad (5.91) \end{aligned}$$

We use the properties of the gamma matrices (Eqs. 5.50–5.52) to simplify the equation. In particular, we invert of the order of matrices in the products

$$\hat{\gamma}^0 \hat{\gamma}^j \hat{\gamma}^0 = -(\hat{\gamma}^0 \hat{\gamma}^0) \hat{\gamma}^j = \hat{\gamma}^j, \quad (5.92)$$

$$\hat{\gamma}^0 \hat{\gamma}^j \hat{\gamma}^0 \hat{\gamma}^j = -(\hat{\gamma}^0 \hat{\gamma}^0)(\hat{\gamma}^j \hat{\gamma}^j) = -(\hat{1})(-\hat{1}) = \hat{1}, \quad (5.93)$$

$$\hat{\gamma}^0 \hat{\gamma}^j \hat{\gamma}^0 \hat{\gamma}^k = -(\hat{\gamma}^0 \hat{\gamma}^0)(\hat{\gamma}^j \hat{\gamma}^k) = -(\hat{1})(\hat{\gamma}^j \hat{\gamma}^k) = -\hat{\gamma}^j \hat{\gamma}^k = \hat{\gamma}^k \hat{\gamma}^j \quad (5.94)$$

and obtain

$$\begin{aligned} \left(i\hbar \frac{\partial}{\partial t} - QV \right)^2 \hat{1}\Psi &= \left(c^2 \left(i\hbar \frac{\partial}{\partial x} + QA_x \right)^2 \hat{1} + c^2 \left(i\hbar \frac{\partial}{\partial y} + QA_y \right)^2 \hat{1} + c^2 \left(i\hbar \frac{\partial}{\partial z} + QA_z \right)^2 \hat{1} + m_0^2 c^4 \hat{1} \right) \Psi \\ &+ m_0 c^3 \left(\left(i\hbar \frac{\partial}{\partial x} + QA_x \right) \hat{\gamma}^1 + \left(i\hbar \frac{\partial}{\partial y} + QA_y \right) \hat{\gamma}^2 + \left(i\hbar \frac{\partial}{\partial z} + QA_z \right) \hat{\gamma}^3 \right) \Psi \\ &- m_0 c^3 \left(\left(i\hbar \frac{\partial}{\partial x} + QA_x \right) \hat{\gamma}^1 + \left(i\hbar \frac{\partial}{\partial y} + QA_y \right) \hat{\gamma}^2 + \left(i\hbar \frac{\partial}{\partial z} + QA_z \right) \hat{\gamma}^3 \right) \Psi \\ &- c^2 \left(\left(i\hbar \frac{\partial}{\partial x} + QA_x \right) \left(i\hbar \frac{\partial}{\partial y} + QA_y \right) - \left(i\hbar \frac{\partial}{\partial y} + QA_y \right) \left(i\hbar \frac{\partial}{\partial x} + QA_x \right) \right) \hat{\gamma}^1 \hat{\gamma}^2 \Psi \\ &- c^2 \left(\left(i\hbar \frac{\partial}{\partial y} + QA_y \right) \left(i\hbar \frac{\partial}{\partial z} + QA_z \right) - \left(i\hbar \frac{\partial}{\partial z} + QA_z \right) \left(i\hbar \frac{\partial}{\partial y} + QA_y \right) \right) \hat{\gamma}^2 \hat{\gamma}^3 \Psi \\ &- c^2 \left(\left(i\hbar \frac{\partial}{\partial z} + QA_z \right) \left(i\hbar \frac{\partial}{\partial x} + QA_x \right) - \left(i\hbar \frac{\partial}{\partial x} + QA_x \right) \left(i\hbar \frac{\partial}{\partial z} + QA_z \right) \right) \hat{\gamma}^3 \hat{\gamma}^1 \Psi, \end{aligned} \quad (5.95)$$

where the second line and the third line cancel each other. To proceed, we need to evaluate the products of operators on the last three lines. Let us look at one of the lines more closely

$$-c^2 \left(\left(i\hbar \frac{\partial}{\partial x} + QA_x \right) \left(i\hbar \frac{\partial}{\partial y} + QA_y \right) - \left(i\hbar \frac{\partial}{\partial y} + QA_y \right) \left(i\hbar \frac{\partial}{\partial x} + QA_x \right) \right) \hat{\gamma}^1 \hat{\gamma}^2 \Psi \quad (5.96)$$

and analyze the operator part (green) and the wave function part (blue) separately. We start by the green operator (to emphasize that we work with the operator, we apply it to some arbitrary function, labeled ψ). The green operator is composed of linear operators, we have to apply them twice (we must be very careful with differentiation)

$$\begin{aligned} &\left(\left(i\hbar \frac{\partial}{\partial x} + QA_x \right) \left(i\hbar \frac{\partial}{\partial y} + QA_y \right) - \left(i\hbar \frac{\partial}{\partial y} + QA_y \right) \left(i\hbar \frac{\partial}{\partial x} + QA_x \right) \right) \psi = \\ &- \hbar^2 \left(\frac{\partial}{\partial x} \frac{\partial \psi}{\partial y} - \frac{\partial}{\partial y} \frac{\partial \psi}{\partial x} \right) + Q^2 (A_x A_y - A_y A_x) \psi + i\hbar Q \left(\frac{\partial(A_y \psi)}{\partial x} + A_x \frac{\partial \psi}{\partial y} - \frac{\partial(A_x \psi)}{\partial y} - A_y \frac{\partial \psi}{\partial x} \right). \end{aligned} \quad (5.97)$$

The first two terms on the second line cancel each other because $\partial^2 \psi / \partial x \partial y = \partial^2 \psi / \partial y \partial x$ and $A_x A_y = A_y A_x$ (A_x, A_y are numbers, not operators). Then we apply the chain rule to calculate the partial derivatives of $A_x \psi$ and $A_y \psi$:

$$\begin{aligned} &- \hbar^2 \left(\frac{\partial}{\partial x} \frac{\partial \psi}{\partial y} - \frac{\partial}{\partial y} \frac{\partial \psi}{\partial x} \right) + Q^2 (A_x A_y - A_y A_x) \psi + i\hbar Q \left(\frac{\partial(A_y \psi)}{\partial x} + A_x \frac{\partial \psi}{\partial y} - \frac{\partial(A_x \psi)}{\partial y} - A_y \frac{\partial \psi}{\partial x} \right) = \\ &i\hbar Q \left(\frac{\partial(A_y \psi)}{\partial x} + A_x \frac{\partial \psi}{\partial y} - \frac{\partial(A_x \psi)}{\partial y} - A_y \frac{\partial \psi}{\partial x} \right) = i\hbar Q \left(\frac{\partial A_y}{\partial x} \psi + A_y \frac{\partial \psi}{\partial x} + A_x \frac{\partial \psi}{\partial y} - \frac{\partial A_x}{\partial y} \psi - A_x \frac{\partial \psi}{\partial y} - A_y \frac{\partial \psi}{\partial x} \right) = i\hbar Q \left(\frac{\partial A_y}{\partial x} - \frac{\partial A_x}{\partial y} \right) \psi. \end{aligned} \quad (5.98)$$

Note that the resulting difference of partial derivatives in the parentheses is nothing else but the z component of the rotation (formally a vector product) of the definition of \vec{B} in Eq. 73. Therefore, we can write

$$- \hbar^2 \left(\frac{\partial}{\partial x} \frac{\partial \psi}{\partial y} - \frac{\partial}{\partial y} \frac{\partial \psi}{\partial x} \right) + Q^2 (A_x A_y - A_y A_x) \psi + i\hbar Q \left(\frac{\partial(A_y \psi)}{\partial x} + A_x \frac{\partial \psi}{\partial y} - \frac{\partial(A_x \psi)}{\partial y} - A_y \frac{\partial \psi}{\partial x} \right) = i\hbar Q \left(\frac{\partial A_y}{\partial x} - \frac{\partial A_x}{\partial y} \right) \psi = i\hbar Q B_z \psi. \quad (5.99)$$

The combinations on the last two lines of Eq. 5.95 are obtained in the same manner.

In addition to the combinations of the operators evaluated above, the last three lines of Eq. 5.95 also contain the products $\hat{\gamma}^1 \hat{\gamma}^2$, $\hat{\gamma}^2 \hat{\gamma}^3$, and $\hat{\gamma}^3 \hat{\gamma}^1$. They can be calculated from Eq. 5.62

$$\hat{\gamma}^1 \hat{\gamma}^2 = \begin{pmatrix} \hat{0} & \hat{\sigma}^1 \\ -\hat{\sigma}^1 & \hat{0} \end{pmatrix} \begin{pmatrix} \hat{0} & \hat{\sigma}^2 \\ -\hat{\sigma}^2 & \hat{0} \end{pmatrix} = - \begin{pmatrix} \hat{\sigma}^1 \hat{\sigma}^2 & \hat{0} \\ \hat{0} & \hat{\sigma}^1 \hat{\sigma}^2 \end{pmatrix} = -i \begin{pmatrix} \hat{\sigma}^3 & \hat{0} \\ \hat{0} & \hat{\sigma}^3 \end{pmatrix}, \quad (5.100)$$

$$\hat{\gamma}^2 \hat{\gamma}^3 = \begin{pmatrix} \hat{0} & \hat{\sigma}^2 \\ -\hat{\sigma}^2 & \hat{0} \end{pmatrix} \begin{pmatrix} \hat{0} & \hat{\sigma}^3 \\ -\hat{\sigma}^3 & \hat{0} \end{pmatrix} = - \begin{pmatrix} \hat{\sigma}^2 \hat{\sigma}^3 & \hat{0} \\ \hat{0} & \hat{\sigma}^2 \hat{\sigma}^3 \end{pmatrix} = -i \begin{pmatrix} \hat{\sigma}^1 & \hat{0} \\ \hat{0} & \hat{\sigma}^1 \end{pmatrix}, \quad (5.101)$$

$$\hat{\gamma}^3 \hat{\gamma}^1 = \begin{pmatrix} \hat{0} & \hat{\sigma}^3 \\ -\hat{\sigma}^3 & \hat{0} \end{pmatrix} \begin{pmatrix} \hat{0} & \hat{\sigma}^1 \\ -\hat{\sigma}^1 & \hat{0} \end{pmatrix} = - \begin{pmatrix} \hat{\sigma}^3 \hat{\sigma}^1 & \hat{0} \\ \hat{0} & \hat{\sigma}^3 \hat{\sigma}^1 \end{pmatrix} = -i \begin{pmatrix} \hat{\sigma}^2 & \hat{0} \\ \hat{0} & \hat{\sigma}^2 \end{pmatrix}, \quad (5.102)$$

where the following important properties of the $\hat{\sigma}^j$ matrices were used in the last steps:

$$\hat{\sigma}^1 \hat{\sigma}^2 = \begin{pmatrix} 0 & 1 \\ 1 & 0 \end{pmatrix} \begin{pmatrix} 0 & -i \\ i & 0 \end{pmatrix} = \begin{pmatrix} i & 0 \\ 0 & -i \end{pmatrix} = i\hat{\sigma}^3 \quad (5.103)$$

$$\hat{\sigma}^2 \hat{\sigma}^3 = \begin{pmatrix} 0 & -i \\ i & 0 \end{pmatrix} \begin{pmatrix} 1 & 0 \\ 0 & -1 \end{pmatrix} = \begin{pmatrix} 0 & i \\ i & 0 \end{pmatrix} = i\hat{\sigma}^1 \quad (5.104)$$

$$\hat{\sigma}^3 \hat{\sigma}^1 = \begin{pmatrix} 1 & 0 \\ 0 & -1 \end{pmatrix} \begin{pmatrix} 0 & 1 \\ 1 & 0 \end{pmatrix} = \begin{pmatrix} 0 & 1 \\ -1 & 0 \end{pmatrix} = i\hat{\sigma}^2. \quad (5.105)$$

Note that we have written the 4×4 matrices $\hat{\gamma}^j \hat{\gamma}^k$ in a *block-diagonal* form, using 2×2 matrices $\hat{\sigma}^l$ and $\hat{0}$. After inserting everything into Eq. 5.95, we get

$$\begin{aligned} \left(i\hbar \frac{\partial}{\partial t} - QV \right)^2 \begin{pmatrix} \hat{1} & \hat{0} \\ \hat{0} & \hat{1} \end{pmatrix} \Psi &= \left(c^2 \left(i\hbar \frac{\partial}{\partial x} + QA_x \right)^2 + c^2 \left(i\hbar \frac{\partial}{\partial y} + QA_y \right)^2 + c^2 \left(i\hbar \frac{\partial}{\partial z} + QA_z \right)^2 + m_0^2 c^4 \right) \begin{pmatrix} \hat{1} & \hat{0} \\ \hat{0} & \hat{1} \end{pmatrix} \Psi \\ &- c^2 \hbar Q \left(B_x \begin{pmatrix} \hat{\sigma}^1 & \hat{0} \\ \hat{0} & \hat{\sigma}^1 \end{pmatrix} + B_y \begin{pmatrix} \hat{\sigma}^2 & \hat{0} \\ \hat{0} & \hat{\sigma}^2 \end{pmatrix} + B_z \begin{pmatrix} \hat{\sigma}^3 & \hat{0} \\ \hat{0} & \hat{\sigma}^3 \end{pmatrix} \right) \Psi. \end{aligned} \quad (5.106)$$

To emphasize the block-diagonal form of the equation, we use 2×2 matrices $\hat{1}$ (unit matrix) and $\hat{0}$ (zero matrix) to write the 4×4 unit matrices on the first line (note that the same symbol $\hat{1}$ represents a 4×4 matrix above and a 2×2 matrix here and below).

Now we have a relativistic equation describing our particle in an electromagnetic field. Let us now separate the mass contribution to the energy from the operator $i\hbar \partial / \partial t$ and let us call the difference \hat{H} (it becomes clear soon why we choose the same symbol as the symbol used for the Hamiltonian in the Schrödinger equation):

$$\hat{H} = i\hbar \frac{\partial}{\partial t} - m_0 c^2, \quad (5.107)$$

Eq. 5.106 can be rewritten as

$$\begin{aligned} \left(\hat{H} + m_0 c^2 - QV \right)^2 \begin{pmatrix} \hat{1} & \hat{0} \\ \hat{0} & \hat{1} \end{pmatrix} \Psi &= \left((\hat{H} - QV)^2 + 2m_0 c^2 (\hat{H} - QV) + m_0^2 c^4 \right) \begin{pmatrix} \hat{1} & \hat{0} \\ \hat{0} & \hat{1} \end{pmatrix} \Psi = \\ &\left(c^2 \left(i\hbar \frac{\partial}{\partial x} + QA_x \right)^2 + c^2 \left(i\hbar \frac{\partial}{\partial y} + QA_y \right)^2 + c^2 \left(i\hbar \frac{\partial}{\partial z} + QA_z \right)^2 + m_0^2 c^4 \right) \begin{pmatrix} \hat{1} & \hat{0} \\ \hat{0} & \hat{1} \end{pmatrix} \Psi \\ &- c^2 \hbar Q \left(B_x \begin{pmatrix} \hat{\sigma}^1 & \hat{0} \\ \hat{0} & \hat{\sigma}^1 \end{pmatrix} + B_y \begin{pmatrix} \hat{\sigma}^2 & \hat{0} \\ \hat{0} & \hat{\sigma}^2 \end{pmatrix} + B_z \begin{pmatrix} \hat{\sigma}^3 & \hat{0} \\ \hat{0} & \hat{\sigma}^3 \end{pmatrix} \right) \Psi, \end{aligned} \quad (5.108)$$

where the two red terms $m_0^2 c^4$ cancel each other. Dividing both sides of the equation by $2m_0 c^2$ gives

$$\begin{aligned} \left(\frac{(\hat{H} - QV)^2}{2m_0 c^2} + \hat{H} - QV \right) \begin{pmatrix} \hat{1} & \hat{0} \\ \hat{0} & \hat{1} \end{pmatrix} \Psi &= \\ \frac{1}{2m_0} \left(\left(i\hbar \frac{\partial}{\partial x} + QA_x \right)^2 + \left(i\hbar \frac{\partial}{\partial y} + QA_y \right)^2 + \left(i\hbar \frac{\partial}{\partial z} + QA_z \right)^2 \right) \begin{pmatrix} \hat{1} & \hat{0} \\ \hat{0} & \hat{1} \end{pmatrix} \Psi \\ - \frac{\hbar Q}{2m_0} \left(B_x \begin{pmatrix} \hat{\sigma}^1 & \hat{0} \\ \hat{0} & \hat{\sigma}^1 \end{pmatrix} + B_y \begin{pmatrix} \hat{\sigma}^2 & \hat{0} \\ \hat{0} & \hat{\sigma}^2 \end{pmatrix} + B_z \begin{pmatrix} \hat{\sigma}^3 & \hat{0} \\ \hat{0} & \hat{\sigma}^3 \end{pmatrix} \right) \Psi. \end{aligned} \quad (5.109)$$

Note that the rest energy of particles $m_0 c^2$ is huge. Unless the eigenvalue of \hat{H} is very large (which is not expected in a standard NMR experiment), the first term with $m_0 c^2$ in the denominator can be safely neglected. For the same reason, the factors $\pm c p_z / (\mathcal{E}_t + m_0 c^2)$ and $c(p_x \pm i p_y) / (\mathcal{E}_t + m_0 c^2)$ in Eq. 5.85 are close to zero for $v \ll c$.

The derived matrix equation represent a set of four equations for four unknowns. The block-diagonal form of all matrices reveals that the first two equations and the last two equations can be solved separately. Therefore, we obtain identical sets of two equations describing particles and antiparticles:

$$\hat{H} \begin{pmatrix} u_1\psi \\ u_2\psi \end{pmatrix} \approx \left(\frac{1}{2m_0} \left(\left(i\hbar \frac{\partial}{\partial x} + QA_x \right)^2 + \left(i\hbar \frac{\partial}{\partial y} + QA_y \right)^2 + \left(i\hbar \frac{\partial}{\partial z} + QA_z \right)^2 + QV \right) \hat{1} - \frac{\hbar Q}{2m_0} (B_x \hat{\sigma}^1 + B_y \hat{\sigma}^2 + B_z \hat{\sigma}^3) \right) \begin{pmatrix} u_1\psi \\ u_2\psi \end{pmatrix}, \quad (5.110)$$

$$\hat{H} \begin{pmatrix} v_1\psi^* \\ v_2\psi^* \end{pmatrix} \approx \left(\frac{1}{2m_0} \left(\left(i\hbar \frac{\partial}{\partial x} + QA_x \right)^2 + \left(i\hbar \frac{\partial}{\partial y} + QA_y \right)^2 + \left(i\hbar \frac{\partial}{\partial z} + QA_z \right)^2 + QV \right) \hat{1} - \frac{\hbar Q}{2m_0} (B_x \hat{\sigma}^1 + B_y \hat{\sigma}^2 + B_z \hat{\sigma}^3) \right) \begin{pmatrix} v_1\psi^* \\ v_2\psi^* \end{pmatrix}, \quad (5.111)$$

where we described the wave functions using the notation introduced in Eq. 5.77. In both matrix equations, the terms multiplied by $\hat{1}$ constitute the Hamiltonian of the non-relativistic Schrödinger equation (Eq. 4.23), and the terms with the $\hat{\sigma}^j$ matrices appear only in our relativistic equations.

5.7.6 The factor of one half in the eigenvalues of \hat{I}_z

The eigenvalues $\pm\hbar/2$ are closely related to the fact that spin is a relativistic effect. Special relativity requires that the Dirac equation must not change if we rotate the coordinate frame or if it moves with a constant speed (Lorentz transformation). This is true in general, but for the sake of simplicity, we just check rotation about the z axis.

We start by writing explicitly the Dirac equation as a set of four equations¹⁰

$$i\hbar \frac{\partial(u_1\psi)}{\partial t} = -i\hbar \frac{\partial(v_1\psi^*)}{\partial z} - i\hbar \frac{\partial(v_2\psi^*)}{\partial x} + i\hbar \frac{\partial(iv_2\psi^*)}{\partial y} + m_0 c^2 u_1\psi, \quad (5.112)$$

$$i\hbar \frac{\partial(u_2\psi)}{\partial t} = +i\hbar \frac{\partial(v_2\psi^*)}{\partial z} - i\hbar \frac{\partial(v_1\psi^*)}{\partial x} - i\hbar \frac{\partial(iv_1\psi^*)}{\partial y} + m_0 c^2 u_2\psi, \quad (5.113)$$

$$i\hbar \frac{\partial(v_1\psi^*)}{\partial t} = -i\hbar \frac{\partial(u_1\psi)}{\partial z} - i\hbar \frac{\partial(u_2\psi)}{\partial x} + i\hbar \frac{\partial(iu_2\psi)}{\partial y} - m_0 c^2 v_1\psi^*, \quad (5.114)$$

$$i\hbar \frac{\partial(v_2\psi^*)}{\partial t} = +i\hbar \frac{\partial(u_2\psi)}{\partial z} - i\hbar \frac{\partial(u_1\psi)}{\partial x} - i\hbar \frac{\partial(iu_1\psi)}{\partial y} - m_0 c^2 v_2\psi^*. \quad (5.115)$$

Let us assume that we have an original coordinate frame t, x, y, z and a rotated frame t', x', y', z' . If we rotate about z by an angle φ ,

$$t' = t \quad (5.116)$$

$$z' = z \quad (5.117)$$

$$x' = \cos \varphi x - \sin \varphi y \quad (5.118)$$

$$y' = \sin \varphi x + \cos \varphi y \quad (5.119)$$

and

$$\frac{\partial f}{\partial t} = \frac{\partial f}{\partial t'} \quad (5.120)$$

$$\frac{\partial f}{\partial z} = \frac{\partial f}{\partial z'} \quad (5.121)$$

$$\frac{\partial f}{\partial x} = \frac{\partial x'}{\partial x} \frac{\partial f}{\partial x'} + \frac{\partial y'}{\partial x} \frac{\partial f}{\partial y'} = \cos \varphi \frac{\partial f}{\partial x'} + \sin \varphi \frac{\partial f}{\partial y'} \quad (5.122)$$

$$\frac{\partial f}{\partial y} = \frac{\partial x'}{\partial y} \frac{\partial f}{\partial x'} + \frac{\partial y'}{\partial y} \frac{\partial f}{\partial y'} = -\sin \varphi \frac{\partial f}{\partial x'} + \cos \varphi \frac{\partial f}{\partial y'} \quad (5.123)$$

and consequently

¹⁰Note that we use the form of the Dirac equation which directly defines the relativistic Hamiltonian (Eq. 5.54).

$$\frac{\partial f}{\partial x} + i \frac{\partial f}{\partial y} = e^{-i\varphi} \left(\frac{\partial f}{\partial x'} + i \frac{\partial f}{\partial y'} \right), \quad (5.124)$$

$$\frac{\partial f}{\partial x} - i \frac{\partial f}{\partial y} = e^{i\varphi} \left(\frac{\partial f}{\partial x'} - i \frac{\partial f}{\partial y'} \right). \quad (5.125)$$

We also need to transform the wavefunction Ψ to the rotated frame. We already know that rotation of a complex function f by an angle ϕ can be written as $f' = f e^{i\phi}$. Let us assume that each of component of Ψ rotates by some angle ($\varphi_1, \varphi_2, \varphi_3, \varphi_4$) – the key step of our analysis will be to relate values of these angles the actual angle of rotating the coordinate frames φ .

Now we have everything that we need to write the set of Eqs. 5.112–5.115 in the rotated coordinate frame:

$$i\hbar \frac{\partial(e^{i\varphi_1} u_1 \psi')}{\partial t'} = -i\hbar \frac{\partial(e^{i\varphi_3} v_1 \psi'^*)}{\partial z'} - i\hbar \frac{\partial(e^{i(\varphi_4+\varphi)} v_2 \psi'^*)}{\partial x'} + i\hbar \frac{\partial(i e^{i(\varphi_4+\varphi)} v_2 \psi'^*)}{\partial y'} + m_0 c^2 e^{i\varphi_1} u_1 \psi', \quad (5.126)$$

$$i\hbar \frac{\partial(e^{i\varphi_2} u_2 \psi')}{\partial t'} = +i\hbar \frac{\partial(e^{i\varphi_4} v_2 \psi'^*)}{\partial z'} - i\hbar \frac{\partial(e^{i(\varphi_3-\varphi)} v_1 \psi'^*)}{\partial x'} - i\hbar \frac{\partial(i e^{i(\varphi_3-\varphi)} v_1 \psi'^*)}{\partial y'} + m_0 c^2 e^{i\varphi_2} u_2 \psi', \quad (5.127)$$

$$i\hbar \frac{\partial(e^{i\varphi_3} v_1 \psi'^*)}{\partial t'} = -i\hbar \frac{\partial(e^{i\varphi_1} u_1 \psi')}{\partial z'} - i\hbar \frac{\partial(e^{i(\varphi_2+\varphi)} u_2 \psi')}{\partial x'} + i\hbar \frac{\partial(i e^{i(\varphi_2+\varphi)} u_2 \psi')}{\partial y'} - m_0 c^2 e^{i\varphi_3} v_1 \psi'^*, \quad (5.128)$$

$$i\hbar \frac{\partial(e^{i\varphi_4} v_2 \psi'^*)}{\partial t'} = +i\hbar \frac{\partial(e^{i\varphi_2} u_2 \psi')}{\partial z'} - i\hbar \frac{\partial(e^{i(\varphi_1-\varphi)} u_1 \psi')}{\partial x'} - i\hbar \frac{\partial(i e^{i(\varphi_1-\varphi)} u_1 \psi')}{\partial y'} - m_0 c^2 e^{i\varphi_4} v_2 \psi'^*. \quad (5.129)$$

According to the first postulate of the special theory of relativity, Eqs. 5.126–5.129 must have the same form as Eqs. 5.112–5.115. In other words, we must eliminate the complex exponential expressions from Eqs. 5.126–5.129. Let us first multiply both sides of the first equation by $e^{-i\varphi_1}$, both sides of the second equation by $e^{-i\varphi_2}$, both sides of the third equation by $e^{-i\varphi_3}$, and both sides of the last equation by $e^{-i\varphi_4}$:

$$i\hbar \frac{\partial(u_1 \psi')}{\partial t'} = -i\hbar \frac{\partial(e^{i(\varphi_3-\varphi_1)} v_1 \psi'^*)}{\partial z'} - i\hbar \frac{\partial(e^{i(\varphi_4-\varphi_1+\varphi)} v_2 \psi'^*)}{\partial x'} + i\hbar \frac{\partial(i e^{i(\varphi_4-\varphi_1+\varphi)} v_2 \psi'^*)}{\partial y'} + m_0 c^2 u_1 \psi', \quad (5.130)$$

$$i\hbar \frac{\partial(u_2 \psi')}{\partial t'} = +i\hbar \frac{\partial(e^{i(\varphi_4-\varphi_2)} v_2 \psi'^*)}{\partial z'} - i\hbar \frac{\partial(e^{i(\varphi_3-\varphi_2-\varphi)} v_1 \psi'^*)}{\partial x'} - i\hbar \frac{\partial(i e^{i(\varphi_3-\varphi_2-\varphi)} v_1 \psi'^*)}{\partial y'} + m_0 c^2 u_2 \psi', \quad (5.131)$$

$$i\hbar \frac{\partial(v_1 \psi'^*)}{\partial t'} = -i\hbar \frac{\partial(e^{i(\varphi_1-\varphi_3)} u_1 \psi')}{\partial z'} - i\hbar \frac{\partial(e^{i(\varphi_2-\varphi_3+\varphi)} u_2 \psi')}{\partial x'} + i\hbar \frac{\partial(i e^{i(\varphi_2-\varphi_3+\varphi)} u_2 \psi')}{\partial y'} - m_0 c^2 v_1 \psi'^*, \quad (5.132)$$

$$i\hbar \frac{\partial(v_2 \psi'^*)}{\partial t'} = +i\hbar \frac{\partial(e^{i(\varphi_2-\varphi_4)} u_2 \psi')}{\partial z'} - i\hbar \frac{\partial(e^{i(\varphi_1-\varphi_4-\varphi)} u_1 \psi')}{\partial x'} - i\hbar \frac{\partial(i e^{i(\varphi_1-\varphi_4-\varphi)} u_1 \psi')}{\partial y'} - m_0 c^2 v_2 \psi'^*. \quad (5.133)$$

This cleared the t' and m_0 terms. The exponential expressions disappear from the z' term if $\varphi_1 = \varphi_3$ and $\varphi_2 = \varphi_4$ (i.e., if the rotation of $u_1 \psi$ and $v_1 \psi^*$ is identical and the same applies to $u_2 \psi$ and $v_2 \psi^*$). In order to fix the x' and y' terms, we assume that $\varphi_1 = -\varphi_2$ and $\varphi_3 = -\varphi_4$, i.e., that the rotation of $u_1 \psi$ and $u_2 \psi$ is opposite and the same applies to $v_1 \psi^*$ and $v_2 \psi^*$. This implies that $u_1 \psi$ and $u_2 \psi$ describe states with opposite spins (and $v_1 \psi^*$ and $v_2 \psi^*$ too). Then, $u_1 \psi'$ and $v_1 \psi'^*$ in the x' and y' terms are multiplied by $e^{i(2\varphi_1-\varphi)}$, and $u_2 \psi'$ and $v_2 \psi'^*$ in the x' and y' terms are multiplied by $e^{-i(2\varphi_1-\varphi)}$. In both cases, the exponential expressions disappear (are equal to one) if $\varphi_1 = \varphi/2$. What does it mean? If we rotate the coordinate system by a certain angle, the components of the wavefunction rotate only by half of this angle! The function describing rotation of the wavefunction about z has the form

$$R_j = e^{i \frac{z_j}{\hbar} \frac{\varphi}{2}}. \quad (5.134)$$

This looks very similar to Eq. 4.92, but with one important difference: rotation by 2π (360°) does not give the same eigenfunction R_j as no rotation ($\varphi = 0$), but changes its sign. Only rotation by 4π (720°) reverts the system to the initial state!

Eq. 4.92 tells us that the eigenvalues of the operator of the spin angular momentum are half-integer multiples of \hbar :

$$I_{z,1} = \frac{\hbar}{2} \quad I_{z,2} = -\frac{\hbar}{2}. \quad (5.135)$$

5.7.7 Eigenfunctions of \hat{I}_x and \hat{I}_y

Eigenfunctions of \hat{I}_x are the following linear combinations of $|\alpha\rangle$ and $|\beta\rangle$:

$$\frac{1}{\sqrt{2}}|\alpha\rangle + \frac{1}{\sqrt{2}}|\beta\rangle = \frac{1}{\sqrt{2}}\begin{pmatrix} 1 \\ 1 \end{pmatrix} \equiv |\rightarrow\rangle, \quad (5.136)$$

$$-\frac{i}{\sqrt{2}}|\alpha\rangle + \frac{i}{\sqrt{2}}|\beta\rangle = \frac{1}{\sqrt{2}}\begin{pmatrix} -i \\ i \end{pmatrix} \equiv |\leftarrow\rangle, \quad (5.137)$$

or these linear combinations multiplied by a phase factor $e^{i\phi}$. E.g., state vectors multiplied by $e^{i\pi/2} = i$ are

$$|\rightarrow\rangle = e^{i\pi/2} \frac{1}{\sqrt{2}}\begin{pmatrix} 1 \\ 1 \end{pmatrix} = i \frac{1}{\sqrt{2}}\begin{pmatrix} 1 \\ 1 \end{pmatrix} = \frac{1}{\sqrt{2}}\begin{pmatrix} i \\ i \end{pmatrix}, \quad |\leftarrow\rangle = e^{i\pi/2} \frac{1}{\sqrt{2}}\begin{pmatrix} -i \\ i \end{pmatrix} = i \frac{1}{\sqrt{2}}\begin{pmatrix} -i \\ i \end{pmatrix} = \frac{1}{\sqrt{2}}\begin{pmatrix} -1 \\ -1 \end{pmatrix}. \quad (5.138)$$

Eigenvalues are again $\hbar/2$ and $-\hbar/2$:

$$\hat{I}_x|\rightarrow\rangle = +\frac{\hbar}{2}|\rightarrow\rangle \quad \frac{\hbar}{2}\begin{pmatrix} 0 & 1 \\ 1 & 0 \end{pmatrix} \frac{1}{\sqrt{2}}\begin{pmatrix} 1 \\ 1 \end{pmatrix} = +\frac{\hbar}{2} \cdot \frac{1}{\sqrt{2}}\begin{pmatrix} 1 \\ 1 \end{pmatrix}, \quad (5.139)$$

$$\hat{I}_x|\leftarrow\rangle = +\frac{\hbar}{2}|\leftarrow\rangle \quad \frac{\hbar}{2}\begin{pmatrix} 0 & 1 \\ 1 & 0 \end{pmatrix} \frac{1}{\sqrt{2}}\begin{pmatrix} -i \\ i \end{pmatrix} = -\frac{\hbar}{2} \cdot \frac{1}{\sqrt{2}}\begin{pmatrix} -i \\ i \end{pmatrix}. \quad (5.140)$$

Eigenfunctions of \hat{I}_y are the following linear combinations of $|\alpha\rangle$ and $|\beta\rangle$:

$$\frac{1-i}{2}|\alpha\rangle + \frac{1+i}{2}|\beta\rangle = \frac{1}{2}\begin{pmatrix} 1-i \\ 1+i \end{pmatrix} \equiv |\otimes\rangle, \quad (5.141)$$

$$-\frac{1+i}{2}|\alpha\rangle + \frac{1-i}{2}|\beta\rangle = \frac{1}{2}\begin{pmatrix} 1+i \\ 1-i \end{pmatrix} \equiv |\odot\rangle, \quad (5.142)$$

or these linear combinations multiplied by a phase factor $e^{i\phi}$. E.g., state vectors multiplied by $e^{i\pi/4} = (1+i)/\sqrt{2}$ are

$$|\otimes\rangle = e^{i\pi/4} \frac{1}{2}\begin{pmatrix} 1-i \\ 1+i \end{pmatrix} = \frac{1+i}{\sqrt{2}} \frac{1}{2}\begin{pmatrix} 1-i \\ 1+i \end{pmatrix} = \frac{1}{\sqrt{2}}\begin{pmatrix} 1 \\ 1 \end{pmatrix}, \quad |\odot\rangle = e^{i\pi/4} \frac{1}{2}\begin{pmatrix} 1+i \\ 1-i \end{pmatrix} = \frac{1+i}{\sqrt{2}} \frac{1}{2}\begin{pmatrix} 1+i \\ 1-i \end{pmatrix} = \frac{1}{\sqrt{2}}\begin{pmatrix} i \\ 1 \end{pmatrix}. \quad (5.143)$$

Eigenvalues are again $\hbar/2$ and $-\hbar/2$:

$$\hat{I}_y|\otimes\rangle = +\frac{\hbar}{2}|\otimes\rangle \quad \frac{\hbar}{2}\begin{pmatrix} 0 & -i \\ i & 0 \end{pmatrix} \frac{1}{2}\begin{pmatrix} 1-i \\ 1+i \end{pmatrix} = +\frac{\hbar}{2} \cdot \frac{1}{2}\begin{pmatrix} 1-i \\ 1+i \end{pmatrix}, \quad (5.144)$$

$$\hat{I}_y|\odot\rangle = -\frac{\hbar}{2}|\odot\rangle \quad \frac{\hbar}{2}\begin{pmatrix} 0 & -i \\ i & 0 \end{pmatrix} \frac{1}{2}\begin{pmatrix} 1+i \\ 1-i \end{pmatrix} = -\frac{\hbar}{2} \cdot \frac{1}{2}\begin{pmatrix} 1+i \\ 1-i \end{pmatrix}. \quad (5.145)$$

An operator representing angular momentum pointing in a general direction, described by angles ϑ (declination) and φ (azimuth) can be written as

$$\hat{I}_z \cos \vartheta + \hat{I}_x \sin \vartheta \cos \varphi + \hat{I}_y \sin \vartheta \sin \varphi. \quad (5.146)$$

Its eigenvalue are again $\hbar/2$ and $-\hbar/2$ and its eigenfunctions are

$$|\vartheta, \varphi\rangle = \begin{pmatrix} \cos \frac{\vartheta}{2} e^{-i\frac{\varphi}{2}} \\ \sin \frac{\vartheta}{2} e^{+i\frac{\varphi}{2}} \end{pmatrix}, \quad |\vartheta + \pi, \varphi\rangle = \begin{pmatrix} -\sin \frac{\vartheta}{2} e^{-i\frac{\varphi}{2}} \\ \cos \frac{\vartheta}{2} e^{+i\frac{\varphi}{2}} \end{pmatrix} \quad (5.147)$$

or the vectors described by Eq. 5.147 multiplied by a phase factor $e^{i\phi}$, e.g.

$$|\vartheta, \varphi\rangle = \begin{pmatrix} \cos \frac{\vartheta}{2} \\ \sin \frac{\vartheta}{2} e^{i\varphi} \end{pmatrix}, \quad |\vartheta + \pi, \varphi\rangle = \begin{pmatrix} -\sin \frac{\vartheta}{2} \\ \cos \frac{\vartheta}{2} e^{i\varphi} \end{pmatrix}. \quad (5.148)$$

5.7.8 Stationary states and energy level diagram

In the presence of a homogeneous magnetic field $\vec{B}_0 = (0, 0, B_0)$, the evolution of the system is given by the Hamiltonian $\hat{H} = -\gamma B_0 \hat{I}_z$. The Schrödinger equation is then

$$i\hbar \frac{\partial}{\partial t} \begin{pmatrix} c_\alpha \\ c_\beta \end{pmatrix} = -\gamma B_0 \frac{\hbar}{2} \begin{pmatrix} 1 & 0 \\ 0 & -1 \end{pmatrix} \begin{pmatrix} c_\alpha \\ c_\beta \end{pmatrix}, \quad (5.149)$$

which is a set of two equations with separated variables

$$\frac{dc_\alpha}{dt} = +i \frac{\gamma B_0}{2} c_\alpha, \quad (5.150)$$

$$\frac{dc_\beta}{dt} = -i \frac{\gamma B_0}{2} c_\beta, \quad (5.151)$$

with the solution

$$c_\alpha = c_\alpha(t=0) e^{+i \frac{\gamma B_0}{2} t} = c_\alpha(t=0) e^{-i \frac{\omega_0}{2} t}, \quad (5.152)$$

$$c_\beta = c_\beta(t=0) e^{-i \frac{\gamma B_0}{2} t} = c_\beta(t=0) e^{+i \frac{\omega_0}{2} t}. \quad (5.153)$$

If the initial state is $|\alpha\rangle$, $c_\alpha(t=0) = 1$, $c_\beta(t=0) = 0$, and

$$c_\alpha = e^{-i \frac{\omega_0}{2} t}, \quad (5.154)$$

$$c_\beta = 0. \quad (5.155)$$

Note that the evolution changes only the phase factor, but the system stays in state $|\alpha\rangle$ (all vectors described by Eq. 5.16 correspond to state $|\alpha\rangle$). It can be shown by calculating the probability that the system is in the $|\alpha\rangle$ or $|\beta\rangle$ state.

$$P_\alpha = c_\alpha^* c_\alpha = e^{+i \frac{\omega_0}{2} t} e^{-i \frac{\omega_0}{2} t} = 1, \quad (5.156)$$

$$P_\beta = c_\beta^* c_\beta = 0. \quad (5.157)$$

If the initial state is $|\beta\rangle$, $c_\alpha(t=0) = 0$, $c_\beta(t=0) = 1$, and

$$c_\alpha = 0, \quad (5.158)$$

$$c_\beta = e^{+i \frac{\omega_0}{2} t}. \quad (5.159)$$

Again, the evolution changes only the phase factor, but the system stays in state $|\beta\rangle$. The probability that the system is in the $|\alpha\rangle$ or $|\beta\rangle$ state is

$$P_\alpha = c_\alpha^* c_\alpha = 0, \quad (5.160)$$

$$P_\beta = c_\beta^* c_\beta = e^{-i \frac{\omega_0}{2} t} e^{+i \frac{\omega_0}{2} t} = 1. \quad (5.161)$$

5.7.9 Oscillatory states

We now analyze evolution of states described by other wave functions that eigenfunctions of the Hamiltonian. We can continue the discussion of the previous section (evolution of evolution of $|\alpha\rangle$ and $|\beta\rangle$ due to $\hat{H} = -\gamma B_0 \hat{I}_z$) and change either the wave function or the Hamiltonian. We start by the latter option, which is easier.

In the presence of a homogeneous magnetic field $\vec{B}_1 = (B_1, 0, 0)$, the evolution of the system is given by the Hamiltonian $\hat{H} = -\gamma B_0 \hat{I}_x$. The Schrödinger equation is then

$$i\hbar \frac{\partial}{\partial t} \begin{pmatrix} c_\alpha \\ c_\beta \end{pmatrix} = -\gamma B_1 \frac{\hbar}{2} \begin{pmatrix} 0 & 1 \\ 1 & 0 \end{pmatrix} \begin{pmatrix} c_\alpha \\ c_\beta \end{pmatrix}, \quad (5.162)$$

which is a set of two equations

$$\frac{dc_\alpha}{dt} = i\frac{\gamma B_1}{2}c_\beta, \quad (5.163)$$

$$\frac{dc_\beta}{dt} = i\frac{\gamma B_1}{2}c_\alpha. \quad (5.164)$$

These equations have similar structure as Eqs. 4.98 and 4.99. Adding and subtracting them leads to the solution

$$c_\alpha + c_\beta = C_+ e^{+i\frac{\gamma B_1}{2}t} = C_+ e^{-i\frac{\omega_1}{2}t}, \quad (5.165)$$

$$c_\alpha - c_\beta = C_- e^{-i\frac{\gamma B_1}{2}t} = C_- e^{+i\frac{\omega_1}{2}t}. \quad (5.166)$$

If the initial state is $|\alpha\rangle$, $c_\alpha(t=0) = 1$, $c_\beta(t=0) = 0$, $C_+ = C_- = 1$, and

$$c_\alpha = \cos\left(\frac{\omega_1}{2}t\right), \quad (5.167)$$

$$c_\beta = -i\sin\left(\frac{\omega_1}{2}t\right). \quad (5.168)$$

Probability that the system is in the $|\alpha\rangle$ or $|\beta\rangle$ state is calculated as

$$P_\alpha = c_\alpha^* c_\alpha = \cos^2\left(\frac{\omega_1}{2}t\right) = \frac{1}{2} + \frac{1}{2}\cos(\omega_1 t), \quad (5.169)$$

$$P_\beta = c_\beta^* c_\beta = \sin^2\left(\frac{\omega_1}{2}t\right) = \frac{1}{2} - \frac{1}{2}\cos(\omega_1 t). \quad (5.170)$$

If the initial state is $|\beta\rangle$, $c_\alpha(t=0) = 0$, $c_\beta(t=0) = 1$, $C_+ = 1$, $C_- = -1$, and

$$c_\alpha = -i\sin\left(\frac{\omega_1}{2}t\right), \quad (5.171)$$

$$c_\beta = \cos\left(\frac{\omega_1}{2}t\right). \quad (5.172)$$

Probability that the system is in the $|\alpha\rangle$ or $|\beta\rangle$ state is calculated as

$$P_\alpha = c_\alpha^* c_\alpha = \sin^2\left(\frac{\omega_1}{2}t\right) = \frac{1}{2} - \frac{1}{2}\cos(\omega_1 t), \quad (5.173)$$

$$P_\beta = c_\beta^* c_\beta = \cos^2\left(\frac{\omega_1}{2}t\right) = \frac{1}{2} + \frac{1}{2}\cos(\omega_1 t). \quad (5.174)$$

In both cases, the system oscillates between the $|\alpha\rangle$ and $|\beta\rangle$ states.

Now we return to the Hamiltonian of the vertical field $\hat{H} = -\gamma B_0 \hat{I}_z$, but analyze the evolution of superposition states called $|\rightarrow\rangle$ and $|\leftarrow\rangle$ in Section 5.7.7. The Schrödinger equation has in this case the same form as in Section 5.7.8 with the solution

$$c_\alpha = c_\alpha(t=0)e^{+i\frac{\gamma B_0}{2}t} = c_\alpha(t=0)e^{-i\frac{\omega_0}{2}t}, \quad (5.175)$$

$$c_\beta = c_\beta(t=0)e^{-i\frac{\gamma B_0}{2}t} = c_\beta(t=0)e^{+i\frac{\omega_0}{2}t}. \quad (5.176)$$

We are interested in evolution of a wave function that can be described as

$$|\Psi\rangle = c_{\rightarrow}|\rightarrow\rangle + c_{\leftarrow}|\leftarrow\rangle. \quad (5.177)$$

According to Eqs. 5.150 and 5.151,

$$c_{\rightarrow} = \frac{c_\alpha}{\sqrt{2}} + \frac{c_\beta}{\sqrt{2}} \quad (5.178)$$

$$c_{\leftarrow} = -i\frac{c_\alpha}{\sqrt{2}} + i\frac{c_\beta}{\sqrt{2}}. \quad (5.179)$$

If the initial state is $|\rightarrow\rangle$, $c_\alpha(t=0) = 1/\sqrt{2}$, $c_\beta(t=0) = 1/\sqrt{2}$, and

$$c_{\rightarrow} = \frac{1}{2}e^{-i\frac{\omega_0}{2}t} + \frac{1}{2}e^{+i\frac{\omega_0}{2}t} = \cos\left(\frac{\omega_0}{2}t\right) \quad (5.180)$$

$$c_{\leftarrow} = -\frac{i}{2}e^{-i\frac{\omega_0}{2}t} + \frac{i}{2}e^{+i\frac{\omega_0}{2}t} = -\sin\left(\frac{\omega_0}{2}t\right). \quad (5.181)$$

Probability that the system is in the $|\rightarrow\rangle$ or $|\leftarrow\rangle$ state is calculated as

$$P_{\rightarrow} = c_{\rightarrow}^* c_{\rightarrow} = \cos^2\left(\frac{\omega_0}{2}t\right) = \frac{1}{2} + \frac{1}{2}\cos(\omega_0 t), \quad (5.182)$$

$$P_{\leftarrow} = c_{\leftarrow}^* c_{\leftarrow} = \sin^2\left(\frac{\omega_0}{2}t\right) = \frac{1}{2} - \frac{1}{2}\cos(\omega_0 t). \quad (5.183)$$

Lecture 6

Ensemble of non-interacting spins

Literature: A nice short introduction is given in K3.1. The topic is clearly described in K6, L11, C2.2. The mixed state is introduced nicely in B17.2, K6.8, L11.1, and C2.2.2. More specific references are given in the individual sections below.

6.1 Mixed state

So far, we worked with systems in so-called *pure states*, when we described the whole studied system by its complete wave function. It is fine if the system consists of one particle or a small number of particles. In the case of a single particle, the wave function $\Psi(x, y, z, c_\alpha)$ depends on the x, y, z coordinates of the particle plus the additional degree of freedom describing the spin state (in terms of the four-components of the solution of the Dirac equation). Extending quantum-mechanical description to more than one particle presents both fundamental and practical problems. A fundamental problem is that particles of the same type cannot be distinguished as in classical mechanics. This issue is briefly discussed in Section 6.7.1. The major practical problem is a high complexity of multiparticle systems. The complete wave function of whole molecule is already very complicated, represented by multidimensional state vectors and their properties are described by operators represented by multidimensional matrices. In the case of macroscopic ensembles of many molecules, the dimensionality of the state vectors and operator matrices is described by astronomic numbers. A typical NMR sample contains approximately 10^{24} particles (electrons, protons, and neutrons). Clearly, we cannot use the brute-force approach requiring determination of the complete wave function. In this lecture, we describe two levels of simplification routinely applied to describe NMR samples.

The *first level of simplification* is separation of the description of spin magnetic moments from the other terms of the wave function. In NMR spectroscopy, we are interested only in properties of molecules associated with spins of the observed nuclei. If we assume that motions of the whole molecule, of its atoms, and of electrons and nuclei in the atoms, do not depend on the spin of the observed nucleus, we can divide the complete wave function into spin wave functions and wave function describing all the other degrees of freedom.

The separation of the spin wave function is trivial in the case of a free particle in the low-speed (i.e., low-energy) limit, as shown in Section 5.4:

$$\Psi = \sqrt{\frac{1}{h^3}} \cdot e^{\frac{i}{\hbar} p_x x} \cdot e^{\frac{i}{\hbar} p_y y} \cdot e^{\frac{i}{\hbar} p_z z} \cdot \begin{pmatrix} c_\alpha \\ c_\beta \end{pmatrix} \quad (6.1)$$

Here, we expressed the wave function as a product of the green vector describing the degree of freedom important in NMR spectroscopy, and of a function dependent of the irrelevant degrees of freedom, shown in red.

In molecules, we first have to be able to separate the nuclear component of the wave function from the electronic one. This is possible if we assume that motions of the electrons in the orbitals are (i) much faster than evolution of the nuclear spin states¹ and (ii) little affected by the magnetic moments of nuclei (i.e., if we assume that the magnetic fields of the nuclear magnetic moments are too weak to influence motions of electrons). Then, we can use *shapes*² of molecular orbitals as a static description of the distribution probability of electron localization, independent of the actual state of the nuclear spin.

Second, we have to consider how the nuclear spin wave function depends on the coordinates of the nucleus (to see if the degree of freedom describing the spin state can be separated from the degrees of freedom describing the position). Infrared spectra tell us that vibrations of nuclei in molecules are much faster (roughly 10^{14} s^{-1}) than the precession of magnetic moments ($\sim 10^9 \text{ s}^{-1}$). Therefore, we can safely use coordinates describing *averaged* positions of nuclei in the molecule. Then, the molecule is defined as a rigid object, and the average coordinates of nuclei define the orientation of the molecule, but also the orientation of the cloud of electrons, discussed above. Instead of investigating the effects of magnetic moments on individual nuclei, it is sufficient to ask how the magnetic moments of nuclei affect the orientation of the molecule. The magnetic fields of the nuclear magnetic moments are weak (the energy of magnetic moments in NMR spectrometers is much lower than the kinetic energy of molecules at the ambient temperature), and we can assume that the influence of the magnetic moments on the orientation of molecules is negligible.³

At this moment, we have finished our discussion of the first level of the simplification of quantum mechanical description of magnetic moments in molecules. We can conclude that (in most cases except for some relaxation effects) wave functions (and consequently of Hamiltonians) can be divided

¹In the currently available NMR spectrometers, the frequency of the magnetic moment precession is $\sim 10^9 \text{ s}^{-1}$. The velocity of the electrons in atoms is not sharply defined (a consequence of the commutation relation between \hat{r}_j and \hat{p}_j , known as the *Heisenberg's uncertainty principle*). Nevertheless, a rough estimate can be made. In a stationary set of bound particles described by the classical mechanics, the total kinetic and potential energy are related as follows. Since our set of particles is stationary, the time derivative of the quantity $\sum_k (\vec{p}_k \cdot \vec{r}_k)$ is equal to zero. The time derivative can be expressed as $\sum_k (\frac{d\vec{p}_k}{dt} \cdot \vec{r}_k + \vec{p}_k \cdot \frac{d\vec{r}_k}{dt}) = \sum_k (\vec{F}_k \cdot \vec{r}_k + m v_k^2) = \mathcal{E}_{\text{pot}} - 2\mathcal{E}_{\text{kin}} = 0$, where \vec{r}_k is the position vector of the k -th particle, \vec{p}_k is its momentum, \vec{v}_k is its velocity, \vec{F}_k is the force acting on it, \mathcal{E}_{kin} and \mathcal{E}_{pot} are the total kinetic and potential energy, respectively. In the case of the electron in the hydrogen atom, $\mathcal{E}_{\text{pot}} = -Q^2/(4\pi\epsilon_0 r)$, where Q is the elementary charge and r is the electron-proton distance, related to the velocity by the uncertainty principle $r_j p_j \sim \hbar$. Therefore, $m v^2 \sim m v Q^2 / (4\pi\epsilon_0 \hbar) \Rightarrow v \sim Q^2 / (4\pi\epsilon_0 \hbar) \approx c/137$, where c is the speed of light. Considering the size of the atom ($\sim 10^{10} \text{ m}$), the "frequency" of the electron is roughly $\sim 10^{16} \text{ s}^{-1}$ in hydrogen and higher in heavier atoms.

²Here, the word "shape" is a synonym for values of the wave function dependent on the x, y, z coordinates in a coordinate frame attached to the molecule, independent of the position and orientation of the molecule as a whole.

³This is a very reasonable assumption in most cases. However, note that it is not true completely: if motions of the magnetic moments and of the molecules were independent, it would be impossible to explain how the magnetic moments reach their equilibrium distribution.

into two parts, one dependent on the spin degrees of freedom, and the other one dependent on the other degrees of freedom that are not important in the NMR spectroscopy. To describe the NMR experiment, it is sufficient to analyze only the spin wave function (spin state vector). However, the number of dimensions of the spin state vector is extremely high, typically $\sim 10^{23}$, and properties of the large sets of magnetic moments in bulk samples are described by operators represented by matrices of the same dimensionality. Another level of simplification is therefore needed.

The *second level of simplification* is related to the question whether individual magnetic moments can be treated independently. This is possible if the spin Hamiltonian can be decomposed into a sum of operators acting separately on individual nuclear magnetic moments, as shown in Section 6.7.2. If this condition is fulfilled, the spin wave function of the whole ensemble can be decomposed to independent spin wave functions of individual nuclei, and the Hamiltonian has the same eigenfunctions ($|\alpha\rangle, |\beta\rangle$ in the case of a vertical field \vec{B}_0) when applied to any of the individual spin wave function. These eigenfunctions can be used as the same basis set for all spin wave functions (state vectors) of individual magnetic moments. Using the same basis for vectors representing spins of different nuclei allows us to use two-dimensional operator matrices (for spin-1/2 nuclei) instead of multidimensional operator matrices. Similar arguments can be applied to the Hamiltonian of magnetic moments in magnetic fields in other directions.

Expected value $\langle A \rangle$ of a quantity A for a single nucleus can be calculated using Eq. 4.9 as a trace of the following product of matrices:

$$\langle A \rangle = \text{Tr} \left\{ \begin{pmatrix} c_\alpha c_\alpha^* & c_\alpha c_\beta^* \\ c_\beta c_\alpha^* & c_\beta c_\beta^* \end{pmatrix} \begin{pmatrix} A_{11} & A_{12} \\ A_{21} & A_{22} \end{pmatrix} \right\}. \quad (6.2)$$

Expected value $\langle A \rangle$ of a quantity A for *multiple nuclei with the same basis* is

$$\begin{aligned} \langle A \rangle &= \text{Tr} \left\{ \begin{pmatrix} c_{\alpha,1} c_{\alpha,1}^* & c_{\alpha,1} c_{\beta,1}^* \\ c_{\beta,1} c_{\alpha,1}^* & c_{\beta,1} c_{\beta,1}^* \end{pmatrix} \begin{pmatrix} A_{11} & A_{12} \\ A_{21} & A_{22} \end{pmatrix} + \begin{pmatrix} c_{\alpha,2} c_{\alpha,2}^* & c_{\alpha,2} c_{\beta,2}^* \\ c_{\beta,2} c_{\alpha,2}^* & c_{\beta,2} c_{\beta,2}^* \end{pmatrix} \begin{pmatrix} A_{11} & A_{12} \\ A_{21} & A_{22} \end{pmatrix} + \dots \right\} \\ &= \text{Tr} \left\{ \left(\begin{pmatrix} c_{\alpha,1} c_{\alpha,1}^* & c_{\alpha,1} c_{\beta,1}^* \\ c_{\beta,1} c_{\alpha,1}^* & c_{\beta,1} c_{\beta,1}^* \end{pmatrix} + \begin{pmatrix} c_{\alpha,2} c_{\alpha,2}^* & c_{\alpha,2} c_{\beta,2}^* \\ c_{\beta,2} c_{\alpha,2}^* & c_{\beta,2} c_{\beta,2}^* \end{pmatrix} + \dots \right) \begin{pmatrix} A_{11} & A_{12} \\ A_{21} & A_{22} \end{pmatrix} \right\} \\ &= N \text{Tr} \left\{ \underbrace{\begin{pmatrix} \overline{c_\alpha c_\alpha^*} & \overline{c_\alpha c_\beta^*} \\ \overline{c_\beta c_\alpha^*} & \overline{c_\beta c_\beta^*} \end{pmatrix}}_{\hat{\rho}} \underbrace{\begin{pmatrix} A_{11} & A_{12} \\ A_{21} & A_{22} \end{pmatrix}}_{\hat{A}} \right\} = N \text{Tr} \{ \hat{\rho} \hat{A} \}. \quad (6.3) \end{aligned}$$

The matrix $\hat{\rho}$ is the (*probability*) *density matrix*, the horizontal bar indicates average over the whole ensemble of nuclei in the sample, and N is the number of non-interacting nuclei described in the same operator basis.

Why probability density? Because the probability $P = \langle \Psi | \Psi \rangle$, the operator of probability can be written as the unit matrix $\hat{1}$: $\langle \Psi | \Psi \rangle \equiv \langle \Psi | \hat{1} | \Psi \rangle$. Therefore, the expectation value of probability can be also calculated using Eq. 4.9 as $\text{Tr} \{ \hat{\rho} \hat{1} \} = \text{Tr} \{ \hat{\rho} \}$.

The most important features of the mixed-state approach are listed below:

Table 6.1: Examples of operators and a density matrix expressed in the same basis. The density matrix is shown in red, the operators are shown in green. The elements of the density matrix are expressed in terms of the $|\vartheta_j, \varphi_j\rangle$ states, as described in Section 6.7.3.

Description of	units	symbol	explicit expression (linear combination of basis matrices)
mixed state	1	$\hat{\rho}$	$1 \times \frac{1}{2} \begin{pmatrix} 1 & 0 \\ 0 & 1 \end{pmatrix} + \overline{\cos \vartheta} \times \frac{1}{2} \begin{pmatrix} 1 & 0 \\ 0 & -1 \end{pmatrix} + \overline{\sin \vartheta \cos \varphi} \times \frac{1}{2} \begin{pmatrix} 0 & 1 \\ 1 & 0 \end{pmatrix} + \overline{\sin \vartheta \sin \varphi} \times \frac{1}{2} \begin{pmatrix} 0 & -i \\ i & 0 \end{pmatrix}$
angular momentum	J s	\hat{I}_z	$0 \times \frac{1}{2} \begin{pmatrix} 1 & 0 \\ 0 & 1 \end{pmatrix} + \hbar \times \frac{1}{2} \begin{pmatrix} 1 & 0 \\ 0 & -1 \end{pmatrix} + 0 \times \frac{1}{2} \begin{pmatrix} 0 & 1 \\ 1 & 0 \end{pmatrix} + 0 \times \frac{1}{2} \begin{pmatrix} 0 & -i \\ i & 0 \end{pmatrix}$
magnetic moment	J T ⁻¹	$\hat{\mu}_z$	$0 \times \frac{1}{2} \begin{pmatrix} 1 & 0 \\ 0 & 1 \end{pmatrix} + \gamma \hbar \times \frac{1}{2} \begin{pmatrix} 1 & 0 \\ 0 & -1 \end{pmatrix} + 0 \times \frac{1}{2} \begin{pmatrix} 0 & 1 \\ 1 & 0 \end{pmatrix} + 0 \times \frac{1}{2} \begin{pmatrix} 0 & -i \\ i & 0 \end{pmatrix}$
energy	J	\hat{H}	$0 \times \frac{1}{2} \begin{pmatrix} 1 & 0 \\ 0 & 1 \end{pmatrix} + \gamma B_z \hbar \times \frac{1}{2} \begin{pmatrix} 1 & 0 \\ 0 & -1 \end{pmatrix} + \gamma B_x \hbar \times \frac{1}{2} \begin{pmatrix} 0 & 1 \\ 1 & 0 \end{pmatrix} + \gamma B_y \hbar \times \frac{1}{2} \begin{pmatrix} 0 & -i \\ i & 0 \end{pmatrix}$

- Two-dimensional basis is sufficient for the whole set of N nuclei (if they do not interact with each other).
- Statistical approach: the possibility to use a 2D basis is paid by losing the information about the *microscopic state*. The same density matrix can describe an astronomic number of possible combinations of individual angular momenta which give the same *macroscopic* result. What is described by the density matrix is called the *mixed state*.
- Choice of the basis of the wave function is encoded in the definition of $\hat{\rho}$ (eigenfunctions of \hat{I}_z).
- The state is described not by a vector, but by a matrix, $\hat{\rho}$ is a matrix like matrices representing the operators.
- Any 2×2 matrix can be written as a linear combination of four 2×2 matrices. Such four matrices can be used as a *basis* of all 2×2 matrices, including matrices representing operators (in the same manner as two selected 2-component vectors serve as a basis for all 2-component vectors). Examples of such linear combinations are presented in Table 6.1. Note that the density matrix and the operators describe different features, they are clearly distinguished by the coefficients of the linear combinations.
- A good choice of a basis is a set of *orthonormal* matrices.⁴
- *Diagonal elements* of $\hat{\rho}$ (or matrices with diagonal elements only) are known as *populations*. They are discussed in Section 6.2.
- *Off-diagonal elements* (or matrices with diagonal elements only) are known as *coherences*. They are discussed in Section 6.3.

⁴Orthonormality for a set of four matrices $\hat{A}_1, \hat{A}_2, \hat{A}_3, \hat{A}_4$ can be defined as $\text{Tr}\{\hat{A}_j^\dagger \hat{A}_k\} = \delta_{jk}$, where j and $k \in \{1, 2, 3, 4\}$, $\delta_{jk} = 1$ for $j = k$ and $\delta_{jk} = 0$ for $j \neq k$, and \hat{A}_j^\dagger is an *adjoint* matrix of \hat{A}_j , i.e., matrix obtained from \hat{A}_j by exchanging rows and columns and replacing all numbers with their complex conjugates.

6.2 Populations

Population is a somewhat confusing name of a diagonal element of the probability density matrix, the correct physical interpretation is clearly described in L11.2.

- In a *pure state*, $c_\alpha c_\alpha^*$ is given by the amplitude of c_α : $c_\alpha c_\alpha^* = |c_\alpha|^2$.
- In a *mixed state*, the coefficients $c_{\alpha,j}$ are different for the observed nucleus in each molecule j .
- The *populations* $\overline{c_\alpha c_\alpha^*}$ and $\overline{c_\beta c_\beta^*}$ are real numbers $\overline{|c_\alpha|^2}$ and $\overline{|c_\beta|^2}$, respectively, and their sum is always one.⁵
- If $c_{\alpha,j}$ and $c_{\beta,j}$ describe stationary states, the populations $\overline{c_\alpha c_\alpha^*}$ and $\overline{c_\beta c_\beta^*}$ do not change in time.
- A population $\overline{c_\alpha c_\alpha^*} > 1/2$ describes *longitudinal polarization*, i.e. polarization of magnetic moments in the z direction (the direction of \vec{B}_0), an excess of magnetic moments with positive μ_z components. The sum of μ_z of all magnetic moments in the sample divided by the volume of the sample is the z component of the bulk magnetization (M_z).
- The value $\overline{c_\alpha c_\alpha^*} = 1/2$ indicates no net polarization in the direction \vec{B}_0 (equal populations of the α and β states). **It does not indicate that all spins in the ensemble must be either in the α state or in the β state! The value $\overline{c_\alpha c_\alpha^*} = 1/2$ describes equally well all combinations of superposition states describing sets of magnetic moments pointing in all possible directions as long as their vector sum has a zero z component. Probability that the system contains 50% spins in the α state and 50% spins in the β state is actually negligible.**
- When $\overline{c_\alpha c_\alpha^*}$ is specified, $\overline{c_\beta c_\beta^*}$ does not carry any additional information because its value is already fully described by the $\overline{c_\alpha c_\alpha^*}$ value: $\overline{c_\beta c_\beta^*} = 1 - \overline{c_\alpha c_\alpha^*}$. It also implies that the real number $\overline{c_\alpha c_\alpha^*}$ carries the same information as the matrix

$$\begin{pmatrix} \overline{c_\alpha c_\alpha^*} & 0 \\ 0 & \overline{c_\beta c_\beta^*} \end{pmatrix}.$$

Consequently, longitudinal polarization is described equally well by the number $\overline{c_\alpha c_\alpha^*}$ and by the displayed matrix.

- Graphical representation of the coherence $\overline{c_\beta c_\alpha^*}$ is shown in Figure 6.2.
- Graphical representations of quantum mechanical objects are helpful but not perfect. An attempt to visualize the population $\overline{c_\alpha c_\alpha^*}$ is presented in Figure 6.1. The polarization is depicted as one possible distribution of magnetic moments and as a vector describing the bulk magnetization as a result of the longitudinal polarization of magnetic moments.

⁵Note that $\sum_{j=1}^N (c_{\alpha,j} c_{\alpha,j}^* + c_{\beta,j} c_{\beta,j}^*) = N$. Therefore, $\overline{c_\alpha c_\alpha^*} + \overline{c_\beta c_\beta^*} = 1$.

6.3 Coherence

Coherence is a very important issue in NMR spectroscopy. It is discussed in K6.9, L11.2, C2.6.

- In a *pure state*, $c_\beta c_\alpha^*$ is given by amplitudes and by the difference of phases of c_α and c_β :
 $c_\beta c_\alpha^* = |c_\alpha||c_\beta|e^{-i(\phi_\alpha - \phi_\beta)}$.
- In a *mixed state*, $c_{\alpha,j} = |c_{\alpha,j}|e^{i\phi_{\alpha,j}}$ and $c_{\beta,j} = |c_{\beta,j}|e^{i\phi_{\beta,j}}$ are different for the observed nucleus in each molecule j .
- The *coherence* $\overline{c_\beta c_\alpha^*}$ is a complex number $|\mathcal{A}|e^{-i\Phi} = \overline{|c_\alpha||c_\beta|} \cdot \overline{e^{-i(\phi_\alpha - \phi_\beta)}}$. Its amplitude $|\mathcal{A}|$ is $\overline{|c_\alpha||c_\beta|}$ and its phase Φ is given by $\overline{e^{-i(\phi_\alpha - \phi_\beta)}} = \overline{\cos(\phi_\alpha - \phi_\beta) - i \sin(\phi_\alpha - \phi_\beta)}$.
- In general, the spin magnetic moment in individual molecules are present in various superposition states corresponding to various linear combinations of the $|\alpha\rangle$ and $|\beta\rangle$ eigenstates ($c_{\alpha,j}|\alpha\rangle + c_{\beta,j}|\beta\rangle$). If there is no macroscopic relationship between the phases $\phi_{\alpha,j}$ and $\phi_{\beta,j}$ in individual molecules, the difference $\phi_{\alpha,j} - \phi_{\beta,j}$ can take any value in the interval $(0, 2\pi)$ with the same probability. Therefore, $\overline{e^{-i(\phi_\alpha - \phi_\beta)}} = \overline{\cos(\phi_\alpha - \phi_\beta) - i \sin(\phi_\alpha - \phi_\beta)} = 0 + 0 = 0$ because the average values of both sine and cosine values are zero in the interval $(0, 2\pi)$. Obviously, $\overline{c_\beta c_\alpha^*} = 0$ in such a case, regardless of the amplitudes. Such an ensemble of states is called *incoherent superposition* of the $|\alpha\rangle$ and $|\beta\rangle$ eigenstates.
- If $e^{-i(\phi_{\alpha,j} - \phi_{\beta,j})}$ does not average to zero, a macroscopic relationship exists between the phases $\phi_{\alpha,j}$ and $\phi_{\beta,j}$. Such an ensemble of states is called *coherent superposition* of the $|\alpha\rangle$ and $|\beta\rangle$ eigenstates. This is why the term *coherence* is used for the off-diagonal elements of the density matrix, whose non-zero values indicate coherent superposition of the $|\alpha\rangle$ and $|\beta\rangle$ eigenstates, or simply *coherence* of the system.
- The non-zero coherence $\overline{c_\beta c_\alpha^*}$ describes *transverse polarization*, i.e. polarization of magnetic moments in the *xy* plane (a plane perpendicular to \vec{B}_0). The magnitude of the transverse polarization is $\overline{|c_\alpha||c_\beta|}$ and its direction is given by the phase of $\overline{c_\beta c_\alpha^*}$. Since the result of polarization of magnetic moments is a bulk magnetization, the direction of the transverse polarization can be described by the x and y components of the magnetization vector \vec{M} : $M_x = |M_\perp| \cos \Phi$, $M_y = |M_\perp| \sin \Phi$, where Φ is the phase of $\overline{c_\beta c_\alpha^*}$ and $M_\perp = \sqrt{M^2 - M_z^2}$.
- If the evolution of the phases $\phi_{\alpha,j}$ and $\phi_{\beta,j}$ is *coherent*, the differences $\phi_{\alpha,j} - \phi_{\beta,j}$ change in time, but identically for all magnetic moments. In such a case, the coherence of the system persists and $\overline{c_\beta c_\alpha^*}$ describes transverse polarization with a constant magnitude and in the direction specified by the actual value of the phase Φ . Section 6.7.3 describes explicitly how the coherence $\overline{c_\beta c_\alpha^*}$ depends on $\phi_{\alpha,j}$ and $\phi_{\beta,j}$.
- $\overline{c_\alpha c_\beta^*}$ does not carry any additional information, it is just a complex conjugate of $\overline{c_\beta c_\alpha^*}$. It also implies that the complex number $\overline{c_\beta c_\alpha^*}$ carries the same information as the matrix

$$\begin{pmatrix} 0 & \overline{c_\alpha c_\beta^*} \\ \overline{c_\beta c_\alpha^*} & 0 \end{pmatrix}.$$

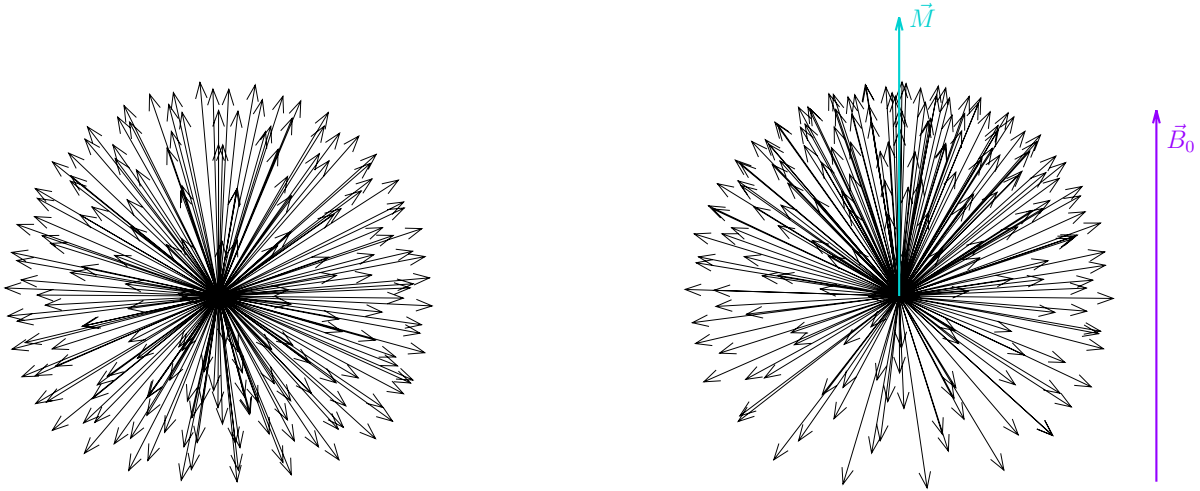


Figure 6.1: Pictorial representation of the populations $\overline{c_\alpha c_\alpha^*} = 1/2$ (left) and $\overline{c_\alpha c_\alpha^*} > 1/2$ (right). The populations are depicted as distributions of magnetic moments (black) and as a magnetization vector (cyan) defining the direction of the longitudinal polarization.

Consequently, the term *coherence* is used for the complex number $\overline{c_\beta c_\alpha^*}$ as well as for the displayed matrix.

- As $\overline{c_\beta c_\alpha^*}$ is a complex number, it carries information of two real numbers, of its amplitude and phase, or of its real and imaginary components $\overline{|c_\alpha||c_\beta| \cos \Phi}$ and $i\overline{|c_\alpha||c_\beta| \sin \Phi}$. The same information is encoded in purely real and purely imaginary matrices

$$\overline{|c_\alpha||c_\beta| \cos \Phi} \begin{pmatrix} 0 & 1 \\ 1 & 0 \end{pmatrix} \quad i\overline{|c_\alpha||c_\beta| \sin \Phi} \begin{pmatrix} 0 & -1 \\ 1 & 0 \end{pmatrix}.$$

- Graphical representation of the coherence $\overline{c_\beta c_\alpha^*}$ is shown in Figure 6.2.

6.4 Basis sets

Usual choices of basis matrices are (C2.7.2):

- *Cartesian operators*, equal to the operators of spin angular momentum divided by \hbar . In this text, these matrices are written as $\mathcal{I}_x, \mathcal{I}_y, \mathcal{I}_z, \mathcal{I}_t$. In a similar fashion, we write $\mathcal{H} = \hat{H}/\hbar$ for Hamiltonians with eigenvalues expressed in units of (angular) frequency, not energy. The normalization factor $\sqrt{2}$ is often omitted (then the basis is still orthogonal, but not orthonormal):

$$\sqrt{2}\mathcal{I}_t = \frac{1}{\sqrt{2}} \begin{pmatrix} 1 & 0 \\ 0 & 1 \end{pmatrix} \quad \sqrt{2}\mathcal{I}_z = \frac{1}{\sqrt{2}} \begin{pmatrix} 1 & 0 \\ 0 & -1 \end{pmatrix}$$

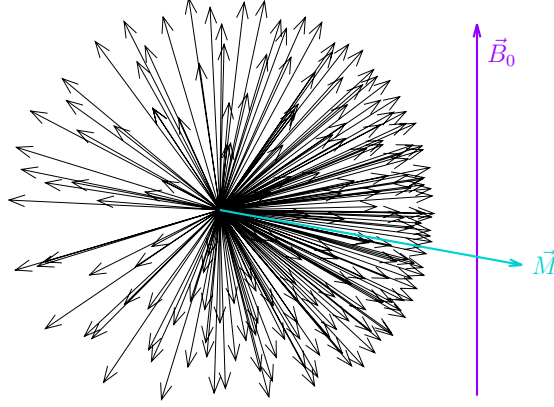


Figure 6.2: Pictorial representation of the coherence $\overline{c_\beta c_\alpha^*}$ as a distribution of magnetic moments (black) and as a magnetization vector (cyan) defining the direction of the transverse polarization.

$$\sqrt{2}\mathcal{I}_x = \frac{1}{\sqrt{2}} \begin{pmatrix} 0 & 1 \\ 1 & 0 \end{pmatrix} \quad \sqrt{2}\mathcal{I}_y = \frac{1}{\sqrt{2}} \begin{pmatrix} 0 & -i \\ i & 0 \end{pmatrix}. \quad (6.4)$$

- Single-element *population*

$$\mathcal{I}_\alpha = \mathcal{I}_t + \mathcal{I}_z = \begin{pmatrix} 1 & 0 \\ 0 & 0 \end{pmatrix} \quad \mathcal{I}_\beta = \mathcal{I}_t - \mathcal{I}_z = \begin{pmatrix} 0 & 0 \\ 0 & 1 \end{pmatrix} \quad (6.5)$$

and *transition* operators

$$\mathcal{I}_+ = \mathcal{I}_x + i\mathcal{I}_y = \begin{pmatrix} 0 & 1 \\ 0 & 0 \end{pmatrix} \quad \mathcal{I}_- = \mathcal{I}_x - i\mathcal{I}_y = \begin{pmatrix} 0 & 0 \\ 1 & 0 \end{pmatrix}. \quad (6.6)$$

- A mixed basis

$$\sqrt{2}\mathcal{I}_t = \frac{1}{\sqrt{2}} \begin{pmatrix} 1 & 0 \\ 0 & 1 \end{pmatrix} \quad \sqrt{2}\mathcal{I}_z = \frac{1}{\sqrt{2}} \begin{pmatrix} 1 & 0 \\ 0 & -1 \end{pmatrix} \quad \mathcal{I}_+ = \begin{pmatrix} 0 & 1 \\ 0 & 0 \end{pmatrix} \quad \mathcal{I}_- = \begin{pmatrix} 0 & 0 \\ 1 & 0 \end{pmatrix}. \quad (6.7)$$

6.5 Liouville - von Neumann equation

In order to describe the evolution of mixed states in time, we must find an equation describing how elements of the density matrix change in time. Derivation of such equation is nicely described in C2.2.3 and reviewed in Section 6.7.4 of our text. The result is

$$\frac{d\hat{\rho}}{dt} = \frac{i}{\hbar}(\hat{\rho}\hat{H} - \hat{H}\hat{\rho}) = \frac{i}{\hbar}[\hat{\rho}, \hat{H}] = -\frac{i}{\hbar}[\hat{H}, \hat{\rho}] \tag{6.8}$$

or in the units of (angular) frequency

$$\frac{d\hat{\rho}}{dt} = i(\hat{\rho}\mathcal{H} - \mathcal{H}\hat{\rho}) = i[\hat{\rho}, \mathcal{H}] = -i[\mathcal{H}, \hat{\rho}]. \tag{6.9}$$

Eqs. 6.8 and 6.9 are known as the *Liouville - von Neumann equation*.

The Liouville - von Neumann equation can be solved using techniques of linear algebra. However, a very simple geometric solution is possible (K7.3, C2.7.3, L11.8) if the Hamiltonian does not change in time and consists solely of matrices which commute (e.g., \mathcal{I}_t and \mathcal{I}_z , but not \mathcal{I}_x and \mathcal{I}_z).

The evolution of $\hat{\rho}$ can be described as a *rotation in an abstract three-dimensional operator space* with the dimensions given by \mathcal{I}_x , \mathcal{I}_y , and \mathcal{I}_z , as shown in Section 6.7.5. An example is given in Fig. 6.3.

If the operator \mathcal{I}_j , defining the density matrix $\hat{\rho} = c\mathcal{I}_j$, and the operator \mathcal{I}_l , defining the Hamiltonian $\mathcal{H} = \omega\mathcal{I}_l$, satisfy the following commutation relation

$$[\mathcal{I}_j, \mathcal{I}_k] = i\mathcal{I}_l, \tag{6.10}$$

then the density matrix evolves as

$$\hat{\rho} = c\mathcal{I}_j \longrightarrow c\mathcal{I}_j \cos(\omega t) + c\mathcal{I}_k \sin(\omega t), \tag{6.11}$$

which corresponds to a rotation about \mathcal{I}_l in an abstract three-dimensional space defined by the basis $\mathcal{I}_j, \mathcal{I}_k, \mathcal{I}_l$.

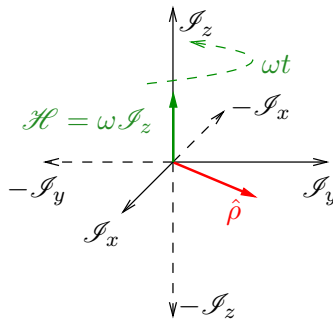


Figure 6.3: Evolution of the density matrix $\hat{\rho} = c\mathcal{I}_x \cos(\omega t) + c\mathcal{I}_y \sin(\omega t)$ under the influence of the Hamiltonian $\mathcal{H} = \omega\mathcal{I}_z$ visualized as a rotations in the space of operators $\mathcal{I}_x, \mathcal{I}_y, \mathcal{I}_z$.

6.6 General strategy of analyzing NMR experiments

The Liouville - von Neumann equation is the most important tool in the analysis of evolution of the spin system during the NMR experiment. The general strategy consists of three steps:

1. Define $\hat{\rho}$ at $t = 0$

2. Describe evolution of $\hat{\rho}$ using the relevant Hamiltonians – this is usually done in several steps
3. Calculate the expectation value of the measured quantity (magnetization components in the x, y plane) according to Eq. 6.3

Obviously, the procedure requires knowledge of

1. relation(s) describing the initial state of the system ($\hat{\rho}(0)$)
2. all Hamiltonians
3. the operator representing the measurable quantity

In the next section, we start from the end and define first the operator of the measurable quantity. Then we spend a lot of time defining all necessary Hamiltonians. Finally, we use the knowledge of the Hamiltonians and basic thermodynamics to describe the initial state.

HOMEWORK

Following Section 6.7.5, and in particular Eq. 6.61, calculate the density matrix after $25 \mu\text{s}$, starting from the state \mathcal{I}_y and evolving under the influence of the Hamiltonian $\mathcal{H} = \omega_0 \mathcal{I}_z$, where $\omega_0 = \pi \times 10^5 \text{ rad/s}$.

6.7 DERIVATIONS

6.7.1 Indistinguishable particles

In classical mechanics, where particles are described by coordinates and momenta, two particles can be always distinguished by tracking their coordinates. This is not possible in quantum mechanics, where particles are described by wave functions. For example, two electrons in a hydrogen molecule are indistinguishable, it is not possible to tell which electron "originally" belonged to which hydrogen atom. This seemingly innocent quantum mechanical feature has dramatic consequences.

Let us investigate a set of three identical spin-1/2 particles, e.g. electrons. Their state is completely described by a wave function Ψ , which depends on their coordinates and spin degrees of freedom:

$$\Psi(x_1, y_1, z_1, c_{\alpha_1}, x_2, y_2, z_2, c_{\alpha_2}, x_3, y_3, z_3, c_{\alpha_3}). \quad (6.12)$$

The probability density that one particle is in a place and in a spin state described by the coordinates $x_1, y_1, z_1, c_{\alpha_1}$, another one in a place and in a spin state described by the coordinates $x_2, y_2, z_2, c_{\alpha_2}$, and a third one in a place and in a spin state described by the coordinates $x_3, y_3, z_3, c_{\alpha_3}$ is given by $\Psi^* \Psi = |\Psi|^2$:

$$\rho = |\Psi(x_1, y_1, z_1, c_{\alpha_1}, x_2, y_2, z_2, c_{\alpha_2}, x_3, y_3, z_3, c_{\alpha_3})|^2. \quad (6.13)$$

If the particles are indistinguishable, $\Psi^* \Psi = |\Psi|^2$ should not be changed by exchanging the particles because we cannot say which one is which.

$$\begin{aligned} \rho &= |\Psi(x_1, y_1, z_1, c_{\alpha_1}, x_2, y_2, z_2, c_{\alpha_2}, x_3, y_3, z_3, c_{\alpha_3})|^2 \\ &= |\Psi(x_2, y_2, z_2, c_{\alpha_2}, x_1, y_1, z_1, c_{\alpha_1}, x_3, y_3, z_3, c_{\alpha_3})|^2 \end{aligned}$$

This is true only if the amplitude of Ψ is not affected by the exchange. The phase of Ψ can differ, but only in a limited way. If the exchange $x_1, y_1, z_1, c_{\alpha_1} \leftrightarrow x_2, y_2, z_2, c_{\alpha_2}$ changes Ψ to $\Psi e^{i\Delta\phi}$, then the second exchange $x_1, y_1, z_1, c_{\alpha_1} \leftrightarrow x_2, y_2, z_2, c_{\alpha_2}$ must return Ψ to its original form because we have returned to the initial state:

$$\Psi e^{i\Delta\phi} \rightarrow (\Psi e^{i\Delta\phi}) e^{i\Delta\phi} = \Psi e^{i2\Delta\phi} = \Psi \quad \Rightarrow \quad e^{i\Delta\phi} = \pm 1. \quad (6.14)$$

Therefore

$$\Psi(x_1, y_1, z_1, c_{\alpha_1}, x_2, y_2, z_2, c_{\alpha_2}, x_3, y_3, z_3, c_{\alpha_3}) = \pm \Psi(x_2, y_2, z_2, c_{\alpha_2}, x_1, y_1, z_1, c_{\alpha_1}, x_3, y_3, z_3, c_{\alpha_3}). \quad (6.15)$$

The wave functions for spin-1/2 particles always change the sign, they are called *antisymmetric*, whereas wave functions keeping the sign upon particle exchange are called *symmetric*. Note that a possible solution of the Schrödinger's equation may be a linear combination of the "correct" symmetric and antisymmetric wave functions, which is not symmetric or antisymmetric. Then, the symmetric and antisymmetric wave functions, correctly describing the system, must be recovered by finding appropriate linear combinations of the "wrong" solutions. For example, if our function Ψ is not symmetric or antisymmetric, we first write all functions obtained by all possible permutations (exchanges) of the coordinates:

$$\begin{aligned} \text{no exchange} &: \Psi(x_1, y_1, z_1, c_{\alpha_1}, x_2, y_2, z_2, c_{\alpha_2}, x_3, y_3, z_3, c_{\alpha_3}) \\ \text{1 exchange} &: \Psi(x_2, y_2, z_2, c_{\alpha_2}, x_1, y_1, z_1, c_{\alpha_1}, x_3, y_3, z_3, c_{\alpha_3}) \\ \text{1 exchange} &: \Psi(x_3, y_3, z_3, c_{\alpha_3}, x_2, y_2, z_2, c_{\alpha_2}, x_1, y_1, z_1, c_{\alpha_1}) \\ \text{1 exchange} &: \Psi(x_1, y_1, z_1, c_{\alpha_1}, x_3, y_3, z_3, c_{\alpha_3}, x_2, y_2, z_2, c_{\alpha_2}) \\ \text{2 exchanges} &: \Psi(x_2, y_2, z_2, c_{\alpha_2}, x_3, y_3, z_3, c_{\alpha_3}, x_1, y_1, z_1, c_{\alpha_1}) \\ \text{2 exchanges} &: \Psi(x_3, y_3, z_3, c_{\alpha_3}, x_1, y_1, z_1, c_{\alpha_1}, x_2, y_2, z_2, c_{\alpha_2}) \end{aligned} \quad (6.16)$$

Then, the sum of all permuted wave functions is symmetric

$$\begin{aligned} \Psi^s = &+ \frac{1}{\sqrt{6}} \Psi(x_1, y_1, z_1, c_{\alpha_1}, x_2, y_2, z_2, c_{\alpha_2}, x_3, y_3, z_3, c_{\alpha_3}) \\ &+ \frac{1}{\sqrt{6}} \Psi(x_2, y_2, z_2, c_{\alpha_2}, x_1, y_1, z_1, c_{\alpha_1}, x_3, y_3, z_3, c_{\alpha_3}) \\ &+ \frac{1}{\sqrt{6}} \Psi(x_3, y_3, z_3, c_{\alpha_3}, x_2, y_2, z_2, c_{\alpha_2}, x_1, y_1, z_1, c_{\alpha_1}) \\ &+ \frac{1}{\sqrt{6}} \Psi(x_1, y_1, z_1, c_{\alpha_1}, x_3, y_3, z_3, c_{\alpha_3}, x_2, y_2, z_2, c_{\alpha_2}) \\ &+ \frac{1}{\sqrt{6}} \Psi(x_2, y_2, z_2, c_{\alpha_2}, x_3, y_3, z_3, c_{\alpha_3}, x_1, y_1, z_1, c_{\alpha_1}) \\ &+ \frac{1}{\sqrt{6}} \Psi(x_3, y_3, z_3, c_{\alpha_3}, x_1, y_1, z_1, c_{\alpha_1}, x_2, y_2, z_2, c_{\alpha_2}) \end{aligned} \quad (6.17)$$

and the sum of the permuted functions multiplied by $(-1)^n$, where n is the number of exchanges, is antisymmetric

$$\begin{aligned}
\Psi^a = & + \frac{1}{\sqrt{6}} \Psi(x_1, y_1, z_1, c_{\alpha_1}, x_2, y_2, z_2, c_{\alpha_2}, x_3, y_3, z_3, c_{\alpha_3}) \\
& - \frac{1}{\sqrt{6}} \Psi(x_2, y_2, z_2, c_{\alpha_2}, x_1, y_1, z_1, c_{\alpha_1}, x_3, y_3, z_3, c_{\alpha_3}) \\
& - \frac{1}{\sqrt{6}} \Psi(x_3, y_3, z_3, c_{\alpha_3}, x_2, y_2, z_2, c_{\alpha_2}, x_1, y_1, z_1, c_{\alpha_1}) \\
& - \frac{1}{\sqrt{6}} \Psi(x_1, y_1, z_1, c_{\alpha_1}, x_3, y_3, z_3, c_{\alpha_3}, x_2, y_2, z_2, c_{\alpha_2}) \\
& + \frac{1}{\sqrt{6}} \Psi(x_2, y_2, z_2, c_{\alpha_2}, x_3, y_3, z_3, c_{\alpha_3}, x_1, y_1, z_1, c_{\alpha_1}) \\
& + \frac{1}{\sqrt{6}} \Psi(x_3, y_3, z_3, c_{\alpha_3}, x_1, y_1, z_1, c_{\alpha_1}, x_2, y_2, z_2, c_{\alpha_2}).
\end{aligned} \tag{6.18}$$

The factor $1/\sqrt{6}$ is a normalization constant, used to obtain $|\Psi^s|^2 = |\Psi^a|^2 = |\Psi|^2$. The symmetry of Ψ^s and antisymmetry of Ψ^a can be checked easily. If we switch any pair of particles, the individual contributions Ψ may change. But the exchange of particles changes the given Ψ to another Ψ , which is already present in the sum, with the same sign (in Ψ^s) or with the opposite sign (in Ψ^a). Therefore, the exchange of particles does not change Ψ^s and changes all signs in Ψ^a .

The minus signs in Eq. 6.18 all indistinguishable particles in a system described by an antisymmetric wave must be in different quantum states (*Pauli exclusion principle*). E.g., if particles 1 and 2 in our three-particle set are in the same state, i.e., if $x_1, y_1, z_1, c_{\alpha_1} = x_2, y_2, z_2, c_{\alpha_2}$, the lines 1 and 2, 3 and 6, and 4 and 5 in Eq. 6.18 cancel each other and the final result is $\Psi^a = 0$. Consequently, $|\Psi^a|^2 = 0$ and the probability of finding the particles anywhere is zero.

Whereas the wave function of a set of indistinguishable particles can change its sign when the particles are exchanged, the Hamiltonian acting on them must stay the same because the Hamiltonian represents the total energy which does not change if we exchange particles. And because the evolution of Ψ is given by the Hamiltonian, a symmetric wave function remains symmetric and an antisymmetric wave function remains antisymmetric during the evolution.

As described in Section 6.1, we usually separate the spatial and spin degrees of freedom:

$$\Psi = \psi_{\text{non-spin}}(x_1, y_1, z_1, x_2, y_2, z_2, x_3, y_3, z_3) \cdot \psi_{\text{spin}}(c_{\alpha_1}, c_{\alpha_2}, c_{\alpha_3}). \tag{6.19}$$

Note that $\psi_{\text{non-spin}}$ must be symmetric and ψ_{spin} antisymmetric, to obtain an antisymmetric Ψ .

6.7.2 Separation of variables

Our task is to find when a wave function ψ_{spin} depending on degrees of freedom of many spins⁶ can be treated as a product of wave functions of individual spins $\psi_{\text{spin}} = \psi^{(1)} \cdot \psi^{(2)} \cdot \psi^{(3)} \dots$, where $\psi^{(1)}$ depends only on the spin degree of freedom of the first nucleus etc. Such separation works if the Hamiltonian can be written as a sum of operators that act only on individual particles (on magnetic moments of nuclei in individual molecules):

$$\hat{H}_{\text{spin}} = \hat{H}^{(1)} + \hat{H}^{(2)} + \hat{H}^{(3)} + \dots \tag{6.20}$$

$$\hat{H}_{\text{spin}} \psi_{\text{spin}} = (\hat{H}^{(1)} + \hat{H}^{(2)} + \hat{H}^{(3)} + \dots) \psi^{(1)} \cdot \psi^{(2)} \cdot \psi^{(3)} \dots = \psi^{(2)} \cdot \psi^{(3)} \dots \hat{H}^{(1)} \psi^{(1)} + \psi^{(1)} \cdot \psi^{(3)} \dots \hat{H}^{(2)} \psi^{(2)} + \psi^{(1)} \cdot \psi^{(2)} \dots \hat{H}^{(3)} \psi^{(3)} + \dots \tag{6.21}$$

Let us assume (see Section 4.9.6)

$$\hat{H}_{\text{spin}} \psi_{\text{spin}} = \mathcal{E}_{\text{spin}} \psi_{\text{spin}}. \tag{6.22}$$

Then, dividing ψ_{spin} to the product $\psi^{(1)} \cdot \psi^{(2)} \cdot \psi^{(3)} \dots$ results in

$$\hat{H}_{\text{spin}} \psi_{\text{spin}} = \psi^{(2)} \cdot \psi^{(3)} \dots \hat{H}^{(1)} \psi^{(1)} + \psi^{(1)} \cdot \psi^{(3)} \dots \hat{H}^{(2)} \psi^{(2)} + \psi^{(1)} \cdot \psi^{(2)} \dots \hat{H}^{(3)} \psi^{(3)} + \dots = \mathcal{E}_{\text{spin}} \psi^{(1)} \cdot \psi^{(2)} \cdot \psi^{(3)} \dots \tag{6.23}$$

If we divide both sides by $\psi_{\text{spin}} = \psi^{(1)} \cdot \psi^{(2)} \cdot \psi^{(3)} \dots$,

$$\frac{\hat{H}^{(1)} \psi^{(1)}}{\psi^{(1)}} + \frac{\hat{H}^{(2)} \psi^{(2)}}{\psi^{(2)}} + \frac{\hat{H}^{(3)} \psi^{(3)}}{\psi^{(3)}} + \dots = \mathcal{E}_{\text{spin}}. \tag{6.24}$$

⁶We are now interested in the spin degrees of freedom, but the same arguments can be applied to any variables.

The right-hand side is the constant $\mathcal{E}_{\text{spin}}$. Therefore, all terms $\hat{H}^{(j)}\psi^{(j)}/\psi^{(j)}$ must be constant if the equation is true for *all* values of the spin degrees of freedom of all nuclei:

$$\begin{aligned} \frac{\hat{H}^{(1)}\psi^{(1)}}{\psi^{(1)}} &= \mathcal{E}^{(1)}, & \frac{\hat{H}^{(2)}\psi^{(2)}}{\psi^{(2)}} &= \mathcal{E}^{(2)}, & \frac{\hat{H}^{(3)}\psi^{(3)}}{\psi^{(3)}} &= \mathcal{E}^{(3)}, & \dots \\ \Rightarrow \hat{H}^{(1)}\psi^{(1)} &= \mathcal{E}^{(1)}\psi^{(1)}, & \hat{H}^{(2)}\psi^{(2)} &= \mathcal{E}^{(2)}\psi^{(2)}, & \hat{H}^{(3)}\psi^{(3)} &= \mathcal{E}^{(3)}\psi^{(3)}, \\ \Rightarrow \mathcal{E}^{(1)} + \mathcal{E}^{(2)} + \mathcal{E}^{(3)} + \dots &= \mathcal{E}_{\text{spin}}. \end{aligned} \quad (6.25)$$

If the nuclei are *indistinguishable* (see Section 6.7.1), all equations $\hat{H}^{(j)}\psi^{(j)} = \mathcal{E}^{(j)}\psi^{(j)}$ and the superscripts can be omitted

$$\hat{H}\psi = \mathcal{E}\psi. \quad (6.26)$$

Nuclear magnetic moments in all molecules are now described by the same spin wave function ψ and by the same Hamiltonian \hat{H} with eigenvalues \mathcal{E}_j and eigenfunctions ψ_j . For example, we have shown (Section 5.4) that the Hamiltonian representing energy of a magnetic moment in a vertical magnetic field described by \vec{B}_0 is

$$-\frac{\gamma B_0 \hbar}{2} \begin{pmatrix} 1 & 0 \\ 0 & -1 \end{pmatrix} = \omega_0 \frac{\hbar}{2} \begin{pmatrix} 1 & 0 \\ 0 & -1 \end{pmatrix}, \quad (6.27)$$

its eigenfunctions are (after separation from the wave functions describing the dependence on x, y, z) the vectors

$$\begin{pmatrix} 1 \\ 0 \end{pmatrix} = |\alpha\rangle, \quad \begin{pmatrix} 0 \\ 1 \end{pmatrix} = |\beta\rangle, \quad (6.28)$$

and its eigenvalues are

$$-\frac{\gamma B_0 \hbar}{2} = +\omega_0 \frac{\hbar}{2} = \mathcal{E}_\alpha, \quad +\frac{\gamma B_0 \hbar}{2} = -\omega_0 \frac{\hbar}{2} = \mathcal{E}_\beta, \quad (6.29)$$

respectively. This Hamiltonian and its eigenfunctions can be used to describe all nuclear magnetic moments of a macroscopic sample if *all consequences of interactions of individual magnetic moments* can be described by modifying only the values $\mathcal{E}_\alpha, \mathcal{E}_\beta$ to some $\mathcal{E}'_\alpha, \mathcal{E}'_\beta$ (actually, only the energy differences $\mathcal{E}_\alpha - \mathcal{E}_\beta$ and $\mathcal{E}'_\alpha - \mathcal{E}'_\beta$ are relevant). Such modification may account for the shielding magnetic fields by electrons, variation of the external field \vec{B}_0 etc. The modification should be general, i.e., we should be able to use a single expression for $\mathcal{E}'_\alpha - \mathcal{E}'_\beta$ of any magnetic moment in the sample.

6.7.3 Phases and coherences

The coherence $\overline{c_\beta c_\alpha^*}$ with the amplitude $\overline{|c_\alpha||c_\beta|}$ and with a phase Φ describes the *transverse polarization* of magnetic moments. In order to analyze coherences explicitly, we use an eigenfunction of the operator representing angular momentum pointing in a general direction, described by angles ϑ (declination) and φ (azimuth), introduced in Section 5.7.7. The eigenfunction (cf. Eq. 5.147) is the following linear combination (superposition) of the α and β eigenstates of \hat{I}_z :

$$|\vartheta_j, \varphi_j\rangle = \begin{pmatrix} \cos \frac{\vartheta_j}{2} e^{-i\frac{\varphi_j}{2}} \\ \sin \frac{\vartheta_j}{2} e^{+i\frac{\varphi_j}{2}} \end{pmatrix} = \begin{pmatrix} c_{\alpha,j} \\ c_{\beta,j} \end{pmatrix} = c_{\alpha,j}|\alpha\rangle + c_{\beta,j}|\beta\rangle. \quad (6.30)$$

If states of all magnetic moments in our ensemble are described by an eigenfunction of this form, the density matrix element $\overline{c_\beta c_\alpha^*}$ is

$$\overline{c_\beta c_\alpha^*} = \overline{\cos \frac{\vartheta}{2} \sin \frac{\vartheta}{2} e^{+i\varphi}} = \frac{1}{2} \overline{\sin \vartheta e^{+i\varphi}}. \quad (6.31)$$

If the distributions of the angles ϑ and φ are independent,

$$\overline{c_\beta c_\alpha^*} = \frac{1}{2} \overline{\sin \vartheta} \cdot \overline{e^{+i\varphi}}. \quad (6.32)$$

What is the physical interpretation of such density matrix elements? If the phase φ is the same for all magnetic moments of the ensemble (it is never true in reality), the direction of the transverse polarization is given by $M_x = |M_\perp| \cos \varphi$ and $M_y = |M_\perp| \sin \varphi$. E.g., $\varphi = 0$ describes polarization of magnetic moments in the x direction, $\varphi = \pi/2$ describes polarization of magnetic moments in the y direction, etc.

What defines the values of φ_j in real samples? In Section 5.7.8, we analyzed how the phases of the c_α and c_β coefficients *evolve* in a magnetic field described by the Hamiltonian $\hat{H} = -\gamma B_0 \hat{I}_z = \omega_0 \hat{I}_z$. We have found (Eqs. 5.152–5.153) that the phases of both coefficients *rotate* with the frequencies given by the eigenvalues of the Hamiltonian (\mathcal{E}_α and \mathcal{E}_β):

$$c_\alpha(t) = c_\alpha(t=0)e^{+i\frac{\gamma B_0}{2}t} = \cos\frac{\vartheta}{2}e^{-i\frac{\varphi(t=0)}{2}}e^{+i\frac{\gamma B_0}{2}t} = \cos\frac{\vartheta}{2}e^{-i\frac{\varphi(t=0)}{2}}e^{-i\frac{\omega_0}{2}t} = \cos\frac{\vartheta}{2}e^{-i\frac{\varphi(t=0)}{2}}e^{+i\frac{\mathcal{E}_\alpha}{\hbar}t}, \quad (6.33)$$

$$c_\beta(t) = c_\beta(t=0)e^{-i\frac{\gamma B_0}{2}t} = \sin\frac{\vartheta}{2}e^{+i\frac{\varphi(t=0)}{2}}e^{-i\frac{\gamma B_0}{2}t} = \sin\frac{\vartheta}{2}e^{+i\frac{\varphi(t=0)}{2}}e^{+i\frac{\omega_0}{2}t} = \sin\frac{\vartheta}{2}e^{+i\frac{\varphi(t=0)}{2}}e^{-i\frac{\mathcal{E}_\beta}{\hbar}t}, \quad (6.34)$$

where we have used the explicit forms of $c_\alpha(t=0)$ and $c_\beta(t=0)$ for $|\vartheta, \varphi\rangle$, (cf. Eq. 5.147). Note that the evolution in the magnetic field \vec{B}_0 changes only the azimuth φ , not the declination ϑ .

If all magnetic moments experience the same magnetic field \vec{B}_0 , the coherence $\overline{c_\beta c_\alpha^*}$ evolves as

$$\overline{c_\beta c_\alpha^*} = \frac{1}{2} \overline{\sin\vartheta} \overline{e^{+i\varphi(t=0)}} e^{+i\omega_0 t}, \quad (6.35)$$

i.e., all azimuths φ_j evolve with the same angular frequency ω_0 .

We have described the evolution of the coherence, but we have not yet specified what defines the distributions of ϑ_j and $\varphi_j(t=0)$, determining $\overline{c_\beta c_\alpha^*}$ at $t=0$, i.e., $\frac{1}{2} \overline{\sin\vartheta} \overline{e^{+i\varphi(t=0)}}$. The general answer is that the magnetic field felt by the magnetic moments determines the statistical distribution of ϑ_j and $\varphi_j(t=0)$. A quantitative analysis of various magnetic fields (the external static field \vec{B}_0 , the influence of the electrons, the field of the applied radio waves \vec{B}_0) is presented in the next lecture.⁷ At this moment, we only comment two results that are derived in the next lecture.

The first example is an equilibrium ensemble of magnetic moments in \vec{B}_0 . At the thermodynamic equilibrium, there is no preferred azimuth of magnetic moments in the vertical field \vec{B}_0 . Therefore, the state of the system is an incoherent superposition of the eigenstates α and β with $e^{+i\varphi(t=0)} = 0$ and consequently $\overline{c_\beta c_\alpha^*} = 0$.

The second example is an ensemble of magnetic moments in \vec{B}_0 after applying a radio-wave pulse that rotated the bulk magnetization to the direction y (cf. Figure 1.4). In such a case, $M_x = |M| \cos\Phi = 0$ and $M_y = |M| \sin\Phi = |M|$, telling us that $\Phi = \pi/2$ immediately after the pulse. Then, the phase factor starts to rotate with the frequency $\omega_0 = -\gamma B_0$:

$$e^{i\Phi} = \overline{e^{+i\varphi}} = \overline{e^{+i\varphi(t=0)}} e^{+i\omega_0 t} = e^{i\frac{\pi}{2}} e^{+i\omega_0 t} = e^{i(\frac{\pi}{2} + \omega_0 t)}. \quad (6.36)$$

Now only the magnitude $\frac{1}{2} \overline{\sin\vartheta}$ remains to be specified. In the next lecture, we derive (i) that the magnitude of the transverse polarization after the pulse is equal to the longitudinal polarization before the pulse and (ii) that the longitudinal polarization at the equilibrium is defined by a statistical relation resembling the Boltzmann's law of classical statistical mechanics.

6.7.4 From Schrödinger to Liouville - von Neumann equation

We start with the Schrödinger equation for a single spin in the matrix representation:

$$i\hbar \frac{d}{dt} \begin{pmatrix} c_\alpha \\ c_\beta \end{pmatrix} = \begin{pmatrix} H_{\alpha,\alpha} & H_{\alpha,\beta} \\ H_{\beta,\alpha} & H_{\beta,\beta} \end{pmatrix} \begin{pmatrix} c_\alpha \\ c_\beta \end{pmatrix} = \begin{pmatrix} H_{\alpha,\alpha}c_\alpha + H_{\alpha,\beta}c_\beta \\ H_{\beta,\alpha}c_\alpha + H_{\beta,\beta}c_\beta \end{pmatrix}. \quad (6.37)$$

Note that the Hamiltonian matrix is written in a general form, the basis functions are not necessarily eigenfunctions of the operator. However, the matrix must be *Hermitian*, i.e., $H_{j,k} = H_{k,j}^*$:

$$H_{\alpha,\beta} = H_{\beta,\alpha}^* \quad H_{\beta,\alpha} = H_{\alpha,\beta}^*. \quad (6.38)$$

If we multiply Eq. 6.37 by the basis functions from left, we obtained the differential equations for c_α and c_β (because the basis functions are orthonormal):

$$(1\ 0) i\hbar \frac{d}{dt} \begin{pmatrix} c_\alpha \\ c_\beta \end{pmatrix} = i\hbar \frac{dc_\alpha}{dt} = H_{\alpha,\alpha}c_\alpha + H_{\alpha,\beta}c_\beta \quad (6.39)$$

$$(0\ 1) i\hbar \frac{d}{dt} \begin{pmatrix} c_\alpha \\ c_\beta \end{pmatrix} = i\hbar \frac{dc_\beta}{dt} = H_{\beta,\alpha}c_\alpha + H_{\beta,\beta}c_\beta. \quad (6.40)$$

In general,

$$\frac{dc_k}{dt} = -\frac{i}{\hbar} \sum_l H_{k,l} c_l \quad (6.41)$$

and its complex conjugate (using Eq. 6.38) is

⁷Setting the beginning of the time scale is somewhat tricky. Therefore we start the analysis by defining the elements of the density matrix (the distribution of ϑ_j and φ_j) for a *stationary macroscopic state*, when the density matrix does not depend on time. Then we can start to vary the magnetic fields and count the time from the first applied change.

$$\frac{dc_k^*}{dt} = +\frac{i}{\hbar} \sum_l H_{k,l}^* c_l^* = +\frac{i}{\hbar} \sum_l H_{l,k} c_l^*. \quad (6.42)$$

Elements of the density matrix consist of the products $c_j c_k^*$. Therefore, we must calculate

$$\frac{d(c_j c_k^*)}{dt} = c_j \frac{dc_k^*}{dt} + c_k^* \frac{dc_j}{dt} = \frac{i}{\hbar} \sum_l H_{l,k} c_j c_l^* - \frac{i}{\hbar} \sum_l H_{j,l} c_l c_k^*. \quad (6.43)$$

For multiple nuclei with the same basis,

$$\frac{d(c_{j,1} c_{k,1}^* + c_{j,2} c_{k,2}^* + \dots)}{dt} = c_{j,1} \frac{dc_{k,1}^*}{dt} + c_{k,1}^* \frac{dc_{j,1}}{dt} + c_{j,2} \frac{dc_{k,2}^*}{dt} + c_{k,2}^* \frac{dc_{j,2}}{dt} + \dots \quad (6.44)$$

$$= \frac{i}{\hbar} \sum_l H_{l,k} (c_{j,1} c_{l,1}^* + c_{j,2} c_{l,2}^* + \dots) - \frac{i}{\hbar} \sum_l H_{j,l} (c_{l,1} c_{k,1}^* + c_{l,2} c_{k,2}^* + \dots). \quad (6.45)$$

Note that

$$\sum_l (c_{j,1} c_{l,1}^* + c_{j,2} c_{l,2}^* + \dots) H_{l,k} = N \sum_l \rho_{j,l} H_{l,k} \quad (6.46)$$

is the j, k element of the product $N \hat{\rho} \hat{H}$, and

$$\sum_l H_{j,l} (c_{l,1} c_{k,1}^* + c_{l,2} c_{k,2}^* + \dots) = N \sum_l H_{j,l} \rho_{l,k} \quad (6.47)$$

is the j, k element of the product $N \hat{H} \hat{\rho}$. Therefore, we can write the equation of motion for the whole density matrix as

$$\frac{d\hat{\rho}}{dt} = \frac{i}{\hbar} (\hat{\rho} \hat{H} - \hat{H} \hat{\rho}) = \frac{i}{\hbar} [\hat{\rho}, \hat{H}] = -\frac{i}{\hbar} [\hat{H}, \hat{\rho}]. \quad (6.48)$$

6.7.5 Rotation in operator space

Let us look at an example⁸ for $\mathcal{H} = \varepsilon_t \mathcal{I}_t + \omega_0 \mathcal{I}_z$ and $\hat{\rho} = c_x \mathcal{I}_x + c_y \mathcal{I}_y + c_z \mathcal{I}_z + c_t \mathcal{I}_t$.

Let us first evaluate the commutators from the Liouville - von Neumann equation:

\mathcal{I}_t is proportional to a unit matrix \Rightarrow it must commute with all matrices:

$$[\mathcal{I}_t, \mathcal{I}_j] = 0 \quad (j = x, y, z, t). \quad (6.49)$$

Commutators of \mathcal{I}_z are given by the definition of angular momentum operators (Eqs. 4.32–4.35):

$$[\mathcal{I}_z, \mathcal{I}_z] = [\mathcal{I}_z, \mathcal{I}_t] = 0 \quad [\mathcal{I}_z, \mathcal{I}_x] = i \mathcal{I}_y \quad [\mathcal{I}_z, \mathcal{I}_y] = -i \mathcal{I}_x. \quad (6.50)$$

Let us write the Liouville - von Neumann equation with the evaluated commutators:

$$\frac{dc_x}{dt} \mathcal{I}_x + \frac{dc_y}{dt} \mathcal{I}_y + \frac{dc_z}{dt} \mathcal{I}_z + \frac{dc_t}{dt} \mathcal{I}_t = i(-i\omega_0 c_x \mathcal{I}_y + i\omega_0 c_y \mathcal{I}_x). \quad (6.51)$$

Written in a matrix representation (noticing that c_z and c_t do not evolve because the $c_z \mathcal{I}_z$ and $c_t \mathcal{I}_t$ components of the density matrix commute with both matrices constituting the Hamiltonian),

$$\frac{dc_x}{dt} \frac{1}{2} \begin{pmatrix} 0 & 1 \\ 1 & 0 \end{pmatrix} + \frac{dc_y}{dt} \frac{1}{2} \begin{pmatrix} 0 & -i \\ i & 0 \end{pmatrix} + 0 + 0 = \omega_0 c_x \frac{1}{2} \begin{pmatrix} 0 & -i \\ i & 0 \end{pmatrix} - \omega_0 c_y \frac{1}{2} \begin{pmatrix} 0 & 1 \\ 1 & 0 \end{pmatrix}, \quad (6.52)$$

$$\frac{1}{2} \begin{pmatrix} 0 & \frac{dc_x}{dt} \\ \frac{dc_x}{dt} & 0 \end{pmatrix} + \frac{1}{2} \begin{pmatrix} 0 & -i \frac{dc_y}{dt} \\ i \frac{dc_y}{dt} & 0 \end{pmatrix} + 0 + 0 = \frac{i}{2} \begin{pmatrix} 0 & -\omega_0 c_x \\ \omega_0 c_x & 0 \end{pmatrix} + \frac{i}{2} \begin{pmatrix} 0 & i\omega_0 c_y \\ i\omega_0 c_y & 0 \end{pmatrix}. \quad (6.53)$$

Adding the matrices,

$$\begin{pmatrix} 0 & \frac{d(c_x - ic_y)}{dt} \\ \frac{d(c_x + ic_y)}{dt} & 0 \end{pmatrix} = i\omega_0 \begin{pmatrix} 0 & -(c_x - ic_y) \\ c_x + ic_y & 0 \end{pmatrix}. \quad (6.54)$$

⁸Various Hamiltonians encountered in NMR spectroscopy are discussed in the next lectures. At this moment, take $\mathcal{H} = \varepsilon_t \mathcal{I}_t + \omega_0 \mathcal{I}_z$ just as an example.

This corresponds to a set of two differential equations

$$\frac{d(c_x - ic_y)}{dt} = -i\omega_0(c_x - ic_y) \quad (6.55)$$

$$\frac{d(c_x + ic_y)}{dt} = +i\omega_0(c_x + ic_y) \quad (6.56)$$

with the same structure as Eqs. 4.101 and 4.102. The solution is

$$c_x - ic_y = (c_x(0) - ic_y(0))e^{-i\omega_0 t} = c_0 e^{-i(\omega_0 t + \phi_0)} \quad (6.57)$$

$$c_x + ic_y = (c_x(0) + ic_y(0))e^{+i\omega_0 t} = c_0 e^{+i(\omega_0 t + \phi_0)} \quad (6.58)$$

with the amplitude c_0 and phase ϕ_0 given by the initial conditions. It corresponds to

$$c_x = c_0 \cos(\omega_0 t + \phi_0) \quad (6.59)$$

$$c_y = c_0 \sin(\omega_0 t + \phi_0). \quad (6.60)$$

We see that coefficients c_x, c_y, c_z play the same roles as coordinates r_x, r_y, r_z in Eqs. 4.98–4.100, respectively, and operators $\mathcal{I}_x, \mathcal{I}_y, \mathcal{I}_z$ play the same role as unit vectors $\vec{i}, \vec{j}, \vec{k}$, defining directions of the axes of the Cartesian coordinate system. Therefore, evolution of $\hat{\rho}$ in our case can be described as a rotation of a three-dimensional vector consisting of the elements c_x, c_y, c_z in an abstract three-dimensional space defined by $\mathcal{I}_x, \mathcal{I}_y$, and \mathcal{I}_z . In our case, if $\phi = 0$, then $\hat{\rho}(0) = c_0 \mathcal{I}_x + c_z \mathcal{I}_z + c_t \mathcal{I}_t$ and it evolves as

$$c_0 \mathcal{I}_x + c_z \mathcal{I}_z + c_t \mathcal{I}_t \longrightarrow c_0 \mathcal{I}_x \cos(\omega_0 t) + c_0 \mathcal{I}_y \sin(\omega_0 t) + c_z \mathcal{I}_z + c_t \mathcal{I}_t. \quad (6.61)$$

Lecture 7

Chemical shift, one-pulse experiment

Literature: The general strategy is clearly outlined in C2.4, Hamiltonians discussed in L8, thermal equilibrium in L11.3, C2.4.1, K6.8.6, relaxation due to the chemical shift in C5.4.4, K9.10 (very briefly, the quantum approach to relaxation is usually introduced using dipole-dipole interactions as an example). The one-pulse experiment is analyzed in K7.2.1, L11.11 and L11.12.

7.1 Operator of the observed quantity

The quantity observed in the NMR experiment is the *bulk magnetization* \vec{M} , i.e., the sum of magnetic moments of all nuclei divided by volume of the sample, assuming isotropic distribution of the nuclei in the sample. Technically, we observe oscillations in the plane perpendicular to the homogeneous field of the magnet \vec{B}_0 . The associated oscillations of the magnetic fields of nuclei induce *electromotive force* in the detector coil, as described by Eq. 55. Since a complex signal is usually recorded (see Section 3.6.3), the operator of complex magnetization $M_+ = M_x + iM_y$ is used ($M_- = M_x - iM_y$ can be used as well).

$$\hat{M}_+ = \mathcal{N}\gamma(\hat{I}_x + i\hat{I}_y) = \mathcal{N}\gamma\hat{I}_+, \quad (7.1)$$

where \mathcal{N} is the number of nuclei in the sample per unit volume.

7.2 Hamiltonian of the static field \vec{B}_0

We already defined the Hamiltonian of the static homogeneous magnetic field \vec{B}_0 , following the classical description of energy of a magnetic moment in a magnetic field (Eq. 55). Since \vec{B}_0 defines direction of the z axis,

$$\hat{H}_{0,\text{lab}} = -\gamma B_0 \hat{I}_z. \quad (7.2)$$

7.3 Hamiltonian of the radio-frequency field \vec{B}_1

The oscillating magnetic field of radio waves irradiating the sample is usually approximated by a magnetic field \vec{B}_1 rotating with the frequency of the radio waves ω_{radio} , and the evolution of the

density matrix is described in a coordinate frame rotating with the opposite angular frequency $\omega_{\text{rot}} = -\omega_{\text{radio}}$, as described in Section 1.5.2. The x axis of the rotating coordinate frame is defined by the direction of the B_1 vector. The phase ϕ_{rot} of this vector is given by the convention described in Section 1.5.2.

In the rotating coordinate system, frequency of the rotation of the coordinate frame¹ is subtracted from the precession frequency and the difference $\Omega = \omega_0 - \omega_{\text{rot}} = -\gamma B_0 - \omega_{\text{rot}}$ is the frequency offset defining the evolution in the rotating frame in the absence of other fields:

In the absence of other fields than \vec{B}_0 :

$$\hat{H}_{0,\text{rot}} = (-\gamma B_0 - \omega_{\text{rot}})\hat{I}_z = \Omega\hat{I}_z. \quad (7.3)$$

During irradiation by the radio wave:

$$\hat{H}_{1,\text{rot}} = (-\gamma B_0 - \omega_{\text{rot}})\hat{I}_z - \gamma B_1\hat{I}_x = \Omega\hat{I}_z + \omega_1\hat{I}_x. \quad (7.4)$$

As the radio frequency ω_{radio} (and consequently ω_{rot}) should be close to the precession frequency of the magnetic moments of the observed nuclei, we can assume $|\Omega| \ll |\gamma B_0|$. If the radio frequency is very close to the resonance, $-\gamma B_0 \approx \omega_{\text{rot}}$, $\Omega \ll \omega_1$, and the \hat{I}_z component of the Hamiltonian can be neglected.

The above description is sufficient for a one-dimensional experiment, discussed in this lecture. However, radio waves are applied in several pulses in many NMR experiments. During different pulses, the phase of the radio waves is often shifted. In such a case, it is the phase of the first pulse which defines the x axis of the rotating coordinate frame. In order to be able to analyze the multiple radio pulses later in our course, we now also describe the form of a Hamiltonian of the magnetic field affecting the magnetic moments during irradiation by a wave shifted by $\pi/2$ from the phase of the first pulse:

$$\hat{H}_{1,\text{rot}} = (-\gamma B_0 - \omega_{\text{rot}})\hat{I}_z - \gamma B_1\hat{I}_y = \Omega\hat{I}_z + \omega_1\hat{I}_y. \quad (7.5)$$

Note that such a radio wave (phase shifted by $\pi/2$ from the first pulse) defines the direction of the y axis of the rotating frame. Therefore, a pulse of such a wave is referred to as a y -pulse. In a similar manner, we describe pulses of waves shifted by π or $3\pi/2$ as $-x$ or $-y$ pulses, respectively.

7.4 Hamiltonian of chemical shift

In addition to the external field, magnetic moments are also influenced by magnetic fields of electrons in the molecules. In order to describe our ensemble of spin magnetic moments by a 2×2 density matrix, the interactions with the electrons must modify only eigenvalues, not eigenfunctions of the already introduced Hamiltonians. The concept of the chemical shift tensor, introduced during our classical treatment of the magnetic fields of moving electrons in Section 1.4, allows us to include the chemical shift into the already defined Hamiltonians without changing their eigenfunctions. The values of μ_x , μ_y , and μ_z in the classical equations are simply replaced by the operators \hat{I}_x , \hat{I}_y , and \hat{I}_z :

¹Formally opposite to ω_{radio} .

$$\begin{aligned}\hat{H}_\delta &= -\gamma(\hat{I}_x B_{e,x} + \hat{I}_y B_{e,y} + \hat{I}_z B_{e,z}) = -\gamma(\hat{I}_x \hat{I}_y \hat{I}_z) \begin{pmatrix} B_{e,x} \\ B_{e,y} \\ B_{e,z} \end{pmatrix} = \\ &= -\gamma(\hat{I}_x \hat{I}_y \hat{I}_z) \begin{pmatrix} \delta_{xx} & \delta_{xy} & \delta_{xz} \\ \delta_{yx} & \delta_{yy} & \delta_{yz} \\ \delta_{zx} & \delta_{zy} & \delta_{zz} \end{pmatrix} \begin{pmatrix} B_{0,x} \\ B_{0,y} \\ B_{0,z} \end{pmatrix} = -\gamma \hat{\underline{I}} \cdot \underline{\delta} \cdot \vec{B}_0.\end{aligned}\quad (7.6)$$

As we have also learnt in Section 1.4, we can decompose the chemical shift tensor $\underline{\delta}$ into isotropic, axially symmetric and asymmetric (rhombic) components. The corresponding decomposition of the chemical shift Hamiltonian to $\hat{H}_{\delta,i}$, $\hat{H}_{\delta,a}$, and $\hat{H}_{\delta,r}$ is presented in Section 7.10.1. The complete Hamiltonian of a magnetic moment of a nucleus not interacting with magnetic moments of other nuclei in the presence of the static field \vec{B}_0 but in the absence of the radio waves is given by

$$\hat{H} = \hat{H}_{0,\text{lab}} + \hat{H}_{\delta,i} + \hat{H}_{\delta,a} + \hat{H}_{\delta,r}. \quad (7.7)$$

If we insert the explicit forms of $\hat{H}_{\delta,i}$, $\hat{H}_{\delta,a}$, and $\hat{H}_{\delta,r}$ (Section 7.10.1) to Eq. 7.7, the Hamiltonian including the chemical shift becomes very complicated. Fortunately, it can be simplified in many cases, as we show in the following sections.

7.5 Secular approximation and averaging

- The components of the induced fields $B_{e,x}$ and $B_{e,y}$ are perpendicular to \vec{B}_0 . The contributions of $\hat{H}_{\delta,i}$ are constant and the contributions of $\hat{H}_{\delta,a}$ and $\hat{H}_{\delta,r}$ fluctuate with the molecular motions changing values of φ , ϑ , and χ . Since the molecular motions do not resonate (in general) with the precession frequency $-\gamma B_0$, the components $B_{e,x}\hat{I}_x$ and $B_{e,y}\hat{I}_y$ of the Hamiltonian oscillate rapidly with a frequency close to $-\gamma B_0$ in the rotating coordinate frame. These oscillations are much faster than the precession about $B_{e,x}$ and $B_{e,y}$ (because the field \vec{B}_0 is much larger than \vec{B}_e) and effectively average to zero on the timescale longer than $1/(\gamma B_0)$ (typically nanoseconds). Therefore, the $B_{e,x}\hat{I}_x$ and $B_{e,y}\hat{I}_y$ terms can be neglected if the effects on the longer timescales are studied. Such a simplification is known as *secular approximation*.² The secular approximation simplifies the Hamiltonian to

$$\hat{H} = -\gamma B_0(1 + \delta_i + (3 \cos^2 \vartheta - 1)\delta_a + \cos(2\chi) \sin^2 \vartheta \delta_r)\hat{I}_z \quad (7.8)$$

²In terms of quantum mechanics, eigenfunctions of $B_{e,x}\hat{I}_x$ and $B_{e,y}\hat{I}_y$ differ from the eigenfunctions of $\hat{H}_{0,\text{lab}}$ ($|\alpha\rangle$ and $|\beta\rangle$). Therefore, the matrix representation of $B_{e,x}\hat{I}_x$ and $B_{e,y}\hat{I}_y$ contains off-diagonal elements. Terms proportional to \hat{I}_z represent so-called *secular* part of the Hamiltonian, which does not change the $|\alpha\rangle$ and $|\beta\rangle$ states (because they are eigenfunctions of \hat{I}_z). Terms proportional to \hat{I}_x and \hat{I}_y are *non-secular* because they change the $|\alpha\rangle$ and $|\beta\rangle$ states ($|\alpha\rangle$ and $|\beta\rangle$ are not eigenfunctions of \hat{I}_x or \hat{I}_y). However, eigenvalues of $B_{e,x}\hat{I}_x$ and $B_{e,y}\hat{I}_y$, defining the off-diagonal elements, are much smaller than the eigenvalues of $\hat{H}_{0,\text{lab}}$ (because the field \vec{B}_e is much smaller than \vec{B}_0). *Secular approximation* represents neglecting such small off-diagonal elements in the matrix representation of the total Hamiltonian and keeping only the diagonal secular terms.

- If the sample is an isotropic liquid, averaging over all molecules of the sample further simplifies the Hamiltonian. As no orientation of the molecule is preferred, all values of χ are equally probable and independent of ϑ . Therefore, the last term in Eq. 7.8 is averaged to zero. Moreover, average values of $a_x^2 = \cos^2 \varphi \sin^2 \vartheta$, of $a_y^2 = \sin^2 \varphi \sin^2 \vartheta$, and of $a_z^2 = \cos^2 \vartheta$ must be the same because none of the directions x, y, z is preferred. The consequence has been already discussed when we described relaxation classically (Eq. 2.45 in Section 2.6.1): $(3 \cos^2 \vartheta - 1) = 0$ and the anisotropic and rhombic contributions can be neglected.

The Hamiltonian describing the effects of the static external magnetic field and coherent effects of the electrons in isotropic liquids reduces to

$$\hat{H} = -\gamma B_0(1 + \delta_i)\hat{I}_z. \quad (7.9)$$

Note that the described simplifications can be used only if they are applicable. Eq. 7.9 is valid only in isotropic liquids, not in liquid crystals, stretched gels, polycrystalline powders, monocrystals, etc.! Moreover, Eq. 7.9 does not describe relaxation processes, as discussed in Section 7.7.

7.6 Thermal equilibrium as the initial state

Knowledge of the Hamiltonian allows us to derive the density matrix at the beginning of the experiment. Usually, we start from the thermal equilibrium. If the equilibrium is achieved, phases of individual magnetic moments are random and the magnetic moments precess incoherently. Therefore, the off-diagonal elements (*coherences*) of the equilibrium density matrix (proportional to \mathcal{I}_x and \mathcal{I}_y) are equal to zero. Values of the diagonal elements (*populations*) are derived in Section 7.10.2 and the complete equilibrium density matrix is

$$\hat{\rho}^{\text{eq}} = \begin{pmatrix} \frac{1}{2} + \frac{\gamma B_0 \hbar}{4k_B T} & 0 \\ 0 & \frac{1}{2} - \frac{\gamma B_0 \hbar}{4k_B T} \end{pmatrix} = \frac{1}{2} \begin{pmatrix} 1 & 0 \\ 0 & 1 \end{pmatrix} + \frac{\gamma B_0 \hbar}{4k_B T} \begin{pmatrix} 1 & 0 \\ 0 & -1 \end{pmatrix} = \mathcal{I}_t + \kappa \mathcal{I}_z, \quad (7.10)$$

where

$$\kappa = \frac{\gamma B_0 \hbar}{2k_B T}. \quad (7.11)$$

Note that we derived the quantum description of a *mixed state*. The difference in two diagonal elements (populations) of the density matrix describes *longitudinal polarization* of the magnetic moments (their sum is equal to one by definition). **Populations do not tell us anything about microscopic states of individual magnetic moments. The two-dimensional density matrix does not imply that all magnetic moments are in one of two eigenstates!**

7.7 Relaxation due to chemical shift anisotropy

The simplified Eq. 7.9 does not describe the effects of fast fluctuations, resulting in relaxation. In order to derive quantum description of relaxation caused by the chemical shift, the Liouville - von

Neumann equation must be solved for the complete Hamiltonian including the axial and rhombic contributions. Bloch, Wangness, and Redfield developed a theory, described in Section 7.10.3, that treats the magnetic moments quantum mechanically and their molecular surroundings classically.³ The theory provides the same definitions of the rate constants describing relaxation due to chemical shift anisotropy as we derived classically in Section 2.6.1. The constant R_1 is

$$R_1 = \frac{3}{4}b^2 \left(\frac{1}{2}J(\omega_0) + \frac{1}{2}J(-\omega_0) \right) \approx \frac{3}{4}b^2 J(\omega_0) \quad (7.12)$$

What is the physical interpretation of the obtained equation? Relaxation of M_z is given by the correlation functions $\overline{c^+(0)c^-(t)}$ and $\overline{c^-(0)c^+(t)}$ (discussed in Section 7.10.3) describing fluctuations of the components of the chemical shift tensor perpendicular to \vec{B}_0 (a_x and a_y). Such fluctuating fields resemble the radio waves with $\vec{B}_1 \perp \vec{B}_0$. If the frequency of such fluctuations matches the precession frequency ω_0 , the resonance condition is fulfilled and, for a short time (comparable to the frequency of molecular collisions) when a fluctuation accidentally resonates with ω_0 , the $-\gamma B_{e,x} \hat{I}_x$ and/or $-\gamma B_{e,x} \hat{I}_y$ components of the chemical shift Hamiltonian are not completely removed by the secular approximation. In analogy to Eq. 7.17, the \mathcal{I}_z component of $\hat{\rho}$ (and consequently $\langle M_z \rangle$) slightly changes due to $-\gamma B_{e,x} \hat{I}_x$ and/or $-\gamma B_{e,x} \hat{I}_y$.

If the molecular motions are assumed to be completely random and independent of the distribution of magnetic moments, M_z is expected to decay to zero, which does not happen in reality. If the coupling between molecular motions and magnetic moment distribution is described correctly by the quantum theory (see footnote 3), a correlation function is obtained that describes correctly the return of $\hat{\rho}$ to its equilibrium form.⁴ This drives the system back to the equilibrium distribution of magnetic moments.

The constant R_2 is also described exactly like when derived classically:

$$R_2 = b^2 \left(\frac{1}{2}J(0) + \frac{3}{8}J(\omega_0) \right) \approx R_0 + \frac{1}{2}R_1. \quad (7.13)$$

What is the physical interpretation of the obtained equation? Two terms in Eq. 7.13 describe two processes contributing to the relaxation of M_+ . The first one is the *loss of coherence* with the rate R_0 , given by the correlation function $\overline{c^z(0)c^z(t)}$ and describing fluctuations of the components of the chemical shift tensor parallel with \vec{B}_0 (a_z). This contribution was analyzed in Section 2.6.1 using the classical approach. The second contribution is due to fluctuations of the components of the chemical shift tensor perpendicular to \vec{B}_0 (a_x and a_y), returning the magnetization vector \vec{M} to its direction in the thermodynamic equilibrium. These fluctuations renew the equilibrium value of M_z , as described above, but also make the M_x and M_y components to disappear. Note however, that only one correlation function $\overline{c^+(0)c^-(t)}$ contributes to the relaxation of M_+ , while both $\overline{c^+(0)c^-(t)}$ and $\overline{c^-(0)c^+(t)}$ contribute to the relaxation of M_z . Therefore only $R_1/2$, not R_1 , contributes to R_2 . If we defined R_2 as a relaxation rate of M_- , only $\overline{c^-(0)c^+(t)}$ would contribute.⁵

³The surroundings can be also treated quantum mechanically, as described in Abragam: The principles of nuclear magnetism, Oxford Press 1961, Chapter VIII, Section II.D.

⁴It can be described as $J(\omega_0) = e^{-\hbar\omega_0/k_B T} J(-\omega_0)$. In the semi-classical Bloch-Wangness-Redfield theory, this is taken into account by working with $\Delta\hat{\rho}$ and $\langle \Delta M_z \rangle$ instead of $\hat{\rho}$ and $\langle M_z \rangle$.

⁵Fluctuations with frequency $+\omega_0$ affect M_+ and fluctuations with frequency $-\omega_0$ affect M_- , but both affect M_z .

7.8 One-pulse experiment

Having the initial form of the density matrix, the Hamiltonians, and the operator of the measured quantity, we can proceed and describe a real NMR experiment for a sample consisting of isolated magnetic moments (not interacting with each other). The basic NMR experiment consists of two parts. In the first part, the radio-wave transmitter is switched on for a short time, needed to rotate the magnetization to the plane perpendicular to the magnetic field \vec{B}_0 . Such application of the radio wave is called *excitation pulse*. In the second part, the radio-wave transmitter is switched off but the receiver is switched on in order to detect rotation of the magnetization vector about the direction of \vec{B}_0 . We start by describing the density matrix before the experiment, then we analyze evolution of the density matrix during these two periods, evaluate the relaxation rate, and finally we calculate the magnetization contributing to the detected signal.

7.8.1 Part 1: excitation by radio wave pulses

At the beginning of the experiment, the density matrix describes thermal equilibrium (Eq. 7.10):

$$\hat{\rho}(0) = \mathcal{I}_t + \kappa \mathcal{I}_z. \quad (7.14)$$

The Hamiltonian governing evolution of the system during the first part of the experiment consists of coherent and fluctuating terms. The fluctuating contributions result in *relaxation*, described by the relaxation rates R_1 and R_2 . The coherent contributions include

$$\mathcal{H} = -\gamma B_0(1 + \delta_i) \mathcal{I}_z - \gamma B_1(1 + \delta_i) \cos(\omega_{\text{rot}} t) \mathcal{I}_x - \gamma B_1(1 + \delta_i) \sin(\omega_{\text{rot}} t) \mathcal{I}_y, \quad (7.15)$$

where the choice of the directions x and y is given by the $\cos(\omega_{\text{rot}} t)$ and $\sin(\omega_{\text{rot}} t)$ terms.

The Hamiltonian simplifies in a coordinate system rotating with $\omega_{\text{rot}} = -\omega_{\text{radio}}$

$$\mathcal{H} = \underbrace{(-\gamma B_0(1 + \delta_i) - \omega_{\text{rot}})}_{\Omega} \mathcal{I}_z + \underbrace{(-\gamma B_1(1 + \delta_i))}_{\omega_1} \mathcal{I}_x, \quad (7.16)$$

but it still contains non-commuting terms (\mathcal{I}_x vs. \mathcal{I}_z). Let us check what can be neglected to keep only commuting terms, which allows us to solve the Liouville - von Neumann equation using the simple geometric approach.

- The value of ω_1 defines how much of the magnetization is rotated to the x, y plane. The maximum effect is obtained for $\omega_1 \tau_p = \pi/2$, where τ_p is the length of the radio-wave pulse. Typical values of τ_p for proton are approximately $10 \mu\text{s}$, corresponding to frequency of rotation of 25 kHz (90° rotation in $10 \mu\text{s}$ corresponds to $40 \mu\text{s}$ for a full circle, $1/40 \mu\text{s} = 25 \text{ kHz}$).

Alternatively, we could define R_2 as a relaxation rate of M_x or M_y . Fluctuations of the $B_{e,y}$ component affect M_x but not M_y , while fluctuations of the $B_{e,x}$ component affect M_y but not M_x . On the other hand, both fluctuations of $B_{e,x}$ and $B_{e,y}$ affect M_z . Working with M_+, M_- or M_x, M_y , the relaxation of M_z due to $B_{e,x}$ and $B_{e,y}$ is always twice faster.

- Typical values of R_1 are 10^{-1} s^{-1} to 10^0 s^{-1} and typical values of R_2 are 10^{-1} s^{-1} to 10^2 s^{-1} for protons in organic molecules and biomacromolecules. Therefore, effects of relaxations can be safely neglected during τ_p .
- When observing a single type of proton (or other nucleus), Ω can be set to zero by the choice of ω_{radio} . However, variation of Ω is what we observe in real samples, containing protons (or other nuclei) with various δ_i . The typical range of proton δ_i is 10 ppm, corresponding to 5 kHz at a 500 MHz spectrometer.⁶ The carrier frequency ω_{radio} is often set to the precession frequency of the solvent. In the case of water, it is roughly in the middle of the spectrum (4.7 ppm at pH 7). So, we need to cover ± 2.5 kHz. We see that $|\Omega| < |\omega_1|$, but the ratio is only 10 % at the edge of the spectrum.

In summary, we see that we can safely ignore fluctuating contributions, but we must be careful when neglecting $\Omega \mathcal{I}_z$. The latter approximation allows us to use the geometric solution of the Liouville - von Neumann equation, but is definitely not perfect for larger Ω resulting in *offset effects*.

Using the simplified Hamiltonian $\mathcal{H} = \omega_1 \mathcal{I}_x$, evolution of $\hat{\rho}$ during τ_p can be described as a rotation about the " \mathcal{I}_x axis":

$$\hat{\rho}(0) = \mathcal{I}_t + \kappa \mathcal{I}_z \longrightarrow \hat{\rho}(\tau_p) = \mathcal{I}_t + \kappa (\mathcal{I}_z \cos(\omega_1 \tau_p) - \mathcal{I}_y \sin(\omega_1 \tau_p)). \quad (7.17)$$

For a 90° pulse,

$$\hat{\rho}(\tau_p) = \mathcal{I}_t - \kappa \mathcal{I}_y. \quad (7.18)$$

7.8.2 Part 2: evolution of chemical shift after excitation

After switching off the transmitter, $\omega_1 \mathcal{I}_x$ disappears from the Hamiltonian, which now contains only commuting terms. On the other hand, signal is typically acquired for a relatively long time (0.1 s to 10 s) to achieve a good frequency resolution. Therefore, the relaxation effects cannot be neglected.

The coherent evolution can be described as a rotation about the " \mathcal{I}_z axis" with the angular frequency Ω

$$\hat{\rho}(t) = \mathcal{I}_t + \kappa (-\mathcal{I}_y \cos(\Omega t) + \mathcal{I}_x \sin(\Omega t)). \quad (7.19)$$

The measured quantity M_+ can be expressed as (Eq. 4.9)

$$\langle M_+ \rangle = \text{Tr}\{\hat{\rho}(t) \hat{M}_+\} = \mathcal{N} \gamma \hbar \text{Tr}\{(\mathcal{I}_t + \kappa (-\mathcal{I}_y \cos(\Omega t) + \mathcal{I}_x \sin(\Omega t))) \mathcal{I}_+\} \quad (7.20)$$

$$= \mathcal{N} \gamma \hbar \text{Tr}\{\mathcal{I}_t \mathcal{I}_+\} - \mathcal{N} \gamma \hbar \kappa \cos(\Omega t) \text{Tr}\{\mathcal{I}_y \mathcal{I}_+\} + \mathcal{N} \gamma \hbar \kappa \sin(\Omega t) \text{Tr}\{\mathcal{I}_x \mathcal{I}_+\}. \quad (7.21)$$

The final expression includes the following three traces:

⁶Chosen as a compromise here: spectra of small molecules are usually recored at 300 MHz–500 MHz, while spectra of biomacromolecules are recorded at ≤ 500 MHz.

$$\text{Tr}\{\mathcal{I}_t\mathcal{I}_+\} = \text{Tr}\left\{\begin{pmatrix} \frac{1}{2} & 0 \\ 0 & \frac{1}{2} \end{pmatrix} \begin{pmatrix} 0 & 1 \\ 0 & 0 \end{pmatrix}\right\} = \text{Tr}\left\{\begin{pmatrix} 0 & \frac{1}{2} \\ 0 & 0 \end{pmatrix}\right\} = 0 \quad (7.22)$$

$$\text{Tr}\{\mathcal{I}_x\mathcal{I}_+\} = \text{Tr}\left\{\begin{pmatrix} 0 & \frac{1}{2} \\ \frac{1}{2} & 0 \end{pmatrix} \begin{pmatrix} 0 & 1 \\ 0 & 0 \end{pmatrix}\right\} = \text{Tr}\left\{\begin{pmatrix} 0 & 0 \\ 0 & \frac{1}{2} \end{pmatrix}\right\} = \frac{1}{2} \quad (7.23)$$

$$\text{Tr}\{\mathcal{I}_y\mathcal{I}_+\} = \text{Tr}\left\{\begin{pmatrix} 0 & -\frac{i}{2} \\ \frac{i}{2} & 0 \end{pmatrix} \begin{pmatrix} 0 & 1 \\ 0 & 0 \end{pmatrix}\right\} = \text{Tr}\left\{\begin{pmatrix} 0 & 0 \\ 0 & \frac{i}{2} \end{pmatrix}\right\} = \frac{i}{2} \quad (7.24)$$

As mentioned above, relaxation effects should be taken into account when analyzing acquisition of the NMR signal. Including the exponential relaxation term and expressing κ

$$\langle M_+ \rangle = \frac{\mathcal{N}\gamma^2\hbar^2 B_0}{4k_B T} e^{-R_2 t} (\sin(\Omega t) - i \cos(\Omega t)). \quad (7.25)$$

which can be rewritten as

$$\langle M_+ \rangle = \frac{\mathcal{N}\gamma^2\hbar^2 B_0}{4k_B T} e^{-R_2 t} \left(\cos\left(\Omega t - \frac{\pi}{2}\right) + i \sin\left(\Omega t - \frac{\pi}{2}\right) \right) = \frac{\mathcal{N}\gamma^2\hbar^2 B_0}{4k_B T} e^{-R_2 t} e^{i\Omega t} e^{-i\frac{\pi}{2}}. \quad (7.26)$$

We know that in order to obtain purely Lorentzian (absorption) real component of the spectrum by Fourier transformation, the signal should evolve as $e^{-R_2 t} e^{i\Omega t}$. We see that magnetization described by Eq. 7.26 is shifted from the ideal signal by a phase of $-\pi/2$. However, this is true only if the evolution starts *exactly* at $t = 0$. In practice, this is impossible to achieve for various technical reasons (instrumental delays and phase shifts, evolution starts already during τ_p , etc.). Therefore, the rotation has an unknown phase shift ϕ (including the $\pi/2$ shift among other contributions), which is removed by an empirical correction during signal processing (corresponding to multiplying Eq. 7.26 by $e^{i\pi/2}$). It tells us that we can ignore the phase shift and write the phase-corrected signal as

$$\langle M_+ \rangle = \frac{\mathcal{N}\gamma^2\hbar^2 B_0}{4k_B T} e^{-R_2 t} (\cos(\Omega t) + i \sin(\Omega t)) = \frac{\mathcal{N}\gamma^2\hbar^2 B_0}{4k_B T} e^{-R_2 t} e^{i\Omega t}. \quad (7.27)$$

Knowing the expected magnetization, we can try to describe the one-dimensional NMR spectrum quantitatively. Factors that should be taken into account are listed and analyzed in Section 7.10.4. The analysis shows that the signal-to-noise ratio is proportional to $\gamma^{5/2} B_0^{3/2}$ and further influenced by relaxation, that strongly depends on the temperature.

7.9 Conclusions

In general, the analysis of an ideal one-pulse experiment leads to the following conclusions:

- The analysis of a one-pulse NMR experiment shows that the density matrix evolves as

$$\hat{\rho}(t) \propto (\mathcal{I}_x \cos(\Omega t + \phi) + \mathcal{I}_y \sin(\Omega t + \phi) + \text{terms orthogonal to } \mathcal{I}_+), \quad (7.28)$$

and that the magnetization rotates during signal acquisition as

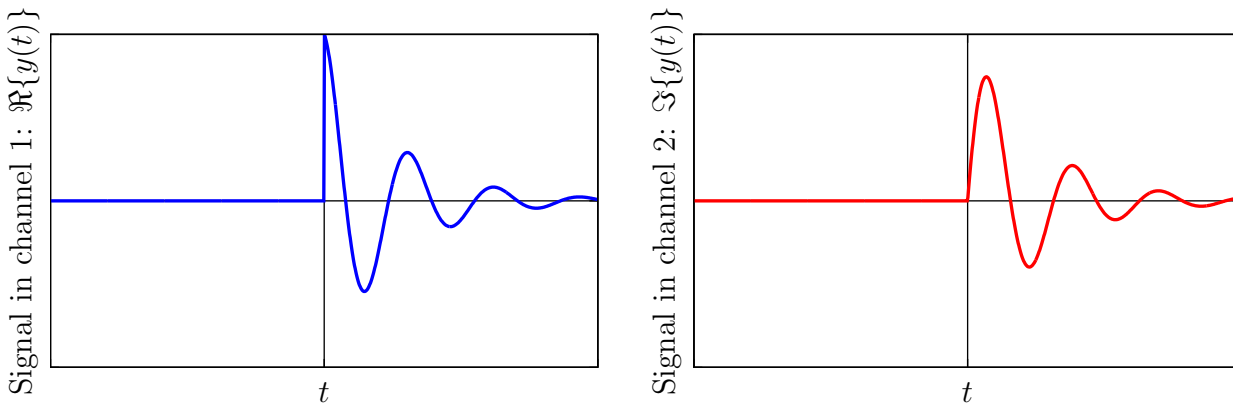
$$\langle M_+ \rangle = |M_+| e^{-R_2 t} e^{i\Omega t} \tag{7.29}$$

(with some unimportant phase shift which is empirically corrected).

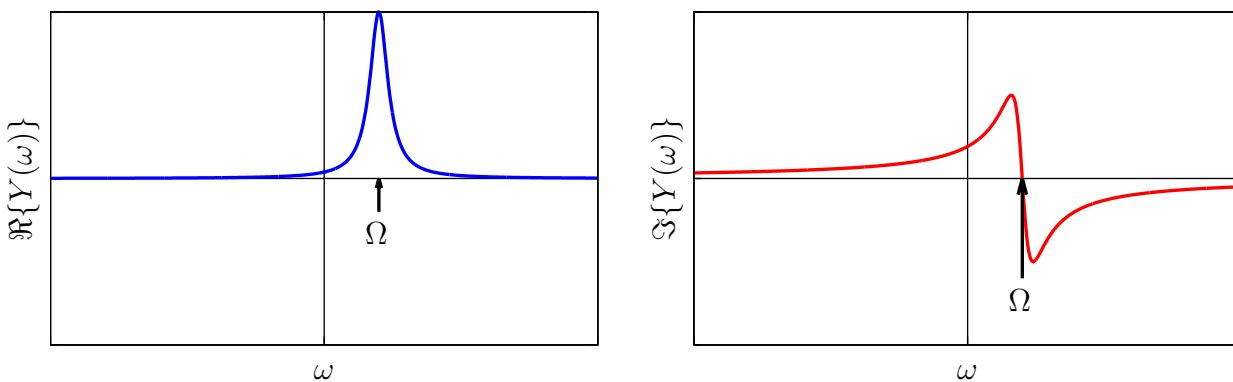
- Fourier transform gives a complex signal proportional to

$$\frac{\mathcal{N} \gamma^2 \hbar^2 B_0}{4k_B T} \left(\frac{R_2}{R_2^2 + (\omega - \Omega)^2} - i \frac{\omega - \Omega}{R_2^2 + (\omega - \Omega)^2} \right). \tag{7.30}$$

- The cosine modulation of \mathcal{I}_x can be taken as the real component of the signal and the sine modulation of \mathcal{I}_y can be taken as the imaginary component of the signal:



After Fourier transformation:



- The signal-to-noise ratio (without relaxation) is proportional to $|\gamma|^{5/2} B_0^{3/2}$, with the optimal temperature given by relaxation properties (close to room temperatures for proteins in aqueous solutions).

HOMEWORK

Analyze the One-pulse experiment (Section 7.8).

7.10 DERIVATIONS

7.10.1 Decomposition of chemical shift Hamiltonian

The Hamiltonian of a homogeneous magnetic field aligned with the z -axis of the coordinate frame can be decomposed into

- isotropic contribution, independent of rotation in space:

$$\hat{H}_{\delta,i} = -\gamma B_0 \delta_i (\hat{I}_z) \quad (7.31)$$

- axial component, dependent on φ and ϑ :

$$\begin{aligned} \hat{H}_{\delta,a} &= -\gamma B_0 \delta_a (3 \sin \vartheta \cos \vartheta \cos \varphi \hat{I}_x + 3 \sin \vartheta \cos \vartheta \sin \varphi \hat{I}_y + (3 \cos^2 \vartheta - 1) \hat{I}_z) \\ &= -\gamma B_0 \delta_a (3 a_x a_z \hat{I}_x + 3 a_y a_z \hat{I}_y + (3 a_z^2 - 1) \hat{I}_z) \end{aligned} \quad (7.32)$$

- rhombic component, dependent on φ , ϑ , and χ :

$$\begin{aligned} \hat{H}_{\delta,r} &= -\gamma B_0 \delta_r ((-2 \cos^2 \chi - 1) \sin \vartheta \cos \vartheta \cos \varphi + 2 \sin \chi \cos \chi \sin \vartheta \cos \vartheta \sin \varphi) \hat{I}_x + \\ &\quad ((-2 \cos^2 \chi - 1) \sin \vartheta \cos \vartheta \sin \varphi - 2 \sin \chi \cos \chi \sin \vartheta \cos \vartheta \cos \varphi) \hat{I}_y + \\ &\quad ((2 \cos^2 \chi - 1) \sin^2 \vartheta) \hat{I}_z \\ &= \gamma B_0 \delta_r ((\cos(2\chi) a_x - \sin(2\chi) a_y) a_z \hat{I}_x + (\cos(2\chi) a_y + \sin(2\chi) a_x) a_z \hat{I}_y + \cos(2\chi) (a_z^2 - 1) \hat{I}_z) \end{aligned}$$

7.10.2 Density matrix in thermal equilibrium

We use the mixed state approach to define the state of the sample in thermal equilibrium. In the large ensemble of nuclei observed in NMR, the equilibrium distribution of magnetic moments is such that orientations in the x and y directions are equally probable, and the orientation in the z direction (defined by the direction of the magnetic induction of the external homogeneous field \vec{B}_0) is slightly favored.

Classically, energy of individual moments depends only on μ_z :

$$\mathcal{E}_j = -\vec{\mu}_j \cdot \vec{B}_0 = -\mu_{z,j} B_0, \quad (7.33)$$

where j identifies the molecule with the observed nuclear magnetic moment, and the overall energy is $\sum_j \mathcal{E}_j$.

Quantum mechanically, the ensemble of magnetic moments represents a mixed state and the expected value of the energy is given by Eq. 6.3, where $\langle A \rangle = \langle \mathcal{E} \rangle$ and $\hat{A} = \hat{H}$. Note that Eq. 6.3 contains an operator (in our case the Hamiltonian) representing the quantity of interest (in our case the energy) for a *single* magnetic moment, although we calculate the expected value for the whole ensemble. If we use eigenfunctions of \hat{I}_z as the basis (the best choice for magnetic moments in the field with \vec{B}_0 defining the z axis), eigenvalues of $H = -\gamma B_0 (1 + \delta_i) \hat{I}_z$ are the diagonal elements of the matrix representation of \hat{H} :

$$\hat{H} = -\gamma B_0 (1 + \delta_i) \hat{I}_z = -\gamma B_0 (1 + \delta_i) \frac{\hbar}{2} \begin{pmatrix} 1 & 0 \\ 0 & -1 \end{pmatrix} = \begin{pmatrix} -\gamma B_0 (1 + \delta_i) \frac{\hbar}{2} & 0 \\ 0 & +\gamma B_0 (1 + \delta_i) \frac{\hbar}{2} \end{pmatrix} = \begin{pmatrix} \mathcal{E}_\alpha & 0 \\ 0 & \mathcal{E}_\beta \end{pmatrix}. \quad (7.34)$$

Eq. 6.3 in this case has the form

$$\langle \mathcal{E} \rangle = \mathcal{N} \text{Tr} \left\{ \underbrace{\begin{pmatrix} \frac{c_\alpha c_\alpha^*}{c_\beta c_\alpha^*} & \frac{c_\alpha c_\beta^*}{c_\beta c_\alpha^*} \\ \frac{c_\beta c_\alpha^*}{c_\beta c_\alpha^*} & \frac{c_\beta c_\beta^*}{c_\beta c_\alpha^*} \end{pmatrix}}_{\hat{\rho}} \underbrace{\begin{pmatrix} \mathcal{E}_\alpha & 0 \\ 0 & \mathcal{E}_\beta \end{pmatrix}}_{\hat{H}} \right\} = \mathcal{N} (\overline{c_\alpha c_\alpha^*} \mathcal{E}_\alpha + \overline{c_\beta c_\beta^*} \mathcal{E}_\beta) = \mathcal{N} (P_\alpha \mathcal{E}_\alpha + P_\beta \mathcal{E}_\beta). \quad (7.35)$$

We see that the expected value of the energy of our mixed state is a weighted average of the energies of the α and β eigenstates of a single magnetic moment. The off-diagonal elements of $\hat{\rho}$, the populations, play a role of *statistical weights* in the derived relation. At the equilibrium, the populations can be evaluated using statistical arguments similar to the Boltzmann law in the classical molecular statistics:

$$P_\alpha^{\text{eq}} = \frac{e^{-\mathcal{E}_\alpha/k_B T}}{e^{-\mathcal{E}_\alpha/k_B T} + e^{-\mathcal{E}_\beta/k_B T}}, \quad (7.36)$$

$$P_\beta^{\text{eq}} = \frac{e^{-\mathcal{E}_\beta/k_B T}}{e^{-\mathcal{E}_\alpha/k_B T} + e^{-\mathcal{E}_\beta/k_B T}}, \quad (7.37)$$

where $k_B = 1.38064852 \times 10^{-23} \text{ m}^2 \text{ kg s}^{-2} \text{ K}^{-1}$ is the Boltzmann constant.

The thermal energy at 0°C is more than 10000 times higher than $\gamma B_0 \hbar / 2$ for the most sensitive nuclei (protons) at spectrometers with the highest magnetic fields (currently 1.2 GHz). The effect of the chemical shift is four orders of magnitude lower (roughly $10^{-8} k_B T$). We see that (i) the effect of the chemical shift δ_i on \mathcal{E}_α and \mathcal{E}_β can be safely neglected, and (ii) that the values in the exponents are much lesser than unity. Therefore, we can approximate the exponential terms by a linear expansion

$$e^{\pm \frac{\gamma B_0 (1 + \delta_i) \hbar}{k_B T}} \approx 1 \pm \frac{\gamma B_0 \hbar}{2 k_B T} \quad (7.38)$$

and calculate the populations as

$$P_\alpha^{\text{eq}} = \frac{e^{-\mathcal{E}_\alpha / k_B T}}{e^{-\mathcal{E}_\alpha / k_B T} + e^{-\mathcal{E}_\beta / k_B T}} = \frac{1 + \frac{\gamma B_0 \hbar}{2 k_B T}}{1 + \frac{\gamma B_0 \hbar}{2 k_B T} + 1 - \frac{\gamma B_0 \hbar}{2 k_B T}} = \frac{1 + \frac{\gamma B_0 \hbar}{2 k_B T}}{2}, \quad (7.39)$$

$$P_\beta^{\text{eq}} = \frac{e^{-\mathcal{E}_\beta / k_B T}}{e^{-\mathcal{E}_\alpha / k_B T} + e^{-\mathcal{E}_\beta / k_B T}} = \frac{1 - \frac{\gamma B_0 \hbar}{2 k_B T}}{1 + \frac{\gamma B_0 \hbar}{2 k_B T} + 1 - \frac{\gamma B_0 \hbar}{2 k_B T}} = \frac{1 - \frac{\gamma B_0 \hbar}{2 k_B T}}{2}. \quad (7.40)$$

7.10.3 Bloch-Wangsness-Redfield theory

The Liouville - von Neumann equation describing the relaxing system of magnetic moments interacting with moving electrons in a so-called *interaction frame* (corresponding to the rotating coordinate frame in the classical description) has the form

$$\frac{d\Delta\hat{\rho}}{dt} = -\frac{i}{\hbar} [\hat{H}_{\delta,a} + \hat{H}_{\delta,r}, \Delta\hat{\rho}], \quad (7.41)$$

where $\hat{H}_{\delta,a}$ and $\hat{H}_{\delta,r}$ are defined by Eqs. 7.32 and 7.33, respectively, and $\Delta\hat{\rho}$ is a difference (expressed in the interaction frame) between density matrix at the given time and density matrix in the thermodynamic equilibrium. Writing $\Delta\hat{\rho}$ in the same bases as used for the Hamiltonian,

$$\Delta\hat{\rho} = d_t \hat{I}_t + d_z \hat{I}_z + d_+ \hat{I}_+ e^{i\omega_0 t} + d_- \hat{I}_- e^{-i\omega_0 t}. \quad (7.42)$$

If the chemical shift is axially symmetric and its size or shape do not change,

$$\frac{d(d_z \hat{I}_z + d_+ \hat{I}_+ e^{i\omega_0 t} + d_- \hat{I}_- e^{-i\omega_0 t})}{dt} = -\frac{i\mathfrak{b}}{\hbar} \left[c^z \hat{I}_z + \sqrt{\frac{3}{8}} c^+ \hat{I}_+ e^{i\omega_0 t} + \sqrt{\frac{3}{8}} c^- \hat{I}_- e^{-i\omega_0 t}, d_z \hat{I}_z + d_+ \hat{I}_+ e^{i\omega_0 t} + d_- \hat{I}_- e^{-i\omega_0 t} \right], \quad (7.43)$$

where $\hat{I}_\pm e^{\pm i\omega_0 t}$ are operators $\hat{I}_\pm = \hat{I}_x \pm i\hat{I}_y$ in the interaction frame, $\omega_0 = -\gamma B_0 (1 + \delta_a)$, and

$$c^z = \frac{1}{2} (3 \cos^2 \vartheta - 1) = \Theta^{\parallel} \quad (7.44)$$

$$c^+ = \sqrt{\frac{3}{2}} \sin \vartheta \cos \vartheta e^{-i\varphi} = \sqrt{\frac{2}{3}} \Theta^\perp e^{-i\varphi} \quad (7.45)$$

$$c^- = \sqrt{\frac{3}{2}} \sin \vartheta \cos \vartheta e^{+i\varphi} = \sqrt{\frac{2}{3}} \Theta^\perp e^{+i\varphi} \quad (7.46)$$

Analogously to the classical analysis, the evolution can be written as

$$\frac{d\Delta\hat{\rho}}{dt} = -\frac{1}{\hbar^2} \int_0^\infty \overline{[\hat{H}_{\delta,a}(0), [\hat{H}_{\delta,a}(t), \Delta\hat{\rho}]]} dt. \quad (7.47)$$

The right-hand side can be simplified dramatically by the *secular approximation*: all terms with $e^{\pm i\omega_0 t}$ are averaged to zero because they rapidly oscillate with the angular frequency ω_0 . Only terms with $(c^z)^2$ and $c^+ c^-$ are non zero (both equal to $1/5$ at $t_j = 0$).⁷ These are the terms with $[\hat{I}_z, [\hat{I}_z, \Delta\hat{\rho}]]$, $[\hat{I}_+, [\hat{I}_-, \Delta\hat{\rho}]]$, and $[\hat{I}_-, [\hat{I}_+, \Delta\hat{\rho}]]$. Moreover, averaging over all molecules makes all three correlation functions identical in isotropic liquids: $c^z(0)c^z(t) = c^+(0)c^-(t) = c^-(0)c^+(t) = c(0)c(t)$.

In order to proceed, the double commutators must be expressed. We start with

$$[\hat{I}_z, \hat{I}_\pm] = [\hat{I}_z, \hat{I}_x] \pm i[\hat{I}_z, \hat{I}_y] = \pm \hbar (\hat{I}_x \pm i\hat{I}_y) = \pm \hbar \hat{I}_\pm \quad (7.48)$$

⁷We have factored out $\sqrt{3/8}$ in order to make $c^+ c^- = \overline{(c^z)^2}$.

and

$$[\hat{I}_+, \hat{I}_-] = [\hat{I}_x, \hat{I}_x] - i[\hat{I}_x, \hat{I}_y] + i[\hat{I}_y, \hat{I}_x] + [\hat{I}_y, \hat{I}_y] = 2\hbar\hat{I}_z. \quad (7.49)$$

Our goal is to calculate relaxation rates for the expectation values of components parallel (M_z) and perpendicular (M_+ or M_-) to \vec{B}_0 .

Let us start with M_z . According to Eq. 4.9,

$$\langle \Delta M_z \rangle = \text{Tr}\{\Delta\hat{\rho}\hat{M}_z\} \quad (7.50)$$

where $\Delta\langle M_z \rangle$ is the difference from the expectation value of M_z in equilibrium. The operator of M_z for one magnetic moment observed is (Eq. 7.1)

$$\hat{M}_z = \mathcal{N}\gamma\hat{I}_z, \quad (7.51)$$

where \mathcal{N} is the number of molecules per volume element detected by the spectrometer. Since the basis matrices are orthogonal, products of \hat{I}_z with the components of the density matrix different from \hat{I}_z are equal to zero and the left-hand side of Eq. 7.47 reduces to

$$\frac{d\langle M_z \rangle}{dt} \hat{I}_z \quad (7.52)$$

when calculating relaxation rate of $\langle M_z \rangle$. In the right-hand side, we need to calculate three double commutators:

$$[\hat{I}_z, [\hat{I}_z, \hat{I}_z]] = 0 \quad [\hat{I}_+, [\hat{I}_-, \hat{I}_z]] = 2\hbar^2\hat{I}_z \quad [\hat{I}_-, [\hat{I}_+, \hat{I}_z]] = 2\hbar^2\hat{I}_z \quad (7.53)$$

After substituting into Eq. 7.47,

$$\frac{d\langle M_z \rangle}{dt} \text{Tr}\{\hat{I}_z\hat{I}_z\} = - \left(\frac{3}{4}b^2 \int_0^\infty \overline{c^+(0)c^-(t)}e^{i\omega_0 t} dt + \frac{3}{4}b^2 \int_0^\infty \overline{c^-(0)c^+(t)}e^{-i\omega_0 t} dt \right) d_z \text{Tr}\{\hat{I}_z\hat{I}_z\} \quad (7.54)$$

$$\frac{d\Delta\langle M_z \rangle}{dt} = - \left(\frac{3}{4}b^2 \int_0^\infty \overline{c^+(0)c^-(t)}e^{i\omega_0 t} dt + \frac{3}{4}b^2 \int_0^\infty \overline{c^-(0)c^+(t)}e^{-i\omega_0 t} dt \right) \Delta\langle M_z \rangle \quad (7.55)$$

The relaxation rate R_1 for M_z , known as *longitudinal relaxation rate* in the literature, is the real part of the expression in the parentheses

$$R_1 = \frac{3}{4}b^2 \Re \left\{ \int_0^\infty \overline{c^+(0)c^-(t)}e^{i\omega_0 t} dt + \int_0^\infty \overline{c^-(0)c^+(t)}e^{-i\omega_0 t} dt \right\} \quad (7.56)$$

As already discussed in the classical description of relaxation, if the fluctuations are random, they are also stationary: the current orientation of the molecule is correlated with the orientation in the past in the same manner as it is correlated with the orientation in the future. Therefore,

$$\int_0^\infty \overline{c^+(0)c^-(t)}e^{i\omega_0 t} dt = \frac{1}{2} \left(\int_0^\infty \overline{c^+(0)c^-(t)}e^{i\omega_0 t} dt + \int_{-\infty}^0 \overline{c^+(0)c^-(t)}e^{i\omega_0 t} dt \right) = \frac{1}{2} \int_{-\infty}^\infty \overline{c^+(0)c^-(t)}e^{i\omega_0 t} dt. \quad (7.57)$$

$$\int_0^\infty \overline{c^-(0)c^+(t)}e^{-i\omega_0 t} dt = \frac{1}{2} \left(\int_0^\infty \overline{c^-(0)c^+(t)}e^{-i\omega_0 t} dt + \int_{-\infty}^0 \overline{c^-(0)c^+(t)}e^{-i\omega_0 t} dt \right) = \frac{1}{2} \int_{-\infty}^\infty \overline{c^-(0)c^+(t)}e^{-i\omega_0 t} dt, \quad (7.58)$$

The right-hand side integrals are identical with the mathematical definition of the Fourier transform of the correlation functions and real parts of such Fourier transforms are the *spectral density functions* $J(\omega)$.

The relaxation rate R_1 can be therefore written in the same form as derived classically:

$$R_1 = \frac{3}{4}b^2 \left(\frac{1}{2}J(\omega_0) + \frac{1}{2}J(-\omega_0) \right) \approx \frac{3}{4}b^2 J(\omega_0) \quad (7.59)$$

Let us continue with M_+ . According to Eq. 4.9,

$$\Delta\langle M_+ \rangle \equiv \langle M_+ \rangle = \text{Tr}\{\Delta\hat{\rho}\hat{M}_+\} \quad (7.60)$$

The expectation value of M_+ in equilibrium is zero, this is why we do not need to calculate the difference for $\langle M_+ \rangle$ and why we did not calculate the difference in the classical analysis.

The operator of M_+ for one magnetic moment observed is

$$\hat{M}_+ = \mathcal{N}\gamma\hat{I}_+ = \mathcal{N}\gamma(\hat{I}_x + i\hat{I}_y). \quad (7.61)$$

Due to the orthogonality of basis matrices, the left-hand side of Eq. 7.47 reduces to

$$\frac{dd_+}{dt} \hat{I}_+ e^{i\omega_0 t} \quad (7.62)$$

when calculating relaxation rate of $\Delta\langle M_+ \rangle \equiv \langle M_+ \rangle$. In the right-hand side, we need to calculate three double commutators:

$$[\hat{I}_z, [\hat{I}_z, \hat{I}_+]] = \hbar^2 \hat{I}_+ \quad [\hat{I}_+, [\hat{I}_-, \hat{I}_+]] = 2\hbar^2 \hat{I}_+ \quad [\hat{I}_-, [\hat{I}_+, \hat{I}_+]] = 0. \quad (7.63)$$

After substituting into Eq. 7.47,

$$\frac{dd_+}{dt} \text{Tr}\{\hat{I}_- \hat{I}_+\} = - \left(b^2 \int_0^\infty \overline{c^z(0)c^z(t)} dt + \frac{3}{4} b^2 \int_0^\infty \overline{c^+(0)c^-(t)} e^{i\omega_0 t} dt \right) d_+ \text{Tr}\{\hat{I}_- \hat{I}_+\} \quad (7.64)$$

$$\frac{d\langle M_+ \rangle}{dt} = - \left(b^2 \int_0^\infty \overline{c^z(0)c^z(t)} dt + \frac{3}{4} b^2 \int_0^\infty \overline{c^+(0)c^-(t)} e^{i\omega_0 t} dt \right) \langle M_+ \rangle \quad (7.65)$$

The relaxation rate R_2 for M_+ , known as *transverse relaxation rate* in the literature, is the real part of the expression in the parentheses.

$$R_2 = b^2 \int_0^\infty \overline{c^z(0)c^z(t)} dt + \Re \left\{ \frac{3}{4} b^2 \int_0^\infty \overline{c^+(0)c^-(t)} e^{i\omega_0 t} dt \right\}. \quad (7.66)$$

Note that the first integral in 7.66 is a real number, equal to R_0 derived by the classical analysis. Using the same arguments as for M_z ,

$$R_2 = b^2 \left(\frac{1}{2} J(0) + \frac{3}{8} J(\omega_0) \right) \approx R_0 + \frac{1}{2} R_1. \quad (7.67)$$

7.10.4 Spectrum and signal-to-noise ratio

In order to describe the one-dimensional NMR spectrum quantitatively, we need to know

1. how is the detected signal related to the magnetization. Here, we analyze a simple experimental setup with a detector coil perpendicular to the external field, and sufficiently far from the sample. In this case, the voltage induced in the coil is described by Eq. 55 (Section 0.1.5).
2. how is the noise defined. Here, we assume that the major source of the noise are the thermal motions of electrons in the detector circuit (we neglect e.g. thermal motions of charges in the sample). We use a fundamental result of statistical mechanics showing that the thermal energy is $k_B T$, where R is the resistance, k_B is the Boltzmann's constant and T is the temperature. As a consequence, the noise power is $k_B T \Delta f$ and the mean square of the voltage variance is $\langle U_{\text{noise}}^2 \rangle = 4Rk_B T \Delta f$, where R is the resistance and Δf is the frequency bandwidth of the detector (the range of frequencies actually detected).
3. how is the time-dependent signal converted to a frequency spectrum. Here, the answer is described in Chapter 2.6.3, the most important step is the Fourier transformation.

According Eq. 55, describing the voltage induced in the detector coil in our setup, the amplitude of the induced voltage is

$$|U_{\text{induced}}| = \frac{\mu_0}{4\pi} \frac{2n|\mu|S}{r^3} |\omega_0|, \quad (7.68)$$

where μ_0 is the magnetic permeability of vacuum, r is the coil from the measured sample,⁸ n and S are the number of turns and the cross-section area of the coil. The amplitude of the magnetic moment μ , rotating with the frequency ω_0 , is equal to the amplitude of the transverse magnetization of the sample, multiplied by the volume sensed by the detector coil. Eq. 7.27 derived in Section 7.8 tells us that the expected value of the magnetization rotating in the plane perpendicular to \vec{B}_0 is (in the laboratory coordinate frame)

$$\langle M_+ \rangle = \frac{\mathcal{N}\gamma^2 \hbar^2 B_0}{4k_B T} e^{-R_2 t} (\cos(\omega_0 t) + i \sin(\omega_0 t)) = \frac{\mathcal{N}\gamma^2 \hbar^2 B_0}{4k_B T} e^{-R_2 t} e^{i\omega_0 t}. \quad (7.69)$$

We start our analysis ignoring the relaxation factor $e^{-R_2 t}$. In such a case,

⁸We assume that this distance is large, which is not true in NMR spectrometers, but later we include the distance in a general parameter defining the geometry.

$$|U_{\text{induced}}| = \frac{\mu_0}{4\pi} \frac{2nS}{r^3} \frac{N\gamma^2 \hbar^2 B_0}{4k_B T} |\omega_0| = \frac{\mu_0}{4\pi} \frac{2nS}{r^3} \frac{N\gamma^2 \hbar^2 B_0}{4k_B T} |\gamma| B_0 = \frac{\mu_0}{4\pi} \left(\frac{\hbar}{2}\right)^2 \frac{2nS}{r^3} \frac{N|\gamma|^3 B_0^2}{k_B T}, \quad (7.70)$$

where N is the number of magnetic moments in the volume sensed by the receiver coil.

As described in Section 3.1.1, the coil (serving both as transmitter and receiver coil) is a part of an LC circuit, acting as a resonator. If the capacitor C_T , wired in parallel with the coil, is tuned to the resonance frequency $\omega_0^2 = LC_T$, than it accumulates the energy given by $\frac{1}{2}LI^2$, where I is the current induced in the coil. On the other hand, the circuit has also some resistance R , and therefore it dissipates a part of the energy as the Joule heat. Balance of the energy accumulation and dissipation is described by the *quality factor* Q , defined as

$$Q = |\omega_0| \frac{\text{energy stored}}{\text{power loss}} = |\omega_0| \frac{\frac{1}{2}LI^2}{\frac{1}{2}RI^2} = |\omega_0|L/R. \quad (7.71)$$

The amplitude of the voltage actually measured across the coil terminals is

$$|U_{\text{measured}}| = Q|U_{\text{induced}}| = \frac{\mu_0}{4\pi} \left(\frac{\hbar}{2}\right)^2 \frac{2nQS}{r^3} \frac{N|\gamma|^3 B_0^2}{k_B T}. \quad (7.72)$$

Now, we move from the signal amplitude to the frequency spectrum and reintroduce relaxation. We derived in Section 3.2.2 (cf. Eq. 3.5) that the height of a peak obtained by Fourier transformation of a signal with an amplitude \mathcal{A} depends on the relaxation rate R_2 and on the acquisition time t_{max} as

$$Y_{\text{max}} = \mathcal{A} \frac{1 - e^{-R_2 t_{\text{max}}}}{R_2} = \frac{\mu_0}{4\pi} \left(\frac{\hbar}{2}\right)^2 \frac{2nQS}{r^3} \frac{N|\gamma|^3 B_0^2}{k_B T} \frac{1 - e^{-R_2 t_{\text{max}}}}{R_2}. \quad (7.73)$$

From the practical point of view, it is not important how large is the detected signal (the measured voltage can be amplified or attenuated if needed). The sensitivity of the measurement is given by the signal-to-noise ratio. Therefore, we also need to calculate the noise in the spectrum. As mentioned above,

$$\langle U_{\text{noise}}^2 \rangle = 4Rk_B T \Delta f = 4Rk_B T \frac{\Delta\omega}{2\pi} \quad (7.74)$$

As the noise voltage fluctuates stochastically, we can describe its correlation function in a similar manner as we described it for the magnetic moment fluctuations in Sections 2.6.1 and 2.6.3, i.e. as $\langle U_{\text{noise}}(0) U_{\text{noise}}(t) \rangle$, and calculate also the corresponding spectral density function:

$$J_U(\omega) = \int_{-\infty}^{\infty} \langle U_{\text{noise}}(0) U_{\text{noise}}(t) \rangle e^{-i\omega t} dt. \quad (7.75)$$

The inverse Fourier transformation allows us to calculate

$$\langle U_{\text{noise}}(0) U_{\text{noise}}(t) \rangle = \frac{1}{2\pi} \int_{-\infty}^{\infty} J_U(\omega) e^{i\omega t} d\omega \quad (7.76)$$

and by setting $t = 0$

$$\langle U_{\text{noise}}^2 \rangle = \langle U_{\text{noise}}(0) U_{\text{noise}}(0) \rangle = \frac{1}{2\pi} \int_{-\infty}^{\infty} J_U(\omega) d\omega. \quad (7.77)$$

When applying a band-pass filter⁹ selecting only frequencies in the range from ω_{low} to $\omega_{\text{high}} = \omega_{\text{low}} + \Delta\omega$,

$$\langle U_{\text{noise}}^2 \rangle = \langle U_{\text{noise}}(0) U_{\text{noise}}(0) \rangle = \frac{1}{2\pi} \int_{-\infty}^{\infty} J_U(\omega) d\omega = \frac{1}{2\pi} \int_{\omega_{\text{low}}}^{\omega_{\text{low}} + \Delta\omega} J_U(\omega) d\omega \quad (7.78)$$

because $J_U(\omega) = 0$ outside the limits ω_{low} and $\omega_{\text{high}} = \omega_{\text{low}} + \Delta\omega$. Comparison with Eq. 7.79, where $4Rk_B T$ is frequency independent, shows that:

$$\langle U_{\text{noise}}^2 \rangle = \frac{1}{2\pi} 4Rk_B T \Delta\omega = \frac{1}{2\pi} 4Rk_B T \int_{\omega_{\text{low}}}^{\omega_{\text{low}} + \Delta\omega} d\omega = \frac{1}{2\pi} \int_{\omega_{\text{low}}}^{\omega_{\text{low}} + \Delta\omega} 4Rk_B T d\omega = \frac{1}{2\pi} \int_{\omega_{\text{low}}}^{\omega_{\text{low}} + \Delta\omega} J_U(\omega) d\omega \quad (7.79)$$

⁹Limiting the detected range of frequencies is important. A completely random noise is present at all frequencies. Without the band-pass filter, this infinite range of frequencies (representing theoretically an infinite noise power) would be aliased (Section 3.2.4) into the spectral width given by the time increment of the digital signal.

and therefore $J_U(\omega) = 4Rk_B T$. This finding helps us to evaluate how noise enters the signal-to-noise ratio of the frequency spectrum. The Fourier transform

$$Y_{\text{noise}} = \int_0^{t_{\text{max}}} U_{\text{noise}}(t) e^{-i\omega t} dt \quad (7.80)$$

is a random quantity that cannot be evaluated easily. However, its mean square can be related to $J_U(\omega)$ if t_{max} is sufficiently long ($t_{\text{max}} \gg 1/\Delta\omega$):

$$\begin{aligned} \langle Y_{\text{noise}}^2 \rangle &= \int_0^{t_{\text{max}}} dt \int_0^{t_{\text{max}}} \langle U_{\text{noise}}(t) U_{\text{noise}}(t-t') \rangle e^{-i\omega(t-t')} dt' \approx \frac{1}{2} \int_0^{t_{\text{max}}} dt \int_{-\infty}^{\infty} \langle U_{\text{noise}}(t) U_{\text{noise}}(t-t') \rangle e^{-i\omega(t-t')} dt' \\ &= \frac{1}{2} J_U(\omega) \int_0^{t_{\text{max}}} dt = 2Rk_B T \int_0^{t_{\text{max}}} dt = 2Rk_B T t_{\text{max}}. \end{aligned} \quad (7.81)$$

We can use Eq. 7.71 to convert R to $|\omega_0|L/Q$. Since the inductance of a solenoid is $L = \mu_0 n^2 S/l$, where l is the length of the solenoid,

$$R = \frac{|\omega_0| S n^2}{Ql} = \frac{|\gamma| B_0 S n^2}{Ql} \quad (7.82)$$

and

$$\langle Y_{\text{noise}}^2 \rangle = \frac{2|\gamma| B_0 k_B T S n^2 t_{\text{max}}}{Ql}. \quad (7.83)$$

We can now combine Eqs. 7.73 and 7.83, and calculate the signal-to-noise ratio as

$$\text{Signal/noise} = \frac{Y_{\text{max}}}{\sqrt{\langle Y_{\text{noise}}^2 \rangle}} = \frac{\frac{\mu_0}{4\pi} \left(\frac{\hbar}{2}\right)^2 \frac{2nQS}{r^3} \frac{N|\gamma|^3 B_0^2}{k_B T} \frac{1 - e^{-R_2 t_{\text{max}}}}{R_2}}{\frac{2|\gamma| B_0 k_B T S n^2 t_{\text{max}}}{Ql}} = \frac{\mu_0}{4\pi} \left(\frac{\hbar}{2}\right)^2 \underbrace{\frac{\sqrt{2Q^3 V_{\text{coil}}}}{r^3}}_K \frac{N|\gamma|^{5/2} B_0^{3/2}}{k_B^{3/2} T^{3/2}} \frac{1 - e^{-R_2(T) t_{\text{max}}}}{R_2(T) t_{\text{max}}^{1/2}}, \quad (7.84)$$

where $V_{\text{coil}} = Sl$ is the coil volume. The signal-to-noise ratio in the spectrum also depends on other tricks applied during signal processing. When deriving Eq. 7.27, we already assumed that the phase correction was applied. Another factor determining the sensitivity of the spectrum in practice is apodization, but we ignore it now for the sake of simplicity. The actual sensitivity is also proportional to square root of the ratio of the time of signal acquisition to the overall time of the experiment.¹⁰

Eq. 7.84 contains many factors. The blue geometry and construction factors do not deserve much attention as they depend on the actual instrumental setup, and can be replaced by a general parameter K . The green factors are most interesting. They show why NMR spectroscopists like to work with high concentrations (resulting in high N), with high- γ nuclei, and at high-field spectrometers. The total acquisition time (purple) and temperature (red) and are set for each experiment. We usually prefer to acquire the signal for $t_{\text{max}} \gg R_2$ in order to avoid truncation artifacts discussed in Section 3.2.2. However, noise also accumulates in time, it grows proportional to $\sqrt{t_{\text{max}}}$. Therefore, an optimum t_{max} should be set (depending on R_2) and/or well chosen apodization should be applied (Section 3.5). For example, if our t_{max} is substantially longer than R_2 and we decide to prolong it further, we accumulate only noise without acquiring any additional signal. The temperature is also a factor that can be controlled easily. At the first glance, lower temperatures seem to be beneficial. However, the dependence of signal-to-noise ratio on the relaxation rate R_2 introduces also additional dependence on the temperature and, in the case of the relaxation caused by the chemical shift anisotropy, on γB_0 . The relaxation seriously reduces sensitivity of detection of magnetic moment precession in large, rigid molecules. In such molecules, the major contribution to R_2 is the loss of coherence (we labeled its rate R_0 in Section 2.2). As shown in Section 2.2, in a large rigid spherical molecule,

$$\frac{1}{R_2} \approx \frac{6D^{\text{rot}}}{b^2} = \frac{3k_B T}{4\pi r^3 \eta(T) b^2}. \quad (7.85)$$

When inserted to Eq. 7.84, $1/R_2$ may seem to change the temperature dependence to $1/T^{1/2}$. However, the temperature dependence of the water viscosity in Eq. 7.85 influences $1/R_2$ more than the linear temperature dependence of the numerator. Therefore, the temperature dependence of sensitivity on the temperature has a maximum (interestingly close to room temperature for medium-size proteins in aqueous solutions).

The factor $1/b^2$ in Eq. 7.85 is equal to $1/(\gamma B_0 \delta_a)^2$ for the for chemical shift anisotropy. It suggests that the signal-to-noise ratio should *decrease* with increasing B_0 . However, relaxation in most chemical groups of molecules is dominated by other mechanisms than the chemical shift anisotropy, in particular by the dipole-dipole interactions with magnetic moments of nearby protons. As the dipole-dipole

¹⁰In many experiments (but not necessarily in the one-dimensional experiment), recycle delay (waiting for the sample to return close to the equilibrium before the next measurement) is much longer than the actual signal acquisition.

interactions do not depend on B_0 , a high field usually *increases* the signal-to-noise ratio. Nevertheless, Eq. 7.85 warns us that using a high magnetic field does not always improve the sensitivity. For example, the relaxation due to the chemical shift anisotropy reduces sensitivity at high fields in the case of ^{13}C nuclei in sp^2 hybridization without attached protons (e.g. in carbonyl groups).

It should be stressed that when deriving Eq. 12.4.6, we made many simplifications. We neglected the effect of the preamplifier, resistance of the sample, and assumed that the receiver coil and sample have the same temperature. In the most sensitive NMR probes, the motions of the electrons are suppressed by cooling the receiver coil to a very low temperature, approximately 20 K. Therefore, we have to include the sample and coil temperature separately. If the effect of preamplifier is included, we get a bit more complex relation

$$\text{Signal/noise} = \frac{Y_{\max}}{\sqrt{\langle Y_{\text{noise}}^2 \rangle}} = \frac{\mu_0}{4\pi} \left(\frac{\hbar}{2}\right)^2 K \frac{N\gamma^{5/2} B_0^{3/2}}{k_B^{3/2} T_{\text{sample}} \sqrt{(T_{\text{coil}} + T_{\text{sample}} R'/R + (1 + R'/R) T')}} \frac{1 - e^{-R_2(T) t_{\max}}}{R_2(T) t_{\max}^{1/2}}, \quad (7.86)$$

where R is the resistance of the coil, R' is the resistance induced by the sample in the coil (proportional to the conductivity and therefore to the ionic strength of the sample), and T' is so called noise temperature of the amplifier.¹¹

The numerical values given by Eqs. 7.84 and 7.86 are of little practical use. However, it is useful to notice how sensitivity depends on individual factors (temperature, field, magnetogyric ratio of the observed nucleus).

¹¹The input noise is amplified by the factor $(1 + T'/T)G$, where G is the gain of the preamplifier.

Lecture 8

Dipolar coupling, product operators

Literature: The product operator formalism for multi-spin systems is described in B17.4, B18, C2.5.1, C2.7, L15. The dipole-dipole Hamiltonian is discussed in L9.3. Relaxation is described in K9, L19–L20, C5 in different manners. All texts are excellent. It is very helpful to read them all if you really want to get an insight. However, relaxation is a difficult topic and absorbing the information requires a lot of time.

8.1 Dipolar coupling

So far, we analyzed effects of various fields on nuclear magnetic moments, but we assumed that individual magnetic moments are independent and their properties can be described by operators composed of two-dimensional matrices. In this lecture, we take into account also mutual interactions – interactions with fields generated by magnetic moments of other nuclei.

As usually, we start by the classical description of the interaction. If spin magnetic moments of two spin-1/2 nuclei interact with each other, the magnetic moment of nucleus 1 is influenced by the magnetic field \vec{B}_2 of the magnetic moment of nucleus 2. Analysis presented in Section 8.9.1 shows that the magnetic field of nucleus 2 contributes to the magnetic field at the position of nucleus 1 as

$$\begin{pmatrix} B_{2,x} \\ B_{2,y} \\ B_{2,z} \end{pmatrix} = \frac{\mu_0}{4\pi r^5} \begin{pmatrix} 3r_x^2 - r^2 & 3r_x r_y & 3r_x r_z \\ 3r_x r_y & 3r_y^2 - r^2 & 3r_y r_z \\ 3r_x r_z & 3r_y r_z & 3r_z^2 - r^2 \end{pmatrix} \cdot \begin{pmatrix} \mu_{2,x} \\ \mu_{2,y} \\ \mu_{2,z} \end{pmatrix}, \quad (8.1)$$

where r_j are components of a vector describing mutual positions of the nuclei in space. A graphical representation of the effect of \vec{B}_2 on nucleus 1 and of its dependence on the orientation of the nuclei (given by the orientation of the molecule) is presented in Figure 8.1. The matrix in Eq. 8.1 can be viewed as a representation of the tensor of dipolar interactions. In contrast to the chemical shift tensor, the tensor of dipolar interactions does not have any isotropic or rhombic component.

Having the classical description of the interaction of two magnetic dipolar moments, derivation of the quantum mechanical Hamiltonian is easy, as shown in Section 8.9.1. The result of Eq. 8.1 is inserted into the general relation $\mathcal{E} = -\vec{\mu}_1 \cdot \vec{B}_2$, the magnetic moments are expressed by the angular momenta ($\vec{\mu}_1 = \gamma_1 \vec{I}_1$, $\vec{\mu}_2 = \gamma_2 \vec{I}_2$), and the energy and angular momentum components are replaced by the corresponding operators. The result is

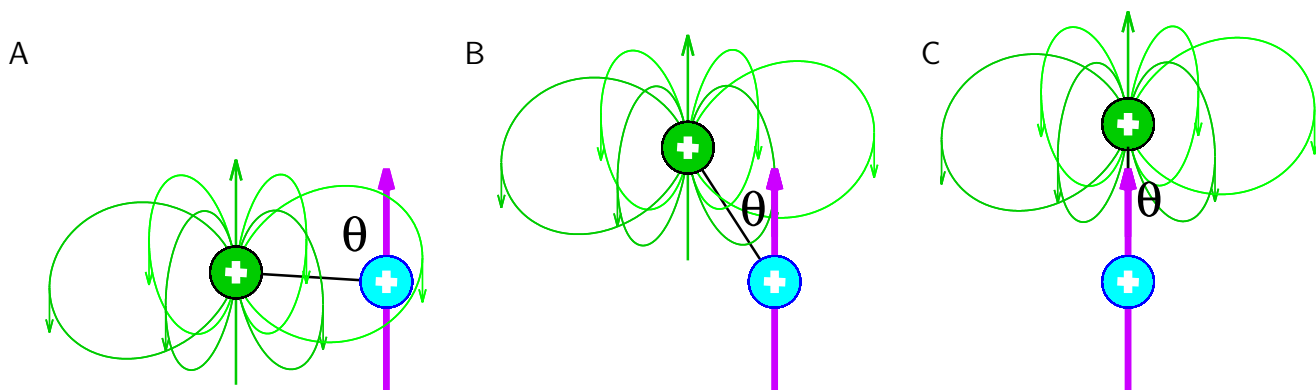


Figure 8.1: A, Classical description of interaction of a spin magnetic moment of the observed nucleus (shown in cyan) with the a spin magnetic moment of another nucleus (shown in green). The thick purple arrow represents \vec{B}_0 , the thin green induction lines represent the magnetic field \vec{B}_2 of the green nucleus (the small green arrows indicate its direction). The black line represents the internuclear vector \vec{r} . As the molecule rotates, the cyan nucleus moves from a position where the field of the spin magnetic moment of the green nucleus \vec{B}_2 has the opposite direction than \vec{B}_0 (A), through a position where \vec{B}_2 is perpendicular to \vec{B}_0 (B), to a position where \vec{B}_2 has the same direction as \vec{B}_0 (C).

$$\hat{H}_D = -\frac{\mu_0\gamma_1\gamma_2}{4\pi r^5} (\hat{I}_{1,x} \hat{I}_{1,y} \hat{I}_{1,z}) \begin{pmatrix} 3r_x^2 - r^2 & 3r_x r_y & 3r_x r_z \\ 3r_x r_y & 3r_y^2 - r^2 & 3r_y r_z \\ 3r_x r_z & 3r_y r_z & 3r_z^2 - r^2 \end{pmatrix} \begin{pmatrix} \hat{I}_{2,x} \\ \hat{I}_{2,y} \\ \hat{I}_{2,z} \end{pmatrix}. \quad (8.2)$$

After defining the Hamiltonian of the dipole-dipole interaction, we can ask how is the total Hamiltonian representing energy of the magnetic moment pairs influenced by the dipolar coupling. In the absence of radio waves,¹ the energy of the magnetic moment pairs depends on \vec{B}_0 , on chemical shifts δ_1 and δ_2 of the coupled nuclei, and on the dipolar coupling. The corresponding Hamiltonian consists of the isotropic component \hat{H}_0 , and of an anisotropic part including axial and rhombic components of the chemical shift Hamiltonian and of the Hamiltonian representing the dipolar coupling, \hat{H}_D . The complete Hamiltonian \hat{H}_D described by Eq. 8.2 is rather complex. However, it can be often greatly simplified, as discussed in Section 8.9.2. The *secular approximation* depends on whether the precession frequencies of the interacting magnetic moments are identical or different. In the former case, \hat{H}_D simplifies to

$$\hat{H}_D = -\frac{\mu_0\gamma_1\gamma_2}{4\pi r^3} \frac{3\langle \cos^2 \vartheta \rangle - 1}{2} \left(2\hat{I}_{1,z}\hat{I}_{2,z} - \hat{I}_{1,x}\hat{I}_{2,x} - \hat{I}_{1,y}\hat{I}_{2,y} \right), \quad (8.3)$$

in the latter case, to

$$\hat{H}_D = -\frac{\mu_0\gamma_1\gamma_2}{4\pi r^3} \frac{3\langle \cos^2 \vartheta \rangle - 1}{2} \left(2\hat{I}_{1,z}\hat{I}_{2,z} \right). \quad (8.4)$$

¹We assume that the field of irradiating radio waves is much stronger than the dipolar interactions of nuclear magnetic moments. Therefore, we neglect the effect of dipolar coupling during the short radio wave pulses.

As derived in Section 8.9.1, \hat{H}_D depends on the orientation of the molecule like the anisotropic component of the chemical shift. It implies that whole \hat{H}_D averages to zero in isotropic liquids (Section 8.9.2).

The Hamiltonian representing energy of an ensemble of pairs of directly interacting spin dipolar magnetic moments in \vec{B}_0 reduces in isotropic liquids to

$$\hat{H} = -\gamma_1 B_0(1 + \delta_{i,1})\hat{I}_{1z} - \gamma_2 B_0(1 + \delta_{i,2})\hat{I}_{2z}. \quad (8.5)$$

The simplified Eq. 8.5 is valid only in isotropic liquids and does not describe relaxation processes. The effect of \hat{H}_D is huge in solid state NMR and can be also be measured e.g. in liquid crystals or mechanically stretched gels. Last but not least, dipole-dipole interactions result in strong relaxation effects, discussed in Section 8.7

8.2 Quantum states of magnetic moment pairs

In order to apply the Hamiltonian defined by Eq. 8.2 to a wave function representing the quantum states of an interacting magnetic moment pair, we have to find

We know how to construct the Hamiltonian of the dipole-dipole interactions from the operators $\hat{I}_{1,x}, \hat{I}_{1,y}, \hat{I}_{1,z}, \hat{I}_{2,x}, \hat{I}_{2,y}, \hat{I}_{2,z}$, but we still did not describe the explicit forms of these operators or of the wave function the Hamiltonian acts on. To fill this gap in our knowledge, we look for a vector representing the wave function representing coupled magnetic moments. Although we are concerned with direct dipole-dipole interactions in this Lecture, we try to formulate our conclusions so that they apply to various couplings of nuclear magnetic moments in general.

We first describe a quantum state of a pair of *non-interacting* spin-1/2 nuclei. The wave function Ψ of such a pair of particles can be decomposed into the spin-part and a part dependent on the other degrees of freedom (spatial coordinates of the nuclei). The spin part can be further separated into a product of wave functions dependent on the spin degrees of freedom of the individual nuclei:

$$\Psi = \psi_{\text{non-spin}}(x_1, y_1, z_1, x_2, y_2, z_2) \cdot \psi_{\text{spin}}(c_{\alpha,1}, c_{\alpha,2}) = \psi_{\text{non-spin}} \cdot \psi_{1,\text{spin}} \cdot \psi_{2,\text{spin}}. \quad (8.6)$$

Writing explicitly first $\psi_{1,\text{spin}}$

$$\Psi = \psi_{\text{non-spin}} \cdot \begin{pmatrix} c_{\alpha,1} \\ c_{\beta,1} \end{pmatrix} \cdot \psi_{2,\text{spin}} = \psi_{\text{non-spin}} \cdot \begin{pmatrix} c_{\alpha,1}\psi_{2,\text{spin}} \\ c_{\beta,1}\psi_{2,\text{spin}} \end{pmatrix} \quad (8.7)$$

and then $\psi_{2,\text{spin}}$

$$\Psi = \psi_{\text{non-spin}} \cdot \begin{pmatrix} c_{\alpha,1} \begin{pmatrix} c_{\alpha,2} \\ c_{\beta,2} \end{pmatrix} \\ c_{\beta,1} \begin{pmatrix} c_{\alpha,2} \\ c_{\beta,2} \end{pmatrix} \end{pmatrix} = \psi_{\text{non-spin}} \cdot \begin{pmatrix} c_{\alpha,1}c_{\alpha,2} \\ c_{\alpha,1}c_{\beta,2} \\ c_{\beta,1}c_{\alpha,2} \\ c_{\beta,1}c_{\beta,2} \end{pmatrix} \equiv \psi_{\text{non-spin}} \cdot \begin{pmatrix} c_{\alpha\alpha} \\ c_{\alpha\beta} \\ c_{\beta\alpha} \\ c_{\beta\beta} \end{pmatrix}, \quad (8.8)$$

we obtain a four-component wave function built as a *direct product*² (or *Kronecker product*) of two-component wave functions (state vectors) of single spin magnetic moments:

²Direct product $\hat{A} \otimes \hat{B}$ is a mathematical operation when each element of the matrix \hat{A} is multiplied by the whole

$$\begin{pmatrix} c_{\alpha,1} \\ c_{\beta,1} \end{pmatrix} \otimes \begin{pmatrix} c_{\alpha,2} \\ c_{\beta,2} \end{pmatrix} = \begin{pmatrix} c_{\alpha,1} \begin{pmatrix} c_{\alpha,2} \\ c_{\beta,2} \end{pmatrix} \\ c_{\beta,1} \begin{pmatrix} c_{\alpha,2} \\ c_{\beta,2} \end{pmatrix} \end{pmatrix} = \begin{pmatrix} c_{\alpha,1}c_{\alpha,2} \\ c_{\alpha,1}c_{\beta,2} \\ c_{\beta,1}c_{\alpha,2} \\ c_{\beta,1}c_{\beta,2} \end{pmatrix} \equiv \begin{pmatrix} c_{\alpha\alpha} \\ c_{\alpha\beta} \\ c_{\beta\alpha} \\ c_{\beta\beta} \end{pmatrix}, \quad (8.9)$$

In the eigenequation, $\psi_{\text{non-spin}}$ is canceled out (see Section 5.4). The introduced four-component function is written in a basis of vectors that are simultaneous eigenfunctions of the angular momentum operators $\hat{I}_1^2, \hat{I}_2^2, \hat{I}_{1z}, \hat{I}_{2z}$. If the magnetic moments are independent, $\hat{I}_1^2 = \hat{I}_2^2$, $\hat{I}_{1z} = \hat{I}_{2z}$, and the pair can be described in a two-component basis of the eigenfunctions of $\hat{I}_z = \hat{I}_{1z} = \hat{I}_{2z}$ (and of $\hat{I}^2 = \hat{I}_1^2 = \hat{I}_2^2$), as described in Section 6.1.

If the magnetic moments of the pair interact, they cannot be described in the two-component basis of independent spin magnetic moments. State of the first spin depends on the state of the second spin. Therefore, the probability density matrix describing a *large ensemble* of pairs that interact mutually, but are isolated from other pairs, must be four-dimensional, built from coefficients of the wave function in Eq. 8.8. In other words, we can use the mixed-state approach, but we must describe the pair of the interacting magnetic moments and its four states as one entity. Furthermore, the Hamiltonian of dipolar interactions (Eq. 8.2) is built from operators representing *products* of individual components of the interacting magnetic moments. Let us now look for a basis that fulfils these requirements.

8.3 Product operators

The wave function (state vector) describing a single interacting pair of magnetic moments is four-dimensional. Therefore, the density matrix that describes an ensemble of such interacting pairs, and consists of averaged combinations of the elements of the four-dimensional state vector, is a 4×4 matrix

$$\hat{\rho} = \begin{pmatrix} \overline{c_{\alpha\alpha}c_{\alpha\alpha}^*} & \overline{c_{\alpha\alpha}c_{\alpha\beta}^*} & \overline{c_{\alpha\alpha}c_{\beta\alpha}^*} & \overline{c_{\alpha\alpha}c_{\beta\beta}^*} \\ \overline{c_{\alpha\beta}c_{\alpha\alpha}^*} & \overline{c_{\alpha\beta}c_{\alpha\beta}^*} & \overline{c_{\alpha\beta}c_{\beta\alpha}^*} & \overline{c_{\alpha\beta}c_{\beta\beta}^*} \\ \overline{c_{\beta\alpha}c_{\alpha\alpha}^*} & \overline{c_{\beta\alpha}c_{\alpha\beta}^*} & \overline{c_{\beta\alpha}c_{\beta\alpha}^*} & \overline{c_{\beta\alpha}c_{\beta\beta}^*} \\ \overline{c_{\beta\beta}c_{\alpha\alpha}^*} & \overline{c_{\beta\beta}c_{\alpha\beta}^*} & \overline{c_{\beta\beta}c_{\beta\alpha}^*} & \overline{c_{\beta\beta}c_{\beta\beta}^*} \end{pmatrix}. \quad (8.10)$$

Basis used for such density matrices and for operators acting on the four-dimensional wave function must consist of $4^2 = 16$ matrices.³ The four-dimensional wave function (state vector) describing

matrix \hat{B} :

$$\hat{A} \otimes \hat{B} = \begin{pmatrix} A_{11} & A_{12} \\ A_{21} & A_{22} \end{pmatrix} \otimes \begin{pmatrix} B_{11} & B_{12} \\ B_{21} & B_{22} \end{pmatrix} = \begin{pmatrix} A_{11} \begin{pmatrix} B_{11} & B_{12} \\ B_{21} & B_{22} \end{pmatrix} & A_{12} \begin{pmatrix} B_{11} & B_{12} \\ B_{21} & B_{22} \end{pmatrix} \\ A_{21} \begin{pmatrix} B_{11} & B_{12} \\ B_{21} & B_{22} \end{pmatrix} & A_{22} \begin{pmatrix} B_{11} & B_{12} \\ B_{21} & B_{22} \end{pmatrix} \end{pmatrix} = \begin{pmatrix} A_{11}B_{11} & A_{11}B_{12} & A_{12}B_{11} & A_{12}B_{12} \\ A_{11}B_{21} & A_{11}B_{22} & A_{12}B_{21} & A_{12}B_{22} \\ A_{21}B_{11} & A_{21}B_{12} & A_{22}B_{11} & A_{22}B_{12} \\ A_{21}B_{21} & A_{21}B_{22} & A_{22}B_{21} & A_{22}B_{22} \end{pmatrix}$$

³In general, the density matrix for n states is a $n \times n$ matrix. Basis used for such density matrices must consist of 4^n matrices.

the interacting pair of magnetic moments was constructed as a direct product of two-dimensional single-spin state vectors. Not surprisingly,⁴ the basis of the 4×4 matrices can be built from direct products of 2×2 basis matrices used for spins without mutual interactions. For example, Cartesian single-spin operators can be used to create a basis for two spins (see Table 8.1) using the following direct products:

$$2 \cdot \mathcal{I}_t^{(1)} \otimes \mathcal{I}_t^{(2)} = \mathcal{I}_t^{(12)} \quad (8.11)$$

$$2 \cdot \mathcal{I}_x^{(1)} \otimes \mathcal{I}_t^{(2)} = \mathcal{I}_{1x}^{(12)} \quad (8.12)$$

$$2 \cdot \mathcal{I}_y^{(1)} \otimes \mathcal{I}_t^{(2)} = \mathcal{I}_{1y}^{(12)} \quad (8.13)$$

$$2 \cdot \mathcal{I}_z^{(1)} \otimes \mathcal{I}_t^{(2)} = \mathcal{I}_{1z}^{(12)} \quad (8.14)$$

$$2 \cdot \mathcal{I}_t^{(1)} \otimes \mathcal{I}_x^{(2)} = \mathcal{I}_{2x}^{(12)} \quad (8.15)$$

$$2 \cdot \mathcal{I}_t^{(1)} \otimes \mathcal{I}_y^{(2)} = \mathcal{I}_{2y}^{(12)} \quad (8.16)$$

$$2 \cdot \mathcal{I}_t^{(1)} \otimes \mathcal{I}_z^{(2)} = \mathcal{I}_{2z}^{(12)} \quad (8.17)$$

$$2 \cdot \mathcal{I}_x^{(1)} \otimes \mathcal{I}_x^{(2)} = 2 \cdot \mathcal{I}_{1x} \mathcal{I}_{2x}^{(12)} \quad (8.18)$$

$$2 \cdot \mathcal{I}_x^{(1)} \otimes \mathcal{I}_y^{(2)} = 2 \cdot \mathcal{I}_{1x} \mathcal{I}_{2y}^{(12)} \quad (8.19)$$

$$2 \cdot \mathcal{I}_x^{(1)} \otimes \mathcal{I}_z^{(2)} = 2 \cdot \mathcal{I}_{1x} \mathcal{I}_{2z}^{(12)} \quad (8.20)$$

$$2 \cdot \mathcal{I}_y^{(1)} \otimes \mathcal{I}_x^{(2)} = 2 \cdot \mathcal{I}_{1y} \mathcal{I}_{2x}^{(12)} \quad (8.21)$$

$$2 \cdot \mathcal{I}_y^{(1)} \otimes \mathcal{I}_y^{(2)} = 2 \cdot \mathcal{I}_{1y} \mathcal{I}_{2y}^{(12)} \quad (8.22)$$

$$2 \cdot \mathcal{I}_y^{(1)} \otimes \mathcal{I}_z^{(2)} = 2 \cdot \mathcal{I}_{1y} \mathcal{I}_{2z}^{(12)} \quad (8.23)$$

$$2 \cdot \mathcal{I}_z^{(1)} \otimes \mathcal{I}_x^{(2)} = 2 \cdot \mathcal{I}_{1z} \mathcal{I}_{2x}^{(12)} \quad (8.24)$$

$$2 \cdot \mathcal{I}_z^{(1)} \otimes \mathcal{I}_y^{(2)} = 2 \cdot \mathcal{I}_{1z} \mathcal{I}_{2y}^{(12)} \quad (8.25)$$

$$2 \cdot \mathcal{I}_z^{(1)} \otimes \mathcal{I}_z^{(2)} = 2 \cdot \mathcal{I}_{1z} \mathcal{I}_{2z}^{(12)}, \quad (8.26)$$

where the numbers in parentheses specify which nuclei constitute the spin system described by the given matrix (these numbers are not written in practice). The matrices on the right-hand side are known as *product operators*. Note that \mathcal{I}_t , equal to⁵ $\frac{1}{2}\hat{1}$, is not written in the product operators for the sake of simplicity. Note also that e.g. $\mathcal{I}_x^{(1)}$ and $\mathcal{I}_x^{(2)}$ are the same 2×2 matrices, but $\mathcal{I}_{1x}^{(12)}$ and $\mathcal{I}_{2x}^{(12)}$ are different 4×4 matrices. Basis matrices for more nuclei are derived in the same manner, e.g. $2 \cdot \mathcal{I}_{1z} \mathcal{I}_{2x}^{(12)} \otimes \mathcal{I}_y^{(3)} = 4 \cdot \mathcal{I}_{1z} \mathcal{I}_{2x} \mathcal{I}_{3y}^{(123)}$.

The basis presented in Table 8.1 represents one of many possible choices. Another possible basis is shown in Table 8.2. Eqs. 6.5 and 6.6 can be used to convert product operators of the basis sets in Tables 8.1 and 8.2.

⁴The relation between the construction of the state vectors and of operators acting on them is described by the group theory. It follows from the analysis of rotation of the state vectors and operators acting on them that the coupling between the state vectors and between the operators is the same.

⁵ $\hat{1}$ is the unit matrix.

8.4 Density matrix of a two-spin system

The introduced formal description of the density matrix would be useless if we did not understand its physical significance. Interpretation of the 4×4 density matrix requires more care than the interpretation of its two-dimensional version. In general, the density matrix ρ is a linear combination of 16 basis matrices \mathcal{I}_j (the actual forms of \mathcal{I}_j depend on the chosen basis):

$$\hat{\rho} = \sum_{j=1}^{16} C_j \mathcal{I}_j \quad (8.27)$$

Each basis matrix \mathcal{I}_j describes one feature of the mixed state (e.g., longitudinal polarization of the first magnetic moment) and the coefficients C_j specifies how much the given feature contributed to the mixed state. Below, we interpret the individual matrices of a commonly used Cartesian basis. Although we discuss direct dipole-dipole interaction in this Lecture, the interpretation of the Cartesian matrices is general and applicable to other interactions between the magnetic moments. The description of the matrices is also summarized in Tables 8.3 and 8.4.

We have listed two basis sets in Tables 8.1 and 8.2. Both of them contain four diagonal matrices. Like in the two-dimensional case, the diagonal elements of $\hat{\rho}$ and diagonal matrices describe *longitudinal polarization* of the magnetic moments. The sum of the diagonal elements is equal to one, like in the two-dimensional density matrix. Therefore, we have three independent *populations*. Two of them, corresponding to contributions of matrices labeled \mathcal{I}_{1z} and \mathcal{I}_{2z} , describe *separately* longitudinal magnetic moment polarization of nuclei 1 and 2, respectively. Contribution of the third diagonal matrix, $2\mathcal{I}_{1z}\mathcal{I}_{2z}$, describes *correlation* between $\mu_{1,z}$ and $\mu_{2,z}$, how much the longitudinal polarization of $\vec{\mu}_1$ is influenced by the longitudinal polarization of $\vec{\mu}_2$, and vice versa.

Twelve off-diagonal elements or matrices composed of them are called *coherences*. Only six off-diagonal elements are independent because each element below the diagonal has its complex conjugate above the diagonal. Note, however, that coherences are complex quantities. The six independent off-diagonal elements thus represent twelve real numbers. Therefore, none of twelve purely real or purely imaginary matrices in Table 8.4 is redundant. Coherences corresponding to contributions of matrices \mathcal{I}_{1x} and \mathcal{I}_{2x} , respectively, describe *transverse polarization in the direction x* of magnetic moments of nuclei 1 and 2, regardless of the state of the other nucleus. Contributions of \mathcal{I}_{1y} and \mathcal{I}_{2y} describe transverse polarization in the direction *y* in the same manner. A contribution of $2\mathcal{I}_{1x}\mathcal{I}_{2z}$ describes how the transverse polarization of $\vec{\mu}_1$ in the *x* direction depends on the longitudinal polarization of $\vec{\mu}_2$. Dependence of the transverse polarization of $\vec{\mu}_2$ in the *x* direction on the longitudinal polarization of $\vec{\mu}_1$ is given by the contribution $2\mathcal{I}_{1z}\mathcal{I}_{2x}$. The same applies to $2\mathcal{I}_{1y}\mathcal{I}_{2z}$, $2\mathcal{I}_{1z}\mathcal{I}_{2y}$ and to direction *y*. Finally, contributions of $2\mathcal{I}_{1x}\mathcal{I}_{2x}$, $2\mathcal{I}_{1y}\mathcal{I}_{2y}$, $2\mathcal{I}_{1x}\mathcal{I}_{2y}$, and $2\mathcal{I}_{1y}\mathcal{I}_{2x}$ describe mutual correlation of transverse polarizations of $\vec{\mu}_1$ and $\vec{\mu}_2$.

8.5 Evolution of coupled spin states

The Liouville - von Neumann equation can be written for coupled magnetic moments in the same form as for spins without mutual interactions (Eq. 6.9):

Table 8.3: Contributions to the two-spin density matrix describing uniform distribution and longitudinal polarizations of spin magnetic moments $\vec{\mu}_1$ and $\vec{\mu}_2$. In the graphical representation, the left and right distribution corresponds to of superimposed $\vec{\mu}_1$ and $\vec{\mu}_2$, respectively. The uniform distribution is shown in black. In order to visualize correlation of the longitudinal polarization, the following color-coding is used. In the case of longitudinal polarization of $\vec{\mu}_1$, magnetic moments of nucleus 1 in 10% molecules with most polarized $\vec{\mu}_1$ are shown in cyan, and magnetic moments of nucleus 2 *in the same molecules* are shown in green. In the case of longitudinal polarization of $\vec{\mu}_2$, magnetic moments of nucleus 2 in 10% molecules with most polarized $\vec{\mu}_1$ are shown in green, and magnetic moments of nucleus 1 *in the same molecules* are shown in cyan. The chosen distributions of orientation symbolize the trend of polarization represented by the given matrix, the depicted degree of polarization is lower than the degree corresponding to the actual matrices: basis matrices describe either no polarization (uniform distribution of orientations) or complete polarization (identical orientations).

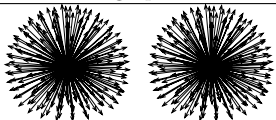
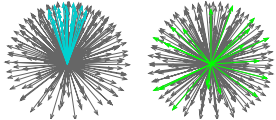
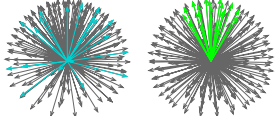
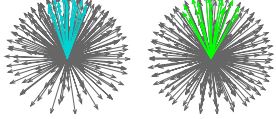
Matrix	graph	description
$\mathcal{I}_t = \frac{1}{2} \begin{pmatrix} +1 & 0 & 0 & 0 \\ 0 & +1 & 0 & 0 \\ 0 & 0 & +1 & 0 \\ 0 & 0 & 0 & +1 \end{pmatrix}$		no polarization of $\vec{\mu}_1$ or $\vec{\mu}_2$
$\mathcal{I}_{1z} = \frac{1}{2} \begin{pmatrix} +1 & 0 & 0 & 0 \\ 0 & +1 & 0 & 0 \\ 0 & 0 & -1 & 0 \\ 0 & 0 & 0 & -1 \end{pmatrix}$		longitudinal polarization of $\vec{\mu}_1$ regardless of $\vec{\mu}_2$
$\mathcal{I}_{2z} = \frac{1}{2} \begin{pmatrix} +1 & 0 & 0 & 0 \\ 0 & -1 & 0 & 0 \\ 0 & 0 & +1 & 0 \\ 0 & 0 & 0 & -1 \end{pmatrix}$		longitudinal polarization of $\vec{\mu}_2$ regardless of $\vec{\mu}_1$
$2\mathcal{I}_{1z}\mathcal{I}_{2z} = \frac{1}{2} \begin{pmatrix} +1 & 0 & 0 & 0 \\ 0 & -1 & 0 & 0 \\ 0 & 0 & -1 & 0 \\ 0 & 0 & 0 & +1 \end{pmatrix}$		correlation of longitudinal polarizations of $\vec{\mu}_1$ and $\vec{\mu}_2$

Table 8.4: Contributions to the two-spin density matrix describing coherences (see Table 8.3 for color coding).

Matrix	graph	description
$\mathcal{I}_{1x} = \frac{1}{2} \begin{pmatrix} 0 & 0 & +1 & 0 \\ 0 & 0 & 0 & +1 \\ +1 & 0 & 0 & 0 \\ 0 & +1 & 0 & 0 \end{pmatrix}$		transverse polarization of $\vec{\mu}_1$ in direction x , regardless of $\vec{\mu}_2$
$2\mathcal{I}_{1x}\mathcal{I}_{2z} = \frac{1}{2} \begin{pmatrix} 0 & 0 & +1 & 0 \\ 0 & 0 & 0 & -1 \\ +1 & 0 & 0 & 0 \\ 0 & -1 & 0 & 0 \end{pmatrix}$		correlation between transverse polarization of $\vec{\mu}_1$ in direction x and longitudinal polarization of $\vec{\mu}_2$
$\mathcal{I}_{1y} = \frac{i}{2} \begin{pmatrix} 0 & 0 & -1 & 0 \\ 0 & 0 & 0 & -1 \\ +1 & 0 & 0 & 0 \\ 0 & +1 & 0 & 0 \end{pmatrix}$		transverse polarization of $\vec{\mu}_1$ in direction y , regardless of $\vec{\mu}_2$
$2\mathcal{I}_{1y}\mathcal{I}_{2z} = \frac{i}{2} \begin{pmatrix} 0 & 0 & -1 & 0 \\ 0 & 0 & 0 & +1 \\ +1 & 0 & 0 & 0 \\ 0 & -1 & 0 & 0 \end{pmatrix}$		correlation between transverse polarization of $\vec{\mu}_1$ in direction y and longitudinal polarization of $\vec{\mu}_2$
$\mathcal{I}_{2x} = \frac{1}{2} \begin{pmatrix} 0 & +1 & 0 & 0 \\ +1 & 0 & 0 & 0 \\ 0 & 0 & 0 & +1 \\ 0 & 0 & +1 & 0 \end{pmatrix}$		transverse polarization of $\vec{\mu}_2$ in direction x , regardless of $\vec{\mu}_1$
$2\mathcal{I}_{1z}\mathcal{I}_{2x} = \frac{1}{2} \begin{pmatrix} 0 & +1 & 0 & 0 \\ +1 & 0 & 0 & 0 \\ 0 & 0 & 0 & -1 \\ 0 & 0 & -1 & 0 \end{pmatrix}$		correlation between transverse polarization of $\vec{\mu}_2$ in direction x and longitudinal polarization of $\vec{\mu}_1$
$\mathcal{I}_{2y} = \frac{i}{2} \begin{pmatrix} 0 & -1 & 0 & 0 \\ +1 & 0 & 0 & 0 \\ 0 & 0 & 0 & -1 \\ 0 & 0 & +1 & 0 \end{pmatrix}$		transverse polarization of $\vec{\mu}_2$ in direction y , regardless of $\vec{\mu}_1$
$2\mathcal{I}_{1z}\mathcal{I}_{2y} = \frac{i}{2} \begin{pmatrix} 0 & -1 & 0 & 0 \\ +1 & 0 & 0 & 0 \\ 0 & 0 & 0 & +1 \\ 0 & 0 & -1 & 0 \end{pmatrix}$		correlation between transverse polarization of $\vec{\mu}_2$ in direction y and longitudinal polarization of $\vec{\mu}_1$
$2\mathcal{I}_{1x}\mathcal{I}_{2x} = \frac{1}{2} \begin{pmatrix} 0 & 0 & 0 & +1 \\ 0 & 0 & +1 & 0 \\ 0 & +1 & 0 & 0 \\ +1 & 0 & 0 & 0 \end{pmatrix}$		correlation between transverse polarization of $\vec{\mu}_1$ and $\vec{\mu}_2$ in direction x
$2\mathcal{I}_{1y}\mathcal{I}_{2y} = \frac{1}{2} \begin{pmatrix} 0 & 0 & 0 & -1 \\ 0 & 0 & +1 & 0 \\ 0 & +1 & 0 & 0 \\ -1 & 0 & 0 & 0 \end{pmatrix}$		correlation between transverse polarization of $\vec{\mu}_1$ and $\vec{\mu}_2$ in direction y
$2\mathcal{I}_{1x}\mathcal{I}_{2y} = \frac{i}{2} \begin{pmatrix} 0 & 0 & 0 & -1 \\ 0 & 0 & +1 & 0 \\ 0 & -1 & 0 & 0 \\ +1 & 0 & 0 & 0 \end{pmatrix}$		correlation between transverse polarization of $\vec{\mu}_1$ in direction x and transverse polarization of $\vec{\mu}_2$ in direction y
$2\mathcal{I}_{1y}\mathcal{I}_{2x} = \frac{i}{2} \begin{pmatrix} 0 & 0 & 0 & -1 \\ 0 & 0 & -1 & 0 \\ 0 & +1 & 0 & 0 \\ +1 & 0 & 0 & 0 \end{pmatrix}$		correlation between transverse polarization of $\vec{\mu}_1$ in direction y and transverse polarization of $\vec{\mu}_2$ in direction x

$$\frac{d\hat{\rho}}{dt} = i(\hat{\rho}\mathcal{H} - \mathcal{H}\hat{\rho}) = i[\hat{\rho}, \mathcal{H}] = -i[\mathcal{H}, \hat{\rho}], \quad (8.28)$$

but the density matrix and Hamiltonian are now⁶ 4×4 matrices. Also Eqs. 6.10 and 6.11 can be generalized to product operators. The same simple geometric solution of the Liouville - von Neumann equation is possible if the Hamiltonian does not vary in time and consists of commuting matrices only. However, the operator space is now 16-dimensional. Therefore, the appropriate three-dimensional subspace must be selected for each rotation. The subspaces are defined by the commutation relations derived in Section 8.9.4. The relations (applicable to any set of n^2 operators of spin systems consisting of n spin-1/2 nuclei) are described by the following equations:

$$[\mathcal{I}_{nx}, \mathcal{I}_{ny}] = i\mathcal{I}_{nz} \quad [\mathcal{I}_{ny}, \mathcal{I}_{nz}] = i\mathcal{I}_{nx} \quad [\mathcal{I}_{nz}, \mathcal{I}_{nx}] = i\mathcal{I}_{ny} \quad (8.29)$$

$$[\mathcal{I}_{nj}, 2\mathcal{I}_{nk}\mathcal{I}_{n'l}] = 2[\mathcal{I}_{nj}, \mathcal{I}_{nk}]\mathcal{I}_{n'l} \quad (8.30)$$

$$[2\mathcal{I}_{nj}\mathcal{I}_{n'l}, 2\mathcal{I}_{nk}\mathcal{I}_{n'm}] = [\mathcal{I}_{nj}, \mathcal{I}_{nk}]\delta_{lm} + [\mathcal{I}_{n'l}, \mathcal{I}_{n'm}]\delta_{jk}, \quad (8.31)$$

where n and n' specify the nucleus, $j, k, l \in \{x, y, z\}$, and $\delta_{jk} = 1$ for $l = m$ and $\delta_{jk} = 0$ for $j \neq k$. Since the dipolar interactions do not have coherent effects in isotropic liquids, we postpone discussion of the rotations in the product operator space to Section 10.3, where we discuss interactions that are not averaged to zero in isotropic samples.

8.6 Operator of the observed quantity for more nuclei

In order to describe the observed signal for a system of n different nuclei, Eq. 7.1, defining the operator of complex magnetization, must be slightly modified

$$\hat{M}_+ = \sum_n \mathcal{N}\gamma_n(\hat{I}_{nx} + i\hat{I}_{ny}) = \sum_n \mathcal{N}\gamma_n\hat{I}_{n+}, \quad (8.32)$$

where the index n distinguishes different types of nuclei. In the case of magnetic moment pairs discussed in this Lecture, $n = 2$.

8.7 Dipolar relaxation

As mentioned above, dipole-dipole interactions do not have coherent effects (do not influence the measured values of precession frequencies) in isotropic liquids. On the other hand, the dipole-dipole interactions represent a very important source of relaxation.

Rotation of the molecule (and internal motions) change the orientation of the inter-nuclear vector and cause fluctuations of the field of the magnetic moment $\vec{\mu}_2$ sensed by the magnetic moment $\vec{\mu}_1$. It leads to the loss of coherence in the same manner as described for the anisotropic part of the chemical

⁶In general, Eq. 6.9 is valid for $n \times n$ matrices describing ensembles of n mutually interacting nuclei.

shift (cf. Eqs 1.42 and 8.57). However, the relaxation effects of the dipole-dipole interactions are more complex, reflecting the higher complexity of the Hamiltonian of the dipolar coupling. A detailed analysis is presented in Section 8.9.5, here we review only the main conclusions.

The following equations describe relaxation due to the dipole-dipole interactions in a pair of nuclei separated by a constant distance r :

$$\begin{aligned}\frac{d\Delta\langle M_{1z}\rangle}{dt} &= -\frac{1}{8}b^2(2J(\omega_{0,1} - \omega_{0,2}) + 6J(\omega_{0,1}) + 12J(\omega_{0,1} + \omega_{0,2}))\Delta\langle M_{1z}\rangle \\ &\quad + \frac{1}{8}b^2(2J(\omega_{0,1} - \omega_{0,2}) - 12J(\omega_{0,1} + \omega_{0,2}))\Delta\langle M_{2z}\rangle \\ &= -R_{a1}\Delta\langle M_{1z}\rangle - R_x\Delta\langle M_{2z}\rangle,\end{aligned}\tag{8.33}$$

$$\begin{aligned}\frac{d\Delta\langle M_{2z}\rangle}{dt} &= -\frac{1}{8}b^2(2J(\omega_{0,1} - \omega_{0,2}) + 6J(\omega_{0,2}) + 12J(\omega_{0,1} + \omega_{0,2}))\Delta\langle M_{2z}\rangle \\ &\quad + \frac{1}{8}b^2(2J(\omega_{0,1} - \omega_{0,2}) - 12J(\omega_{0,1} + \omega_{0,2}))\Delta\langle M_{1z}\rangle \\ &= -R_{a2}\Delta\langle M_{2z}\rangle - R_x\Delta\langle M_{1z}\rangle,\end{aligned}\tag{8.34}$$

$$\begin{aligned}\frac{d\langle M_{1+}\rangle}{dt} &= -\frac{1}{8}b^2(4J(0) + 6J(\omega_{0,2}) + J(\omega_{0,1} - \omega_{0,2}) + 3J(\omega_{0,1}) + 6J(\omega_{0,1} + \omega_{0,2}))\langle M_{1+}\rangle \\ &= -R_{2,1}\langle M_{1+}\rangle = -\left(R_{0,1} + \frac{1}{2}R_{a1}\right)\langle M_{1+}\rangle,\end{aligned}\tag{8.35}$$

where

$$b = -\frac{\mu_0\gamma_1\gamma_2\hbar}{4\pi r^3}.\tag{8.36}$$

The relaxation rate R_1 of the dipole-dipole relaxation is the rate of relaxation of the z -component of the total magnetization $\langle M_z \rangle = \langle M_{1z} \rangle + \langle M_{2z} \rangle$. R_1 is derived by solving the set of Eqs. 8.33 and 8.34. The solution is simple if $J(\omega_{0,1}) = J(\omega_{0,2}) = J(\omega_0) \Rightarrow R_{a1} = R_{a2} = R_a$ (this is correct e.g. if both nuclei have the same γ , if the molecule rotates as a sphere, and if internal motions are negligible or identical for both nuclei).⁷ Then,

$$\frac{d\Delta\langle M_z \rangle}{dt} = -\frac{1}{8}b^2(6J(\omega) + 24J(2\omega))\Delta\langle M_z \rangle = -\underbrace{(R_a + R_x)}_{R_1}\Delta\langle M_z \rangle.\tag{8.37}$$

There are several remarkable differences between relaxation due to the chemical shift anisotropy and dipole-dipole interactions:

- The rate constants describing the return to the equilibrium polarization is more complex than for the chemical shift anisotropy relaxation. In addition to the $3b^2J(\omega_{0,1})/4$ term, describing effect of stochastic molecular motions resonating with the precession frequency of $\vec{\mu}_1$, the

⁷The general solution gives $R_1 = \frac{1}{2}\left(R_{a1} + R_{a2} + \sqrt{(R_{a1} - R_{a2})^2 + 4R_x^2}\right)$.

auto-relaxation rate R_{a1} contains terms depending on the sum and difference of the precession frequency of $\vec{\mu}_1$ and $\vec{\mu}_2$. These terms account for temporary resonance of random molecular rotation with the mutual difference in the precession of $\vec{\mu}_1$ and $\vec{\mu}_2$. For example, if the molecule rotates for a short time about the vertical axis with an angular frequency ω_{mol} which is accidentally close to $\omega_{0,1} - \omega_{0,2}$, the horizontal component of \vec{B}_2 in the place of nucleus 1 rotates with frequency $\omega_{0,2} + \omega_{\text{mol}} \approx \omega_{0,2} + \omega_{0,1} - \omega_{0,2} = \omega_{0,1}$ and thus resonates with the precession of $\vec{\mu}_1$. Consequently, \vec{B}_2 temporally resembles a radio wave and contributes to redistribution of $\mu_{1,z}$ towards equilibrium. Quantum mechanically, such effects are described by the orientation-dependent coefficients preceding $2\hat{I}_{1x}\hat{I}_{2x}$, $2\hat{I}_{1y}\hat{I}_{2y}$, $2\hat{I}_{1x}\hat{I}_{2y}$, $2\hat{I}_{1y}\hat{I}_{2x}$ components in \hat{H}_D , contributing to $J(\omega_{0,1} \pm \omega_{0,2})$.

- Return to the equilibrium polarization of nucleus 1 depends also on the actual polarization of nucleus 2. This effect, resembling chemical kinetics of a reversible reaction, is known as *cross-relaxation*, or *nuclear Overhauser effect* (NOE), and described by the *cross-relaxation constant* R_x . The value of R_x is proportional to r^{-6} and thus provides information about inter-atomic distances. NOE is a useful tool in analysis of small molecules and the most important source of structural information for large biological molecules.
- The relaxation constant R_0 , describing the loss of coherence, contains an additional term, depending on the frequency of the other nucleus, $3b^2J(\omega_{0,2})/4$. This term has the following physical significance. The field generated by the second magnetic moment depends on its state. For example, $\vec{\mu}_2$ in a pure $|\alpha\rangle$ state⁸ reduces the field and consequently precession frequency of nucleus 2 if the internuclear vector is horizontal (Figure 8.1A), whereas $\vec{\mu}_2$ in a pure $|\beta\rangle$ state has the opposite effect.⁹ Fluctuations of $\omega_{0,1}$ due to the changes of the state of $\vec{\mu}_2$ (described by $J(\omega_{0,2})$) contribute to the loss of coherence.¹⁰

In real samples, contributions to relaxation due to the chemical shift anisotropy and due to dipole-dipole interactions (often with several spin magnetic moments close in space) are combined. The constants R_1 and R_2 (and other) are therefore sums of the relaxation rate constants described here and in Section 7.7. At moderate \vec{B}_0 fields (up to 15–20 T, depending on the molecule), relaxation is usually dominated by dipole-dipole interactions with protons.

8.8 Thermal equilibrium with dipolar coupling

As shown in Section 8.9.6, if we neglect the chemical shifts ($\delta_{i,1} \ll 1$, $\delta_{i,2} \ll 1$), the density matrix describing two different nuclei coupled only through dipolar interactions is

⁸Note that we mentioned the $|\alpha\rangle$ and $|\beta\rangle$ eigenstates as an example, $\vec{\mu}_2$ can be in reality in many superposition states.

⁹The interaction is described here for nuclei with positive γ_1 and γ_2 , e.g. protons.

¹⁰Such changes have a similar effect as the *chemical or conformational exchange*, modifying the size of the chemical shift tensor (the chemical/conformational exchange was briefly discussed in Section 2.4). Therefore, $3b^2J(\omega_{0,2})/4$ adds to R_0 like the exchange contribution.

$$\hat{\rho}^{\text{eq}} = \begin{pmatrix} \frac{1}{4} + \frac{\gamma_1 B_0 \hbar}{8k_B T} + \frac{\gamma_2 B_0 \hbar}{8k_B T} & 0 & 0 & 0 \\ 0 & \frac{1}{4} + \frac{\gamma_1 B_0 \hbar}{8k_B T} - \frac{\gamma_2 B_0 \hbar}{8k_B T} & 0 & 0 \\ 0 & 0 & \frac{1}{4} - \frac{\gamma_1 B_0 \hbar}{8k_B T} + \frac{\gamma_2 B_0 \hbar}{8k_B T} & 0 \\ 0 & 0 & 0 & \frac{1}{4} - \frac{\gamma_1 B_0 \hbar}{8k_B T} - \frac{\gamma_2 B_0 \hbar}{8k_B T} \end{pmatrix} \quad (8.38)$$

$$= \frac{1}{4} \begin{pmatrix} 1 & 0 & 0 & 0 \\ 0 & 1 & 0 & 0 \\ 0 & 0 & 1 & 0 \\ 0 & 0 & 0 & 1 \end{pmatrix} + \frac{\gamma_1 B_0 \hbar}{8k_B T} \begin{pmatrix} +1 & 0 & 0 & 0 \\ 0 & +1 & 0 & 0 \\ 0 & 0 & -1 & 0 \\ 0 & 0 & 0 & -1 \end{pmatrix} + \frac{\gamma_2 B_0 \hbar}{8k_B T} \begin{pmatrix} +1 & 0 & 0 & 0 \\ 0 & -1 & 0 & 0 \\ 0 & 0 & +1 & 0 \\ 0 & 0 & 0 & -1 \end{pmatrix} \quad (8.39)$$

$$= \frac{1}{2} (\mathcal{I}_t + \kappa_1 \mathcal{I}_{1,z} + \kappa_2 \mathcal{I}_{2,z}), \quad (8.40)$$

where

$$\kappa_j = \frac{\gamma_j B_0 \hbar}{2k_B T}. \quad (8.41)$$

HOMEWORK

To prepare for the next lecture, analyze evolution of the density matrix described in Section 9.2.

8.9 DERIVATIONS

8.9.1 Tensor and Hamiltonian of dipolar coupling

As shown in Section 0.2.2, magnetic induction can be expressed as a curl (rotation) of the vector potential ($\vec{B} = \vec{\nabla} \times \vec{A}$). Therefore, the magnetic induction of the field of nucleus \vec{B}_2 is given by the classical electrodynamics as

$$\vec{B}_2 = \vec{\nabla} \times \vec{A}_2, \quad (8.42)$$

where

$$\vec{\nabla} \equiv \left(\frac{\partial}{\partial x}, \frac{\partial}{\partial y}, \frac{\partial}{\partial z} \right). \quad (8.43)$$

Let us assume (classically) that the source of the magnetic moment of nucleus 2 is a current loop. It can be derived from Maxwell equations¹¹ that the vector potential A_2 in a distance much larger than radius of the loop is

$$\vec{A}_2 = \frac{\mu_0}{4\pi} \frac{\vec{\mu}_2 \times \vec{r}}{r^3}, \quad (8.44)$$

where \vec{r} is a vector defining the mutual position of nuclei 1 and 2 (inter-nuclear vector). The individual components of \vec{A} are

$$A_{2,x} = \frac{\mu_0}{4\pi} \left(\mu_{2,y} \frac{r_z}{r^3} - \mu_{2,z} \frac{r_y}{r^3} \right), \quad (8.45)$$

$$A_{2,y} = \frac{\mu_0}{4\pi} \left(\mu_{2,z} \frac{r_x}{r^3} - \mu_{2,x} \frac{r_z}{r^3} \right), \quad (8.46)$$

$$A_{2,z} = \frac{\mu_0}{4\pi} \left(\mu_{2,x} \frac{r_y}{r^3} - \mu_{2,y} \frac{r_x}{r^3} \right). \quad (8.47)$$

Calculation of \vec{B}_2 thus includes two vector products

$$\vec{B}_2 = \frac{\mu_0}{4\pi} \vec{\nabla} \times \frac{\vec{\mu}_2 \times \vec{r}}{r^3}. \quad (8.48)$$

As a consequence, each component of \vec{B}_2 depends on all components of $\vec{\mu}_2$:

$$B_{2,x} = \frac{\mu_0}{4\pi} \left(\frac{\partial A_{2,z}}{\partial r_y} - \frac{\partial A_{2,y}}{\partial r_z} \right) = \frac{\mu_0}{4\pi} \left(\mu_{2,x} \left(\frac{\partial}{\partial r_y} \frac{r_z}{r^3} + \frac{\partial}{\partial r_z} \frac{r_y}{r^3} \right) - \mu_{2,y} \frac{\partial}{\partial r_y} \frac{r_x}{r^3} - \mu_{2,z} \frac{\partial}{\partial r_z} \frac{r_x}{r^3} \right), \quad (8.49)$$

$$B_{2,y} = \frac{\mu_0}{4\pi} \left(\frac{\partial A_{2,x}}{\partial r_z} - \frac{\partial A_{2,z}}{\partial r_x} \right) = \frac{\mu_0}{4\pi} \left(\mu_{2,y} \left(\frac{\partial}{\partial r_z} \frac{r_x}{r^3} + \frac{\partial}{\partial r_x} \frac{r_z}{r^3} \right) - \mu_{2,z} \frac{\partial}{\partial r_z} \frac{r_y}{r^3} - \mu_{2,x} \frac{\partial}{\partial r_x} \frac{r_y}{r^3} \right), \quad (8.50)$$

$$B_{2,z} = \frac{\mu_0}{4\pi} \left(\frac{\partial A_{2,y}}{\partial r_x} - \frac{\partial A_{2,x}}{\partial r_y} \right) = \frac{\mu_0}{4\pi} \left(\mu_{2,z} \left(\frac{\partial}{\partial r_x} \frac{r_y}{r^3} + \frac{\partial}{\partial r_y} \frac{r_x}{r^3} \right) - \mu_{2,x} \frac{\partial}{\partial r_x} \frac{r_z}{r^3} - \mu_{2,y} \frac{\partial}{\partial r_y} \frac{r_z}{r^3} \right). \quad (8.51)$$

To proceed, we have to evaluate the partial derivatives $\frac{\partial}{\partial r_j} \frac{r_j}{r^3}$ and $\frac{\partial}{\partial r_j} \frac{r_k}{r^3}$:

$$\frac{\partial}{\partial r_j} \frac{r_j}{r^3} = \frac{\partial}{\partial r_j} \frac{r_j}{\left(\sqrt{r_x^2 + r_y^2 + r_z^2} \right)^3} = \frac{\partial}{\partial r_j} \frac{r_j}{(r_x^2 + r_y^2 + r_z^2)^{3/2}} = \frac{1 \cdot r^3 - r_j \cdot \frac{3}{2} r \cdot 2r_j}{r^6} = \frac{1}{r^3} - \frac{3r_j^2}{r^5}, \quad (8.52)$$

$$\frac{\partial}{\partial r_j} \frac{r_k}{r^3} = \frac{\partial}{\partial r_j} \frac{r_k}{\left(\sqrt{r_x^2 + r_y^2 + r_z^2} \right)^3} = \frac{\partial}{\partial r_j} \frac{r_k}{(r_x^2 + r_y^2 + r_z^2)^{3/2}} = \frac{0 \cdot r^3 - r_k \cdot \frac{3}{2} r \cdot 2r_j}{r^6} = -\frac{3r_j r_k}{r^5} \quad (8.53)$$

After inserting the partial derivatives from Eqs. 8.52 and 8.53 to Eqs. 8.49–8.51,

$$B_{2,x} = \frac{\mu_0}{4\pi r^5} ((3r_x^2 - r^2)\mu_{2,x} + 3r_x r_y \mu_{2,y} + 3r_x r_z \mu_{2,z}) \quad (8.54)$$

$$B_{2,y} = \frac{\mu_0}{4\pi r^5} (3r_x r_y \mu_{2,x} + (3r_y^2 - r^2)\mu_{2,y} + 3r_y r_z \mu_{2,z}) \quad (8.55)$$

$$B_{2,z} = \frac{\mu_0}{4\pi r^5} (3r_x r_z \mu_{2,x} + 3r_y r_z \mu_{2,y} + (3r_z^2 - r^2)\mu_{2,z}), \quad (8.56)$$

¹¹The derivation is presented in The Feynman Lectures on Physics, Vol. 2, Chapter 14 (the general description is presented in Section 14.2. and the current loop is discussed in Section 14.5), using an analogy with the description of the electric dipole in Section 14.3. of Vol. 2.

which can be described by a matrix equation

$$\begin{pmatrix} B_{2,x} \\ B_{2,y} \\ B_{2,z} \end{pmatrix} = \frac{\mu_0}{4\pi r^5} \begin{pmatrix} 3r_x^2 - r^2 & 3r_x r_y & 3r_x r_z \\ 3r_x r_y & 3r_y^2 - r^2 & 3r_y r_z \\ 3r_x r_z & 3r_y r_z & 3r_z^2 - r^2 \end{pmatrix} \cdot \begin{pmatrix} \mu_{2,x} \\ \mu_{2,y} \\ \mu_{2,z} \end{pmatrix}. \quad (8.57)$$

The matrix in Eq. 8.57 represents a tensor describing the geometric relations of the dipolar coupling and has the same form as the matrix in Eq. 1.42, describing the anisotropic contribution to the chemical shift tensor: the vector defining the symmetry axis of the chemical shift tensor \vec{a} is just replaced with the inter-nuclear vector \vec{r} in Eq. 8.57. Like the anisotropic part of the chemical shift tensor, the matrix in Eq. 8.57 simplifies to

$$\frac{\mu_0}{4\pi r^3} \begin{pmatrix} -1 & 0 & 0 \\ 0 & -1 & 0 \\ 0 & 0 & 2 \end{pmatrix} \quad (8.58)$$

in a coordinate system with axis $z \parallel \vec{r}$. Rotation to the laboratory frame is described by angles φ and ϑ defining orientation of \vec{r} in the laboratory frame

$$\begin{pmatrix} -1 & 0 & 0 \\ 0 & -1 & 0 \\ 0 & 0 & 2 \end{pmatrix} \rightarrow \frac{1}{r^2} \begin{pmatrix} 3r_x^2 - r^2 & 3r_x r_y & 3r_x r_z \\ 3r_x r_y & 3r_y^2 - r^2 & 3r_y r_z \\ 3r_x r_z & 3r_y r_z & 3r_z^2 - r^2 \end{pmatrix}, \quad (8.59)$$

where $r_x = r \sin \vartheta \cos \varphi$, $r_y = r \sin \vartheta \sin \varphi$, and $r_z = r \cos \vartheta$.

As usually, Hamiltonian of the dipolar coupling can be obtained using the classical description of the energy. Classical electrodynamics tells us that the energy of the interaction of the magnetic moment of nucleus 1 with the field generated by the magnetic moment of nucleus 2, described by Eq. 8.57 is

$$\begin{aligned} \mathcal{E} = -\vec{\mu}_1 \cdot \vec{B}_2 = & -\frac{\mu_0}{4\pi r^3} \left((3r_x^2 - r^2)\mu_{1x}\mu_{2x} + (3r_y^2 - r^2)\mu_{1y}\mu_{2y} + (3r_z^2 - r^2)\mu_{1z}\mu_{2z} + \right. \\ & + 3r_x r_y \mu_{1x}\mu_{2y} + 3r_x r_z \mu_{1x}\mu_{2z} + 3r_y r_z \mu_{1y}\mu_{2z} \\ & \left. + 3r_y r_x \mu_{1y}\mu_{2x} + 3r_z r_x \mu_{1z}\mu_{2x} + 3r_z r_y \mu_{1z}\mu_{2y} \right). \end{aligned} \quad (8.60)$$

Describing the magnetic moments by the operators $\hat{\mu}_{1,j}\gamma_1\hat{I}_{1,j}$ and $\hat{\mu}_{2,j}\gamma_2\hat{I}_{2,j}$, where j is x , y , and z , the Hamiltonian of dipolar coupling \hat{H}_D can be written as

$$\begin{aligned} \hat{H}_D = & -\frac{\mu_0}{4\pi r^3} \left((3r_x^2 - r^2)\hat{I}_{1x}\hat{I}_{2x} + (3r_y^2 - r^2)\hat{I}_{1y}\hat{I}_{2y} + (3r_z^2 - r^2)\hat{I}_{1z}\hat{I}_{2z} + \right. \\ & + 3r_x r_y \hat{I}_{1x}\hat{I}_{2y} + 3r_x r_z \hat{I}_{1x}\hat{I}_{2z} + 3r_y r_z \hat{I}_{1y}\hat{I}_{2z} \\ & \left. + 3r_y r_x \hat{I}_{1y}\hat{I}_{2x} + 3r_z r_x \hat{I}_{1z}\hat{I}_{2x} + 3r_z r_y \hat{I}_{1z}\hat{I}_{2y} \right) \\ = & -\frac{\mu_0\gamma_1\gamma_2}{4\pi r^5} (\hat{I}_{1,x} \hat{I}_{1,y} \hat{I}_{1,z}) \begin{pmatrix} 3r_x^2 - r^2 & 3r_x r_y & 3r_x r_z \\ 3r_x r_y & 3r_y^2 - r^2 & 3r_y r_z \\ 3r_x r_z & 3r_y r_z & 3r_z^2 - r^2 \end{pmatrix} \begin{pmatrix} \hat{I}_{2,x} \\ \hat{I}_{2,y} \\ \hat{I}_{2,z} \end{pmatrix} = \hat{I}_1 \cdot \underline{D} \cdot \hat{I}_2, \end{aligned} \quad (8.61)$$

where \underline{D} is the tensor of direct dipole-dipole interactions (dipolar coupling).

The Hamiltonian can be written in spherical coordinates as

$$\begin{aligned} \hat{H}_D = & -\frac{\mu_0\gamma_1\gamma_2}{4\pi r^3} \left((3\sin^2\vartheta \cos^2\varphi - 1)\hat{I}_{1x}\hat{I}_{2x} + (3\sin^2\vartheta \sin^2\varphi - 1)\hat{I}_{1y}\hat{I}_{2y} + (3\cos^2\vartheta - 1)\hat{I}_{1z}\hat{I}_{2z} + \right. \\ & + 3\sin^2\vartheta \sin\varphi \cos\varphi \hat{I}_{1x}\hat{I}_{2y} + 3\sin\vartheta \cos\vartheta \cos\varphi \hat{I}_{1x}\hat{I}_{2z} + 3\sin\vartheta \cos\vartheta \sin\varphi \hat{I}_{1y}\hat{I}_{2z} \\ & \left. + 3\sin^2\vartheta \sin\varphi \cos\varphi \hat{I}_{1y}\hat{I}_{2x} + 3\sin\vartheta \cos\vartheta \cos\varphi \hat{I}_{1z}\hat{I}_{2x} + 3\sin\vartheta \cos\vartheta \sin\varphi \hat{I}_{1z}\hat{I}_{2y} \right). \end{aligned} \quad (8.62)$$

8.9.2 Secular approximation and averaging of dipolar Hamiltonian

Like the chemical-shift Hamiltonian, the Hamiltonian of dipolar coupling can be simplified in many cases.

- Magnetic moments with the same γ and chemical shift precess about the z axis with *the same precession frequency*. In addition to the precession, the magnetic moments move with random molecular motions, described by re-orientation of \vec{r} . In a coordinate system rotating with the common precession frequency, \vec{r} quickly rotates about the z axis in addition to the random molecular motions. On a time scale slower than nanoseconds, the rapid oscillations of r_x , r_y , and r_z are neglected (secular approximation). The values of r_x^2 and r_y^2 do not oscillate about zero, but about a value $\langle r_x^2 \rangle = \langle r_y^2 \rangle$, which is equal to¹² $(r^2 - \langle r_z^2 \rangle)/2$ because $\langle r_x^2 + r_y^2 + r_z^2 \rangle = \langle r^2 \rangle = r^2$. Therefore, the secular approximation (i.e., neglecting the oscillations and keeping the average values) simplifies the Hamiltonian to

$$\hat{H}_D = -\frac{\mu_0\gamma_1\gamma_2}{4\pi r^5} (3\langle r_z^2 \rangle - r^2) \left(\hat{I}_{1,z}\hat{I}_{2,z} - \frac{1}{2}\hat{I}_{1,x}\hat{I}_{2,x} - \frac{1}{2}\hat{I}_{1,y}\hat{I}_{2,y} \right) \quad (8.63)$$

$$= -\frac{\mu_0\gamma_1\gamma_2}{4\pi r^3} \frac{3\langle \cos^2 \vartheta \rangle - 1}{2} \left(2\hat{I}_{1,z}\hat{I}_{2,z} - \hat{I}_{1,x}\hat{I}_{2,x} - \hat{I}_{1,y}\hat{I}_{2,y} \right). \quad (8.64)$$

- Magnetic moments with different γ and/or chemical shift precess with *different precession frequencies*. Therefore, the x and y components of $\vec{\mu}_2$ rapidly oscillate in a frame rotating with the precession frequency of $\vec{\mu}_1$ and vice versa. When neglecting the oscillating terms (secular approximation), the Hamiltonian reduces to

$$\hat{H}_D = -\frac{\mu_0\gamma_1\gamma_2}{4\pi r^5} (3\langle r_z^2 \rangle - r^2) \hat{I}_{1,z}\hat{I}_{2,z} = -\frac{\mu_0\gamma_1\gamma_2}{4\pi r^3} \frac{3\langle \cos^2 \vartheta \rangle - 1}{2} 2\hat{I}_{1,z}\hat{I}_{2,z}. \quad (8.65)$$

- Averaging over all molecules in isotropic liquids has the same effect as described for the anisotropic part of the chemical shielding tensor because both tensors have the same form. Terms with different coordinates average to zero because they contain products of sine and cosine functions of 2ϑ , φ and 2φ . As the angles ϑ and φ are independent, their functions average independently. And as 2ϑ and φ can have in isotropic liquids any value in the interval $(0, 2\pi)$ with equal probability, the averages of their sine and cosine functions are equal to zero

$$\overline{r_x r_y} = \overline{3 \sin^2 \vartheta \sin \varphi \cos \varphi} = \frac{3}{2} \overline{(1 - \cos(2\vartheta))} \cdot \frac{1}{2} \overline{\sin(2\varphi)} = \frac{3}{4} \overline{\sin(2\varphi)} - \frac{3}{4} \overline{\cos(2\vartheta)} \cdot \overline{\sin(2\varphi)} = 0 - 0 \cdot 0 = 0, \quad (8.66)$$

$$\overline{r_x r_z} = \overline{3 \sin \vartheta \cos \vartheta \cos \varphi} = \frac{3}{2} \overline{(\sin(2\vartheta))} \cdot \overline{\cos \varphi} = \frac{3}{4} \overline{\sin(2\vartheta)} \cdot \overline{\cos \varphi} = 0 \cdot 0 = 0, \quad (8.67)$$

$$\overline{r_y r_z} = \overline{3 \sin \vartheta \cos \vartheta \sin \varphi} = \frac{3}{2} \overline{(\sin(2\vartheta))} \cdot \overline{\sin \varphi} = \frac{3}{4} \overline{\sin(2\vartheta)} \cdot \overline{\sin \varphi} = 0 \cdot 0 = 0. \quad (8.68)$$

The terms with the same coordinates are identical because no direction is preferred:

$$\overline{r_x^2} = \overline{r_y^2} = \overline{r_z^2}. \quad (8.69)$$

Finally,

$$r_x^2 + r_y^2 + r_z^2 = r^2 \Rightarrow \overline{r_x^2 + r_y^2 + r_z^2} = \overline{3r_z^2} = r^2 \Rightarrow \overline{3r_z^2} - r^2 = 0. \quad (8.70)$$

8.9.3 Interacting and non-interacting magnetic moments

We have decomposed a wave function of a pair of magnetic moments to (Eq. 8.8)

$$\Psi = \psi_{\text{non-spin}} \cdot \begin{pmatrix} c_{\alpha,1} \begin{pmatrix} c_{\alpha,2} \\ c_{\beta,2} \end{pmatrix} \\ c_{\beta,1} \begin{pmatrix} c_{\alpha,2} \\ c_{\beta,2} \end{pmatrix} \end{pmatrix} = \psi_{\text{non-spin}} \cdot \begin{pmatrix} c_{\alpha,1}c_{\alpha,2} \\ c_{\alpha,1}c_{\beta,2} \\ c_{\beta,1}c_{\alpha,2} \\ c_{\beta,1}c_{\beta,2} \end{pmatrix} \equiv \psi_{\text{non-spin}} \cdot \begin{pmatrix} c_{\alpha\alpha} \\ c_{\alpha\beta} \\ c_{\beta\alpha} \\ c_{\beta\beta} \end{pmatrix}, \quad (8.71)$$

What tells us if we can describe the state of the individual magnetic moments in the two-dimensional basis $|\alpha\rangle, |\beta\rangle$? We inspect eigenfunctions and eigenvalues of the Hamiltonian including the influence of \vec{B}_0 , chemical shifts, and dipolar coupling, in the secular approximation:

$$\hat{H} = -\gamma_1 B_0 (1 + \delta_{i,1}) \hat{I}_{1z} - \gamma_2 B_0 (1 + \delta_{i,2}) \hat{I}_{2z} - \frac{\mu_0\gamma_1\gamma_2}{4\pi r^3} \frac{3\langle \cos^2 \vartheta \rangle - 1}{2} \left(2\hat{I}_{1,z}\hat{I}_{2,z} - \hat{I}_{1,x}\hat{I}_{2,x} - \hat{I}_{1,y}\hat{I}_{2,y} \right)$$

¹²Note that $\langle r_x^2 \rangle = \langle r_y^2 \rangle \neq \langle r_z^2 \rangle$ in general.

$$= \omega_{0,1}\hat{I}_{1z} + \omega_{0,2}\hat{I}_{2z} + D \left(2\hat{I}_{1,z}\hat{I}_{2,z} - \hat{I}_{1,x}\hat{I}_{2,x} - \hat{I}_{1,y}\hat{I}_{2,y} \right) \quad (8.72)$$

If the magnetic moments are too distant to interact mutually ($r \rightarrow \infty \Rightarrow D \rightarrow 0$), the Hamiltonian simplifies to a sum of two operators acting separately on each magnetic moment

$$\hat{H} = \omega_{0,1}\hat{I}_{1z} + \omega_{0,2}\hat{I}_{2z}. \quad (8.73)$$

As discussed in Section 6.7.2, action of such Hamiltonian can be described by two independent eigenequations

$$\omega_{0,1}\hat{I}_{1z}\psi^{(1)} = \mathcal{E}^{(1)}\psi^{(1)} \quad \omega_{0,2}\hat{I}_{2z}\psi^{(2)} = \mathcal{E}^{(2)}\psi^{(2)}. \quad (8.74)$$

The eigenfunctions can be found immediately:

$$\begin{aligned} \frac{\omega_{0,1}\hbar}{2} \begin{pmatrix} 1 & 0 & 0 & 0 \\ 0 & 1 & 0 & 0 \\ 0 & 0 & -1 & 0 \\ 0 & 0 & 0 & -1 \end{pmatrix} \cdot \begin{pmatrix} 1 \\ c_{\alpha,2} \\ c_{\beta,2} \\ 0 \end{pmatrix} &= \frac{\omega_{0,1}\hbar}{2} \begin{pmatrix} 1 \\ c_{\alpha,2} \\ c_{\beta,2} \\ 0 \end{pmatrix} & \frac{\omega_{0,2}\hbar}{2} \begin{pmatrix} 1 & 0 & 0 & 0 \\ 0 & -1 & 0 & 0 \\ 0 & 0 & 1 & 0 \\ 0 & 0 & 0 & -1 \end{pmatrix} \begin{pmatrix} c_{\alpha,1} \\ 1 \\ c_{\beta,1} \\ 0 \end{pmatrix} &= \frac{\omega_{0,2}\hbar}{2} \begin{pmatrix} c_{\alpha,1} \\ 1 \\ c_{\beta,1} \\ 0 \end{pmatrix} \\ \frac{\omega_{0,1}\hbar}{2} \begin{pmatrix} 1 & 0 & 0 & 0 \\ 0 & 1 & 0 & 0 \\ 0 & 0 & -1 & 0 \\ 0 & 0 & 0 & -1 \end{pmatrix} \cdot \begin{pmatrix} 0 \\ c_{\alpha,2} \\ c_{\beta,2} \\ 1 \end{pmatrix} &= -\frac{\omega_{0,1}\hbar}{2} \begin{pmatrix} 0 \\ c_{\alpha,2} \\ c_{\beta,2} \\ 1 \end{pmatrix} & \frac{\omega_{0,2}\hbar}{2} \begin{pmatrix} 1 & 0 & 0 & 0 \\ 0 & -1 & 0 & 0 \\ 0 & 0 & 1 & 0 \\ 0 & 0 & 0 & -1 \end{pmatrix} \begin{pmatrix} c_{\alpha,1} \\ 0 \\ c_{\beta,1} \\ 1 \end{pmatrix} &= -\frac{\omega_{0,2}\hbar}{2} \begin{pmatrix} c_{\alpha,1} \\ 0 \\ c_{\beta,1} \\ 1 \end{pmatrix}, \end{aligned} \quad (8.75)$$

or, using direct products,

$$\begin{aligned} \frac{\omega_{0,1}\hbar}{2} \begin{pmatrix} 1 & 0 \\ 0 & -1 \end{pmatrix} \otimes \begin{pmatrix} 1 & 0 \\ 0 & 1 \end{pmatrix} \cdot \begin{pmatrix} 1 \\ 0 \end{pmatrix} \otimes \begin{pmatrix} c_{\alpha,2} \\ c_{\beta,2} \end{pmatrix} &= \frac{\omega_{0,1}\hbar}{2} \begin{pmatrix} 1 \\ 0 \end{pmatrix} \otimes \begin{pmatrix} c_{\alpha,2} \\ c_{\beta,2} \end{pmatrix} & \frac{\omega_{0,1}\hbar}{2} \begin{pmatrix} 1 & 0 \\ 0 & 1 \end{pmatrix} \otimes \begin{pmatrix} 1 & 0 \\ 0 & -1 \end{pmatrix} \cdot \begin{pmatrix} c_{\alpha,1} \\ c_{\beta,1} \end{pmatrix} \otimes \begin{pmatrix} 1 \\ 0 \end{pmatrix} &= \frac{\omega_{0,2}\hbar}{2} \begin{pmatrix} c_{\alpha,1} \\ c_{\beta,1} \end{pmatrix} \otimes \begin{pmatrix} 1 \\ 0 \end{pmatrix} \\ \frac{\omega_{0,1}\hbar}{2} \begin{pmatrix} 1 & 0 \\ 0 & -1 \end{pmatrix} \otimes \begin{pmatrix} 1 & 0 \\ 0 & 1 \end{pmatrix} \cdot \begin{pmatrix} 0 \\ 1 \end{pmatrix} \otimes \begin{pmatrix} c_{\alpha,2} \\ c_{\beta,2} \end{pmatrix} &= -\frac{\omega_{0,1}\hbar}{2} \begin{pmatrix} 0 \\ 1 \end{pmatrix} \otimes \begin{pmatrix} c_{\alpha,2} \\ c_{\beta,2} \end{pmatrix} & \frac{\omega_{0,1}\hbar}{2} \begin{pmatrix} 1 & 0 \\ 0 & 1 \end{pmatrix} \otimes \begin{pmatrix} 1 & 0 \\ 0 & -1 \end{pmatrix} \cdot \begin{pmatrix} c_{\alpha,1} \\ c_{\beta,1} \end{pmatrix} \otimes \begin{pmatrix} 0 \\ 1 \end{pmatrix} &= -\frac{\omega_{0,2}\hbar}{2} \begin{pmatrix} c_{\alpha,1} \\ c_{\beta,1} \end{pmatrix} \otimes \begin{pmatrix} 0 \\ 1 \end{pmatrix}, \end{aligned} \quad (8.76)$$

$$\begin{aligned} \frac{\omega_{0,1}\hbar}{2} \begin{pmatrix} 1 & 0 \\ 0 & -1 \end{pmatrix} \cdot \begin{pmatrix} 1 \\ 0 \end{pmatrix} \psi^{(2)} &= +\frac{\omega_{0,1}\hbar}{2} \begin{pmatrix} 1 \\ 0 \end{pmatrix} \psi^{(2)} & \frac{\omega_{0,1}\hbar}{2} \begin{pmatrix} 1 & 0 \\ 0 & -1 \end{pmatrix} \cdot \begin{pmatrix} 1 \\ 0 \end{pmatrix} \psi^{(1)} &= +\frac{\omega_{0,2}\hbar}{2} \begin{pmatrix} 1 \\ 0 \end{pmatrix} \psi^{(1)} \\ \frac{\omega_{0,1}\hbar}{2} \begin{pmatrix} 1 & 0 \\ 0 & -1 \end{pmatrix} \cdot \begin{pmatrix} 0 \\ 1 \end{pmatrix} \psi^{(2)} &= -\frac{\omega_{0,1}\hbar}{2} \begin{pmatrix} 0 \\ 1 \end{pmatrix} \psi^{(2)} & \frac{\omega_{0,1}\hbar}{2} \begin{pmatrix} 1 & 0 \\ 0 & -1 \end{pmatrix} \cdot \begin{pmatrix} 0 \\ 1 \end{pmatrix} \psi^{(1)} &= -\frac{\omega_{0,2}\hbar}{2} \begin{pmatrix} 0 \\ 1 \end{pmatrix} \psi^{(1)}, \end{aligned} \quad (8.77)$$

$$\begin{aligned} \frac{\omega_{0,1}\hbar}{2} \begin{pmatrix} 1 & 0 \\ 0 & -1 \end{pmatrix} \cdot \begin{pmatrix} 1 \\ 0 \end{pmatrix} &= +\frac{\omega_{0,1}\hbar}{2} \begin{pmatrix} 1 \\ 0 \end{pmatrix} & \frac{\omega_{0,1}\hbar}{2} \begin{pmatrix} 1 & 0 \\ 0 & -1 \end{pmatrix} \cdot \begin{pmatrix} 1 \\ 0 \end{pmatrix} &= +\frac{\omega_{0,2}\hbar}{2} \begin{pmatrix} 1 \\ 0 \end{pmatrix} \\ \frac{\omega_{0,1}\hbar}{2} \begin{pmatrix} 1 & 0 \\ 0 & -1 \end{pmatrix} \cdot \begin{pmatrix} 0 \\ 1 \end{pmatrix} &= -\frac{\omega_{0,1}\hbar}{2} \begin{pmatrix} 0 \\ 1 \end{pmatrix} & \frac{\omega_{0,1}\hbar}{2} \begin{pmatrix} 1 & 0 \\ 0 & -1 \end{pmatrix} \cdot \begin{pmatrix} 0 \\ 1 \end{pmatrix} &= -\frac{\omega_{0,2}\hbar}{2} \begin{pmatrix} 0 \\ 1 \end{pmatrix}. \end{aligned} \quad (8.78)$$

We see that the eigenfunctions of the left equation are $\begin{pmatrix} 1 \\ 0 \end{pmatrix}$ and $\begin{pmatrix} 0 \\ 1 \end{pmatrix}$ for any $\psi^{(2)} = \begin{pmatrix} c_{\alpha,2} \\ c_{\beta,2} \end{pmatrix}$, and that the eigenfunctions of the right equation are also $\begin{pmatrix} 1 \\ 0 \end{pmatrix}$ and $\begin{pmatrix} 0 \\ 1 \end{pmatrix}$ for any $\psi^{(1)} = \begin{pmatrix} c_{\alpha,1} \\ c_{\beta,1} \end{pmatrix}$. The energy differences, given by the differences of the eigenvalues, are $\omega_{0,1}\hbar$ and $\omega_{0,2}\hbar$. As the left equation does not depend on $\psi^{(2)}$ and the right equation does not depend on $\psi^{(1)}$, the original set of four equations, represented by the 4-dimensional matrices, was redundant. If the nuclei are identical, the left and right equations can be replaced by a single equation with $\omega_{0,1} = \omega_{0,2} = \omega$ (cf treatment of indistinguishable nuclei in Section 6.7.2). Such case is equivalent to the mixed state described by the 2×2 density matrix in Section 6.1.

If the magnetic moments interact ($D \neq 0$) and the Hamiltonian cannot be simplified to Eq. 8.73, we have to work with four-dimensional matrices and state vectors. The Hamiltonian then has the following matrix representation

$$\hat{H} = \hbar \begin{pmatrix} \frac{\omega_{0,1} + \omega_{0,2}}{2} + \frac{D}{2} & 0 & 0 & 0 \\ 0 & \frac{\omega_{0,1} - \omega_{0,2}}{2} - \frac{D}{2} & -D & 0 \\ 0 & -D & -\frac{\omega_{0,1} - \omega_{0,2}}{2} + \frac{D}{2} & 0 \\ 0 & 0 & 0 & -\frac{\omega_{0,1} + \omega_{0,2}}{2} + \frac{D}{2} \end{pmatrix}. \quad (8.79)$$

If $\omega_{0,1}$ and $\omega_{0,2}$ differ substantially, secular approximation allows us to neglect also the $-\hat{I}_{1,x}\hat{I}_{2,x} - \hat{I}_{1,y}\hat{I}_{2,y}$ terms and to obtain a diagonal Hamiltonian matrix

$$\hat{H} \approx \hbar \begin{pmatrix} \frac{\omega_{0,1} + \omega_{0,2}}{2} + \frac{D}{2} & 0 & 0 & 0 \\ 0 & \frac{\omega_{0,1} - \omega_{0,2}}{2} - \frac{D}{2} & 0 & 0 \\ 0 & 0 & -\frac{\omega_{0,1} - \omega_{0,2}}{2} + \frac{D}{2} & 0 \\ 0 & 0 & 0 & -\frac{\omega_{0,1} + \omega_{0,2}}{2} + \frac{D}{2} \end{pmatrix} \quad (8.80)$$

with four-dimensional eigenvectors

$$\begin{pmatrix} 1 \\ 0 \\ 0 \\ 0 \end{pmatrix}, \quad \begin{pmatrix} 0 \\ 1 \\ 0 \\ 0 \end{pmatrix}, \quad \begin{pmatrix} 0 \\ 0 \\ 1 \\ 0 \end{pmatrix}, \quad \begin{pmatrix} 0 \\ 0 \\ 0 \\ 1 \end{pmatrix}. \quad (8.81)$$

If $\omega_{0,1}$ and $\omega_{0,2}$ are similar, the off-diagonal elements warn us that the vectors listed above (direct products of $|\alpha\rangle$ and $|\beta\rangle$) are no longer eigenfunctions of the Hamiltonian in Eq 8.80. **Note that the analysis presented in this Lecture and in the following Lectures cannot be applied to such spin systems.** We return to the interacting magnetic moments with very similar $\omega_{0,1}$ and $\omega_{0,2}$ in the end of our course (Section 12.2).

8.9.4 Commutators of product operators

The product operators are direct products of 2×2 matrices $\mathcal{I}_x, \mathcal{I}_y, \mathcal{I}_z, \mathcal{I}_t$. Therefore, commutators of product operators can be derived from their relations and from the general properties of the direct product of matrices. In general expressions used in this section letters j, k, l, m replace one of the subscript x, y, z (but not t), n, n' distinguish nuclei (1 or 2), and $\delta_{jk} = 1$ for $j = k$, and $\delta_{jk} = 0$ for $j \neq k$.

Products of the 2×2 matrices $\mathcal{I}_x, \mathcal{I}_y, \mathcal{I}_z$ are related in the following manner (cf Eqs. 4.32–4.35)

$$\mathcal{I}_x \cdot \mathcal{I}_y - \mathcal{I}_y \cdot \mathcal{I}_x = [\mathcal{I}_x, \mathcal{I}_y] = i\mathcal{I}_z, \quad (8.82)$$

$$\mathcal{I}_y \cdot \mathcal{I}_z - \mathcal{I}_z \cdot \mathcal{I}_y = [\mathcal{I}_y, \mathcal{I}_z] = i\mathcal{I}_x, \quad (8.83)$$

$$\mathcal{I}_z \cdot \mathcal{I}_x - \mathcal{I}_x \cdot \mathcal{I}_z = [\mathcal{I}_z, \mathcal{I}_x] = i\mathcal{I}_y, \quad (8.84)$$

$$\mathcal{I}_j \cdot \mathcal{I}_k + \mathcal{I}_k \cdot \mathcal{I}_j = \delta_{jk} \mathcal{I}_t. \quad (8.85)$$

The following properties of the direct (Kronecker) products allow us to find the commutation relation also for the product operators.

$$(\hat{A} \otimes \hat{B}) + (\hat{A} \otimes \hat{C}) = \hat{A} \otimes (\hat{B} + \hat{C}), \quad (8.86)$$

$$(\hat{A} \otimes \hat{B}) \cdot (\hat{C} \otimes \hat{D}) = (\hat{A} \cdot \hat{C}) \otimes (\hat{B} \cdot \hat{D}). \quad (8.87)$$

First, we derive commutation relations among operators of the form \mathcal{I}_{nj} . Eq. 8.86 shows that

$$2\mathcal{I}_t \otimes (\mathcal{I}_j \cdot \mathcal{I}_k) \pm 2\mathcal{I}_t \otimes (\mathcal{I}_k \cdot \mathcal{I}_j) = 2\mathcal{I}_t \otimes (\mathcal{I}_j \cdot \mathcal{I}_k \pm \mathcal{I}_k \cdot \mathcal{I}_j), \quad (8.88)$$

$$2(\mathcal{I}_j \cdot \mathcal{I}_k) \otimes \mathcal{I}_t \pm 2(\mathcal{I}_j \cdot \mathcal{I}_k) \otimes \mathcal{I}_t = 2(\mathcal{I}_j \cdot \mathcal{I}_k \pm \mathcal{I}_k \cdot \mathcal{I}_j) \otimes \mathcal{I}_t. \quad (8.89)$$

Therefore, the relations among $\mathcal{I}_{1x}, \mathcal{I}_{1y}, \mathcal{I}_{1z}$ and $\mathcal{I}_{2x}, \mathcal{I}_{2y}, \mathcal{I}_{2z}$ can be obtained simply by replacing subscripts x, y, z in Eqs. 8.82–8.85 by the subscripts $1x, 1y, 1z$ and $2x, 2y, 2z$. This is written in a concise form in Eq. 8.29.

Second, we derive commutation relations between operators \mathcal{I}_{nj} and $2\mathcal{I}_{nk}\mathcal{I}_{n'l}$. Their commutator is

$$[\mathcal{I}_{nj}, 2\mathcal{I}_{nk}\mathcal{I}_{n'l}] = 2\mathcal{I}_{nj}\mathcal{I}_{nk}\mathcal{I}_{n'l} - 2\mathcal{I}_{nk}\mathcal{I}_{n'l}\mathcal{I}_{nj}. \quad (8.90)$$

Eq. 8.87 implies

$$\mathcal{I}_{1j}\mathcal{I}_{2k} = (\mathcal{I}_j \otimes \mathcal{I}_t) \cdot (\mathcal{I}_t \otimes \mathcal{I}_k) = (\mathcal{I}_j \cdot \mathcal{I}_t) \otimes (\mathcal{I}_t \cdot \mathcal{I}_k) = \frac{1}{4}\mathcal{I}_j \otimes \mathcal{I}_k, \quad (8.91)$$

$$\mathcal{I}_{2k}\mathcal{I}_{1j} = (\mathcal{I}_t \otimes \mathcal{I}_k) \cdot (\mathcal{I}_j \otimes \mathcal{I}_t) = (\mathcal{I}_t \cdot \mathcal{I}_j) \otimes (\mathcal{I}_k \cdot \mathcal{I}_t) = \frac{1}{4}\mathcal{I}_j \otimes \mathcal{I}_k. \quad (8.92)$$

Therefore, $\mathcal{I}_{1j}\mathcal{I}_{2k} - \mathcal{I}_{2k}\mathcal{I}_{1j} = 0$, i.e., \mathcal{I}_{1j} and \mathcal{I}_{2k} (operators of magnetic moment components of *different* nuclei) *commute* and can be applied in any order:

$$\mathcal{I}_{1j}\mathcal{I}_{2k} = \mathcal{I}_{2k}\mathcal{I}_{1j} \quad (8.93)$$

This allows us to switch the last two operators in Eq. 8.90 and obtain the relation described by Eq. 8.30:

$$2\mathcal{I}_{nj}\mathcal{I}_{nk}\mathcal{I}_{n'l} - 2\mathcal{I}_{nk}\mathcal{I}_{n'l}\mathcal{I}_{nj} = 2\mathcal{I}_{nj}\mathcal{I}_{nk}\mathcal{I}_{n'l} - 2\mathcal{I}_{nk}\mathcal{I}_{nj}\mathcal{I}_{n'l} = 2[\mathcal{I}_{nj}, \mathcal{I}_{nk}]\mathcal{I}_{n'l}. \quad (8.94)$$

Third, we derive commutation relations between operators $2\mathcal{I}_{nj}\mathcal{I}_{n'l}$ and $2\mathcal{I}_{nk}\mathcal{I}_{n'm}$

$$[2\mathcal{I}_{nj}\mathcal{I}_{n'l}, 2\mathcal{I}_{nk}\mathcal{I}_{n'm}] = 4\mathcal{I}_{nj}\mathcal{I}_{n'l}\mathcal{I}_{nk}\mathcal{I}_{n'm} - 4\mathcal{I}_{nk}\mathcal{I}_{n'm}\mathcal{I}_{nj}\mathcal{I}_{n'l}. \quad (8.95)$$

We start by switching the commuting operators of magnetic moment components of different nuclei $\mathcal{I}_{n'l}$, \mathcal{I}_{nk} and $\mathcal{I}_{n'm}\mathcal{I}_{nj}$.

$$[2\mathcal{I}_{nj}\mathcal{I}_{n'l}, 2\mathcal{I}_{nk}\mathcal{I}_{n'm}] = 4\mathcal{I}_{nj}\mathcal{I}_{nk}\mathcal{I}_{n'l}\mathcal{I}_{n'm} - 4\mathcal{I}_{nk}\mathcal{I}_{nj}\mathcal{I}_{n'm}\mathcal{I}_{n'l}. \quad (8.96)$$

Then we use Eqs. 8.82–8.85 to express

$$2\mathcal{I}_{nj}\mathcal{I}_{nk} = (\mathcal{I}_{nj}\mathcal{I}_{nk} - \mathcal{I}_{nk}\mathcal{I}_{nj}) + (\mathcal{I}_{nj}\mathcal{I}_{nk} + \mathcal{I}_{nk}\mathcal{I}_{nj}) = [\mathcal{I}_{nj}, \mathcal{I}_{nk}] + \delta_{jk}\mathcal{I}_t, \quad (8.97)$$

$$-2\mathcal{I}_{nk}\mathcal{I}_{nj} = (\mathcal{I}_{nj}\mathcal{I}_{nk} - \mathcal{I}_{nk}\mathcal{I}_{nj}) - (\mathcal{I}_{nj}\mathcal{I}_{nk} + \mathcal{I}_{nk}\mathcal{I}_{nj}) = [\mathcal{I}_{nj}, \mathcal{I}_{nk}] - \delta_{jk}\mathcal{I}_t, \quad (8.98)$$

$$2\mathcal{I}_{n'l}\mathcal{I}_{n'm} = (\mathcal{I}_{n'l}\mathcal{I}_{n'm} - \mathcal{I}_{n'm}\mathcal{I}_{n'l}) + (\mathcal{I}_{n'l}\mathcal{I}_{n'm} + \mathcal{I}_{n'm}\mathcal{I}_{n'l}) = [\mathcal{I}_{n'l}, \mathcal{I}_{n'm}] + \delta_{lm}\mathcal{I}_t, \quad (8.99)$$

$$-2\mathcal{I}_{n'm}\mathcal{I}_{n'l} = (\mathcal{I}_{n'l}\mathcal{I}_{n'm} - \mathcal{I}_{n'm}\mathcal{I}_{n'l}) - (\mathcal{I}_{n'l}\mathcal{I}_{n'm} + \mathcal{I}_{n'm}\mathcal{I}_{n'l}) = [\mathcal{I}_{n'l}, \mathcal{I}_{n'm}] - \delta_{lm}\mathcal{I}_t. \quad (8.100)$$

Inserting the obtained expressions into Eq. 8.101 results in Eq. 8.31

$$[2\mathcal{I}_{nj}\mathcal{I}_{n'l}, 2\mathcal{I}_{nk}\mathcal{I}_{n'm}] = 4\mathcal{I}_{nj}\mathcal{I}_{nk}\mathcal{I}_{n'l}\mathcal{I}_{n'm} - 4\mathcal{I}_{nk}\mathcal{I}_{nj}\mathcal{I}_{n'm}\mathcal{I}_{n'l} = ([\mathcal{I}_{nj}, \mathcal{I}_{nk}] + \delta_{jk}\mathcal{I}_t)([\mathcal{I}_{n'l}, \mathcal{I}_{n'm}] + \delta_{lm}\mathcal{I}_t) - ([\mathcal{I}_{nj}, \mathcal{I}_{nk}] - \delta_{jk}\mathcal{I}_t)([\mathcal{I}_{n'l}, \mathcal{I}_{n'm}] - \delta_{lm}\mathcal{I}_t) = [\mathcal{I}_{nj}, \mathcal{I}_{nk}]\delta_{lm} + [\mathcal{I}_{n'l}, \mathcal{I}_{n'm}]\delta_{jk}. \quad (8.101)$$

Note that

$$j = k \Rightarrow [\mathcal{I}_{nj}, \mathcal{I}_{nk}] = 0, \quad \delta_{jk} = 1 \quad (8.102)$$

$$l = m \Rightarrow [\mathcal{I}_{n'l}, \mathcal{I}_{n'm}] = 0, \quad \delta_{lm} = 1. \quad (8.103)$$

8.9.5 Dipole-dipole relaxation

The Bloch-Wangsness-Redfield theory (see Section 7.10.3) describes also the relaxation due to the dipole-dipole interactions. The Liouville - von Neumann equation has the same form as Eq. 7.41, only the chemical shift Hamiltonian is replaced by the Hamiltonian describing the interactions of spin magnetic moments:

$$\frac{d\Delta\hat{\rho}}{dt} = -\frac{i}{\hbar}[\hat{H}_D, \Delta\hat{\rho}], \quad (8.104)$$

In order to describe the dipole-dipole relaxation on the quantum level, it is useful to work in spherical coordinates and to convert the product operators constituting the Hamiltonian \hat{H}_D to a different basis. The operators $\hat{I}_{1x}\hat{I}_{2z}$, $\hat{I}_{1y}\hat{I}_{2z}$, $\hat{I}_{1z}\hat{I}_{2x}$, $\hat{I}_{1z}\hat{I}_{2y}$ are transformed using the relation $\hat{I}_{\pm} = \hat{I}_x \pm i\hat{I}_y$:

$$\hat{I}_{1x}\hat{I}_{2z} = \frac{1}{2}(+\hat{I}_{1+}\hat{I}_{2z} + \hat{I}_{1-}\hat{I}_{2z}), \quad (8.105)$$

$$\hat{I}_{1y}\hat{I}_{2z} = \frac{i}{2}(-\hat{I}_{1+}\hat{I}_{2z} + \hat{I}_{1-}\hat{I}_{2z}), \quad (8.106)$$

$$\hat{I}_{1z}\hat{I}_{2x} = \frac{1}{2}(+\hat{I}_{1z}\hat{I}_{2+} + \hat{I}_{1z}\hat{I}_{2-}), \quad (8.107)$$

$$\hat{I}_{1z}\hat{I}_{2y} = \frac{i}{2}(-\hat{I}_{1z}\hat{I}_{2+} + \hat{I}_{1z}\hat{I}_{2-}). \quad (8.108)$$

Since

$$\cos\varphi + i\sin\varphi = e^{i\varphi}, \quad (8.109)$$

$$\cos\varphi - i\sin\varphi = e^{-i\varphi}, \quad (8.110)$$

$$\begin{aligned} & 3\sin\vartheta\cos\vartheta(\hat{I}_{1x}\hat{I}_{2z}\cos\varphi + \hat{I}_{1y}\hat{I}_{2z}\sin\varphi + \hat{I}_{1z}\hat{I}_{2x}\cos\varphi + \hat{I}_{1z}\hat{I}_{2y}\sin\varphi) \\ &= \frac{3}{2}\sin\vartheta\cos\vartheta(\hat{I}_{1+}\hat{I}_{2z}e^{-i\varphi} + \hat{I}_{1-}\hat{I}_{2z}e^{i\varphi} + \hat{I}_{1z}\hat{I}_{2+}e^{-i\varphi} + \hat{I}_{1z}\hat{I}_{2-}e^{i\varphi}) \end{aligned} \quad (8.111)$$

The $\hat{I}_{1x}\hat{I}_{2x}, \hat{I}_{1y}\hat{I}_{2y}, \hat{I}_{1x}\hat{I}_{2y}, \hat{I}_{1y}\hat{I}_{2x}$ are transformed in a similar fashion

$$\begin{aligned}\hat{I}_{1x}\hat{I}_{2y} &= \frac{i}{4}(+\hat{I}_{1+}\hat{I}_{2-} - \hat{I}_{1-}\hat{I}_{2+} - \hat{I}_{1+}\hat{I}_{2+} + \hat{I}_{1-}\hat{I}_{2-}), \\ \hat{I}_{1y}\hat{I}_{2x} &= \frac{i}{4}(-\hat{I}_{1+}\hat{I}_{2-} + \hat{I}_{1-}\hat{I}_{2+} - \hat{I}_{1+}\hat{I}_{2+} + \hat{I}_{1-}\hat{I}_{2-}), \\ \hat{I}_{1x}\hat{I}_{2x} &= \frac{1}{4}(+\hat{I}_{1+}\hat{I}_{2-} + \hat{I}_{1-}\hat{I}_{2+} + \hat{I}_{1+}\hat{I}_{2+} + \hat{I}_{1-}\hat{I}_{2-}), \\ \hat{I}_{1y}\hat{I}_{2y} &= \frac{1}{4}(+\hat{I}_{1+}\hat{I}_{2-} + \hat{I}_{1-}\hat{I}_{2+} - \hat{I}_{1+}\hat{I}_{2+} - \hat{I}_{1-}\hat{I}_{2-}),\end{aligned}$$

and

$$\begin{aligned}3 \sin^2 \vartheta (\hat{I}_{1x}\hat{I}_{2x} \cos^2 \varphi + \hat{I}_{1y}\hat{I}_{2y} \sin^2 \varphi + \hat{I}_{1x}\hat{I}_{2y} \sin \varphi \cos \varphi + \hat{I}_{1y}\hat{I}_{2x} \sin \varphi \cos \varphi) - (\hat{I}_{1x}\hat{I}_{2x} + \hat{I}_{1y}\hat{I}_{2y}) \\ = \frac{3}{4} \sin^2 \vartheta (\hat{I}_{1+}\hat{I}_{2-} (\cos^2 \varphi + \sin^2 \varphi + i \sin \varphi \cos \varphi - i \sin \varphi \cos \varphi) \\ + \hat{I}_{1-}\hat{I}_{2+} (\cos^2 \varphi + \sin^2 \varphi - i \sin \varphi \cos \varphi + i \sin \varphi \cos \varphi) \\ + \hat{I}_{1+}\hat{I}_{2+} (\cos^2 \varphi - \sin^2 \varphi - i \sin \varphi \cos \varphi - i \sin \varphi \cos \varphi) \\ + \hat{I}_{1-}\hat{I}_{2-} (\cos^2 \varphi - \sin^2 \varphi + i \sin \varphi \cos \varphi + i \sin \varphi \cos \varphi)) \\ - \frac{1}{4} (2\hat{I}_{1+}\hat{I}_{2-} + 2\hat{I}_{1-}\hat{I}_{2+}) \\ = \frac{1}{4} \hat{I}_{1+}\hat{I}_{2-} (3 \sin^2 \vartheta - 2) + \frac{1}{4} \hat{I}_{1-}\hat{I}_{2+} (3 \sin^2 \vartheta - 2) \\ + \frac{3}{4} \hat{I}_{1+}\hat{I}_{2+} \sin^2 \vartheta e^{-i2\varphi} + \frac{3}{4} \hat{I}_{1-}\hat{I}_{2-} \sin^2 \vartheta e^{i2\varphi} \\ = -\frac{1}{4} \hat{I}_{1+}\hat{I}_{2-} (3 \cos^2 \vartheta - 1) - \frac{1}{4} \hat{I}_{1-}\hat{I}_{2+} (3 \cos^2 \vartheta - 1) \\ + \frac{3}{4} \hat{I}_{1+}\hat{I}_{2+} \sin^2 \vartheta e^{-i2\varphi} + \frac{3}{4} \hat{I}_{1-}\hat{I}_{2-} \sin^2 \vartheta e^{i2\varphi}.\end{aligned}\quad (8.112)$$

Using Eqs. 8.111 and 8.112 and moving to the interaction frame ($\hat{I}_{n\pm} \rightarrow \hat{I}_{n\pm} e^{\pm i\omega_0 n t}$), Eq. 8.62 is converted to

$$\begin{aligned}\hat{H}_D^I &= -\frac{\mu_0 \gamma_1 \gamma_2}{4\pi r^3} \left(\hat{I}_{1z}\hat{I}_{2z} (3 \cos^2 \vartheta - 1) \right. \\ &\quad - \frac{1}{4} \hat{I}_{1+}\hat{I}_{2-} (3 \cos^2 \vartheta - 1) e^{i(\omega_0, 1 - \omega_0, 2)t} - \frac{1}{4} \hat{I}_{1-}\hat{I}_{2+} (3 \cos^2 \vartheta - 1) e^{-i(\omega_0, 1 - \omega_0, 2)t} \\ &\quad + \frac{3}{2} \hat{I}_{1+}\hat{I}_{2z} \sin \vartheta \cos \vartheta e^{-i\varphi} e^{i(\omega_0, 1)t} + \frac{3}{2} \hat{I}_{1-}\hat{I}_{2z} \sin \vartheta \cos \vartheta e^{i\varphi} e^{-i(\omega_0, 1)t} \\ &\quad + \frac{3}{2} \hat{I}_{1z}\hat{I}_{2+} \sin \vartheta \cos \vartheta e^{-i\varphi} e^{i(\omega_0, 2)t} + \frac{3}{2} \hat{I}_{1z}\hat{I}_{2-} \sin \vartheta \cos \vartheta e^{i\varphi} e^{-i(\omega_0, 2)t} \\ &\quad \left. + \frac{3}{4} \hat{I}_{1+}\hat{I}_{2+} \sin^2 \vartheta e^{-i2\varphi} e^{i(\omega_0, 1 + \omega_0, 2)t} + \frac{3}{4} \hat{I}_{1-}\hat{I}_{2-} \sin^2 \vartheta e^{i2\varphi} e^{-i(\omega_0, 1 + \omega_0, 2)t} \right) \\ &= -b \left(2c^{zz} \hat{I}_{1z}\hat{I}_{2z} - \frac{1}{2} c^{+-} \hat{I}_{1+}\hat{I}_{2-} - \frac{1}{2} c^{-+} \hat{I}_{1-}\hat{I}_{2+} \right. \\ &\quad \left. + \sqrt{\frac{3}{2}} \left(c^{+z} \hat{I}_{1+}\hat{I}_{2z} + c^{-z} \hat{I}_{1-}\hat{I}_{2z} + c^{z+} \hat{I}_{1z}\hat{I}_{2+} + c^{z-} \hat{I}_{1z}\hat{I}_{2-} + c^{++} \hat{I}_{1+}\hat{I}_{2+} + c^{--} \hat{I}_{1-}\hat{I}_{2-} \right) \right).\end{aligned}\quad (8.113)$$

The difference of the density matrix from its equilibrium form, written in a bases including the operators used to define \hat{H}_D , is in general

$$\begin{aligned}\Delta \hat{\rho} &= d_t \hat{I}_t + d_{1z} \hat{I}_{1z} + d_{1+} \hat{I}_{1+} + d_{1-} \hat{I}_{1-} + d_{2z} \hat{I}_{2z} + d_{2+} \hat{I}_{2+} + d_{2-} \hat{I}_{2-} \\ &\quad + d_{zz} \hat{I}_{1z}\hat{I}_{2z} + d_{+-} \hat{I}_{1+}\hat{I}_{2-} + d_{-+} \hat{I}_{1-}\hat{I}_{2+} + d_{+z} \hat{I}_{1+}\hat{I}_{2z} + d_{-z} \hat{I}_{1-}\hat{I}_{2z} + d_{z+} \hat{I}_{1z}\hat{I}_{2+} + d_{z-} \hat{I}_{1z}\hat{I}_{2-} + d_{++} \hat{I}_{1+}\hat{I}_{2+} + d_{--} \hat{I}_{1-}\hat{I}_{2-}.\end{aligned}\quad (8.114)$$

However, here we analyze only evolution of $d_{1z}\hat{I}_{1z}$, $d_{2z}\hat{I}_{2z}$, $d_{1+}\hat{I}_{1+}$, needed to describe relaxation of $\Delta\langle M_{1,z} \rangle$, $\Delta\langle M_{1,z} \rangle$, and $\langle M_{1,+} \rangle$. Similarly to Eq. 7.47, the dipole-dipole relaxation is described by

$$\frac{d\Delta\hat{\rho}}{dt} = -\frac{1}{\hbar^2} \int_0^\infty [\hat{H}_D(0), [\hat{H}_D(t), \Delta\hat{\rho}]] dt. \quad (8.115)$$

The right-hand side can be simplified dramatically by the *secular approximation* as in Eq. 7.47: all terms with $e^{\pm i\omega_0 n t}$ are averaged to zero. Only terms with $(c^{zz})^2$, $c^{z+}c^{z-}$, $c^{+z}c^{-z}$, $c^{+-}c^{-+}$, and $c^{++}c^{--}$ are non zero (all equal to 1/5 at $t_j = 0$).¹³ This reduces the number of double commutators to be expressed from 81 to 9 for each density matrix component. The double commutators needed to describe relaxation rates of the contributions of the first nucleus to the magnetization $\langle M_{1z} \rangle$ and $\langle M_{1+} \rangle$ are

$$[\hat{I}_{1z}\hat{I}_{2z}, [\hat{I}_{1z}\hat{I}_{2z}, \hat{I}_{1z}]] = 0, \quad (8.116)$$

$$[\hat{I}_{1-}\hat{I}_{2+}, [\hat{I}_{1+}\hat{I}_{2-}, \hat{I}_{1z}]] = \hbar^2(\hat{I}_{1z} - \hat{I}_{2z}), \quad (8.117)$$

$$[\hat{I}_{1+}\hat{I}_{2-}, [\hat{I}_{1-}\hat{I}_{2+}, \hat{I}_{1z}]] = \hbar^2(\hat{I}_{1z} - \hat{I}_{2z}), \quad (8.118)$$

$$[\hat{I}_{1+}\hat{I}_{2z}, [\hat{I}_{1-}\hat{I}_{2z}, \hat{I}_{1z}]] = \frac{1}{2}\hbar^2\hat{I}_{1z}, \quad (8.119)$$

$$[\hat{I}_{1-}\hat{I}_{2z}, [\hat{I}_{1+}\hat{I}_{2z}, \hat{I}_{1z}]] = \frac{1}{2}\hbar^2\hat{I}_{1z}, \quad (8.120)$$

$$[\hat{I}_{1z}\hat{I}_{2+}, [\hat{I}_{1z}\hat{I}_{2-}, \hat{I}_{1z}]] = 0, \quad (8.121)$$

$$[\hat{I}_{1z}\hat{I}_{2-}, [\hat{I}_{1z}\hat{I}_{2+}, \hat{I}_{1z}]] = 0, \quad (8.122)$$

$$[\hat{I}_{1+}\hat{I}_{2+}, [\hat{I}_{1-}\hat{I}_{2-}, \hat{I}_{1z}]] = \hbar^2(\hat{I}_{1z} + \hat{I}_{2z}), \quad (8.123)$$

$$[\hat{I}_{1-}\hat{I}_{2-}, [\hat{I}_{1+}\hat{I}_{2+}, \hat{I}_{1z}]] = \hbar^2(\hat{I}_{1z} + \hat{I}_{2z}), \quad (8.124)$$

$$[\hat{I}_{1z}\hat{I}_{2z}, [\hat{I}_{1z}\hat{I}_{2z}, \hat{I}_{2z}]] = 0, \quad (8.125)$$

$$[\hat{I}_{1-}\hat{I}_{2+}, [\hat{I}_{1+}\hat{I}_{2-}, \hat{I}_{2z}]] = \hbar^2(\hat{I}_{2z} - \hat{I}_{1z}), \quad (8.126)$$

$$[\hat{I}_{1+}\hat{I}_{2-}, [\hat{I}_{1-}\hat{I}_{2+}, \hat{I}_{2z}]] = \hbar^2(\hat{I}_{2z} - \hat{I}_{1z}), \quad (8.127)$$

$$[\hat{I}_{1+}\hat{I}_{2z}, [\hat{I}_{1-}\hat{I}_{2z}, \hat{I}_{2z}]] = \frac{1}{2}\hbar^2\hat{I}_{2z}, \quad (8.128)$$

$$[\hat{I}_{1-}\hat{I}_{2z}, [\hat{I}_{1+}\hat{I}_{2z}, \hat{I}_{2z}]] = \frac{1}{2}\hbar^2\hat{I}_{2z}, \quad (8.129)$$

$$[\hat{I}_{1z}\hat{I}_{2+}, [\hat{I}_{1z}\hat{I}_{2-}, \hat{I}_{2z}]] = 0, \quad (8.130)$$

$$[\hat{I}_{1z}\hat{I}_{2-}, [\hat{I}_{1z}\hat{I}_{2+}, \hat{I}_{2z}]] = 0, \quad (8.131)$$

$$[\hat{I}_{1+}\hat{I}_{2+}, [\hat{I}_{1-}\hat{I}_{2-}, \hat{I}_{2z}]] = \hbar^2(\hat{I}_{2z} + \hat{I}_{1z}), \quad (8.132)$$

$$[\hat{I}_{1-}\hat{I}_{2-}, [\hat{I}_{1+}\hat{I}_{2+}, \hat{I}_{2z}]] = \hbar^2(\hat{I}_{2z} + \hat{I}_{1z}), \quad (8.133)$$

¹³Averaging over all molecules makes all correlation functions identical in isotropic liquids.

$$[\hat{I}_{1z}\hat{I}_{2z}, [\hat{I}_{1z}\hat{I}_{2z}, \hat{I}_{1+}]] = \frac{1}{4}\hbar^2\hat{I}_{1+}, \quad (8.134)$$

$$[\hat{I}_{1+}\hat{I}_{2-}, [\hat{I}_{1-}\hat{I}_{2+}, \hat{I}_{1+}]] = \hbar^2\hat{I}_{1+}, \quad (8.135)$$

$$[\hat{I}_{1-}\hat{I}_{2+}, [\hat{I}_{1+}\hat{I}_{2-}, \hat{I}_{1+}]] = 0, \quad (8.136)$$

$$[\hat{I}_{1+}\hat{I}_{2z}, [\hat{I}_{1-}\hat{I}_{2z}, \hat{I}_{1+}]] = \frac{1}{2}\hbar^2\hat{I}_{1+}, \quad (8.137)$$

$$[\hat{I}_{1-}\hat{I}_{2z}, [\hat{I}_{1+}\hat{I}_{2z}, \hat{I}_{1+}]] = 0, \quad (8.138)$$

$$[\hat{I}_{1z}\hat{I}_{2+}, [\hat{I}_{1z}\hat{I}_{2-}, \hat{I}_{1+}]] = \frac{1}{2}\hbar^2\hat{I}_{1+}, \quad (8.139)$$

$$[\hat{I}_{1z}\hat{I}_{2-}, [\hat{I}_{1z}\hat{I}_{2+}, \hat{I}_{1+}]] = \frac{1}{2}\hbar^2\hat{I}_{1+}, \quad (8.140)$$

$$[\hat{I}_{1+}\hat{I}_{2+}, [\hat{I}_{1-}\hat{I}_{2-}, \hat{I}_{1+}]] = 0, \quad (8.141)$$

$$[\hat{I}_{1-}\hat{I}_{2-}, [\hat{I}_{1+}\hat{I}_{2+}, \hat{I}_{1+}]] = \frac{1}{2}\hbar^2\hat{I}_{1+}. \quad (8.142)$$

The relaxation rates can be then derived as described for the relaxation due to the chemical shift in Section 7.10.3. For ΔM_{1z} ,

$$\langle \Delta M_{1z} \rangle = \text{Tr}\{\Delta \hat{\rho} \hat{M}_{1z}\} = \mathcal{N}\gamma \text{Tr}\{\Delta \hat{\rho} \hat{I}_{1z}\}. \quad (8.143)$$

As discussed in Section 7.10.3, the orthogonality of basis matrices reduces the left-hand side of Eq. 8.115 to

$$\frac{d d_{1z}}{dt} \hat{I}_{1z}. \quad (8.144)$$

Expressing the terms with the non-zero double commutators in the right-hand side of Eq. 8.115 results in six integrals

$$\begin{aligned} \frac{d d_{1z}}{dt} \text{Tr}\{\hat{I}_{1z}\hat{I}_{1z}\} = & - \left(\frac{1}{4}b^2 \int_0^\infty \overline{c^{+-}(0)c^{-+}(t)} e^{i(\omega_{0,1}-\omega_{0,2})t} dt + \frac{1}{4}b^2 \int_0^\infty \overline{c^{-+}(0)c^{+-}(t)} e^{-i(\omega_{0,1}-\omega_{0,2})t} dt \right) d_{1z} (\text{Tr}\{\hat{I}_{1z}\hat{I}_{1z}\} - \text{Tr}\{\hat{I}_{2z}\hat{I}_{2z}\}) \\ & - \left(\frac{3}{4}b^2 \int_0^\infty \overline{c^{+z}(0)c^{-z}(t)} e^{i\omega_{0,1}t} dt + \frac{3}{4}b^2 \int_0^\infty \overline{c^{-z}(0)c^{+z}(t)} e^{-i\omega_{0,1}t} dt \right) d_{1z} \text{Tr}\{\hat{I}_{1z}\hat{I}_{1z}\} \\ & - \left(\frac{3}{2}b^2 \int_0^\infty \overline{c^{++}(0)c^{--}(t)} e^{i(\omega_{0,1}+\omega_{0,2})t} dt + \frac{3}{2}b^2 \int_0^\infty \overline{c^{--}(0)c^{++}(t)} e^{-i(\omega_{0,1}+\omega_{0,2})t} dt \right) (d_{1z} (\text{Tr}\{\hat{I}_{1z}\hat{I}_{1z}\} + \text{Tr}\{\hat{I}_{2z}\hat{I}_{2z}\})). \end{aligned} \quad (8.145)$$

As both sides of the equation contain the same coefficients, $d_{nz} \text{Tr}\{\hat{I}_{nz}\hat{I}_{nz}\}$ can be converted to $\Delta \langle M_{nz} \rangle$:

$$\begin{aligned} \frac{d \Delta \langle M_{1z} \rangle}{dt} = & - \left(\frac{1}{4}b^2 \int_0^\infty \overline{c^{+-}(0)c^{-+}(t)} e^{i(\omega_{0,1}-\omega_{0,2})t} dt + \frac{1}{4}b^2 \int_0^\infty \overline{c^{-+}(0)c^{+-}(t)} e^{-i(\omega_{0,1}-\omega_{0,2})t} dt \right) (\Delta \langle M_{1z} \rangle - \Delta \langle M_{2z} \rangle) \\ & - \left(\frac{3}{4}b^2 \int_0^\infty \overline{c^{+z}(0)c^{-z}(t)} e^{i\omega_{0,1}t} dt + \frac{3}{4}b^2 \int_0^\infty \overline{c^{-z}(0)c^{+z}(t)} e^{-i\omega_{0,1}t} dt \right) \Delta \langle M_{1z} \rangle \\ & - \left(\frac{3}{2}b^2 \int_0^\infty \overline{c^{++}(0)c^{--}(t)} e^{i(\omega_{0,1}+\omega_{0,2})t} dt + \frac{3}{2}b^2 \int_0^\infty \overline{c^{--}(0)c^{++}(t)} e^{-i(\omega_{0,1}+\omega_{0,2})t} dt \right) (\Delta \langle M_{1z} \rangle + \Delta \langle M_{2z} \rangle). \end{aligned} \quad (8.146)$$

If the fluctuations are random and consequently stationary, the current orientation of the molecule is correlated with the orientation in the past in the same manner as it is correlated with the orientation in the future (see Section 7.10.3), and the bounds of the integrals can be changed

$$\begin{aligned}
\frac{d\Delta\langle M_{1z} \rangle}{dt} = & - \left(\frac{1}{8}b^2 \int_{-\infty}^{\infty} \overline{c^{+-}(0)c^{-+}(t)} e^{i(\omega_{0,1}-\omega_{0,2})t} dt + \frac{1}{8}b^2 \int_{-\infty}^{\infty} \overline{c^{-+}(0)c^{+-}(t)} e^{-i(\omega_{0,1}-\omega_{0,2})t} dt \right) (\Delta\langle M_{1z} \rangle - \Delta\langle M_{2z} \rangle) \\
& - \left(\frac{3}{8}b^2 \int_{-\infty}^{\infty} \overline{c^{+z}(0)c^{-z}(t)} e^{i\omega_{0,1}t} dt + \frac{3}{8}b^2 \int_{-\infty}^{\infty} \overline{c^{-z}(0)c^{+z}(t)} e^{-i\omega_{0,1}t} dt \right) \Delta\langle M_{1z} \rangle \\
& - \left(\frac{3}{4}b^2 \int_{-\infty}^{\infty} \overline{c^{++}(0)c^{--}(t)} e^{i(\omega_{0,1}+\omega_{0,2})t} dt + \frac{3}{4}b^2 \int_{-\infty}^{\infty} \overline{c^{--}(0)c^{++}(t)} e^{-i(\omega_{0,1}+\omega_{0,2})t} dt \right) (\Delta\langle M_{1z} \rangle + \Delta\langle M_{2z} \rangle). \quad (8.147)
\end{aligned}$$

Collecting the real parts of integrals preceding $\Delta\langle M_z \rangle$ of the same nucleus, noting that they are identical with the definitions of the spectral density functions, and assuming $J(\omega) \approx J(-\omega)$,

$$\begin{aligned}
\frac{d\Delta\langle M_{1z} \rangle}{dt} = & - \frac{1}{8}b^2(2J(\omega_{0,1}-\omega_{0,2}) + 6J(\omega_{0,1}) + 12J(\omega_{0,1}+\omega_{0,2}))\Delta\langle M_{1z} \rangle \\
& + \frac{1}{8}b^2(2J(\omega_{0,1}-\omega_{0,2}) - 12J(\omega_{0,1}+\omega_{0,2}))\Delta\langle M_{2z} \rangle \\
= & - R_{a1}\Delta\langle M_{1z} \rangle - R_x\Delta\langle M_{2z} \rangle. \quad (8.148)
\end{aligned}$$

The corresponding expression for relaxation of $\Delta\langle M_{2z} \rangle$ is obtained in the same manner (or simply by switching subscripts 1 and 2 in the result):

$$\begin{aligned}
\frac{d\Delta\langle M_{2z} \rangle}{dt} = & - \frac{1}{8}b^2(2J(\omega_{0,2}-\omega_{0,1}) + 6J(\omega_{0,2}) + 12J(\omega_{0,2}+\omega_{0,1}))\Delta\langle M_{2z} \rangle \\
& + \frac{1}{8}b^2(2J(\omega_{0,2}-\omega_{0,1}) - 12J(\omega_{0,2}+\omega_{0,1}))\Delta\langle M_{1z} \rangle \\
= & - R_{a2}\Delta\langle M_{2z} \rangle - R_x\Delta\langle M_{1z} \rangle. \quad (8.149)
\end{aligned}$$

The same approach is applied to M_{1+} .

$$\Delta\langle M_{1+} \rangle \equiv \langle M_{1+} \rangle = \text{Tr}\{\Delta\hat{\rho}\hat{M}_{1+}\}. \quad (8.150)$$

The operator of M_{1+} for one magnetic moment observed is

$$\hat{M}_{1+} = \mathcal{N}\gamma_1\hat{I}_{1+} = \mathcal{N}\gamma_1(\hat{I}_{1x} + i\hat{I}_{1y}). \quad (8.151)$$

Due to the orthogonality of basis matrices, the left-hand side of Eq. 8.115 reduces to

$$\frac{dd_{1+}}{dt} \hat{I}_{1+} e^{i\omega_{0,1}t} \quad (8.152)$$

The terms with the non-zero double commutators in the right-hand side of Eq. 8.115 give six integrals

$$\begin{aligned}
\frac{dd_{1+}}{dt} \text{Tr}\{\hat{I}_{1-}\hat{I}_{1+}\} = & -b^2 \left(\int_0^{\infty} \overline{c^{zz}(0)c^{zz}(t)} dt + \frac{3}{4} \int_0^{\infty} \overline{c^{z+}(0)c^{z-}(t)} e^{i\omega_{0,2}t} dt + \frac{3}{4} \int_0^{\infty} \overline{c^{z-}(0)c^{z+}(t)} e^{-i\omega_{0,2}t} dt \right. \\
& \left. + \frac{1}{4} \int_0^{\infty} \overline{c^{+-}(0)c^{-+}(t)} e^{i(\omega_{0,1}-\omega_{0,2})t} dt + \frac{3}{4} \int_0^{\infty} \overline{c^{+z}(0)c^{-z}(t)} e^{i\omega_{0,1}t} dt + \frac{3}{2} \int_0^{\infty} \overline{c^{--}(0)c^{++}(t)} e^{-i(\omega_{0,1}+\omega_{0,2})t} dt \right) d_{1+} \text{Tr}\{\hat{I}_{1-}\hat{I}_{1+}\}. \quad (8.153)
\end{aligned}$$

The same coefficients in both sides of the equation allow us to replace $d_{1+} \text{Tr}\{\hat{I}_{1-}\hat{I}_{1+}\}$ by $\langle M_{1+} \rangle$:

$$\begin{aligned}
\frac{\langle M_{1+} \rangle}{dt} = & -b^2 \left(\int_0^{\infty} \overline{c^{zz}(0)c^{zz}(t)} dt + \frac{3}{4} \int_0^{\infty} \overline{c^{z+}(0)c^{z-}(t)} e^{i\omega_{0,2}t} dt + \frac{3}{4} \int_0^{\infty} \overline{c^{z-}(0)c^{z+}(t)} e^{-i\omega_{0,2}t} dt \right. \\
& \left. + \frac{1}{4} \int_0^{\infty} \overline{c^{+-}(0)c^{-+}(t)} e^{i(\omega_{0,1}-\omega_{0,2})t} dt + \frac{3}{4} \int_0^{\infty} \overline{c^{+z}(0)c^{-z}(t)} e^{i\omega_{0,1}t} dt + \frac{3}{2} \int_0^{\infty} \overline{c^{--}(0)c^{++}(t)} e^{-i(\omega_{0,1}+\omega_{0,2})t} dt \right) \langle M_{1+} \rangle. \quad (8.154)
\end{aligned}$$

Like in the expression for $\Delta\langle M_{1z} \rangle$, the bounds of the integrals can be changed

$$\begin{aligned} \frac{d\langle M_{1+} \rangle}{dt} = & -b^2 \left(\frac{1}{2} \int_{-\infty}^{\infty} \overline{c^{zz}(0)c^{zz}(t)} dt + \frac{3}{8} \int_{-\infty}^{\infty} \overline{c^{z+}(0)c^{z-}(t)} e^{i\omega_{0,2}t} dt + \frac{3}{8} \int_{-\infty}^{\infty} \overline{c^{z-}(0)c^{z+}(t)} e^{-i\omega_{0,2}t} dt \right. \\ & \left. + \frac{1}{8} \int_{-\infty}^{\infty} \overline{c^{+-}(0)c^{+-}(t)} e^{i(\omega_{0,1}-\omega_{0,2})t} dt + \frac{3}{8} \int_{-\infty}^{\infty} \overline{c^{+z}(0)c^{-z}(t)} e^{i\omega_{0,1}t} dt + \frac{3}{4} \int_{-\infty}^{\infty} \overline{c^{--}(0)c^{++}(t)} e^{-i(\omega_{0,1}+\omega_{0,2})t} dt \right) \langle M_{1+} \rangle \end{aligned} \quad (8.155)$$

and the real parts of the integrals can be identified with the spectral density values (assuming $J(\omega) \approx J(-\omega)$), providing the final equation describing relaxation of the transverse magnetization of the first nucleus:

$$\frac{d\langle M_{1+} \rangle}{dt} = -\frac{1}{8}b^2(4J(0)+6J(\omega_{0,2})+J(\omega_{0,1}-\omega_{0,2})+3J(\omega_{0,2})+6J(\omega_{0,1}+\omega_{0,2}))\langle M_{1+} \rangle = -R_{2,1}\langle M_{1+} \rangle = -\left(R_{0,1} + \frac{1}{2}R_{a1}\right)\langle M_{1+} \rangle. \quad (8.156)$$

8.9.6 Two magnetic moments in thermal equilibrium

The initial density matrix describing an ensemble of pairs of nuclear magnetic moments is derived in a similar manner as outlined in Section 7.10.2 for an ensemble of isolated nuclei. Again, we start from the thermal equilibrium and use the Hamiltonian. The difference from the case of isolated nuclei is that Hamiltonian must be represented by a 4×4 density matrix in order to describe a pair of mutually interacting nuclei. If secular approximation is applicable, the matrix representation of the Hamiltonian is diagonal. In general, the Hamiltonian should include effects of the external field \vec{B}_0 , of chemical shifts of both nuclei, and of their coupling. However, the dipolar coupling in isotropic liquids is averaged to zero. It is therefore sufficient to write the total Hamiltonian as

$$\begin{aligned} \hat{H} = & -\gamma_1 B_0(1 + \delta_{i,1})\hat{I}_{1,z} - \gamma_2 B_0(1 + \delta_{i,2})\hat{I}_{2,z} = -\gamma_1 B_0(1 + \delta_{i,1})\frac{\hbar}{2} \begin{pmatrix} 1 & 0 & 0 & 0 \\ 0 & 1 & 0 & 0 \\ 0 & 0 & -1 & 0 \\ 0 & 0 & 0 & -1 \end{pmatrix} - \gamma_2 B_0(1 + \delta_{i,2})\frac{\hbar}{2} \begin{pmatrix} 1 & 0 & 0 & 0 \\ 0 & -1 & 0 & 0 \\ 0 & 0 & 1 & 0 \\ 0 & 0 & 0 & -1 \end{pmatrix} \\ = & \frac{B_0\hbar}{2} \begin{pmatrix} -\gamma_1(1 + \delta_{i,1}) - \gamma_2(1 + \delta_{i,2}) & 0 & 0 & 0 \\ 0 & -\gamma_1(1 + \delta_{i,1}) + \gamma_2(1 + \delta_{i,2}) & 0 & 0 \\ 0 & 0 & +\gamma_1(1 + \delta_{i,1}) - \gamma_2(1 + \delta_{i,2}) & 0 \\ 0 & 0 & 0 & +\gamma_1(1 + \delta_{i,1}) + \gamma_2(1 + \delta_{i,2}) \end{pmatrix} \\ = & \begin{pmatrix} \mathcal{E}_{\alpha\alpha} & 0 & 0 & 0 \\ 0 & \mathcal{E}_{\alpha\beta} & 0 & 0 \\ 0 & 0 & \mathcal{E}_{\beta\alpha} & 0 \\ 0 & 0 & 0 & \mathcal{E}_{\beta\beta} \end{pmatrix}, \end{aligned} \quad (8.157)$$

where the diagonal elements (eigenvalues) are the energies of the eigenstates of a single pair of magnetic moments.

As explained for the isolated nuclei, the off-diagonal elements of the equilibrium density matrix (coherences) are equal to zero. The four diagonal elements (populations) represent statistical weights in the relation describing the expected energy of the ensemble of pairs of coupled magnetic moments

$$\langle E \rangle = P_{\alpha\alpha}\mathcal{E}_{\alpha\alpha} + P_{\alpha\beta}\mathcal{E}_{\alpha\beta} + P_{\beta\alpha}\mathcal{E}_{\beta\alpha} + P_{\beta\beta}\mathcal{E}_{\beta\beta}, \quad (8.158)$$

The values of the populations are obtained as described in Section 7.10.2:

$$P_{\alpha\alpha}^{\text{eq}} = \frac{e^{-\mathcal{E}_{\alpha\alpha}/k_B T}}{e^{-\mathcal{E}_{\alpha\alpha}/k_B T} + e^{-\mathcal{E}_{\alpha\beta}/k_B T} + e^{-\mathcal{E}_{\beta\alpha}/k_B T} + e^{-\mathcal{E}_{\beta\beta}/k_B T}} \approx \frac{1 - \frac{\mathcal{E}_{\alpha\alpha}}{k_B T}}{4}, \quad (8.159)$$

$$P_{\alpha\beta}^{\text{eq}} = \frac{e^{-\mathcal{E}_{\alpha\beta}/k_B T}}{e^{-\mathcal{E}_{\alpha\alpha}/k_B T} + e^{-\mathcal{E}_{\alpha\beta}/k_B T} + e^{-\mathcal{E}_{\beta\alpha}/k_B T} + e^{-\mathcal{E}_{\beta\beta}/k_B T}} \approx \frac{1 - \frac{\mathcal{E}_{\alpha\beta}}{k_B T}}{4}, \quad (8.160)$$

$$P_{\beta\alpha}^{\text{eq}} = \frac{e^{-\mathcal{E}_{\beta\alpha}/k_B T}}{e^{-\mathcal{E}_{\alpha\alpha}/k_B T} + e^{-\mathcal{E}_{\alpha\beta}/k_B T} + e^{-\mathcal{E}_{\beta\alpha}/k_B T} + e^{-\mathcal{E}_{\beta\beta}/k_B T}} \approx \frac{1 - \frac{\mathcal{E}_{\beta\alpha}}{k_B T}}{4}, \quad (8.161)$$

$$P_{\beta\beta}^{\text{eq}} = \frac{e^{-\mathcal{E}_{\beta\beta}/k_B T}}{e^{-\mathcal{E}_{\alpha\alpha}/k_B T} + e^{-\mathcal{E}_{\alpha\beta}/k_B T} + e^{-\mathcal{E}_{\beta\alpha}/k_B T} + e^{-\mathcal{E}_{\beta\beta}/k_B T}} \approx \frac{1 - \frac{\mathcal{E}_{\beta\beta}}{k_B T}}{4}, \quad (8.162)$$

and approximating the exponential terms by their linear expansions

$$P_{\alpha\alpha}^{\text{eq}} \approx \frac{1 - \frac{\mathcal{E}_{\alpha\alpha}}{k_{\text{B}}T}}{4} = \frac{1}{4} + \gamma_1(1 + \delta_{i,1}) \frac{B_0\hbar}{8k_{\text{B}}T} + \gamma_2(1 + \delta_{i,2}) \frac{B_0\hbar}{8k_{\text{B}}T} \approx \frac{1}{4} + \gamma_1 \frac{B_0\hbar}{8k_{\text{B}}T} + \gamma_2 \frac{B_0\hbar}{8k_{\text{B}}T}, \quad (8.163)$$

$$P_{\alpha\beta}^{\text{eq}} \approx \frac{1 - \frac{\mathcal{E}_{\alpha\beta}}{k_{\text{B}}T}}{4} = \frac{1}{4} + \gamma_1(1 + \delta_{i,1}) \frac{B_0\hbar}{8k_{\text{B}}T} - \gamma_2(1 + \delta_{i,2}) \frac{B_0\hbar}{8k_{\text{B}}T} \approx \frac{1}{4} + \gamma_1 \frac{B_0\hbar}{8k_{\text{B}}T} - \gamma_2 \frac{B_0\hbar}{8k_{\text{B}}T}, \quad (8.164)$$

$$P_{\beta\alpha}^{\text{eq}} \approx \frac{1 - \frac{\mathcal{E}_{\beta\alpha}}{k_{\text{B}}T}}{4} = \frac{1}{4} - \gamma_1(1 + \delta_{i,1}) \frac{B_0\hbar}{8k_{\text{B}}T} + \gamma_2(1 + \delta_{i,2}) \frac{B_0\hbar}{8k_{\text{B}}T} \approx \frac{1}{4} - \gamma_1 \frac{B_0\hbar}{8k_{\text{B}}T} + \gamma_2 \frac{B_0\hbar}{8k_{\text{B}}T}, \quad (8.165)$$

$$P_{\beta\beta}^{\text{eq}} \approx \frac{1 - \frac{\mathcal{E}_{\beta\beta}}{k_{\text{B}}T}}{4} = \frac{1}{4} - \gamma_1(1 + \delta_{i,1}) \frac{B_0\hbar}{8k_{\text{B}}T} - \gamma_2(1 + \delta_{i,2}) \frac{B_0\hbar}{8k_{\text{B}}T} \approx \frac{1}{4} - \gamma_1 \frac{B_0\hbar}{8k_{\text{B}}T} - \gamma_2 \frac{B_0\hbar}{8k_{\text{B}}T}. \quad (8.166)$$

$$(8.167)$$

Lecture 9

Two-dimensional spectroscopy, NOESY

Literature: A very nice explanation of the principles of two-dimensional spectroscopy can be found in K8.1–K8.2. The idea of 2D spectroscopy, but for a different type of experiment (COSY) is also presented in C4.1, L5.6 and L5.9.

9.1 Two-dimensional spectroscopy

NMR spectroscopy based on application of short radio-wave pulses gives us an opportunity to display frequencies of multiple magnetic moments in multiple dimensions of a single multidimensional spectrum. The great advantage of this approach is the possibility to immediately see various *correlations* among the observed nuclear magnetic moments and use this information in the structural analysis of the studied molecule. When working with large molecules (proteins, nucleic acids), spectra with three and more frequency dimensions are recorded routinely. In our course, we analyze only two-dimensional experiments, but we try to understand in detail how various correlations of interacting magnetic moments are encoded in the spectra. Before we reach this point, we have to learn the basic principle.

In order to explain principles of 2D spectroscopy, we first analyze an experiment consisting of three 90° pulses and two delays preceding the data acquisition. Later we learn that this experiment is abbreviated NOESY and serves as a source of information about interatomic distances, but now we use it just as a simple example. Application of three radio-wave pulse is already an advanced experimental approach, deserving a clear formal presentation. The experiment can be described as

$${}_a(\pi/2)_{x_b} - t_1 - {}_c(\pi/2)_{x_d} - \tau_m - {}_e(\pi/2)_{x_f} - t_2(\text{acquire}).$$

However, a pictorial representation shown in Figure 9.1 is more usual and practical.

In the drawing presented in Figure 9.1, each application of radio waves is represented by a black rectangle. In our experiments, all rectangles have the same width because all pulses have the same duration. Later we discuss experiments that combine 90° and 180° . In schemes of such experiments, 90° and 180° pulses are represented by narrow and wide rectangles, respectively. Durations of the delays between the pulses are described by time variables t_1 and τ_m , the time-dependence of the acquired signal is labeled t_2 . In our analysis, we describe the density matrix just before and after pulses, as indicated by arrows labeled by letters "a" to "f" in Figure 9.1.

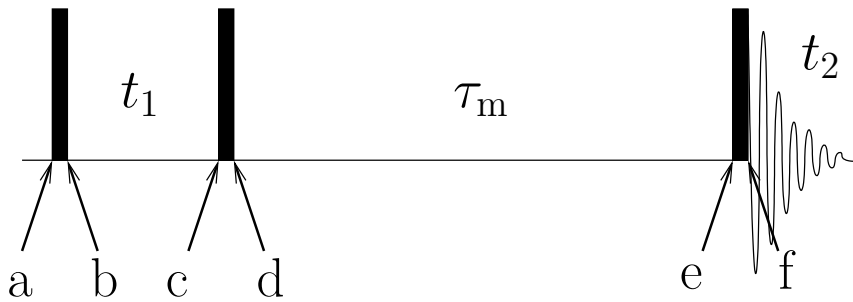


Figure 9.1: Schematic drawing of a two-dimensional NMR experiment.

9.2 Evolution in the absence of dipolar coupling

We start with an analysis for two non-interacting magnetic moments, e.g. of two protons that have different chemical shift $\delta_{i,1}$ and $\delta_{i,2}$, and are far from each other in a molecule.¹ The pair of protons is an example of a homonuclear system, where all nuclei have the same magnetogyric ratio γ . Before we analyze evolution of the density matrix in a 2D experiment, we must define its initial form. Like in the case of the isolated nuclear magnetic moments, we assume that the experiments starts from thermal equilibrium. Therefore, we use $\hat{\rho}^{\text{eq}}$, derived in Sections 8.8 and 8.9.6, as $\hat{\rho}(t=0)$. Since we have neglected the very small effect of different chemical shifts in Eq. 8.40, the values of κ are also the same for both protons. As in the one-pulse experiment, we follow the coherent evolution of $\hat{\rho}$ step-by-step, and add the effect of relaxation *ad hoc*.

- $\hat{\rho}(a) = \frac{1}{2}\mathcal{I}_t + \frac{1}{2}\kappa(\mathcal{I}_{1z} + \mathcal{I}_{2z})$

We start from the thermal equilibrium described by Eq. 8.40. Note that the matrices are different than for the single-spin mixed state, but the constant is the same. Moreover, only $\mathcal{I}_t, \mathcal{I}_{1z}, \mathcal{I}_{2z}$ contribute to $\hat{\rho}(a)$. If the magnetic moments do not interact, no $2\mathcal{I}_{1j}\mathcal{I}_{2k}$ operator (where $j, k \in x, y, z$) contributes to any Hamiltonian. As a consequence, the \mathcal{I}_{1z} and \mathcal{I}_{2z} components of the density matrix evolve separately, following the same rules as described for \mathcal{I}_z . Therefore, we can use Eq. 6.11 to analyze the evolution, we just repeat the analysis twice for \mathcal{I}_{1z} and \mathcal{I}_{2z} , treating both as \mathcal{I}_z in Eq. 6.11.

- $\hat{\rho}(b) = \frac{1}{2}\mathcal{I}_t + \frac{1}{2}\kappa(-\mathcal{I}_{1y} - \mathcal{I}_{2y})$

Here we describe the effect of the 90° pulse. For detailed analysis, see the one-pulse experiment.

- $\hat{\rho}(c) = \frac{1}{2}\mathcal{I}_t + \frac{1}{2}\kappa(-\cos(\Omega_1 t_1)\mathcal{I}_{1y} + \sin(\Omega_1 t_1)\mathcal{I}_{1x} - \cos(\Omega_2 t_1)\mathcal{I}_{2x} + \sin(\Omega_2 t_1)\mathcal{I}_{2y})$

Here we describe evolution during t_1 exactly as in the one-pulse experiment. To keep the equations short, we replace the goniometric terms describing the evolution by (time-dependent) coefficients c_{11}, c_{21}, s_{11} , and s_{21} :

$$\hat{\rho}(c) = \frac{1}{2}\mathcal{I}_t + \frac{1}{2}\kappa(-c_{11}\mathcal{I}_{1y} + s_{11}\mathcal{I}_{1x} - c_{21}\mathcal{I}_{2y} + s_{21}\mathcal{I}_{2x})$$

The coefficients c_{11}, c_{21}, s_{11} , and s_{21} deserve some attention. First, note that the first subscript specifies the nucleus and the second subscript specifies the time period (so-far, it is always 1

¹Protons in propynal (H-C≡C-CO-H) may serve as an example.

because we have analyzed only evolution during t_1). Second, we include the effect of relaxation into the coefficients:

$$\begin{aligned} c_{11} &\rightarrow e^{-R_{2,1}t_1} \cos(\Omega_1 t_1) & s_{11} &\rightarrow e^{-R_{2,1}t_1} \sin(\Omega_1 t_1) \\ c_{21} &\rightarrow e^{-R_{2,2}t_1} \cos(\Omega_2 t_1) & s_{21} &\rightarrow e^{-R_{2,2}t_1} \sin(\Omega_2 t_1) \end{aligned}$$

- $\hat{\rho}(d) = \frac{1}{2}\mathcal{I}_t + \frac{1}{2}\kappa(-c_{11}\mathcal{I}_{1z} + s_{11}\mathcal{I}_{1x} - c_{21}\mathcal{I}_{2z} + s_{21}\mathcal{I}_{2x})$

Here we analyze the effect of the second 90° pulse, similarly to the step a \rightarrow b. The x -pulse does not affect the x magnetization, but rotates the $-y$ magnetization further to $-z$. The final magnetization is parallel with \vec{B}_0 , but the equilibrium polarization is inverted.

- $\hat{\rho}(e) = ?$

This is a new case, it should be analyzed carefully. Here we perform the analysis for a large molecule such as a small protein: In proteins, M_x, M_y relax with $R_2 > 10\text{s}^{-1}$ and M_z with $R_1 \approx 1\text{s}^{-1}$. The delay τ_m is usually longer than 0.1 s. Let us assume $\tau_m = 0.2\text{s}$ and $R_2 = 20\text{s}^{-1}$. After 0.2 s, $e^{-R_2\tau_m} = e^{-20 \times 0.2} = e^{-4} \approx 0.02$. We see that M_x, M_y relaxes almost completely. Therefore, $\mathcal{I}_{1x}, \mathcal{I}_{1y}, \mathcal{I}_{2x}, \mathcal{I}_{2y}$ can be neglected. On the other hand, $e^{-R_1\tau_m} = e^{-1 \times 0.2} = e^{-0.2} \approx 0.82$. We see that M_z does not relax too much. Therefore, we continue analysis with $\mathcal{I}_{1z}, \mathcal{I}_{2z}$. The $\mathcal{I}_{1z}, \mathcal{I}_{2z}$ terms do not evolve because they commute with $\mathcal{H} = \Omega_1\mathcal{I}_{1z} + \Omega_2\mathcal{I}_{2z}$. Consequently,

$$\hat{\rho}(e) = \frac{1}{2}\mathcal{I}_t + \frac{1}{2}\kappa(-e^{-R_1\tau_m}c_{11}\mathcal{I}_{1z} - e^{-R_1\tau_m}c_{21}\mathcal{I}_{2z}) = \frac{1}{2}\mathcal{I}_t - \mathcal{A}_1\mathcal{I}_{1z} - \mathcal{A}_2\mathcal{I}_{2z}.$$

We further simplified the notation by introducing the factors \mathcal{A}_1 and \mathcal{A}_2 . Again, we include the relaxation effects into \mathcal{A}_1 and \mathcal{A}_2 when we express the measurable signal:

$$\begin{aligned} \mathcal{A}_1 &\rightarrow \frac{\kappa}{2}e^{-R_{1,1}\tau_m}c_{11} = \frac{\kappa}{2}e^{-R_{1,1}\tau_m}e^{-R_{2,1}t_1} \cos(\Omega_1 t_1) \\ \mathcal{A}_2 &\rightarrow \frac{\kappa}{2}e^{-R_{1,2}\tau_m}c_{21} = \frac{\kappa}{2}e^{-R_{1,2}\tau_m}e^{-R_{2,2}t_1} \cos(\Omega_2 t_1) \end{aligned}$$

- $\hat{\rho}(f) = \frac{1}{2}\mathcal{I}_t + \mathcal{A}_1\mathcal{I}_{1y} + \mathcal{A}_2\mathcal{I}_{2y}$

Here we analyze the effect of the third pulse, in the same manner as we analyzed the first pulse.

- $\hat{\rho}(t_2) = \frac{1}{2}\mathcal{I}_t + \mathcal{A}_1(\cos(\Omega_1 t_2)\mathcal{I}_{1y} - \sin(\Omega_1 t_2)\mathcal{I}_{1x}) + \mathcal{A}_2(\cos(\Omega_2 t_2)\mathcal{I}_{2y} - \sin(\Omega_2 t_2)\mathcal{I}_{2x})$

In the last step, we analyze evolution during the data acquisition.

9.3 Signal modulation in a two-dimensional experiment

Having $\hat{\rho}(t_2)$, we can calculate $\langle M_+ \rangle$. As the size of the matrices increased, it is more convenient to use the orthonormality of the basis than to calculate all matrix products.² It follows from the definition of orthonormal matrices that for the two-spin matrices

$$\text{Tr}\{\mathcal{I}_{nx}(\mathcal{I}_{nx} + i\mathcal{I}_{ny})\} = 1, \quad (9.1)$$

$$\text{Tr}\{\mathcal{I}_{ny}(\mathcal{I}_{nx} + i\mathcal{I}_{ny})\} = i, \quad (9.2)$$

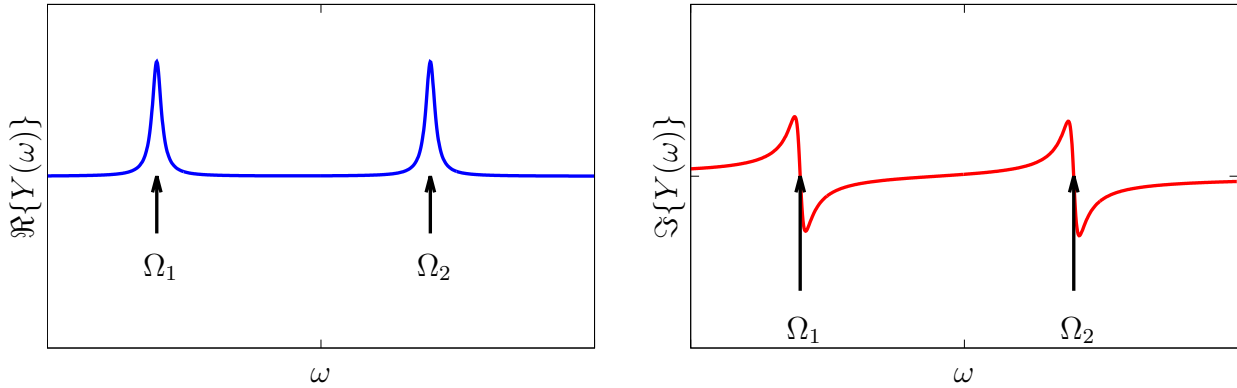
²Orthonormality for a set of matrices \hat{A}_j is defined as $\text{Tr}\{\hat{A}_j^\dagger \hat{A}_k\} = \delta_{jk}$, where $\delta_{jk} = 1$ for $j = k$, $\delta_{jk} = 0$ for $j \neq k$, and \hat{A}_j^\dagger is an adjoint matrix of \hat{A}_j , i.e., matrix obtained from \hat{A}_j by exchanging rows and columns and replacing all numbers with their complex conjugates.

and traces of products with other matrices are zero. Applying the orthonormality relations to the product of \hat{M}_+ with the obtained $\hat{\rho}(t_2)$ and introducing relaxation, we get

$$\begin{aligned}
\langle M_+ \rangle &= \text{Tr}\{\hat{\rho}(t_2)\hat{M}_+\} \\
&= \mathcal{N}\gamma\hbar \left(\mathcal{A}_1(e^{-R_{2,1}t_2} \cos(\Omega_1 t_2) \text{Tr}\{\mathcal{I}_{1y}(\mathcal{I}_{1+} + \mathcal{I}_{2+})\} - e^{-R_{2,1}t_2} \sin(\Omega_1 t_2) \text{Tr}\{\mathcal{I}_{1x}(\mathcal{I}_{1+} + \mathcal{I}_{2+})\}) \right. \\
&\quad \left. + \mathcal{A}_2(e^{-R_{2,2}t_2} \cos(\Omega_2 t_2) \text{Tr}\{\mathcal{I}_{2y}(\mathcal{I}_{1+} + \mathcal{I}_{2+})\} - e^{-R_{2,2}t_2} \sin(\Omega_2 t_2) \text{Tr}\{\mathcal{I}_{2x}(\mathcal{I}_{1+} + \mathcal{I}_{2+})\}) \right) \\
&= \mathcal{N}\gamma\hbar\mathcal{A}_1 \left(e^{-R_{2,1}t_2} \cos(\Omega_1 t_2) - \frac{i}{2}e^{-R_{2,1}t_2} \sin(\Omega_1 t_2) \right) \\
&\quad + \mathcal{N}\gamma\hbar\mathcal{A}_2 \left(e^{-R_{2,2}t_2} \cos(\Omega_2 t_2) - \frac{i}{2}e^{-R_{2,2}t_2} \sin(\Omega_2 t_2) \right). \tag{9.3}
\end{aligned}$$

Note that the resulting phase is shifted by $\pi/2$ similarly to Eq. 7.28, but in the opposite direction. After applying the phase correction, Fourier transform of the signal provides spectrum in the form (cf. Eq. 7.30)

$$\mathcal{N}\gamma\hbar \left(\left(\frac{\mathcal{A}_1 R_{2,1}}{R_{2,1}^2 + (\omega - \Omega_1)^2} + \frac{\mathcal{A}_2 R_{2,2}}{R_{2,2}^2 + (\omega - \Omega_2)^2} \right) - i \left(\frac{\mathcal{A}_1(\omega - \Omega_1)}{R_{2,1}^2 + (\omega - \Omega_1)^2} + \frac{\mathcal{A}_2(\omega - \Omega_2)}{R_{2,2}^2 + (\omega - \Omega_2)^2} \right) \right). \tag{9.4}$$



In the one-dimensional experiment, \mathcal{A}_1 and \mathcal{A}_2 just scale the peak height. However, they depend on the length of the delay t_1 in our two-dimensional experiment. If the measurement is repeated many times and t_1 is increased by an increment Δt each time, the obtained series of 1D spectra is *amplitude modulated* by $c_{11} = e^{-R_{2,1}t_2} \cos(\Omega_1 t_1)$ and $c_{21} = e^{-R_{2,2}t_2} \cos(\Omega_2 t_1)$. Since the data are stored in a computer in a digital form, they can be treated as a two-dimensional array (table), depending on the real time t_2 in one direction and on the length of the incremented delay t_1 in the other directions. These directions are referred to as the *direct dimension* and the *indirect dimension*. The Fourier transformation can be performed in each dimension providing *direct frequency dimension* and *indirect frequency dimension*.

Since we acquire signal as a series of complex numbers, it is useful to introduce the complex numbers in the indirect dimension as well. It is possible e.g. by repeating the measurement twice for

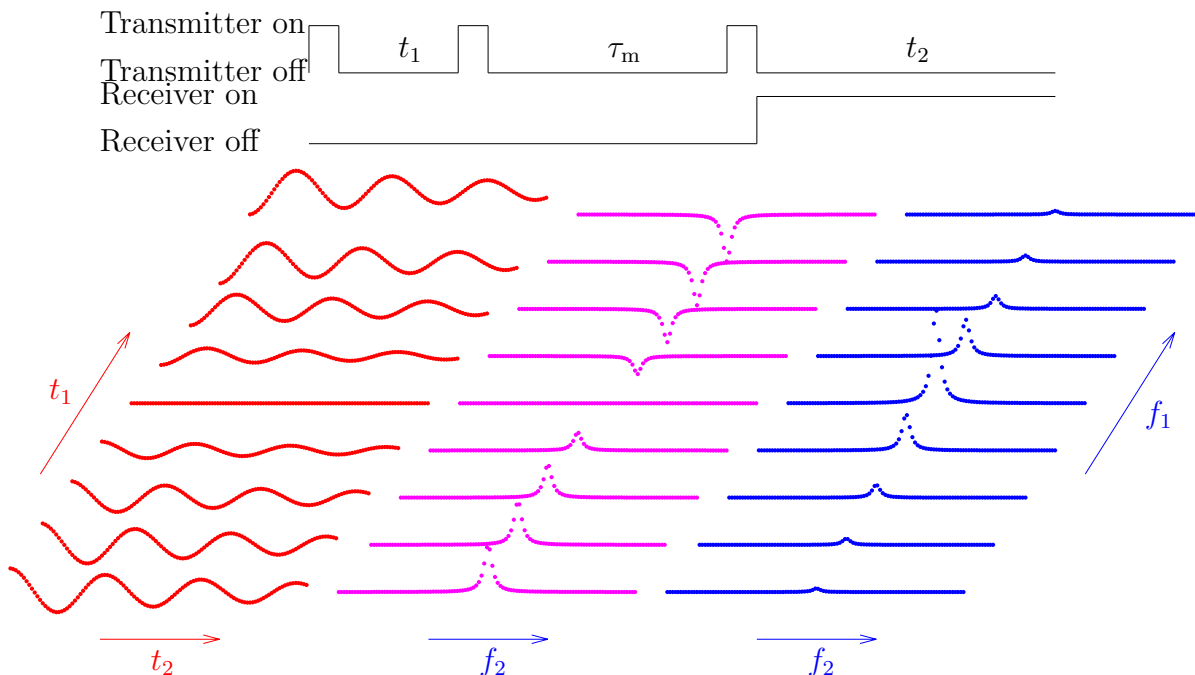


Figure 9.2: Principle of two-dimensional spectroscopy (experiment NOESY). The acquired signal is shown in red, the signal after the Fourier transformation in the direct dimension is shown in magenta, and the signal after the Fourier transformation in both dimensions is shown in blue.

each value of t_1 , each time with a different phase of the radio waves applied during the second pulse. First we acquire the signal with the second pulse applied with the same phase as the first pulse. Such a phase is labeled x in the NMR literature. Then, we repeat the acquisition with the phase of the radio waves shifted by 90° during the second pulse. Such a phase is labeled y in the literature. The former case was already analyzed above. In the latter case, the \mathcal{I}_{1y} and \mathcal{I}_{2y} components are not affected and relax during τ_m , while the \mathcal{I}_{1x} and \mathcal{I}_{2x} are rotated to $-\mathcal{I}_{1z}$ and $-\mathcal{I}_{2z}$, respectively, and converted to the measurable signal by the third pulse. Because the \mathcal{I}_{1x} and \mathcal{I}_{2x} coherences are modulated by s_{11} and s_{21} , \mathcal{A}_1 and \mathcal{A}_2 oscillate as a sine function, not a cosine function, in the even spectra. So, we obtain cosine modulation in odd spectra and sine modulation in even spectra. The cosine- and sine- signals are then treated as the real and imaginary component of the complex signal in the indirect dimension. Complex Fourier transformation in both dimensions provides a two-dimensional *hypercomplex* spectrum, with each point described by two complex numbers. The advantage of such spectrum is that the positive and negative values of the frequency offset can be distinguished in both dimensions. The method described in this paragraph was introduced by States, Haberkorn, and Ruben. In practice, other methods are also used to discriminate the positive and negative frequency offsets in the indirect dimension, but they are not described here.

9.4 NOESY

If the two-dimensional spectra looked exactly as described in the preceding section, they would not be very useful because they would not bring any new information. The same frequencies would be measured in the direct and indirect dimension and all peaks would be found along the diagonal of the spectrum. What makes the experiment really useful is the interaction between magnetic moments during τ_m . Such approach is known as Nuclear Overhauser effect spectroscopy (NOESY) and is used frequently to measure distances between protons in molecules.

As described by Eq. 8.33, relaxation of nucleus 1 is influenced by the state of nucleus 2 (and vice versa):

$$-\frac{d\Delta\langle M_{1z} \rangle}{dt} = R_{a1}\Delta\langle M_{1z} \rangle + R_x\Delta\langle M_{2z} \rangle \quad (9.5)$$

$$-\frac{d\Delta\langle M_{2z} \rangle}{dt} = R_{a2}\Delta\langle M_{2z} \rangle + R_x\Delta\langle M_{1z} \rangle. \quad (9.6)$$

This set of equations is solved and the solution is analyzed in Section 9.5.1. The analysis shows that the amplitudes \mathcal{A}_1 and \mathcal{A}_2 depend on *both frequencies* Ω_1 and Ω_2 (contain both c_{11} and c_{21}). Therefore, the spectrum contains both diagonal peaks (with the frequencies of the given magnetic moment in both dimensions) and off-diagonal *cross-peaks* (with the frequencies of the given magnetic moment in the direct dimension and the frequency of its interaction partner in the indirect dimension³).

The presence of the cross-peaks provides very useful *qualitative information* about the studied molecules. It tells us which nuclei are close in space. Such knowledge of spatial proximity often allows us to assign measured frequencies to the hydrogen atoms in the studied molecule. But we often go further and analyze the intensities of the cross-peaks *quantitatively*. As shown in Section 9.5.2, the height of the NOESY cross-peaks Y_{\max} depends on two factors: on the dynamics of the molecule and on the distance of the interacting nuclei. Depending on the motions on the molecules, the peak height can be positive or negative. If the molecular motions are slow the cross-peaks have the same sign as diagonal peaks. However, if the molecular motions are fast (e.g., if the molecule is small), the sign is opposite. Obviously, there is a range of molecular motions that make the peak height close to zero. In such case, other NMR techniques than NOESY should be applied. If the dynamics of the molecule is favorable (sufficiently fast or slow), the dependence on the distance between the interacting nuclei can be used to estimate distances in the molecule. For short τ_m , the cross-peak height is approximately proportional to r^{-6} . The studied molecules (especially large molecules like proteins or nucleic acid fragments) often contain pairs of protons with a well-defined geometry. For example, the distance between geminal protons in the CH_2 group is 0.17 nm, distances between protons in the *ortho*- and *meta*- positions in aromatic rings are 0.25 nm and 0.42 nm, respectively. Such distances can be used as a reference for the measurement of unknown distances. If we assume that two protons have a similar dynamics as a reference pair of protons, the ratio of the heights⁴ of the cross-peaks of the investigated and reference proton pairs is

³The direct and indirect dimensions are defined in Section 9.3

⁴Volume (integral) of the peak gives more accurate distances because it is not influenced by the relaxation during measurement. On the other hand, measurement of peak volumes may be difficult in crowded spectra of large molecules.

$$\frac{Y_{\max}}{Y_{\max,\text{ref}}} = \left(\frac{r_{\text{ref}}}{r}\right)^6. \quad (9.7)$$

Therefore, the unknown distance r can be calculated as

$$r = r_{\text{ref}} \sqrt[6]{\frac{Y_{\max,\text{ref}}}{Y_{\max}}}. \quad (9.8)$$

It is quite remarkable that the dipole-dipole interaction allows us to measure distances nine orders of magnitude shorter than the wave length of the used electromagnetic waves.

HOMework

Analyze the intensities of the NOESY cross-peaks (Sections 9.4, 9.5.1, and 9.5.2, using Eq. 8.33 from Section 8.7.)

9.5 DERIVATIONS

9.5.1 Quantitative analysis of cross-relaxation in NOESY

As described by Eq. 8.33, relaxation of nucleus 1 is influenced by the state of nucleus 2 (and vice versa):

$$-\frac{d\Delta\langle M_{1z} \rangle}{dt} = R_{a1}\Delta\langle M_{1z} \rangle + R_x\Delta\langle M_{2z} \rangle \quad (9.9)$$

$$-\frac{d\Delta\langle M_{2z} \rangle}{dt} = R_{a2}\Delta\langle M_{2z} \rangle + R_x\Delta\langle M_{1z} \rangle. \quad (9.10)$$

The analysis greatly simplifies if the auto-relaxation rates are identical for both magnetic moments.⁵ Then,

$$-\frac{d\Delta\langle M_{1z} \rangle}{dt} = R_a\Delta\langle M_{1z} \rangle + R_x\Delta\langle M_{2z} \rangle, \quad (9.11)$$

$$-\frac{d\Delta\langle M_{2z} \rangle}{dt} = R_a\Delta\langle M_{2z} \rangle + R_x\Delta\langle M_{1z} \rangle. \quad (9.12)$$

Such set of differential equations can be solved easily e.g. by the substitutions $\Delta_+ = \Delta\langle M_{1z} \rangle + \Delta\langle M_{2z} \rangle$ and $\Delta_- = \Delta\langle M_{2z} \rangle - \Delta\langle M_{1z} \rangle$. The result is

$$\Delta_+ = \Delta_+(0)e^{-(R_a+R_x)t}, \quad (9.13)$$

$$\Delta_- = \Delta_-(0)e^{-(R_a-R_x)t}. \quad (9.14)$$

Returning back to $\Delta\langle M_{1z} \rangle$ and $\Delta\langle M_{2z} \rangle$,

$$\Delta\langle M_{1z} \rangle = ((1-\zeta)\Delta\langle M_{1z} \rangle(0) + \zeta\Delta\langle M_{2z} \rangle(0))e^{-(R_a+R_x)t}, \quad (9.15)$$

$$\Delta\langle M_{2z} \rangle = ((1-\zeta)\Delta\langle M_{2z} \rangle(0) + \zeta\Delta\langle M_{1z} \rangle(0))e^{-(R_a+R_x)t}, \quad (9.16)$$

where $\zeta = (1 - e^{2R_x t})/2$. Therefore, the amplitudes \mathcal{A}_1 and \mathcal{A}_2 in our two-dimensional experiment are

$$\mathcal{A}_1 = \frac{\kappa}{2}((1-\zeta)c_{11} + \zeta c_{21})e^{-(R_a+R_x)\tau_m}, \quad (9.17)$$

$$\mathcal{A}_2 = \frac{\kappa}{2}((1-\zeta)c_{21} + \zeta c_{11})e^{-(R_a+R_x)\tau_m}. \quad (9.18)$$

9.5.2 Intensity of NOESY cross-peaks

The intensity (measured as peak height or peak integral, i.e., volume) of the cross-peaks is proportional to the amplitudes \mathcal{A}_1 and \mathcal{A}_2 . Here we analyze how \mathcal{A}_1 and \mathcal{A}_2 decay during τ_m . The overall loss of signal ("leakage") due to the R_1 relaxation is given by $e^{-(R_a-R_x)\tau_m}$ and intensities of the cross-peaks are given by the factor

$$\zeta e^{-(R_a+R_x)\tau_m} = -\frac{1}{2}(e^{R_x\tau_m} - e^{-R_x\tau_m})e^{-R_a\tau_m}. \quad (9.19)$$

For short τ_m , $e^{R_x\tau_m} - e^{-R_x\tau_m} \approx 1 + R_x\tau_m - 1 + R_x\tau_m$ and $e^{-R_a\tau_m}$ is close to one. Therefore, the expression describing the cross-peak intensities can be approximated as

$$-\frac{1}{2}(e^{R_x\tau_m} - e^{-R_x\tau_m})e^{-R_a\tau_m} \approx -R_x\tau_m \quad (9.20)$$

and R_x can be expressed explicitly using Eqs. 8.33 and 8.36

$$-\frac{1}{2}(e^{R_x\tau_m} - e^{-R_x\tau_m})e^{-R_a\tau_m} \approx -R_x\tau_m = \left(\frac{\mu_0}{8\pi}\right)^2 \frac{\gamma^4 \hbar^2}{r^6} (J(0) - 6J(2\omega_0))\tau_m, \quad (9.21)$$

where the difference of the precession frequencies due to different chemical shifts was neglected (assuming $\omega_{0,1} = \omega_{0,2} = \omega_0$ because $\gamma_1 = \gamma_2$ and $|\omega_{0,1} - \omega_{0,2}|$ is $\sim 10^{-5}\omega_{0,1}$ or lower). The obtained result shows that the cross-peak intensity is proportional to r^{-6} and

⁵This is a reasonable assumption for protons with similar dynamics and in similar chemical environment.

to $J(0) - 6J(2\omega_0)$ in the linear approximation. In order to investigate the impact of the dependence on $J(0) - 6J(2\omega_0)$, we calculate the spectral density function for a simple correlation function of a rigid spherical molecule (Eq. 2.3):

$$J(\omega) = \Re \left\{ \int_{-\infty}^{\infty} \frac{1}{5} e^{-t/\tau_C} e^{-i\omega t} dt \right\} = 2\Re \left\{ \int_0^{\infty} \frac{1}{5} e^{-\frac{i\omega\tau_C+1}{\tau_C}t} dt \right\} = \frac{2}{5} \Re \left\{ \frac{\tau_C}{i\omega\tau_C + 1} \right\} = \frac{2}{5} \Re \left\{ \frac{\tau_C}{1 + i\omega\tau_C} \frac{1 - i\omega\tau_C}{1 - i\omega\tau_C} \right\} = \frac{2}{5} \frac{\tau_C}{1 + (\omega\tau_C)^2}. \quad (9.22)$$

Setting $\omega = 0$, we obtain $J(0) = \frac{2}{5}\tau_C$.

If the molecular motions are slow, τ_C is long and $2\omega_0\tau_C \gg 1 \Rightarrow J(2\omega_0) \ll \frac{2}{5}\tau_C \Rightarrow J(0) > 6J(2\omega_0)$. Therefore the cross-peak intensity proportional to $J(0) - 6J(2\omega_0)$ is positive (i.e., cross-peaks have the same sign as diagonal peaks).

If the molecular motions are fast, $2\omega_0\tau_C \ll 1 \Rightarrow J(2\omega_0) \approx \frac{2}{5}\tau_C \Rightarrow J(0) = \frac{2}{5}\tau_C < 6J(2\omega_0) \approx 6 \times \frac{2}{5}\tau_C$. Therefore the cross-peak intensity proportional to $J(0) - 6J(2\omega_0)$ is negative (i.e., cross-peaks and diagonal peaks have the opposite sign).

Lecture 10

J -coupling, spin echoes

Literature: The through-bond coupling (J -coupling) is described in L14 and L15, the Hamiltonian is presented in L9.4 and J -coupled spins are described in L14.2, L14.3, and L14.5. Spin echoes are nicely described in K7.8 and also presented in LA.10.

10.1 Through-bond coupling

Magnetic moments of nuclei connected by covalent bonds interact also indirectly, via interactions with magnetic moments of the electrons of the bonds. This type of interaction is known as J -coupling, *through-bond coupling*, or *indirect spin-spin coupling*. A magnetic moment μ_2 is a source of a magnetic field that perturbs the distribution of electrons. Such a distortion (perturbation of the electron spin states or modification of electron orbital magnetic moments by altering the magnetic field felt by the electrons) modifies a magnetic field at the site of μ_1 . The fact that such indirect interaction exists is itself not surprising. But it is less obvious (and was surprising when first observed) why the indirect interaction *is not averaged to zero* in isotropic liquids. Before we discuss this mystery, we write down a general form of a Hamiltonian representing a contribution of the coupling to the magnetic energy of a pair of interacting nuclear magnetic moments. For example, if nucleus 2 generates (indirectly, via interactions with the electrons as described above) a field \vec{B}_2 at the site of nucleus 1, then coupling with $\vec{\mu}_2$ contributes to the energy of the magnetic moment $\vec{\mu}_1$ by $-\vec{\mu}_1 \cdot \vec{B}_2$. In general, each component of the field felt by magnetic moment 1 (e.g. of ^1H) depends on all components of the magnetic moment 2 (e.g. of ^{13}C), similarly to the through-space dipole-dipole coupling. Therefore, the interaction is described by a tensor (like chemical shift or dipolar coupling):

$$\begin{aligned} \hat{H}_J &= -\gamma(\hat{I}_{x1}B_{2,x} + \hat{I}_{y1}B_{2,y} + \hat{I}_{z1}B_{2,z}) = -\gamma(\hat{I}_{1x} \hat{I}_{1y} \hat{I}_{1z}) \begin{pmatrix} B_{2,x} \\ B_{2,y} \\ B_{2,z} \end{pmatrix} = \\ &= 2\pi(\hat{I}_{1x} \hat{I}_{1y} \hat{I}_{1z}) \begin{pmatrix} J_{xx} & J_{xy} & J_{xz} \\ J_{yx} & J_{yy} & J_{yz} \\ J_{zx} & J_{zy} & J_{zz} \end{pmatrix} \begin{pmatrix} \hat{I}_{1x} \\ \hat{I}_{1y} \\ \hat{I}_{1z} \end{pmatrix} = 2\pi\hat{I}_1 \cdot \underline{J} \cdot \hat{I}_2. \end{aligned} \quad (10.1)$$

To proceed, we should investigate the physical origin of the interaction. As briefly discussed in Section 10.9.1, the major contribution to the J -coupling in most molecules is an interaction

mediated by electrons occurring *at the same positions* as the nuclei. Obviously, interaction of such electrons with the nuclei does not change as the molecule rotates. As a consequence, the J -tensor has a dominant isotropic (orientation-independent) component, whereas the anisotropic part is usually small (and difficult to distinguish from the dipolar coupling). Therefore, only the isotropic component of the tensor is considered and the anisotropic component is neglected in practice. The isotropic component is defined as described in Section 1.5.3 for the chemical shift tensor.¹

$$2\pi \begin{pmatrix} J_{XX} & 0 & 0 \\ 0 & J_{YY} & 0 \\ 0 & 0 & J_{ZZ} \end{pmatrix} = 2\pi \frac{J_{XX} + J_{YY} + J_{ZZ}}{3} \begin{pmatrix} 1 & 0 & 0 \\ 0 & 1 & 0 \\ 0 & 0 & 1 \end{pmatrix} = 2\pi J \begin{pmatrix} 1 & 0 & 0 \\ 0 & 1 & 0 \\ 0 & 0 & 1 \end{pmatrix}. \quad (10.2)$$

The unit matrix tells us that we can replace the tensor \underline{J} (represented by a 3 matrix) in the Hamiltonian by a *scalar* value (single number) J . Accordingly, the J -coupling is often called *scalar coupling* (implying that the anisotropic component is neglected). The value of the constant J can be positive or negative, depends on the actual distribution of electrons, and its calculation requires advanced quantum chemistry methods. The factor of 2π reflects the convention to express J in the units of Hz. Note that the J -coupling does not depend on the external magnetic field \vec{B}_0 . Therefore, it does not make sense to express J in relative units (ppm). Proton-proton J -coupling is significant (exceeding 10 Hz) up to three bonds and observable for 4 or 5 bonds in special cases (planar geometry like in aromatic systems). Interactions of other nuclei are weaker, but the one-bond couplings are always significant (as strong as 700 Hz for ^{31}P - ^1H , 140 Hz to 200 Hz for ^{13}C - ^1H , -90 Hz for ^{15}N - ^1H in amides, 30 Hz to 60 Hz for ^{13}C - ^{13}C , -10 Hz to -15 Hz for ^{13}C - ^{15}N). Typical values of two-bond (2J) and three-bond (3J) ^1H - ^1H couplings are -15 Hz and 0 Hz to 20 Hz, respectively. As the value of J is given by the distribution of electrons in bonds, it reports the local geometry of the molecule. In particular, three-bond scalar couplings can be used to measure torsion angles in molecules.

10.2 Secular approximation, averaging, and relaxation

If the anisotropic part of the J -tensor is neglected, the J -coupling does not depend on orientation (*scalar* coupling) and no ensemble averaging is needed. The secular approximation is applied like in the case of the dipolar coupling.

¹Note that it is sufficient to consider only the average of the diagonal elements of the tensor $J = (J_{XX} + J_{YY} + J_{ZZ})/3$ if the anisotropy $(2J_{ZZ} - J_{YY} - J_{XX})/6$ and rhombicity $(J_{XX} - J_{YY})/2$ are equal to zero.

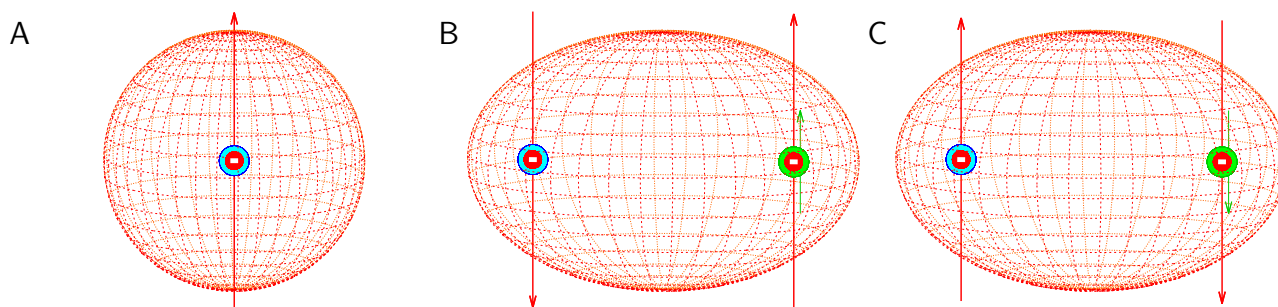


Figure 10.1: J -coupling. A, probability of finding an electron in the hydrogen atom at particular coordinates is described by the probability density ρ . The probability density described by the orbital $1s$ (depicted as a sphere) has non-zero value at the position of the nucleus (shown in cyan). Therefore, there is a non-zero probability of finding electron (red circle) exactly at the site of the nucleus. The field produced at the site of the nucleus by the electron's magnetic moment (red arrow) does not depend on the orientation of the atom if the positions of the nucleus and electron coincide. Therefore, the interaction of the nucleus with the electron is not averaged to zero if the atom rotates isotropically. B and C, the probability density described by the sigma orbitals (depicted as an ellipsoid) in molecules has also non-zero values at the sites of nuclei. The spin state of the electrons in the bonding sigma orbital is a superposition of the $|\alpha\rangle \otimes |\beta\rangle$ and $|\beta\rangle \otimes |\alpha\rangle$ eigenstates (indicated by the opposite direction of the red arrows), perturbed by the magnetic moment of the nuclei. The parallel orientations of magnetic moments is energetically favorable for a nucleus and an electron sharing its position.

The Hamiltonian of *scalar coupling*, i.e., of J -coupling with the small anisotropic contribution neglected, has one of the following forms.

- In the case of magnetic moments with the same γ and chemical shift, precessing about the z axis with the same precession frequency,

$$\hat{H}_J = \pi J \left(2\hat{I}_{1z}\hat{I}_{2z} + 2\hat{I}_{1x}\hat{I}_{2x} + 2\hat{I}_{1y}\hat{I}_{2y} \right). \quad (10.3)$$

- In the case of magnetic moments with different γ and/or chemical shift, precessing about the z axis with different precession frequencies,

$$\hat{H}_J = 2\pi J\hat{I}_{1z}\hat{I}_{2z} = \pi J \left(2\hat{I}_{1z}\hat{I}_{2z} \right). \quad (10.4)$$

In principle, the anisotropic part of the J -tensor would contribute to relaxation like the anisotropic part of the chemical shift tensor, but it is small and usually neglected. The scalar coupling (described by the isotropic part of the J -tensor) does not depend on the orientation. Therefore, it can contribute to the relaxation only through a conformational or chemical exchange. Conformational effects are usually small: one-bond and two-bond couplings do not depend on torsion angles and three-bond coupling constants are small. In summary, relaxation due to the J -coupling is rarely observed. However, the J -coupling influences relaxation of the sample in another way. As described in Section 10.3, J -coupling creates density matrix components relaxing with different rates than \mathcal{S}_{1+} and

\mathcal{I}_{2+} , analyzed in Sections 8.7 and 8.9.5.

10.3 Density matrix evolution in the presence of J -coupling

In order to extend description of NMR experiments to J -coupled pair of nuclear magnetic moments, we should update the analysis of the density matrix evolution derived in the previous lectures. As always, analysis starts by the definition of the initial density matrix form. Derivation of the density matrix in the thermal equilibrium, presented in Section 10.9.3, is very similar to that described for two nuclei interacting through space (dipolar coupling) in Section 8.8. In principle, the diagonal elements of the density matrix are slightly influenced by the J -coupling, but this influence is at least five orders of magnitude weaker than the dominant effect of the external magnetic field \vec{B}_0 . Therefore, the J -coupling contribution can be neglected together with the effect of the chemical shifts, and the same equilibrium density matrix can be used as the starting point of the analysis of NMR experiments in the presence of J -coupling, as it was used for systems with no or dipolar coupling:

$$\hat{\rho}^{\text{eq}} = \frac{1}{2} (\mathcal{I}_t + \kappa_1 \mathcal{I}_{1,z} + \kappa_2 \mathcal{I}_{2,z}), \quad (10.5)$$

where

$$\kappa_j = \frac{\gamma_j B_0 \hbar}{2k_B T}. \quad (10.6)$$

Also the second step, the analysis of the effect of the 90° radio wave pulse (see the schematic drawing in Figure 10.2A), gives the same result as for uncoupled systems. Again, the reason is that the fields indirectly produced by the coupled magnetic moments are too weak (much weaker than the radio-frequency field) to have a noticeable effect during the short pulse. Therefore, our analysis of the evolution in the presence of the J -coupling starts from $\hat{\rho}(b) = \frac{1}{2} \mathcal{I}_t + \frac{1}{2} \kappa (-\mathcal{I}_{1y} - \mathcal{I}_{2y})$, where the letter "b" refers to the labeling of the time course in Figure 10.2.

In the presence of the scalar coupling, the general Hamiltonian describing evolution after a 90° pulse is complicated even in a coordinate system rotating with $\omega_{\text{rot}} = -\omega_{\text{radio}}$

$$\mathcal{H} = \underbrace{-\gamma_1 B_0 (1 + \delta_{i,1})}_{\Omega_1} \mathcal{I}_{1z} - \underbrace{\gamma_2 B_0 (1 + \delta_{i,2})}_{\Omega_2} \mathcal{I}_{2z} + \pi J (2\mathcal{I}_{1z} \mathcal{I}_{2z} + 2\mathcal{I}_{1x} \mathcal{I}_{2x} + 2\mathcal{I}_{1y} \mathcal{I}_{2y}). \quad (10.7)$$

However, if the precession frequencies differ, the secular approximation simplifies the Hamiltonian to a form where all components commute. In such case, Eq. 6.10 can be applied and the Liouville - von Neumann equation can be solved geometrically as rotations in three-dimensional subspaces of the 16-dimensional operator space. The relevant subspaces are defined by the commutation relations summarized in Eqs. 8.29–8.31 and presented graphically in Figure 10.3. Rotations described by different components of the Hamiltonian are independent and can be performed consecutively, in any order.

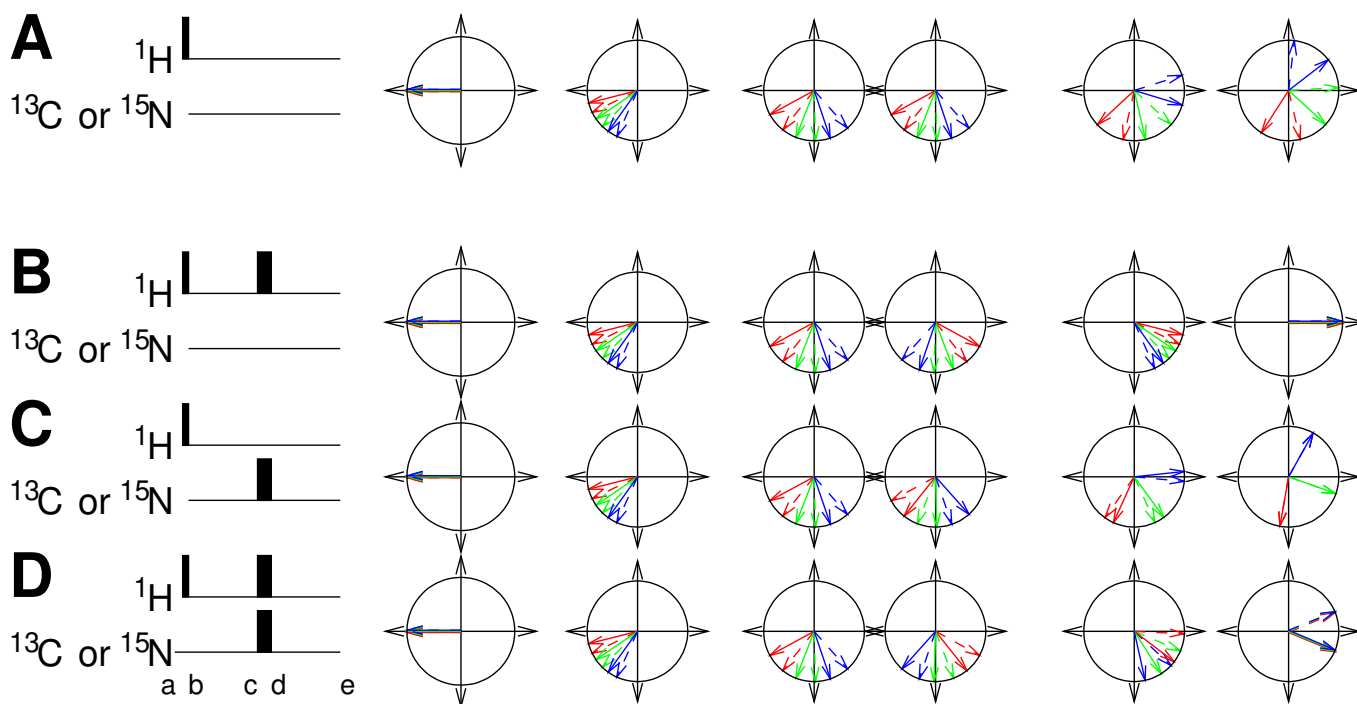


Figure 10.2: Graphical analysis of evolution of density matrix for ^1H (nucleus 1) and ^{13}C (nucleus 2) in an isolated $-\text{CH}-$ group. In individual rows, evolution of coherences is shown for three protons (distinguished by colors) with slightly different precession frequency due to the different chemical shifts δ_i . The protons are bonded to ^{13}C . Solid arrows represent fractions of proton magnetization in 10% molecules with ^{13}C magnetic moments most polarized in the direction of \vec{B}_0 . Dashed arrow represent fractions of proton magnetization in 10% molecules with ^{13}C magnetic moments most aligned in the opposite direction. The first column shows the arrows at the beginning of the echo (after the initial 90° pulse at the proton frequency), the second column shows the arrows in the middle of the first delay τ , the third and fourth columns show the arrows immediately before and after the 180° pulse(s) in the middle of the echo, respectively, the fifth column shows the arrows in the middle of the second delay τ , the sixth column shows the arrows at the end of the echo. Row A corresponds to an experiment when no 180° pulse is applied, row B corresponds to the echo with the 180° pulse applied at the proton frequency, row C corresponds to the echo with the 180° pulse applied at the ^{13}C frequency, and row D corresponds to the echo with the 180° pulses applied at both frequencies (see the schematic drawings in left part of the figure). The x -axis points down, the y -axis points to the right.

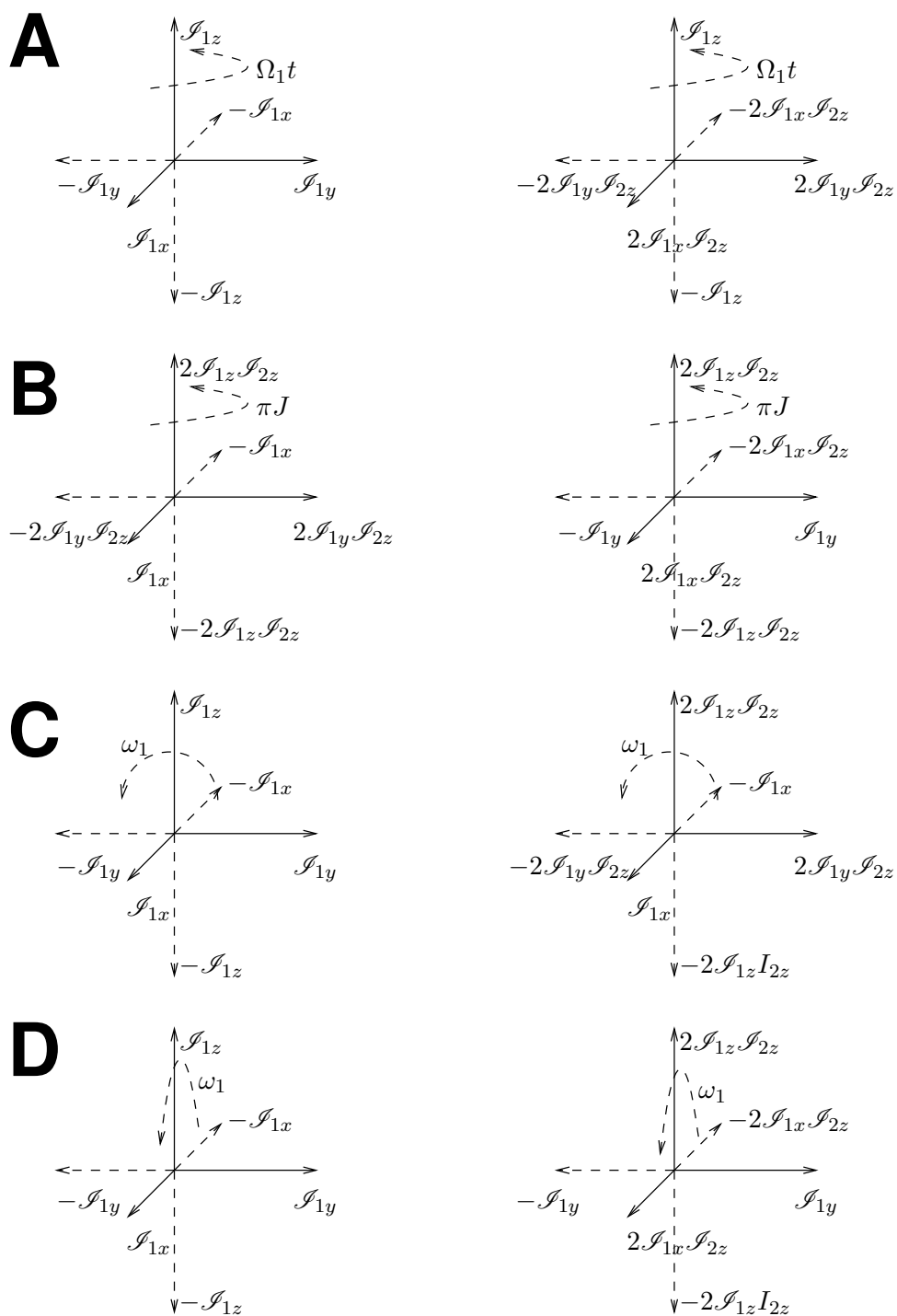


Figure 10.3: Rotations in product operator space. A, effects of the Hamiltonian describing the chemical shift; B, effects of the Hamiltonian describing the J coupling; C, effects of the Hamiltonian describing the radio wave pulses with the phase 0 (x); D effects of the Hamiltonian describing the radio wave pulses with the phase $\pi/2$ (y). The rotations are shown for the magnetic moment 1, a similar diagram for the magnetic moment 2 can be obtained by switching the subscripts 1 and 2 of the operators \mathcal{I}_{1j} and \mathcal{I}_{2k} .

For a density matrix $\hat{\rho}(b) = \frac{1}{2}\mathcal{I}_t + \frac{1}{2}\kappa(-\mathcal{I}_{1y} - \mathcal{I}_{2y})$ after a 90° pulse, the evolution due to the chemical shift (described by Ω_1 and Ω_2) and scalar coupling (described by πJ) can be analyzed as follows

$$\mathcal{I}_{1t} \longrightarrow \mathcal{I}_{1t} \longrightarrow \mathcal{I}_{1t} \quad (10.8)$$

$$-\mathcal{I}_{1y} \longrightarrow \begin{cases} -c_1\mathcal{I}_{1y} \longrightarrow \begin{cases} -c_1c_J \mathcal{I}_{1y} \\ +c_1s_J 2\mathcal{I}_{1x}\mathcal{I}_{2z} \end{cases} \\ +s_1\mathcal{I}_{1x} \longrightarrow \begin{cases} +s_1c_J \mathcal{I}_{1x} \\ +s_1s_J 2\mathcal{I}_{1y}\mathcal{I}_{2z} \end{cases} \end{cases} \quad (10.9)$$

$$-\mathcal{I}_{2y} \longrightarrow \begin{cases} -c_2\mathcal{I}_{2y} \longrightarrow \begin{cases} -c_2c_J \mathcal{I}_{2y} \\ +c_2s_J 2\mathcal{I}_{2x}\mathcal{I}_{1z} \end{cases} \\ +s_2\mathcal{I}_{2x} \longrightarrow \begin{cases} +s_2c_J \mathcal{I}_{2x} \\ +s_2s_J 2\mathcal{I}_{2y}\mathcal{I}_{1z} \end{cases} \end{cases} \quad (10.10)$$

where the first arrows represent rotation "about" \mathcal{I}_{1z} or \mathcal{I}_{2z} by the angle $\Omega_1 t$ or $\Omega_2 t$, the second arrows represent rotation "about" $2\mathcal{I}_{1z}\mathcal{I}_{2z}$ by the angle $\pi J t$, and

$$c_1 = \cos(\Omega_1 t) \quad s_1 = \sin(\Omega_1 t) \quad (10.11)$$

$$c_2 = \cos(\Omega_2 t) \quad s_2 = \sin(\Omega_2 t) \quad (10.12)$$

$$c_J = \cos(\pi J t) \quad s_J = \sin(\pi J t). \quad (10.13)$$

As mentioned above, the same result is obtained if we first "rotate about" $2\mathcal{I}_{1z}\mathcal{I}_{2z}$, and then "about" \mathcal{I}_{1z} or \mathcal{I}_{2z} .

The last step is the evaluation of the expectation value of the transverse magnetization. Only \mathcal{I}_{1x} , \mathcal{I}_{1y} , \mathcal{I}_{2x} , \mathcal{I}_{2y} contribute to the expected value of M_+ , giving non-zero trace when multiplied by \hat{I}_+ (orthogonality, see Section 9.3):

$$\text{Tr} \{ \mathcal{I}_{1x}(\mathcal{I}_{1x} + i\mathcal{I}_{1y}) \} = \text{Tr} \{ \mathcal{I}_{2x}(\mathcal{I}_{2x} + i\mathcal{I}_{2y}) \} = 1, \quad (10.14)$$

$$\text{Tr} \{ \mathcal{I}_{1y}(\mathcal{I}_{1x} + i\mathcal{I}_{1y}) \} = \text{Tr} \{ \mathcal{I}_{2y}(\mathcal{I}_{2x} + i\mathcal{I}_{2y}) \} = i, \quad (10.15)$$

Well-known goniometric relations $\cos(a \pm b) = \cos a \cos b \mp \sin a \sin b$ and $\sin(a \pm b) = \sin a \cos b \pm \cos a \sin b$ allow us to convert the products $c_n c_J$ (modulating \mathcal{I}_{ny}) and $s_n c_J$ (modulating \mathcal{I}_{nx}) in 10.9 and 10.10 to sums of cosine and sine functions, respectively:

$$c_1 c_J = \frac{1}{2} \cos((\Omega_1 + \pi J)t) + \frac{1}{2} \cos((\Omega_1 - \pi J)t) \quad (10.16)$$

$$s_1 c_J = \frac{1}{2} \sin((\Omega_1 + \pi J)t) + \frac{1}{2} \sin((\Omega_1 - \pi J)t) \quad (10.17)$$

$$c_2 c_J = \frac{1}{2} \cos((\Omega_2 + \pi J)t) + \frac{1}{2} \cos((\Omega_2 - \pi J)t) \quad (10.18)$$

$$s_2 c_J = \frac{1}{2} \sin((\Omega_2 + \pi J)t) + \frac{1}{2} \sin((\Omega_2 - \pi J)t) \quad (10.19)$$

The expected value of M_+ calculated from the complete density matrix is then

$$\begin{aligned}
\langle M_+ \rangle &= \text{Tr} \left\{ \hat{\rho}(t) \hat{M}_+ \right\} = \mathcal{N} \gamma \hbar \text{Tr} \left\{ \hat{\rho}(t) (\mathcal{I}_{1x} + i \mathcal{I}_{1y} + \mathcal{I}_{2x} + i \mathcal{I}_{2y}) \right\} \\
&= -i \mathcal{N} \gamma \hbar \frac{\kappa}{4} (\cos((\Omega_1 + \pi J)t) + \cos((\Omega_1 - \pi J)t) + \cos((\Omega_2 + \pi J)t) + \cos((\Omega_2 - \pi J)t)) \\
&\quad + \mathcal{N} \gamma \hbar \frac{\kappa}{4} (\sin((\Omega_1 + \pi J)t) + \sin((\Omega_1 - \pi J)t) + \sin((\Omega_2 + \pi J)t) + \sin((\Omega_2 - \pi J)t)) \\
&= \mathcal{N} \gamma \hbar \frac{\kappa}{4} (-i) (\cos((\Omega_1 - \pi J)t) + i \sin((\Omega_1 - \pi J)t) + \cos((\Omega_1 + \pi J)t) + i \sin((\Omega_1 + \pi J)t)) \\
&\quad + \mathcal{N} \gamma \hbar \frac{\kappa}{4} (-i) (\cos((\Omega_2 - \pi J)t) + i \sin((\Omega_2 - \pi J)t) + \cos((\Omega_2 + \pi J)t) + i \sin((\Omega_2 + \pi J)t)) \\
&= \frac{\mathcal{N} \gamma^2 \hbar^2 B_0}{8k_B T} e^{-i\frac{\pi}{2}} \left(e^{i(\Omega_1 - \pi J)t} + e^{i(\Omega_1 + \pi J)t} e^{i(\Omega_2 - \pi J)t} + e^{i(\Omega_2 + \pi J)t} \right) \quad (10.20)
\end{aligned}$$

At this moment, we should also include relaxation. We have analyzed relaxation in Sections 7.7, 7.10.3, and 8.7, 8.9.5. However, the density matrix in the presence of the J -coupling evolves into new terms $2\mathcal{I}_{1x}\mathcal{I}_{2z}$, $2\mathcal{I}_{1y}\mathcal{I}_{2z}$, $2\mathcal{I}_{1z}\mathcal{I}_{2x}$, and $2\mathcal{I}_{1z}\mathcal{I}_{2y}$, and these terms relax differently. Their relaxation rates can be derived using the Bloch-Wangsness-Redfield approach, but we do not do it in this course. If both dipole-dipole interactions and chemical shift anisotropy contribute the relaxation, another complication appears: relaxation of \mathcal{I}_{1+} depends on $2\mathcal{I}_{1+}\mathcal{I}_{2z}$ and vice versa, and the same applies to \mathcal{I}_{2+} and $2\mathcal{I}_{1z}\mathcal{I}_{2+}$.² To keep our analysis as simple as possible, we (i) assume that the contribution of the chemical shift anisotropy is negligible, (ii) describe relaxation of the inter-converting $\hat{\rho}$ contributions \mathcal{I}_{1+} , $2\mathcal{I}_{1+}\mathcal{I}_{2z}$ and \mathcal{I}_{2+} , $2\mathcal{I}_{1z}\mathcal{I}_{2+}$ by average rate constants, and (iii) assume that the average rate constants are identical for both nuclei (we use the symbol \bar{R}_2).

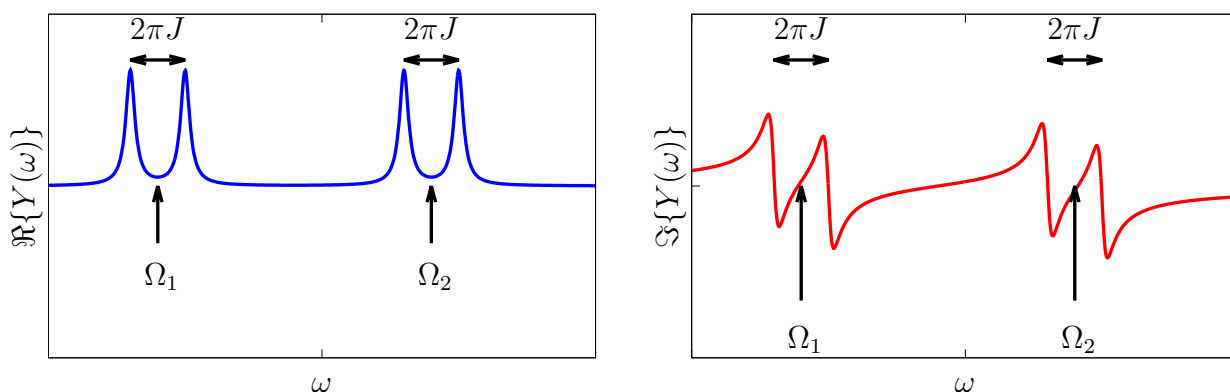
Including relaxation and applying a phase shift by 90° , we obtain description of the time evolution of the expected value of M_+

$$\langle M_+ \rangle = \frac{\mathcal{N} \gamma^2 \hbar^2 B_0}{8k_B T} \left(e^{-\bar{R}_{2,1}t} \left(e^{i(\Omega_1 - \pi J)t} + e^{i(\Omega_1 + \pi J)t} \right) + e^{-\bar{R}_{2,2}t} \left(e^{i(\Omega_2 - \pi J)t} + e^{i(\Omega_2 + \pi J)t} \right) \right) \quad (10.21)$$

which gives four peaks in the spectrum after the Fourier transformation:

²The mutual dependence of relaxation is described by constants known as *cross-correlated cross-relaxation* rate constants, resembling R_x in Eqs. 8.33 and 8.34

$$\begin{aligned}
& \frac{\mathcal{N}\gamma^2\hbar^2 B_0}{8k_B T} \left(\frac{\bar{R}_{2,1}}{\bar{R}_{2,1}^2 + (\omega - \Omega_1 + \pi J)^2} + \frac{\bar{R}_{2,1}}{\bar{R}_{2,1}^2 + (\omega - \Omega_1 - \pi J)^2} \right. \\
& \quad \left. + \frac{\bar{R}_{2,2}}{\bar{R}_{2,2}^2 + (\omega - \Omega_2 + \pi J)^2} + \frac{\bar{R}_{2,2}}{\bar{R}_{2,2}^2 + (\omega - \Omega_2 - \pi J)^2} \right) \\
& -i \frac{\mathcal{N}\gamma^2\hbar^2 B_0}{8k_B T} \left(\frac{\omega - \Omega_1 + \pi J}{\bar{R}_{2,1}^2 + (\omega - \Omega_1 + \pi J)^2} + \frac{\omega - \Omega_1 - \pi J}{\bar{R}_{2,1}^2 + (\omega - \Omega_1 - \pi J)^2} \right. \\
& \quad \left. + \frac{\omega - \Omega_2 + \pi J}{\bar{R}_{2,2}^2 + (\omega - \Omega_2 + \pi J)^2} + \frac{\omega - \Omega_2 - \pi J}{\bar{R}_{2,2}^2 + (\omega - \Omega_2 - \pi J)^2} \right).
\end{aligned} \tag{10.22}$$



The four peaks in the spectrum form two doublets, one at an average angular frequency Ω_1 , the other one at an average angular frequency Ω_2 . Both doubles are split by an angular frequency difference $\pi J - (-\pi J) = 2\pi J$, or by the value of J if the frequencies are plotted in Hz.

10.4 Homo- and heteronuclear magnetic moment pairs

So far, we did not distinguish *homonuclear* pairs of magnetic moments (magnetic moments of the same type of nuclei, e.g., two protons) and *heteronuclear* pairs of magnetic moments (magnetic moments of different isotopes, e.g., proton and ^{13}C). It is useful to distinguish these two cases when we analyze advanced NMR experiments. Although the density matrix has the same form in both cases, the Hamiltonians describing the effects of radio waves may differ. The reason is technical. Differences in chemical shifts are usually small and allow us to irradiate the sample by a radio wave with a frequency sufficiently close to the precession frequencies of both nuclei. Therefore, the resonance conditions can be matched reasonably well for both nuclei and they are affected by the radio waves in a similar manner. On the other hand, precession frequencies of different isotopes differ substantially and the frequency of the radio waves can resonate only with one of the isotopes. As

a consequence, each of the magnetic moments of the pair is affected selectively, which is frequently exploited in the NMR experiments. The selective irradiation of either nucleus 1 or nucleus 2 also implies that the peaks of nuclei 1 and 2 are not observed in the same spectrum. The signals of nucleus 1 and nucleus 2 are recorded in two experiments with different frequencies (resonating with the precession frequency of nucleus 1 in one spectrum and of nucleus 2 in the other one) of the radio waves, as shown in Figure 10.4. The sensitivities (signal-to-noise ratios) of the experiments are in the ratio $|\gamma_1/\gamma_2|^{5/2}$ (Eq. 7.84). For example, sensitivity of ^{13}C and ^{15}N spectra is reduced by a factor of 32 (see Figure 10.4) and 300, respectively, compared to proton spectra, even if the molecules contain 100 % ^{13}C and ^{15}N isotopes.

In order to distinguish the heteronuclear systems from homonuclear ones in our written notes, we save the symbols \mathcal{I}_{1j} and \mathcal{I}_{2j} for homonuclear pairs (most often two protons) and use symbols \mathcal{I}_j and \mathcal{S}_j for operators of nucleus 1 and 2, respectively, if $\gamma_1 \neq \gamma_2$. For example, a graphical description of rotations in the 16D operator space of a heteronuclear pair is derived from Figure 10.3 by changing \mathcal{I}_{1j} to \mathcal{I}_j and \mathcal{I}_{2j} to \mathcal{S}_j , or vice versa. Both labeling systems are mixed if we describe more complex chemical groups. For example, we use symbols \mathcal{I}_{1j} , \mathcal{I}_{2j} , and \mathcal{S}_j for the operators representing contributions to density matrix describing (mixed) states of nuclear magnetic moments in the $^{13}\text{C}^1\text{H}_2$ group.

10.5 Spin echoes

In many NMR experiments, the J -coupling is not just detected, but creatively employed to deliberately change quantum states (mixed states) of the studied system. Such a manipulation resembles the dream of the medieval alchemists, transmutation of chemical elements,³ and is sometimes called "spin alchemy".

Spin echoes are basic tools of spin alchemy, consisting of a 180° (π) radio-wave pulse sandwiched by two delays of equal duration τ . In the case of a heteronuclear pair, we can apply the 180° pulse selectively to magnetic moment 1, to magnetic moment 2, or simultaneously to both (see Figure 10.2). Such a collection of spin echoes gives us the possibility to control evolution of the chemical shift and scalar coupling separately. In the case of a homonuclear pair, the radio waves affect both magnetic moments simultaneously, as shown in Figure 10.2D.⁴

Below, we analyze three types of spin echoes applied to a heteronuclear system (^1H and ^{13}C in our example). For the sake of simplicity, we do not discuss relaxation effects, although relaxation is usually observable. On the other hand, we have to extend the analyzed system to see how the echoes

³Transmutation of the mercury isotope $^{197}_{80}\text{Hg}$ (which can be prepared from the stable isotope $^{198}_{80}\text{Hg}$) to a common isotope of gold $^{197}_{79}\text{Au}$ is a nuclear reaction known as electron capture: a proton in the nucleus absorbs an inner-shell electron, emits a neutrino ν_e and changes to neutron. Since proton and neutron can be described as different quantum states of an object called nucleon, the transmutation of mercury to gold can be viewed as a change of the quantum state. Interestingly, proton and neutron differ in the *isospin projection* quantum number I_3 , whereas the quantum states manipulated in NMR spectroscopy differ in the *spin projection* quantum number s_z . The similar nomenclature is used to emphasize similar symmetry (the same mathematical description) of two different physical phenomena.

⁴If the chemical shift of nuclei in a homonuclear pair differ substantially, a selective application of 180° pulses to either magnetic moment is possible. In such a case, power of the radio waves should be low, and their amplitude is often modulated during the pulse to achieve a higher selectivity.

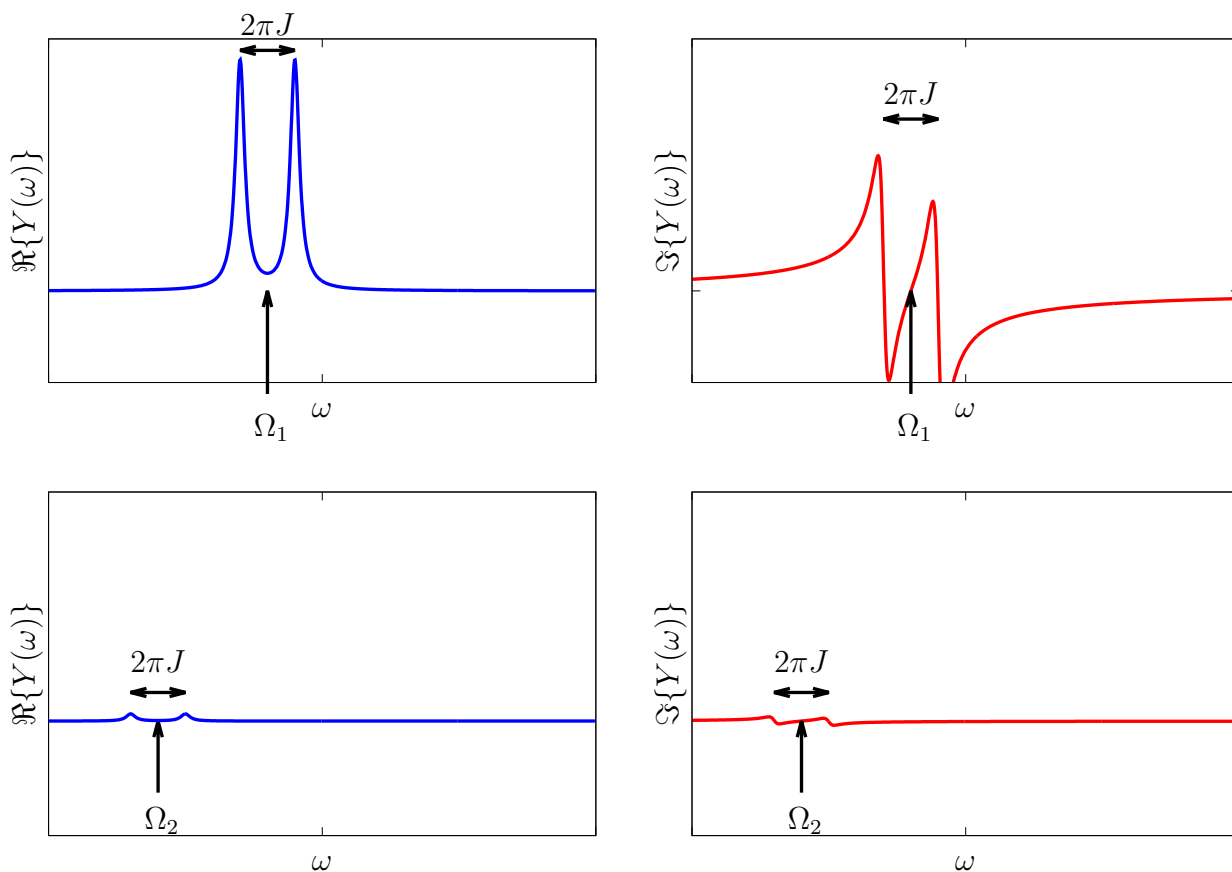


Figure 10.4: Spectra of a heteronuclear pair. Top, real and imaginary component of a spectrum recorded after applying a radio wave pulse close to the precession frequency of nucleus 1. Bottom, real and imaginary component of a spectrum recorded after applying a radio wave pulse close to the precession frequency of nucleus 2. Note that the frequency offsets Ω_1 and Ω_2 are measured from different carrier frequencies (close to $\omega_{0,1}$ and $\omega_{0,2}$, respectively). The spectra are plotted so that the noise is the same in both spectra, the relative intensities correspond to a pair of ^1H (nucleus 1) and ^{13}C (nucleus 2). The value of J is the same in the top and bottom spectra.

Table 10.1: Examples of two graphical representations of coherences: as distributions (used in Table 8.4) and as arrows (used in Figure 10.2). The color coding of distributions is similar to that used in Tables 8.3–8.4, but both distributions corresponding to the fractions of most polarized and least polarized magnetic moments are highlighted. The solid and dashed arrows presented in the last column correspond to partial transverse magnetization of $\vec{\mu}_1$ selected based on fractions of most (solid arrow) and least (dashed arrow) polarized $\vec{\mu}_2$ (shown in upper and lower pictures in the third column, respectively). The direction of the arrow is given by the average direction of the cyan arrows in the cyan boxes, the type (solid or dashed) of the arrow is given by the average direction of the green arrows in the green boxes (up or down, respectively).

Matrix	depicted as distributions 10% most/least polarized $\vec{\mu}_1$		depicted as distributions 10% most/least polarized $\vec{\mu}_2$		depicted as arrows
$\mathcal{I}_{1y} = \frac{i}{2} \begin{pmatrix} 0 & 0 & -1 & 0 \\ 0 & 0 & 0 & -1 \\ +1 & 0 & 0 & 0 \\ 0 & +1 & 0 & 0 \end{pmatrix}$					
$2\mathcal{I}_{1y}\mathcal{I}_{2z} = \frac{i}{2} \begin{pmatrix} 0 & 0 & -1 & 0 \\ 0 & 0 & 0 & +1 \\ +1 & 0 & 0 & 0 \\ 0 & -1 & 0 & 0 \end{pmatrix}$					

affect evolution due to the chemical shift differences. Therefore, we include *three pairs with different chemical shifts of the observed nucleus* in the analysis. Algebraic analysis of the corresponding density matrix evolution is straightforward, but somewhat tedious. An alternative graphical analysis is presented in Figure 10.2. We have introduced a graphical representation of the product operators (density matrix contributions) in Table 8.4, where each coherence is visualized as a colored plot of the magnetic moment distributions. In order to depict transverse polarization of three magnetic moments in a single diagram, the graphical representation is further simplified in Figure 10.2. The distributions of magnetic moments, with the most polarized ones highlighted, are replaced by single arrows representing (partial) magnetizations of sets of the observed nuclei 1 attached to 10% fractions of nuclei 2 with magnetic moments most aligned along \vec{B}_0 (solid arrow) and against \vec{B}_0 (dashed arrow). The solid and dashed arrows have the same direction if the transverse polarization of magnetic moment 1 is not correlated with the longitudinal polarization of magnetic moment 2 (contributions of \mathcal{I}_x and \mathcal{I}_y to the density matrix), and the opposite directions if the transverse polarization of magnetic moment 1 is correlated with the longitudinal polarization of magnetic moment 2 (contributions of $2\mathcal{I}_x\mathcal{I}_z$ and $2\mathcal{I}_y\mathcal{I}_z$ to the density matrix). The visualizations of coherences used in Table 8.4 and in Figure 10.2 are compared in Table 10.1. Note that the solid and dashed arrows represent vectors of partial magnetizations, and are thus affected by the radio waves in the same way as the magnetization vectors. Our graphical analysis can be thus viewed as an extension of the *vector model*, presented e.g. by Keeler in K4.

To see how the echoes influence polarization of the sample, we should compare the effect of the echoes with the free evolution. Evolution of a single homonuclear pair of magnetic moments in the presence of scalar coupling was described in Section 10.3. To convert the description to our set of three heteronuclear pairs, we should follow evolution of a density matrix starting from

$$\hat{\rho}(a) = \frac{1}{2^5} \mathcal{I}_t + \sum_{n=1}^3 \frac{1}{2^5} \kappa_1 \mathcal{I}_{nz} + \sum_{n=1}^3 \frac{1}{2^5} \kappa_2 \mathcal{I}_{nz}. \quad (10.23)$$

However, complexity of such analysis might obscure the effects of the analyzed spin echoes. Therefore, we write the evolution for one heteronuclear pair and depict the set of three pairs only in the graphical analysis, as shown in Figure 10.2A.

- $\hat{\rho}(a) = \frac{1}{2} \mathcal{I}_t + \frac{1}{2} \kappa_1 \mathcal{I}_z + \frac{1}{2} \kappa_2 \mathcal{I}_z$
thermal equilibrium, the constants κ_1 and κ_2 are different because the nuclei have different γ .
- $\hat{\rho}(b) = \frac{1}{2} \mathcal{I}_t - \frac{1}{2} \kappa_1 \mathcal{I}_y + \frac{1}{2} \kappa_2 \mathcal{I}_z$
90° pulse applied to nucleus I only
- $\hat{\rho}(e) = \frac{1}{2} \mathcal{I}_t + \frac{1}{2} \kappa_1 (-c_1 c_J \mathcal{I}_y + s_1 c_J \mathcal{I}_x + c_1 s_J 2 \mathcal{I}_x \mathcal{I}_z + s_1 s_J 2 \mathcal{I}_y \mathcal{I}_z) + \frac{1}{2} \kappa_2 \mathcal{I}_z$
free evolution during 2τ ($t \rightarrow 2\tau$ in c_1 etc.)

The $2\mathcal{I}_x \mathcal{I}_z$, $2\mathcal{I}_y \mathcal{I}_z$ coherences do not give non-zero trace when multiplied by \mathcal{I}_+ (they are not measurable per se), but *cannot be ignored* if the pulse sequence continues because they can *evolve* into measurable coherences later (note that the scalar coupling Hamiltonian $2\pi J \mathcal{I}_z \mathcal{I}_z$ converts them to \mathcal{I}_y , \mathcal{I}_x , respectively).

The graphical analysis in Figure 10.2A shows how the coherences evolve with different chemical shifts (arrows of different colors rotate with different frequency) and how is the evolution influenced by the J -coupling (solid arrows rotate slower⁵ than dashed arrows of the same color).

10.6 Refocusing echo

The *refocusing echo* consists of a 90° pulse exciting magnetic moment 1 and a 180° pulse applied to the excited nucleus in the middle of the echo (see the schematic drawing in Figure 10.2B). The middle 180° pulse flips all arrows from left to right (rotation about the vertical axis x by 180°). The faster arrows start to evolve with a handicap at the beginning of the second delay τ and they reach the slower arrows at the end of the echo regardless of the actual speed of rotation.

Even without a detailed analysis of product operators, we see that the final state of the system does not depend on chemical shift or scalar coupling: the evolution of both chemical shift and scalar coupling is *refocused* during this echo.

The evolution of the density matrix can be guessed from the graphical analysis. The frequency of the applied radio waves resonates with proton precession frequency and is far from the precession frequency of ^{13}C . Therefore, magnetic moments of ^{13}C should stay in their equilibrium distribution,

⁵This is true for nuclei with $\gamma > 0$.

described by \mathcal{I}_t and \mathcal{I}_z . The initial state of protons was described (after the 90° pulse) by $-\mathcal{I}_y$ in terms of product operators and by three arrows with the same $-y$ orientation. As the arrows only changed their direction at the end of the experiment (all arrows have the $+y$ orientation at the end of the echo), we can deduce that the final state of protons is $+\mathcal{I}_y$. Taken together, each pair of magnetic moment ends in the state described by

- $\hat{\rho}(e) = \frac{1}{2}\mathcal{I}_t + \frac{1}{2}\kappa_1\mathcal{I}_y + \frac{1}{2}\kappa_2\mathcal{I}_z$

10.7 Decoupling echo

The *decoupling echo* consists of a 90° pulse exciting magnetic moment 1 and a 180° pulse applied to the other nucleus in the middle of the echo (see the schematic drawing in Figure 10.2C). The graphical analysis is shown in Figure 10.2C. The middle 180° is applied at the ^{13}C frequency. It does not affect proton coherences, depicted as arrows in Figure 10.2C, but *inverts longitudinal polarizations* (populations) of ^{13}C (solid arrows change to dashed ones and vice versa). The faster arrows become slower, the slower arrows become faster, and they meet at the end of the echo.

Without a detailed analysis of product operators, we see that the final state of the system does not depend on scalar coupling (the difference between solid and dashed arrows disappeared) but the evolution due to the chemical shift took place (arrows of different colors rotated by different angles $2\Omega_1\tau$). As the effects of the scalar coupling are masked, this echo is known as the *decoupling echo*.

We again derive the final density matrix from the graphical analysis. As the arrows at the end of the echo have the same orientations as if the nuclei were not coupled at all, we can deduce that the final state of protons is identical to the density matrix evolving due to the chemical shift only. Magnetic moments of ^{13}C nuclei were affected only by the middle 180° pulse that *inverted* longitudinal polarization. The density matrix at the end of the echo is

- $\hat{\rho}(e) = \frac{1}{2}\mathcal{I}_t + \frac{1}{2}\kappa_1(c_1\mathcal{I}_y - s_1\mathcal{I}_x) - \frac{1}{2}\kappa_2\mathcal{I}_z$

10.8 Simultaneous echo

The last echo consists of a 90° pulse exciting magnetic moment 1 and 180° pulses applied to both nuclei in the middle of the echo (see the schematic drawing in Figure 10.2D). As both nuclei are affected, it can be applied to heteronuclear or homonuclear pairs. The homonuclear version includes one 180° pulses of radio waves with a frequency close to the precession frequency of both magnetic moments. In the heteronuclear variant, two 180° pulses are applied simultaneously to both nuclei. The graphical analysis of the heteronuclear application is shown in Figure 10.2D. The 180° pulses are applied at ^1H and ^{13}C frequencies in the middle of the echo, resulting in combination of both effects described in Figs. 10.2B and C. The proton pulse flips arrows representing proton coherences and the ^{13}C pulse inverts longitudinal polarizations (populations) of ^{13}C nuclei (solid arrows change to dashed ones and vice versa). As a result, the average direction of dashed and solid arrows is refocused at the end of the echo but the difference due to the coupling is preserved (the handicapped arrows were made slower by the inversion of longitudinal polarization of ^{13}C).

Without a detailed analysis of product operators, we see that the effect of the chemical shift is removed (the average direction of arrows of the same color is just reversed), but the final state of the system depends on scalar coupling (the solid and dashed arrows collapsed). We can deduce from the graphical analysis that the final state of the density matrix is obtained by rotation "about" $2\mathcal{I}_z\mathcal{S}_z$, but not "about" \mathcal{I}_z in the product operator space, and by changing the sign of the resulting coherences:

- $\hat{\rho}(e) = \frac{1}{2}\mathcal{I}_t + \frac{1}{2}\kappa_1 (c_J\mathcal{I}_y - s_J2\mathcal{I}_x\mathcal{S}_z) - \frac{1}{2}\kappa_2\mathcal{S}_z$

HOMEWORK

Analyze the spin echoes (Sections 10.5–10.8).

10.9 DERIVATIONS

10.9.1 Interaction between nuclei mediated by bond electrons

In principle, both orbital and spin magnetic moments of electrons can mediate the J -coupling, but the contribution of the orbital magnetic moments is usually negligible (coupling between hydrogen nuclei in water is an interesting exception). In order to describe the mediation of the J -coupling by the electron spin, we first investigate the interaction between electron and proton in the hydrogen atom.

A classical picture of interactions of nuclear and electronic spin magnetic moments is presented in Figure 10.5. Energy of the interaction between the (spin) magnetic moment of nucleus $\vec{\mu}_n$ and the magnetic field generated by the spin magnetic moment of electron \vec{B}_e is given by (cf. Eq. 8.48)

$$\mathcal{E} = -\vec{\mu}_n \cdot \vec{B}_e = -\frac{\mu_0}{4\pi} \vec{\mu}_n \cdot \vec{\nabla} \times \frac{\vec{\mu}_e \times \vec{r}}{r^3} = -\frac{\mu_0}{4\pi} \vec{\mu}_n \cdot \vec{\nabla} \times \left(\vec{\nabla} \times \frac{\vec{\mu}_e}{r} \right). \quad (10.24)$$

In principle, the interaction with an electron does not differ from an interaction between two nuclear magnetic moments, described in Sections 8.1 and 8.9.1. Depending on the mutual orientation of the nucleus and electron, the direction of \vec{B}_e varies (Figure 10.5A–C). If the distribution of electrons is spherically symmetric, or if the molecules tumble isotropically, the interactions of the spin magnetic moments of the electron and the nucleus average to zero. With one exception, depicted in Figure 10.5D. If the electron is present *exactly* at the nucleus, the vector of the electron spin magnetic moment $\vec{\mu}_e$ has the same direction as \vec{B}_e and \mathcal{E} is proportional to the scalar product $-\vec{\mu}_n \cdot \vec{\mu}_e$. The exact co-localization of electron and nucleus may look strange in the classical, but the interaction between the nucleus and electron *inside* the nucleus can be simulated by a hypothetical current loop giving the correct magnetic moment when treated classically. To include the distribution of the electron around the nucleus into our classical model, the total energy of the integration must be calculated by integrating Eq. 10.24 over the electron coordinates. As mentioned above, the integral tends to zero for $r > 0$ in isotropic samples. However, the integral has a non-zero value in the limit $r \rightarrow 0$, as discussed e.g. in Abragam: The principles of nuclear magnetism, Oxford Press 1961, Chapter VI, Section II.A.

Here, we present a quantum-mechanical analysis, following the original paper by Fermi in Z. Phys. 60 (1930) 320–333. Fermi started from the eigenfunctions of the Dirac Hamiltonian for an electron in an electromagnetic field (Eq. 5.90) of nuclei of alkali metals. We investigate the simplest example, the ground state of hydrogen atom. The 1s atomic orbital of the hydrogen atom is particularly interesting because it has a non-zero value in the center, at the place of the nucleus (cf. Figure 10.1A). The eigenfunctions describing an electron in the 1s orbital are

$$\Psi(1s_{1/2}, +1/2) = \begin{pmatrix} \psi(1s) \\ 0 \\ \frac{i}{2} \frac{1}{4\pi\epsilon_0} \frac{Q^2}{\hbar c} \cos\vartheta \psi(1s) \\ \frac{i}{2} \frac{1}{4\pi\epsilon_0} \frac{Q^2}{\hbar c} \sin\vartheta e^{i\varphi} \psi(1s) \end{pmatrix} = \begin{pmatrix} 1 \\ 0 \\ \frac{i}{2a_0} \frac{\hbar}{mc} \frac{z}{r} \\ \frac{i}{2a_0} \frac{\hbar}{mc} \frac{x+iy}{r} \end{pmatrix} \psi(1s), \quad (10.25)$$

$$\Psi(1s_{1/2}, -1/2) = \begin{pmatrix} 0 \\ -\psi(1s) \\ -\frac{i}{2} \frac{1}{4\pi\epsilon_0} \frac{Q^2}{\hbar c} \sin\vartheta e^{-i\varphi} \psi(1s) \\ \frac{i}{2} \frac{1}{4\pi\epsilon_0} \frac{Q^2}{\hbar c} \cos\vartheta \psi(1s) \end{pmatrix} = \begin{pmatrix} 0 \\ -1 \\ -\frac{i}{2a_0} \frac{\hbar}{mc} \frac{x-iy}{r} \\ \frac{i}{2a_0} \frac{\hbar}{mc} \frac{z}{r} \end{pmatrix} \psi(1s), \quad (10.26)$$

where $\psi(1s)$ is the familiar non-relativistic (Schrödinger) orbital 1s (note that the 1s orbital is a real wave function, i.e. $\psi^*(1s) = \psi(1s)$).

Contribution of the interaction between magnetic moments of the nucleus and of the electron at the site of the nucleus to the expected energy can be calculated by applying Eq. 4.5 to the spin magnetic part of the Hamiltonian in Eq. 5.90

$$\mathcal{E} = \int_{V \rightarrow 0} \Psi^* Q c (-A_{n,x} \hat{\gamma}^0 \hat{\gamma}^1 - A_{n,y} \hat{\gamma}^0 \hat{\gamma}^2 - A_{n,z} \hat{\gamma}^0 \hat{\gamma}^3) \Psi \, dx \, dy \, dz, \quad (10.27)$$

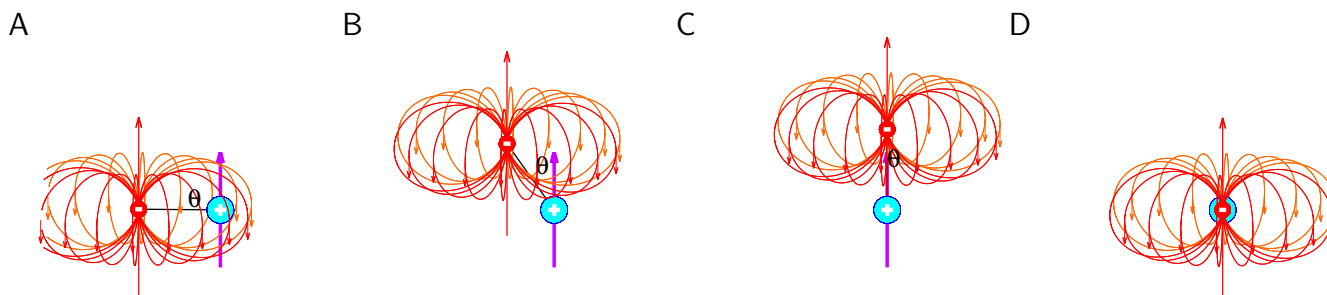


Figure 10.5: Classical description of interactions of nuclear and electronic spin magnetic moments.

where \vec{A}_n is the vector potential of the nucleus. Using Eq. 8.44, the vector potential can be expressed in terms of the nuclear magnetic moment and electron coordinates

$$\mathcal{E} = -\frac{\mu_0 Qc}{4\pi} \int_{V \rightarrow 0} \frac{1}{r^3} \Psi^* \left((z\mu_{n,y} - y\mu_{n,z})\hat{\gamma}^0\hat{\gamma}^1 + (x\mu_{n,z} - z\mu_{n,x})\hat{\gamma}^0\hat{\gamma}^2 + (y\mu_{n,x} - x\mu_{n,y})\hat{\gamma}^0\hat{\gamma}^3 \right) \Psi \, dx \, dy \, dz. \quad (10.28)$$

The integral with $\Psi(1s_{1/2}, +1/2)$ includes the following three terms

$$\begin{aligned} \Psi^* \frac{z\mu_{n,y} - y\mu_{n,z}}{r^3} \hat{\gamma}^0\hat{\gamma}^1 \Psi &= \frac{z\mu_{n,y} - y\mu_{n,z}}{r^3} \left(1 \ 0 \ -\frac{i}{2a_0} \frac{\hbar}{mc} \frac{z}{r} \ -\frac{i}{2a_0} \frac{\hbar}{mc} \frac{x-iy}{r} \right) \begin{pmatrix} 0 & 0 & 0 & 1 \\ 0 & 0 & 1 & 0 \\ 0 & 1 & 0 & 0 \\ 1 & 0 & 0 & 0 \end{pmatrix} \begin{pmatrix} 1 \\ 0 \\ \frac{i}{2a_0} \frac{\hbar}{mc} \frac{z}{r} \\ \frac{i}{2a_0} \frac{\hbar}{mc} \frac{x+iy}{r} \end{pmatrix} \psi^2(1s) \\ &= \frac{z\mu_{n,y} - y\mu_{n,z}}{r^3} \left(1 \ 0 \ -\frac{i}{2a_0} \frac{\hbar}{mc} \frac{z}{r} \ -\frac{i}{2a_0} \frac{\hbar}{mc} \frac{x-iy}{r} \right) \begin{pmatrix} \frac{i}{2a_0} \frac{\hbar}{mc} \frac{x+iy}{r} \\ \frac{i}{2a_0} \frac{\hbar}{mc} \frac{z}{r} \\ 0 \\ 1 \end{pmatrix} \psi^2(1s) = \frac{-z\mu_{n,y} + y\mu_{n,z}}{a_0 r^3} \frac{\hbar}{mc} \frac{y}{r} \psi^2(1s), \end{aligned} \quad (10.29)$$

$$\begin{aligned} \Psi^* \frac{x\mu_{n,z} - z\mu_{n,x}}{r^3} \hat{\gamma}^0\hat{\gamma}^2 \Psi &= \frac{x\mu_{n,z} - z\mu_{n,x}}{r^3} \left(1 \ 0 \ -\frac{i}{2a_0} \frac{\hbar}{mc} \frac{z}{r} \ -\frac{i}{2a_0} \frac{\hbar}{mc} \frac{x-iy}{r} \right) \begin{pmatrix} 0 & 0 & 0 & -i \\ 0 & 0 & i & 0 \\ 0 & -i & 0 & 0 \\ i & 0 & 0 & 0 \end{pmatrix} \begin{pmatrix} 1 \\ 0 \\ \frac{i}{2a_0} \frac{\hbar}{mc} \frac{z}{r} \\ \frac{i}{2a_0} \frac{\hbar}{mc} \frac{x+iy}{r} \end{pmatrix} \psi^2(1s) \\ &= \frac{x\mu_{n,z} - z\mu_{n,x}}{r^3} \left(1 \ 0 \ -\frac{i}{2a_0} \frac{\hbar}{mc} \frac{z}{r} \ -\frac{i}{2a_0} \frac{\hbar}{mc} \frac{x-iy}{r} \right) \begin{pmatrix} \frac{1}{2a_0} \frac{\hbar}{mc} \frac{x+iy}{r} \\ -\frac{1}{2a_0} \frac{\hbar}{mc} \frac{z}{r} \\ 0 \\ i \end{pmatrix} \psi^2(1s) = \frac{x\mu_{n,z} - z\mu_{n,x}}{a_0 r^3} \frac{\hbar}{mc} \frac{x}{r} \psi^2(1s), \end{aligned} \quad (10.30)$$

$$\begin{aligned} \Psi^* \frac{y\mu_{n,x} - x\mu_{n,y}}{r^3} \hat{\gamma}^0\hat{\gamma}^3 \Psi &= \frac{y\mu_{n,x} - x\mu_{n,y}}{r^3} \left(1 \ 0 \ -\frac{i}{2a_0} \frac{\hbar}{mc} \frac{z}{r} \ -\frac{i}{2a_0} \frac{\hbar}{mc} \frac{x-iy}{r} \right) \begin{pmatrix} 0 & 0 & 1 & 0 \\ 0 & 0 & 0 & -1 \\ 1 & 0 & 0 & 0 \\ 0 & -1 & 0 & 0 \end{pmatrix} \begin{pmatrix} 1 \\ 0 \\ \frac{i}{2a_0} \frac{\hbar}{mc} \frac{z}{r} \\ \frac{i}{2a_0} \frac{\hbar}{mc} \frac{x+iy}{r} \end{pmatrix} \psi^2(1s) \\ &= \frac{y\mu_{n,x} - x\mu_{n,y}}{r^3} \left(1 \ 0 \ -\frac{i}{2a_0} \frac{\hbar}{mc} \frac{z}{r} \ -\frac{i}{2a_0} \frac{\hbar}{mc} \frac{x-iy}{r} \right) \begin{pmatrix} \frac{i}{2a_0} \frac{\hbar}{mc} \frac{z}{r} \\ -\frac{i}{2a_0} \frac{\hbar}{mc} \frac{x+iy}{r} \\ 1 \\ 0 \end{pmatrix} \psi^2(1s) = 0. \end{aligned} \quad (10.31)$$

Inserting results of Eqs. 10.29–10.31 into Eq. 10.28,

$$\mathcal{E} = -\frac{\mu_0}{4\pi} \frac{Q\hbar}{m} \frac{1}{a_0} \int_{V \rightarrow 0} \frac{1}{r^2} \left(\frac{x^2 + y^2}{r^2} \mu_{n,z} - \frac{zx}{r^2} \mu_{n,x} - \frac{zy}{r^2} \mu_{n,y} \right) \psi^2(1s) \, dx \, dy \, dz. \quad (10.32)$$

Expressed in spherical coordinates $x = r \sin \vartheta \cos \varphi$, $y = r \sin \vartheta \sin \varphi$, $z = r \cos \vartheta$, $dV = dx \, dy \, dz = r^2 \sin \vartheta dr d\vartheta d\varphi$,

$$\begin{aligned} \mathcal{E} &= -\frac{\mu_0}{4\pi} \frac{Q\hbar}{m} \frac{\mu_{n,z}}{a_0} \int_0^{r_0 \rightarrow 0} \psi^2(1s) dr \int_0^\pi \sin \vartheta d\vartheta (1 - \cos^2 \vartheta) \int_0^{2\pi} d\varphi \\ &\quad - \frac{\mu_0}{4\pi} \frac{Q\hbar}{m} \frac{\mu_{n,x}}{a_0} \int_0^{r_0 \rightarrow 0} \psi^2(1s) dr \int_0^\pi \sin \vartheta d\vartheta \sin \vartheta \int_0^{2\pi} d\varphi \cos \varphi \\ &\quad - \frac{\mu_0}{4\pi} \frac{Q\hbar}{m} \frac{\mu_{n,y}}{a_0} \int_0^{r_0 \rightarrow 0} \psi^2(1s) dr \int_0^\pi \sin \vartheta d\vartheta \sin \vartheta \int_0^{2\pi} d\varphi \sin \varphi \end{aligned} \quad (10.33)$$

Only the first term differs from zero because $\cos \varphi$ and $\sin \varphi$ are periodic functions and their integrals over the whole period

$$\int_0^{2\pi} d\varphi \cos \varphi = 0, \quad \int_0^{2\pi} d\varphi \sin \varphi = 0. \quad (10.34)$$

The first term can be evaluated using the substitution $u = \cos \vartheta$

$$\mathcal{E} = -\frac{\mu_0}{4\pi} \frac{Q\hbar}{m} \mu_{n,z} 2\pi \int_0^{r_0 \rightarrow 0} \frac{\psi^2(1s)}{a_0} dr \int_{-1}^1 (1-u^2) du = -\frac{\mu_0}{4\pi} \frac{Q\hbar}{m} \mu_{n,z} 2\pi \int_0^{r_0 \rightarrow 0} \frac{\psi^2(1s)}{a_0} dr \left[u - \frac{u^3}{3} \right]_{-1}^1 = -\frac{\mu_0}{4\pi} \frac{Q\hbar}{m} \mu_{n,z} \frac{8\pi}{3} \int_0^{r_0 \rightarrow 0} \frac{\psi^2(1s)}{a_0} dr, \quad (10.35)$$

where the integral gives the value of $\psi^2(1s)$ at the site of the nucleus ($\psi^2(1s, r=0)$). Note that $Q\hbar/2m$ is the eigenvalue of the component of the magnetic moment of the electron parallel to the magnetic field. This time, it is the magnetic field of the nucleus (\vec{B}_0 does not play any role here). If we use the direction of $\vec{\mu}_n$ as the z -axis of our coordinate system,

$$\mathcal{E} = -2 \frac{\mu_0}{4\pi} \vec{\mu}_e \cdot \vec{\mu}_n \frac{8\pi}{3} \psi^2(1s, r=0). \quad (10.36)$$

Accordingly, the corresponding Hamiltonian is

$$\hat{H}_F = -\frac{2\mu_0\gamma_n\gamma_e}{3} \left(\hat{I}_n \cdot \hat{I}_e \right) \psi^2(1s, r=0), \quad (10.37)$$

where \hat{I}_n and \hat{I}_e are operators of the spin of the nucleus and the electron, respectively, γ_n and γ_e are magnetogyric ratios of the spin of the nucleus and the electron, respectively, and the integral is equal to one inside the nucleus and to zero outside the nucleus. This type of interaction is known as the *Fermi contact interaction* and does not depend on orientation of the molecule in the magnetic field, as documented by the scalar vector in Eq. 10.37.

We can now proceed from the nucleus-electron interactions to interactions between two sigma-bonded nuclei mediated by electrons of the bond. The electrons in the bonding sigma orbital also have non-zero probability density at the positions of the nuclei (Figure 10.6). If the nuclei did not have any magnetic moments, the eigenfunction of the electrons is the linear combination $\frac{1}{\sqrt{2}}|\alpha\rangle \otimes |\beta\rangle - \frac{1}{\sqrt{2}}|\beta\rangle \otimes |\alpha\rangle$, as discussed in Section 10.9.2 and shown schematically in Figure 10.6A. Due to the Fermi interaction, parallel orientation of the nuclear and electron spin magnetic moments has (Figure 10.6B) a lower energy and the opposite orientation (Figure 10.6C) has a higher energy than the unperturbed stationary state. Thus the orientation of the magnetic moment of the first nucleus is indirectly influenced by the orientation of the second magnetic moment: the energy is proportional to the scalar product $\vec{\mu}_1 \cdot \vec{\mu}_2$, where $\vec{\mu}_1$ and $\vec{\mu}_2$ are the nuclear magnetic moments. The exact value of the energy depends on the actual distribution of the electrons in the bonding orbital, the calculation of the energy requires advanced quantum chemical methods. Such methods can be applied to more complex systems too. In general, the described indirect interaction is described by the Hamiltonian

$$\hat{H}_J = 2\pi J (\hat{I}_{1x}\hat{I}_{2x} + \hat{I}_{1y}\hat{I}_{2y} + \hat{I}_{1z}\hat{I}_{2z}), \quad (10.38)$$

where $2\pi J$ is a constant describing the strength of the indirect, electron mediated interaction and \hat{I}_{nj} are operators of the components of the angular momenta of the nuclei.

10.9.2 Two electrons in a sigma orbital

A wave function describing two electrons must be antisymmetric, as stated in Section 6.7.1. Assuming that the spin degrees of freedom can be separated (see the discussion in Sections 6.1 and 6.7.2), we can decompose the wave function into (i) a symmetric non-spin part σ^s and an antisymmetric spin part ψ^a , or to an antisymmetric non-spin part σ^a and a symmetric spin part ψ^s . We try to express the spin wave function in a suitable basis. In the case of a single particle in a field described by the Hamiltonian $-\gamma B_0 \hat{I}_z$, we used a basis consisting of eigenfunctions of the operator \hat{I}_z , i.e., the eigenvectors $|\alpha\rangle = \begin{pmatrix} 1 \\ 0 \end{pmatrix}$ and $|\beta\rangle = \begin{pmatrix} 0 \\ 1 \end{pmatrix}$. These eigenvectors are also eigenfunctions of the operator of I^2 because the matrix representation of I^2 is proportional to the unit matrix (see Eq. 5.10) and $\hat{I}\psi = \psi$ for any ψ . For a pair of two electrons, we could use the eigenfunctions of \hat{I}_{1z} , \hat{I}_1^2 , \hat{I}_{2z} , and \hat{I}_2^2 (i.e., eigenvectors listed in Eq. 8.81). However, it is more useful to chose eigenfunctions of operators representing the z -component and the square of the *total spin angular momentum* $\vec{I} = \vec{I}_1 + \vec{I}_2$, in combination with \hat{I}_1^2 and \hat{I}_2^2 . Note that all operators of the set \hat{I}_1^2 , \hat{I}_2^2 , \hat{I}^2 , and \hat{I}_z commute (the first two operators are proportional to the unit matrix that commutes with any matrix of the same size, commutation of the last two operators is given by Eq. 4.35). The explicit forms of the chosen operators are obtained using the matrix representations of the product operators in Tables 8.3 and 8.4:

$$\hat{I}_1^2 \psi_k = \frac{3\hbar^2}{4} \begin{pmatrix} 1 & 0 & 0 & 0 \\ 0 & 1 & 0 & 0 \\ 0 & 0 & 1 & 0 \\ 0 & 0 & 0 & 1 \end{pmatrix} \begin{pmatrix} c_{1k} \\ c_{2k} \\ c_{3k} \\ c_{4k} \end{pmatrix}, \quad (10.39)$$

$$\hat{I}_2^2 \psi_k = \frac{3\hbar^2}{4} \begin{pmatrix} 1 & 0 & 0 & 0 \\ 0 & 1 & 0 & 0 \\ 0 & 0 & 1 & 0 \\ 0 & 0 & 0 & 1 \end{pmatrix} \begin{pmatrix} c_{1k} \\ c_{2k} \\ c_{3k} \\ c_{4k} \end{pmatrix}, \quad (10.40)$$

$$\begin{aligned} \hat{I}^2 \psi_k &= (\hat{I}_1 + \hat{I}_2)^2 \psi_k = (\hat{I}_1^2 + \hat{I}_2^2 + 2\hat{I}_1 \cdot \hat{I}_2) \psi_k = \\ &= (\hat{I}_1^2 + \hat{I}_2^2 + 2\hat{I}_{1x}\hat{I}_{2x} + 2\hat{I}_{1y}\hat{I}_{2y} + 2\hat{I}_{1z}\hat{I}_{2z}) \psi_k = \hbar^2 \begin{pmatrix} 2 & 0 & 0 & 0 \\ 0 & 1 & 1 & 0 \\ 0 & 1 & 1 & 0 \\ 0 & 0 & 0 & 2 \end{pmatrix} \begin{pmatrix} c_{1k} \\ c_{2k} \\ c_{3k} \\ c_{4k} \end{pmatrix}, \end{aligned} \quad (10.41)$$

$$\hat{I}_z \psi_k = (\hat{I}_{1z} + \hat{I}_{2z}) \psi_k = \hbar \begin{pmatrix} 1 & 0 & 0 & 0 \\ 0 & 0 & 0 & 0 \\ 0 & 0 & 0 & 0 \\ 0 & 0 & 0 & 1 \end{pmatrix} \begin{pmatrix} c_{1k} \\ c_{2k} \\ c_{3k} \\ c_{4k} \end{pmatrix}. \quad (10.42)$$

The eigenfunctions of \hat{I}_{1z} , \hat{I}_1^2 , \hat{I}_{2z} , and \hat{I}_2^2 clearly cannot be eigenfunctions of the operator \hat{I}^2 , represented by a non-diagonal matrix. Therefore, we have to look for a new basis, where the operator \hat{I}^2 is represented by a diagonal matrix $\hat{I}^{2'}$. For this purpose, we use a procedure that is not very elegant, but does not require any special approaches of matrix algebra.

From the mathematical point of view, we have to find a *transformation* matrix \hat{T} so that

$$\hat{T} \hat{I}^{2'} = \hat{I}^2 \hat{T}. \quad (10.43)$$

Then, the *diagonalized* matrix $\hat{I}^{2'}$ representing the \hat{I}^2 operator is obtained by multiplying the equation from left by a matrix \hat{T}^{-1} , inverse to \hat{T} (i.e., $\hat{T}^{-1}\hat{T} = \hat{1}$):

$$\mathcal{H}' = \hat{T}^{-1} \mathcal{H} \hat{T}. \quad (10.44)$$

Multiplying by \hat{T} from left gives

$$\hat{T} \mathcal{H}' = \mathcal{H} \hat{T}. \quad (10.45)$$

The desired eigenvalues are diagonal elements of the *diagonalized* matrix

$$\begin{pmatrix} \lambda'_1 & 0 & 0 & 0 \\ 0 & \lambda'_2 & 0 & 0 \\ 0 & 0 & \lambda'_3 & 0 \\ 0 & 0 & 0 & \lambda'_4 \end{pmatrix}. \quad (10.46)$$

The eigenvalues λ'_k and eigenvectors $|\psi'_k\rangle$ can be obtained by comparing the eigenvalue equation

$$\mathcal{H}' |\psi'_k\rangle = \omega'_k |\psi'_k\rangle \quad (10.47)$$

with the left-hand side of Eq. 10.45

$$\hat{T} \mathcal{H}' = \begin{pmatrix} T_{11} & T_{12} & T_{13} & T_{14} \\ T_{21} & T_{22} & T_{23} & T_{24} \\ T_{31} & T_{32} & T_{33} & T_{34} \\ T_{41} & T_{42} & T_{43} & T_{44} \end{pmatrix} \begin{pmatrix} \lambda'_1 & 0 & 0 & 0 \\ 0 & \lambda'_2 & 0 & 0 \\ 0 & 0 & \lambda'_3 & 0 \\ 0 & 0 & 0 & \lambda'_4 \end{pmatrix} = \begin{pmatrix} \lambda'_1 T_{11} & \lambda'_2 T_{12} & \lambda'_3 T_{13} & \lambda'_4 T_{14} \\ \lambda'_1 T_{21} & \lambda'_2 T_{22} & \lambda'_3 T_{23} & \lambda'_4 T_{24} \\ \lambda'_1 T_{31} & \lambda'_2 T_{32} & \lambda'_3 T_{33} & \lambda'_4 T_{34} \\ \lambda'_1 T_{41} & \lambda'_2 T_{42} & \lambda'_3 T_{43} & \lambda'_4 T_{44} \end{pmatrix}. \quad (10.48)$$

The eigenvalue equation can be written as a set of four equations for $k = 1, 2, 3, 4$

$$\mathcal{H}' |\psi'_k\rangle = \hbar^2 \begin{pmatrix} 2 & 0 & 0 & 0 \\ 0 & 1 & 1 & 0 \\ 0 & 1 & 1 & 0 \\ 0 & 0 & 0 & 2 \end{pmatrix} \begin{pmatrix} T_{1k} \\ T_{2k} \\ T_{3k} \\ T_{4k} \end{pmatrix} = \hbar^2 \begin{pmatrix} 2T_{1k} \\ T_{2k} + T_{3k} \\ T_{2k} + T_{3k} \\ 2T_{4k} \end{pmatrix} = \lambda'_k \begin{pmatrix} T_{1k} \\ T_{2k} \\ T_{3k} \\ T_{4k} \end{pmatrix} = \lambda'_k |\psi'_k\rangle. \quad (10.49)$$

The first row of the middle equality allows us to identify

$$\lambda'_1 = 2\hbar^2 \quad (10.50)$$

if we set $T_{21} = T_{31} = T_{41} = 0$, i.e.,

$$|\psi'_1\rangle = \begin{pmatrix} T_{11} \\ 0 \\ 0 \\ 0 \end{pmatrix}. \quad (10.51)$$

Similarly,

$$\lambda'_4 = 2\hbar^2 \quad (10.52)$$

for

$$|\psi'_4\rangle = \begin{pmatrix} 0 \\ 0 \\ 0 \\ T_{44} \end{pmatrix}. \quad (10.53)$$

The λ'_2 and λ'_3 values can be calculated from the equations

$$\lambda'_k T_{2k} = \hbar^2 (T_{2k} + T_{3k}) \quad (10.54)$$

$$\lambda'_k T_{3k} = \hbar^2 (T_{2k} + T_{3k}), \quad (10.55)$$

(setting $T_{12} = T_{42} = T_{13} = T_{43} = 0$).

T_{3k} can be expressed from the first equation

$$T_{3k} = \frac{\lambda'_k - \hbar^2}{\hbar^2} T_{2k} \quad (10.56)$$

and inserted into the second equation

$$\lambda'_k \frac{\lambda'_k - \hbar^2}{\hbar^2} T_{2k} = (\lambda'_k - \hbar^2) T_{2k} + \hbar^2 T_{2k} = \lambda'_k T_{2k}, \quad (10.57)$$

$$(\lambda'_k)^2 - 2\hbar^2 \lambda'_k = \lambda'_k (\lambda'_k - 2\hbar^2) = 0, \quad (10.58)$$

directly giving

$$\lambda'_2 = 0, \quad \lambda'_3 = 2\hbar^2. \quad (10.59)$$

We have identified all diagonal elements of the diagonalized operator

$$\hat{I}^{2'} = 2\hbar^2 \begin{pmatrix} 1 & 0 & 0 & 0 \\ 0 & 0 & 0 & 0 \\ 0 & 0 & 1 & 0 \\ 0 & 0 & 0 & 1 \end{pmatrix}. \quad (10.60)$$

The new basis is given by Eqs. 10.54, 10.55, and the normalization condition

$$\langle \psi'_k | \psi'_k \rangle = 1 \Rightarrow \sum_{j=1}^4 T_{jk}^2 = 1. \quad (10.61)$$

The normalization condition immediately defines $T_{11} = T_{44} = 1$.

Substituting λ'_2 into Eqs. 10.54 and 10.55 gives

$$T_{22} + T_{32} = 0 \quad \Rightarrow \quad T_{22} = -T_{32}. \quad (10.62)$$

The normalization condition $1 = T_{22}^2 + T_{32}^2 = 2T_{22}^2$ requires

$$T_{22} = \frac{1}{\sqrt{2}}, \quad T_{32} = -\frac{1}{\sqrt{2}}. \quad (10.63)$$

Substituting λ'_3 into Eqs. 10.54 and 10.55 gives

$$2\hbar^2 T_{23} = \hbar^2 (T_{23} + T_{33}) \quad (10.64)$$

$$2\hbar^2 T_{33} = \hbar^2 (T_{23} + T_{33}) \quad (10.65)$$

$$\Rightarrow \quad T_{23} = T_{33}. \quad (10.66)$$

$$\Rightarrow T_{23} = T_{23}. \quad (10.67)$$

The normalization condition $1 = T_{23}^2 + T_{33}^2 = 2T_{23}^2$ requires

$$T_{23} = \frac{1}{\sqrt{2}}, \quad T_{33} = \frac{1}{\sqrt{2}}. \quad (10.68)$$

Taken together, the new basis consists of the following eigenvectors

$$|\psi'_1\rangle = \begin{pmatrix} 1 \\ 0 \\ 0 \\ 0 \end{pmatrix} = |\alpha\rangle \otimes |\alpha\rangle, \quad |\psi'_2\rangle = \begin{pmatrix} 0 \\ \frac{1}{\sqrt{2}} \\ -\frac{1}{\sqrt{2}} \\ 0 \end{pmatrix} = \frac{1}{\sqrt{2}}(|\alpha\rangle \otimes |\beta\rangle - |\beta\rangle \otimes |\alpha\rangle), \quad |\psi'_3\rangle = \begin{pmatrix} 0 \\ \frac{1}{\sqrt{2}} \\ \frac{1}{\sqrt{2}} \\ 0 \end{pmatrix} = \frac{1}{\sqrt{2}}(|\alpha\rangle \otimes |\beta\rangle + |\beta\rangle \otimes |\alpha\rangle), \quad |\psi'_4\rangle = \begin{pmatrix} 0 \\ 0 \\ 0 \\ 1 \end{pmatrix} = |\beta\rangle \otimes |\beta\rangle. \quad (10.69)$$

Among them, $|\psi'_1\rangle$, $|\psi'_3\rangle$, and $|\psi'_4\rangle$, are symmetric and are multiplied by the antisymmetric σ^a , whereas $|\psi'_2\rangle$ is antisymmetric and is multiplied by the symmetric σ^s . Calculations of the non-spin functions σ^a and σ^s is not easy⁶ and requires advanced quantum chemistry. The result of such calculation is the *bonding sigma orbital* σ^s with lower energy and the *antibonding sigma orbital* σ^a with higher energy. Therefore, we are interested in $\sigma^s|\psi'_2\rangle = \sigma^s(|\alpha\rangle \otimes |\beta\rangle - |\beta\rangle \otimes |\alpha\rangle)/\sqrt{2}$ if we study ground state of the molecule. The corresponding eigenvalues are $3\hbar^2/4$ for \hat{I}_1^2 and \hat{I}_1^2 , zero for \hat{I}^2 and \hat{I}_z .

10.9.3 Two J -coupled nuclei in thermal equilibrium

Before we analyze evolution of the density matrix in a 2D experiment, we must define its initial form. Again, we start from the thermal equilibrium and use the Hamiltonian. The difference from the case of isolated nuclei is that we need to define a 4×4 density matrix in order to describe a pair of mutually interacting nuclei. As explained above, the off-diagonal elements of the equilibrium density matrix (proportional to \mathcal{S}_x and \mathcal{S}_y) are equal to zero. The four diagonal elements describe average populations of four stationary states of a system composed of (isolated) nuclear pairs: $\alpha\alpha$, $\alpha\beta$, $\beta\alpha$, and $\beta\beta$. These populations are:

$$P_{\alpha\alpha}^{\text{eq}} = \frac{e^{-\mathcal{E}_{\alpha\alpha}/k_B T}}{e^{-\mathcal{E}_{\alpha\alpha}/k_B T} + e^{-\mathcal{E}_{\alpha\beta}/k_B T} + e^{-\mathcal{E}_{\beta\alpha}/k_B T} + e^{-\mathcal{E}_{\beta\beta}/k_B T}} \approx \frac{1 - \frac{\mathcal{E}_{\alpha\alpha}}{k_B T}}{4}, \quad (10.70)$$

$$P_{\alpha\beta}^{\text{eq}} = \frac{e^{-\mathcal{E}_{\alpha\beta}/k_B T}}{e^{-\mathcal{E}_{\alpha\alpha}/k_B T} + e^{-\mathcal{E}_{\alpha\beta}/k_B T} + e^{-\mathcal{E}_{\beta\alpha}/k_B T} + e^{-\mathcal{E}_{\beta\beta}/k_B T}} \approx \frac{1 - \frac{\mathcal{E}_{\alpha\beta}}{k_B T}}{4}, \quad (10.71)$$

$$P_{\beta\alpha}^{\text{eq}} = \frac{e^{-\mathcal{E}_{\beta\alpha}/k_B T}}{e^{-\mathcal{E}_{\alpha\alpha}/k_B T} + e^{-\mathcal{E}_{\alpha\beta}/k_B T} + e^{-\mathcal{E}_{\beta\alpha}/k_B T} + e^{-\mathcal{E}_{\beta\beta}/k_B T}} \approx \frac{1 - \frac{\mathcal{E}_{\beta\alpha}}{k_B T}}{4}, \quad (10.72)$$

$$P_{\beta\beta}^{\text{eq}} = \frac{e^{-\mathcal{E}_{\beta\beta}/k_B T}}{e^{-\mathcal{E}_{\alpha\alpha}/k_B T} + e^{-\mathcal{E}_{\alpha\beta}/k_B T} + e^{-\mathcal{E}_{\beta\alpha}/k_B T} + e^{-\mathcal{E}_{\beta\beta}/k_B T}} \approx \frac{1 - \frac{\mathcal{E}_{\beta\beta}}{k_B T}}{4}. \quad (10.73)$$

In principle, the total Hamiltonian also includes the term \hat{H}_J , which describes the J coupling and which is not averaged to zero.

$$\hat{H} = -\gamma_1 B_0(1 + \delta_{i,1})\hat{I}_{1,z} - \gamma_2 B_0(1 + \delta_{i,2})\hat{I}_{2,z} + 2\pi J \hat{I}_{1,z} \hat{I}_{2,z} = \quad (10.74)$$

$$-\gamma_1 B_0(1 + \delta_{i,1}) \frac{\hbar}{2} \begin{pmatrix} 1 & 0 & 0 & 0 \\ 0 & 1 & 0 & 0 \\ 0 & 0 & -1 & 0 \\ 0 & 0 & 0 & -1 \end{pmatrix} - \gamma_2 B_0(1 + \delta_{i,2}) \frac{\hbar}{2} \begin{pmatrix} 1 & 0 & 0 & 0 \\ 0 & -1 & 0 & 0 \\ 0 & 0 & 1 & 0 \\ 0 & 0 & 0 & -1 \end{pmatrix} + \frac{\pi J \hbar}{2} \begin{pmatrix} 1 & 0 & 0 & 0 \\ 0 & -1 & 0 & 0 \\ 0 & 0 & -1 & 0 \\ 0 & 0 & 0 & 1 \end{pmatrix}. \quad (10.75)$$

where the diagonal elements (eigenvalues) are the energies of the individual states. Therefore, the populations (diagonal elements of the density matrix) should be given by

⁶The major difficulty is a mutual interactions of the electron charges

$$P_{\alpha\alpha}^{\text{eq}} \approx \frac{1 - \frac{\mathcal{E}_{\alpha\alpha}}{k_{\text{B}}T}}{4} = \frac{1}{4} + \gamma_1(1 + \delta_{i,1}) \frac{B_0\hbar}{8k_{\text{B}}T} + \gamma_2(1 + \delta_{i,2}) \frac{B_0\hbar}{8k_{\text{B}}T} - \frac{\pi J\hbar}{16k_{\text{B}}T}, \quad (10.76)$$

$$P_{\alpha\beta}^{\text{eq}} \approx \frac{1 - \frac{\mathcal{E}_{\alpha\beta}}{k_{\text{B}}T}}{4} = \frac{1}{4} + \gamma_1(1 + \delta_{i,1}) \frac{B_0\hbar}{8k_{\text{B}}T} - \gamma_2(1 + \delta_{i,2}) \frac{B_0\hbar}{8k_{\text{B}}T} + \frac{\pi J\hbar}{16k_{\text{B}}T}, \quad (10.77)$$

$$P_{\beta\alpha}^{\text{eq}} \approx \frac{1 - \frac{\mathcal{E}_{\beta\alpha}}{k_{\text{B}}T}}{4} = \frac{1}{4} - \gamma_1(1 + \delta_{i,1}) \frac{B_0\hbar}{8k_{\text{B}}T} + \gamma_2(1 + \delta_{i,2}) \frac{B_0\hbar}{8k_{\text{B}}T} + \frac{\pi J\hbar}{16k_{\text{B}}T}, \quad (10.78)$$

$$P_{\beta\beta}^{\text{eq}} \approx \frac{1 - \frac{\mathcal{E}_{\beta\beta}}{k_{\text{B}}T}}{4} = \frac{1}{4} - \gamma_1(1 + \delta_{i,1}) \frac{B_0\hbar}{8k_{\text{B}}T} - \gamma_2(1 + \delta_{i,2}) \frac{B_0\hbar}{8k_{\text{B}}T} - \frac{\pi J\hbar}{16k_{\text{B}}T}. \quad (10.79)$$

$$(10.80)$$

However, the values of J in typical organic compounds are at least five orders of magnitude lower than the frequencies measured even at low-field magnets. As a consequence, the contribution of J -coupling can be safely neglected, and the initial density matrix is identical to that derived for a pair of nuclei interacting through space (Eq. 8.40).

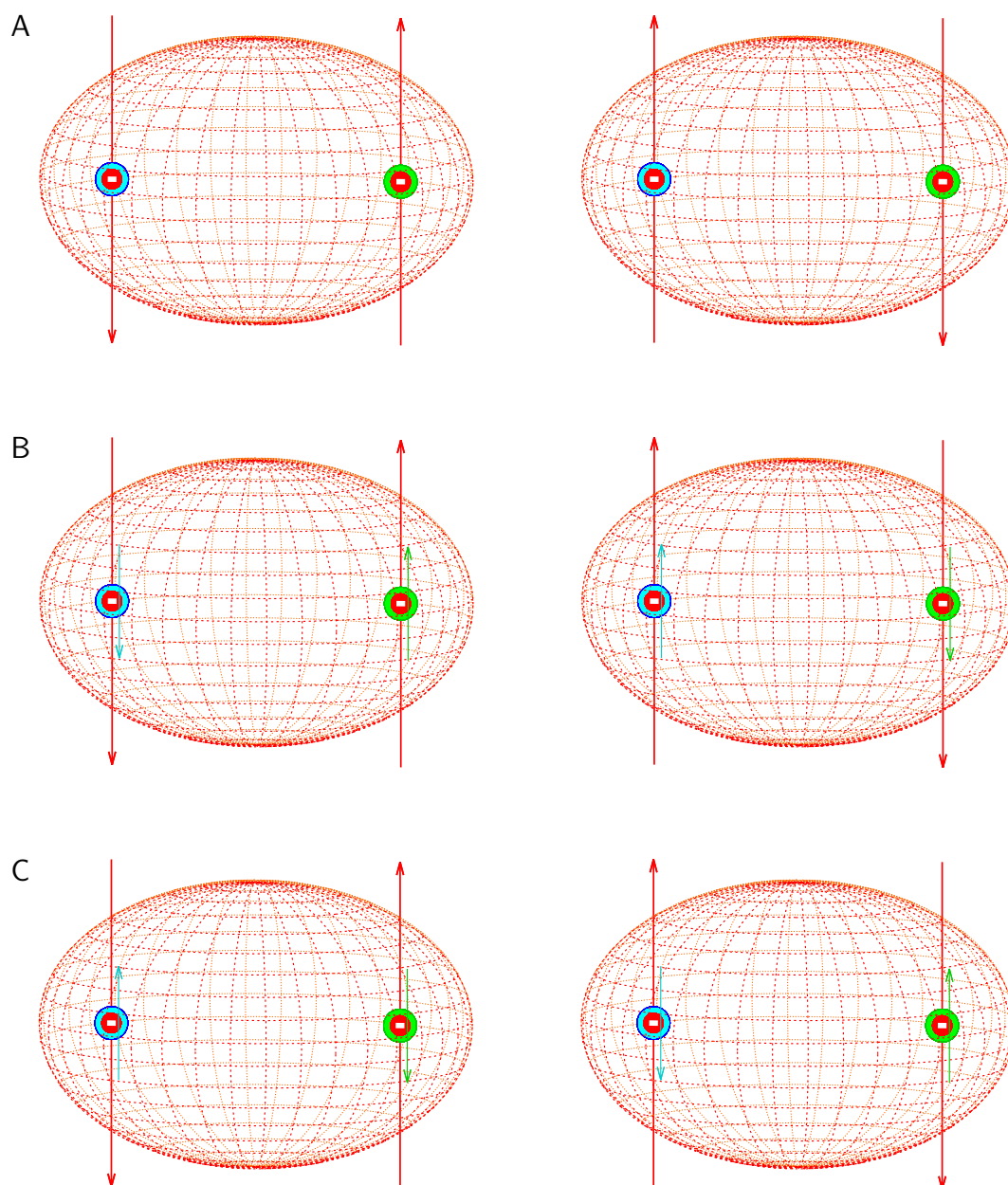


Figure 10.6: J -coupling. A, the stationary spin state of the electrons in the bonding sigma orbital without nuclear magnetic moments is a superposition of the $|\alpha\rangle \otimes |\beta\rangle$ and $|\beta\rangle \otimes |\alpha\rangle$ eigenstates (indicated by the opposite direction of the red arrows). B, energetically favorable state of electrons interacting with nuclear magnetic moments (green and cyan arrows). C, energetically unfavorable state of electrons interacting with nuclear magnetic moments.

Lecture 11

Correlated spectroscopy using J -coupling

Literature: INEPT, HSQC, and APT experiments are nicely described in K7.10, K8.7, and K12.4.4., respectively. INEPT is discussed in detail in L16.3., HSQC in C7.1.1. Decoupling trains are reviewed in C3.5. COSY is described in detail in L16.1, C6.2.1., and K8.3 (with a detailed discussion of DQF-COSY in K8.4).

11.1 INEPT

INEPT is a heteronuclear NMR experiment based on the simultaneous echo. It differs from the simple simultaneous echo in two issues:

- The length of the delay τ is set to $1/4|J|$
- The echo is followed by two 90° radio wave pulses, one applied at the same frequency as the excitation pulse (the 90° pulse preceding the echo) – this one must be phase-shifted by 90° from the excitation pulse, and the other one applied at the frequency of the other nucleus (^{13}C or ^{15}N in Fig. 11.1).

With $\tau = 1/4J$, $2\pi\tau = \pi/2$, $c_J = 0, s_J = 1$ if $J > 0$, and $s_J = -1$ if $J < 0$. Therefore, the density matrix at the end of the echo is¹

$$\hat{\rho}(\text{e}) = \frac{1}{2}\mathcal{I}_t - \frac{1}{2}\kappa_1(2\mathcal{I}_x\mathcal{I}_z) - \frac{1}{2}\kappa_2\mathcal{I}_z$$

$$\longrightarrow \hat{\rho}(\text{f}) = \frac{1}{2}\mathcal{I}_t + \frac{1}{2}\kappa_1(2\mathcal{I}_z\mathcal{I}_z) - \frac{1}{2}\kappa_2\mathcal{I}_z \text{ after the first pulse and}$$

$$\longrightarrow \hat{\rho}(\text{g}) = \frac{1}{2}\mathcal{I}_t - \frac{1}{2}\kappa_1(2\mathcal{I}_z\mathcal{I}_y) + \frac{1}{2}\kappa_2\mathcal{I}_y \text{ after the second pulse.}$$

If the experiment continues by acquisition, the density matrix evolves as

¹The analysis is done for $J > 0$. If $J < 0$ (e.g. for one-bond ^1H - ^{15}N coupling), all blue terms have the opposite sign.

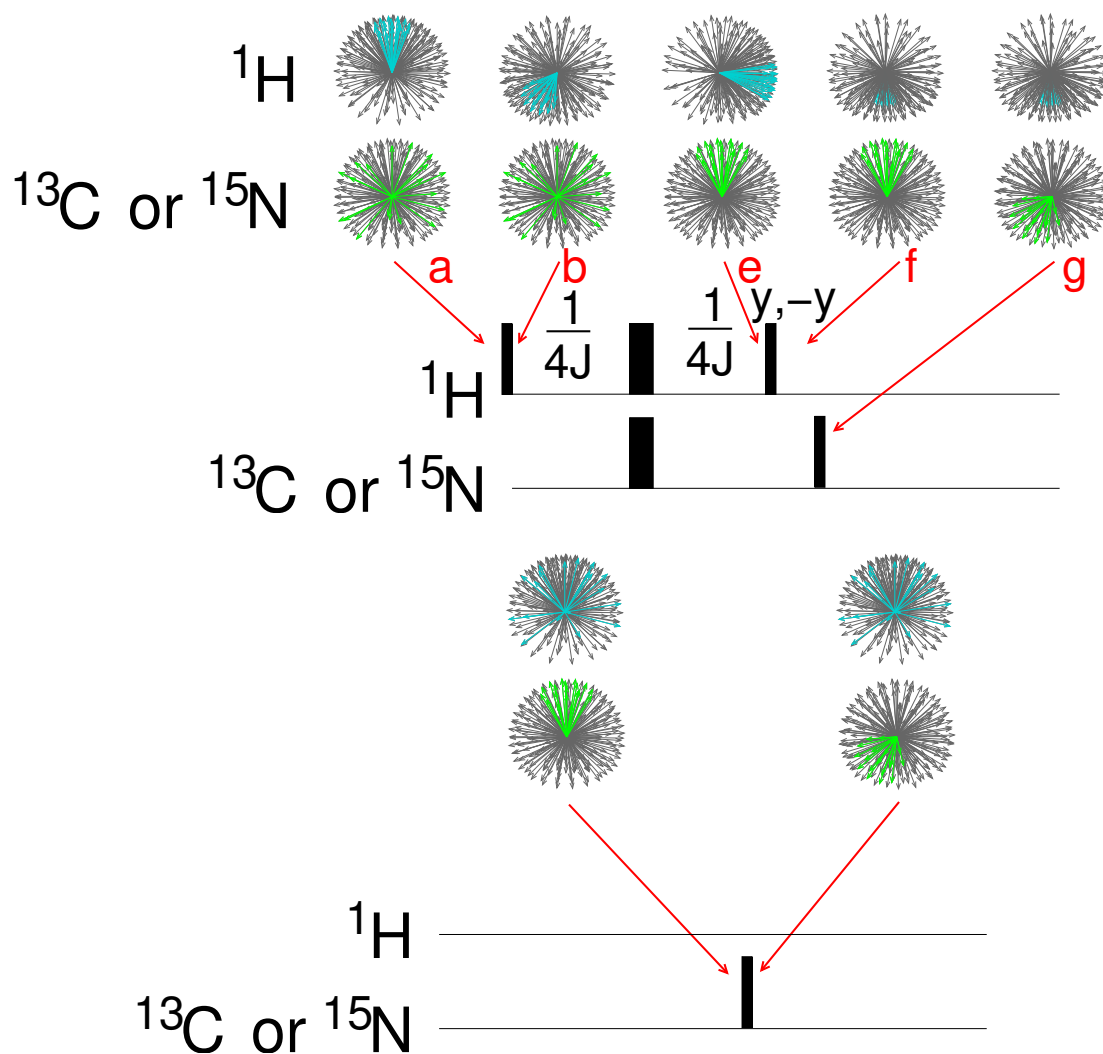


Figure 11.1: INEPT pulse sequence applied to ^1H and ^{13}C or ^{15}N (top) and direct excitation of ^{13}C or ^{15}N (bottom). The narrow and wide rectangles represent 90° and 180° radio wave pulses, respectively. The label $y, -y$ above the pulse indicates application of phase cycling to the labeled pulse (irradiation by a radio wave with the phases alternating between values of 90° and 270° , relative to the first pulse in the sequence, in subsequent measurements). Distributions of magnetic moments corresponding to the density matrix contributions other than \mathcal{S}_i are shown schematically above the pulse sequences for time instants labeled by the red letters and arrows. For a better visibility, the distributions are shown in a coordinate frame rotated by 90° counterclockwise about z , compared with the orientation used in Table 8.4.

$$\mathcal{I}_t \longrightarrow \mathcal{I}_t \longrightarrow \mathcal{I}_t \quad (11.1)$$

$$-2\mathcal{I}_z\mathcal{I}_y \longrightarrow \begin{cases} -c_2 2\mathcal{I}_z\mathcal{I}_y \longrightarrow \begin{cases} -c_2c_J 2\mathcal{I}_z\mathcal{I}_y \\ +c_2s_J \mathcal{I}_x \end{cases} \\ +s_2 2\mathcal{I}_x\mathcal{I}_z \longrightarrow \begin{cases} +s_2c_J 2\mathcal{I}_z\mathcal{I}_x \\ +s_2s_J \mathcal{I}_y \end{cases} \end{cases} \quad (11.2)$$

$$\mathcal{I}_y \longrightarrow \begin{cases} +c_2\mathcal{I}_y \longrightarrow \begin{cases} +c_2c_J \mathcal{I}_y \\ -c_2s_J 2\mathcal{I}_x\mathcal{I}_z \end{cases} \\ -s_2\mathcal{I}_x \longrightarrow \begin{cases} -s_2c_J \mathcal{I}_x \\ -s_2s_J 2\mathcal{I}_y\mathcal{I}_z \end{cases} \end{cases} \quad (11.3)$$

Both the "blue" coherence $2\mathcal{I}_z\mathcal{I}_y$ and the "green" coherence \mathcal{I}_y evolve into "measurable" product operators, giving non-zero trace when multiplied by \mathcal{I}_+ .

After calculating the traces, including relaxation (treated as in Section 10.3), and applying a phase shift by 90° , the expected value of M_{2+} evolves as

$$\frac{\kappa_1}{4}e^{-\bar{R}_2t} (e^{-i(\Omega_2-\pi J)t} - e^{-i(\Omega_2+\pi J)t}) + \frac{\kappa_2}{4}e^{-\bar{R}_2t} (e^{-i(\Omega_2-\pi J)t} + e^{-i(\Omega_2+\pi J)t}) \quad (11.4)$$

The real part of the spectrum obtained by the Fourier transformation is

$$\Re\{Y(\omega)\} = \frac{\mathcal{N}\gamma_1^2\hbar^2B_0}{8k_B T} \left(+\frac{\bar{R}_2}{\bar{R}_2^2 + (\omega - \Omega_2 + \pi J)^2} - \frac{\bar{R}_2}{\bar{R}_2^2 + (\omega - \Omega_2 - \pi J)^2} \right) + \frac{\mathcal{N}\gamma_2^2\hbar^2B_0}{8k_B T} \left(+\frac{\bar{R}_2}{\bar{R}_2^2 + (\omega - \Omega_2 + \pi J)^2} + \frac{\bar{R}_2}{\bar{R}_2^2 + (\omega - \Omega_2 - \pi J)^2} \right) \quad (11.5)$$

- The "blue" coherence $2\mathcal{I}_z\mathcal{I}_y$ gives a signal with *opposite phase* of the peaks at $\Omega_2 - \pi J$ and $\Omega_2 + \pi J$. Accordingly, it is called the *anti-phase* coherence.
- The "green" coherence \mathcal{I}_y gives a signal with the *same phase* of the peaks at $\Omega_2 - \pi J$ and $\Omega_2 + \pi J$. Accordingly, it is called the *in-phase* coherence.
- More importantly, the "blue" coherence $2\mathcal{I}_z\mathcal{I}_y$ gives a signal proportional to γ_1^2 while the "green" coherence \mathcal{I}_y gives a signal proportional to γ_2^2 . The amplitude of the "green" signal corresponds to the amplitude of a regular 1D ^{15}N spectrum. The "blue" signal "inherited" the amplitude with γ_1^2 from the excited nucleus, proton. In the case of ^1H and ^{15}N , $|\gamma_1|$ is approximately ten times higher than $|\gamma_2|$. Therefore, the blue signal is two orders of magnitude stronger. This is why this experiment is called *Insensitive Nuclei Enhanced by Polarization Transfer (INEPT)*.
- As described, the "blue" and "green" signals are combined, which results in different heights of the $\Omega_2 - \pi J$ and $\Omega_2 + \pi J$ peaks (Figure 11.2). The "blue" and "green" signals can be separated if we repeat the measurement twice with the phase of the proton y pulse shifted by

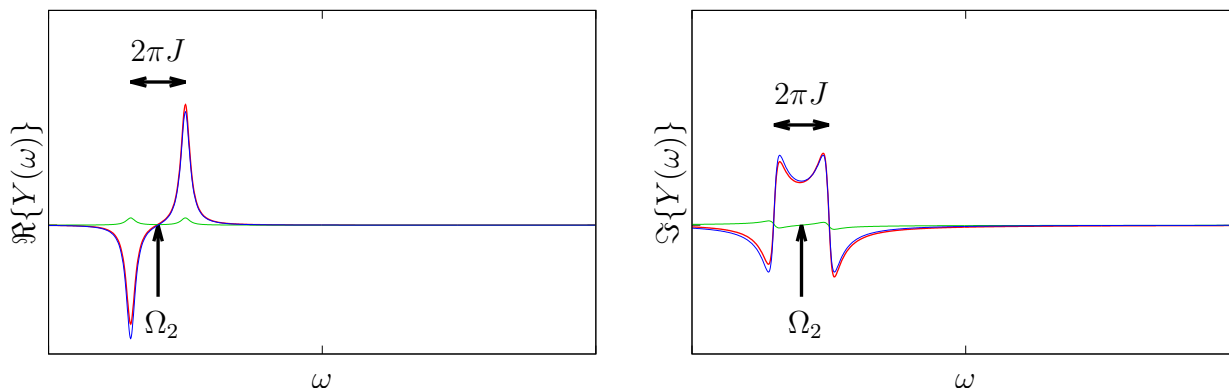


Figure 11.2: Real (left) and imaginary (right) components of an INEPT spectrum of a ^1H - ^{13}C pair. The blue and green curves are contributions of the INEPT transfer and direct excitation to the final spectrum (red). Note that the direct contribution makes the final peak heights slightly unbalanced. The blue spectrum is obtained if the phase sampling is applied, direct measurement of ^{13}C magnetization provides the green spectrum. The scale is the same as in Figure 10.4.

180° (i.e., with $-y$). The mentioned pulse converts the $2\mathcal{I}_x\mathcal{I}_z$ operator in $\hat{\rho}(e)$ to $-2\mathcal{I}_z\mathcal{I}_z$ if the relative phase of the radio wave is $+90^\circ$ (y), but to $+2\mathcal{I}_z\mathcal{I}_z$ if the phase is -90° ($-y$):

$$\hat{\rho}(e) = \frac{1}{2}\mathcal{I}_t - \frac{1}{2}\kappa_1(2\mathcal{I}_x\mathcal{I}_z) - \frac{1}{2}\kappa_2\mathcal{I}_z \longrightarrow$$

$$\hat{\rho}(f) = \frac{1}{2}\mathcal{I}_t \pm \frac{1}{2}\kappa_1(2\mathcal{I}_z\mathcal{I}_z) - \frac{1}{2}\kappa_2\mathcal{I}_z \longrightarrow$$

$$\hat{\rho}(g) = \frac{1}{2}\mathcal{I}_t \mp \frac{1}{2}\kappa_1(2\mathcal{I}_z\mathcal{I}_y) + \frac{1}{2}\kappa_2\mathcal{I}_y$$

Such alteration of the phase does not affect the "green" signal, but changes the sign of the "blue" signal. If we subtract the spectra, we obtained a pure "blue" signal. This trick, repeating acquisition with different phases, is known as *phase cycling* and is used routinely in NMR spectroscopy to remove unwanted signals.

Another application of the simultaneous echo, known as ATP (attached proton test) and useful for analysis of the CH_n groups, is presented in Section 11.6.1.

11.2 HSQC

Heteronuclear Single-Quantum Correlation (HSQC) spectroscopy is a 2D experiment using scalar coupling to correlate frequencies of two magnetic moments with different γ (Figure 11.3A). The experiment consists of

- excitation pulse, usually applied at the proton frequency
- INEPT module, transferring polarization to the coupled nucleus (usually ^{15}N or ^{13}C)
- evolution period of incremented duration t_1 , introducing signal modulation by frequency of the other nucleus

- another INEPT module, transferring polarization back to proton
- signal acquisition

The pulse sequence is already rather complex and tracking the complete density matrix evolution may be very demanding. In practice, the analysis is simplified (i) by working with the already known effects of the complete building blocks (spin echoes, INEPT) and (ii) by ignoring evolution of the density matrix contributions that cannot influence the measured transverse magnetization. The latter simplification is based on the following considerations.

- Only product operators representing *uncorrelated transverse polarizations* ($\mathcal{I}_x, \mathcal{I}_y, \mathcal{S}_x, \mathcal{S}_y$), known as *in-phase single-quantum coherences*, directly contribute to the measurable signal. Furthermore, only signal oscillating relatively close to the carrier frequency of the radio waves passes the audio filters of the spectrometer (see footnote 9 in Section 7.10.4). Therefore, the operator of the measured quantity represents only the actually detected transverse magnetization (M_{1+} in our case). This limits coherences contributing to the signal to $\mathcal{I}_x, \mathcal{I}_y$ (if nucleus 1 is detected). Only traces of their products with \hat{M}_{1+} are not zero. The coherences $\mathcal{S}_x, \mathcal{S}_y$ can be converted to the "measurable" operators $\mathcal{I}_x, \mathcal{I}_y$ by a combination of J -coupling and 90° pulses.
- Product operators representing *transverse polarizations correlated with longitudinal polarizations*, known as *anti-phase single-quantum coherences* ($2\mathcal{I}_x\mathcal{S}_z, 2\mathcal{I}_y\mathcal{S}_z$ if nucleus 1 is detected), do not contribute to the measurable signal (traces of their products with \hat{M}_{1+} are equal to zero), but they can evolve to the "measurable" in-phase single-quantum coherences if the J -coupling is present (without application of any radio-wave pulses).
- Conversion of the operators $2\mathcal{I}_z\mathcal{S}_x, 2\mathcal{I}_z\mathcal{S}_y$ to the single-quantum coherences of the measured nucleus 1 requires evolution of the J -coupling and application of a 90° pulse (at the precession frequency of nucleus 1).
- Product operators representing *two² correlated transverse polarizations* ($2\mathcal{I}_x\mathcal{S}_x, 2\mathcal{I}_y\mathcal{S}_y, 2\mathcal{I}_x\mathcal{S}_y, 2\mathcal{I}_y\mathcal{S}_x$), known as *multiple-quantum coherences*, do not contribute to the measurable signal (traces of their products with \hat{M}_{1+} are equal to zero), and can be converted to the "measurable" in-phase single quantum coherences only by applying 90° pulse and by a subsequent action of the J -coupling.
- Product operators representing *longitudinal polarizations* ($\mathcal{I}_z, \mathcal{S}_z, 2\mathcal{I}_z\mathcal{S}_z$), known as *populations*, do not contribute to the measurable signal (traces of their products with \hat{M}_{1+} are equal to zero), and can be converted to single quantum coherences only by applying 90° pulse (\mathcal{I}_z) and, in the case of \mathcal{S}_z and $2\mathcal{I}_z\mathcal{S}_z$, by a subsequent action of the J -coupling.
- Based on the arguments discussed above, all operators other than $\mathcal{I}_x, \mathcal{I}_y, 2\mathcal{I}_x\mathcal{S}_z, 2\mathcal{I}_y\mathcal{S}_z$ can be ignored *after the last 90° pulse* applied at the frequency of the given nucleus.

²In spin systems consisting of more than two coupled magnetic moments, product operators representing more than two correlated transverse polarizations also belong to this category.

- The product operator \mathcal{I}_t never evolves to a measurable coherence because it commutes with all Hamiltonians. It can be ignored right from the beginning.

We now analyze the evolution of the density matrix during the HSQC experiments using the simplified approach described above.

- After a 90° pulse at the proton frequency, polarization is transferred to the other nucleus (usually ^{15}N or ^{13}C). The density matrix at the end of the INEPT is

$$\hat{\rho}(\text{e}) = \frac{1}{2}\mathcal{I}_t - \frac{1}{2}\kappa_1(2\mathcal{I}_z\mathcal{I}_y) + \frac{1}{2}\kappa_2\mathcal{I}_y$$

- During an echo with a decoupling 180° pulse at the proton frequency (cyan pulse in Figure 11.3, top), anti-phase single quantum coherences evolve according to the chemical shift

$$\hat{\rho}(\text{e}) \longrightarrow \hat{\rho}(\text{f}) = \frac{1}{2}\mathcal{I}_t + \frac{1}{2}\kappa_1(c_{21}2\mathcal{I}_z\mathcal{I}_y - s_{21}2\mathcal{I}_z\mathcal{I}_x) + \frac{1}{2}\kappa_2(c_{21}\mathcal{I}_y - s_{21}\mathcal{I}_x).$$

- Two 90° pulses convert $2\mathcal{I}_z\mathcal{I}_y$ to $-2\mathcal{I}_y\mathcal{I}_z$ and $-2\mathcal{I}_z\mathcal{I}_x$ to $2\mathcal{I}_y\mathcal{I}_x$. The magenta operator is a contribution to the density matrix which represents a *multiple-quantum coherence*, which can be converted to a "measurable" in-phase single quantum coherence only by applying a 90° pulse (and by a subsequent action of the J -coupling). Since our pulse sequence does not contain any more 90° pulses, we ignore $2\mathcal{I}_y\mathcal{I}_x$. The 90° pulse applied at the precession frequency of ^{13}C or ^{15}N converts \mathcal{I}_y to the longitudinal polarization \mathcal{I}_z . The \mathcal{I}_x is not affected by the 90° pulses applied with the 0° (x) phase. As the pulse sequence does not contain any more 90° pulses, we can ignore the green terms. Also, we ignore the red term \mathcal{I}_t which never evolves to a measurable coherence because it commutes with all Hamiltonians. The density matrix can be written as

$$\hat{\rho}(\text{g}) = -\frac{1}{2}\kappa_1c_{21}2\mathcal{I}_y\mathcal{I}_z + \text{unmeasurable contributions}$$

- The last echo allows the scalar coupling to evolve but refocuses evolution of the scalar coupling. If the delays $\tau = 1/4J$, the measurable components of the density matrix evolve to $\frac{1}{2}\kappa_1 \cos(\Omega_2 t_1)\mathcal{I}_x$ (rotation "about" $2\mathcal{I}_z\mathcal{I}_z$ by 90° and change of the sign by the last 180° pulse applied at the proton frequency):

$$\hat{\rho}(\text{h}) = \frac{1}{2}\kappa_1c_{21}\mathcal{I}_x + \text{unmeasurable contributions}$$

- During acquisition, both chemical shift and scalar coupling evolve in the experiment depicted in Figure 11.3A:

$$\frac{1}{2}\kappa_1c_{21}\mathcal{I}_x \longrightarrow \begin{cases} +\frac{1}{2}\kappa_1c_{21}c_{12}\mathcal{I}_x \longrightarrow \begin{cases} +\frac{1}{2}\kappa_1c_{21}c_{12}c_J\mathcal{I}_x \\ +\frac{1}{2}\kappa_1c_{21}c_{12}s_J2\mathcal{I}_y\mathcal{I}_z \end{cases} \\ +\frac{1}{2}\kappa_1c_{21}s_{12}\mathcal{I}_y \longrightarrow \begin{cases} +\frac{1}{2}\kappa_1c_{21}s_{12}c_J\mathcal{I}_y \\ -\frac{1}{2}\kappa_1c_{21}s_{12}s_J2\mathcal{I}_x\mathcal{I}_z \end{cases} \end{cases} \quad (11.6)$$

HSQC experiments are usually two-dimensional. The second dimension is introduced by repeating the measurement with t_1 being incremented. Moreover, each increment is measured twice with a different phase of one of the 90° radio-wave pulses applied to ^{13}C or ^{15}N (labeled in Figure 11.3 by

writing x/y above the pulse, do not confuse with the label x, y in Figure 11.1 that indicates phase cycling, i.e. storing a single record obtained by adding or subtracting data acquired with a different phase). In the records acquired with the phase shifted by 90° (y), the pulses influence the density matrix as follows:

- Two 90° pulses convert $2\mathcal{I}_z\mathcal{I}_y$ to $-2\mathcal{I}_y\mathcal{I}_y$ and $-2\mathcal{I}_z\mathcal{I}_x$ to $-2\mathcal{I}_y\mathcal{I}_z$. The 90° pulse applied at the precession frequency of ^{13}C or ^{15}N with a phase shift of 90° (y) converts $-\mathcal{I}_x$ to \mathcal{I}_z and leaves \mathcal{I}_y untouched. As discussed above, only $2\mathcal{I}_y\mathcal{I}_z$ evolves to a measurable coherence:
 $\hat{\rho}(g) = -\frac{1}{2}\kappa_1 s_{21} 2\mathcal{I}_y\mathcal{I}_z + \text{unmeasurable contributions}$

The density matrix then evolves as described above for the records acquired with the phase 0° (x), the only difference is the factor s_{21} instead of c_{21} :

$$\frac{1}{2}\kappa_1 s_{21} \mathcal{I}_x \longrightarrow \begin{cases} +\frac{1}{2}\kappa_1 s_{21} c_{12} \mathcal{I}_x \longrightarrow \begin{cases} +\frac{1}{2}\kappa_1 s_{21} c_{12} c_J \mathcal{I}_x \\ +\frac{1}{2}\kappa_1 s_{21} c_{12} s_J 2\mathcal{I}_y\mathcal{I}_z \end{cases} \\ +\frac{1}{2}\kappa_1 s_{21} s_{12} \mathcal{I}_y \longrightarrow \begin{cases} +\frac{1}{2}\kappa_1 s_{21} s_{12} c_J \mathcal{I}_y \\ -\frac{1}{2}\kappa_1 s_{21} s_{12} s_J 2\mathcal{I}_x\mathcal{I}_z \end{cases} \end{cases} \quad (11.7)$$

The subsequent records acquired with the 0° (x) and 90° (y) phases of the 90° ^{13}C or ^{15}N pulse are stored as real (modulated by $c_{21} = \cos(\Omega_2 t_1)$) and imaginary (modulated by $s_{21} = \sin(\Omega_2 t_1)$) component of a complex signal, respectively, like in the NOESY experiment. In our analysis, we combine c_{21} and s_{21} as $c_{21} + is_{21} = e^{i\Omega_2 t_1}$:

$$\frac{1}{2}\kappa_1 e^{i\Omega_2 t_1} \mathcal{I}_x \longrightarrow \begin{cases} +\frac{1}{2}\kappa_1 e^{i\Omega_2 t_1} c_{12} \mathcal{I}_x \longrightarrow \begin{cases} +\frac{1}{2}\kappa_1 e^{i\Omega_2 t_1} c_{12} c_J \mathcal{I}_x \\ +\frac{1}{2}\kappa_1 e^{i\Omega_2 t_1} c_{12} s_J 2\mathcal{I}_y\mathcal{I}_z \end{cases} \\ +\frac{1}{2}\kappa_1 e^{i\Omega_2 t_1} s_{12} \mathcal{I}_y \longrightarrow \begin{cases} +\frac{1}{2}\kappa_1 e^{i\Omega_2 t_1} s_{12} c_J \mathcal{I}_y \\ -\frac{1}{2}\kappa_1 e^{i\Omega_2 t_1} s_{12} s_J 2\mathcal{I}_x\mathcal{I}_z \end{cases} \end{cases} \quad (11.8)$$

As described in Section 10.3, we continue by calculating the trace of $\hat{\rho}(t_2)\hat{M}_{1+}$ and including relaxation (with different rates $\bar{R}_{2,1}$ and $\bar{R}_{2,2}$ in the direct and indirect dimensions,³, respectively). The result shows that the expected value of M_{1+} evolves as

$$\langle M_{1+} \rangle = \frac{\mathcal{N}\gamma_1^2 \hbar^2 B_0}{8k_B T} e^{-\bar{R}_{2,2} t_1} e^{-\bar{R}_{2,1} t_2} e^{i\Omega_2 t_1} (e^{i(\Omega_1 - \pi J)t_2} - e^{i(\Omega_1 + \pi J)t_2}) \quad (11.9)$$

The real part of the spectrum obtained by the Fourier transformation is

³The relaxation rates differ because single-quantum coherences of ^{13}C or ^{15}N evolve during t_1 , whereas proton single-quantum coherences evolve during t_2 . Moreover, the single-quantum coherences oscillate between in-phase and anti-phase terms during t_1 and t_2 , and the relaxation rates of in-phase and anti-phase single-quantum coherences differ as described in Section 10.3. The actually observed relaxation rates $\bar{R}_{2,1}$ and $\bar{R}_{2,2}$ are averages of the in-phase and anti-phase values, despite the fact that (i) the density matrix is purely anti-phase (consisting of $2\mathcal{I}_z\mathcal{I}_x$ and $2\mathcal{I}_z\mathcal{I}_y$ operators) at the end of t_1 (due to the presence of the cyan decoupling pulse) and that (ii) only the in-phase (\mathcal{I}_x and \mathcal{I}_y) coherence contributes to the signal in t_2 .

$$\Re\{Y(\omega)\} = \frac{\mathcal{N}\gamma_1^2\hbar^2 B_0}{8k_B T} \frac{\overline{R}_{2,2}^2}{\overline{R}_{2,1}^2 + (\omega - \Omega_1)^2} \left(\frac{\overline{R}_{2,1}^2}{\overline{R}_{2,1}^2 + (\omega - \Omega_2 + \pi J)^2} + \frac{\overline{R}_{2,1}^2}{\overline{R}_{2,1}^2 + (\omega - \Omega_2 - \pi J)^2} \right) \quad (11.10)$$

11.3 Decoupling trains

If we perform the experiments as depicted in Figure 11.3A and analyzed above, we obtain a 2D spectrum with peaks at the frequency offset Ω_2 in the indirect dimension and a doublet at $\Omega_1 \pm \pi J$ in the direct (proton) dimension (Figure 11.4). Note that the splitting by $\pm\pi J$ was removed by the cyan decoupling pulse in the indirect dimension. Splitting of peaks in the direct dimension is undesirable, but the remedy is not simple. We acquire signal in real time and cannot remove the splitting by a decoupling echo. In principle, we can divide the acquisition time into short fragments and apply a 180° pulse at the frequency of ^{13}C (or ^{15}N) in the middle of each such echo (green pulses in Figure 11.3B). In practice, imperfections of such a long series of echoes, affecting especially magnetic moments with large Ω_2 , are significant. However, more sophisticated series of pulses have much better performance. Typical examples of decoupling pulse sequences are

- WALTZ - a series of 90° , 180° , and 270° pulses with phase of 0° (x), or 180° ($-x$), repeating in complex patterns
- DIPSI - a similar series of pulses with non-integer rotation angles
- GARP - computer-optimized sequence of pulses with non-integer rotation angles and phases.

In the schematic drawings of pulse sequences, the decoupling (and other) trains of many pulses are depicted as rectangles with abbreviations of the used sequences (Figure 11.3C).

11.4 Benefits of HSQC

At the end of the discussion of the HSQC experiment, we summarize the advantages of recording a 2D HSQC spectrum instead of 1D proton and ^{13}C or ^{15}N spectra.

- ^{13}C or ^{15}N frequency is measured with *high sensitivity* (higher by $(\gamma_1/\gamma_2)^{5/2}$ than provided by the direct detection, cf. Section 7.10.4).
- Expansion to the second dimension and reducing the number of peaks in spectrum (only ^{13}C or ^{15}N -bonded protons and only protonated ^{13}C or ^{15}N nuclei are visible) provides *high resolution*.
- ^1H - ^{13}C and ^1H - ^{15}N correlation is *important structural information* (it tells us which proton is attached to which ^{13}C or ^{15}N).

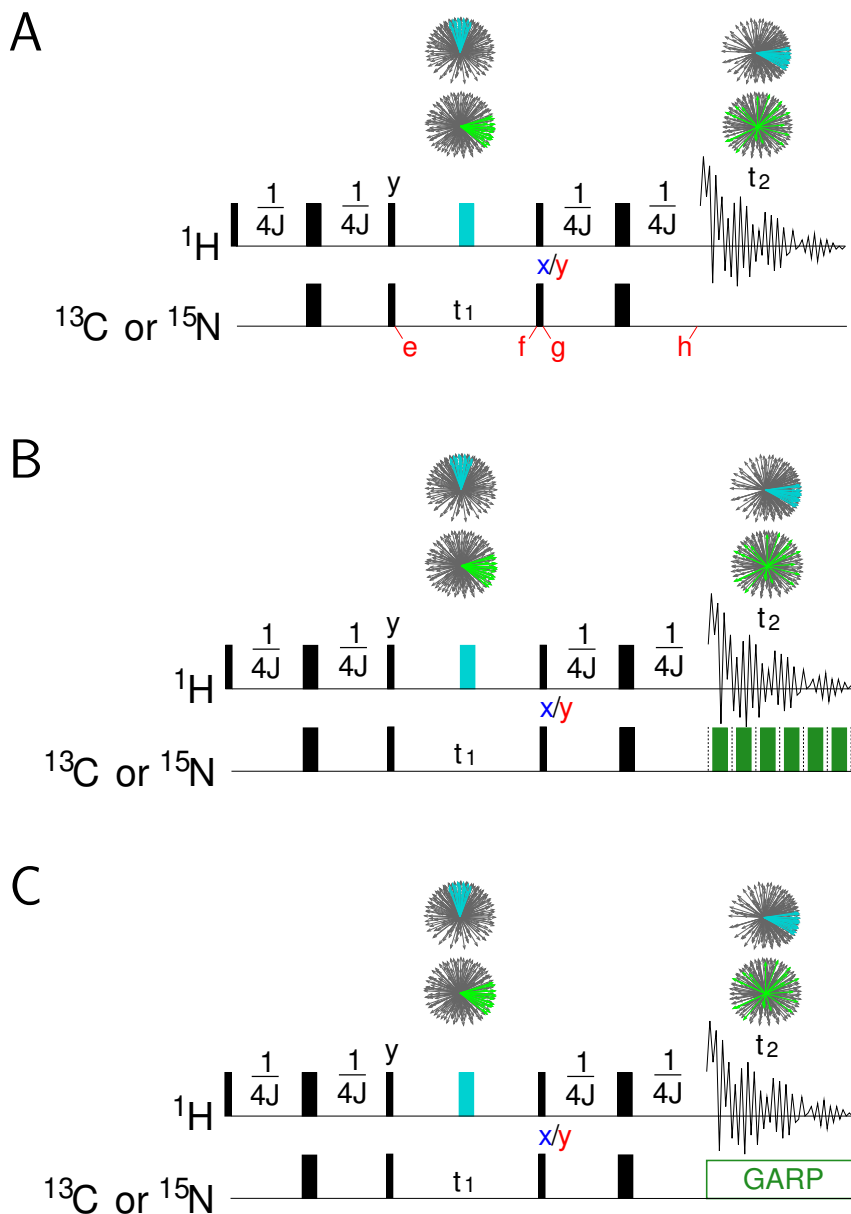


Figure 11.3: HSQC experiment. A, basic HSQC pulse sequence. B, general idea of the decoupling in the direct dimension. C, Standard presentation of the HSQC pulse sequence with decoupling in the direct dimension. The decoupling pulse applied to proton and to ^{13}C (or ^{15}N) are shown in cyan and green, respectively. The label x/y indicates repeated acquisition with the phase of the given pulse set first to 0° (x) and then to 90° (y), in order to obtain a cosine-modulated and sine-modulated 1D records for each t_1 increment. Other symbols are used as explained in Figure 11.1.

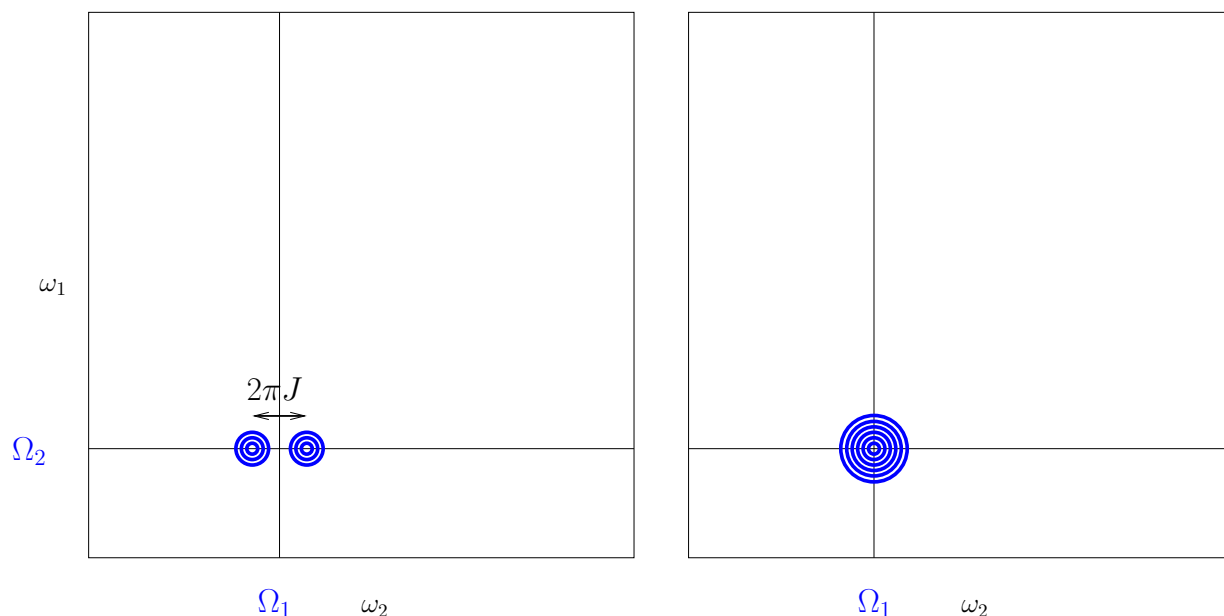


Figure 11.4: HSQC spectrum of a ^1H - ^{13}C (or ^1H - ^{15}N) pair. The two-dimensional peaks are displayed as contour plots. Frequency offsets of the proton and ^{13}C (or ^{15}N) are Ω_1 and Ω_2 , respectively. The left spectrum was obtained using the pulse sequence shown in Figure 11.3A, the right spectrum was acquired with the decoupling applied in the direct dimension (Figure 11.3B,C).

11.5 COSY

We started the discussion of experiments based on scalar couplings with heteronuclear correlations because they are easier to analyze. The basic (and very popular) *homonuclear* experiment is COSY (COrelated SpectroscopY). Its pulse sequence is very simple, consisting of only two 90° pulses separated by an incremented delay t_1 (which provides the second dimension), but the evolution of the density matrix is relatively complex. Here, we analyze evolution for a pair of interacting nuclei (protons). In the text, we discuss only the components of the density matrix that contribute to the measurable signal. The complete analysis is summarized in Table 11.1.

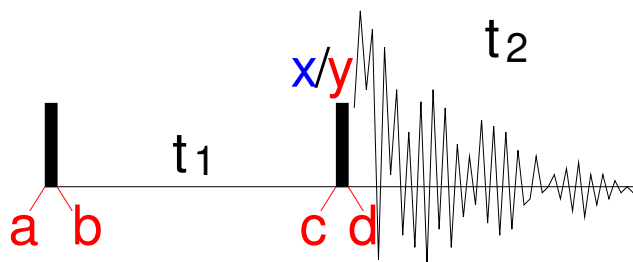


Figure 11.5: COSY pulse sequence. The rectangles represent 90° radio wave pulses applied at a frequency sufficiently close to the precession frequencies of both interacting magnetic moments.

- $\hat{\rho}(a) = \frac{1}{2}\mathcal{I}_t + \frac{1}{2}\kappa(\mathcal{I}_{1z} + \mathcal{I}_{2z})$
thermal equilibrium, the matrices are different than for the noninteracting spin, but the constant is the same.
- $\hat{\rho}(b) = \frac{1}{2}\mathcal{I}_t + \frac{1}{2}\kappa(-\mathcal{I}_{1y} - \mathcal{I}_{2y})$
90° pulse, see the one-pulse experiment
- $\hat{\rho}(c) = \frac{1}{2}\mathcal{I}_t$
 $+\frac{1}{2}\kappa(-c_{11}c_{J1}\mathcal{I}_{1y} + s_{11}c_{J1}\mathcal{I}_{1x} + c_{11}s_{J1}2\mathcal{I}_{1x}\mathcal{I}_{2z} + s_{11}s_{J1}2\mathcal{I}_{1y}\mathcal{I}_{2z})$
 $+\frac{1}{2}\kappa(-c_{21}c_{J1}\mathcal{I}_{2y} + s_{21}c_{J1}\mathcal{I}_{2x} + c_{21}s_{J1}2\mathcal{I}_{1z}\mathcal{I}_{2x} + s_{21}s_{J1}2\mathcal{I}_{1z}\mathcal{I}_{2y})$,
where $c_{11} = \cos(\Omega_1 t_1)$, $s_{11} = \sin(\Omega_1 t_1)$, $c_{21} = \cos(\Omega_2 t_1)$, $s_{21} = \sin(\Omega_2 t_1)$, $c_{J1} = \cos(\pi J t_1)$, and $s_{J1} = \sin(\pi J t_1)$ – evolution of the chemical shift and coupling.

- The second 90° pulse creates the following coherences

$$\hat{\rho}(d) = \frac{1}{2}\mathcal{I}_t$$

$$+\frac{1}{2}\kappa(-c_{11}c_{J1}\mathcal{I}_{1z} + \boxed{s_{11}c_{J1}\mathcal{I}_{1x}} - c_{11}s_{J1}2\mathcal{I}_{1x}\mathcal{I}_{2y} - \boxed{s_{11}s_{J1}2\mathcal{I}_{1z}\mathcal{I}_{2y}})$$

$$+\frac{1}{2}\kappa(-c_{21}c_{J1}\mathcal{I}_{2z} + \boxed{s_{21}c_{J1}\mathcal{I}_{2x}} - c_{21}s_{J1}2\mathcal{I}_{1y}\mathcal{I}_{2x} - \boxed{s_{21}s_{J1}2\mathcal{I}_{1y}\mathcal{I}_{2z}}).$$

The red terms contain polarization operators, not coherences, they do not contribute to the signal. The green terms contain in-phase single-quantum coherences, only they give non-zero trace when multiplied with $\hat{M}_+ \propto (\mathcal{I}_{1x} + i\mathcal{I}_{1y} + \mathcal{I}_{2x} + i\mathcal{I}_{2y})$. The blue terms contain anti-phase single-quantum coherences, they do not contribute to the signal directly, but they evolve into in-phase coherences during acquisition due to the scalar coupling. The magenta terms contain multiple-quantum coherences. They do not contribute to the signal, but can be converted to single-quantum coherences by 90° pulses.⁴ Such pulses are not applied in the discussed pulse sequence, but are used in some versions of the experiment.

- The terms in black frames evolve with the chemical shift of the first nucleus during acquisition:

$$\boxed{s_{11}c_{J1}\mathcal{I}_{1x} \rightarrow s_{11}c_{J1}c_{J2}c_{J2}\mathcal{I}_{1x} + s_{11}c_{J1}s_{12}c_{J2}\mathcal{I}_{1y} + \text{unmeasurable anti-phase coherences}}$$

$$\boxed{-s_{21}s_{J1}2\mathcal{I}_{1y}\mathcal{I}_{2z} \rightarrow s_{21}s_{J1}c_{12}s_{J2}\mathcal{I}_{1x} + s_{21}s_{J1}s_{12}s_{J2}\mathcal{I}_{1y} + \text{unmeasurable anti-phase coherences}},$$

where $c_{j2} = \cos(\Omega_n t_2)$, $s_{n2} = \sin(\Omega_n t_2)$, $c_{J2} = \cos(\pi J t_2)$, and $s_{J2} = \sin(\pi J t_2)$. Using the following trigonometric relations

$$c_{nk}c_{Jk} = \frac{c_{nk}^- + c_{nk}^+}{2} \quad s_{nk}s_{Jk} = \frac{c_{nk}^- - c_{nk}^+}{2} \quad c_{nk}s_{Jk} = \frac{-s_{nk}^- + s_{nk}^+}{2} \quad s_{nk}c_{Jk} = \frac{s_{nk}^- + s_{nk}^+}{2}, \quad (11.11)$$

where $c_{nk}^\pm = \cos((\Omega_n \pm \pi J)t_k)$ and $s_{nk}^\pm = \sin((\Omega_n \pm \pi J)t_k)$, the terms contributing to the signal can be written as

$$\left(\underbrace{(s_{11}^- + s_{11}^+)(c_{12}^- + c_{12}^+)}_{[\Omega_1, \Omega_1]} + \underbrace{(c_{21}^- - c_{21}^+)(-s_{12}^- + s_{12}^+)}_{[\Omega_2, \Omega_1]} \right) \mathcal{I}_{1x} + \left(\underbrace{(s_{11}^- + s_{11}^+)(s_{12}^- + s_{12}^+)}_{[\Omega_1, \Omega_1]} + \underbrace{(c_{21}^- - c_{21}^+)(c_{12}^- - c_{12}^+)}_{[\Omega_2, \Omega_1]} \right) \mathcal{I}_{1y}$$

⁴We have not analyzed evolution of the multiple quantum coherences so far. To do it, it is sufficient (i) to recognize that multiple quantum coherences commute with $2\mathcal{I}_{1z}\mathcal{I}_{2z}$ (therefore they are not influenced by the weak J -coupling), and (ii) to analyze "rotation" of individual constituents of the product operators (e.g. of \mathcal{I}_{1x} and \mathcal{I}_{2y}) "about" \mathcal{I}_{nj} individually and calculate the product of the results of the rotation.

The first and second line show coherences providing the real and imaginary component of the complex signal acquired in the direct dimension (t_2).

- Evaluation of the traces of $\hat{M}_+ \hat{\rho}(t_2)$ gives the following modulation of the signal:

$$\underbrace{(s_{11}^- + s_{11}^+) (e^{i(\Omega_1 - \pi J)t_2} + e^{i(\Omega_1 + \pi J)t_2})}_{[\Omega_1, \Omega_1]} + i \underbrace{(c_{21}^- - c_{21}^+) (e^{i(\Omega_1 - \pi J)t_2} - e^{i(\Omega_1 + \pi J)t_2})}_{[\Omega_2, \Omega_1]}$$

The imaginary signal in the indirect dimension is obtained by repeating acquisition for each increment of t_1 with a different phase of the second 90° pulse (shifted by 90° , which corresponds to the direction y in the rotating coordinate system).

- The second 90° pulse with the y phase creates the following coherences

$$\begin{aligned} \hat{\rho}(d) &= \frac{1}{2} \mathcal{I}_t \\ &+ \frac{1}{2} \kappa \left(- \boxed{c_{11} c_{J1} \mathcal{I}_{1y}} - s_{11} c_{J1} \mathcal{I}_{1z} - \boxed{c_{11} s_{J1} 2 \mathcal{I}_{1z} \mathcal{I}_{2x}} + s_{11} s_{J1} 2 \mathcal{I}_{1y} \mathcal{I}_{2x} \right) \\ &+ \frac{1}{2} \kappa \left(- \boxed{c_{21} c_{J1} \mathcal{I}_{2y}} - s_{21} c_{J1} \mathcal{I}_{2z} - \boxed{c_{21} s_{J1} 2 \mathcal{I}_{1x} \mathcal{I}_{2z}} + s_{21} s_{J1} 2 \mathcal{I}_{1x} \mathcal{I}_{2y} \right). \end{aligned}$$

- The terms in black frames evolve with the chemical shift of the first nucleus during acquisition:

$$\begin{aligned} \boxed{c_{11} c_{J1} \mathcal{I}_{1y} \rightarrow c_{11} c_{J1} s_{12} c_{J2} \mathcal{I}_{1x} - c_{11} c_{J1} c_{12} c_{J2} \mathcal{I}_{1y} + \text{unmeasurable anti-phase coherences}} \\ \boxed{-s_{21} s_{J1} 2 \mathcal{I}_{1x} \mathcal{I}_{2z} \rightarrow c_{21} s_{J1} s_{12} s_{J2} \mathcal{I}_{1x} - c_{21} s_{J1} c_{12} s_{J2} \mathcal{I}_{1y} + \text{unmeasurable anti-phase coherences}}. \end{aligned}$$

The terms contributing to the signal can be written as

$$\left(\underbrace{(c_{11}^- + c_{11}^+) (s_{12}^- + s_{12}^+)}_{[\Omega_1, \Omega_1]} + \underbrace{(-s_{21}^- - s_{21}^+) (c_{12}^- - c_{12}^+)}_{[\Omega_2, \Omega_1]} \right) \mathcal{I}_{1x} - \left(\underbrace{(c_{11}^- + c_{11}^+) (c_{12}^- + c_{12}^+)}_{[\Omega_1, \Omega_1]} + \underbrace{(-s_{21}^- + s_{21}^+) (-s_{12}^- + s_{12}^+)}_{[\Omega_2, \Omega_1]} \right) \mathcal{I}_{1y}.$$

- Evaluation of the traces of $\hat{M} + \hat{\rho}(t_2)$ gives the following modulation of the signal:

$$-i \underbrace{(c_{11}^- + c_{11}^+) (e^{i(\Omega_1 - \pi J)t_2} + e^{i(\Omega_1 + \pi J)t_2})}_{[\Omega_1, \Omega_1]} + \underbrace{(-s_{21}^- + s_{21}^+) (e^{i(\Omega_1 - \pi J)t_2} - e^{i(\Omega_1 + \pi J)t_2})}_{[\Omega_2, \Omega_1]}$$

Now we combine signals obtained with the different phases of the second pulse.

- The *hypercomplex* signal (sum of the signals recorded with the x and y phases of the second pulse) is modulated as

$$\begin{aligned} e^{-i\frac{\pi}{2}} \underbrace{(e^{i(\Omega_1 - \pi J)t_1} + e^{i(\Omega_1 + \pi J)t_1})}_{[\Omega_1, \Omega_1]} (e^{i(\Omega_1 - \pi J)t_2} + e^{i(\Omega_1 + \pi J)t_2}) \\ + \underbrace{(e^{i(\Omega_2 - \pi J)t_1} - e^{i(\Omega_2 + \pi J)t_1})}_{[\Omega_2, \Omega_1]} (e^{i(\Omega_1 - \pi J)t_2} - e^{i(\Omega_1 + \pi J)t_2}), \end{aligned}$$

where we replaced $-i$ by $e^{-i\pi/2}$.

- The green component of the signal evolves with the same chemical shift in both dimensions, providing *diagonal* signal (at frequencies $[\Omega_1, \Omega_1]$ and $[\Omega_2, \Omega_2]$ in the 2D spectrum). The blue (originally anti-phase) component of the signal also evolves with Ω_1 in the direct dimension (t_2), but with Ω_2 in the indirect dimension (t_1). It provides *off-diagonal* signal, a *cross-peak* at

frequencies $[\Omega_1, \Omega_2]$ and $[\Omega_2, \Omega_1]$ in the 2D spectrum. Note that the blue and green components have the phase different by 90° . Therefore, either diagonal peaks or cross-peaks have the undesirable dispersive shape (it is not possible to phase both diagonal peaks or cross-peaks, they always have phases differing by 90°). Typically, the spectrum is phased so that the cross-peaks have a nice absorptive shape (see Figure 11.6) because they carry a useful chemical information: they show which protons are connected by 2 or 3 covalent bonds.

- The diagonal peaks are not interesting, but their dispersive shape may obscure cross-peaks close to the diagonal. The problem with the phase can be solved if one more 90° pulse is introduced. Such a pulse converts the magenta multiple-quantum coherences to anti-phase single-quantum coherences, which evolve into the measurable signal. The point is that other coherences can be removed by phase cycling. The obtained spectrum contains diagonal peaks and cross-peaks, but (in contrast to the simple two-pulse variant of the COSY experiment) both diagonal peaks and cross-peaks have the same phase.⁵ This version of the experiment, known as *double-quantum filtered COSY* (DQF-COSY), is analyzed in Section 11.6.2. Its disadvantage is a lower sensitivity – we lose a half of the signal.
- Also, note that each peak is split into doublets in both dimensions. More complex multiplets are obtained if more than two nuclei are coupled. The distance of peaks in the multiplets is given by the interaction constant J . In the case of nuclei connected by three bonds, J depends on the torsion angle defined by these three bonds. So, COSY spectra can be used to determine torsion angles in the molecule.
- The terms in cyan frames evolve with the chemical shift of the second nucleus during acquisition as

$$s_{21}c_{J1}\mathcal{I}_{2x} \rightarrow s_{21}c_{J1}c_{12}c_{J2}\mathcal{I}_{2x} + s_{21}c_{J1}s_{12}c_{J2}\mathcal{I}_{2y} + \text{unmeasurable anti-phase coherences}$$

$$-s_{11}s_{J1}2\mathcal{I}_{1z}\mathcal{I}_{2y} \rightarrow s_{11}s_{J1}c_{12}s_{J2}\mathcal{I}_{2x} + s_{11}s_{J1}s_{12}s_{J2}\mathcal{I}_{2y} + \text{unmeasurable anti-phase coherences}$$

and give a similar type of signal for the other nucleus:

$$e^{-i\frac{\pi}{2}} \underbrace{\left(e^{i(\Omega_2 - \pi J)t_1} + e^{i(\Omega_2 + \pi J)t_1} \right) \left(e^{i(\Omega_2 - \pi J)t_2} + e^{i(\Omega_2 + \pi J)t_2} \right)}_{[\Omega_2, \Omega_2]} \\ + \underbrace{\left(e^{i(\Omega_1 - \pi J)t_1} - e^{i(\Omega_1 + \pi J)t_1} \right) \left(e^{i(\Omega_2 - \pi J)t_2} - e^{i(\Omega_2 + \pi J)t_2} \right)}_{[\Omega_1, \Omega_2]}.$$

This signal represents the other diagonal and off-diagonal peak in the spectrum. The complete signal, including the quantitative factor, can be written as

⁵We cannot use phase cycling to remove the green terms resulting in the unwanted diagonal peaks because phase cycling can distinguish multiple-quantum coherences from single-quantum ones, but it cannot distinguish anti-phase single quantum coherences from in-phase single quantum coherences.

$$\begin{aligned}
\langle M_+ \rangle = & \mathcal{N} \gamma \hbar \frac{\kappa}{8} \left(e^{-\bar{R}_2 t_1} \left(-e^{i(\Omega_1 - \pi J)t_1} + e^{i(\Omega_1 + \pi J)t_1} \right) e^{-\bar{R}_2 t_2} \left(-e^{i(\Omega_1 - \pi J)t_2} + e^{i(\Omega_1 + \pi J)t_2} \right) \right) e^{-i\frac{\pi}{2}} \\
& + \mathcal{N} \gamma \hbar \frac{\kappa}{8} \left(e^{-\bar{R}_2 t_1} \left(-e^{i(\Omega_2 - \pi J)t_1} + e^{i(\Omega_2 + \pi J)t_1} \right) e^{-\bar{R}_2 t_2} \left(-e^{i(\Omega_1 - \pi J)t_2} + e^{i(\Omega_1 + \pi J)t_2} \right) \right) \\
& + \mathcal{N} \gamma \hbar \frac{\kappa}{8} \left(e^{-\bar{R}_2 t_1} \left(-e^{i(\Omega_1 - \pi J)t_1} + e^{i(\Omega_1 + \pi J)t_1} \right) e^{-\bar{R}_2 t_2} \left(-e^{i(\Omega_2 - \pi J)t_2} + e^{i(\Omega_2 + \pi J)t_2} \right) \right) \\
& + \mathcal{N} \gamma \hbar \frac{\kappa}{8} \left(e^{-\bar{R}_2 t_1} \left(-e^{i(\Omega_2 - \pi J)t_1} + e^{i(\Omega_2 + \pi J)t_1} \right) e^{-\bar{R}_2 t_2} \left(-e^{i(\Omega_2 - \pi J)t_2} + e^{i(\Omega_2 + \pi J)t_2} \right) \right) e^{-i\frac{\pi}{2}}.
\end{aligned} \tag{11.12}$$

HOMEWORK

Analyze the COSY experiment (Section 11.5).

Table 11.1: Evolution of the density matrix during DQF-COSY. Modulations of the density matrix components (omitting the $\kappa/2$ factor and the \mathcal{S}_t component) having the origin in \mathcal{S}_{1z} and \mathcal{S}_{2z} are shown in black and cyan, respectively. The product operators are color-coded as in the text.

Real in t_1 :						
	$\hat{\rho}(a)$	$\hat{\rho}(b)$	$\hat{\rho}(c)$	$\hat{\rho}(d)$	$\hat{\rho}(t_2)$	$\text{Tr}\{\hat{\rho}(t_2)(\mathcal{S}_{1x} + \mathcal{S}_{2x} + i\mathcal{S}_{1y} + i\mathcal{S}_{2y})\}$
\mathcal{S}_{1z}	+1	0	0	$-c_{11}c_{J1}$	$+c_{11}c_{J1}$	0
\mathcal{S}_{1x}		0	$+s_{11}c_{J1}$	$+s_{11}c_{J1}$	$+s_{11}c_{J1}c_{12}c_{J2} + s_{21}s_{J1}c_{12}s_{J2}$	$+s_{11}c_{J1}c_{12}c_{J2} + s_{21}s_{J1}c_{12}s_{J2}$
\mathcal{S}_{1y}		-1	$-c_{11}c_{J1}$	0	$+s_{11}c_{J1}s_{12}c_{J2} + s_{21}s_{J1}s_{12}s_{J2}$	$i(+s_{11}c_{J1}s_{12}c_{J2} + s_{21}s_{J1}s_{12}s_{J2})$
$2\mathcal{S}_{1y}\mathcal{S}_{2z}$			$+s_{11}s_{J1}$	$-s_{21}s_{J1}$	$+s_{11}c_{J1}c_{12}s_{J2} - s_{21}s_{J1}c_{12}c_{J2}$	0
$2\mathcal{S}_{1x}\mathcal{S}_{2z}$			$+c_{11}s_{J1}$	0	$-s_{11}c_{J1}s_{12}s_{J2} + s_{21}s_{J1}s_{12}c_{J2}$	0
$2\mathcal{S}_{1x}\mathcal{S}_{2y}$				$-c_{11}s_{J1}$	$-c_{11}s_{J1}c_{12}c_{22} + c_{21}s_{J1}s_{12}s_{22}$	0
$2\mathcal{S}_{1x}\mathcal{S}_{2x}$					$+c_{11}s_{J1}c_{12}s_{22} + c_{21}s_{J1}s_{12}c_{22}$	0
$2\mathcal{S}_{1y}\mathcal{S}_{2y}$					$-c_{21}s_{J1}c_{12}s_{22} - c_{11}s_{J1}s_{12}c_{22}$	0
$2\mathcal{S}_{1y}\mathcal{S}_{2x}$				$-c_{21}s_{J1}$	$-c_{21}s_{J1}c_{12}c_{22} + c_{11}s_{J1}s_{12}s_{22}$	0
$2\mathcal{S}_{1z}\mathcal{S}_{2x}$			$+c_{21}s_{J1}$	0	$-s_{21}c_{J1}s_{22}s_{J2} + s_{11}s_{J1}s_{22}c_{J2}$	0
$2\mathcal{S}_{1z}\mathcal{S}_{2y}$			$+s_{21}s_{J1}$	$-s_{11}s_{J1}$	$+s_{21}c_{J1}c_{22}s_{J2} - s_{11}s_{J1}c_{22}c_{J2}$	0
\mathcal{S}_{2y}		-1	$-c_{21}c_{J1}$	0	$+s_{21}c_{J1}s_{22}c_{J2} + s_{11}s_{J1}s_{22}s_{J2}$	$i(+s_{21}c_{J1}s_{22}c_{J2} + s_{11}s_{J1}s_{22}s_{J2})$
\mathcal{S}_{2x}		0	$+s_{21}c_{J1}$	$+s_{21}c_{J1}$	$+s_{21}c_{J1}c_{22}c_{J2} + s_{11}s_{J1}c_{22}s_{J2}$	$+s_{21}c_{J1}c_{22}c_{J2} + s_{11}s_{J1}c_{22}s_{J2}$
\mathcal{S}_{2z}	+1	0	0	$-c_{21}c_{J1}$	$+c_{21}c_{J1}$	0
Imaginary in t_1 :						
	$\hat{\rho}(a)$	$\hat{\rho}(b)$	$\hat{\rho}(c)$	$\hat{\rho}(d)$	$\hat{\rho}(t_2)$	
\mathcal{S}_{1z}	+1	0	0	$-s_{11}c_{J1}$	$+s_{11}c_{J1}$	0
\mathcal{S}_{1x}		0	$+s_{11}c_{J1}$	0	$+c_{11}c_{J1}s_{12}c_{J2} + c_{21}s_{J1}s_{12}s_{J2}$	$+c_{11}c_{J1}s_{12}c_{J2} + c_{21}s_{J1}s_{12}s_{J2}$
\mathcal{S}_{1y}		-1	$-c_{11}c_{J1}$	$-c_{11}c_{J1}$	$-c_{11}c_{J1}c_{12}c_{J2} - c_{21}s_{J1}c_{12}s_{J2}$	$i(-c_{11}c_{J1}c_{12}c_{J2} - c_{21}s_{J1}c_{12}s_{J2})$
$2\mathcal{S}_{1y}\mathcal{S}_{2z}$			$+s_{11}s_{J1}$	0	$+c_{11}c_{J1}s_{12}s_{J2} - c_{21}s_{J1}s_{12}c_{J2}$	0
$2\mathcal{S}_{1x}\mathcal{S}_{2z}$			$+c_{11}s_{J1}$	$-c_{21}s_{J1}$	$+c_{11}c_{J1}c_{12}s_{J2} - c_{21}s_{J1}c_{12}c_{J2}$	0
$2\mathcal{S}_{1x}\mathcal{S}_{2y}$				$+s_{11}s_{J1}$	$+s_{11}s_{J1}c_{12}c_{22} + c_{21}s_{J1}s_{12}s_{22}$	0
$2\mathcal{S}_{1x}\mathcal{S}_{2x}$					$-s_{11}s_{J1}c_{12}s_{22} - s_{21}s_{J1}s_{12}c_{22}$	0
$2\mathcal{S}_{1y}\mathcal{S}_{2y}$					$+s_{21}s_{J1}c_{12}s_{22} + s_{11}s_{J1}s_{12}c_{22}$	0
$2\mathcal{S}_{1y}\mathcal{S}_{2x}$				$+s_{21}s_{J1}$	$+s_{21}s_{J1}c_{12}c_{22} + c_{11}s_{J1}s_{12}s_{22}$	0
$2\mathcal{S}_{1z}\mathcal{S}_{2x}$			$+c_{21}s_{J1}$	$-c_{11}s_{J1}$	$+c_{21}c_{J1}c_{22}s_{J2} - c_{11}s_{J1}c_{22}c_{J2}$	0
$2\mathcal{S}_{1z}\mathcal{S}_{2y}$			$+s_{21}s_{J1}$	0	$+c_{21}c_{J1}s_{22}s_{J2} - c_{11}s_{J1}s_{22}c_{J2}$	0
\mathcal{S}_{2y}		-1	$-c_{21}c_{J1}$	$-c_{21}c_{J1}$	$-c_{21}c_{J1}c_{22}c_{J2} - c_{11}s_{J1}c_{22}s_{J2}$	$i(-c_{21}c_{J1}c_{22}c_{J2} - c_{11}s_{J1}c_{22}s_{J2})$
\mathcal{S}_{2x}		0	$+s_{21}c_{J1}$	0	$+c_{21}c_{J1}s_{22}c_{J2} + c_{11}s_{J1}s_{22}s_{J2}$	$+c_{21}c_{J1}s_{22}c_{J2} + c_{11}s_{J1}s_{22}s_{J2}$
\mathcal{S}_{2z}	+1	0	0	$-s_{21}c_{J1}$	$+s_{21}c_{J1}$	0

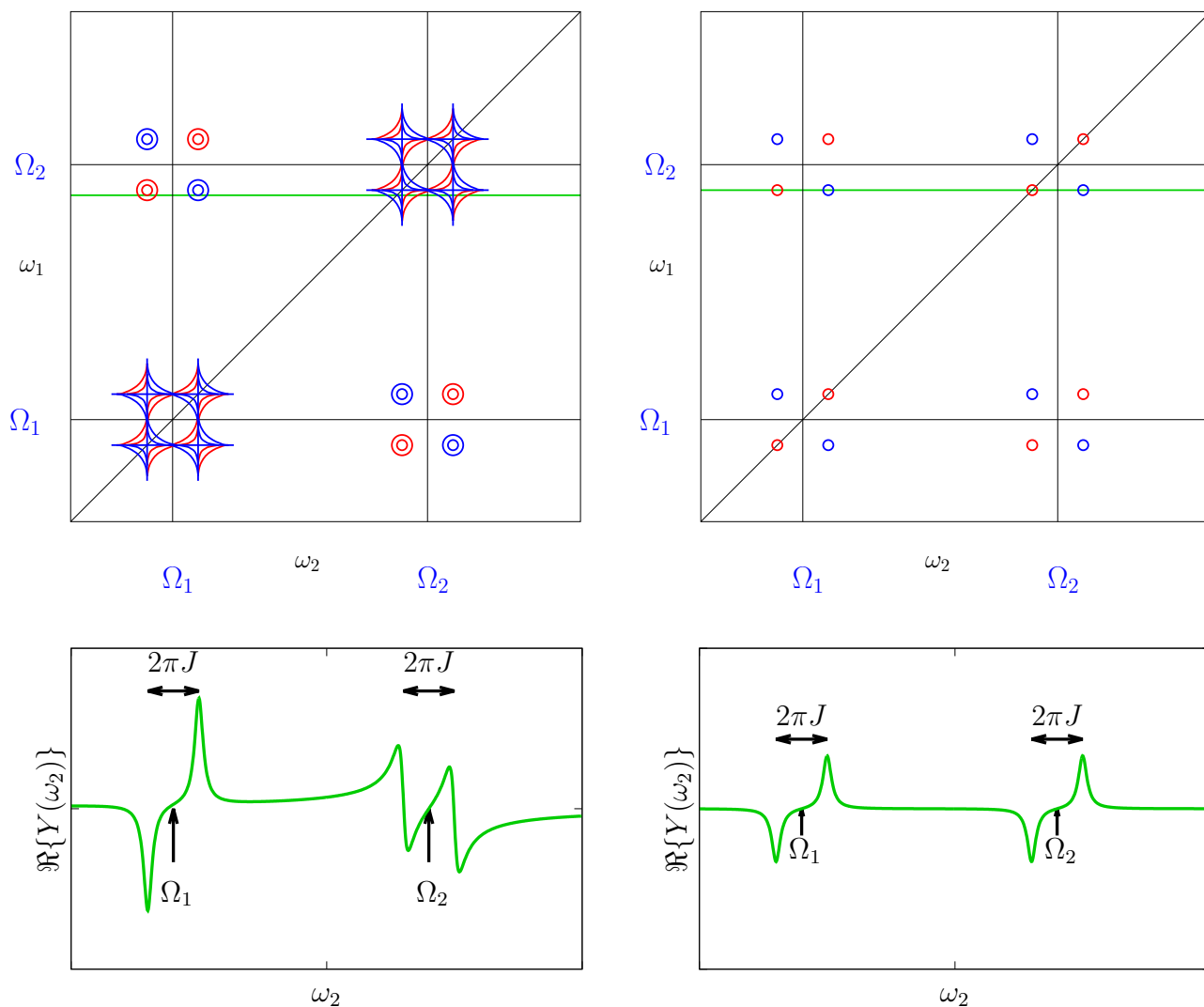


Figure 11.6: COSY spectrum of a ^1H - ^1H pair. The two-dimensional peaks are displayed as contour plots, the positive and negative contours are shown in blue and red, respectively. A one-dimensional slice taken from the 2D spectrum at the position indicated by the green line is displayed below the 2D plot. Frequency offsets of the protons are Ω_1 and Ω_2 . The left spectra were obtained by the pulse sequence displayed in Figure 11.5, the right spectra by the pulse sequence DQF-COSY.

11.6 DERIVATIONS

11.6.1 APT

The attached proton test (APT) is useful for analysis of systems with multiple protons, most often CH_n (C, CH, CH_2 , CH_3). The experiment consists of ^{13}C excitation, simultaneous echo (discussed in Section 10.8), and ^{13}C acquisition with proton decoupling. In the following analysis, the ^{13}C operators are labeled \mathcal{S}_x , \mathcal{S}_y , \mathcal{S}_z , and relaxation is ignored for the sake of simplicity.

$$\bullet \hat{\rho}(\text{a}) = \frac{1}{2^n} \mathcal{S}_t + \frac{\kappa_1}{2^n} \sum_{k=1}^n (\mathcal{S}_{kz}) + \frac{\kappa_2}{2^n} \mathcal{S}_z$$

The probability density matrix at equilibrium is described in a similar manner as for one or two magnetic moments, the extension to the multinuclear system is reflected by the scaling constant $1/2^n$, where n is the number of protons attached to ^{13}C .

$$\bullet \hat{\rho}(\text{b}) = \frac{1}{2^n} \mathcal{S}_t + \frac{\kappa_1}{2^n} \sum_{k=1}^n (\mathcal{S}_{kz}) - \frac{\kappa_2}{2^n} \mathcal{S}_y$$

Excitation of ^{13}C is an analogy of cases discussed above.

- Understanding the next step is critical for the analysis. The general conclusions of Section 10.8 apply, but the actual form of the density matrix must be derived for each system. The general conclusions are: evolution of Ω_2 (^{13}C frequency offset) due to the ^{13}C chemical shift is refocused, scalar coupling evolves for 2τ as $\cos(2\pi J\tau)$ and $\sin(2\pi J\tau)$, nucleus 1 (proton) is never excited (no proton 90° pulse), therefore only \mathcal{S}_{kz} contributions are present for protons.
- The actual analysis for $^{13}\text{CH}_2$ and $^{13}\text{CH}_3$ groups requires extension of the density matrix to $2^{n+1} \times 2^{n+1}$ dimensions. Construction of the basis matrices for such 4^{n+1} -dimensional operator space involves additional direct products with the matrices \mathcal{S}_t , \mathcal{S}_x , \mathcal{S}_y , \mathcal{S}_z . Evolution of the $2^{n+1} \times 2^{n+1}$ matrices is governed by their commutation rules, three-dimensional subspaces where "rotations" of operators take place are defined by these commutation rules (Eqs. 8.29–8.31).

- When the rules are applied, the analysis gives

$$\hat{\rho}(\text{e}) = \frac{1}{2^n} \mathcal{S}_t + \frac{\kappa_1}{2^n} \sum_{k=1}^n (\mathcal{S}_{kz}) + \frac{\kappa_2}{2^n} \begin{cases} n=0: & \mathcal{S}_y \\ n=1: & c\mathcal{S}_y - s2\mathcal{S}_{1z}\mathcal{S}_x \\ n=2: & c^2\mathcal{S}_y - sc(2\mathcal{S}_{1z}\mathcal{S}_x + 2\mathcal{S}_{2z}\mathcal{S}_x) - s^24\mathcal{S}_{1z}\mathcal{S}_{2z}\mathcal{S}_y \\ n=3: & c^3\mathcal{S}_y - sc^2(2\mathcal{S}_{1z}\mathcal{S}_x + 2\mathcal{S}_{2z}\mathcal{S}_x + 2\mathcal{S}_{3z}\mathcal{S}_x) \\ & -s^2c(4\mathcal{S}_{1z}\mathcal{S}_{2z}\mathcal{S}_y + 4\mathcal{S}_{1z}\mathcal{S}_{3z}\mathcal{S}_y + 4\mathcal{S}_{2z}\mathcal{S}_{3z}\mathcal{S}_y) \\ & +s^38\mathcal{S}_{1z}\mathcal{S}_{2z}\mathcal{S}_{3z}\mathcal{S}_x \end{cases}$$

where $s = \sin(2\pi J\tau)$ and $c = \cos(2\pi J\tau)$.

- Since decoupling is applied during acquisition, only the \mathcal{S}_y coherences give a measurable signal. Note that the fact that the proton decoupling is used tells us in advance that the terms containing \mathcal{S}_{kz} need not be analyzed. Therefore the knowledge of exact commutation rules is not necessary, the only important conclusion is that the observable contributions to the density matrix are modulated by $\cos^n(2\pi J\tau)$ for CH_n . During acquisition, these terms evolve under the influence of chemical shift, exactly like in a one-pulse experiment. If τ is set to $\tau = 2J$, then $c = \cos \pi = -1$. Therefore, signals of C and CH_2 are positive and signals of CH and CH_3 are negative \Rightarrow useful chemical information.

11.6.2 Double-quantum filtered COSY

The double-quantum filtered variant of the COSY experiment (DQF-COSY) provides spectra with the same phases of diagonal peaks and cross peaks. The modification of the experiment consists of (i) adding a third 90° pulse and (ii) phase cycle of the first two pulses (Figure 11.7). In DQF-COSY, the initial density matrix

$$\hat{\rho}(\text{a}) = \frac{1}{2}(\mathcal{S}_t + \kappa_1\mathcal{S}_{1z} + \kappa_2\mathcal{S}_{2z})$$

evolves as shown in Table 11.2. The experiment is repeated for times with different phases of the radio waves (see values ϕ_1 and ϕ_2 in Table 11.2). As the consecutive measured records are subtracted before storing the data (indicated by the multiplying factor m in Table 11.2), contribution of all coherences are canceled except for the multiple-quantum terms $2\mathcal{S}_{1x}\mathcal{S}_{1y}$ and $2\mathcal{S}_{1y}\mathcal{S}_{1x}$. It is therefore sufficient to analyze only the following component of $\hat{\rho}(\text{d})$:

$$\hat{\rho}(\text{d}) = \frac{\kappa}{2} \left(\frac{1}{2}(c_{11}s_{J1} + c_{21}s_{J1})2\mathcal{S}_{1x}\mathcal{S}_{1y} + \frac{1}{2}(c_{11}s_{J1} + c_{21}s_{J1})2\mathcal{S}_{1y}\mathcal{S}_{1x} \right)$$

It is converted by the third 90° pulse to

$$\hat{\rho}(\text{e}) = \frac{\kappa}{2} \left(\frac{1}{2}(c_{11}s_{J1} + c_{21}s_{J1})2\mathcal{S}_{1x}\mathcal{S}_{1z} + \frac{1}{2}(c_{11}s_{J1} + c_{21}s_{J1})2\mathcal{S}_{1z}\mathcal{S}_{1x} \right),$$

which evolves during t_2 as

$$\hat{\rho}(t_2) = \frac{\kappa}{2} \left(\frac{1}{2}(c_{11}s_{J1} + c_{21}s_{J1})c_{12}s_{J2}\mathcal{S}_{1y} - \frac{1}{2}(c_{11}s_{J1} + c_{21}s_{J1})s_{12}s_{J2}\mathcal{S}_{1x} + \frac{1}{2}(c_{11}s_{J1} + c_{21}s_{J1})c_{22}s_{J2}\mathcal{S}_{2y} - \frac{1}{2}(c_{11}s_{J1} + c_{21}s_{J1})s_{22}s_{J2}\mathcal{S}_{2x} \right)$$

plus unmeasurable anti-quantum coherences.

Considering orthogonality of the matrices,

$$\begin{aligned} & \text{Tr}\{\hat{\rho}(t_2)(\mathcal{I}_{1x} + i\mathcal{I}_{1y} + \mathcal{I}_{2x} + i\mathcal{I}_{2y})\} = \\ & \frac{\kappa}{2} \left(i \frac{1}{2} (c_{11}s_{J1} + c_{21}s_{J1}) c_{12}s_{J2} - \frac{1}{2} (c_{11}s_{J1} + c_{21}s_{J1}) s_{12}s_{J2} + i \frac{1}{2} (c_{11}s_{J1} + c_{21}s_{J1}) c_{22}s_{J2} - \frac{1}{2} (c_{11}s_{J1} + c_{21}s_{J1}) s_{22}s_{J2} \right). \end{aligned} \quad (11.13)$$

Using the trigonometric relations (Eq. 11.11), the averaged signal (i.e., the signal recorded for the full phase cycle, divided by four) is proportional to

$$\begin{aligned} & \text{Tr}\{\hat{\rho}(t_2)(\mathcal{I}_{1x} + i\mathcal{I}_{1y} + \mathcal{I}_{2x} + i\mathcal{I}_{2y})\} \\ & = \frac{\kappa}{4} (i(c_{11}s_{J1} + c_{21}s_{J1})c_{12}s_{J2} - (c_{11}s_{J1} + c_{21}s_{J1})s_{12}s_{J2} + i(c_{11}s_{J1} + c_{21}s_{J1})c_{22}s_{J2} - (c_{11}s_{J1} + c_{21}s_{J1})s_{22}s_{J2}) \\ & = i \frac{\kappa}{4} \left(\frac{-s_{11}^- + s_{11}^+}{2} \frac{-s_{12}^- + s_{12}^+}{2} + \frac{-s_{21}^- + s_{21}^+}{2} \frac{-s_{12}^- + s_{12}^+}{2} + \frac{-s_{11}^- + s_{11}^+}{2} \frac{-s_{22}^- + s_{22}^+}{2} + \frac{-s_{21}^- + s_{21}^+}{2} \frac{-s_{22}^- + s_{22}^+}{2} \right. \\ & \quad \left. - i \left(\frac{-s_{11}^- + s_{11}^+}{2} \frac{c_{12}^- - c_{12}^+}{2} + \frac{-s_{21}^- + s_{21}^+}{2} \frac{c_{12}^- - c_{12}^+}{2} + \frac{-s_{11}^- + s_{11}^+}{2} \frac{c_{22}^- - c_{22}^+}{2} + \frac{-s_{21}^- + s_{21}^+}{2} \frac{c_{22}^- - c_{22}^+}{2} \right) \right) \end{aligned} \quad (11.14)$$

In order to obtain a hypercomplex two-dimensional spectrum, the measurements is repeated with ϕ_2 advanced by 90° for each t_1 increment. The components of $\hat{\rho}(d)$ contributing to the signal, $= -\frac{\kappa}{2} (\frac{1}{2}(s_{11}s_{J1} + s_{21}s_{J1})2\mathcal{I}_{1x}\mathcal{I}_{1y} + (s_{11}s_{J1} + s_{21}s_{J1})2\mathcal{I}_{1y}\mathcal{I}_{1x})$ are converted by the third 90° pulse to $\hat{\rho}(e) = -\frac{\kappa}{2} (\frac{1}{2}(s_{11}s_{J1} + s_{21}s_{J1})2\mathcal{I}_{1x}\mathcal{I}_{1z} + \frac{1}{2}(s_{11}s_{J1} + s_{21}s_{J1})2\mathcal{I}_{1z}\mathcal{I}_{1x})$, which evolves during t_2 as $\hat{\rho}(t_2) = -\frac{\kappa}{2} (\frac{1}{2}(s_{11}s_{J1} + s_{21}s_{J1})c_{12}s_{J2}\mathcal{I}_{1y} - \frac{1}{2}(s_{11}s_{J1} + s_{21}s_{J1})s_{12}s_{J2}\mathcal{I}_{1x} + \frac{1}{2}(s_{11}s_{J1} + s_{21}s_{J1})c_{22}s_{J2}\mathcal{I}_{2y} - \frac{1}{2}(s_{11}s_{J1} + s_{21}s_{J1})s_{22}s_{J2}\mathcal{I}_{2x})$ plus unmeasurable anti-quantum coherences.

Considering orthogonality of the matrices,

$$\begin{aligned} & \text{Tr}\{\hat{\rho}(t_2)(\mathcal{I}_{1x} + i\mathcal{I}_{1y} + \mathcal{I}_{2x} + i\mathcal{I}_{2y})\} = \\ & -\frac{\kappa}{2} \left(i \frac{1}{2} (s_{11}s_{J1} + s_{21}s_{J1}) c_{12}s_{J2} - \frac{1}{2} (s_{11}s_{J1} + s_{21}s_{J1}) s_{12}s_{J2} + i \frac{1}{2} (s_{11}s_{J1} + s_{21}s_{J1}) c_{22}s_{J2} - \frac{1}{2} (s_{11}s_{J1} + s_{21}s_{J1}) s_{22}s_{J2} \right). \end{aligned} \quad (11.15)$$

Including the factor of two and using the trigonometric relations (Eq. 11.11),

$$\begin{aligned} & \text{Tr}\{\hat{\rho}(t_2)(\mathcal{I}_{1x} + i\mathcal{I}_{1y} + \mathcal{I}_{2x} + i\mathcal{I}_{2y})\} \\ & = -\frac{\kappa}{4} (i(s_{11}s_{J1} + s_{21}s_{J1})c_{12}s_{J2} - (s_{11}s_{J1} + s_{21}s_{J1})s_{12}s_{J2} + i(s_{11}s_{J1} + s_{21}s_{J1})c_{22}s_{J2} - (s_{11}s_{J1} + s_{21}s_{J1})s_{22}s_{J2}) \\ & = -i \frac{\kappa}{4} \left(\frac{c_{11}^- - c_{11}^+}{2} \frac{-s_{12}^- + s_{12}^+}{2} + \frac{c_{21}^- - c_{21}^+}{2} \frac{-s_{12}^- + s_{12}^+}{2} + \frac{c_{11}^- - c_{11}^+}{2} \frac{-s_{22}^- + s_{22}^+}{2} + \frac{c_{21}^- - c_{21}^+}{2} \frac{-s_{22}^- + s_{22}^+}{2} \right. \\ & \quad \left. - i \left(\frac{c_{11}^- - c_{11}^+}{2} \frac{c_{12}^- - c_{12}^+}{2} + \frac{c_{21}^- - c_{21}^+}{2} \frac{c_{12}^- - c_{12}^+}{2} + \frac{c_{11}^- - c_{11}^+}{2} \frac{c_{22}^- - c_{22}^+}{2} + \frac{c_{21}^- - c_{21}^+}{2} \frac{c_{22}^- - c_{22}^+}{2} \right) \right) \end{aligned} \quad (11.16)$$

Multiplying Eq. 11.16 by "i" and combining it with Eq. 11.14, applying phase correction, and introducing relaxation, modulation of the signal of the DQF-COSY experiment is obtained:

$$\begin{aligned} \langle M_+ \rangle & = \mathcal{N}\gamma\hbar \frac{\kappa}{16} \left(e^{-\bar{R}_2 t_1} \left(-e^{i(\Omega_1 - \pi J)t_1} + e^{i(\Omega_1 + \pi J)t_1} \right) e^{-\bar{R}_2 t_2} \left(-e^{i(\Omega_1 - \pi J)t_2} + e^{i(\Omega_1 + \pi J)t_2} \right) \right) \\ & \quad + \mathcal{N}\gamma\hbar \frac{\kappa}{16} \left(e^{-\bar{R}_2 t_1} \left(-e^{i(\Omega_2 - \pi J)t_1} + e^{i(\Omega_2 + \pi J)t_1} \right) e^{-\bar{R}_2 t_2} \left(-e^{i(\Omega_1 - \pi J)t_2} + e^{i(\Omega_1 + \pi J)t_2} \right) \right) \\ & \quad + \mathcal{N}\gamma\hbar \frac{\kappa}{16} \left(e^{-\bar{R}_2 t_1} \left(-e^{i(\Omega_1 - \pi J)t_1} + e^{i(\Omega_1 + \pi J)t_1} \right) e^{-\bar{R}_2 t_2} \left(-e^{i(\Omega_2 - \pi J)t_2} + e^{i(\Omega_2 + \pi J)t_2} \right) \right) \\ & \quad + \mathcal{N}\gamma\hbar \frac{\kappa}{16} \left(e^{-\bar{R}_2 t_1} \left(-e^{i(\Omega_2 - \pi J)t_1} + e^{i(\Omega_2 + \pi J)t_1} \right) e^{-\bar{R}_2 t_2} \left(-e^{i(\Omega_2 - \pi J)t_2} + e^{i(\Omega_2 + \pi J)t_2} \right) \right), \end{aligned} \quad (11.17)$$

where the lines with the same colors of the sums of exponentials correspond to diagonal peaks at $[\Omega_1, \Omega_1]$ and $[\Omega_2, \Omega_2]$ and the lines with different colors correspond to cross-peaks at $[\Omega_2, \Omega_1]$ and $[\Omega_1, \Omega_2]$. Comparison with Eq. 11.12 shows that (i) a phase shift between diagonal peaks and cross-peaks is present only in standard COSY but not in DQF-COSY, and (ii) the DQF-COSY signal intensity is half of the value obtained in standard COSY. The spectrum is plotted in Figure 11.6. Note that diagonal peaks and cross-peaks have the same phase (form anti-phase doublets).

Lecture 12

Strong coupling

Literature: Strong coupling for a pair of nuclei is discussed in K12.1, L14.1-L14.3, C2.5.2, and analyzed in detail in LA.8. The idea of the magnetic equivalence is presented in K12.2, L14.4 (for two nuclei), L17.5 (in larger molecules, with some details discussed in LA.9). The TOCSY experiment discussed in Section 12.3 (mixing the \mathcal{I}_{ny} coherences) is described in L18.14, another variant (mixing the \mathcal{I}_{nz} coherences) is presented in K8.11, C4.2.1.2, and C6.5.

12.1 Strong J -coupling

We have seen in Section 10.2 that secular approximation substantially simplifies Hamiltonian of the J -coupling if γ and/or chemical shifts differ. However, the description of the system of interacting nuclei changes dramatically if $\gamma_1 = \gamma_2$ and chemical shifts are similar.

As usually, the density matrix at the beginning of the experiment is given by the thermal equilibrium. As mentioned in Section 10.9.3, the effect of the J -coupling on populations is negligible. Therefore, the initial form of the density matrix and its form after the 90° excitation pulse are the same as in the case of a weak coupling:

$$\hat{\rho}(b) = \frac{1}{2}\mathcal{I}_t - \frac{\kappa}{2}\mathcal{I}_{1y} - \frac{\kappa}{2}\mathcal{I}_{2y}. \quad (12.1)$$

In order to describe evolution, we need to know the Hamiltonian. For a pair of nuclei, the Hamiltonian is given by Eq. 10.3. In the presence of (very similar) chemical shifts

$$\mathcal{H} = +\omega_{0,1}\mathcal{I}_{1z} + \omega_{0,2}\mathcal{I}_{2z} + \pi J (2\mathcal{I}_{1z}\mathcal{I}_{2z} + 2\mathcal{I}_{1x}\mathcal{I}_{2x} + 2\mathcal{I}_{1y}\mathcal{I}_{2y}). \quad (12.2)$$

In this Hamiltonian, \mathcal{I}_{1z} and \mathcal{I}_{2z} do not commute with $2\mathcal{I}_{1x}\mathcal{I}_{2x}$ and $2\mathcal{I}_{1y}\mathcal{I}_{2y}$. Therefore, we cannot analyze the evolution of the density matrix by analyzing effects of individual components of the Hamiltonian separately and in any order, as we did in the case of weak the coupling Hamiltonian $\omega_{0,1}\mathcal{I}_{1z} + \omega_{0,2}\mathcal{I}_{2z} + \pi J \cdot 2\mathcal{I}_{1z}\mathcal{I}_{2z}$ consisting of three mutually commuting components.

If we use matrices listed in Tables 8.3 and 8.4, the matrix representation of the Hamiltonian is

$$\mathcal{H} = \frac{\pi}{2} \begin{pmatrix} \Sigma + J & 0 & 0 & 0 \\ 0 & \Delta - J & 2J & 0 \\ 0 & 2J & -\Delta - J & 0 \\ 0 & 0 & 0 & -\Sigma + J \end{pmatrix}, \quad (12.3)$$

where $\Sigma = (\omega_{0,1} + \omega_{0,2})/\pi$ and $\Delta = (\omega_{0,1} - \omega_{0,2})/\pi$. Obviously, the matrix is not diagonal. In order to find eigenvalues of the Hamiltonian, corresponding to frequencies observed in the spectra, we have to find a new basis where the Hamiltonian represented by a diagonal matrix. This is done in Section 12.4.1. The diagonalized matrix \mathcal{H}' can be written as a linear combination of matrices listed in Table 8.3

$$\mathcal{H}' = \omega'_{0,1} \mathcal{I}_{1z} + \omega'_{0,2} \mathcal{I}_{2z} + \pi J \cdot 2 \mathcal{I}_{1z} \mathcal{I}_{2z}, \quad (12.4)$$

where

$$\omega'_{0,1} = \frac{1}{2} \left(\omega_{0,1} + \omega_{0,2} + \sqrt{(\omega_{0,1} - \omega_{0,2})^2 + 4\pi^2 J^2} \right) \quad (12.5)$$

$$\omega'_{0,2} = \frac{1}{2} \left(\omega_{0,1} + \omega_{0,2} - \sqrt{(\omega_{0,1} - \omega_{0,2})^2 + 4\pi^2 J^2} \right). \quad (12.6)$$

We see that \mathcal{H}' consists of the same product operators as the Hamiltonian describing a weak coupling, only the frequencies differ. The density matrix $\hat{\rho}(b)$ and the operator of the measured quantity \hat{M}_+ should be also expressed in the basis found in Section 12.4.1. The transformed density matrix $\hat{\rho}'$ consists of the same product operators as the density matrix in the original basis, they are just combined with different coefficients. We can thus repeat the analysis presented for a weak J -coupling in Section 10.3 using the same rotations in the operators space as presented in Figure 10.3. The analysis of a strongly j -coupled system differs only in three issues: (i) we start to rotate from a different combination of product operators, (ii) the angles of rotations differ, being given by the frequencies $\omega'_{0,1}, \omega'_{0,2}$ instead of $\omega_{0,1}, \omega_{0,2}$, and (iii) we have to calculate a trace of the density matrix multiplied by the transformed operator of transverse magnetization, \hat{M}'_+ . The analysis is presented in Section 12.4.2. Fourier transformation of the result (Eq. 12.52) is

$$\begin{aligned} \Re\{Y(\omega)\} &= \left(1 - \frac{J}{\sqrt{\Delta^2 + 4J^2}}\right) \frac{\mathcal{N}\gamma^2\hbar^2 B_0}{8k_B T} \frac{\bar{R}_2}{\bar{R}_2^2 + (\omega - \Omega'_2 - \pi J)^2} \\ &+ \left(1 + \frac{J}{\sqrt{\Delta^2 + 4J^2}}\right) \frac{\mathcal{N}\gamma^2\hbar^2 B_0}{8k_B T} \frac{\bar{R}_2}{\bar{R}_2^2 + (\omega - \Omega'_2 - \pi J)^2} \\ &+ \left(1 + \frac{J}{\sqrt{\Delta^2 + 4J^2}}\right) \frac{\mathcal{N}\gamma^2\hbar^2 B_0}{8k_B T} \frac{\bar{R}_2}{\bar{R}_2^2 + (\omega - \Omega'_1 + \pi J)^2} \\ &+ \left(1 - \frac{J}{\sqrt{\Delta^2 + 4J^2}}\right) \frac{\mathcal{N}\gamma^2\hbar^2 B_0}{8k_B T} \frac{\bar{R}_2}{\bar{R}_2^2 + (\omega - \Omega'_1 + \pi J)^2} \end{aligned}$$

$$\begin{aligned}
\Im\{Y(\omega)\} = & -i \left(1 - \frac{J}{\sqrt{\Delta^2 + 4J^2}}\right) \frac{\mathcal{N}\gamma^2\hbar^2 B_0}{8k_B T} \frac{\omega - \Omega'_2 - \pi J}{R_2^2 + (\omega - \Omega'_2 - \pi J)^2} \\
& -i \left(1 + \frac{J}{\sqrt{\Delta^2 + 4J^2}}\right) \frac{\mathcal{N}\gamma^2\hbar^2 B_0}{8k_B T} \frac{\omega - \Omega'_2 - \pi J}{R_2^2 + (\omega - \Omega'_2 - \pi J)^2} \\
& -i \left(1 + \frac{J}{\sqrt{\Delta^2 + 4J^2}}\right) \frac{\mathcal{N}\gamma^2\hbar^2 B_0}{8k_B T} \frac{\omega - \Omega'_1 + \pi J}{R_2^2 + (\omega - \Omega'_1 + \pi J)^2} \\
& -i \left(1 - \frac{J}{\sqrt{\Delta^2 + 4J^2}}\right) \frac{\mathcal{N}\gamma^2\hbar^2 B_0}{8k_B T} \frac{\omega - \Omega'_1 + \pi J}{R_2^2 + (\omega - \Omega'_1 + \pi J)^2}.
\end{aligned} \tag{12.7}$$

Spectra for three different values of $|\Omega_1 - \Omega_2|$ are plotted in Figure 12.1. The features that distinguish spectra of strongly coupled nuclear magnetic moments from those of weakly coupled pairs are

- The centers of doublets of peaks of individual nuclei are shifted from the precession frequencies of the nuclei Ω_1 and Ω_2 by a factor of $\pm \left(\Omega_1 - \Omega_2 - \sqrt{(\Omega_1 - \Omega_2)^2 + 4\pi^2 J^2}\right) / 2$.
- The intensities of the inner peaks of the doublet of doublets are increased and the intensities of the outer peaks are decreased by a factor of $2\pi J / \sqrt{(\Omega_1 - \Omega_2)^2 + 4\pi^2 J^2}$.

The square root $\sqrt{(\Omega_1 - \Omega_2)^2 + 4\pi^2 J^2}$ specifies the limit between *weak* and *strong* J -coupling. If $|\Omega_1 - \Omega_2| \gg 2\pi|J|$, the factors modifying the peak intensities are negligible and the J -coupling is considered *weak*. The other limit, $|\Omega_1 - \Omega_2| \rightarrow 0$, deserves a special attention and is discussed in more details in the next section.

12.2 Magnetic equivalence

If two interacting nuclear magnetic moments have the same precession frequencies (due to a molecular symmetry¹ or accidentally), and if they are not distinguished by different couplings to other nuclei, they are *magnetically equivalent*.

Following the trends in Figure 12.1 suggests that only one peak appears in a spectrum of a pair of magnetically equivalent nuclei. This explains why we do not observe e.g. splitting due to the relatively large J -coupling of protons in water ($|^2J| \approx 7$ Hz).

From the theoretical point of view, a pair of magnetically equivalent nuclei represents a fundamentally different system than a pair of weakly coupled nuclei (even for identical J constant). The eigenstates of the Hamiltonian of the magnetically equivalent nuclei in \vec{B}_0 are not direct products of the $|\alpha\rangle$ and $|\beta\rangle$ eigenstates (as we described in Section 8.9.3). The pair of magnetically equivalent

¹Nuclei can be inequivalent even if the whole molecule is symmetric (i.e., achiral). Existence of a plane of symmetry is not sufficient, the plane must bisect the particular pair of nuclei. Otherwise, the nuclei are *diastereotopic* and magnetically inequivalent.

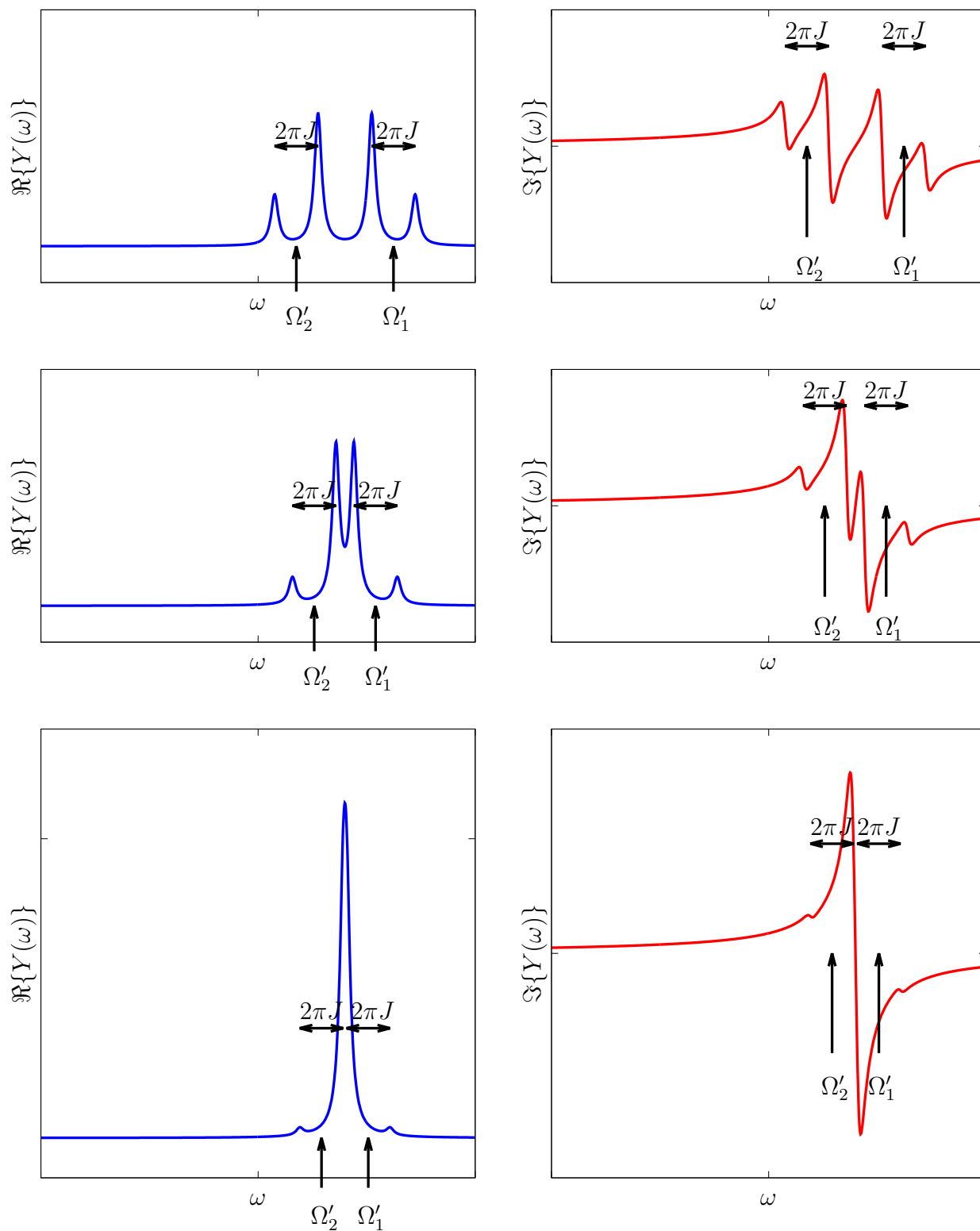


Figure 12.1: One-dimensional spectra of strongly J -coupled ^1H - ^1H pairs. The spectra are plotted for $\Omega_1 - \Omega_2 = 4\pi J$ (top), $\Omega_1 - \Omega_2 = 2\pi J$ (middle), and $\Omega_1 - \Omega_2 = 0.8\pi J$ (bottom).

Table 12.1: Eigenvalues of selected operators for a pair of magnetically equivalent nuclei. The operators \hat{I}_1^2 , \hat{I}_2^2 , $\hat{I}^{2'}$, and \hat{I}'_z are defined in Section 10.9.2, $\mathcal{H}' = (\omega_0 + \pi J)\mathcal{I}_{1z} + (\omega_0 - \pi J)\mathcal{I}_{2z} + \pi J \cdot 2\mathcal{I}_{1z}\mathcal{I}_{2z}$.

Eigenfunction	\hat{I}_1^2	\hat{I}_2^2	$\hat{I}^{2'}$	\hat{I}'_z	\mathcal{H}'
$ \alpha\rangle \otimes \alpha\rangle$	$3\hbar^2/4$	$3\hbar^2/4$	$2\hbar^2$	$+\hbar$	$+\omega_0 + \frac{\pi}{2}J$
$\frac{1}{\sqrt{2}} \alpha\rangle \otimes \beta\rangle + \frac{1}{\sqrt{2}} \beta\rangle \otimes \alpha\rangle$	$3\hbar^2/4$	$3\hbar^2/4$	$2\hbar^2$	0	$+\frac{\pi}{2}J$
$\frac{1}{\sqrt{2}} \alpha\rangle \otimes \beta\rangle - \frac{1}{\sqrt{2}} \beta\rangle \otimes \alpha\rangle$	$3\hbar^2/4$	$3\hbar^2/4$	0	0	$-\frac{3\pi}{2}J$
$ \beta\rangle \otimes \beta\rangle$	$3\hbar^2/4$	$3\hbar^2/4$	$2\hbar^2$	$-\hbar$	$-\omega_0 + \frac{\pi}{2}J$

nuclei is similar to a pair of electrons discussed in Section 10.9.2. The eigenfunctions and eigenvalues for important operators are listed in Table 12.1.

The eigenfunctions help us to understand the difference between quantum states of non-interacting or weakly J -coupled pairs on one hand, and magnetically equivalent pairs on the other hand. We have discussed in detail that the stationary states $|\alpha\rangle \otimes |\alpha\rangle$, $|\alpha\rangle \otimes |\beta\rangle$, $|\beta\rangle \otimes |\alpha\rangle$, $|\beta\rangle \otimes |\beta\rangle$ are important in single pairs of nuclei, but are rarely present in large macroscopic ensembles. Now we see that in the case of magnetically equivalent nuclei, $|\alpha\rangle \otimes |\beta\rangle$ and $|\beta\rangle \otimes |\alpha\rangle$ do not even describe stationary states of a single pair. Instead, the stationary states are their combinations.

The eigenvalues of the operator representing square of the total angular momentum $\hat{I}^{2'}$ tells us that three eigenstates have the same size of the total angular momentum ($\sqrt{2}\hbar$) and one does not have any angular momentum (and therefore any magnetic moment). The energy differences (eigenvalues of \mathcal{H}' multiplied by \hbar) between the three "magnetic states" are the same in isotropic liquids (but they differ if the dipole-dipole coupling is not averaged to zero), which explains why we see only one frequency in the spectrum. The "non-magnetic" state does not have any magnetic moment and thus does not contribute to observable magnetization.

The analysis is more demanding if a magnetically equivalent pair is a part of a larger molecule. Nevertheless, it can be shown that J -couplings between magnetically equivalent nuclei in larger molecules do not affect the NMR spectra (Sections 12.4.3 and 12.4.4).

12.3 TOCSY

At the first glance, molecules whose nuclei have very similar chemical shifts (by accident or as a result of molecular symmetry), and are therefore very strongly J -coupled, seem to represent a special case. However, tricks discussed in the previous lectures allow us to exploit advantages of strong J -coupling even if the chemical shifts are very different. We have learnt that we can use a spin echo to suppress the effect of the chemical shift evolution, which is exactly what we need: no chemical shift evolution corresponds to zero difference in frequency offset. If we apply the simultaneous echo (actually, the only echo applicable to homonuclear pairs) that keeps the J -coupling evolution but refocuses evolution of the chemical shift, the state of the system of nuclei at the end of the echo is the same as a state of a system of nuclei with identical chemical shifts. Note, however, that a single application of a spin echo is not sufficient. Our goal is to make the strong coupling to act continuously for a certain period of time, comparable to $1/J$, not just in one moment. Therefore, we have to apply

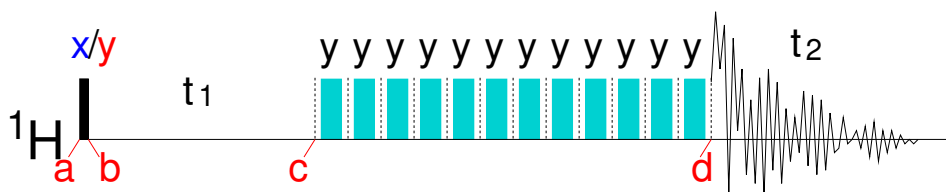


Figure 12.2: TOCSY pulse sequence. The narrow black and wide cyan rectangles represent 90° and 180° radio wave pulses applied at a frequency sufficiently close to the precession frequencies of all interacting magnetic moments.

a series of radio-frequency pulses to keep the strong coupling active for a whole *mixing* period. In principle, a series of very short coupling echoes with very short 180° should work (Figure 12.2). However, specially designed sequences of pulses with much weaker offset effects are used in practice.² Two-dimensional experiment utilizing a mixing mimicking the strong coupling is known as Totally Correlated Spectroscopy (TOCSY). There are numerous variants of the experiment, here we present only the simplest version (Figure 12.2) illustrating the basic idea.

In order to describe the major advantage of the TOCSY experiment, we analyze a simple system of three nuclei (e.g. three protons) where nuclei 1 and 2 are coupled, nuclei 2 and 3 are also coupled, but there is no coupling between nuclei 1 and 3 (a more general analysis and matrix representations of the product operators for ensembles presented in Section 12.4.6). Let us assume that both coupling constants are identical ($J_{12} = J_{23} = J$). Before the TOCSY mixing period, density matrix of our system evolves like in the NOESY or COSY experiment. The starting, equilibrium, density matrix

$$\hat{\rho}(a) = \frac{1}{4}(\mathcal{I}_t + \kappa\mathcal{I}_{1z} + \kappa\mathcal{I}_{2z} + \kappa\mathcal{I}_{3z})$$

is converted to

$$\hat{\rho}(b) = \frac{1}{4}(\mathcal{I}_t - \kappa\mathcal{I}_{1y} - \kappa\mathcal{I}_{2y} - \kappa\mathcal{I}_{3y})$$

by a 90° excitation pulse and evolves during the incremented evolution period t_1 . For the sake of simplicity, we pay attention to the fate of the coherences modulated by the chemical shift of nucleus 1:

$$\hat{\rho}(c) = -\frac{\kappa}{4} \cos(\Omega_1 t_1) \cos(\pi J t_1) \mathcal{I}_{1y} + \dots$$

Let us assume that the TOCSY pulse train is applied with the 90° or -90° (y or $-y$) phases of the radio waves. As a consequence, the pulses keep the \mathcal{I}_{1y} , \mathcal{I}_{2y} , \mathcal{I}_{3y} components of the density matrix intact and rotate other coherences "about" the \mathcal{I}_{ny} "axis". Because the trains contain many (hundreds) of pulses, the imperfections of the pulses and stochastic molecular motions randomize the direction of the polarizations in the xz plane (an effect similar to the loss of coherence in the xy plane during evolution in the \vec{B}_0 field). Therefore, we assume that only the \mathcal{I}_{1y} , \mathcal{I}_{2y} , \mathcal{I}_{3y} coherences, "locked" in the y direction of the rotating frame, survive the TOCSY mixing pulse train.³

The Hamiltonian describing the evolution of our simple system during the TOCSY mixing period is

$$\mathcal{H}_{\text{TOCSY}} = \pi J (2\mathcal{I}_{1z}\mathcal{I}_{2z} + 2\mathcal{I}_{1x}\mathcal{I}_{2x} + 2\mathcal{I}_{1y}\mathcal{I}_{2y} + 2\mathcal{I}_{2z}\mathcal{I}_{3z} + 2\mathcal{I}_{2x}\mathcal{I}_{3x} + 2\mathcal{I}_{2y}\mathcal{I}_{3y}). \quad (12.8)$$

Note that the Hamiltonian is fully symmetric in our coordinate system. In our version of the TOCSY experiment, we decided to preserve only the \mathcal{I}_{ny} coherences by the choice of the phase of

²Technically, our task is very similar to decoupling during acquisition, shown in Section 11.3.

³If coherences other than \mathcal{I}_{ny} are not destroyed completely, their contribution can be removed by phase cycling.

the applied pulses. However, the Hamiltonian itself acts on the \mathcal{I}_{nx} , \mathcal{I}_{ny} , and \mathcal{I}_{nz} in a completely identical way.⁴ Therefore, the effect of the Hamiltonian is called *isotropic mixing* (working equally in all directions).

All components of the Hamiltonian in Eq. 12.8 commute (because the echo removed the chemical shift components) and it is possible to inspect their effects separately. Such analysis is straightforward for two interacting nuclei, but gets complicated for three or more nuclei. Nevertheless, a useful insight can be gained from the inspection of commutation relations of the $\mathcal{H}_{\text{TOCSY}}$ Hamiltonian, derived in Section 12.4.5. First, $\mathcal{H}_{\text{TOCSY}}$ does not commute with \mathcal{I}_{1y} . It tells us that $-\frac{\kappa}{4} \cos(\Omega_1 t_1) \cos(\pi J t_1) \mathcal{I}_{1y}$ partially evolves to other coherences (or populations) during the TOCSY mixing (Eq. 12.60). Second, $\mathcal{H}_{\text{TOCSY}}$ does not commute with $\mathcal{I}_{1y} + \mathcal{I}_{2y}$ either (Eq. 12.63). We see, that the lost portion of $-\frac{\kappa}{4} \cos(\Omega_1 t_1) \cos(\pi J t_1) \mathcal{I}_{1y}$ is not completely converted to $-\frac{\kappa}{4} \cos(\Omega_1 t_1) \cos(\pi J t_1) \mathcal{I}_{2y}$. Finally, $\mathcal{H}_{\text{TOCSY}}$ *does* commute⁵ with $\mathcal{I}_{1y} + \mathcal{I}_{2y} + \mathcal{I}_{3y}$ (Eq. 12.64). If $\mathcal{I}_{1y} + \mathcal{I}_{2y} + \mathcal{I}_{3y}$ does not change and \mathcal{I}_{1y} is not completely converted to \mathcal{I}_{2y} , the missing portion of \mathcal{I}_{1y} must be compensated by formation of $-\frac{\kappa}{4} \cos(\Omega_1 t_1) \cos(\pi J t_1) \mathcal{I}_{3y}$. The fraction of the density matrix converted to \mathcal{I}_{2y} and \mathcal{I}_{3y} depends on the length of the TOCSY pulse train (*mixing time*), on actual values of the J constants (they are not identical in real case), on relaxation, and on the evolution during the pulses (their duration is not negligible compared to the lengths of individual echoes in the train if the goal is to have the echoes as short as possible). In our analysis, we describe the fraction that stays in the \mathcal{I}_{1y} by a factor a_{11} , the efficiency of the transfer from nucleus 1 to nucleus 2 by a factor a_{12} , and the efficiency of the transfer from nucleus 1 to nucleus 3 by a factor a_{13} .

Detailed analysis of the evolution of the density matrix (the procedure, presented in Section 12.4.6, is very similar to those described in previous lectures for other 2D experiments) shows that the coherence \mathcal{I}_{1y} provides three components of the signal (see Eq. 12.73)

$$\begin{aligned} & \frac{\kappa}{8} a_{11} e^{-\bar{R}_2 t_1} \left(e^{-i(\Omega_1 - \pi J) t_1} + e^{-i(\Omega_1 + \pi J) t_1} \right) e^{-\bar{R}_2 t_2} \left(e^{-i(\Omega_1 - \pi J) t_2} + e^{-i(\Omega_1 + \pi J) t_2} \right) \\ & + \frac{\kappa}{8} a_{12} e^{-\bar{R}_2 t_1} \left(e^{-i(\Omega_1 - \pi J) t_1} + e^{-i(\Omega_1 + \pi J) t_1} \right) e^{-\bar{R}_2 t_2} \left(e^{-i(\Omega_2 - \pi J) t_2} + e^{-i(\Omega_2 + \pi J) t_2} \right) \\ & + \frac{\kappa}{8} a_{13} e^{-\bar{R}_2 t_1} \left(e^{-i(\Omega_1 - \pi J) t_1} + e^{-i(\Omega_1 + \pi J) t_1} \right) e^{-\bar{R}_2 t_2} \left(e^{-i(\Omega_3 - \pi J) t_2} + e^{-i(\Omega_3 + \pi J) t_2} \right). \end{aligned} \quad (12.9)$$

These components represent one diagonal peak (at the frequencies $[\Omega_1, \Omega_2]$) and two cross-peaks (Figure 12.3), including a cross-peak at the frequencies of protons that are not directly J -coupled ($[\Omega_1, \Omega_3]$). This is a fundamental difference between COSY and TOCSY spectra. Appearance of cross-peaks in the COSY spectra requires a direct J -coupling, whereas cross-peaks in the TOCSY spectra correlate all peaks of a *spin-system* (a network of nuclei connected by J -coupling), even if the coupling of a particular pair is negligible (Figure 12.3). Structural information in COSY and TOCSY spectra is complementary. The TOCSY experiment describes the complete spin systems in a single spectrum, COSY spectra distinguish directly J -coupled nuclei (usually vicinal and geminal protons).

⁴We could select \mathcal{I}_{nx} coherences equally well by applying pulses with a phase of 0° (x). The \mathcal{I}_{nz} can be selected by applying additional 90° before and after the TOCSY pulse train (this approach is described in K8.11 and C6.5).

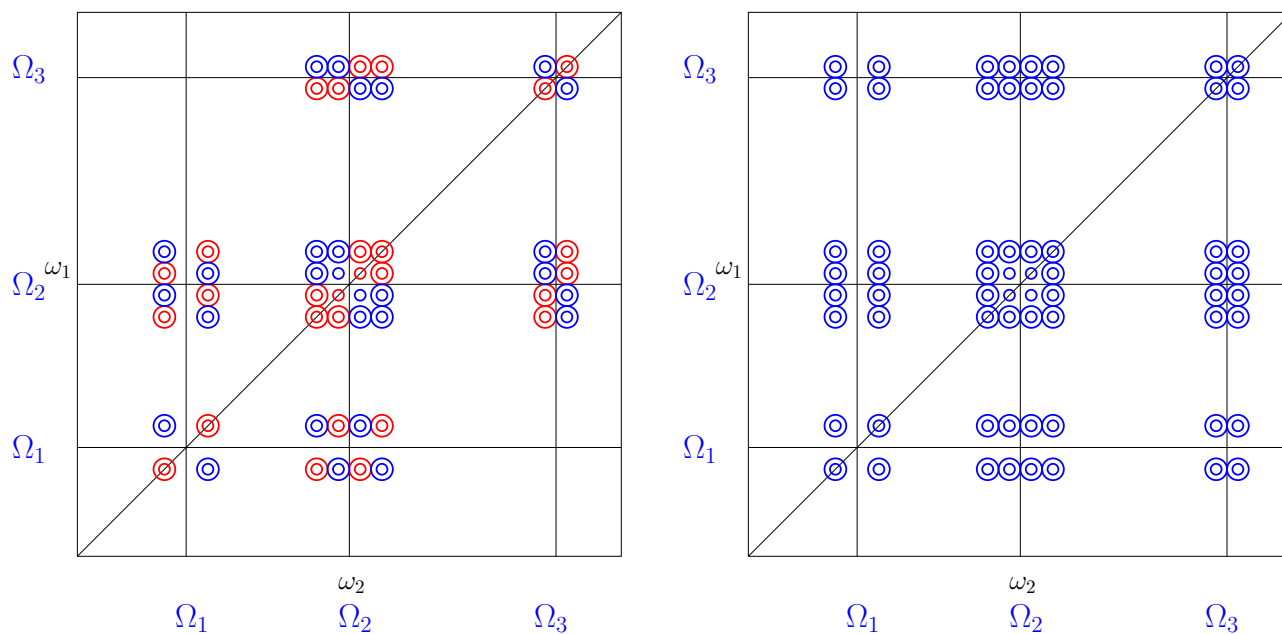


Figure 12.3: DQF-COSY (left) and TOCSY (right) spectra of a molecule with three protons with the J -coupling constants $|J_{12}| > |J_{23}|$ and $J_{13} = 0$. Note the presence of a cross-peak correlating the not coupled protons 1 and 3 in the TOCSY, but not in the DQF-COSY spectrum.

HOMEWORK

Using results of Section 12.4.1, analyze evolution of the density matrix in the presence of a strong J -coupling (Section 12.4.2).

In practice, the pulse trains are optimized for the given purpose.

⁵In general, $\mathcal{H}_{\text{TOCSY}}$ commutes with the operators of all three components I_j of the total angular momentum, where $j \in \{x, y, z\}$ and I_j is a sum of I_{nj} for all nuclei n .

12.4 DERIVATIONS

12.4.1 Diagonalization of the J -coupling Hamiltonian matrix

The matrix representation of the Hamiltonian describing chemical shift and strong J -coupling, written in the basis constructed from the α and β states of the interacting nuclei (i.e., $|\alpha\alpha\rangle, |\beta\alpha\rangle, |\alpha\beta\rangle, |\beta\beta\rangle$), is

$$\mathcal{H} = \frac{\pi}{2} \begin{pmatrix} \Sigma + J & 0 & 0 & 0 \\ 0 & \Delta - J & 2J & 0 \\ 0 & 2J & -\Delta - J & 0 \\ 0 & 0 & 0 & -\Sigma + J \end{pmatrix}, \quad (12.10)$$

where $\Sigma = (\omega_{0,1} + \omega_{0,2})/\pi$ and $\Delta = (\omega_{0,1} - \omega_{0,2})/\pi$. We are looking for a new, diagonal matrix representation of our Hamiltonian \mathcal{H}' . A similar task is solved in Section 10.9.2, the matrix in Eq. 12.10 just have more complicated elements. From the mathematical point of view, *diagonalization* of our Hamiltonian can be described using a transformation matrix \hat{T} :

$$\mathcal{H}' = \hat{T}^{-1} \mathcal{H} \hat{T}. \quad (12.11)$$

Multiplying by \hat{T} from left gives

$$\hat{T} \mathcal{H}' = \mathcal{H} \hat{T}. \quad (12.12)$$

The desired eigenvalues ω'_k and eigenvectors $|\psi'_k\rangle$ can be obtained by comparing the eigenvalue equation

$$\mathcal{H}' |\psi'_k\rangle = \omega'_k |\psi'_k\rangle \quad (12.13)$$

with the left-hand side of Eq. 12.12

$$\begin{pmatrix} T_{11} & T_{12} & T_{13} & T_{14} \\ T_{21} & T_{22} & T_{23} & T_{24} \\ T_{31} & T_{32} & T_{33} & T_{34} \\ T_{41} & T_{42} & T_{43} & T_{44} \end{pmatrix} \begin{pmatrix} \omega'_1 & 0 & 0 & 0 \\ 0 & \omega'_2 & 0 & 0 \\ 0 & 0 & \omega'_3 & 0 \\ 0 & 0 & 0 & \omega'_4 \end{pmatrix} = \begin{pmatrix} \omega'_1 T_{11} & \omega'_2 T_{12} & \omega'_3 T_{13} & \omega'_4 T_{14} \\ \omega'_1 T_{21} & \omega'_2 T_{22} & \omega'_3 T_{23} & \omega'_4 T_{24} \\ \omega'_1 T_{31} & \omega'_2 T_{32} & \omega'_3 T_{33} & \omega'_4 T_{34} \\ \omega'_1 T_{41} & \omega'_2 T_{42} & \omega'_3 T_{43} & \omega'_4 T_{44} \end{pmatrix}. \quad (12.14)$$

The eigenvalue equation can be written as a set of four equations for $k = 1, 2, 3, 4$

$$\mathcal{H}' |\psi'_k\rangle = \frac{\pi}{2} \begin{pmatrix} \Sigma + J & 0 & 0 & 0 \\ 0 & \Delta - J & 2J & 0 \\ 0 & 2J & -\Delta - J & 0 \\ 0 & 0 & 0 & -\Sigma + J \end{pmatrix} \begin{pmatrix} T_{1k} \\ T_{2k} \\ T_{3k} \\ T_{4k} \end{pmatrix} = \frac{\pi}{2} \begin{pmatrix} (\Sigma + J)T_{1k} \\ (\Delta - J)T_{2k} + 2JT_{3k} \\ 2JT_{2k} - (\Delta + J)T_{3k} \\ (-\Sigma + J)T_{4k} \end{pmatrix} = \omega'_k \begin{pmatrix} T_{1k} \\ T_{2k} \\ T_{3k} \\ T_{4k} \end{pmatrix} = \omega'_k |\psi'_k\rangle. \quad (12.15)$$

The first row of the middle equality allows us to identify

$$\omega'_1 = \frac{\pi}{2} (\Sigma + J) = \frac{\omega_{0,1} + \omega_{0,2}}{2} + \frac{\pi}{2} J \quad (12.16)$$

if we set $T_{21} = T_{31} = T_{41} = 0$, i.e.,

$$|\psi'_1\rangle = \begin{pmatrix} T_{11} \\ 0 \\ 0 \\ 0 \end{pmatrix}. \quad (12.17)$$

Similarly,

$$\omega'_4 = \frac{\pi}{2} (-\Sigma + J) = -\frac{\omega_{0,1} + \omega_{0,2}}{2} + \frac{\pi}{2} J \quad (12.18)$$

for

$$|\psi'_4\rangle = \begin{pmatrix} 0 \\ 0 \\ 0 \\ T_{44} \end{pmatrix}. \quad (12.19)$$

The ω'_2 and ω'_3 values can be calculated from the equations

$$2\omega'_k T_{2k} = \pi(\Delta - J)T_{2k} + 2\pi J T_{3k} \quad (12.20)$$

$$2\omega'_k T_{3k} = 2\pi J T_{2k} - \pi(\Delta + J)T_{3k}, \quad (12.21)$$

(setting $T_{12} = T_{42} = T_{13} = T_{43} = 0$).

T_{3k} can be expressed from the first equation

$$T_{3k} = \frac{2\omega'_k + \pi(J - \Delta)}{2\pi J} T_{2k} \quad (12.22)$$

and inserted into the second equation

$$(2\omega'_k + \pi(J + \Delta))(2\omega'_k + \pi(J - \Delta))T_{2k} = (2\pi J)^2 T_{2k}, \quad (12.23)$$

directly giving

$$\omega'_k = -\frac{\pi}{2} \left(J \pm \sqrt{4J^2 + \Delta^2} \right). \quad (12.24)$$

Choosing

$$\omega'_2 = -\frac{\pi}{2} \left(J - \sqrt{4J^2 + \Delta^2} \right) = \frac{\sqrt{(\omega_{0,1} - \omega_{0,2})^2 + 4\pi^2 J^2}}{2} - \frac{\pi}{2} J \quad (12.25)$$

and

$$\omega'_3 = -\frac{\pi}{2} \left(J + \sqrt{4J^2 + \Delta^2} \right) = -\frac{\sqrt{(\omega_{0,1} - \omega_{0,2})^2 + 4\pi^2 J^2}}{2} - \frac{\pi}{2} J. \quad (12.26)$$

completely defines the diagonalized Hamiltonian

$$\begin{aligned} \mathcal{H}' &= \frac{\pi}{2} \begin{pmatrix} \Sigma + J & 0 & 0 & 0 \\ 0 & \sqrt{\Delta^2 + 4J^2} - J & 0 & 0 \\ 0 & 0 & -\sqrt{\Delta^2 + 4J^2} - J & 0 \\ 0 & 0 & 0 & -\Sigma + J \end{pmatrix} = \frac{\omega'_{0,1}}{2} \begin{pmatrix} 1 & 0 & 0 & 0 \\ 0 & 1 & 0 & 0 \\ 0 & 0 & -1 & 0 \\ 0 & 0 & 0 & -1 \end{pmatrix} + \frac{\omega'_{0,1}}{2} \begin{pmatrix} 1 & 0 & 0 & 0 \\ 0 & -1 & 0 & 0 \\ 0 & 0 & 1 & 0 \\ 0 & 0 & 0 & -1 \end{pmatrix} + \pi J \begin{pmatrix} 1 & 0 & 0 & 0 \\ 0 & -1 & 0 & 0 \\ 0 & 0 & -1 & 0 \\ 0 & 0 & 0 & 1 \end{pmatrix} \\ &= \omega'_{0,1} \mathcal{I}_{1z} + \omega'_{0,2} \mathcal{I}_{2z} + \pi J 2 \mathcal{I}_{1z} \mathcal{I}_{2z}, \end{aligned} \quad (12.27)$$

where

$$\omega'_{0,1} = \frac{\pi}{2} (\Sigma + \sqrt{\Delta^2 + 4J^2}) = \frac{1}{2} \left(\omega_{0,1} + \omega_{0,2} + \sqrt{(\omega_{0,1} - \omega_{0,2})^2 + 4\pi^2 J^2} \right) \quad (12.28)$$

$$\omega'_{0,2} = \frac{\pi}{2} (\Sigma - \sqrt{\Delta^2 + 4J^2}) = \frac{1}{2} \left(\omega_{0,1} + \omega_{0,2} - \sqrt{(\omega_{0,1} - \omega_{0,2})^2 + 4\pi^2 J^2} \right). \quad (12.29)$$

The new basis is given by Eqs. 12.20, 12.21, and the normalization condition

$$\langle \psi'_k | \psi'_k \rangle = 1 \Rightarrow \sum_{j=1}^4 T_{jk}^2 = 1. \quad (12.30)$$

The normalization conditions immediately defines $T_{11} = T_{44} = 1$. Substituting ω'_2 into Eqs. 12.20 and 12.21, respectively, gives

$$\frac{T_{32}}{T_{22}} = \frac{\sqrt{4J^2 + \Delta^2} - \Delta}{2J} \quad (12.31)$$

$$\frac{T_{22}}{T_{32}} = \frac{\sqrt{4J^2 + \Delta^2} + \Delta}{2J}. \quad (12.32)$$

Consequently,

$$\frac{T_{32}^2}{T_{22}^2} = \frac{\sqrt{4J^2 + \Delta^2} - \Delta}{\sqrt{4J^2 + \Delta^2} + \Delta} \quad (12.33)$$

and applying the normalization condition $T_{32}^2 = 1 - T_{22}^2$

$$\frac{1 + T_{22}^2}{T_{22}^2} = \frac{\sqrt{4J^2 + \Delta^2} - \Delta}{\sqrt{4J^2 + \Delta^2} + \Delta} \quad (12.34)$$

defines

$$T_{22}^2 = \frac{1}{1 - \frac{\sqrt{4J^2 + \Delta^2} - \Delta}{\sqrt{4J^2 + \Delta^2} + \Delta}} = \frac{\sqrt{4J^2 + \Delta^2} + \Delta}{2\sqrt{4J^2 + \Delta^2}} \quad (12.35)$$

and

$$T_{32}^2 = 1 - T_{22}^2 = \frac{\sqrt{4J^2 + \Delta^2} - \Delta}{2\sqrt{4J^2 + \Delta^2}}. \quad (12.36)$$

Similarly, T_{23}^2 and T_{33}^2 can be calculated by substituting ω'_3 into Eqs. 12.20 and 12.21:

$$T_{23}^2 = \frac{\sqrt{4J^2 + \Delta^2} - \Delta}{2\sqrt{4J^2 + \Delta^2}} \quad (12.37)$$

$$T_{33}^2 = \frac{\sqrt{4J^2 + \Delta^2} + \Delta}{2\sqrt{4J^2 + \Delta^2}}. \quad (12.38)$$

If we use

$$T_{22} = T_{33} = \sqrt{\frac{1}{2} + \frac{\Delta}{2\sqrt{4J^2 + \Delta^2}}} \equiv c_\xi, \quad T_{23} = \sqrt{\frac{1}{2} - \frac{\Delta}{2\sqrt{4J^2 + \Delta^2}}} \equiv s_\xi, \quad T_{32} = -\sqrt{\frac{1}{2} + \frac{\Delta}{2\sqrt{4J^2 + \Delta^2}}} \equiv -s_\xi, \quad (12.39)$$

we obtain a transformation matrix

$$\hat{T} = \begin{pmatrix} 1 & 0 & 0 & 0 \\ 0 & c_\xi & -s_\xi & 0 \\ 0 & s_\xi & c_\xi & 0 \\ 0 & 0 & 0 & 1 \end{pmatrix}, \quad (12.40)$$

which is its own inverse ($\hat{T}^{-1} = \hat{T} \Rightarrow \hat{T}^{-1}\hat{T} = \hat{T}\hat{T} = \hat{1}$). Later, we also use the following relations between c_ξ and s_ξ :

$$c_\xi^2 + s_\xi^2 = \frac{1}{2} + \frac{\Delta}{2\sqrt{4J^2 + \Delta^2}} + \frac{1}{2} - \frac{\Delta}{2\sqrt{4J^2 + \Delta^2}} = 1 \quad (12.41)$$

$$2c_\xi s_\xi = 2\sqrt{\frac{1}{4} - \frac{\Delta^2}{4(4J^2 + \Delta^2)}} = \sqrt{\frac{4J^2 + \Delta^2 + \Delta^2}{4J^2 + \Delta^2}} = \frac{2J}{\sqrt{4J^2 + \Delta^2}}. \quad (12.42)$$

Finally, the new basis consists of the following eigenvectors

$$|\psi'_1\rangle = \begin{pmatrix} 1 \\ 0 \\ 0 \\ 0 \end{pmatrix}, \quad |\psi'_2\rangle = \begin{pmatrix} 0 \\ \sqrt{\frac{1}{2} + \frac{\Delta}{2\sqrt{4J^2 + \Delta^2}}} \\ \sqrt{\frac{1}{2} - \frac{\Delta}{2\sqrt{4J^2 + \Delta^2}}} \\ 0 \end{pmatrix} \equiv \begin{pmatrix} 0 \\ c_\xi \\ s_\xi \\ 0 \end{pmatrix}, \quad |\psi'_3\rangle = \begin{pmatrix} 0 \\ -\sqrt{\frac{1}{2} - \frac{\Delta}{2\sqrt{4J^2 + \Delta^2}}} \\ \sqrt{\frac{1}{2} + \frac{\Delta}{2\sqrt{4J^2 + \Delta^2}}} \\ 0 \end{pmatrix} \equiv \begin{pmatrix} 0 \\ -s_\xi \\ c_\xi \\ 0 \end{pmatrix}, \quad |\psi'_4\rangle = \begin{pmatrix} 0 \\ 0 \\ 0 \\ 1 \end{pmatrix}. \quad (12.43)$$

We can also use the transformation matrix to express the density matrix ($\hat{\rho}' = \hat{T}\hat{\rho}\hat{T}$) and the operator of the measured quantity ($\hat{M}'_+ = \hat{T}\hat{M}_+\hat{T}$) in the new basis (cf. Eq. 12.11). In particular, we are interested in the transformed operators $\mathcal{J}'_{1y} + \mathcal{J}'_{2y}$ and $\mathcal{J}'_{1+} + \mathcal{J}'_{2+} = \mathcal{J}'_{1x} + \mathcal{J}'_{2x} + i(\mathcal{J}'_{1y} + \mathcal{J}'_{2y})$:

$$\begin{aligned} \mathcal{J}'_{1y} + \mathcal{J}'_{2y} &= \hat{T}(\mathcal{J}_{1y} + \mathcal{J}_{2y})\hat{T} = \begin{pmatrix} 1 & 0 & 0 & 0 \\ 0 & c_\xi & -s_\xi & 0 \\ 0 & s_\xi & c_\xi & 0 \\ 0 & 0 & 0 & 1 \end{pmatrix} \frac{i}{2} \begin{pmatrix} 0 & -1 & -1 & 0 \\ 1 & 0 & 0 & -1 \\ 1 & 0 & 0 & -1 \\ 0 & 1 & 1 & 0 \end{pmatrix} \begin{pmatrix} 1 & 0 & 0 & 0 \\ 0 & c_\xi & -s_\xi & 0 \\ 0 & s_\xi & c_\xi & 0 \\ 0 & 0 & 0 & 1 \end{pmatrix} = \frac{i}{2} \begin{pmatrix} 0 & -(c_\xi + s_\xi) & -(c_\xi - s_\xi) & 0 \\ c_\xi + s_\xi & 0 & 0 & -(c_\xi + s_\xi) \\ c_\xi - s_\xi & 0 & 0 & -(c_\xi - s_\xi) \\ 0 & c_\xi + s_\xi & c_\xi - s_\xi & 0 \end{pmatrix} \\ &= c_\xi \frac{i}{2} \begin{pmatrix} 0 & -1 & -1 & 0 \\ +1 & 0 & 0 & -1 \\ +1 & 0 & 0 & -1 \\ 0 & +1 & +1 & 0 \end{pmatrix} + s_\xi \frac{i}{2} \begin{pmatrix} 0 & -1 & +1 & 0 \\ +1 & 0 & 0 & -1 \\ -1 & 0 & 0 & +1 \\ 0 & +1 & -1 & 0 \end{pmatrix} = c_\xi(\mathcal{J}_{1y} + \mathcal{J}_{2y}) + s_\xi(2\mathcal{J}_{1z}\mathcal{J}_{2y} - 2\mathcal{J}_{1y}\mathcal{J}_{2z}), \end{aligned} \quad (12.44)$$

$$\begin{aligned}
\mathcal{S}'_{1x} + \mathcal{S}'_{2x} &= \hat{T}(\mathcal{S}_{1x} + \mathcal{S}_{2x})\hat{T} = \begin{pmatrix} 1 & 0 & 0 & 0 \\ 0 & c_\xi & -s_\xi & 0 \\ 0 & s_\xi & c_\xi & 0 \\ 0 & 0 & 0 & 1 \end{pmatrix} \frac{1}{2} \begin{pmatrix} 0 & 1 & 1 & 0 \\ 1 & 0 & 0 & 1 \\ 1 & 0 & 0 & 1 \\ 0 & 1 & 1 & 0 \end{pmatrix} \begin{pmatrix} 1 & 0 & 0 & 0 \\ 0 & c_\xi & -s_\xi & 0 \\ 0 & s_\xi & c_\xi & 0 \\ 0 & 0 & 0 & 1 \end{pmatrix} = \frac{1}{2} \begin{pmatrix} 0 & c_\xi + s_\xi & c_\xi - s_\xi & 0 \\ c_\xi + s_\xi & 0 & 0 & c_\xi + s_\xi \\ c_\xi - s_\xi & 0 & 0 & c_\xi - s_\xi \\ 0 & c_\xi + s_\xi & c_\xi - s_\xi & 0 \end{pmatrix} \\
&= c_\xi \frac{1}{2} \begin{pmatrix} 0 & +1 & +1 & 0 \\ +1 & 0 & 0 & +1 \\ +1 & 0 & 0 & +1 \\ 0 & +1 & +1 & 0 \end{pmatrix} + s_\xi \frac{1}{2} \begin{pmatrix} 0 & +1 & -1 & 0 \\ +1 & 0 & 0 & +1 \\ -1 & 0 & 0 & -1 \\ 0 & +1 & -1 & 0 \end{pmatrix} = c_\xi(\mathcal{S}_{1x} + \mathcal{S}_{2x}) + s_\xi(2\mathcal{S}_{1z}\mathcal{S}_{2x} - 2\mathcal{S}_{1x}\mathcal{S}_{2z}), \tag{12.45}
\end{aligned}$$

$$\mathcal{S}'_{1+} + \mathcal{S}'_{2+} = \begin{pmatrix} 0 & c_\xi + s_\xi & c_\xi - s_\xi & 0 \\ 0 & 0 & 0 & c_\xi + s_\xi \\ 0 & 0 & 0 & c_\xi - s_\xi \\ 0 & 0 & 0 & 0 \end{pmatrix} = c_\xi(\mathcal{S}_{1x} + \mathcal{S}_{2x} + i\mathcal{S}_{1y} + i\mathcal{S}_{2y}) + s_\xi(2\mathcal{S}_{1z}\mathcal{S}_{2x} - 2\mathcal{S}_{1x}\mathcal{S}_{2z} + i2\mathcal{S}_{1z}\mathcal{S}_{2y} - i2\mathcal{S}_{1y}\mathcal{S}_{2z}) \tag{12.46}$$

12.4.2 Strong J -coupling and density matrix evolution

When the density matrix at the beginning of the evolution is written in the new basis (where the Hamiltonian matrix is diagonal), it consists of multiple contributions. We analyze its evolution separately for the operators contributing to the signal of individual nuclei, and write the progress of the analysis in a table. The density matrix can be divided as

$$\hat{\rho}' = -\frac{\kappa}{2}\mathcal{S}'_{1y} - \frac{\kappa}{2}\mathcal{S}'_{2y} = \hat{\rho}'_1 + \hat{\rho}'_2 \tag{12.47}$$

Starting with $\hat{\rho}'_1$,

Contribution	$\hat{\rho}'_1(\text{b})$	$\omega'_{0,1}\mathcal{S}_{1z}$ →	$\pi J \cdot 2\mathcal{S}_{1z}\mathcal{S}_{2z}$ →	$\text{Tr}\{\hat{\rho}'_1(t)\mathcal{S}'_{1+}\}$
\mathcal{S}_{1y}	$+\frac{\kappa}{2}c_\xi$	$+\frac{\kappa}{2}c_\xi c'_1$	$+\frac{\kappa}{2}c_\xi c'_1 c_J + \frac{\kappa}{2}s_\xi s'_1 s_J$	$\left. \begin{aligned} &+i\frac{\kappa}{2}c_\xi^2 c'_1 c_J + i\frac{\kappa}{2}c_\xi s_\xi s'_1 s_J \\ &+i\frac{\kappa}{2}s_\xi^2 c'_1 c_J + i\frac{\kappa}{2}c_\xi s_\xi s'_1 s_J \end{aligned} \right\} = i\frac{\kappa}{2} \left(c'_1 c_J + \frac{2J}{\sqrt{4J^2 + \Delta^2}} s'_1 s_J \right)$
$2\mathcal{S}_{1y}\mathcal{S}_{2z}$	$-\frac{\kappa}{2}s_\xi$	$-\frac{\kappa}{2}s_\xi c'_1$	$-\frac{\kappa}{2}s_\xi c'_1 c_J - \frac{\kappa}{2}c_\xi s'_1 s_J$	
\mathcal{S}_{1x}	0	$-\frac{\kappa}{2}c_\xi s'_1$	$-\frac{\kappa}{2}c_\xi s'_1 c_J + \frac{\kappa}{2}s_\xi c'_1 s_J$	$\left. \begin{aligned} &-\frac{\kappa}{2}c_\xi^2 s'_1 c_J + \frac{\kappa}{2}c_\xi s_\xi c'_1 s_J \\ &-\frac{\kappa}{2}s_\xi^2 s'_1 c_J + \frac{\kappa}{2}c_\xi s_\xi c'_1 s_J \end{aligned} \right\} = -\frac{\kappa}{2} \left(s'_1 c_J - \frac{2J}{\sqrt{4J^2 + \Delta^2}} c'_1 s_J \right)$
$2\mathcal{S}_{1x}\mathcal{S}_{2z}$	0	$+\frac{\kappa}{2}s_\xi s'_1$	$+\frac{\kappa}{2}s_\xi s'_1 c_J - \frac{\kappa}{2}c_\xi c'_1 s_J$	

Using the following trigonometric relations

$$c'_1 c_J = \frac{c_1^- + c_1^+}{2} \quad s'_1 s_J = \frac{c_1^- - c_1^+}{2} \quad c'_1 s_J = \frac{-s_1^- + s_1^+}{2} \quad s'_1 c_J = \frac{s_1^- + s_1^+}{2}, \tag{12.48}$$

where $c_1^\pm = \cos((\omega'_{0,1} - \omega_{\text{rot}} \pm \pi J)t) = \cos((\Omega_1^\pm \pm \pi J)t)$ and $s_1^\pm = \sin((\omega'_{0,1} - \omega_{\text{rot}} \pm \pi J)t) = \sin((\Omega_1^\pm \pm \pi J)t)$ ($\omega_{\text{rot}} = -\omega_{\text{radio}}$),

$$\begin{aligned}
\text{Tr}\{\hat{\rho}'_1(t)\mathcal{S}'_{1+}\} &= i\frac{\kappa}{2} \left(c'_1 c_J + \frac{2J}{\sqrt{4J^2 + \Delta^2}} s'_1 s_J \right) - \frac{\kappa}{2} \left(s'_1 c_J - \frac{2J}{\sqrt{4J^2 + \Delta^2}} c'_1 s_J \right) \\
&= i\frac{\kappa}{2} \left(\frac{c_1^- + c_1^+}{2} + \frac{2J}{\sqrt{4J^2 + \Delta^2}} \frac{c_1^- - c_1^+}{2} \right) - \frac{\kappa}{2} \left(\frac{s_1^- + s_1^+}{2} + \frac{2J}{\sqrt{4J^2 + \Delta^2}} \frac{s_1^- - s_1^+}{2} \right) \\
&= i\frac{\kappa}{4} \left(\left(1 + \frac{2J}{\sqrt{4J^2 + \Delta^2}} \right) c_1^- + \left(1 - \frac{2J}{\sqrt{4J^2 + \Delta^2}} \right) c_1^+ + i \left(\left(1 + \frac{2J}{\sqrt{4J^2 + \Delta^2}} \right) s_1^- + \left(1 - \frac{2J}{\sqrt{4J^2 + \Delta^2}} \right) s_1^+ \right) \right) \\
&= \frac{\kappa}{4} e^{i\frac{\pi}{2}} \left(\left(1 + \frac{2J}{\sqrt{4J^2 + \Delta^2}} \right) e^{i(\Omega_1^- - \pi J)t} + \left(1 - \frac{2J}{\sqrt{4J^2 + \Delta^2}} \right) e^{i(\Omega_1^+ + \pi J)t} \right). \tag{12.49}
\end{aligned}$$

We now repeat the analysis for nucleus 2.

Contribution	$\hat{\rho}'_2(\text{b})$	$\omega'_{0,2}\mathcal{S}_{2z}$ →	$\pi J \cdot 2\mathcal{S}_{1z}\mathcal{S}_{2z}$ →	$\text{Tr}\{\hat{\rho}'_2(t)\mathcal{S}'_{2+}\}$
\mathcal{S}_{2y}	$+\frac{\kappa}{2}c_\xi$	$+\frac{\kappa}{2}c_\xi c'_2$	$+\frac{\kappa}{2}c_\xi c'_2 c_J - \frac{\kappa}{2}s_\xi s'_2 s_J$	$\left. \begin{aligned} &+i\frac{\kappa}{2}c_\xi^2 c'_2 c_J - i\frac{\kappa}{2}c_\xi s_\xi s'_2 s_J \\ &+i\frac{\kappa}{2}s_\xi^2 c'_2 c_J - i\frac{\kappa}{2}c_\xi s_\xi s'_2 s_J \end{aligned} \right\} = i\frac{\kappa}{2} \left(c'_2 c_J - \frac{2J}{\sqrt{4J^2 + \Delta^2}} s'_2 s_J \right)$
$2\mathcal{S}_{1z}\mathcal{S}_{2y}$	$+\frac{\kappa}{2}s_\xi$	$+\frac{\kappa}{2}s_\xi c'_2$	$+\frac{\kappa}{2}s_\xi c'_2 c_J - \frac{\kappa}{2}c_\xi s'_2 s_J$	
\mathcal{S}_{2x}	0	$-\frac{\kappa}{2}c_\xi s'_2$	$-\frac{\kappa}{2}c_\xi s'_2 c_J - \frac{\kappa}{2}s_\xi c'_2 s_J$	$\left. \begin{aligned} &-\frac{\kappa}{2}c_\xi^2 s'_2 c_J - \frac{\kappa}{2}c_\xi s_\xi c'_2 s_J \\ &-\frac{\kappa}{2}s_\xi^2 s'_2 c_J - \frac{\kappa}{2}c_\xi s_\xi c'_2 s_J \end{aligned} \right\} = -\frac{\kappa}{2} \left(s'_2 c_J + \frac{2J}{\sqrt{4J^2 + \Delta^2}} c'_2 s_J \right)$
$2\mathcal{S}_{1z}\mathcal{S}_{2x}$	0	$-\frac{\kappa}{2}s_\xi s'_2$	$-\frac{\kappa}{2}s_\xi s'_2 c_J - \frac{\kappa}{2}c_\xi c'_2 s_J$	

Using the following trigonometric relations

$$c'_2 c_J = \frac{c_2^- + c_2^+}{2} \quad s'_2 s_J = \frac{c_2^- - c_2^+}{2} \quad c'_2 s_J = \frac{-s_2^- + s_2^+}{2} \quad s'_2 c_J = \frac{s_2^- + s_2^+}{2}, \tag{12.50}$$

where $c_2^{\pm} = \cos((\omega'_{0,2} - \omega_{\text{rot}} \pm \pi J)t) = \cos((\Omega'_2 \pm \pi J)t)$ and $s_2^{\pm} = \sin((\omega'_{0,2} - \omega_{\text{rot}} \pm \pi J)t) = \sin((\Omega'_2 \pm \pi J)t)$,

$$\begin{aligned}
\text{Tr}\{\hat{\rho}'_2(t)\mathcal{I}'_{2+}\} &= i\frac{\kappa}{2} \left(c_2' c_J - \frac{2J}{\sqrt{4J^2 + \Delta^2}} s_2' s_J \right) - \frac{\kappa}{2} \left(s_2' c_J + \frac{2J}{\sqrt{4J^2 + \Delta^2}} c_2' s_J \right) \\
&= i\frac{\kappa}{2} \left(\frac{c_2'^- + c_2'^+}{2} - \frac{2J}{\sqrt{4J^2 + \Delta^2}} \frac{c_2'^- - c_2'^+}{2} \right) - \frac{\kappa}{2} \left(\frac{s_2'^- + s_2'^+}{2} - \frac{2J}{\sqrt{4J^2 + \Delta^2}} \frac{s_2'^- - s_2'^+}{2} \right) \\
&= i\frac{\kappa}{4} \left(\left(1 - \frac{2J}{\sqrt{4J^2 + \Delta^2}}\right) c_2'^- + \left(1 + \frac{2J}{\sqrt{4J^2 + \Delta^2}}\right) c_2'^+ + i \left(\left(1 - \frac{2J}{\sqrt{4J^2 + \Delta^2}}\right) s_2'^- + \left(1 + \frac{2J}{\sqrt{4J^2 + \Delta^2}}\right) s_2'^+ \right) \right) \\
&= \frac{\kappa}{4} e^{i\frac{\pi}{2}} \left(\left(1 - \frac{2J}{\sqrt{4J^2 + \Delta^2}}\right) e^{i(\Omega'_2 - \pi J)t} + \left(1 + \frac{2J}{\sqrt{4J^2 + \Delta^2}}\right) e^{i(\Omega'_2 + \pi J)t} \right). \tag{12.51}
\end{aligned}$$

Combining results presented in Eqs. 12.51 and 12.49, applying phase correction, and including relaxation, we obtain the following description of the evolution of the signal:

$$\langle M_+ \rangle = \frac{\mathcal{N}\gamma^2 \hbar^2 B_0}{8k_B T} e^{-\bar{R}_2 t} \left((1 - 2c_\xi s_\xi) e^{i(\Omega'_1 - \pi J)t} + (1 + 2c_\xi s_\xi) e^{i(\Omega'_1 + \pi J)t} + (1 + 2c_\xi s_\xi) e^{i(\Omega'_2 - \pi J)t} + (1 - 2c_\xi s_\xi) e^{i(\Omega'_2 + \pi J)t} \right), \tag{12.52}$$

where $2c_\xi s_\xi = 2J/\sqrt{4J^2 + \Delta^2}$.

12.4.3 \mathcal{H}_j and operators of components of total \vec{I} commute

We show that the operator of each component of the total angular momentum (e.g., $\hat{I}_x \propto \mathcal{I}_x = \mathcal{I}_{1x} + \mathcal{I}_{2x} + \mathcal{I}_{3x} + \dots$) commutes with the strong coupling Hamiltonian \mathcal{H}_J for any number of nuclei in the coupled system and for any values of the J constants. For $j = x, k = y, l = z$ or for any cyclic permutation ($j = y, k = z, l = x$ or $j = z, k = x, l = y$),

$$\begin{aligned}
[\mathcal{I}_j, \mathcal{H}_J] &= \sum_n \sum_{n' \neq n} 2\pi J_{nn'} [\mathcal{I}_{nj}, (\mathcal{I}_{nj} \mathcal{I}_{n'j} + \mathcal{I}_{nk} \mathcal{I}_{n'k} + \mathcal{I}_{nl} \mathcal{I}_{n'l})] \\
&= \sum_n \sum_{n' \neq n} 2\pi J_{nn'} ([\mathcal{I}_{nj}, \mathcal{I}_{nk}] \mathcal{I}_{n'k} + [\mathcal{I}_{nj}, \mathcal{I}_{nl}] \mathcal{I}_{n'l}) = \sum_n \sum_{n' \neq n} 2\pi J_{nn'} ([\mathcal{I}_{nj}, \mathcal{I}_{nk}] \mathcal{I}_{n'k} - [\mathcal{I}_{nl}, \mathcal{I}_{nj}] \mathcal{I}_{n'l}) \\
&= \sum_n \sum_{n' \neq n} 2i\pi J_{nn'} (\mathcal{I}_{nl} \mathcal{I}_{n'k} - \mathcal{I}_{nk} \mathcal{I}_{n'l}) = 0
\end{aligned} \tag{12.53}$$

where n and n' are two different nuclei. The commutator is equal to zero because for any pair of nuclei p and q , the term $2i\pi J_{nn'} (\mathcal{I}_{nl} \mathcal{I}_{n'k} - \mathcal{I}_{nk} \mathcal{I}_{n'l})$ appears twice in the sum, with the opposite sign: once for $n = p$ and $n' = q$ as $2i\pi J_{pq} (\mathcal{I}_{pl} \mathcal{I}_{qk} - \mathcal{I}_{pk} \mathcal{I}_{ql})$, and once for $n = q$ and $n' = p$ as $2i\pi J_{pq} (\mathcal{I}_{ql} \mathcal{I}_{pk} - \mathcal{I}_{qk} \mathcal{I}_{pl})$.

12.4.4 J -coupling of magnetically equivalent nuclei

In general, the free evolution of multiple spin-1/2 magnetic moments is governed by the Hamiltonian

$$\mathcal{H} = \sum_n \omega_{0,n} \mathcal{I}_{nz} + \pi J_{nn'} \sum_n \sum_{n'} (2\mathcal{I}_{nx} \mathcal{I}_{n'x} + 2\mathcal{I}_{ny} \mathcal{I}_{n'y} + 2\mathcal{I}_{nz} \mathcal{I}_{n'z}) = \sum_n \omega_{0,n} \mathcal{I}_{nz} + \mathcal{H}_J \tag{12.54}$$

If the nuclei are magnetically equivalent,

$$\mathcal{H} = \omega_0 \sum_n \mathcal{I}_{nz} + \mathcal{H}_J = \omega_0 \mathcal{I}_z + \mathcal{H}_J, \tag{12.55}$$

where \mathcal{I}_z and \mathcal{H}_J commute, as shown in Section 12.4.3. Therefore, the effect of chemical shift and J -coupling can be analyzed separately. Note that \mathcal{H}_J commutes also with M_+ , which is proportional to $\mathcal{I}_x + i\mathcal{I}_y$.

In order to analyze the effect of the J -coupling on the spectrum, we evaluate $\langle M_+ \rangle$ as

$$\langle M_+ \rangle = \text{Tr}\{\hat{\rho} \hat{M}_+\} = \sum_j \sum_k \rho_{jk} M_{+jk}, \tag{12.56}$$

where we expressed the trace explicitly in terms of the elements of the matrices $\hat{\rho}$ and \hat{M}_+ . If the system evolves due to the J -coupling, $\langle M_+ \rangle$ should change, i.e., the time derivative of $\langle M_+ \rangle$ should differ from zero.

$$\frac{d\langle M_+ \rangle}{dt} = \sum_j \sum_k \frac{d\rho_{jk} M_{+jk}}{dt} = \text{Tr} \left\{ \frac{d\hat{\rho}}{dt} \hat{M}_+ \right\}. \quad (12.57)$$

According to the Liouville - von Neumann equation,

$$\frac{d\hat{\rho}}{dt} = i[\hat{\rho}, \mathcal{H}_J] \Rightarrow \frac{d\langle M_+ \rangle}{dt} = i\text{Tr} \left\{ [\hat{\rho}, \mathcal{H}_J] \hat{M}_+ \right\} = i\text{Tr} \left\{ \hat{\rho} \mathcal{H}_J \hat{M}_+ \right\} - i\text{Tr} \left\{ \mathcal{H}_J \hat{\rho} \hat{M}_+ \right\}. \quad (12.58)$$

Because \mathcal{H}_J commutes with \hat{M}_+ (and therefore $\mathcal{H}_J \hat{M}_+ = \hat{M}_+ \mathcal{H}_J$), and because $\text{Tr}\{\hat{A}\hat{B}\} = \text{Tr}\{\hat{B}\hat{A}\}$,

$$\frac{d\langle M_+ \rangle}{dt} = i\text{Tr} \left\{ \hat{\rho} \hat{M}_+ \mathcal{H}_J \right\} - i\text{Tr} \left\{ \mathcal{H}_J \hat{\rho} \hat{M}_+ \right\} = i\text{Tr} \left\{ (\hat{\rho} \hat{M}_+) \mathcal{H}_J \right\} - i\text{Tr} \left\{ \mathcal{H}_J (\hat{\rho} \hat{M}_+) \right\} = i\text{Tr} \left\{ (\hat{\rho} \hat{M}_+) \mathcal{H}_J \right\} - i\text{Tr} \left\{ (\hat{\rho} \hat{M}_+) \mathcal{H}_J \right\} = 0. \quad (12.59)$$

We see that $\langle M_+ \rangle$ does not change due to the J -coupling regardless of the actual form of $\hat{\rho}$. This proves that J -coupling between magnetically equivalent nuclei does not have any effect on the spectrum (is invisible).

12.4.5 Commutation relations of the TOCSY mixing Hamiltonian

The commutators of the \mathcal{I}_{jy} operators with the $\mathcal{H}_{\text{TOCSY}}$ Hamiltonian for a set of three protons with $J_{12} = J_{23} > 0$ and $J_{13} = 0$ are given by

$$[\mathcal{I}_{1y}, \mathcal{H}_{\text{TOCSY}}] = \pi J [\mathcal{I}_{1y}, 2\mathcal{I}_{1x}\mathcal{I}_{2x} + 2\mathcal{I}_{1y}\mathcal{I}_{2y} + 2\mathcal{I}_{1z}\mathcal{I}_{2z}] = 2\pi J [\mathcal{I}_{1y}, \mathcal{I}_{1x}] \mathcal{I}_{2x} + 2\pi J [\mathcal{I}_{1y}, \mathcal{I}_{1z}] \mathcal{I}_{2z} = -2i\pi J (\mathcal{I}_{1z}\mathcal{I}_{2x} - \mathcal{I}_{1x}\mathcal{I}_{2z}), \quad (12.60)$$

$$\begin{aligned} [\mathcal{I}_{2y}, \mathcal{H}_{\text{TOCSY}}] &= \pi J [\mathcal{I}_{2y}, 2\mathcal{I}_{1x}\mathcal{I}_{2x} + 2\mathcal{I}_{1y}\mathcal{I}_{2y} + 2\mathcal{I}_{1z}\mathcal{I}_{2z} + 2\mathcal{I}_{2x}\mathcal{I}_{3x} + 2\mathcal{I}_{2y}\mathcal{I}_{3y} + 2\mathcal{I}_{2z}\mathcal{I}_{3z}] \\ &= 2\pi J \mathcal{I}_{1x} [\mathcal{I}_{2y}, \mathcal{I}_{2x}] + 2\pi J \mathcal{I}_{1z} [\mathcal{I}_{2y}, \mathcal{I}_{2z}] + 2\pi J [\mathcal{I}_{2y}, \mathcal{I}_{2x}] \mathcal{I}_{3x} + 2\pi J [\mathcal{I}_{2y}, \mathcal{I}_{2z}] \mathcal{I}_{3z} \\ &= -2i\pi J (\mathcal{I}_{1x}\mathcal{I}_{2z} - \mathcal{I}_{1z}\mathcal{I}_{2x}) - 2i\pi J (\mathcal{I}_{2x}\mathcal{I}_{3z} - \mathcal{I}_{2z}\mathcal{I}_{3x}), \end{aligned} \quad (12.61)$$

$$[\mathcal{I}_{3y}, \mathcal{H}_{\text{TOCSY}}] = \pi J [\mathcal{I}_{3y}, 2\mathcal{I}_{2x}\mathcal{I}_{3x} + 2\mathcal{I}_{2y}\mathcal{I}_{3y} + 2\mathcal{I}_{2z}\mathcal{I}_{3z}] = 2\pi J \mathcal{I}_{2x} [\mathcal{I}_{3y}, \mathcal{I}_{3x}] + 2\pi J \mathcal{I}_{2z} [\mathcal{I}_{3y}, \mathcal{I}_{3z}] = -2i\pi J (\mathcal{I}_{2x}\mathcal{I}_{3z} - \mathcal{I}_{2z}\mathcal{I}_{3x}). \quad (12.62)$$

A sum of the first two commutators (Eqs. 12.60 and 12.61) shows that

$$[\mathcal{I}_{1y} + \mathcal{I}_{2y}, \mathcal{H}_{\text{TOCSY}}] = 2i\pi J (\mathcal{I}_{2x}\mathcal{I}_{3z} - \mathcal{I}_{2z}\mathcal{I}_{3x}) \quad (12.63)$$

and a sum of all three commutators (Eqs. 12.60–12.62) shows that

$$[\mathcal{I}_{1y} + \mathcal{I}_{2y} + \mathcal{I}_{3y}, \mathcal{H}_{\text{TOCSY}}] = 0 \quad (12.64)$$

in agreement with Eq. 12.53.

12.4.6 Density matrix evolution in the TOCSY experiment

As discussed in Section 12.3, the TOCSY pulse sequence starts by a 90° excitation pulse that converts $\hat{\rho}(a) = \frac{1}{4}(\mathcal{I}_t + \kappa\mathcal{I}_{1z} + \kappa\mathcal{I}_{2z} + \kappa\mathcal{I}_{3z}) = \frac{1}{4}\mathcal{I}_t + \frac{\kappa}{4} \sum_j \mathcal{I}_{jz}$

to

$$\hat{\rho}(b) = \frac{1}{4}(\mathcal{I}_t - \kappa\mathcal{I}_{1y} - \kappa\mathcal{I}_{2y} - \kappa\mathcal{I}_{3y}) = \frac{1}{4}\mathcal{I}_t - \frac{\kappa}{4} \sum_j \mathcal{I}_{jy},$$

which evolves during the incremented evolution period t_1 . An example of a set of nuclei interacting via couplings described by constants $J_{12} = J_{23} = J$ and $J_{13} = 0$ is presented in Section 12.3, here we analyze a general case that evolves (considering only \mathcal{I}_{jy} coherences that survive the TOCSY mixing) as

$$\hat{\rho}(c) = -\frac{\kappa}{4} \sum_j C_{j1} \mathcal{I}_{jy},$$

where

$$\begin{aligned}
C_{11} &= \cos(\Omega_1 t_1) \cos(\pi J_{12} t_1) \cos(\pi J_{13} t_1) = \frac{1}{2} \cos(\Omega_1 t_1) (\cos(\pi J_{12} t_1 - \pi J_{13} t_1) - \cos(\pi J_{12} t_1 + \pi J_{13} t_1)) \\
&= \frac{1}{4} (\cos((\Omega_1 - \pi J_{12} - \pi J_{13}) t_1) + \cos((\Omega_1 - \pi J_{12} + \pi J_{13}) t_1) + \cos((\Omega_1 + \pi J_{12} - \pi J_{13}) t_1) + \cos((\Omega_1 + \pi J_{12} + \pi J_{13}) t_1)) \\
C_{21} &= \cos(\Omega_2 t_1) \cos(\pi J_{12} t_1) \cos(\pi J_{23} t_1) = \frac{1}{2} \cos(\Omega_1 t_1) (\cos(\pi J_{12} t_1 - \pi J_{23} t_1) - \cos(\pi J_{12} t_1 + \pi J_{23} t_1)) \\
&= \frac{1}{4} (\cos((\Omega_1 - \pi J_{12} - \pi J_{23}) t_1) + \cos((\Omega_1 - \pi J_{12} + \pi J_{23}) t_1) + \cos((\Omega_1 + \pi J_{12} - \pi J_{23}) t_1) + \cos((\Omega_1 + \pi J_{12} + \pi J_{23}) t_1)) \\
C_{31} &= \cos(\Omega_3 t_1) \cos(\pi J_{13} t_1) \cos(\pi J_{23} t_1) = \frac{1}{2} \cos(\Omega_1 t_1) (\cos(\pi J_{13} t_1 - \pi J_{23} t_1) - \cos(\pi J_{13} t_1 + \pi J_{23} t_1)) \\
&= \frac{1}{4} (\cos((\Omega_1 - \pi J_{13} - \pi J_{23}) t_1) + \cos((\Omega_1 - \pi J_{13} + \pi J_{23}) t_1) + \cos((\Omega_1 + \pi J_{13} - \pi J_{23}) t_1) + \cos((\Omega_1 + \pi J_{13} + \pi J_{23}) t_1)).
\end{aligned} \tag{12.65}$$

The $-\frac{\kappa}{4} C_{j1} \mathcal{J}_{jy}$ components of the density matrix, converted to $\hat{\rho}(d) = -\frac{\kappa}{4} \sum_j \sum_k a_{jk} C_{j1} \mathcal{J}_{ky}$ during the TOCSY mixing period (see Section 12.3), further evolve during t_2 to $\hat{\rho}(t_2) = -\frac{\kappa}{4} \sum_j \sum_k a_{jk} C_{j1} (C_{k2} \mathcal{J}_{ky} - S_{k2} \mathcal{J}_{kx})$, where

$$\begin{aligned}
C_{12} &= \cos(\Omega_1 t_2) \cos(\pi J_{12} t_2) \cos(\pi J_{13} t_2) = \frac{1}{2} \cos(\Omega_1 t_2) (\cos(\pi J_{12} t_2 - \pi J_{13} t_2) - \cos(\pi J_{12} t_2 + \pi J_{13} t_2)) \\
&= \frac{1}{4} (\cos((\Omega_1 - \pi J_{12} - \pi J_{13}) t_2) + \cos((\Omega_1 - \pi J_{12} + \pi J_{13}) t_2) + \cos((\Omega_1 + \pi J_{12} - \pi J_{13}) t_2) + \cos((\Omega_1 + \pi J_{12} + \pi J_{13}) t_2)) \\
C_{22} &= \cos(\Omega_2 t_2) \cos(\pi J_{12} t_2) \cos(\pi J_{23} t_2) = \frac{1}{2} \cos(\Omega_1 t_2) (\cos(\pi J_{12} t_2 - \pi J_{23} t_2) - \cos(\pi J_{12} t_2 + \pi J_{23} t_2)) \\
&= \frac{1}{4} (\cos((\Omega_1 - \pi J_{12} - \pi J_{23}) t_2) + \cos((\Omega_1 - \pi J_{12} + \pi J_{23}) t_2) + \cos((\Omega_1 + \pi J_{12} - \pi J_{23}) t_2) + \cos((\Omega_1 + \pi J_{12} + \pi J_{23}) t_2)) \\
C_{32} &= \cos(\Omega_3 t_2) \cos(\pi J_{13} t_2) \cos(\pi J_{23} t_2) = \frac{1}{2} \cos(\Omega_1 t_2) (\cos(\pi J_{13} t_2 - \pi J_{23} t_2) - \cos(\pi J_{13} t_2 + \pi J_{23} t_2)) \\
&= \frac{1}{4} (\cos((\Omega_1 - \pi J_{13} - \pi J_{23}) t_2) + \cos((\Omega_1 - \pi J_{13} + \pi J_{23}) t_2) + \cos((\Omega_1 + \pi J_{13} - \pi J_{23}) t_2) + \cos((\Omega_1 + \pi J_{13} + \pi J_{23}) t_2)).
\end{aligned} \tag{12.66}$$

and

$$\begin{aligned}
S_{12} &= \sin(\Omega_1 t_2) \cos(\pi J_{12} t_2) \cos(\pi J_{13} t_2) = \frac{1}{2} \sin(\Omega_1 t_2) (\cos(\pi J_{12} t_2 - \pi J_{13} t_2) - \cos(\pi J_{12} t_2 + \pi J_{13} t_2)) \\
&= \frac{1}{4} (\sin((\Omega_1 - \pi J_{12} - \pi J_{13}) t_2) + \sin((\Omega_1 - \pi J_{12} + \pi J_{13}) t_2) + \sin((\Omega_1 + \pi J_{12} - \pi J_{13}) t_2) + \sin((\Omega_1 + \pi J_{12} + \pi J_{13}) t_2)) \\
S_{22} &= \sin(\Omega_2 t_2) \cos(\pi J_{12} t_2) \cos(\pi J_{23} t_2) = \frac{1}{2} \sin(\Omega_1 t_2) (\cos(\pi J_{12} t_2 - \pi J_{23} t_2) - \cos(\pi J_{12} t_2 + \pi J_{23} t_2)) \\
&= \frac{1}{4} (\sin((\Omega_1 - \pi J_{12} - \pi J_{23}) t_2) + \sin((\Omega_1 - \pi J_{12} + \pi J_{23}) t_2) + \sin((\Omega_1 + \pi J_{12} - \pi J_{23}) t_2) + \sin((\Omega_1 + \pi J_{12} + \pi J_{23}) t_2)) \\
S_{32} &= \sin(\Omega_3 t_2) \cos(\pi J_{13} t_2) \cos(\pi J_{23} t_2) = \frac{1}{2} \sin(\Omega_1 t_2) (\cos(\pi J_{13} t_2 - \pi J_{23} t_2) - \cos(\pi J_{13} t_2 + \pi J_{23} t_2)) \\
&= \frac{1}{4} (\sin((\Omega_1 - \pi J_{13} - \pi J_{23}) t_2) + \sin((\Omega_1 - \pi J_{13} + \pi J_{23}) t_2) + \sin((\Omega_1 + \pi J_{13} - \pi J_{23}) t_2) + \sin((\Omega_1 + \pi J_{13} + \pi J_{23}) t_2)).
\end{aligned} \tag{12.67}$$

Considering the orthogonality of the matrices and the normalization used in our analysis,⁶ the nonzero traces are

$$\text{Tr}\{\mathcal{J}_{nx} \mathcal{J}_{n+}\} = 2, \quad \text{Tr}\{\mathcal{J}_{ny} \mathcal{J}_{n+}\} = 2i. \tag{12.68}$$

$$\text{Tr}\{\hat{\rho}(t_2) \hat{M}_+\} = -\mathcal{N} \gamma \hbar \frac{\kappa}{2} \sum_j \sum_k a_{jk} C_{j1} (iC_{k2} - S_{k2}) = -i\mathcal{N} \gamma \hbar \frac{\kappa}{2} \sum_j \sum_k a_{jk} C_{j1} (C_{k2} + iS_{k2}) = -i\mathcal{N} \gamma \hbar \frac{\kappa}{2} \sum_j \sum_k a_{jk} C_{j1} E_{k2}, \tag{12.69}$$

⁶Our normalization corresponds to $\Lambda = 2$ in Tables 12.2–12.5. If orthonormal matrices are used ($\Lambda = 8$ in the case of 8×8 matrices), $\text{Tr}\{\mathcal{J}_{nx} \mathcal{J}_{n+}\} = 1$ and $\text{Tr}\{\mathcal{J}_{ny} \mathcal{J}_{n+}\} = i$.

where

$$\begin{aligned}
E_{12} &= C_{12} + iS_{12} = \frac{1}{4} \left(e^{i(\Omega_1 - \pi J_{12} - \pi J_{13})t_2} + e^{i(\Omega_1 - \pi J_{12} + \pi J_{13})t_2} + e^{i(\Omega_1 + \pi J_{12} - \pi J_{13})t_2} + e^{i(\Omega_1 + \pi J_{12} + \pi J_{13})t_2} \right) \\
E_{22} &= C_{22} + iS_{22} = \frac{1}{4} \left(e^{i(\Omega_1 - \pi J_{12} - \pi J_{23})t_2} + e^{i(\Omega_1 - \pi J_{12} + \pi J_{23})t_2} + e^{i(\Omega_1 + \pi J_{12} - \pi J_{23})t_2} + e^{i(\Omega_1 + \pi J_{12} + \pi J_{23})t_2} \right) \\
E_{32} &= C_{32} + iS_{32} = \frac{1}{4} \left(e^{i(\Omega_1 - \pi J_{13} - \pi J_{23})t_2} + e^{i(\Omega_1 - \pi J_{13} + \pi J_{23})t_2} + e^{i(\Omega_1 + \pi J_{13} - \pi J_{23})t_2} + e^{i(\Omega_1 + \pi J_{13} + \pi J_{23})t_2} \right).
\end{aligned} \tag{12.70}$$

As the previously discussed two-dimensional experiments, TOCSY is also applied so that a hypercomplex 2D spectrum is obtained. Therefore, acquisition is repeated for each t_1 increment with the phase of the radio wave shifted by 90° (y) during the 90° pulse. The original density matrix

$$\hat{\rho}(a) = \frac{1}{4}(\mathcal{I}_t + \kappa\mathcal{I}_{1z} + \kappa\mathcal{I}_{2z} + \kappa\mathcal{I}_{3z}) = \frac{1}{4}\mathcal{I}_t + \frac{\kappa}{4}\sum_j \mathcal{I}_{jz}$$

is then converted to

$$\hat{\rho}(b) = \frac{1}{4}(\mathcal{I}_t + \kappa\mathcal{I}_{1x} + \kappa\mathcal{I}_{2x} + \kappa\mathcal{I}_{3x}) = \frac{1}{4}\mathcal{I}_t + \frac{\kappa}{4}\sum_j \mathcal{I}_{jx},$$

which evolves during t_1 to the \mathcal{I}_{jy} components, selected during the TOCSY mixing, with the following modulation: $\hat{\rho}(c) = \frac{\kappa}{4}\sum_j S_{j1}\mathcal{I}_{jy}$,

where

$$\begin{aligned}
S_{12} &= \sin(\Omega_1 t_2) \cos(\pi J_{12} t_2) \cos(\pi J_{13} t_2) = \frac{1}{2} \cos(\Omega_1 t_2) (\cos(\pi J_{12} t_2 - \pi J_{13} t_2) - \cos(\pi J_{12} t_2 + \pi J_{13} t_2)) \\
&= \frac{1}{4} (\sin((\Omega_1 - \pi J_{12} - \pi J_{13})t_2) + \sin((\Omega_1 - \pi J_{12} + \pi J_{13})t_2) + \sin((\Omega_1 + \pi J_{12} - \pi J_{13})t_2) + \sin((\Omega_1 + \pi J_{12} + \pi J_{13})t_2)) \\
S_{22} &= \sin(\Omega_2 t_2) \cos(\pi J_{12} t_2) \cos(\pi J_{23} t_2) = \frac{1}{2} \sin(\Omega_1 t_2) (\cos(\pi J_{12} t_2 - \pi J_{23} t_2) - \cos(\pi J_{12} t_2 + \pi J_{23} t_2)) \\
&= \frac{1}{4} (\sin((\Omega_1 - \pi J_{12} - \pi J_{23})t_2) + \sin((\Omega_1 - \pi J_{12} + \pi J_{23})t_2) + \sin((\Omega_1 + \pi J_{12} - \pi J_{23})t_2) + \sin((\Omega_1 + \pi J_{12} + \pi J_{23})t_2)) \\
S_{32} &= \cos(\Omega_3 t_2) \cos(\pi J_{13} t_2) \cos(\pi J_{23} t_2) = \frac{1}{2} \cos(\Omega_1 t_2) (\cos(\pi J_{13} t_2 - \pi J_{23} t_2) - \cos(\pi J_{13} t_2 + \pi J_{23} t_2)) \\
&= \frac{1}{4} (\sin((\Omega_1 - \pi J_{13} - \pi J_{23})t_2) + \sin((\Omega_1 - \pi J_{13} + \pi J_{23})t_2) + \sin((\Omega_1 + \pi J_{13} - \pi J_{23})t_2) + \sin((\Omega_1 + \pi J_{13} + \pi J_{23})t_2)).
\end{aligned} \tag{12.71}$$

The $\frac{\kappa}{4}S_{j1}\mathcal{I}_{jy}$ components of the density matrix, converted to $\hat{\rho}(d) = \frac{\kappa}{4}\sum_j \sum_k a_{jk}S_{j1}\mathcal{I}_{ky}$ during the TOCSY mixing period, evolve during t_2 to

$$\hat{\rho}(t_2) = -\frac{\kappa}{4}\sum_j \sum_k a_{jk}S_{j1}(C_{k2}\mathcal{I}_{ky} - S_{k2}\mathcal{I}_{kx}), \text{ and}$$

$$\text{Tr}\{\hat{\rho}(t_2)\hat{M}_+\} = \mathcal{N}\gamma\hbar\frac{\kappa}{2}\sum_j \sum_k a_{jk}S_{j1}(iC_{k2} - S_{k2}) = i\mathcal{N}\gamma\hbar\frac{\kappa}{2}\sum_j \sum_k a_{jk}S_{j1}(C_{k2} + iS_{k2}) = i\mathcal{N}\gamma\hbar\frac{\kappa}{2}\sum_j \sum_k a_{jk}S_{j1}E_{k2}, \tag{12.72}$$

If we multiply Eq. 12.72 by "i" and combine it with Eq. 12.69, apply phase correction, and introduce relaxation, we obtain a *hypercomplex* signal

$$\langle M_+ \rangle = \mathcal{N}\gamma\hbar\frac{\kappa}{2}\sum_j \sum_k a_{jk}e^{-\bar{R}_2 t_1}(C_{j1} + iS_{j1})e^{-\bar{R}_2 t_1}E_{k2} = \mathcal{N}\gamma\hbar\frac{\kappa}{2}\sum_j \sum_k a_{jk}e^{-\bar{R}_2 t_1}E_{j1}e^{-\bar{R}_2 t_1}E_{k2}. \tag{12.73}$$

where

$$\begin{aligned}
E_{11} &= C_{11} + iS_{11} = \frac{1}{4} \left(e^{i(\Omega_1 - \pi J_{12} - \pi J_{13})t_1} + e^{i(\Omega_1 - \pi J_{12} + \pi J_{13})t_1} + e^{i(\Omega_1 + \pi J_{12} - \pi J_{13})t_1} + e^{i(\Omega_1 + \pi J_{12} + \pi J_{13})t_1} \right) \\
E_{21} &= C_{21} + iS_{21} = \frac{1}{4} \left(e^{i(\Omega_1 - \pi J_{12} - \pi J_{23})t_1} + e^{i(\Omega_1 - \pi J_{12} + \pi J_{23})t_1} + e^{i(\Omega_1 + \pi J_{12} - \pi J_{23})t_1} + e^{i(\Omega_1 + \pi J_{12} + \pi J_{23})t_1} \right) \\
E_{31} &= C_{31} + iS_{31} = \frac{1}{4} \left(e^{i(\Omega_1 - \pi J_{13} - \pi J_{23})t_1} + e^{i(\Omega_1 - \pi J_{13} + \pi J_{23})t_1} + e^{i(\Omega_1 + \pi J_{13} - \pi J_{23})t_1} + e^{i(\Omega_1 + \pi J_{13} + \pi J_{23})t_1} \right).
\end{aligned} \tag{12.74}$$

Lecture 13

Field gradients

Literature: The use of magnetic field gradients in NMR spectroscopy is nicely reviewed in K11 (in particular, K11.11–11.14, presented more systematically and in more detail than here) and also presented in L4.7 and L12.4 (with detailed analysis in LA12), C4.3.3., and B19.5. Magnetic resonance imaging is discussed in B22, the basic ideas of slice selection and frequency encoding are also described in L12.5. A very nice introduction has been written by Lars G. Hanson (currently available at <http://www.drmmr.dk/>).

13.1 Pulsed field gradients in NMR spectroscopy

Resonance frequencies of nuclei depend on properties of the molecule (inherent properties of nuclei and interactions of nuclei with their microscopic environment) and on the external magnetic field. The external magnetic field is what we control and the molecular properties is what we study. We try to keep the external magnetic field as homogeneous as possible so that all nuclei feel the same external field \vec{B}_0 and their frequencies are modulated by their molecular environment only. Now we learn a trick of the spin alchemy which is based on violating this paradigm. It is possible to create a magnetic field that is inhomogeneous in a controlled way. We will discuss an example when the field is linearly increasing along the z axis (Figure 13.1 left, Sections 13.4.1 and 13.4.2). A *linear gradient of magnetic field* (or simply "a gradient" in the NMR jargon) is applied in the z direction. The nuclei close to the bottom of the sample tube feel a weaker magnetic field and have a lower precession frequency, whereas the nuclei close to the top feel a stronger field and have a higher precession frequency in such case. We can say that *frequency carries information about position along the z axis*.

If the gradient in the z direction is applied when the total magnetization vector rotates in the xy plane, nuclei at different height of the sample acquire different frequencies of rotation (an analysis of the density matrix evolution is presented in Section 13.4.1). In the individual slices, the coherence is preserved. But after a while, vectors of local transverse polarization (magnetization) rotating at different frequencies in different slices of the sample would point to all possible directions and they would no longer add up to a measurable total magnetization. We can say (i) that the gradient allows us to distinguish magnetic moments in different slices, or (ii) that the gradient destroys the bulk (net) *transverse* magnetization. The longitudinal polarizations are not influenced. We postpone discussion of the first point of view (selectivity introduced by the gradient) to Section 13.2 and now

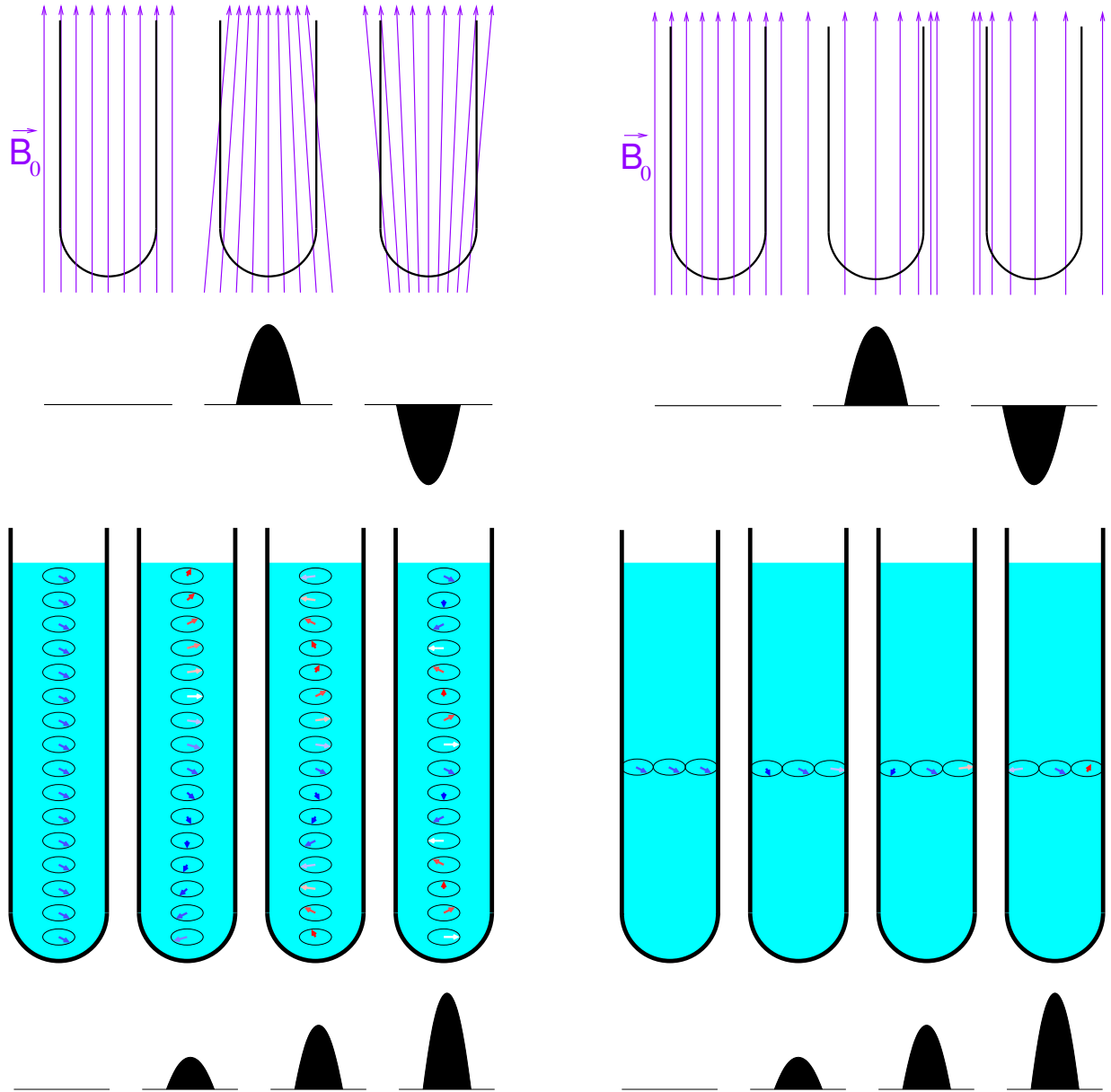


Figure 13.1: Magnetic field gradients in the vertical (z , left) and horizontal (y , right). Top, magnetic induction lines and the corresponding schematic drawings of the gradients (used to present the gradients in pulse sequence diagrams) are shown in purple and black, respectively. Bottom, local transverse polarizations (magnetization) at different positions in the sample tube for increasing gradients (indicated by the black schematic drawings below the sample tubes). The arrows representing the transverse polarizations (magnetization) vectors are color-coded so that blue corresponds to M_x , red corresponds to $-M_x$, and white corresponds to $\pm M_y$. The round shape of the gradient symbols indicates that the gradients were applied with smoothly changing amplitudes as discussed in Section 13.4.2.

explore the consequences of the loss of net magnetization.

At the first glance, it seems that dephasing of coherences and the consequent loss of the signal are completely useless and should be avoided in NMR experiments. It is not true, gradients are very useful if they are applied correctly. The first trick is to apply gradients that destroy coherences we are not interested in. Such gradients have *cleaning* effects and remove unwanted contributions from the spectra.

Another trick is to recover the magnetization back. If we apply the same gradient for the same time, but in the opposite direction ($-z$) later in the pulse sequence, the magnetic vectors are refocused and the signal appears again. We see how an *echo* can be created from two opposite gradients. There are also other ways of creating gradient echoes, presented in Figure 13.2. Instead of using two opposite gradients, two identical gradients can be applied during the refocusing echo (described in Section 10.6), one in the first half of the echo and the other one in the other half (echo "a" in Figure 13.2). The gradients do nothing else but adding another source of frequency variation, on the top of the chemical shift and scalar coupling effects. Magnetic moments of the nuclei affected by the 180° pulse in the middle of the echo get always refocused, no matter what was the origin of the frequency variability. On the other hand, magnetic moments of nuclei not affected by the 180° pulse (e.g., ^{13}C or ^{15}N nuclei if radio waves are applied at the proton frequency) feel two identical gradients and get dephased. We see the selective cleaning effect of the gradient echo, e.g. preserving the \mathcal{I}_y and $2\mathcal{I}_x\mathcal{I}_z$ coherences but destroying unwanted \mathcal{I}_x and \mathcal{I}_y coherences. Gradients incorporated into the decoupling echo (described in Section 10.7) have exactly the opposite effect (echo "b" in Figure 13.2). In this spirit, gradients are frequently added to the echoes in the pulse sequence to clean imperfections of the used pulses.

Application of a cleaning gradient and of gradient echoes in a real NMR experiment is presented in Figure 13.3 (magenta and cyan symbols, respectively). Note that the cleaning (magenta) gradient is applied when no coherence (transverse polarization) should contribute to the density matrix ($\hat{\rho}(d) = \mathcal{I}_t - \frac{\kappa_1}{2}2\mathcal{I}_z\mathcal{I}_z$, cf. the magnetic moment distribution at "d" in Figure 13.3). The cyan gradients are applied during the simultaneous echoes and refocus coherences that evolve due to the J -coupling.

Figure 13.3 also shows another, more tricky use of gradients implemented in an improved version of the HSQC experiment (blue/red and green symbols). The idea is to apply one gradient during the time when the desired coherence rotates in the operator space (and the corresponding transverse polarization rotates in the real space) with the frequency of ^{13}C (or ^{15}N) and the other gradient during the time when the total magnetization rotates with the frequency of protons. In order to do it, we must generate a space in the pulse sequence by including a refocusing echo (a typical example of using refocusing echoes in situation when we need more space but do not want to change evolution). The two applied gradients are not identical, they change the magnetic fields to different extent. The deviations of the field must be exactly in the ratio of resonance frequencies of ^{13}C and ^1H . Then, the gradients form a *heteronuclear gradient echo*. Note what happens to various coherences of protons. The coherence which contributed to the polarization transfer to ^{13}C and back experiences the gradients as an echo and gets refocused. On the other hand, population of protons which polarization was not transferred to ^{13}C (e.g. protons of water that are not ^{13}C -bonded) feels just two gradients of different strengths and its coherence is destroyed. The gradient echo makes the experiment selective for protons correlated with carbons and suppresses the signal of uncorrelated protons.

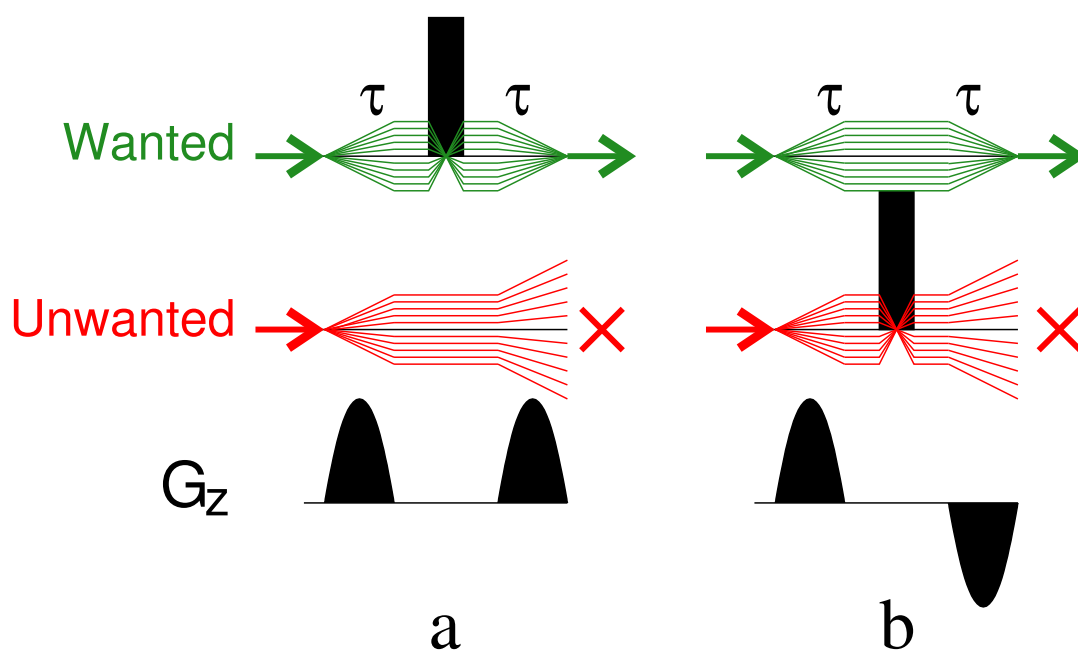


Figure 13.2: Gradient echoes. Black rectangles and round shapes indicate pluses of radio waves and magnetic field gradients, respectively. Evolution of the phase of the desired and undesired transverse coherence (describing direction of the corresponding transverse polarization) is shown as green and red lines, respectively. Values of the phase at different positions in the sample tubes correspond to the distances of the green and red lines from the central black line.

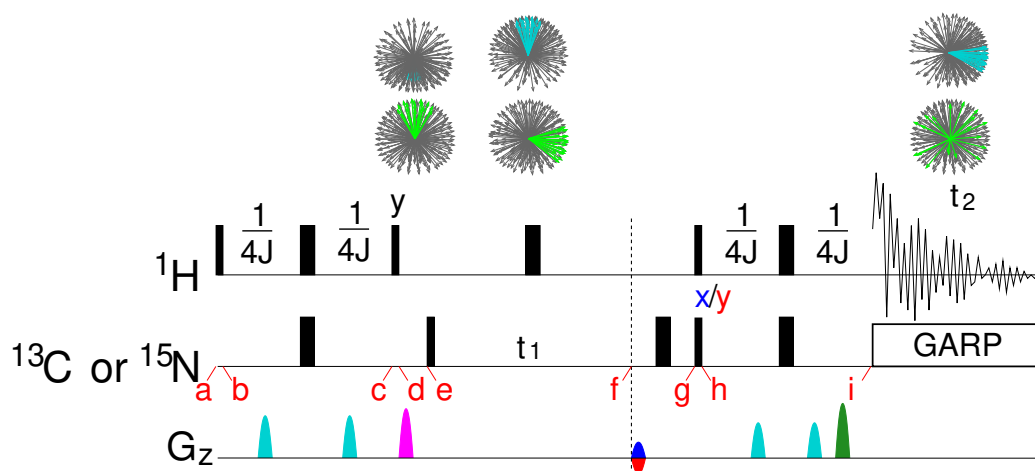


Figure 13.3: Gradient enhanced HSQC experiment. Cleaning gradients and gradient echoes are shown in magenta and cyan, respectively. The heteronuclear gradient echo consists of a gradient shown in green, applied during the last echo (when density matrix evolves with the proton frequency), and of another gradient applied during the refocusing echo between time instants "f" and "g" (when density matrix evolves with the ^{13}C or ^{15}N frequency). The latter gradient is shown in blue in Figure 13.3 for recording the real component of hypercomplex data and in red for recording the imaginary component.

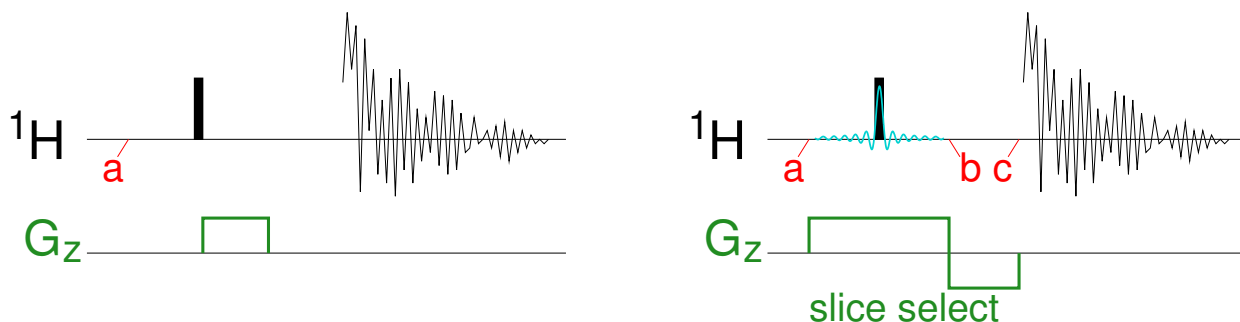


Figure 13.4: Slice selection pulse sequence: the basic idea (left) and real application (right). Gradients of B_0 in the z direction are shown in green. The 90° radio wave pulses are shown schematically as filled black rectangles, the actual modulation of the radio-wave amplitude is depicted in cyan.

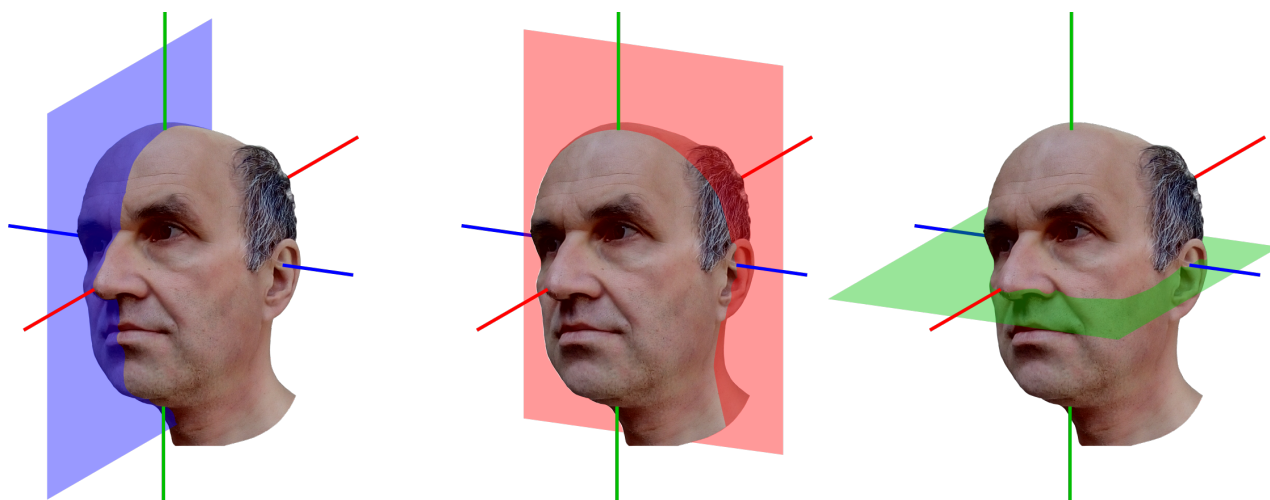


Figure 13.5: Selection of sagittal, coronal, and axial slices by G_x , G_y , and G_z gradients, respectively.

13.2 Magnetic resonance imaging

We now explore selectivity of gradients, mentioned in Section 13.1. During a field gradient in the z direction, the actual precession frequency depends on the position of the molecule along the z axis. This relationship can be used to selectively acquire NMR signal only from molecules in a certain slice perpendicular to the z axis. As discussed in Section 13.4.1, the pulse sequence presented in Figure 13.4 allows us to detect transverse magnetization in a vertical slice of a given thickness. The gradient can be also applied in the x and y directions (right part of Figure 13.1). It is therefore possible to select signal in sagittal, coronal, and axial slices of a human body as shown in Figure 13.5

Gradients also allow us to investigate variations of local magnetization inside the selected slice. One possibility, called *frequency encoding* and presented in Figure 13.6, is to apply a gradient during signal acquisition and to convert the frequency of the Fourier-transformed spectrum to the position

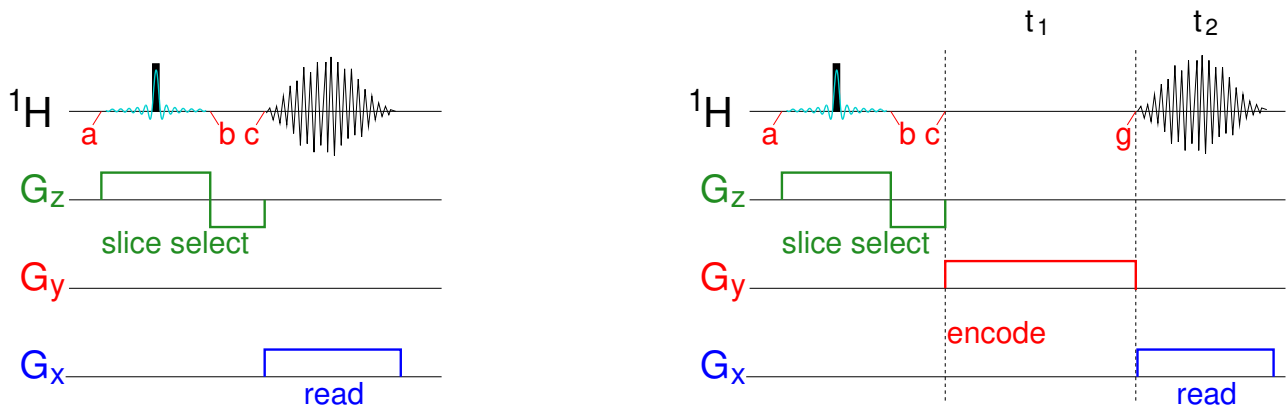


Figure 13.6: Pulse sequences allowing frequency encoded 1D (left) and 2D (right) imaging in the selected slice. Gradients of B_0 in the x , y , and z direction are shown in blue, red, and green, respectively. The 90° radio wave pulses are shown schematically as filled black rectangles, the actual modulation of the radio-wave amplitude is depicted in cyan.

information (see Section 13.4.3 for details). Another option, called *phase encoding* and presented in Figure 13.6, is to vary the strength of a gradient applied for a constant time (see Section 13.4.4 for details).

The *slice-selective* imaging techniques, discussed above, have one disadvantage. It is difficult to select a very thin slice. Therefore, the imaging has limited resolution in one dimension. An alternative approach exists that is not restricted in this sense. It is possible to apply gradient encoding to all three dimensions. An example of such a pulse sequence is shown in the right panel in Figure 13.7. However, such a high-resolution 3D imaging is considerably more time consuming. To save time, shorter than 90° pulses are often applied. Such short pulses leave a large portion of magnetization in the z direction. Therefore, a next short pulse, generating some transverse polarization can be applied immediately after signal acquisition without the need to wait for the return to the equilibrium. In this fashion, several acquisitions may be performed in one T_R period before the longitudinal magnetization is completely "consumed". This significantly reduces the measurement time.

Reconstruction of the two-dimensional image from frequency- and phase-encoded data can be described in the same manner. Both frequency and phase encoding gradient introduce variation of the magnetic field, and consequently of the precession frequency, in the selected slice (xy plane in our example). Linear variations of the magnetic field create "waves" of phases of the transverse polarization, as shown in Figures 13.8 and 13.9. The waves propagate in the x or y direction, respectively, if the gradients G_x and G_y are applied separately. Simultaneous application of both gradients generates waves spreading in a direction given by the relative ratio of the gradient strengths (Figure 13.8B). Each imaging experiment consists of a series of measurements with different setting of the gradients. Each combination of the gradients can be described by two parameters, k_x and k_y , that can be combined in a vector (vector \vec{k} in Figure 13.8B). The values of k_x and k_y vary as the acquisition time proceeds in the case of the frequency encoding gradient, or as the strength of the phase encoding gradient is incremented (see Sections 13.4.3 and 13.4.4 for details). Each panel

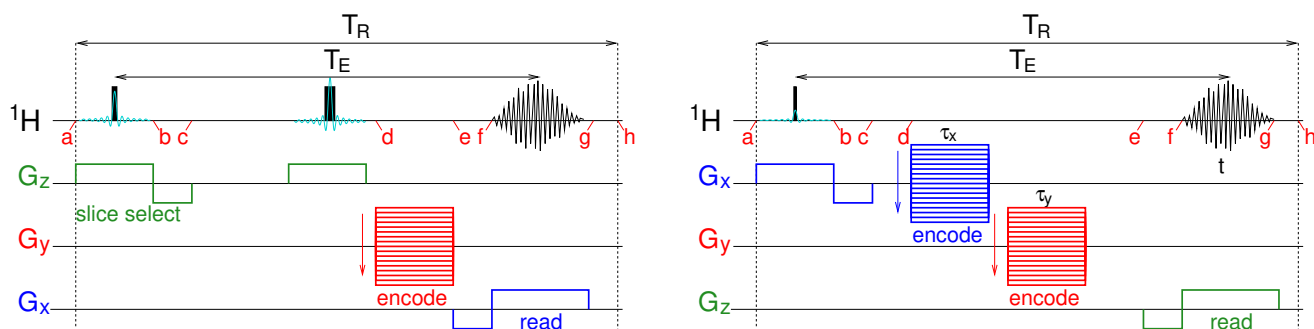


Figure 13.7: Examples of slice-selective 2D imaging experiment, combining phase and frequency encoding (left) and of 3D phase encoding imaging experiment (right). The frequency and phase encode gradients are labeled "read" and "encode" respectively. T_E and T_R are echo time and repetition time, respectively. Gradients of B_0 in the x , y , and z direction are shown in blue, red, and green, respectively. The radio wave pulses (90° in the left panel and 10° in the right panel) are shown schematically as filled black rectangles, the actual modulation of the radio-wave amplitude is depicted in cyan.

in Figure 13.9 represents a phase wave for a particular value of k_x and k_y . In terms of the phase waves, the direction of \vec{k} defines the direction of the wave propagation and the magnitude of \vec{k} says how dense the waves are. We see that \vec{k} behaves as a *wave vector* describing any other physical waves (e.g. electromagnetic waves), and we can expect that signal reconstruction is based on similar principles as analysis of diffraction patterns providing structure of the diffracting objects.

Instead of describing the image reconstruction technically (it is done in Sections 13.4.3 and 13.4.4), here we try to get a general idea by inspecting Figure 13.8. For the sake of simplicity, we assume that all observed nuclei have the same chemical shift. The chemical shift differences (e.g. between aliphatic protons of lipids and protons in water) result in artifacts, displacements of the apparent positions of the observed molecules in the image. Figure 13.8A shows transverse polarization phases in the absence of gradients. The phases are aligned at the beginning of the experiment and move coherently, i.e., do not move at all in the coordinate frame rotating with the frequency $-\omega_{\text{radio}}$ (Figure 13.8A). In the absence of the gradients ($k_x = k_y = 0$), the coherent arrangement of the phases depicted in Figure 13.8A does not change (except for relaxation effects and technical imperfections). We therefore record a signal proportional to the number of observed nuclei in the slice and to the magnetic moment distribution in equilibrium (our constant κ). Application of gradients redistributes the phases as shown in Figure 13.8B. Local transverse polarizations (magnetizations) pointing in opposite directions at different sites of the slice cancel each other, and the net transverse magnetization of the whole slice is very small (equal to zero in Figure 13.8B). We see that the gradients greatly reduce signal in slices with a uniform distribution of magnetic moments (of the *spin density*). What happens if the magnetic moments (the spin density) are not distributed uniformly, but have some *structure*? For example, if bones (containing much less protons than soft tissues) intersect the slice? If the structure is periodic (e.g. like ribs) and if it has a period and orientation matching the period and direction of the phase waves, the signal may greatly increase because protons are concentrated in the regions of the slice with a similar phase of transverse polarization (magnetization). An example is shown in

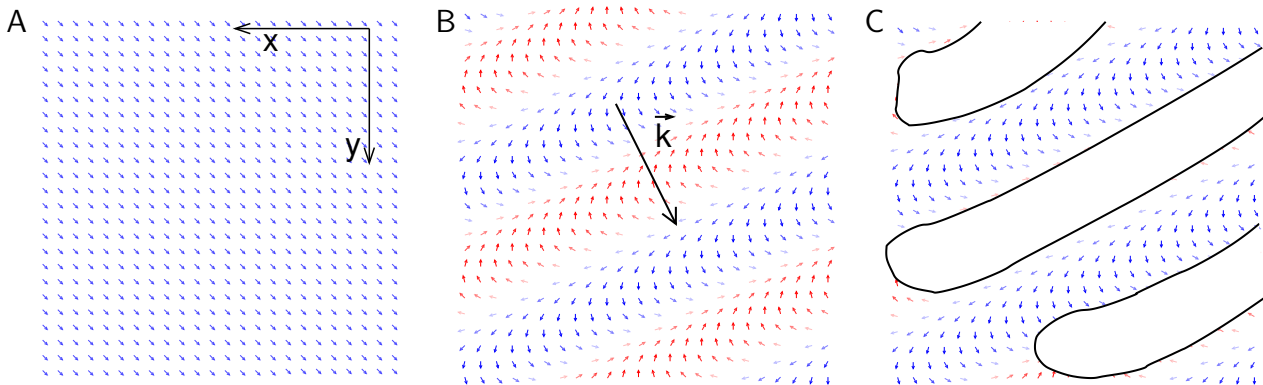


Figure 13.8: Coherent phase distribution (A) and a phase wave generated by the gradients G_x and G_y in selected axial slice with a uniform spin density (B) and with a low-spin density structure (C). The wave vector \vec{k} is depicted in Panel B.

Figure 13.8C.

The example of the Figure 13.8C represents an extreme case of signal enhancement. Most structures in the human body are not periodic as the ribs. But any deviation from uniform distribution of protons perturbs the regular patterns of phase waves resulting in net transverse magnetization close to zero. Each wave interferes with the given structure differently. Therefore, the signal obtained for different k_x and k_y varies. Mathematically, the set of all values of k_x , k_y (and k_z in some experiments) forms a two-dimensional (or three-dimensional) space, called *k-space*. Each combination of gradients represents one point in the *k-space*. If we plot the values of the signal obtained for different gradient settings in the order of increasing k_x and k_y , we obtain a picture of the imaged object in the *k-space*. The task of image reconstruction is to convert this picture into dependence of the spin density on the coordinates x and y . A very simple example is provided in Figure 13.10. Although the signal is calculated only for 25 different \vec{k} values in Figure 13.10, it exhibits some general features. For example, comparison of data collected for shapes with increasing complexity documents that higher values of k_x , k_y (data further from the middle of the *k-space*) reflect finer structural details.

In reality, there is a straightforward relation between the shape of the imaged object in a real space (described by coordinates x , y , and z in some experiments) and the shape of the object's picture in the *k-space* (described by "coordinates" k_x , k_y , and k_z in some experiments). As shown in Sections 13.4.3 and 13.4.4, the dependence of the signal on the distribution of magnetic moments (spin density) in the x, y plane (and in space in general) has a form of the Fourier transformation. Therefore, the distribution of spin density, defining the shape of the object, can be calculated simply by applying the inverse Fourier transformation.

13.3 Weighting

NMR spectroscopy of diluted chemical compounds is often limited by the inherently low sensitivity of NMR experiments. However, the highest possible sensitivity is not the ultimate goal of imaging. It is much more important to obtain a *high contrast*. It does not help us to get a very bright image

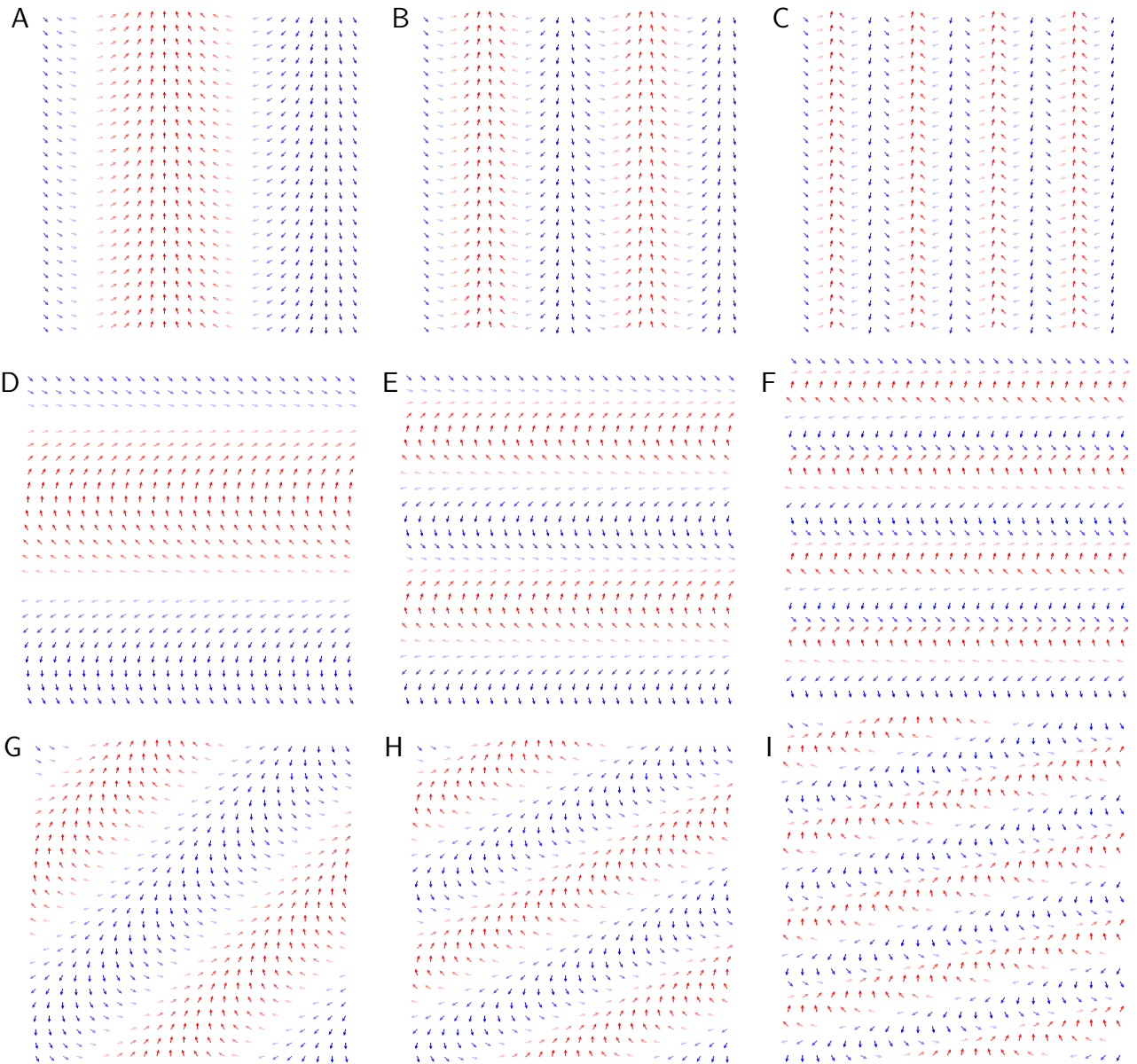


Figure 13.9: Phase waves generated in the selected axial slice by the gradients G_x and G_y .

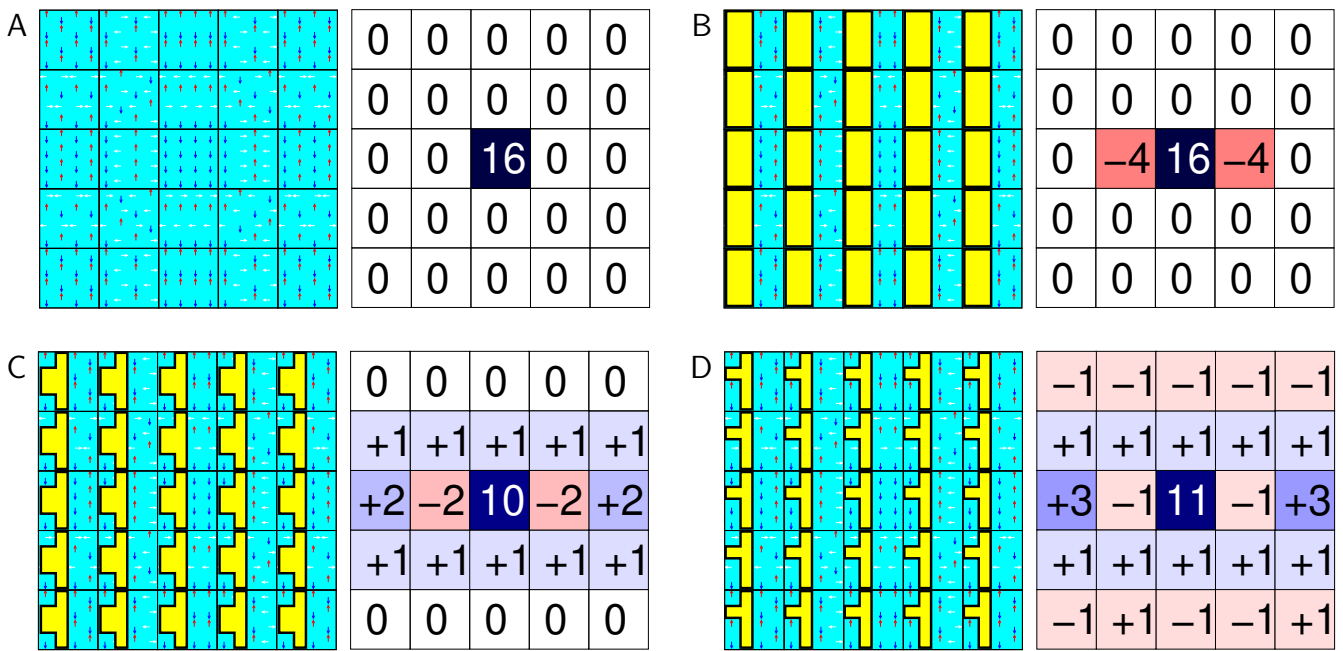


Figure 13.10: A simple example of image reconstruction. In each panel, phase waves (left) and obtained relative signal intensities (right) are shown for 25 different gradient settings (25 small squares). The phases are presented as arrows, color-coded as in Figure 13.1 ($+M_x$ in blue, $-M_x$ in red, $\pm M_{xy}$ in white). The signal intensities are displayed as numbers and corresponding colors (positive and negative intensities are shown in blue and red). Imaging of an object with uniform proton density (A) and with structures of three different shapes (B–D) is presented. Matter with high and low proton density is shown in cyan and yellow, respectively. The depicted waves correspond to the k_x values of $2\Delta k_x$, Δk_x , 0 , $-\Delta k_x$, and $-2\Delta k_x$ (top-to-bottom) and to k_y values of $2\Delta k_y$, Δk_y , 0 , $-\Delta k_y$, and $-2\Delta k_y$ (right-to-left).

of the human body if we cannot distinguish individual organs and finer structural details. So far, we discussed how magnetic resonance imaging reflects the variations in the local concentration of magnetic moments (spin density). But the signal is also influenced by relaxation. Relaxation gives us a unique opportunity to distinguish regions of the body where protons are present in similar concentrations but in molecules with different dynamics and consequently different relaxation. Among numerous, often sophisticated imaging techniques, three major approaches can be recognized.

- *Spin density weighting.* The highest possible signal, depending only on the spin density is obtained if the experiment starts from thermodynamic equilibrium and the transverse relaxation does not decrease the signal significantly. This is the case if (i) the time between the individual measurements is much longer than $1/R_1$ (where R_1 is the relaxation constant of *longitudinal relaxation* which drives the system back to the equilibrium) and (ii) the duration of the experiment is much shorter than $1/R_2$ (where R_2 is the relaxation constant of *transverse relaxation* which is the source of the signal decay). Therefore, the spin density weighted experiments are run with a *short echo time* T_E and *long repetition time* T_R .
- *T_2 weighting.* The signal strongly depending on the relaxation constant R_2 (or on the relaxation time $T_2 = 1/R_2$) is obtained if (i) the time between the individual measurements is much longer than $1/R_1$ and (ii) the duration of the experiment is such that the differences in the factors $e^{-R_2 T_E}$ of different molecules are most pronounced. Therefore, the T_2 weighted experiments are run with a *long echo time* T_E and *long repetition time* T_R . As R_2 is mostly given by $J(0)$ and $J(0)$ is proportional to the rotational correlation time (cf. Eq 2.6), the T_2 -weighted signal is most attenuated for slowly reorienting molecules (molecules in firm tissues).
- *T_1 weighting.* The signal strongly depending on the relaxation constant R_1 (or on the relaxation time $T_1 = 1/R_1$) is obtained if (i) the time between the individual measurements is comparable to $1/R_1$ and (ii) the duration of the experiment is much shorter than $1/R_2$. Therefore, the T_1 weighted experiments are run with a *short echo time* T_E and *short repetition time* T_R . In contrast to R_2 , the major contribution to R_1 is $J(\omega_0)$, which has a maximum (in the approximation of Eq. 9.22) for a rotational correlation time equal to $1/\omega_0$, i.e. 3.75 ns at 1 T or 1.25 ns at 3 T. Therefore, the highest contrast of T_1 -weighted signal is obtained for molecules with intermediate (low-nanosecond) dynamics (molecules in semi-firm tissues).

HOMEWORK

13.4 DERIVATIONS

13.4.1 Coherence dephasing and slice selection by field gradients

Quantitatively, the magnetic field gradient in the direction z is defined as $G_z = \Delta B_0 / \Delta z$. The same applies to gradients applied in other directions: $G_x = \Delta B_0 / \Delta x$, $G_y = \Delta B_0 / \Delta y$. Note that all gradient describe linear perturbations of the *vertical* magnetic field \vec{B}_0 . As the precession frequency ω_0 , and consequently the frequency offset $\Omega = \omega_0 - \omega_{\text{rot}} = \omega_0 - (-\omega_{\text{radio}})$, are proportional to B_0 , the gradient makes the frequency dependent on the position:

$$\Omega'(x) = \Omega - \gamma G_x x, \quad \Omega'(y) = \Omega - \gamma G_y y, \quad \Omega'(z) = \Omega - \gamma G_z z, \quad (13.1)$$

where we set the origins of the axes x , y , z at the place where the gradient has no effect. For the sake of simplicity, we analyze the effect of gradients for magnetic moments not influenced by interactions with electrons and other magnetic dipoles (i.e., we assume that all molecules have the same chemical shift and the dipole-dipole and J couplings are not present or can be neglected). We start with a density matrix describing an ensemble of magnetic moments uniformly rotated by a 90° radio wave pulse from the equilibrium distribution $\hat{\rho}(0) = \mathcal{I}_t - \kappa \mathcal{I}_y$ (Figure 13.4). Then we apply a gradient, e.g. in the z direction. The density matrix at evolves as

$$\hat{\rho}(t) = \mathcal{I}_t - \kappa \overline{\mathcal{I}_y \cos(\Omega'(z)t)} + \kappa \overline{\mathcal{I}_x \sin(\Omega'(z)t)} = \mathcal{I}_t - \kappa \overline{\mathcal{I}_y \cos((\Omega - \gamma G_z z)t)} + \kappa \overline{\mathcal{I}_x \sin((\Omega - \gamma G_z z)t)} = \mathcal{I}_t - \kappa \overline{\mathcal{I}_y \cos \phi(z, t)} + \kappa \overline{\mathcal{I}_x \sin \phi(z, t)}, \quad (13.2)$$

where the horizontal bar indicates ensemble averaging. The expected value of the transverse magnetization is

$$\begin{aligned} \langle M_+ \rangle(t) &= \text{Tr}\{\hat{\rho}(t) \hat{M}_+\} = -\mathcal{N} \frac{\gamma^2 \hbar^2 B_0}{2k_B T} \overline{\text{Tr}\{\mathcal{I}_y \mathcal{I}_+\} \cos((\Omega - \gamma G_z z)t)} + \mathcal{N} \frac{\gamma^2 \hbar^2 B_0}{2k_B T} \overline{\text{Tr}\{\mathcal{I}_x \mathcal{I}_+\} \sin((\Omega - \gamma G_z z)t)} \\ &= \mathcal{N} \frac{\gamma^2 \hbar^2 B_0}{4k_B T} e^{i\frac{\pi}{2}} e^{i(\Omega - \gamma G_z z)t}, \end{aligned} \quad (13.3)$$

Performing phase correction and including relaxation,

$$\langle M_+ \rangle(t) = \mathcal{N} \frac{\gamma^2 \hbar^2 B_0}{4k_B T} e^{-R_2 t} e^{i(\Omega t - \gamma G_z z)t} = \mathcal{N} \frac{\gamma^2 \hbar^2 B_0}{4k_B T} e^{-R_2 t} \left(\overline{\cos(i(\Omega - \gamma G_z z)t)} + \overline{\sin(i(\Omega - \gamma G_z z)t)} \right). \quad (13.4)$$

If the gradient is sufficiently strong, the sine and cosine terms oscillate rapidly and their ensemble averages tend to zero. However, if the value of $\gamma G_z z$ matches the chemical shift (position-independent frequency offset), $\Omega = \gamma G_z z$,

$$\langle M_+ \rangle(t) = \mathcal{N} \frac{\gamma^2 \hbar^2 B_0}{4k_B T} e^{-R_2 t} e^{i(0)t} = \mathcal{N} \frac{\gamma^2 \hbar^2 B_0}{4k_B T} e^{-R_2 t}. \quad (13.5)$$

Therefore, non-negligible signal is obtained only from a slice of the signal at

$$z = \frac{\Omega}{\gamma G_z} = \frac{\omega_0 - \omega_{\text{rot}}}{\gamma G_z} = \frac{\omega_0 - (-\omega_{\text{radio}})}{\gamma G_z}. \quad (13.6)$$

Thickness of the slice depends on the value of G_z (the stronger G_z the thinner the slice) and the position z can be varied by changing the carrier frequency of the radio wave ω_{radio} .

In NMR spectroscopy of samples with relatively low concentration of the studied substance, the signal, obtained only from the selected slice, often decreases below the limit of detection. This is the principle of the action of cleaning gradients (e.g. the magenta gradient in Figure 13.3). If the concentration of the detected compound is sufficiently high and the transverse magnetization in the selected slice is observable, signal from different slices can be compared and further investigated. This is interesting especially if the number of magnetic moments per volume element, or the *spin density* $\mathcal{N}(z)$ varies in the z direction.

$$\langle M_+ \rangle(t) = \frac{\gamma^2 \hbar^2 B_0}{4k_B T} e^{-R_2 t} \overline{\mathcal{N}(z) e^{i(\Omega t - \gamma G_z z)t}} \approx \begin{cases} \frac{\gamma^2 \hbar^2 B_0}{4k_B T} e^{-R_2 t} \mathcal{N}(z) & \text{if } z \approx \frac{\omega_0 - (-\omega_{\text{radio}})}{\gamma G_z} \\ 0 & \text{if } z \neq \frac{\omega_0 - (-\omega_{\text{radio}})}{\gamma G_z} \end{cases} \quad (13.7)$$

In practice, we prefer to select signal from a region of a well defined thickness. This is achieved by applying simultaneously the gradient and a radio wave with the amplitude modulated so that magnetic moments with frequencies in a certain interval are rotated by an angle close to 90° , whereas magnetic moments with frequencies outside the selected interval are almost unaffected (the amplitude modulation is shown in cyan in Figure 13.4). Then, the condition $z \approx (\omega_0 - (-\omega_{\text{radio}})) / (\gamma G_z)$ is fulfilled in an interval of z defined by the range of the frequencies affected by the radio-wave pulse. The amplitude-modulated radio-wave pulse is usually relatively long and magnetic moments with slightly different precession frequencies (within the selected range) have enough time to rotate significantly during the pulse. This rotation, different for different vertical positions inside the selected slice, is refocused by a negative gradient. It can be shown that the gradients make an exact echo if the negative gradient corresponds to the second half of the positive gradient (between the middle and end of the amplitude-modulated radio-wave pulse, see Figure 13.4).

Such filtering of the signal according to the z coordinate of the observed molecule is the basis of slice-selective imaging techniques. The gradients applied in the x or y direction can be used in the same manner to select slices perpendicular to the x or y axis, respectively. In human body imaging, the coordinate system is used so that G_x , G_y , and G_z selects sagittal, coronal, and axial slices, respectively (see Figure 13.5).

13.4.2 Field gradients with smooth amplitude

In NMR pulse sequences, the gradient is usually not switched on and off suddenly. Instead, the linear magnetic field perturbation is increased and decreased in a smooth fashion, following for example a function $\sin(\pi t/\tau_z)$ for a gradient that starts at $t = 0$ and is finished at $t = \tau_z$. In such a case, the total rotation angle of the transverse polarization (the phase ϕ) is

$$\phi(z, t) = \Omega t - \gamma z \frac{\Delta B_0(t = \tau_z/2)}{\Delta z} \int_0^{\tau_z} \sin \frac{\pi t}{\tau_z} dt. \quad (13.8)$$

Because the ratio

$$\frac{\int_0^t f(t') dt'}{t} \quad (13.9)$$

is constant (definition of the average value of $f(t)$), it is convenient to absorb the effect of the smooth amplitude of the gradient into the value of G_z :

$$\phi(z, \tau_z) = \Omega \tau_z - \gamma z \underbrace{\frac{\Delta B_0(t = \tau_z/2)}{\Delta z} \int_0^{\tau_z} \sin \frac{\pi t}{\tau_z} dt}_{G_z} \tau_z = \Omega \tau_z - \gamma G_z z \tau_z. \quad (13.10)$$

The equations describing the slice selection can be modified for the gradients with a smooth amplitude (*shaped gradients*) by changing t to τ_z .

13.4.3 Frequency encoding gradients

We now proceed to the imaging in the slice selected at $z \approx (\omega_0 - (-\omega_{\text{radio}}))/(\gamma G_z)$. In order to describe imaging in the x direction based on *frequency encoding*, we analyze how the density matrix evolves during the G_x gradient in Figure 13.6. The density matrix at the beginning of G_x is $\hat{\rho}(c) = \mathcal{I}_t - \kappa \mathcal{I}_y$ in the selected slice and $\hat{\rho}(c) = \mathcal{I}_t$ everywhere else. During G_x , $\hat{\rho}(t)$ in the slice evolves as

$$\hat{\rho}(t) = \mathcal{I}_t - \kappa \mathcal{I}_y \cos((\Omega t - \gamma G_x x)t) + \kappa \mathcal{I}_x \sin((\Omega t - \gamma G_x x)t), \quad (13.11)$$

which can be also written as

$$\hat{\rho}(x) = \mathcal{I}_t - \kappa \mathcal{I}_y \cos((\Omega t - \gamma G_x t x)) + \kappa \mathcal{I}_x \sin((\Omega t - \gamma G_x t x)) = \mathcal{I}_t - \kappa \mathcal{I}_y \cos((\Omega t - k_x x)) + \kappa \mathcal{I}_x \sin((\Omega t - k_x x)), \quad (13.12)$$

where k_x is the x -component of the *wave vector* \vec{k} in Figure 13.8. Introducing relaxation and performing phase correction,

$$\langle M_+ \rangle(t) = \frac{\gamma^2 \hbar^2 B_0}{4k_B T} e^{-R_2 \tau_z} e^{i\Omega t - R_2 t} \overline{\mathcal{N}(x) e^{-i\gamma G_x x t}}. \quad (13.13)$$

Expressing the ensemble averaging explicitly,

$$\langle M_+ \rangle(t) = \frac{\gamma^2 \hbar^2 B_0}{4k_B T} e^{-R_2 \tau_z} e^{i\Omega t - R_2 t} \int_0^{L_x} \mathcal{N}(x) e^{-i\gamma G_x x t} dx = \frac{\gamma^2 \hbar^2 B_0}{4k_B T} e^{-R_2 \tau_z} e^{i\Omega t - R_2 t} \int_0^{L_x} \mathcal{N}(x) e^{-ik_x x} dx, \quad (13.14)$$

where L_x is the size of the imaged object in the x direction.

Fourier transformation of $\langle M_+ \rangle(t)$ gives a spectrum corresponding to

$$Y(\omega) = \frac{\gamma^2 \hbar^2 B_0}{4k_B T} e^{-R_2 \tau_z} \int_0^{L_x} \mathcal{N}(x) \left(\frac{R_2}{R_2^2 + (\Omega - \gamma G_x x - \omega)^2} + i \frac{\Omega - \gamma G_x x - \omega}{R_2^2 + (\Omega - \gamma G_x x - \omega)^2} \right) dx, \quad (13.15)$$

with the spatial distribution encoded in the apparent frequency $\Omega' = \Omega - \gamma G_x x$.

In reality, the signal is stored as N discrete data points sampled with a time increment Δt . The value $k_x = \gamma G_x t = \gamma G_x \cdot n \Delta t$ can be written as $n \Delta k_x$, where $\Delta k_x = \gamma G_x \cdot \Delta t$. The sampled time points correspond to $n \Delta t = n \Delta k_x / (\gamma G_x)$. Considering $\Delta t \Delta f = 1/N$ (Eq. 3.7), $\Delta k_x = \gamma G_x / (N \Delta f)$. The second integral in Eq. 13.14 has the form of the Fourier transformation (as $\mathcal{N}(x) = 0$ for $x < 0$ and $x > L$, the integration can be extended to $\pm\infty$). The distribution of the spin density $\mathcal{N}(x)$ can be evaluated at discrete values of $x = j \Delta x$ by the inverse discrete Fourier transformation of the signal sampled at $n \Delta t = n \Delta k_x / (\gamma G_x)$:

$$\mathcal{N}(x) = \mathcal{N}_j = \frac{4k_B T \Delta k_x}{\gamma^2 \hbar^2 B_0 e^{-R_2 \tau_z}} \sum_{n=0}^{N-1} \langle M_+ \rangle_n e^{-(i\Omega - R_2) \frac{\Delta k_x \cdot n}{\gamma G_x}} e^{i2\pi \frac{j \cdot n}{N}}. \quad (13.16)$$

Note that all features of discrete Fourier transformation (e.g. aliasing) are relevant for image reconstruction. Extending the discussion to the two-dimensional experiment (right panel in Figure 13.6), is straightforward:

$$x = j_x \Delta x \quad k_x = \gamma G_x t = \gamma G_x \cdot n_x \Delta t_2 \quad \Delta k_x = \gamma G_x \cdot \Delta t_2 = \gamma G_x / (N_x \Delta f_2) \quad (13.17)$$

$$y = j_y \Delta y \quad k_y = \gamma G_y t = \gamma G_y \cdot n_y \Delta t_1 \quad \Delta k_y = \gamma G_y \cdot \Delta t_1 = \gamma G_y / (N_y \Delta f_1), \quad (13.18)$$

and

$$\mathcal{N}(x, y) = \mathcal{N}_{j_x, j_y} = \Delta k_x \Delta k_y \frac{4k_B T}{\gamma^2 \hbar^2 B_0 e^{-R_2 \tau_z}} \sum_{n_x=0}^{N_x-1} \sum_{n_y=0}^{N_y-1} \langle M_+ \rangle_{n_x, n_y} e^{-i(\Omega - R_2) \left(\frac{\Delta k_x \cdot n_x}{\gamma G_x} + \frac{\Delta k_y \cdot n_y}{\gamma G_y} \right)} e^{i2\pi \left(\frac{j_x \cdot n_x}{N_x} + \frac{j_y \cdot n_y}{N_y} \right)}. \quad (13.19)$$

13.4.4 Phase encoding gradients

In order to describe imaging in the y direction based on *phase encoding*, we analyze how the density matrix evolves during the G_y gradient in the pulse sequence presented in the left panel in Figure 13.7. The gradient is placed in a refocusing echo of the duration T_E . We ignore the possible phase shift and assume that the density matrix at the beginning of G_y is $\hat{\rho}(d) = \mathcal{I}_t + \kappa \mathcal{I}_y$ inside the selected slice and $\hat{\rho}(d) = \mathcal{I}_t$ everywhere else. During G_y , $\hat{\rho}(d)$ evolves to

$$\hat{\rho}(e) = \mathcal{I}_t + \kappa \mathcal{I}_y \overline{\cos((\Omega - \gamma G_y y) \tau_y)} - \kappa \mathcal{I}_x \overline{\sin((\Omega - \gamma G_y y) \tau_y)}, \quad (13.20)$$

where τ_y is the duration of the gradient. Expressing $\hat{\rho}(e)$ as a function of y ,

$$\hat{\rho}(y) = \mathcal{I}_t + \kappa \mathcal{I}_y \overline{\cos((\Omega \tau_y - \gamma G_y \tau_y y)} - \kappa \mathcal{I}_x \overline{\sin((\Omega \tau_y - \gamma G_y \tau_y y)} = \mathcal{I}_t + \kappa \mathcal{I}_y \overline{\cos((\Omega \tau_y - k_y y)} - \kappa \mathcal{I}_x \overline{\sin((\Omega \tau_y - k_y y)}. \quad (13.21)$$

During imaging, τ_y is kept constant and the phase shift $\Omega \tau_y$ is refocused by the echo. The parameter that is varied is the strength of the gradient G_y , gradually decreased from the originally positive value to a negative one by increments ΔG_y .

Then, a negative *pre-phasing* gradient G_x is applied for a time period equal to the half of the total acquisition time $N_x \Delta t / 2$. Ignoring the phase shifts $\Omega \tau_x$ and $-\Omega N_x \Delta t / 2$ that get refocused at T_E , the density matrix at the beginning of data acquisition is

$$\begin{aligned} \hat{\rho}(f) = & \mathcal{I}_t + \kappa \mathcal{I}_y \overline{\left(\cos(-\gamma G_y \tau_y y) \cos\left(+\gamma G_x \frac{N_x}{2} \Delta t x\right) - \sin(-\gamma G_y \tau_y y) \sin\left(+\gamma G_x \frac{N_x}{2} \Delta t x\right) \right)} \\ & - \kappa \mathcal{I}_x \overline{\left(\sin(-\gamma G_y \tau_y y) \cos\left(+\gamma G_x \frac{N_x}{2} \Delta t x\right) - \cos(-\gamma G_y \tau_y y) \sin\left(+\gamma G_x \frac{N_x}{2} \Delta t x\right) \right)} \end{aligned} \quad (13.22)$$

and further evolves during the acquisition as

$$\hat{\rho}(x, y) = \mathcal{I}_t + \kappa \mathcal{I}_y \overline{c_x c_y - s_x s_y} - \kappa \mathcal{I}_x \overline{s_x c_y + c_x s_y}, \quad (13.23)$$

where

$$s_x = \sin(k_x x) = -\sin\left(\left(\frac{N_x}{2} - n_x\right) \Delta k_x x\right) \quad c_x = \cos(k_x x) = \cos\left(\left(\frac{N_x}{2} - n_x\right) \Delta k_x x\right) \quad (13.24)$$

$$s_y = \sin(k_y y) = -\sin\left(\left(\frac{N_y}{2} - n_y\right) \Delta k_y y\right) \quad c_y = \cos(k_y y) = \cos\left(\left(\frac{N_y}{2} - n_y\right) \Delta k_y y\right) \quad (13.25)$$

$$x = j_x \Delta x \quad k_x = k_x(0) + \gamma G_x t = -\left(\frac{N_x}{2} - n_x\right) \gamma G_x \Delta t \quad \Delta k_x = -\gamma G_x \cdot \Delta t = \gamma G_x / (N_x \Delta f) \quad (13.26)$$

$$y = j_y \Delta y \quad k_y = k_y(0) - n_y \gamma \Delta G_y \tau_y = \left(\frac{N_y}{2} - n_y\right) \gamma \tau_y \Delta G_y \quad \Delta k_y = -\gamma \Delta G_y \cdot \tau_y. \quad (13.27)$$

The pre-phasing gradient makes the evolution of the density matrix to start from negative k_x and pass $k_x = 0$ in the middle of the experiment. The modulation by $k_x x$ and $k_y y$ thus has the same form.

Using standard trigonometric relations,

$$\hat{\rho}(x, y) = \mathcal{I}_t + \kappa \mathcal{I}_y \overline{\left(\left(\frac{N_x}{2} - n_x\right) \Delta k_x x + \left(\frac{N_y}{2} - n_y\right) \Delta k_y y \right)} + \kappa \mathcal{I}_x \overline{\left(\left(\frac{N_x}{2} - n_x\right) \Delta k_x x + \left(\frac{N_y}{2} - n_y\right) \Delta k_y y \right)}, \quad (13.28)$$

Introducing relaxation and performing phase correction,

$$\langle M_+ \rangle(k_x, k_y) = \frac{\gamma^2 \hbar^2 B_0}{4k_B T} e^{-R_2(T_E - (\frac{N_x}{2} - n_x) \frac{\Delta k_x}{\gamma G_x})} \overline{\mathcal{N}(x, y) e^{-i((\frac{N_x}{2} - n_x) \Delta k_x x + (\frac{N_y}{2} - n_y) \Delta k_y y)}}. \quad (13.29)$$

Expressing the ensemble averaging explicitly,

$$\langle M_+ \rangle(k_x, k_y) = \frac{\gamma^2 \hbar^2 B_0}{4k_B T} e^{-R_2(T_E - (\frac{N_x}{2} - n_x) \frac{\Delta k_x}{\gamma G_x})} \int_0^{L_x} \int_0^{L_y} \mathcal{N}(x, y) e^{-i((\frac{N_x}{2} - n_x) \Delta k_x x + (\frac{N_y}{2} - n_y) \Delta k_y y)} dx dy. \quad (13.30)$$

Inverse discrete Fourier transformation converts the signal into the two-dimensional image

$$\mathcal{N}(x, y) = \mathcal{N}_{j_x, j_y} = \frac{4k_B T \Delta k_x \Delta k_y}{\gamma^2 \hbar^2 B_0 e^{-R_2 T_E}} \sum_{n_x = -\frac{N_x}{2}}^{\frac{N_x}{2} - 1} \sum_{n_y = -\frac{N_y}{2}}^{\frac{N_y}{2} - 1} \langle M_+ \rangle_{n_x, n_y} e^{-R_2(\frac{N_x}{2} - n_x) \frac{\Delta k_x}{\gamma G_x}} e^{i2\pi \left(\frac{j_x \cdot n_x}{N_x} + \frac{j_y \cdot n_y}{N_y} \right)}. \quad (13.31)$$

The analysis can be easily extended to the *three-dimensional* imaging experiment presented in the right panel in Figure 13.7, where two phase-encoding gradients G_x and G_y are applied (the frequency encoding gradient is G_z). The evolution of the density matrix matrix from $\hat{\rho}(d)$ introduces the modulation

$$\hat{\rho}(x, y) = \mathcal{I}_t + \kappa \overline{\mathcal{I}_y C_x C_y C_z - s_x s_y C_z - s_x C_y s_z - C_x C_y C_z} - \kappa \overline{\mathcal{I}_x s_x C_y C_z + C_x s_y C_z + C_x C_y s_z - s_x s_y s_z}, \quad (13.32)$$

where

$$s_x = \sin(k_x x) = -\sin\left(\left(\frac{N_x}{2} - n_x\right) \Delta k_x x\right) \quad c_x = \cos(k_x x) = \cos\left(\left(\frac{N_x}{2} - n_x\right) \Delta k_x x\right) \quad (13.33)$$

$$s_y = \sin(k_y y) = -\sin\left(\left(\frac{N_y}{2} - n_y\right) \Delta k_y y\right) \quad c_y = \cos(k_y y) = \cos\left(\left(\frac{N_y}{2} - n_y\right) \Delta k_y y\right) \quad (13.34)$$

$$s_z = \sin(k_z z) = -\sin\left(\left(\frac{N_z}{2} - n_z\right) \Delta k_z z\right) \quad c_z = \cos(k_z z) = \cos\left(\left(\frac{N_z}{2} - n_z\right) \Delta k_z z\right) \quad (13.35)$$

$$x = j_x \Delta x \quad k_x = k_x(0) - n_x \gamma \Delta G_x \tau_x = \left(\frac{N_x}{2} - n_x\right) \gamma \tau_x \Delta G_x \quad \Delta k_x = -\gamma \Delta G_x \cdot \tau_x \quad (13.36)$$

$$y = j_y \Delta y \quad k_y = k_y(0) - n_y \gamma \Delta G_y \tau_y = \left(\frac{N_y}{2} - n_y\right) \gamma \tau_y \Delta G_y \quad \Delta k_y = -\gamma \Delta G_y \cdot \tau_y \quad (13.37)$$

$$z = j_z \Delta z \quad k_z = k_z(0) + \gamma G_z t = -\left(\frac{N_z}{2} - n_z\right) \gamma G_z \Delta t \quad \Delta k_z = -\gamma G_z \cdot \Delta t = \gamma G_z / (N_z \Delta f). \quad (13.38)$$

The corresponding signal is

$$\langle M_+ \rangle(k_x, k_y, k_z) = \frac{\gamma^2 \hbar^2 B_0}{4k_B T} e^{-R_2(T_E - (\frac{N_z}{2} - n_z) \frac{\Delta k_z}{\gamma G_z})} \int_0^{L_x} \int_0^{L_y} \int_0^{L_z} \mathcal{N}(x, y, z) e^{-i((\frac{N_x}{2} - n_x) \Delta k_x x + (\frac{N_y}{2} - n_y) \Delta k_y y + (\frac{N_z}{2} - n_z) \Delta k_z z)} dx dy dz, \quad (13.39)$$

and the inverse discrete Fourier transformation converts it into the three-dimensional image

$$\mathcal{N}(x, y, z) = \mathcal{N}_{j_x, j_y, j_z} = \frac{4k_B T \Delta k_x \Delta k_y \Delta k_z}{\gamma^2 \hbar^2 B_0 e^{-R_2 T_E}} \sum_{n_x = -\frac{N_x}{2}}^{\frac{N_x}{2} - 1} \sum_{n_y = -\frac{N_y}{2}}^{\frac{N_y}{2} - 1} \sum_{n_z = -\frac{N_z}{2}}^{\frac{N_z}{2} - 1} \langle M_+ \rangle_{n_x, n_y, n_z} e^{-R_2(\frac{N_z}{2} - n_z) \frac{\Delta k_z}{\gamma G_z}} e^{i2\pi \left(\frac{j_x \cdot n_x}{N_x} + \frac{j_y \cdot n_y}{N_y} + \frac{j_z \cdot n_z}{N_z} \right)}. \quad (13.40)$$